НАУЧНО-ПРАКТИЧЕСКИЙ ЖУРНАЛ

ISSN 1682-0363 (print)
ISSN 1819-3684 (online)

# БЮЛЛЕТЕНЬ СИБИРСКОЙ МЕДИЦИНЫ

# BULLETIN OF SIBERIAN MEDICINE


Том 24
№ 3. 2025

# Издательский дом Сибирского государственного медицинского университета представляет серию книг

# «Наследие томской медицины»

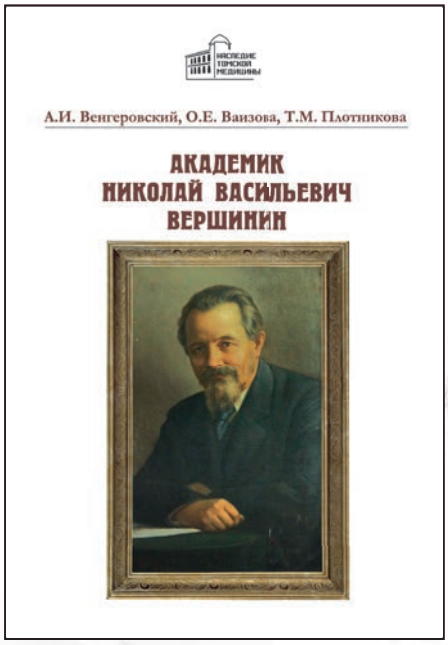


В книге представлены биография и обзор научной, педагогической и общественной деятельности выдающегося фармаколога, академика АМН СССР, заслуженного деятеля науки РСФСР, лауреата Сталинской (Государственной) премии Николая Васильевича Вершинина (1867–1951).

Для врачей, студентов, ученых, всех интересующихся историей медицины.


Книга посвящена памяти доктора медицинских наук, профессора Владимира Демьяновича Суходоло (1919–2000), участника обороны Ленинграда, инвалида Великой Отечественной войны, работавшего в Сибирском государственном медицинском университете (СибГМУ, Томском медицинском институте) в 1948–2000 гг. С уважением, восхищением и любовью профессора В.Д. Суходоло вспоминают ученики, коллеги, друзья, члены семьи, родные.

Для тех, кто интересуется историей медицины, Сибирского государственного медицинского университета, Томска.

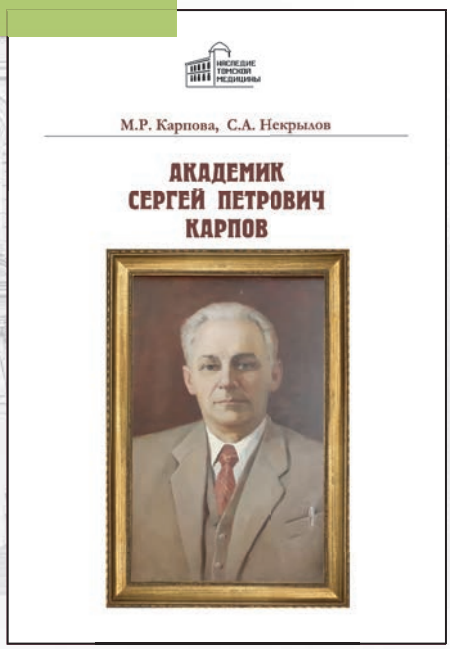


В книге представлены биография и обзор научной, педагогической и общественной деятельности выдающегося микробиолога, вирусолога и эпидемиолога, академика АМН СССР, заслуженного деятеля науки РСФСР Сергея Петровича Карпова (1903–1976).

Для врачей, студентов, ученых, всех интересующихся историей медицины.

# BULLETIN OF SIBERIAN MEDICINE

Peer-reviewed scientific-practical journal
Issued quarterly

## Volume 24, No. 3, 2025

ISSN 1682-0363 (print)
ISSN 1819-3684 (online)

**FOUNDER AND PUBLISHER:**
Siberian State Medical University, Ministry of Healthcare of the Russian Federation

Registered by the Ministry of Mass Media and Communications of the Russian Federation
Certificate of registration
No. 77-7366 of 26.03.2001

The journal "Bulletin of Siberian Medicine" is included in the list of peer-reviewed scientific journals and publications issued in the Russian Federation, which should publish main scientific results of doctoral and Candidate of Sciences theses

Bulletin of Siberian Medicine is indexed in:
Scopus
Web of Science (WoS (ESCI))
Science Index
RSCI
Ulrich's International Periodicals Directory
Cyberleninka
DOAS

Editorial Board Office:
107 Lenina Ave., 634050 Tomsk, Russian Federation
Telephone: +7-(382-2)-51-41-53.
http://bulletin.ssmu.ru
E-mail: bulletin.tomsk@mail.ru

Publisher: Siberian State Medical University.
2, Moscow Trakt, Tomsk, 634050,
Russian Federation.
Editors: E.E. Stepanova, Yu.P. Gotfrid
Translators: D.A. Guryanova, E.D. Zaitseva, E.Yu. Skvortsova, M.E. Chirikova
Electronic makeup, cover design: L.D. Krivtsova

Printed in Litburo LLC,
4 Koroleva Str., Tomsk, 634055 Russian Federation

Signed to print on 29.09.2025
Format 60 × 84/8. Offset print.
Coated paper. Times font.
P.s. 23. C.p.s. 22,5.
500 copies. Order No. 723.

The price – free.
Date of publication 30.09.2025.

# БЮЛЛЕТЕНЬ СИБИРСКОЙ МЕДИЦИНЫ

Научно-практический журнал
Выходит 4 раза в год

## Том 24, № 3, 2025

ISSN 1682-0363 (print)
ISSN 1819-3684 (online)

**УЧРЕДИТЕЛЬ И ИЗДАТЕЛЬ:**
ФГБОУ ВО «Сибирский государственный медицинский университет» Минздрава России

Журнал основан в 2001 году
Зарегистрирован в Министерстве РФ по делам печати, телерадиовещания и средств массовых коммуникаций
Свидетельство регистрации ПИ № 77-7366 от 26.03.2001 г.

Журнал входит в Перечень ведущих рецензируемых научных журналов и изданий, выпускаемых в РФ, в которых должны быть опубликованы основные научные результаты диссертаций на соискание ученой степени доктора и кандидата наук

Индексация:
Scopus
Web of Science (WoS (ESCI))
РИНЦ (Science Index)
RSCI
Ulrich's International Periodicals Directory
Cyberleninka
DOAS

Редакция:
634050, г. Томск, пр. Ленина, 107.
Тел.: (382-2)-51-41-53.
http://bulletin.ssmu.ru
E-mail: bulletin.tomsk@mail.ru

Оригинал-макет:
Издательство СибГМУ.
634050, г. Томск, Московский тракт, 2.
Редакторы: Е.Е. Степанова, Ю.П. Готфрид
Перевод: Д.А. Гурьянова, Е.Д. Зайцева, Е.Ю. Скворцова, М.Е. Чирикова
Электронная верстка, дизайн обложки: Л.Д. Кривцова

Отпечатано в ООО «Литбюро»,
634055, г. Томск, ул. Королёва, 4.

Подписано в печать 29.09.2025 г.
Формат 60 × 84/8. Печать офсетная.
Бумага мелованная. Гарнитура «Times».
Печ. л. 23. Усл. печ. л. 22,5.
Тираж 500 экз. Заказ 723.

Цена – свободная.
Дата выхода в свет 30.09.2025.

# СОДЕРЖАНИЕ

# CONTENTS

## ОРИГИНАЛЬНЫЕ СТАТЬИ



## ORIGINAL ARTICLES

УДК 579.861.2.083.13
https://doi.org/10.20538/1682-0363-2025-3-5-13

# Estimation of combined *ex vivo* effect of thermal ablation and vancomycin on the growth of *Staphylococcus aureus culture*

**Gorokhova A.V.[1], Nasibov T.F.[1], Mushtovatova L.S.[1], Bochkareva O.P.[1], Anisenya I.I.[2, 3], Sitnikov P.K.[2, 3], Bariev U.A.[1], Leshenkova A.V.[1], Ryzhkova A.Yu.[1], Pakhmurin D.O.[1, 2], Khlusov I.A.[1, 2]**

*[1] Siberian State Medical University (SibSMU)*
*2 Moskovsky trakt, 634050 Tomsk, Russian Federation*

*[2] Tomsk State University of Control Systems and Radioelectronics (TSUCSR)*
*40 Lenin Ave., 634050 Tomsk, Russian Federation*

*[3] Cancer Research Institute, Tomsk National Research Medical Center (NRMC),*
*Russian Academy of Sciences5 Kooperativny St., 634009 Tomsk, Russian Federation*

## ABSTRACT

**Aim.** To study the *ex vivo* effect of high temperature exposure (55–56 °C) combined with vancomycin on culture behavior of pathogenic *Staphylococcus aureus* (*S. aureus*).

**Materials and methods.** Liquid cultures of methicillin-resistant *S. aureus* (MRSA) strain 43300 were heated *ex vivo* at 55–56 °C for 0–60 min, either with or without vancomycin (20 μg/ml), followed by incubation at 37°C up to 120 min. A control suspension (100 or 250 microbial cells per 1 ml of isotonic saline) was maintained at 37°C. Then, cultures were seeded on solid agar medium, and colony-forming units (CFU) were calculated using computer morphometry after 48-h growth. Each experimental subgroup (growth control, thermal ablation, antibiotic, and thermal ablation + antibiotic) included at least three replicates.

**Results.** A semi-lethal heat exposure time (LD50) of 12.25 min was determined for a liquid microbial culture at 100 cells/ml. When the density was increased to 250 cells/ml, 30-min thermal ablation (55–56°C) was insufficient for MRSA growth suppression. Vancomycin (20 μg/ml) alone did not affect CFU output. However, combined heat and antibiotic treatment resulted in 28% bacteriostatic effect ($p < 0.001$) on agar medium.

**Conclusion.** The study revealed a bacteriostatic effect of combined use of high-temperature exposure with vancomycin, which were ineffective when used separately. The obtained results have practical significance for reconstructive surgery of bone tissue, but require additional studies to clarify the mechanisms of the discovered phenomenon.

**Keywords**: MRSA, liquid culture, high temperature exposure, antibacterial therapy, colony-forming units, bacteriostatic effect

**Conflict of interest.** The authors declare no obvious or potential conflicts of interest related to the publication of this article.

**Source of financing.** The work was supported by the Ministry of Science and Higher Education of the Russian Federation (project No. FEWM-2024-0003).

**Compliance with the principles of ethics.** The study was approved by the IACUC Committee of Siberian State Medical University (Minutes No. 1 dated April 3, 2024).

**For citation:** Gorokhova A.V., Nasibov T.F., Mushtovatova L.S., Bochkareva O.P., Anisenya I.I., Sitnikov P.K., Bariev U.A., Leshenkova A.V., Ryzhkova A.Yu., Pakhmurin D.O., Khlusov I.A. Estimation of combined *ex vivo* effect of thermal ablation and vancomycin on the growth of *Staphylococcus aureus culture*. *Bulletin of Siberian Medicine.* 2025;24(3):5–13. https://doi.org/10.20538/1682-0363-2025-3-5-13.

✉ *Khlusov Igor A.,* khlusov63@mail.ru

# Оценка комбинированного *ex vivo* воздействия термоабляции и ванкомицина на рост культуры *Staphylococcus aureus*

**Горохова А.В.[1], Насибов Т.Ф.[1], Муштоватова Л.С.[1], Бочкарева О.П.[1], Анисеня И.И.[2, 3], Ситников П.К.[2, 3], Бариев У.А.[1], Лешенкова А.В.[1], Рыжкова А.Ю.[1], Пахмурин Д.О.[1, 2], Хлусов И.А.[1, 2]**

*[1] Сибирский государственный медицинский университет (СибГМУ)Россия, 634050, г. Томск, Московский тракт, 2[2] Томский государственный университет систем управления и радиоэлектроники (ТУСУР)*

*Россия, 634050, г. Томск, пр. Ленина, 40[3] Научно-исследовательский институт (НИИ) онкологии Томского национального исследовательского медицинского центра (НМИЦ) Российской академии наукРоссия, 634009, г. Томск, пер. Кооперативный, 5*

**РЕЗЮМЕ**

**Цель.** Изучить *ex vivo* влияние высокотемпературного воздействия (55–56 °C) в сочетании с ванкомицином на поведение культуры патогенного золотистого стафилококка (*S. aureus*).

**Материалы и методы.** Жидкую культуру метициллинрезистентного *S. aureus* (MRSA) штамм 43300 нагревали *ex vivo* (55–56 °C, 0–60 мин) с или без добавления ванкомицина (20 мкг/мл), затем инкубировали (37 °C, до 120 мин). В качестве контроля использовалась микробная взвесь (100 или 250 микробных тел на 1 мл изотонического хлорида натрия) при 37 °C. После экстремального воздействия культуры *S. aureus* высевали на плотную питательную среду, через 48 ч определяли выход колониеобразующих единиц (КОЕ) методом компьютерной морфометрии цифровых изображений бактериальных культур в чашках Петри. Для каждой экспериментальной подгруппы (контроль роста; термоабляция; антибиотик; термоабляция + антибиотик) проводили не менее трех повторений.

**Результаты.** Отработан временной интервал высокотемпературного воздействия для определения полулетальной дозы нагревания (LD50) в отношении жидкой микробной культуры, который составил 12,25 мин при плотности разведения 100 микробных тел/мл растворителя. При увеличении плотности бактериальной культуры до 250 микробных тел/мл растворителя 30 мин ее нагревания до 55–56 °C недостаточно для подавления роста MRSA на агаре. Ванкомицин в терапевтической дозе 20 мкг/мл не влияет на выход КОЕ использованного патогенного штамма 43300. В то же время комбинированное *ex vivo* воздействие термоабляции и антибиотика оказывает бактериостатический эффект на уровне 28% ($p < 0{,}001$) подавления роста бактерий на агаровой питательной среде.

**Заключение.** Выявлен бактериостатический эффект комбинированного применения высокотемпературного воздействия с ванкомицином, неэффективных по отдельности. Полученные результаты имеют практическую значимость для реконструктивной хирургии костной ткани, однако требуют проведения дополнительных исследований для уточнения механизмов обнаруженного феномена.

**Ключевые слова:** MRSA, жидкая культура, высокотемпературное воздействие, антибактериальная терапия, колониеобразующие единицы, бактериостатический эффект

**Конфликт интересов.** Авторы декларируют отсутствие явных и потенциальных конфликтов интересов, связанных с публикацией настоящей статьи.

**Источник финансирования.** Работа выполнена при финансовой поддержке Министерства науки и высшего образования Российской Федерации (проект № FEWM-2024-0003).

**Соответствие принципам этики.** Исследование одобрено комиссией IACUC СибГМУ (заключение № 1 от 03.04.2024).

**Для цитирования:** Горохова А.В., Насибов Т.Ф., Муштоватова Л.С., Бочкарева О.П., Анисеня И.И., Ситников П.К., Бариев У.А., Лешенкова А.В., Рыжкова А.Ю., Пахмурин Д.О., Хлусов И.А. Оценка комбинированного ex vivo воздействия термоабляции и ванкомицина на рост культуры *Staphylococcus aureus*. *Бюллетень сибирской медицины.* 2025;24(3):5–13. https://doi.org/10.20538/1682-0363-2025-3-5-13.

## INTRODUCTION

*Staphylococcus aureus* (*S. aureus*) is the most common pathogenic microorganism in surgical hospitals. In diseases caused by *S. aureus*, the duration of hospitalization, cost of treatment, and mortality are 2 times higher than in infections caused by other types of microorganisms. The frequency of isolation of methicillin-resistant (or oxacillin-resistant) strains of *S. aureus* (MRSA) from inflammation foci has increased sharply (from 1–40 (according to various sources) to 54%) since the beginning of the 21st century [1].

The problem of treating MRSA-associated infectious diseases attracts great attention worldwide. For the query "MRSA and treatment", the PubMed database of the US National Institutes of Health (https://pubmed.ncbi.nlm.nih.gov/) showed 25,642 studies published from 1955 to 2024. The maximum number of articles was published in 2021 (1,596 results).

*S. aureus*, including MRSA, are the main causative agents of implant-associated infections (IAI; up to 50–80%) [2–4], which include periprosthetic infections [5, 6] and infections associated with bone fractures [7]. According to other sources, *S. aureus* and *P. aeruginosa* are isolated in 60% of clinical cases of all IAI [8].

Vancomycin (VMN) is one of the leading antibacterial drugs used experimentally and clinically for the prevention and pharmacotherapy of osteomyelitis caused by MRSA [9]. In general, MRSA strains are highly sensitive to VMN [1]. However, a single administration of VMN, even in high doses (up to 1 g), sometimes is insufficient to suppress MRSA-associated infections [10].

Hyperthermia is considered as one of the promising approaches in the combination therapy of infections caused by MRSA [11]. Nevertheless, only 69 publications related to the topic were found in the PubMed database, starting from 2003 (https://pubmed.ncbi.nlm.nih.gov/?term=mrsa%20and%20hyperthermia&timeline=expanded; query date is October 21, 2024). The query "MRSA and thermal ablation" revealed only 3 results since 2016 related to photodynamic therapy (https://pubmed.ncbi.nlm.nih.gov/?term=mrsa+and+thermal+ablation; query date is October 21, 2024).

In this regard, the *in vitro* study of the effect of high-temperature exposure (thermal ablation at 55–56 °C) in combination with vancomycin on the MRSA culture is of absolute relevance.

## MATERIALS AND METHODS

Freshly prepared (according to the attached manufacturer's instructions) nutrient agar for the cultivation of microorganisms (NACM) (BTN-agar, Biotekhinnovatsiya, Russia) in plastic Petri dishes with a lid (MiniMed, Belarus) with a diameter of 90 mm was tested for sterility of the medium by a thermostat programmed at 37 °C for 24 hours. NACM showed the absence of microbial growth (sterility).

The original MRSA culture (strain 43300) was obtained from the Bacteriological Laboratory of Siberian State Medical University, which has a sanitary and epidemiological inspection report (dated July 20, 2015 No. 70.TS.06.000.M.000268.07.15) for manipulations with pathogens of infectious diseases of III–IV pathogenicity groups.

The original MRSA culture was diluted to achieve a bacterial concentration of 100 or 250 microbial bodies in 1 ml of a sterile 0.9% sodium chloride solution in plastic sterile conical tubes with a cap of 15 ml (MiniMed, Belarus).

General heating of the microbial suspension in test tubes was carried out in two electric dry-air thermostats ShS-80N (SG-term, Russia), set to the required temperature of 37 °C or 55–56 °C. The exposure time was selected based on the determination of the semi-lethal time of heating the liquid MRSA culture in a preliminary experiment.

After heating the liquid MRSA cultures, 0.2 ml (20 or 50 microbial bodies) of the bacterial suspension were transferred to the NACM in Petri dishes. At least 3 tubes/Petri dishes with staphylococcal culture were used for each experimental subgroup (growth control at 37 °C; thermal ablation at 55–56 °C; antibiotic at 37 °C; and thermal ablation at 55–56 °C + antibiotic vancomycin (VMN, Belmedpreparaty, Belarus) 20 μg/ml).

MRSA agar cultures on Petri dishes showed an increase in colony-forming units (CFUs) after just 24 hours of cultivation at 37 °C and 100% humidity. However, small (dust-like) CFUs made morphometric studies difficult. Therefore, microbial cultures were left to grow for another 24 hours (total cultivation time was 48 hours), after which the potential bacteriostatic effect was assessed by reducing the area of CFUs grown on NACM.

The relative area of bacterial cultures was assessed according to the computer morphometry method of digital images [12] using ImageJ software tools version 1.38 (National Institutes of Health, USA;

http://www.rsb.info.nih.gov/ij). Digital photographs were taken using a Canon PowerShot A2200 camera (Canon Inc., China) with a resolution of 14.1 megapixels.

Due to the massive but uneven growth of MRSA on a solid nutrient medium (agar), the following method was used for a more accurate calculation of the relative (specific) area (RA) of bacterial cultures:

1. Each Petri dish was conditionally divided into 8 segments (Fig. 1).2. In each segment, the area of bacterial cultures (*S*c) was calculated in square millimeters.3. The area of each segment (*S*s) was calculated in square millimeters.4. The relative area of bacterial cultures (*S*r) was calculated for each segment using the formula *S*r = *S*c/*S*s, and the calculated shares were summed up.

As a result of the calculations, the RA in the Petri dish occupied by bacterial cultures was obtained.

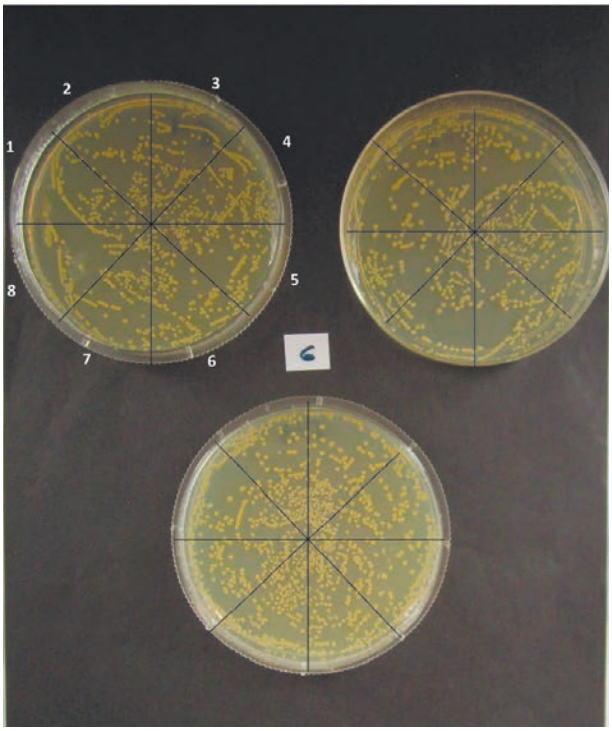


Fig. 1. Examples of dividing a Petri dish into segments when counting the area of grown MRSA colonies

The prepared liquid suspensions of MRSA in isotonic NaCl solution after mixing were cultured (with or without vancomycin) in the following time interval (in the main experiment): 2 hours (120 min) at 37 °C; 30 min at 55–56 °C + 90 min at 37 °C.

The total time interval (120 min) for pre-incubation of liquid cultures of *Staphylococcus aureus* was chosen in accordance with previous studies [13], as well as taking into account a preliminary study of the semi-lethal dose of thermal ablation at 55–56 °C (see below).

Statistical analysis of the data was conducted in the RStudio environment (ver. 2024.04.2+764) in the R programming language (version 4.4.1) using the MVN [14], PMCMRplus [15], and brunnermunzel [16] packages. The normality of distribution of quantitative variables was checked by the Shapiro–Wilk test with the Royston correction AS R94 for large samples ($3 \leq n \leq 5{,}000$) [17]. The description of normally distributed quantitative characteristics is given as the mean value and standard deviation ($M \pm SD$); non-normally distributed quantitative variables and ordinal characteristics were in the form of the median and the first and third quartiles $Me\ (Q_1; Q_3)$.

For quantitative independent data that do not comply with the normal distribution, the comparison was performed using the Brunner–Munzel test [18, 19]. The peculiarity of the Brunner–Munzel test is that it does not require the assumptions: (a) equal deviations and (b) equal distributions, while the Mann–Whitney *U*-test is quite sensitive to their violations. At the same time, met, the Brunner–Munzel test corresponds to the Mann–Whitney *U*-test, which shows its reliability and universality [20, 21].

For quantitative non-normal independent data, multiple comparisons were performed using the Van der Waerden test. The choice of the Van der Waerden test is based on the fact that it provides high power (at the ANOVA level, at which the assumptions of normality are met) [22], and at the same time has sufficient reliability [23, 24]. The Dunn's post-hoc test was used as a one-versus-all (control-versus-all) a posteriori test.

## RESULTS

The visual picture of bacterial CFU cultivation on a solid nutrient medium (agar) showed a significant inhibitory effect of thermal ablation on the growth of MRSA (Fig. 2).

Statistical processing of the results of MRSA colony growth on agar after preliminary heating of liquid microbial cultures made it possible to establish that at 55–56 °C, a statistically significant drop in the CFU area was observed already after 15 minutes of extreme exposure (5.5% (11/198 mm$^2$/dish) of the control); and by minute 30, the growth of MRSA colonies on agar was completely absent (Fig. 3).

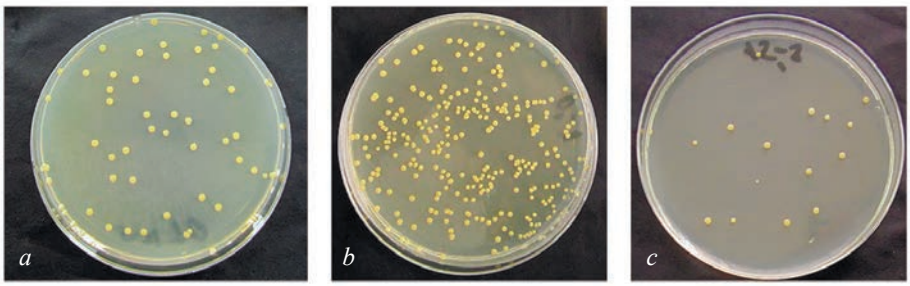


Fig. 2. Examples of 48-hour growth of MRSA colonies on agar in Petri dishes after preliminary extreme effects on liquid bacterial culture (concentration of 100 microbial bodies per 1 ml of 0.9% sodium chloride solution; 20 microbial bodies per Petri dish) at different temperatures: *a* – 37 °C, 120 min; *b* – 37 °C, 120 min; *c* – 55–56 °C 15 min + 105 min at 37 °C

The exposure dose of thermal energy causing 50% death of MRSA CFUs *in vitro* (LD50) was determined using calculated curves with reliable ($p < 0.001$) exponential (Fig. 3) approximation of the data. The calculated LD50 when heating a liquid MRSA culture (100 microbial bodies per 1 ml of 0.9% sodium chloride solution) to 55–56 °C was 12.25 min (Fig. 3).

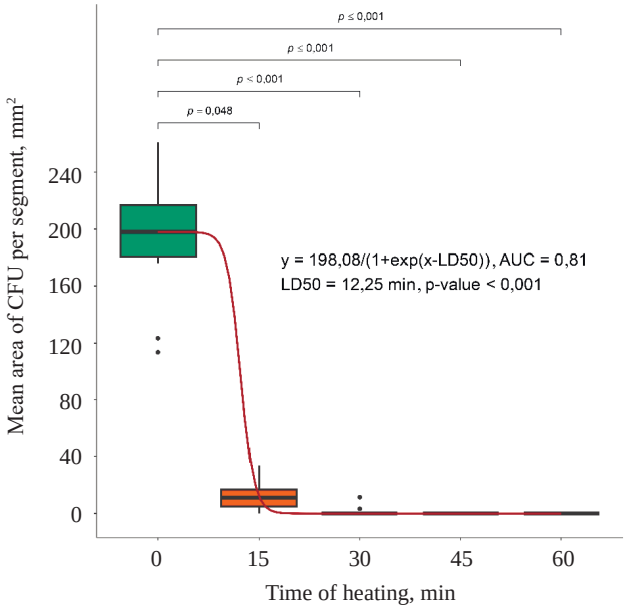


Fig. 3. Graphical approximation of experimental data on the area of CFUs ($mm^2$) grown in a 48-hour MRSA culture on agar after heating the liquid bacterial culture at 55–56 °C to determine (by the time of extreme exposure) the exposure semi-lethal dose (LD50) of thermal energy. The results are expressed as *Me* ($Q_1$; $Q_3$). Multiple comparisons, Van der Waerden test (p<0.001); pairwise comparisons, Dunn's test ($p = 0.048$ between the time 0 and 15 min)

Thus, heating to 55–56 °C quickly inhibited the vital activity of pathogenic bacteria at a concentration of MRSA in a liquid culture of 100 microbial bodies per 1 ml of 0.9% sodium chloride solution, which was expressed in a significant bacteriostatic effect on a solid nutrient medium (Fig. 2, *c*). At the same time, when MRSA was seeded on an agar medium from 20 microbial bodies subjected to heating in a liquid culture, only 11 CFUs germinated, there was a risk of a false positive result with the combined inhibitory effect of thermal ablation and antibiotic.

In addition, the control culture of staphylococcus at a concentration of 100 microbial bodies and a temperature of 37 °C gave an unstable yield of CFUs (Fig. 2, *a, b*). At the control points (0 min of liquid culture thermal ablation; 2-hour preincubation of bacteria in liquid culture, and 48-hour growth at 37 °C) with the same bacterial culture seeding density (20 microbial bodies per Petri dish), the CFU growth density in the controls differed by 3.33 times (CFU area 59.31 (20.47; 80.38) $mm^2$/dish (Fig. 2, *a*) and 198.08 (180.85; 216.97) $mm^2$/dish, Fig. 2, *b*).

In connection with the listed circumstances, the main experiment was carried out on the MRSA culture with a density of 250 microbial bodies per 1 ml of liquid suspension in 0.9% NaCl solution, 50 microbial bodies in 0.2 ml on the agar medium of Petri dishes. The thermal ablation time of liquid bacterial cultures at 55–56 °C was 30 min, which corresponds to LD100 at a culture density of 100 microbial bodies per 1 ml of sodium chloride (Fig. 3).

Nevertheless, a paradoxical effect of MRSA growth stimulation on agar was obtained, since after heating the liquid bacterial suspension, the proportion of grown colonies increased to 0.22 (22% of the Petri dish area) from 0.13 (13%) in the control (37 °C), respectively ($p < 0.001$; Brunner–Munzel test, Fig. 4).

Perhaps the increased (from 100 mt/ml to 250 mt/ml) density of the microbial liquid culture is important, which during hyperthermia can lead to an increase in the survival rate of MRSA due to a decrease in the amount of absorbed heat flux (thermal energy per unit surface area of microbial bodies).

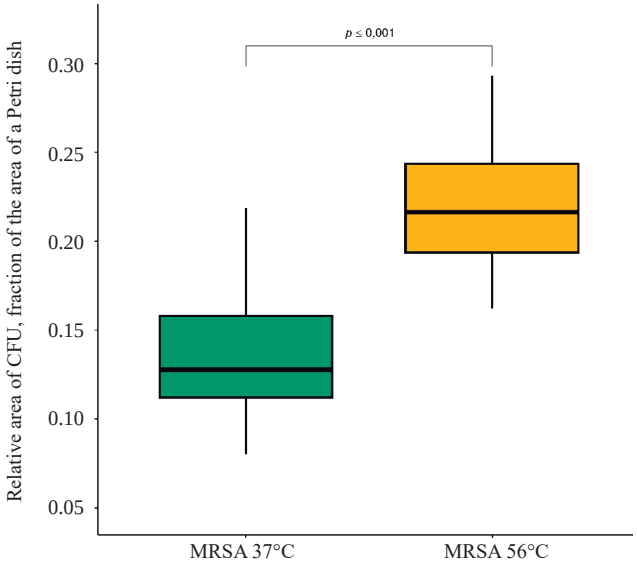


Fig. 4. Comparison of MRSA colony growth on agar in Petri dishes after preliminary heating of liquid bacterial cultures to different temperatures. Pairwise comparison, the Brunner–Munzel test

Notably, VMN at a therapeutic concentration (20 μg/ml) under conditions of 2-hour co-cultivation with a liquid bacterial culture at a temperature of 37 °C did not have an inhibitory effect on the growth of MRSA on agar. Visually, the number of CFUs did not differ from that in the control culture (Fig. 5).

Computer morphometry of digital images of MRSA CFUs on agar also did not show statistically significant changes after exposure to VMN to a liquid microbial culture at 37 °C (Table). In other words, the used MRSA culture was resistant to a single 2-hour exposure to VMN at a dose of 20 μg/ml at 37 °C.

Table

**Area (% of the Control) of MRSA Colony-Forming Units after Extreme Effects in Liquid Culture Followed by 48-Hour Cultivation on Agar in Petri Dishes at 37 °C**

| Group, $n = 3$ | Sample size in each group, $n_1$ | Relative area of bacterial culture, $Me\ (Q_1; Q_3)$ | Pairwise comparison, the Brunner–Munzel test |
|---|---|---|---|
| MRSA 37 °C, growth control | 24 | 100.00 (87.58; 123.44) | 5.13; $p = 0.16$ |
| MRSA + VMN 37 °C | 24 | 97.23 (81.95; 116.85) | |

Note. VMN is vancomycin, 20 μg/ml; $n$ is the number of Petri dishes in each group, divided into 8 segments in each dish ($n_1$) for more accurate determination of the parameter

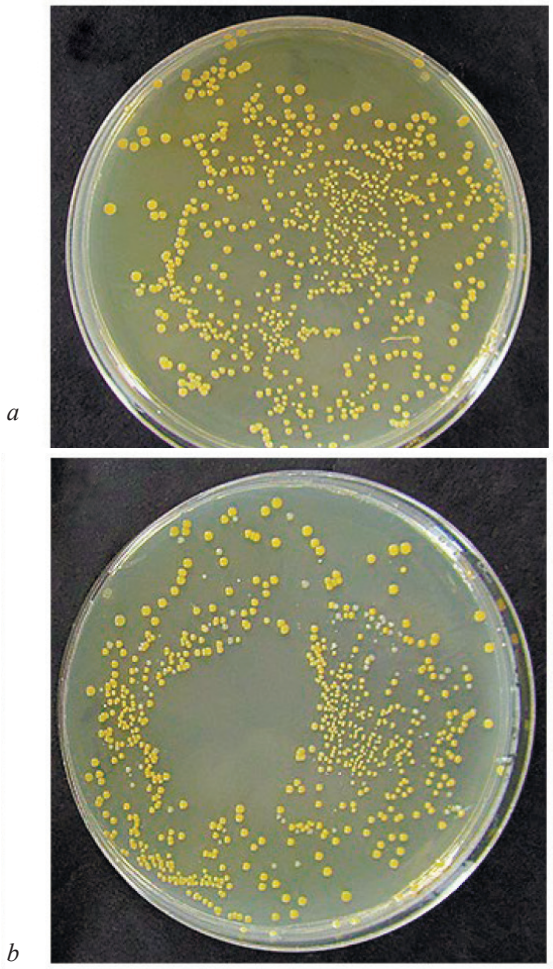


Fig. 5. Examples of 48-hour growth of MRSA colonies on agar in Petri dishes after 2-hour cultivation of the liquid culture at 37 °C with antibiotic: *a* – MRSA growth control; *b* – MRSA + VMN 20 μg/ml

In turn, under conditions of 30-minute heating of the liquid bacterial culture at a temperature of 55–56 °C, VMN at a therapeutic concentration (20 μg/ml) visually reduced the number of CFUs grown on agar, compared to the control culture (Fig. 6).

Computer morphometry of digital images showed a statistically significant ($p < 0.001$) decrease in the yield of MRSA CFUs on agar (by 28% compared to the control) after the exposure to VMN on the liquid microbial culture under conditions of its thermal ablation at 55–56 °C (Fig. 7).

Thus, heating liquid cultures of MRSA for 30 minutes at a temperature of 55–56 °C significantly increased the colony-forming ability of MRSA on a solid nutrient medium (agar-agar, Fig. 4). Addition of vancomycin (20 μg/ml) to the liquid culture without heating did not affect the yield of microbial CFUs on agar (Table).

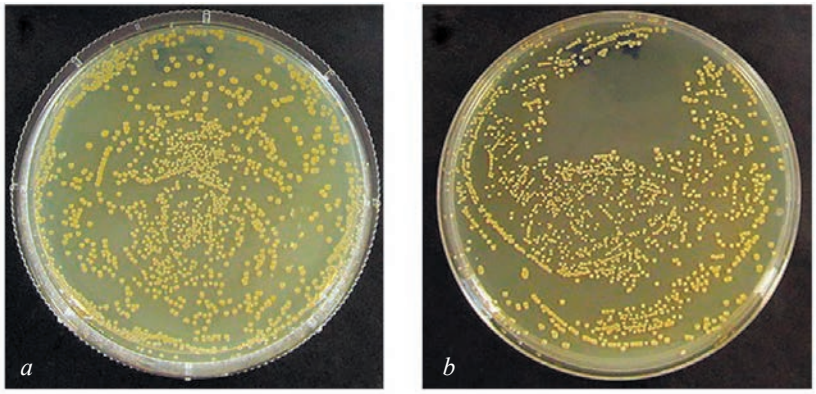


Fig. 6. Examples of 48-hour growth of MRSA colonies on agar in Petri dishes after preliminary thermal ablation of the liquid culture at 55–56 °C: *a* – MRSA growth control without antibiotic; *b* – MRSA + VMN 20 μg/ml

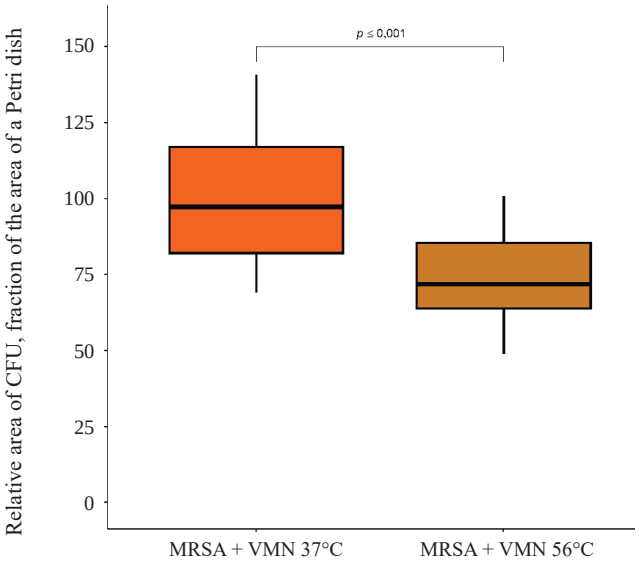


Fig. 7. Graphic representation (% of the control) of the areas of MRSA CFUs after adding vancomycin (20 μg/ml) and heating the liquid culture at 37 °C or 55–56 °C, followed by culturing for 48 hours on agar in Petri dishes at 37°C. Pairwise comparison, the Brunner–Munzel test.

In turn, heating the microbial suspension to a temperature of 55–56 °C (Fig. 7) in the presence of VMN has a noticeable bacteriostatic effect in comparison with the effect of the antibiotic at 37 °C. Presumably, the use of high-temperature exposure (above 55 °C) can improve the results of standard antibacterial therapy in the treatment and prevention of MRSA-induced osteomyelitis.

## DISCUSSION

MRSA is resistant to all beta-lactam antibiotics, including inhibitor-protected penicillins and cephalosporins of all generations. Another clinically important feature of methicillin-resistant staphylococci is the high frequency of associated resistance to antibacterial drugs of different groups (aminoglycosides, macrolides, and lincosamides) [1]. Due to the high frequency of antibiotic use in the complex treatment of surgical patients, pathogenic MRSA strain 43300 was chosen for *in vitro* experiments.

Vancomycin (VMN) at a therapeutic concentration in human serum in the range of 10–20 μg/ml [25] is one of the leading antibacterial drugs used for the prevention and pharmacotherapy of osteomyelitis caused by MRSA [9].

However, the MRSA strain 43300 used in the work turned out to be insensitive to the therapeutic dose of VMN (20 μg/ml) at a temperature of 37 °C (Table), corresponding to the temperature of the human body, especially during inflammatory processes. The increased yield of bacterial CFUs at a relatively high density of the microbial liquid culture (250 microbial bodies per 1 ml) under conditions of 30-minute heating of the microbial suspension to 55–56 °C, which usually causes coagulation necrosis, turned out to be unexpected (Fig. 4).

A possible explanation for the obtained phenomenon is the fact that an increase in genetic diversity with an increase in the number of microbial bodies in the culture leads to the emergence and accumulation of bacteria carrying antibiotic resistance genes [26]. In turn, this increases the overall chances of the bacterial strain to survive in extreme conditions. In particular, there is significant variability in the thermosensitivity of *S. aureus* to 45 °C [27]. Similar to osteogenic cells, which are activated by moderate hyperthermia (~42 °C) due to hyperexpression of heat shock proteins [28], some "thermotolerant" MRSA may ensure the survival of the strain at high temperatures.

## CONCLUSION

Antibiotic therapy is considered to be themainstay in the prevention and treatment of infectious complications in bone fractures and their surgical treatment [7]. However, the increasing antibiotic resistance of bacterial

strains and the increasing contribution of MRSA to infectious inflammation make the development of new approaches to the treatment of infectious complications a key challenge in biomedicine.

In this regard, an important result of the *in vitro* study is the practical feasibility of the simultaneous administration of vancomycin and thermal ablation of liquid MRSA cultures, which are ineffective separately, but have an almost 30% bacteriostatic effect when used together. The obtained data have practical significance for specialists involved in the treatment of diseases of the skeletal bones and their complications. However, the obtained results require additional research to clarify the mechanisms of the discovered phenomenon.

## REFERENCES


1. Naumenko Z.S., Rozova L.V. Resistance of Staphylococcus Aureus to Antibacterial Drugs. *Orthopaedic Genius.* 2007;(2):36–38. (In Russ.).
2. Bozhkova S.A., Tikhilov R.M., Krasnova M.V., Rukina A.N. Orthopedic Implant-Associated Infection: the Main Etiological Agents, Local Resistance and Antimicrobial Therapy Recommendations. *Traumatology and Orthopedics of Russia.* 2013;19(4):5–15. (In Russ.). DOI: 10.21823/2311-2905-2013--4-5-15.
3. Bozhkova S., Tikhilov R., Labutin D., Denisov A., Shubnyakov I., Razorenov V. et al. Failure of the first step of two-stage revision due to polymicrobial prosthetic joint infection of the hip. *Journal of Orthopaedics and Traumatology: Official Journal of the Italian Society of Orthopaedics and Traumatology*. 2016;17(4):369–376. DOI: 10.1007/s10195-016-0417-8.
4. Masters E.A., Ricciardi B.F., Bentley K.L. de M., Moriarty T.F., Schwarz E.M., Muthukrishnan G. Skeletal infections: microbial pathogenesis, immunity and clinical management. *Nature Reviews. Microbiology.* 2022;20(7):385–400. DOI: 10.1038/s41579-022-00686-0.
5. Parvizi J., Gehrke T., International consensus group on periprosthetic joint infection. Definition of periprosthetic joint infection. *The Journal of Arthroplasty.* 2014;29(7):1331. DOI: 10.1016/j.arth.2014.03.009.
6. Manning L., Allen B., Davis J.S. Design Characteristics and Recruitment Rates for Randomized Trials of Peri-Prosthetic Joint Infection Management: A Systematic Review. *Antibiotics (Basel, Switzerland)*. 2023;12(10):1486. DOI: 10.3390/antibiotics12101486.
7. He S.Y., Yu B., Jiang N. Current concepts of fracture-related infection. *International Journal of Clinical Practice.* 2023;2023:4839701. DOI: 10.1155/2023/4839701.
8. Rahim M.I., Rohde M., Rais B., Seitz J.M., Mueller P.P. Susceptibility of metallic magnesium implants to bacterial biofilm infections. *Journal of Biomedical Materials Research. Part A.* 2016;104(6):1489–1499. DOI: 10.1002/jbm.a.35680.
9. Rybak M.J., Lomaestro B.M., Rotschafer J.C., Moellering R.C., Craig W.A., Billeter M. et al. Therapeutic monitoring of vancomycin in adults summary of consensus recommendations from the American Society of Health-System Pharmacists, the Infectious Diseases Society of America, and the Society of Infectious Diseases Pharmacists. *Pharmacotherapy.* 2009;29(11):275–1279. DOI: 10.1592/phco.29.11.1275.
10. Bue M., Hanberg P., Koch J., Jensen L.K., Lundorff M., Aalbaek B. et al. Single-dose bone pharmacokinetics of vancomycin in a porcine implant-associated osteomyelitis model. *Journal of Orthopaedic Research: Official Publication of the Orthopaedic Research Society.* 2018;36(4):1093–1098. DOI: 10.1002/jor.23776.
11. Palau M., Muñoz E., Larrosa N., Gomis X., Márquez E., Len O. et al. Hyperthermia prevents *in vitro* and *in vivo* biofilm formation on endotracheal tubes. *Microbiology Spectrum.* 2023;11(1):e0280722. DOI: 10.1128/spectrum.02807-22.
12. Shakhov V.P., Khlusov I.A., Dambaev G.Ts., Zaitsev K.V., Salmina (Egorova) A.B., Shakhova S.S. et al. Introduction to Cell Culture Methods, Organ and Tissue Bioengineering. Novosibirsk: STT, 2004. (In Russ.).
13. Prosolov K.A., Mitrichenko D.V., Prosolov A.B., Nikolaeva O.O., Lastovka V.V., Belyavskaya O.A. et al. Zn-doped CaP-based coatings on Ti–6Al–4V and Ti–6Al–7Nb alloys prepared by magnetron sputtering: controllable biodegradation, bacteriostatic, and osteogenic activities. *Coatings.* 2021;11(7):809. DOI: 10.3390/coatings11070809.
14. Korkmaz S., Göksülük D., Zararsiz G.. MVN: An r package for assessing multivariate normality. *R JOURNAL.* 2014;6(2):151–162. DOI: 10.32614/RJ-2014-031.
15. Pohlert T. PMCMRplus: Calculate pairwise multiple comparisons of mean rank sums extended. 2018. DOI: 10.32614/CRAN.package.PMCMRplus.
16. Brunnermunzel package. RDocumentation. [Accessed 18th October 2024]. Available online: https://www.rdocumentation.org/packages/brunnermunzel/versions/2.0.
17. Royston P. Remark AS R94: a remark on algorithm AS 181: the W-test for normality. *Journal of the Royal Statistical Society. Series C (Applied Statistics).* 1995;44(4):547–551. DOI: 10.2307/2986146.
18. Munzel U., Brunner E. Nonparametric tests in the unbalanced multivariate one-way design. *Biometrical Journal.* 2000;42(7):837–854. DOI: 10.1002/1521-4036(200011)42:7<837::AID-BIMJ837>3.0.CO;2-S.
19. Brunner E., Munzel U. The nonparametric behrens-fisher problem: asymptotic theory and a small-sample approximation. *Biometrical Journal.* 2000;42(1):17–25. DOI: 10.1002/(SICI)1521-4036(200001)42:1<17::AID-BIMJ17>3.0.CO;2-U.
20. Karch J.D. Psychologists should use Brunner-Munzel's instead of Mann-Whitney's U test as the default nonparametric procedure. *Advances in Methods and Practices in Psychological Science.* 2021;4. DOI: 10.1177/2515245921999602.
21. Noguchi K., Konietschke F., Marmolejo-Ramos F., Pauly M. Permutation tests are robust and powerful at 0.5% and 5% significance levels. *Behavior Research Methods.* 2021;53(6):2712–2724. DOI: 10.3758/s13428-021-01595-5.
22. Elamir E. On uses of Van der Waerden test: a graphical approach. *Preprint arXiv.* 2022. DOI: 10.48550/arXiv.2203.02148.
23. Macunluoglu A.C., Ocakoğlu G. Comparison of the performances of non-parametric k-sample test procedures as an alternative to one-way analysis of variance. *The Europe-*

*an Research Journal.* 2023;9(4) 687–696. DOI: 10.18621/eurj.1037546.
24. Luepsen H. Comparison of nonparametric analysis of variance methods: A vote for van der Waerden. *Communications in Statistics – Simulation and Computation*. 2018;47(9):2547. DOI: 10.1080/03610918.2017.1353613.
25. Hirano R., Sakamoto Y., Kitazawa J., Yamamoto S., Tachibana N. Pharmacist-managed dose adjustment feedback using therapeutic drug monitoring of vancomycin was useful for patients with methicillin-resistant *Staphylococcus aureus* infections: a single institution experience. *Infection and Drug Resistance.* 2016;9:243–252. DOI: 10.2147/IDR.S109485.
26. Lehtinen S., Blanquart F., Croucher N.J., Turner P., Lipsitch M., Fraser C. Evolution of antibiotic resistance is linked to any genetic mechanism affecting bacterial duration of carriage. *Proceedings of the National Academy of Sciences of the United States of America.* 2017;114(5):1075–1080. DOI: 10.1073/pnas.1617849114.
27. Sturtevant R.A., Sharma P., Pavlovsky L., Stewart E.J., Solomon M.J., Younger J.G. Thermal augmentation of vancomycin against staphylococcal biofilms. *Shock (Augusta, Ga.).* 2015;44(2):121–127. DOI: 10.1097/SHK.0000000000000369.
28. Zhao Y., Peng X., Xu X., Wu M., Sun F., Xin Q. et al. Chitosan based photothermal scaffold fighting against bone tumor-related complications: *Recurrence, infection, and defects. Carbohydrate Polymers.* 2023;300:120264. DOI: 10.1016/j.carbpol.2022.120264.

## Author Contribution

All authors confirm that their authorship complies with the international ICMJE criteria (all authors made a significant contribution to the conception and design, conduct of the study, preparation of the manuscript, read, and approved the final version of the manuscript before publication). Gorokhova A.V. — morphometric processing, interpretation, and visualization of data. Nasibov T.F. – drafting and editing of the manuscript and statistical analysis. Mushtovatova L.S. — conception and design, conducting the experimental study. Bochkareva O.P., Bariev U.A. — conducting the experimental study. Anisenya I.I., Sitnikov P.K. — conducting the experimental study and experimental data interpretation. Leshenkova A.V. — conducting the experimental study and data visualization. Ryzhkova A.Yu. — conducting the experimental study, collecting and analyzing literary sources. Pakhmurin D.O. — final approval of the content for publication of the manuscript, conducting the experimental study. Khlusov I.A. — coordination of the study, writing and editing the article.

## Author Information

**Gorokhova Anna V.** – Laboratory Assistant, Morphology and General Pathology Division, Siberian State Medical University, Tomsk, a.gorokhova3062@gmail.com, https://orcid.org/0000-0001-8401-7181

**Nasibov Temur F.** – Laboratory Assistant, Morphology and General Pathology Division, Siberian State Medical University, Tomsk, temur.nsbv@gmail.com, https://orcid.org/0000-0002-8056-3967

**Mushtovatova Lyudmila S.** – Cand. Sci. (Biology), Associate Professor, Microbiology and Virology Division, Siberian State Medical University, Tomsk, mls2013@mail.ru, https://orcid.org/0000-0002-4339-5204

**Bochkareva Olga P.** – Cand. Sci. (Med.), Associate Professor, Microbiology and Virology Division, Siberian State Medical University, Tomsk, bpo97@rambler.ru, https://orcid.org/0000-0002-9063-0326

**Anisenya Ilya I.** – Cand. Sci. (Med.), Senior Researcher, General Cancer Department, Tomsk National Research Medical Center; Researcher, MedTech Laboratory, Tomsk State University of Control Systems and Radioelectronics, Tomsk, aii@mail.tsu.ru, https://orcid.org/0000-0003-3882-4665

**Sitnikov Pavel K.** – Oncologist, General Cancer Department, Tomsk National Research Medical Center; Junior Researcher, MedTech Laboratory, Tomsk State University of Control Systems and Radioelectronics, Tomsk, sitnikov.pavel.k@yandex.ru, https://orcid.org/0000-0003-0674-2067;

**Bariev Usman A.** – Laboratory Assistant, Laboratory of Cellular and Microfluidic Technologies, Siberian State Medical University, Tomsk, bariev.usman.20002@gmail.com, https://orcid.org/0009-0002-7547-2558;

**Leshenkova A.V.** – Student, Department of Biomedicine, Siberian State Medical University, Tomsk, nasya14.a@gmail.com, https://orcid.org/0009-0003-5358-9795;

**Ryzhkova A.Yu.** – Student, Department of Biomedicine, Siberian State Medical University, Tomsk, alya.ryzhkova.20031@gmail.com, https://orcid.org/0000-0002-7862-7992;

**Pakhmurin Denis O.** – Cand. Sci. (Tech.), Associate Professor, Head of the MedTech Laboratory, Tomsk State University of Control Systems and Radioelectronics; Associate Professor, Medical and Biological Cybernetics Division, Siberian State Medical University, Tomsk, pdo@ie.tusur.ru, https://orcid.org/0000-0002-5191-6938

**Khlusov Igor A.**– Dr. Sci. (Med.), Professor, Microbiology and Virology Division, Head of the Laboratory of Cellular and Microfluidic Technologies, Siberian State Medical University, Tomsk, khlusov63@mail.ru, https://orcid.org/0000-0003-3465-8452

(✉) **Khlusov Igor A.,** khlusov63@mail.ru

Received on March 5, 2025;
approved after peer review 14.03.2025;
accepted on March 20, 2025

УДК 616.447.085.032:616.61-002.2-06
https://doi.org/10.20538/1682-0363-2025-3-14-24

# The effect of local injections of paricalcitol into the parathyroid glands on parathyroid hormone levels, vascular calcification, and bone mineral density in patients with chronic kidney disease

**Zhulina E.M., Brykun M.V., Saprina T.V., Vorojcova I.N., Tskhay V.F., Komkova T.B.**

*Siberian State Medical University (SibSMU)*
*2 Moskovsky trakt, 634050 Tomsk, Russian Federation*

## ABSTRACT

**Aim.** To study the effects of local paricalcitol injections into the parathyroid glands on bone turnover in patients with chronic kidney disease (CKD) and secondary hyperparathyroidism (SHPT) with moderately elevated parathyroid hormone (PTH) levels (300–600 pg/ml).

**Materials and methods**. The study included 48 patients with end-stage CKD and SHPT with PTH levels of 300–600 pg/ml. All patients received standard medical therapy before the study, including correction of hyperphosphatemia, hypocalcemia, and disorders of calcium-phosphorus metabolism. The main group ($n$ = 14) comprised patients for whom ultrasound-guided paricalcitol injections into the parathyroid glands were technically feasible. The dynamics of PTH levels, vascular calcification, bone mineral density (BMD), and levels of PTH, b-CrossLaps, and FGF23 were assessed.

**Results**. Multivariate logistic regression analysis demonstrated that osteoporosis and vascular calcification were significantly associated with age, PTH levels, dialysis duration, comorbidity index, b-CrossLaps, and FGF23. Threshold values for age and PTH were 33 years and 301 pg/ml for the development of osteoporosis and 29 years and 301 pg/ml for vascular calcification. Correlation analysis revealed a statistically significant relationship between FGF23 and dialysis duration, b-CrossLaps and PTH levels, as well as between FGF23 and b-CrossLaps. The comorbidity index also increased with age and PTH levels. After 3 and 6 months of treatment, PTH levels significantly decreased, while the volume of the parathyroid glands remained unchanged. No serious complications were observed after the injections, and transient local pain was reported in only 8 (57%) patients.

**Conclusion**. Ultrasound-guided paricalcitol injections into the parathyroid glands contribute to reducing PTH levels, improving bone remodeling parameters, and creating conditions for preventing cardiovascular complications. These findings require further investigation in larger-scale studies.

**Keywords:** secondary hyperparathyroidism, chronic kidney disease, mineral and bone disorders, paricalcitol, local injections

**Conflict of interest.** The authors declare the absence of obvious or potentialor potential conflicts of interest related to the publication of this article.

**Source of financing.** The study was carried out with the support of the contest of scientific projects conducted by young scientists of Siberian State Medical University (SibSMU) (No. NIOKTR 21-22-07-03-42).

**For citation:** Zhulina E.M., Brykun M.V., Saprina T.V., Vorojcova I.N., Tskhay V.F., Komkova T.B. The effect of local injections of paricalcitol into the parathyroid glands on parathyroid hormone levels, vascular calcification, and bone mineral density in patients with chronic kidney disease. *Bulletin of Siberian Medicine.* 2025;24(3):14–24. https://doi.org/10.20538/1682-0363-2025-3-14-24.

✉ *Zhulina Elizaveta M.,* elisaveta.zhulina@gmail.com

# Влияние местных инъекций парикальцитола в околощитовидные железы на уровень паратгормона, сосудистую кальцификацию и минеральную плотность костной ткани у пациентов с хронической болезнью почек

**Жулина Е.М., Брыкун М.В., Саприна Т.В., Ворожцова И.Н., Цхай В.Ф., Комкова Т.Б.**

*Сибирский государственный медицинский университет (СибГМУ)*
*Россия, 634050, г. Томск, Московский тракт, 2*

**РЕЗЮМЕ**

**Цель.** Изучить влияние местных инъекций парикальцитола в околощитовидные железы на костный обмен у пациентов с хронической болезнью почек (ХБП) и вторичным гиперпаратиреозом (ВГПТ) при умеренном повышении уровня паратгормона (ПТГ) (300–600 пг/мл).

**Материалы и методы.** В исследование включены 48 пациентов с терминальной стадией ХБП и ВГПТ с концентрацией паратгормона 300–600 пг/мл. Все пациенты до начала исследования получали стандартное медикаментозное лечение, включающее коррекцию гиперфосфатемии, гипокальциемии и нарушения кальциево-фосфорного обмена. В основную группу ($n$ = 14) вошли пациенты, которым было технически возможно проведение инъекций парикальцитола под ультразвуковым контролем в околощитовидные железы. Оценивались динамика уровня ПТГ, кальцификация сосудов, минеральная плотность костной ткани, уровни ПТГ, b-CrossLaps и FGF23.

**Результаты.** Многомерный логистический регрессионный анализ показал, что остеопороз и сосудистая кальцификация достоверно связаны с возрастом, уровнем ПТГ, длительностью диализа, индексом коморбидности, b-CrossLaps и FGF23. Пороговые значения возраста пациента и ПТГ составили 33 года и 301 пг/мл для развития остеопороза и 29 лет и 301 пг/мл – для сосудистой кальцификации. Корреляционный анализ выявил статистически значимую связь между FGF23 и продолжительностью диализной терапии, b-CrossLaps и уровнем ПТГ, а также между FGF23 и b-CrossLaps. Индекс коморбидности также увеличивался с возрастом и уровнем ПТГ. Через 3 и 6 мес лечения уровень ПТГ значительно снизился, а объем околощитовидных желез остался без изменений. После инъекций не наблюдалось серьезных осложнений, а кратковременная местная болезненность отмечалась только у 8 (57%) пациентов.

**Заключение.** Инъекции парикальцитола в околощитовидные железы под ультразвуковым контролем способствуют снижению уровня ПТГ, улучшению показателей ремоделирования костной ткани и создают предпосылки для предотвращения сердечно-сосудистых осложнений, что требует дальнейшего изучения в рамках более масштабных исследований.

**Ключевые слова:** вторичный гиперпаратиреоз, хроническая болезнь почек, минеральные и костные расстройства, парикальцитол, местные инъекции

**Конфликт интересов.** Авторы декларируют отсутствие явных и потенциальных конфликтов интересов, связанных с публикацией настоящей статьи.

**Источник финансирования.** Конкурс научных проектов молодых ученых ФГБОУ ВО СибГМУ (№ НИОКТР 21-22-07-03-42).

**Для цитирования:** Жулина Е.М., Брыкун М.В., Саприна Т.В., Ворожцова И.Н., Цхай В.Ф., Комкова Т.Б. Влияние местных инъекций парикальцитола в околощитовидные железы на уровень паратгормона, сосудистую кальцификацию и минеральную плотность костной ткани у пациентов с хронической болезнью почек. *Бюллетень сибирской медицины.* 2025;24(3):14–24. https://doi.org/10.20538/1682-0363-2025-3-14-24.

## INTRODUCTION

The pathogenesis of secondary hyperparathyroidism (SHPT) in patients with chronic kidney disease (CKD) involves several factors related to the effects of parathyroid hormone (PTH), calcium (Ca) levels, phosphorus (P) levels, fibroblast growth factor 23 (FGF23), and the bone resorption biomarker b-CrossLaps. These factors affect mineral metabolism, osteoclast and osteoblast activity, and bone tissue quality [1, 2]. In CKD, PTH is produced by the chief cells of the parathyroid glands (PTG) in

response to hypocalcemia and hyperphosphatemia. It stimulates bone resorption, leading to elevated calcium and phosphorus levels in the blood. A decrease in glomerular filtration rate (GFR) results in a significant reduction in phosphate clearance, causing its accumulation in the body.

Phosphate ions form complexes with calcium, lowering the concentration of ionized calcium in the blood. This, in turn, activates calcium-sensing receptors (CaSRs) on the parathyroid cells, stimulating the secretion of PTH and leading to hypercalcemia as a compensatory response. A decrease in ionized calcium disrupts the synthesis of calcitriol from vitamin D3, which reduces calcium absorption in the intestine and promotes metastatic calcification. Additionally, phosphorus directly stimulates PTH secretion and the hyperplasia of parathyroid cells, as well as causes dysfunction of calcitriol receptors, leading to resistance to this hormone. Hyperphosphatemia also contributes to the reduction in the number of CaSRs, impairing the ability of calcium to stimulate calcitriol synthesis in the kidneys [3].

Furthermore, phosphorus stimulates the production of the growth factor FGF23, which inhibits the activity of 1-alpha-hydroxylase and lowers the level of the active form of vitamin D. The regulation of vitamin D receptors in the parathyroid glands deteriorates, leading to vitamin D resistance. FGF23 affects the production and regulation of PTH, osteoclast and osteoblast activity, and bone remodeling. The bone resorption marker b-CrossLaps reflects osteoclast activity and bone tissue destruction. In SHPT elevated levels of b-CrossLaps are associated with bone resorption and worsening bone quality [4–8]. Renal osteodystrophy is the cause of serious conditions, including fractures and a decline in quality of life [8, 9]. Compared to the general population, the risk of fractures among CKD patients increases steadily as kidney disease progresses [10, 11].

Extraskeletal calcification, particularly cardiovascular calcification, predicts subsequent cardiovascular mortality and all-cause mortality in patients with end-stage renal disease [12].

Today, vascular calcification is considered an actively regulated and cell-mediated process [13], with a crucial aspect being the imbalance between promoters and inhibitors of calcification. In CKD, calcification inducers such as hyperphosphatemia, hypercalcemia, oxidative stress, inflammatory cytokines, and uremic toxins increase, while calcification inhibitors like fetuin-A, albumin, and ionized magnesium decrease. Moreover, in CKD, the function of vitamin K-dependent proteins that prevent calcification is impaired [14]. Vascular smooth muscle cells, macrophages, endothelial cells, and vascular interstitial cells are involved in the calcification process [13, 15]. Osteoblast-like cells in the vascular bed and heart valves synthesize and secrete bone-related proteins, including osteopontin, osteocalcin, and collagen, which collectively accelerate the calcification of the extracellular matrix [14].

Several studies have shown that osteoporosis is a risk factor for cardiovascular diseases [16]. Arterial calcification and osteoporosis are often observed in the same individuals and progress simultaneously in patients with chronic and end-stage kidney diseases. The associations between bone and arterial anomalies suggest a direct or indirect effect of bone cells and turnover on the arterial system. Understanding these associations is crucial for developing effective therapeutic strategies aimed at improving outcomes for CKD patients [17].

Data obtained from dialysis patients with PTH levels of 300-600 pg/ml, treated with cinacalcet and vitamin D analogs, showed a lower risk of death and cardiovascular complications with earlier treatment of SHPT. This effect is observed when achieving lower target PTH levels compared to higher ones [18].

A higher PTH concentration directly correlates with a higher mortality rate from cardiovascular diseases [19].

Recent studies show that an increase in PTH levels before the start of dialysis predicts a higher PTH level after 9–12 months [20]. Untreated SHPT leads to a progressive increase in PTH levels [21, 22], and parathyroid hyperplasia with progressive SHPT due to delayed treatment is accompanied by a progressive decrease in sensitivity to calcium and vitamin D regulation, leading to a subsequent risk of treatment resistance in the later stages of the disease [23].

Therefore, there remains a need to find a method for early and sustained control of SHPT which would not only ensure safety but also guarantee long-term effect on the system, minimizing patient dependence on treatment adherence [22]. This approach could significantly improve long-term outcomes for bone tissue and cardiovascular outcomes.

The **aim** of this research is to study the effect of local paricalcitol injections into the parathyroid glands

on bone remodeling markers in CKD patients with SHPT and PTH levels of 300–600 pg/ml.

## MATERIALS AND METHODS

The study sample consisted of 48 patients with secondary hyperparathyroidism (SHPT) and end-stage chronic kidney disease (CKD). All patients were undergoing renal replacement therapy and received conservative medical treatment for SHPT prior to the study, which included correction of hyperphosphatemia (Sevelamer, daily dose of 2,400 mg, administered to 41% of patients in the control group and 50% in the main group, $p > 0.05$); use of calcimimetics (Cinacalcet, daily dose of 30 mg, prescribed to all patients in both groups); calcium-phosphorus metabolism regulators (Alfacalcidol, 0.25–1 mcg 3 times a week; paricalcitol, 5 mcg 3 times a week; prescribed to all patients in both groups); correction of hypocalcemia (calcium carbonate, daily doses of 4.0–6.0 g, administered to 28.5% of patients in the main group and 17.6% in the control group).

The difference in calcium intake between the groups may be attributed to individual patient characteristics, including the level of hypocalcemia and response to the therapy. The group with more pronounced hypocalcemia required more extensive correction with calcium-containing preparations. It is also important to note that combined therapy, which includes calcimimetics and vitamin D, may reduce the need for calcium supplements. These differences may reflect both clinical characteristics of the patients and variability in the approaches to prescribing medications.

It is worth noting that adherence to the prescribed treatment among the patients was low. So, 64.2% of patients in the main group and 67.6% of patients in the control group took Cinacalcet as prescribed by their doctor. Only 12 patients in the main group and 30 patients in the control group took vitamin D receptor activators. Patients with CKD often experience apathy and fatigue from prolonged medication use, leading to treatment non-compliance despite having the medications on hand. This may also be associated with potential side effects of the drugs, such as dyspepsia, nausea, or discomfort, which further reduce patients' willingness to continue treatment. For some patients, the high cost of medications or limited access to them may also contribute to poor therapy adherence.

The Charlson Comorbidity Index (CCI) [24] was used to assess the prognosis of the patients and the impact of comorbidity on clinical outcomes. The use of this index allowed for an objective evaluation of the risk associated with comorbid conditions and ensured comparability of results between the groups.

Inclusion criteria were as follows: end-stage CKD, diagnosed SHPT, PTH concentration in blood of 300–600 pg/ml, and verified parathyroid glands based on scintigraphy data combined with single-photon emission computed tomography (SPECT).

Exclusion criteria were the following: planned or previous surgical intervention on neck organs, surgical treatment of SHPT in the medical history, oncological diseases, pregnancy, and severe somatic symptom disorder.

Patients were divided into two groups based on the results of ultrasound examination of the parathyroid glands (SonoScape equipment, S35, China, B-mode). The main group consisted of patients ($n = 14$) in whom the possibility of performing injections into the parathyroid glands was identified after the examination. The control group included patients ($n = 34$) who presented one or more technical difficulties in performing the procedure: the parathyroid glands were not visualized by ultrasound, or they were located atypically, or there was abundant blood flow with a risk of bleeding during the puncture.

In the main group, patients received ultrasound-guided paricalcitol (5 mcg/ml) injections into the parathyroid glands, at a dosage of up to 0.5 ml. The volume of the administered drug was determined depending on the initial volume of the gland (1/3 of its volume). Each patient in this group underwent two punctures, with an interval of 1 day between injections. In the control group, all patients continued to receive standard conservative treatment for SHPT.

Echocardiography was used to evaluate vascular calcification, including the presence of linear calcifications, as well as valve calcification.

The blood tests included the following parameters.

Intact parathyroid hormone (PTH) was determined using the chemiluminescent immunoassay method (Cobas 6000, Roche Diagnostics, Switzerland). Measurement range was 1.2–5,000 pg/ml. Reference values were 15–65 pg/ml.

B-CrossLaps was determined using the Serum CrossLaps reagent kit for enzyme-linked immunosorbent assay (BioMedica, Serbia). Measurement range was 0.020–2.494 ng/ml. Analytical sensitivity was 0.020 ng/ml.

FGF23 was determined using the FGF23 (C-terminal) reagent kit for enzyme-linked immunosorbent assay (BioMedica, Serbia). Measurement

range was 0.1–20 pmol/l. Analytical sensitivity was 0.08 pmol/l.

Bone mineral density was measured by densitometry of the lumbar spine and femoral neck using a computed tomography scanner (General Electric Optima CT660-128, USA).

The verification of the parathyroid glands was conducted using scintigraphy combined with single-photon emission computed tomography (SPECT) (Symbia Intevo Bold system, Germany).

Statistical processing of the findings was carried out using Statistica software (v 13.5.0.17, TIBCO Software Inc.), and IBM SPSS Statistics (v 30.0.0, IBM Corp.). The data were checked for normal distribution using the Shapiro–Wilk test. None of the studied parameters showed a normal distribution, so non-parametric statistical methods were used for the analysis. Descriptive data were presented as the median and the interquartile range *Me* ($Q_{25}$;$Q_{75}$). For all statistical methods, the corresponding null hypothesis was tested. The critical level of significance ($p$) was set at 0.05. A $p$-value < 0.05 was considered statistically significant, indicating a rejection of the null hypothesis. The Kruskal–Wallis test (Analysis of Variance, ANOVA) and Dunn's post-hoc test were used to compare differences between groups.

Risk factors for osteoporosis and vascular calcification were assessed using binary logistic regression analysis. Univariate logistic regression analysis was conducted first, calculating the odds ratio (OR) and 95% confidence interval (95% CI) to evaluate the effect of individual factors on the likelihood of developing osteoporosis and vascular calcification. Variables with a significance level of $p < 0.05$ were included in the multivariate binary logistic regression model to assess their independent contribution to the development of osteoporosis and vascular calcification. Predictor selection in the multivariate model was performed using the backward selection.

To evaluate the diagnostic value of predictors for the development of osteoporosis and vascular calcification, ROC (Receiver Operating Characteristic) analysis was used, with the construction of characteristic curves and the calculation of the area under the curve (AUC). The Youden's J statistic was applied to determine the optimal threshold for each parameter. Values greater than 0.7 were interpreted as good predictive ability, and values above 0.8 were interpreted as very good.

To identify relationships between quantitative variables in the analysis of serum markers, the non-parametric Spearman's rank correlation coefficient was used. The Mann–Whitney U-test was applied to compare laboratory parameters between groups of patients and to test the null hypothesis of no differences between two independent samples. For the evaluation of parameters over time and differences between them, as well as for testing the null hypothesis of equality of medians in dynamic changes within the group, the non-parametric Friedman test (Friedman ANOVA) [25] was used, followed by pairwise comparisons using the Wilcoxon signed-rank test.

## RESULTS

*Characteristics of the Study Groups* A total of 48 patients participated in this study.

In the main group ($n$ = 14), the median age of the patients was 59 (49;65) years, with 71.4% being men. All patients received renal replacement therapy through hemodialysis. The median duration of dialysis was 60 (27;96) months. The median baseline PTH level was 504 (489;601) pg/ml. Osteoporosis was present in 64.3% (9) of the patients, and vascular calcification was present in 64.3% (9) of the patients.

In the comparison group ($n$ = 34), the median age of the patients was 56 (43;68) years, with 44.1% being men. All patients received renal replacement therapy through hemodialysis. The median duration of dialysis was 36 (12;69) months. The median baseline PTH level was 365 (320;425) pg/ml. Osteoporosis was present in 85.2% (29) of the patients, and vascular calcification was present in 58.8% (20) of the patients (Table 1).

Table 1

**Demographic and Laboratory Parameters in Both Groups**

| Parameters | Main group ($n$ = 14) | Comparison group ($n$ = 34) | $p$ |
|---|---|---|---|
| Age, years, *Me* ($Q_{25}$;$Q_{75}$) | 59 (49;65) | 56 (43;68) | 0.83 |
| Male, % | 71.4 | 44.1 | - |
| Duration of dialysis, months, *Me* ($Q_{25}$;$Q_{75}$) | 60 (27;96) | 36 (12;69) | 0.21 |
| PTH level, pg/ml, *Me* ($Q_{25}$;$Q_{75}$) | 504 (489;601) | 365 (320;425) | 0.17 |
| b-CrossLaps level, ng/ml, *Me* ($Q_{25}$;$Q_{75}$) | 1.1 (0.9;2.2) | 1.9 (1.1;2.5) | 0.19 |
| FGF23 level, pmol/l, *Me* ($Q_{25}$;$Q_{75}$) | 14.8 (5;18) | 18.1 (5;20) | 0.50 |
| Presence of osteoporosis, % | 64.3 | 85.2 | 0.83 |
| Presence of vascular calcification, % | 64.3 | 58.8 | 0.78 |
| Volume of parathyroid glands, $mm^3$, *Me* ($Q_{25}$;$Q_{75}$) | 16 (15.2;16.5) | 15.5 (15.2;15.9) | 0.23 |

### Factors Associated with Osteoporosis and Vascular Calcification

According to the multivariate binary logistic regression analysis, osteoporosis was significantly positively associated with age, PTH levels, duration of dialysis therapy, comorbidity index, b-CrossLaps, and FGF23. The comorbidity index was identified as the most significant factor. Vascular calcification was also significantly positively associated with these factors but to a lesser extent (Table 2).

Table 2

**Association of Osteoporosis and Vascular Calcification with Demographic Data and Biochemical Variables Based on Multivariate Logistic Regression Analysis (Binary)**

| Parameters | Osteoporosis | | | Vascular calcification | | |
|---|---|---|---|---|---|---|
| | *p* | OR | CI | *p* | OR | CI |
| Age, years | 0.00 | 5.84 | 1.7–6.2 | 0.02 | 1.05 | 0.97 – 1.12 |
| Duration of dialysis, months | 0.00 | 1.63 | 1.05–1.89 | 0.01 | 1.01 | 0.99 – 1.03 |
| PTH level, pg/ml | 0.01 | 1.01 | 1.01–1.30 | 0.03 | 1.37 | 0.78 – 2.41 |
| Comorbidity index | 0.00 | 2.50 | 1.80–3.20 | 0.02 | 1.00 | 0.99 – 1.00 |
| b-CrossLaps level, ng/ml | 0.01 | 1.30 | 1.10–1.50 | 0.01 | 2.11 | 0.80 – 5.67 |
| FGF23 level, pmol/l | 0.01 | 1.25 | 1.10–1.40 | 0.03 | 1.01 | 0.91 – 1.12 |

Based on ROC analysis, important predictive factors for osteoporosis were age ≥33 years (sensitivity 88%, specificity 70%; AUC = 0.88; $p = 0.00$), dialysis duration ≥12 months (sensitivity 84%, specificity 78%; AUC = 0.84; $p = 0.00$), comorbidity index ≥3 (sensitivity 92%, specificity 89%; AUC = 0.92; $p = 0.00$), and FGF23 ≥0.78 pmol/l (sensitivity 73%, specificity 75%; AUC = 0.73; $p = 0.01$). The least effective factors were PTH ≥301 pg/ml (sensitivity 62%, specificity 71%; AUC = 0.62; $p = 0.01$) and b-CrossLaps ≥0.52 ng/ml (sensitivity 66%, specificity 64%; AUC = 0.66; $p = 0.01$).

For vascular calcification, the most significant factors were the comorbidity index ≥3 (sensitivity 71%, specificity 60%; AUC = 0.71; $p = 0.01$), age ≥29 years (sensitivity 68%, specificity 61%; AUC = 0.71; $p = 0.01$), dialysis duration ≥5 months (sensitivity 64%, specificity 55%; AUC = 0.64; $p = 0.04$), and b-CrossLaps ≥0.19 ng/ml (sensitivity 60%, specificity 55%; AUC = 0.60; $p = 0.04$). Factors such as FGF23 ≥0.92 pmol/l (sensitivity 54%, specificity 61%; AUC = 0.54; $p = 0.01$) and PTH ≥301 pg/ml (sensitivity 58%, specificity 65%; AUC = 0.58; $p = 0.01$) were less significant (Table 3).

Table 3

**Association of Osteoporosis and Vascular Calcification with Demographic Data and Biochemical Variables Based on ROC analysis**

| Parameters | Osteoporosis | | | Vascular calcification | | |
|---|---|---|---|---|---|---|
| | *p* | AUC | Threshold value | *p* | AUC | Threshold value |
| Age, years | 0.00 | 0.88 | 33 | 0.01 | 0.71 | 29 |
| Duration of dialysis, months | 0.00 | 0.84 | 12 | 0.04 | 0.64 | 5 |
| PTH level, pg/ml | 0.01 | 0.62 | 301 | 0.01 | 0.58 | 301 |
| Comorbidity index | 0.00 | 0.92 | 3 | 0.01 | 0.71 | 3 |
| b-CrossLaps level, ng/ml | 0.01 | 0.66 | 0.52 | 0.04 | 0.60 | 0.19 |
| FGF23 level, pmol/l | 0.01 | 0.73 | 0.78 | 0.01 | 0.54 | 0.92 |

### Analysis of Serum Markers

The results of the univariate correlation analysis between bone turnover markers and demographic variables showed a direct statistically significant correlation between FGF23 and dialysis duration, b-CrossLaps and PTH concentration, as well as FGF23 and b-CrossLaps. The Charlson Comorbidity Index was also associated with age, and PTH level exacerbated the comorbidity index (Table 4).

Table 4

**Univariate Correlations between Bone Turnover Markers and Characteristics of Patients with CKD**

| Parameter | Age, years | Dialysis duration, months | PTH, pg/ml | Comorbidity index | b-CrossLaps, ng/ml | FGF23, pmol/l |
|---|---|---|---|---|---|---|
| Age, years | – | 0.19 | 0.12 | 0.73* | 0.14 | 0.09 |
| Dialysis duration, months | 0.19 | – | 0.06 | 0.20 | 0.26 | 0.43* |
| PTH, pg/ml | 0.12 | 0.06 | – | 0.36* | 0.35* | 0.20 |
| Comorbidity index | 0.73* | 0.20 | 0.36* | – | 0.16 | 0.03 |
| b-CrossLaps, ng/ml | 0.14 | 0.26 | 0.35* | 0.16 | – | 0.34* |
| FGF23, pmol/l | 0.09 | 0.43* | 0.20 | 0.03 | 0.34* | – |

* – significance level $p < 0.05$.

**Dynamics of Bone Turnover Markers**

After the ultrasound-guided paricalcitol injections into the parathyroid glands, a persistent and statistically significant reduction in PTH levels was observed in the main group ($p < 0.05$). Within the first 3 months of treatment, the median PTH concentration decreased from 504 (489.25;601) pg/ml to 426.55 (363.75;510.75) pg/ml, which is a reduction by 15.3% ($p < 0.01$). After 6 months of follow-up after the injections, the PTH level also decreased to 171.9 (115.5;266.9) pg/ml, which was 65.8% of the baseline level ($p < 0.01$). In the comparison group, a statistically significant increase in the median PTH concentration was noted ($p < 0.01$) from 365 (320;425) to 498 (353;694), which represented a 36.4% increase from the baseline level over 6 months (Fig. 1).

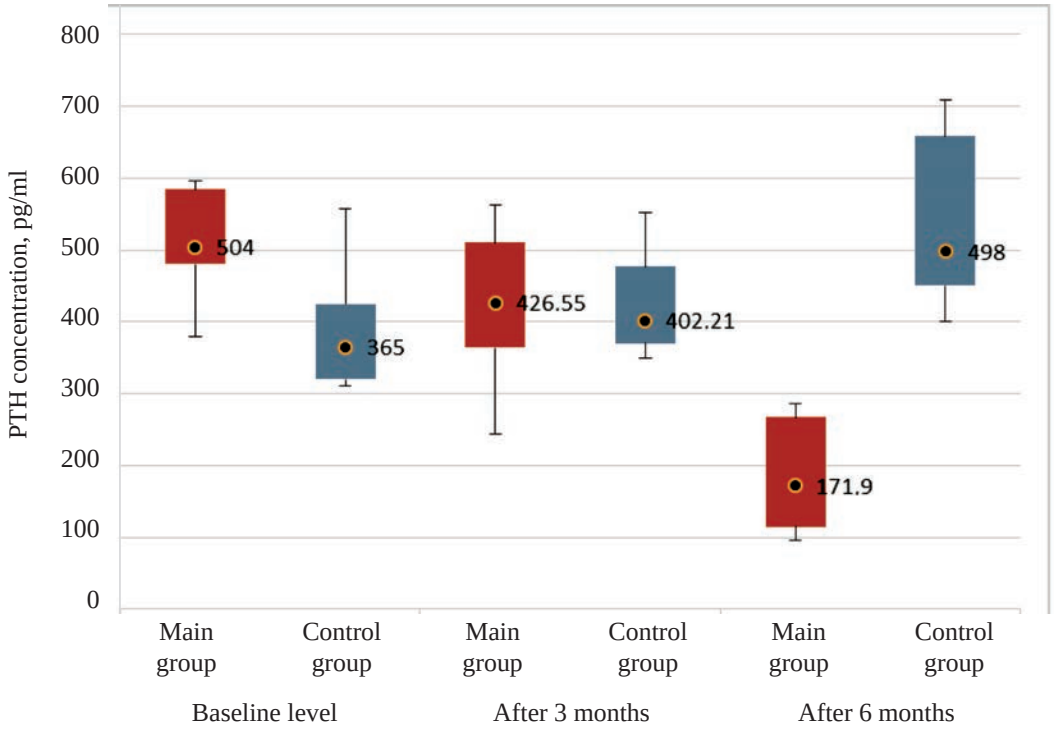


Fig. 1. Dynamics of parathyroid hormone concentration in both groups over 6 months

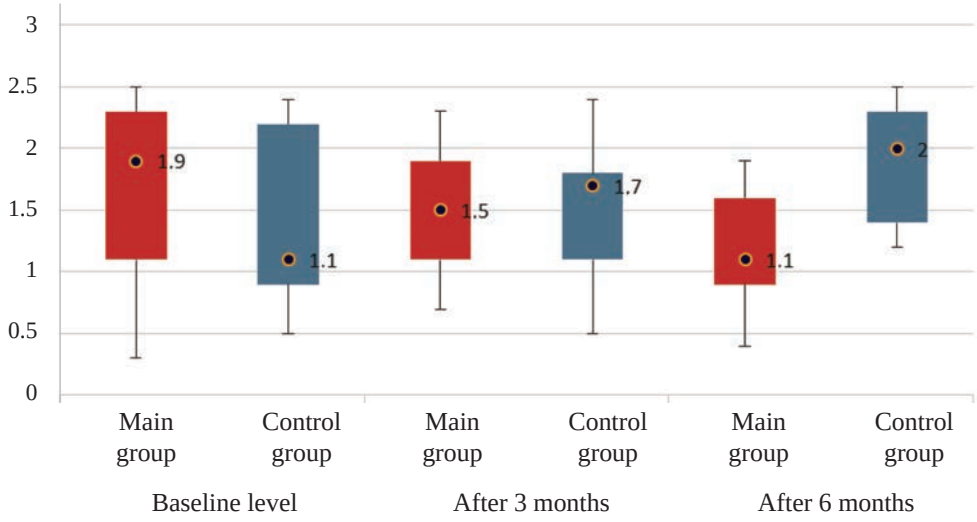


Fig. 2. Dynamics of b-CrossLaps concentration in both groups over 6 months, ng/ml. ANOVA Chi-Square in the main group was 24.03, and in the comparison group it was 38.80. Here and in Fig. 3, $p < 0.01$.

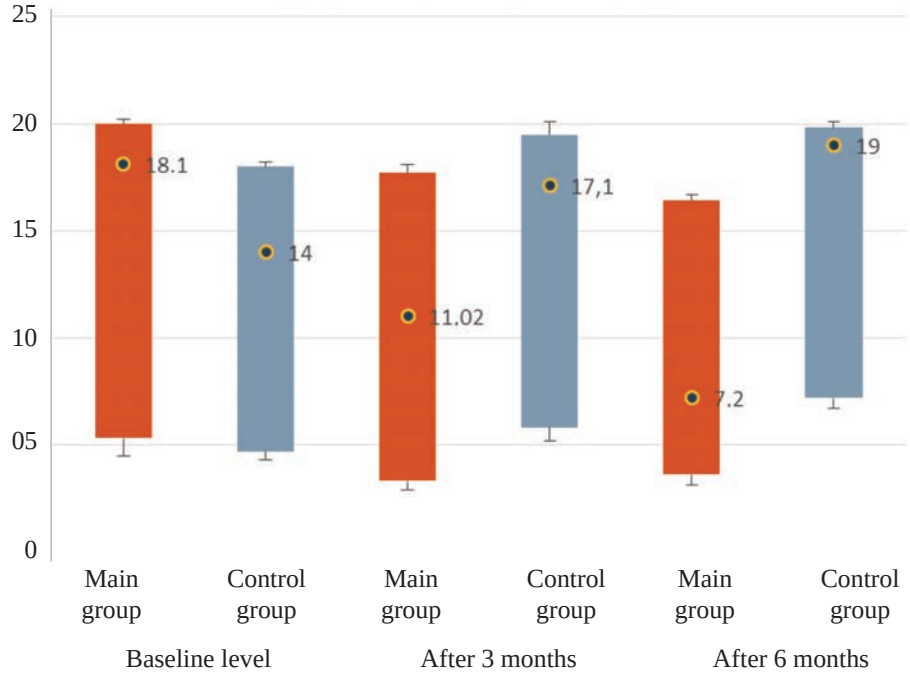


Figure 3. Dynamics of FGF23 concentration in both groups over 6 months, pmol/l. ANOVA Chi-Square in the main group was 33.00, and in the comparison group it was 65.61

In the comparison group, during the 6-month follow-up period, there was a trend towards an increase in bone resorption markers. Specifically, the level of b-CrossLaps increased significantly from 1.55 (0.9;2.2) ng/ml to 2 (1.3;2.4) ng/ml ($p$ = 0.01), and FGF23 increased from 14.75 (4.73;18) pmol/l to 20 (7.2;20) pmol/l ($p$ < 0.01).

In contrast, in the main group, b-CrossLaps significantly decreased from 1.9 (1.19;2.5) ng/ml to 1.1 (0.98;1.59) ng/ml ($p$ = 0.03), and FGF23 decreased from 18.1 (5.3;20.0) pmol/l to 7.2 (3.0;16.4) pmol/l ($p$ < 0.01) (Fig. 2, 3).

After local injections, the median volume of the parathyroid glands in the main group did not change significantly after 6 months and was 15.8 (15.2;16.0) mm³ ($p$ = 0.24).

In our study, there were no cases of hoarseness, bleeding, or intramuscular hematomas following parathyroid gland injections in any of the observed cases. Local pain occurred in 8 (57%) patients in the main group during the procedure but resolved within 2–3 minutes after its completion.

## DISCUSSION

Cardiovascular diseases are the leading cause of death in patients with CKD. Among patients with advanced CKD, cardiovascular diseases are predominantly associated with poorly controlled hypertension and left ventricular hypertrophy (LVH). Common causes of mortality include heart failure, stroke, and sudden cardiac death [26, 27]. Numerous studies have shown that the highest serum FGF23 concentrations are linked to LVH and mortality in CKD patients and those on dialysis [28, 29]. Furthermore, studies have demonstrated that a 30% or greater decrease in serum FGF23 levels is associated with lower rates of heart failure, sudden cardiac death, and cardiovascular mortality [30].

Additionally, there is evidence linking the progression of aortic valve stenosis to an imbalance in bone resorption and an increase in PTH levels in SHPT [31]. Patients with PTH levels exceeding target values have a 29% higher risk of complications [32]. At the same time, both PTH levels below 150 pg/ml and above 300 pg/ml are associated with all-cause and cardiovascular mortality [33].

Surgical treatment is highly effective and remains the mainstay for treating refractory SHPT with PTH levels exceeding 800 pg/ml. However, this approach has several drawbacks. A single-center retrospective study demonstrated a high incidence (71.2%) of hungry bone syndrome following surgical treatment of SHPT, with no statistically significant differences between total and subtotal parathyroidectomy [34]. Moreover,

low PTH levels (<50 pg/ml) after parathyroidectomy are associated with an increased risk of adynamic bone disease, vascular calcification, and mortality in hemodialysis patients [35].

The use of radiofrequency ablation (RFA) for parathyroid glands is becoming increasingly common as a minimally invasive treatment for SHPT. In patients with PTH levels above 800 pg/ml, severe hypocalcemia occurred in 22.1%, while recurrent laryngeal nerve damage was reported in 5.77% after the first session and 21.15% after the second session [36]. However, when this method was applied in patients with lower PTH levels (130–585 pg/ml), its effectiveness reached 70% at 6 months, with complications including a higher incidence of hoarseness (20%), permanent hypoparathyroidism (10%), and severe hypocalcemia (40%) [37].

Our study presents findings comparable to those of minimally invasive SHPT treatments but without severe complications such as recurrent laryngeal nerve paralysis, bleeding, or hematomas.

The dynamics of bone resorption markers in minimally invasive SHPT treatments remain unexplored. Currently, no literature data are available on their changes in SHPT correction with PTH levels up to 600 pg/ml. This gap highlights the need for further research.

## CONCLUSION

The study demonstrated that local ultrasound-guided paricalcitol injections into the parathyroid glands result in a sustained and statistically significant reduction in PTH levels, a key factor in improving patient outcomes and preventing cardiovascular complications. Additionally, this approach positively affects bone remodeling processes, preventing further bone tissue degradation.

The absence of severe complications such as hoarseness, bleeding, or hematomas confirms the high safety of this procedure. Thus, this method can be recommended for the early correction of secondary hyperparathyroidism in CKD patients, potentially improving their prognosis and quality of life.

### REFERENCES


1. Komaba H., Goto S., Fukagawa M. Critical issues of PTH assays in CKD. *Bone.* 2009;44(4):666–670. DOI: 10.1016/j.bone.2008.12.016.
2. Shimada T., Hasegawa H., Yamazaki Y., Muto T., Hino R., Yasuhiro Y. et al. FGF23 is a potent regulator of vitamin D metabolism and phosphate homeostasis. *J. Bone Miner. Res*. 2004;19(3):429–435.
3. Nadzhfarova K.N., Kovalev Yu.R., Kurnikova E.A., Isakov V.A. Chronic Kidney Disease and Secondary Hyperparathyroidism: Causal Relationships. *Medicine: Theory and Practice.* 2019;4(2):27–34. (In Russ.).
4. Sagliker Y., Balal M., Sagliker Ozkaynak P.S., Paydas S., Sagliker C., Sagliker H.S. et al. Sagliker syndrome: uglifying human face appearance in late and severe secondary hyperparathyroidism in chronic renal failure. *Semin Nephrol*. 2004;24(5):449–455. DOI:10.1016/j.semnephrol.2004.06.021.
5. Quarles L.D. Role of FGF23 in vitamin D and phosphate metabolism: implications in chronic kidney disease. *Exp. Cell Res*. 2012;318(9):1040–1048. DOI: 10.1016/j.yexcr.2012.02.027.
6. Silver J., Naveh-Many T. FGF23 and the parathyroid glands. *Pediatr. Nephrol*. 2011;26(9):1441–1445.
7. Arnlov J., Carlsson A.C., Sundstrom J., Ingelsson E., Larsson A., Lind L. et al. Serum FGF23 and risk of cardiovascular events in relation to mineral metabolism and cardiovascular pathology. *Clin. J. Am. Soc. Nephrol*. 2013;8(5):781–786. DOI: 10.2215/CJN.09570912.
8. Garimella P., Ix J., Katz R., Chonchol M., Kestenbaum B., Siscovick D. et al. Fibroblast growth factor 23, the ankle-brachial index, and incident peripheral artery disease in the Cardiovascular Health Study. *Atherosclerosis*. 2014;233(1):91–96. DOI: 10.1016/j.atherosclerosis.2013.12.015.
9. Graciolli F.G., Neves K.R., Barreto F., Barreto D., Reis L., Canziani M., Sabbagh Y. et al. The complexity of chronic kidney disease-mineral and bone disorder across stages of chronic kidney disease. *Kidney Int.* 2017;91(6):1436–1446. DOI: 10.1016/j.kint.2016.12.029.
10. Arneson T.J., Li S., Liu J., Kilpatrick R.D., Newsome B.B., St. Peter W.L. Trends in hip fracture rates in US hemodialysis patients, 1993-2010. *Am. J. Kidney Dis.* 2013;62(4):747–754. DOI: 10.1053/j.ajkd.2013.02.368.
11. Goto N.A., Weststrate A.C.G., Oosterlaan F.M., Verhaar M.C., Willems H.C., Emmelot-Vonk M.H. et al. The association between chronic kidney disease, falls, and fractures: a systematic review and meta-analysis. *Osteoporos. Int.* 2020;31(1):13–29. DOI: 10.1007/s00198-019-05190-5.
12. Bansal N. Evolution of cardiovascular disease during the transition to end-stage renal disease. *Semin. Nephrol*. 2017;37(2):120–31. DOI: 10.1016/j.semnephrol.2016.12.002.
13. Shanahan C.M., Crouthamel M.H., Kapustin A., Giachelli C. Arterial calcification in chronic kidney disease: key roles for calcium and phosphate. *Circ. Res*. 2011;109(6):697–711. DOI: 10.1161/CIRCRESAHA.110.234914.
14. Yamada S., Nakano T. Role of chronic kidney disease (CKD)-mineral and bone disorder (MBD) in the pathogenesis of cardiovascular disease in CKD. *J. Atheroscler. Thromb*. 2023;30(8):835–850. DOI: 10.5551/jat.RV22006.
15. Naik V., Leaf E.M., Hu J.H., Yang H., Nguyen N., Giachelli C. et al. Sources of cells that contribute to atherosclerotic intimal calcification: an in *vivo* genetic fate mapping study. *Cardiovasc. Res*. 2012;94(3):545–554. DOI: 10.1093/cvr/cvs126.
16. Lv J., Xie W., Wang S., Zhu Y., Wang Y., Zhang P. et al. Associated factors of osteoporosis and vascular calcification in patients awaiting kidney transplantation. *Int. Urol. Nephrol*. 2023;55(12):3217–3224. DOI: 10.1007/s11255-023-03606-0.

17. Evenepoel P., Opdebeeck B., David K., D'Haese P.C. Bone-vascular axis in chronic kidney disease. *Adv. Chronic Kidney Dis*. 2019;26(6):472–483. DOI: 10.1053/j.ackd.2019.09.006.
18. Platt A., Wilson J., Hall R., Ephraim P., Morton S., Shafi T. et al. Comparative effectiveness of alternative treatment approaches to secondary hyperparathyroidism in patients receiving maintenance hemodialysis: An observational trial emulation. *Am. J. Kidney Dis*. 2024;83(1):58–70. DOI: 10.1053/j.ajkd.2023.05.016.
19. Magagnoli L., Cozzolino M., Caskey F.J., Evans M., Torino C., Porto G. et al. Association between CKD-MBD and mortality in older patients with advanced CKD-results from the EQUAL study. *Nephrol. Dial Transplant*. 2023;38(11):2562–2575. DOI: 10.1093/ndt/gfad100.
20. Tabibzadeh N., Karaboyas A., Robinson B.M., Csomor P.A., Spiegel D.M., Evenepoel P. et al. The risk of medically uncontrolled secondary hyperparathyroidism depends on parathyroid hormone levels at haemodialysis initiation. *Nephrol. Dial. Transplant*. 2021;36(1):160–169. DOI: 10.1093/ndt/gfaa195.
21. Bover J., Gunnarsson J., Csomor P., Kaiser E., Cianciolo G., Lauppe R. Impact of nutritional vitamin D supplementation on parathyroid hormone and 25-hydroxyvitamin D levels in non-dialysis chronic kidney disease: a meta-analysis. *Clin. Kidney J*. 2021;14(10):2177–2186. DOI: 10.1093/ckj/sfab035.
22. Ketteler M., Bover J., Mazzaferro S. Treatment of secondary hyperparathyroidism in non-dialysis CKD: an appraisal 2022s. *Nephrol. Dial. Transplant*. 2023;38(6):1397–1404. DOI: 10.1093/ndt/gfac236.
23. Ketteler M., Ambühl P. Where are we now? Emerging opportunities and challenges in the management of secondary hyperparathyroidism in patients with non-dialysis chronic kidney disease. *J. Nephrol*. 2021;34(5):1405–1418. DOI: 10.1007/s40620-021-01082-2.
24. Charlson M.E., Pompei P., Ales K.L. A new method of classifying prognostic comorbidity in longitudinal studies: development and validation. *J. Chron. Dis*. 1987;40:373–383.
25. Friedman M. A comparison of alternative tests of significance for the problem of m rankings. *The Annals of Mathematical Statistics*. 1940;11(1):86–92. DOI: 10.1214/aoms/1177731944.
26. Wheeler D.C., London G.M., Parfrey P.S., Block G.A., Correa-Rotter R., Dehmel B. et al. Effects of cinacalcet on atherosclerotic and nonatherosclerotic cardiovascular events in patients receiving hemodialysis: the evaluation of cinacalcet HCl Therapy to lower cardiovascular events (EVOLVE) trial. *J. Am. Heart Assoc*. 2014;3(6):e001363. DOI: 10.1161/JAHA.114.001363.
27. Eckardt K.U., Gillespie I.A., Kronenberg F., Richards S., Stenvinkel P., Anker S.D. et al. High cardiovascular event rates occur within the first weeks of starting hemodialysis. *Kidney Int*. 2015;88(5):1117–1125. DOI: 10.1038/ki.2015.117.
28. Kirkpantur A., Balci M., Gurbuz O.A., Afsar B., Canbakan B., Akdemir R. et al. Serum fibroblast growth factor-23 (FGF23) levels are independently associated with left ventricular mass and myocardial performance index in maintenance haemodialysis patients. *Nephrol. Dial. Transplant*. 2011;26(4):1346–1354. DOI: 10.1093/ndt/gfq539.
29. Mitsnefes M.M., Betoko A., Schneider M.F., Salusky I.B., Wolf M.S., Juppner H. et al. FGF23 and left ventricular hypertrophy in children with CKD. *Clin. J. Am. Soc. Nephrol*. 2018;13(1):45–52. DOI: 10.2215/CJN.02110217.
30. Moe S.M., Chertow G.M., Parfrey P.S., Kubo Y., Block G.A., Correa-Rotter R. et al. Cinacalcet, fibroblast growth factor-23, and cardiovascular disease in hemodialysis: The Evaluation of cinacalcet HCl therapy to lower cardiovascular events (EVOLVE) Trial. *Circulation*. 2015;132(1):27–39. DOI: 10.1161/CIRCULATIONAHA.114.013876.
31. Hekimian G., Boutten A., Flamant M., Duval X., Dehoux M., Benessiano J. et al. Progression of aortic valve stenosis is associated with bone remodelling and secondary hyperparathyroidism in elderly patients--the COFRASA study. *Eur. Heart J*. 2013;34(25):1915–1922. DOI: 10.1093/eurheartj/ehs450.
32. Zemchenkov A.Yu., Gerasimchuk R.P., Vishnevsky K.A., Zemchenkov G.A. Hyperphosphatemia in Patients with Chronic Kidney Disease on Dialysis: Risks and Correction Possibilities. *Clinical Nephrology*. 2013;4:13–46. (In Russ.).
33. Zhou X., Guo,Y., Luo Y. The optimal range of serum intact parathyroid hormone for a lower risk of mortality in the incident hemodialysis patients. *Renal Failure*. 2021;43(1):599–605. DOI: 10.1080/0886022X.2021.1903927.
34. Yeh H., Yeh H., Chiang C.C., Yen J.C., Wang I.K., Liu S.H. et al. Hungry bone syndrome in peritoneal dialysis patients after parathyroid surgery. *Endocr. Connect*. 2023;12(10):e230107. DOI: 10.1530/EC-23-0107.
35. Jean G., Lataillade D., Genet L., Legrand E., Kuentz .F, Moreau-Gaudry X. et al. Association between very low PTH levels and poor survival rates in haemodialysis patients: results from the French ARNOS cohort. *Nephron. Clin. Pract.* 2011;118(2):211–216.
36. Jiang T., Deng E., Chai H., Weng N., He H., Zhang Z. et al. Radiofrequency ablation for patients with recurrent or persistent secondary hyperparathyroidism after parathyroidectomy: initial experience. *Endocrine*. 2023;83(3):681–690. DOI: 10.1007/s12020-023-03513-5.
37. Lin L.P., Lin M., Wu S.S., Liu W.H., Zhang L., Ruan Y.P. et al. Complications after radiofrequency ablation of hyperparathyroidism secondary to chronic kidney disease. *Ren. Fail.* 2023;45(1):2215334. DOI: 10.1080/0886022X.2023.2215334.

## Author Contribution

Zhulina E.M. – conception and design, data analysis and interpretation, and drafting of the manuscript. Brykun M.V. – data analysis and interpretation. Saprina T.V. – conception and design, editing, and final approval of the manuscript for publication. Vorojcova I.N., Tskhay V.F., Komkova T.B. – justification of the manuscript and critical revision for important intellectual content.

## Author Information

**Zhulina Elizaveta M.** – Assistant, Intermediate-Level Therapy Division with Clinical Pharmacology and Endocrinology Courses, Siberian State Medical University, Tomsk, elisaveta.zhulina@gmail.com, http://orcid.org/0000-0002-0798-1089

**Brykun Maria V.** – Student, Siberian State Medical University, Tomsk, aryabrykun@gmail.com, http://orcid.org/0009-0004-7680-4272

**Saprina Tatiana V.** – Dr. Sci. (Med.), Associate Professor, Intermediate-Level Therapy Division with Clinical Pharmacology and Endocrinology Courses, Siberian State Medical University, Tomsk, tanja.v.saprina@mail.ru, http://orcid.org/0000-0001-9011-8720;

**Vorojcova Irina N.** – Dr. Sci. (Med.), Professor, Professor of the Intermediate-Level Therapy Division with Clinical Pharmacology and Endocrinology Courses, Siberian State Medical University, Tomsk, vorozhcova.in@ssmu.ru, https://orcid.org/0000-0002-0424-4825

**Tskhay Valentina F.** – Dr. Sci. (Med.), Professor, Surgical Conditions Division with a Traumatology and Orthopedics Course, Siberian State Medical University, Tomsk, tskhay.vf@ssmu.ru, http://orcid.org/0000-0002-9892-2825

**Komkova Tatiana B.** – Dr. Sci. (Med.), Professor, Head of the Surgical Conditions Division with a Traumatology and Orthopedics Course, Siberian State Medical University, Tomsk, komkova.tb@ssmu.ru, http://orcid.org/0000-0002-4164-6823

(✉) **Zhulina Elizaveta M.,** elisaveta.zhulina@gmail.com

Received on January 23, 2025;
approved after peer review on February 25, 2025;
accepted on February 27, 2025

УДК 616.98:578.834.1]-06:616.1-098
https://doi.org/10.20538/1682-0363-2025-3-25-33

# Cardiometabolic and echocardiographic characteristics of the cardiovascular phenotype of post COVID-19 condition

**Zorina V.V.[1], Garbuzova E.V.[2], Afanaseva A.D.[2], Shchepina Yu.V.[2], Palekhina Yu.Y.[2], Shramko V.S.[2], Shakhtschneider E.V.[1, 2], Logvinenko I.I.[2]**

*[1] Institute of Cytology and Genetics, Siberian Branch, Russian Academy of Sciences (ICG SB RAS)*

*10 Lavrentjev Ave., 630090 Novosibirsk, Russian Federation*

*[2] Research Institute of Internal and Preventive Medicine, Branch of the Institute of Cytology and Genetics, Siberian Branch, Russian Academy of Sciences (RIIPM, Branch of ICG SB RAS)*
*175/1 B. Bogatkov St., 630089 Novosibirsk, Russian Federation*

## ABSTRACT

**Aim.** To study the cardiometabolic and echocardiographic characteristics of COVID-19 convalescents, including patients with the cardiovascular phenotype of )post COVID-19 condition (PCC).

**Materials and methods.** The sample included 270 COVID-19 convalescents (62 without PCC and 208 with PCC). In the subgroup with PCC, 16 convalescents had a cardiovascular phenotype. The study took into account the data of anamnesis, anthropometry, several clinical and biochemical blood parameters, and instrumental diagnostic data (electrocardiography and echocardiography).

**Results.** In COVID-19 convalescents with PCC ($n$ = 208), fasting plasma glucose levels were 1.10 times higher ($p < 0.001$), abdominal obesity (AO) was 5.52 times more common ($p < 0.001$), arterial hypertension (AH) was 4.96 times more common ($p < 0.001$), diastolic dysfunction grade I was 5.55 times more common ($p = 0.002$), and left ventricular hypertrophy was 7 times more common ($p = 0.005$). The indices of maximum blood flow velocity and pressure gradient in the pulmonary artery in convalescents with PCC were 1.08-fold ($p = 0.020$) and 1.14-fold ($p = 0.043$) lower, respectively. In COVID-19 convalescents with PCC ($n$ = 16) and a cardiovascular phenotype, total cholesterol (TC) was 1.11 times higher ($p = 0.039$), low-density lipoprotein cholesterol (LDL-C) was 1.21 times higher ($p = 0.004$), high-density lipoprotein cholesterol (HDL-C) was 1.22 times lower ($p = 0.040$), non-high-density lipoprotein cholesterol (non-HDL-C) was 1.24 times higher ($p = 0.005$) compared with patients without a cardiovascular phenotype. An increase in TC, LDL-C, and non-HDL-C and a decrease in HDL-C are associated with the cardiovascular phenotype of PCC regardless of gender, age, body mass index, and lipid-lowering therapy.

**Conclusion.** According to the study, echocardiographic changes and cardiometabolic risk factors, such as AO, AH, and carbohydrate metabolism disorders, were more common in patients with PCC. The cardiovascular phenotype of PCC is associated with an increase in TC, LDL-C, non-HDL-C, and a decrease in HDL-C.

**Keywords:** COVID-19 convalescents, post COVID-19 condition, cardiovascular phenotype

**Conflict of interests.** The authors declare the absence of obvious or potential conflicts of interest related to the publication of this article.

**Source of financing.** The study was carried out as part of the state-financed research No. FWNR-2024-0002 and with the support of the scholarship of the President of the Russian Federation SP 2974.2022.4

**Compliance with the principles of ethics.** The study was approved by the Ethics Committee of the Research Institute of Internal and Preventive Medicine, branch of ICG SB RAS, Novosibirsk (Minutes No. 71 dated November 10, 2020).

**For citation:** Zorina V.V., Garbuzova E.V., Afanaseva A.D., Shchepina Yu.V., Palekhina Yu.Y., Shramko V.S., Shakhtschneider E.V., Logvinenko I.I. Cardiometabolic and echocardiographic characteristics of the

✉ *Zorina Valentina V.,* walentina.zorina@bk.ru

cardiovascular phenotype of post COVID-19 condition. *Bulletin of Siberian Medicine.* 2025;24(3):25–33. https://doi.org/10.20538/1682-0363-2025-3-25-33.

# Кардиометаболические и эхокардиографические характеристики сердечно-сосудистого фенотипа постковидного синдрома

**Зорина В.В.[1], Гарбузова Е.В.[2], Афанасьева А.Д.[2], Щепина Ю.В.[2], Палехина Ю.Ю.[2], Шрамко В.С.[2], Шахтшнейдер Е.В.[1, 2], Логвиненко И.И.[2]**

*[1] Институт цитологии и генетики Сибирского отделения Российской академии наук (ИЦиГ СО РАН) Россия, 630090, г. Новосибирск, пр. Академика Лаврентьева, 10*

*[2] Научно-исследовательский институт терапии и профилактической медицины (НИИТПМ) – филиал Института цитологии и генетики Сибирского отделения Российской академии наук (ИЦиГ СО РАН) Россия, 630089, г. Новосибирск, ул. Бориса Богаткова, 175/1*

## РЕЗЮМЕ

**Цель.** Изучить кардиометаболические и эхокардиографические характеристики реконвалесцентов COVID-19, в том числе пациентов с сердечно-сосудистым фенотипом постковидного синдрома (ПКС).

**Материалы и методы.** Выборка 270 реконвалесцентов COVID-19: 62 без ПКС и 208 с ПКС. В подгруппе с ПКС 16 реконвалесцентов имели сердечно-сосудистый фенотип. В ходе исследования учитывались данные анамнеза, антропометрии, ряда клинических, биохимических показателей крови, данных инструментальной диагностики (электрокардиографии и эхокардиографии).

**Результаты.** У реконвалесцентов COVID-19 с ПКС ($n$ = 208) уровень глюкозы плазмы крови натощак был выше в 1,10 раза ($p$ < 0,001), чаще встречались: абдоминальное ожирение (АО) в 5,52 раза ($p$ < 0,001), артериальная гипертензия (АГ) в 4,96 раза ($p$ < 0,001), диастолическая дисфункция I степени в 5,55 раза ($p$ = 0,002) и гипертрофия левого желудочка в 7 раз ($p$ = 0,005), показатели максимальной скорости кровотока и градиента давления в легочной артерии у реконвалесцентов с ПКС были ниже в 1,08 ($p$ = 0,020) и 1,14 раза ($p$ = 0,043) соответственно. У реконвалесцентов COVID-19 с ПКС ($n$ = 16), имеющих сердечно-сосудистый фенотип, общий холестерин (ОХС) выше в 1,11 раза ($p$ = 0,039), холестерин липопротеинов низкой плотности (ХС-ЛНП) выше в 1,21 раза ($p$ = 0,004), холестерин липопротеинов высокой плотности (ХС-ЛВП) ниже в 1,22 раза ($p$ = 0,040), холестерин липопротеинов невысокой плотности (ХС-неЛВП) выше в 1,24 раза ($p$ = 0,005) по сравнению с пациентами без сердечно-сосудистого фенотипа. Увеличение ОХС, ХС-ЛНП, ХС-неЛВП и уменьшение ХС-ЛВП ассоциированы с сердечно-сосудистым фенотипом ПКС независимо от пола, возраста, индекса массы тела и гиполипидемической терапии.

**Заключение.** По данным исследования у пациентов с ПКС чаще встречались эхокардиографические изменения и кардиометаболические факторы риска, такие как АО, АГ и нарушения углеводного обмена. Сердечно-сосудистый фенотип ПКС ассоциирован с увеличением ОХС, ХС-ЛНП, ХС-неЛВП и уменьшением ХС-ЛВП.

**Ключевые слова:** реконвалесценты COVID-19, постковидный синдром, сердечно-сосудистый фенотип

**Конфликт интересов.** Авторы декларируют отсутствие явных и потенциальных конфликтов интересов, связанных с публикацией настоящей статьи.

**Источник финансирования.** Исследование выполнено в рамках бюджетной темы № FWNR-2024-0002 и при поддержке стипендии Президента РФ СП 2974.2022.4.

**Соответствие принципам этики.** Все участники подписали информированное согласие на участие в исследовании и обработку персональных данных. Исследование одобрено этическим комитетом НИИТПМ – филиал ИЦиГ СО РАН (протокол № 71 от 10.11.2020).

**Для цитирования:** Зорина В.В., Гарбузова Е.В., Афанасьева А.Д., Щепина Ю.В., Палехина Ю.Ю., Шрамко В.С., Шахтшнейдер Е.В., Логвиненко И.И. Кардиометаболические и эхокардиографические характеристики сердечно-сосудистого фенотипа постковидного синдрома. *Бюллетень сибирской медицины.* 2025;24(3):25–33. https://doi.org/10.20538/1682-0363-2025-3-25-33.

## INTRODUCTION

According to the World Health Organization (WHO), 10–20% of new coronavirus infection (COVID-19) convalescents have consequences that manifest as new diseases, as well as decompensation of existing chronic non-communicable diseases, known as post COVID-19 condition (PCC).

In the acute course of COVID-19, the respiratory system is mainly affected through target cells having angiotensin-converting enzyme 2 (ACE2) receptors. However, ACE2 receptors are found in the cytoplasmic membrane of not only alveolar cells but also enterocytes of the small intestine, smooth muscle cells of the arteries, endothelial cells of the arteries and veins, and cells of tissues of the brain, esophagus, adrenal glands, bladder, etc. [1, 2].

Clinical cardiovascular manifestations are an important aspect of PCC [3]. Their structuring will greatly contribute to the search for a comprehensive, targeted approach to COVID-19 convalescents in order to diagnose and prevent complications early.

**Aim.** To study the cardiometabolic and echocardiographic characteristics of COVID-19 convalescents, including patients with the cardiovascular phenotype of post COVID-19 condition (PCC).

## MATERIALS AND METHODS

A one-stage observational study of COVID-19 convalescents was performed at the Research Institute of Internal and Preventive Medicine, branch of the Institute of Cytology and Genetics, Siberian Branch of the Russian Academy of Sciences.

The study included 270 COVID-19 convalescents whose average age was 53.2 ±13.2 years. All the subjects were divided into subgroups depending on the presence of PCC: 62 without PCC (58.1% were men) and 208 with PCC (45.2% were men). The group of COVID-19 convalescents with PCC was formed taking into account the WHO criteria [4]. In the group of people with PCC, a cardiovascular phenotype was identified (16 people, 56.3% were men), represented by new onsets of cardiovascular diseases (CVD), as well as decompensation of pre-existing diseases of the cardiovascular system before COVID-19 infection. The structure of the cardiovascular phenotype is shown in Figure 1.

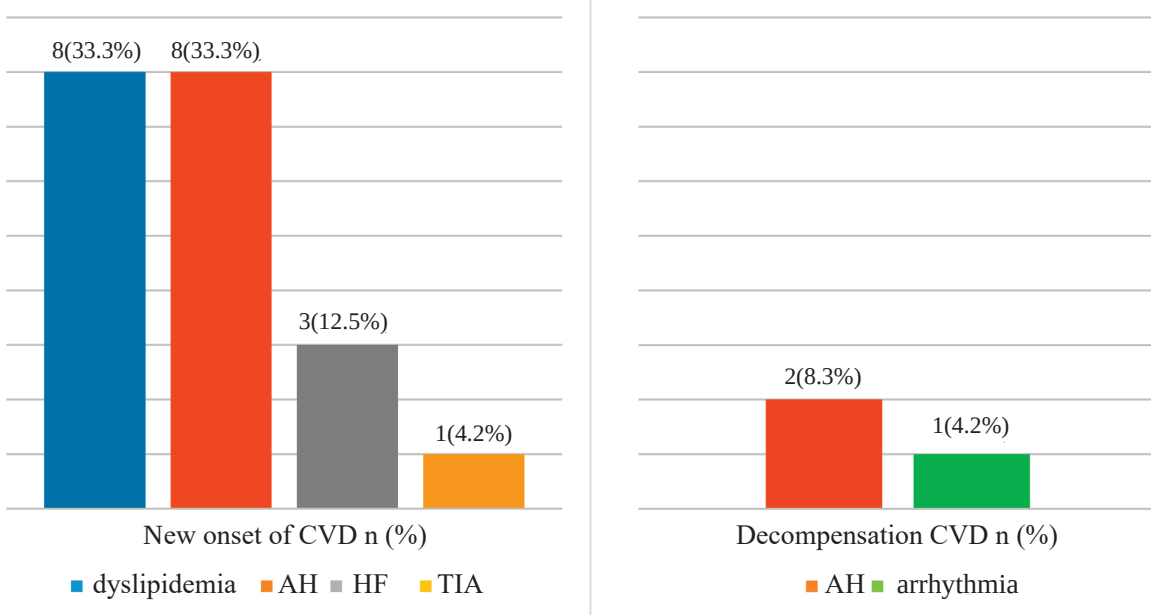


Fig. 1. The structure of the cardiovascular phenotype

Arterial hypertension (AH) was recorded at systolic blood pressure (SBP) ≥ 140 mm Hg and/or diastolic blood pressure (DBP) ≥ 90 mm Hg. Body mass index (BMI) was calculated using the formula: BMI (kg/m$^2$) = body weight (kg)/height (m$^2$) [5]. Abdominal obesity (AO) was recorded according to measurements of waist circumference > 94 cm (men) and > 80 cm (women).

Echocardiography (Echo) was performed in all patients using a Toshiba Aplio 500 color ultrasound scanner (Japan). The left ventricular myocardial mass (LVMM) was determined using the Penn Convention

formula [6]: LVMM (g) = 1.04 × ([LVEDD + IVSD + PWD]$^3$–[LVEDD]$^3$) – 13.6. Body surface area (BSA) according to the Du Bois and Du Bois formula: BSA (m$^2$) = 0.007184 × weight (kg)$^{0.425}$ × height (cm)$^{0.725}$ [7]. The calculation of the relative wall thickness (RWT) of the left ventricle (LV) was carried out according to the formula: RWT (units) = PWD × 2 / LVEDD [8]. The LV myocardial mass index (LVMI) was calculated using the formula: LVMI (g/m$^2$) = LVMM / BSA. The criteria for left ventricular hypertrophy (LVH) were the following parameters: (LVH (LVMM, g/height, m), ASE formula for overweight and obese patients: for men > 50 g/m$^{2.7}$, for women > 47 g/m$^{2.7}$, and for patients with normal body weight, indexing was carried out using BSA > 115 g/m$^2$ (men) and > 95 g/m$^2$ (women) [9].

Left ventricular diastolic dysfunction (LVDD) was assessed using Echo criteria: grade 1 LVDD was established if the ratio of LV filling pressure in the early diastole and atrial systole was (E/A) < 0.8, and the LV filling pressure in the early diastole (E) was < 50 cm/s; grade 2 LVDD was established if two of the following three criteria were positive: 1) the ratio of the early LV diastolic filling pressure and the left ventricular posterior wall in the early diastole (E/e' > 14); 2) left atrial volume indexed for body surface area (> 34 ml/m$^2$); 3) maximum tricuspid regurgitation rate > 2.8 m/s. Grade 3 LVDD was established when the E/A ratio was > 2 [10].

The erythrocyte sedimentation rate (ESR) was determined by the indirect Panchenkov's method (a space-dependent neutron kinetics model utilizing an integral representation of the Boltzmann equation). Biochemical parameters of blood (aspartate aminotransferase (AST), alanine aminotransferase (ALT), uric acid, fibrinogen, prothrombin index (PTI), activated partial thromboplastin time (APTT), C-reactive protein (CRP), fasting blood glucose, creatinine, total cholesterol (TC), high lipoprotein cholesterol densities (HDL-C), triglycerides (TG) were determined using Thermo Fisher Scientific kits (Finland) on a Konelab Prime 30i biochemical analyzer (Thermo Fisher Scientific, Finland). Low-density lipoprotein cholesterol (LDL-C) was calculated using the Friedewald formula: LDL-C (in mmol/l) = TC – HDL-C – TG/2.2. Non-high-density lipoprotein cholesterol (non-HDL-C) was calculated using the formula: TC – HDL-C [11].

Statistical processing of the obtained results was performed using the SPSS software package (version 13.0). The results are presented as the median of the lower and upper quartiles *Me* [25;75]. We used the Mann–Whitney test to compare groups and univariate logistic regression analysis to evaluate the odds ratio. Spearman's rank correlation coefficient was used to assess correlations. The groups were compared regarding frequency using conjugation tables and the Pearson's chi-squared test. When testing statistical hypotheses, the critical level of significance was at $p < 0.05$.

## RESULTS

According to demographic data, the age of convalescents with PCC was 1.18 times higher ($p = 0.003$) than that of convalescents without PCC (Fig. 2). No statistically significant differences were revealed regarding gender ($p = 0.075$).

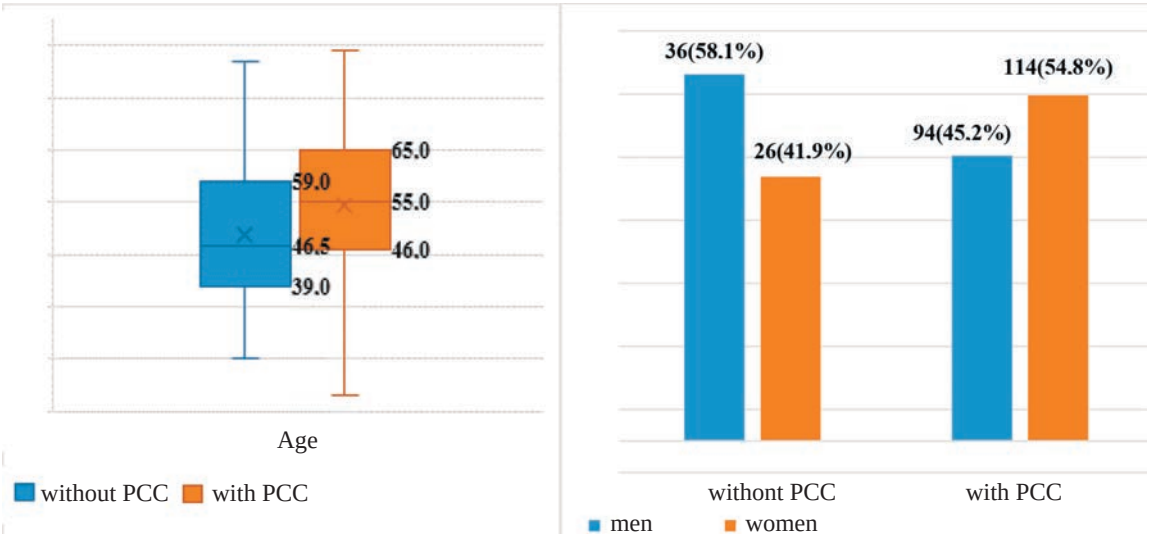


Fig. 2. Demographic data of COVID-19 convalescents with and without PCC

The analysis of anamnestic data revealed that at the outpatient and inpatient stages of treatment for the acute period of COVID-19, patients received various groups of medications. The analysis included records of only those patients for whom it was possible to clarify the data on medication intake. Thus, anticoagulant therapy was received by 6 (9.7% of 19) convalescents without PCC and 33 (15.9% of 72) convalescents with PCC ($p$ = 0.264), oxygen therapy — by 2 (3.2% of 29) convalescents without PCC and 14 (6.7% of 84) with PCC ($p$ = 0.193), glucocorticoid therapy — by 7 (11.3% of 25) convalescents without PCC and 30 (14.4% of 75) with PCC ($p$ = 0.282), antibiotics – by 17 (27.4% of 26) convalescents without PCC and 62 (29.8% of 83) with PCC ($p$ = 0.353), antiviral therapy — by 13 (21.0% of 25) convalescents without PCC and 35 (16.8% of 78) with PCC ($p$ = 0.534).

Statistical processing of laboratory data revealed that in the group of people with PCC, fasting blood glucose and fibrinogen levels were 1.10 times higher ($p$ < 0.001) and 1.13 times higher ($p$ = 0.007), respectively (Fig. 3).

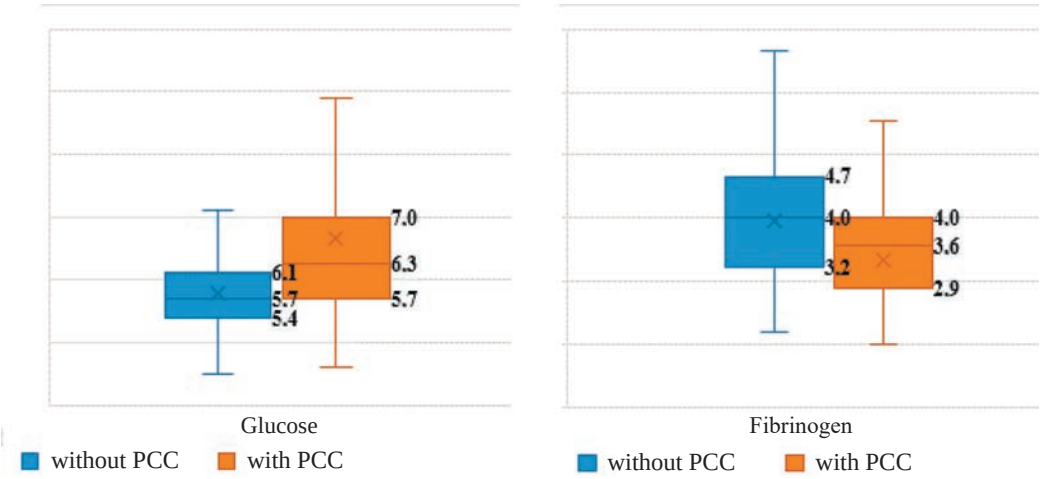


Fig. 3. Fasting blood glucose and fibrinogen levels in COVID-19 convalescents with and without PCC

According to Echo data, LVRWT was 1.07 times larger in patients with PCC, grade 1 LVDD was 5.55 times more common, LVH was 7 times more common compared with people without PCC. In individuals with PCC, AO and AH were also more common — by 5.52 and 4.96 times, respectively, than in individuals without PCC. When comparing the maximum blood flow velocity and the pressure gradient in the pulmonary artery in individuals with PCC, the parameters were 1.08 and 1.14 times lower, respectively (Table 1).

Table 1

**Characterization of Morphofunctional Parameters of Individuals with and without PCC**

| Parameters | COVID-19 convalescents without PCC, $n$ = 62 | Convalescents of COVID-19 with PCC, $n$ = 208 | $p$ |
|---|---|---|---|
| QT, s | 0.36 [0.33;0.37] | 0.35 [0.34;0.37] | 0.565 |
| QRS, s | 0.08 [0.08;0.09] | 0.08 [0.08;0.09] | 0.975 |
| Ao, mm | 32.65 [30.00;35.00] | 32.00[29.73;35.00] | 0.469 |
| LA diameter, mm | 37.10 [34.00;40.00] | 38.00 [35.00;42.00] | 0.074 |
| LA length, mm | 49.00 [45.00;52.00] | 50.00 [46.00;55.00] | 0.069 |
| RV, mm | 27.50 [21.25;32.75] | 26.00 [21.00;31.00] | 0.537 |
| IVSD, mm | 10.15 [8.90;11.00] | 10.50 [9.50;12.00] | 0.075 |
| LV, mm | 50.10 [48.00;52.88] | 51.00 [47.00;54.00] | 0.347 |
| LVESD, mm | 31.00 [29.00;33.00] | 31.90 [29.00;34.00] | 0.429 |
| PWd, mm | 8.80 [8.00;9.48] | 9.00 [8.30;10.00] | 0.060 |
| RA diameter, mm | 35.00 [32.00;37.75] | 35.00 [32.00;38.00] | 0.679 |
| RA length, mm | 46.00 [43.00;52.00] | 48.00 [44.00;51.00] | 0.146 |
| Mitral valve, m/s, Vmax | 0.69 [0.52;0.82] | 0.67 [0.55;0.75] | 0.463 |
| Mitral valve, gradient, mm Hg | 1.90 [1.10;2.70] | 1.80 [1.20;2.20] | 0.434 |
| Aortic valve, m/s, Vmax | 1.23 [1.15;1.43] | 1.30 [1.19;1.45] | 0.264 |
| Aortic valve, gradient, mm Hg | 6.05 [5.35;8.20] | 6.80 [5.70;8.40] | 0.284 |
| Pulmonary artery, m/s, Vmax | 0.90 [0.80;1.04] | 0.83 [0.73;0.96] | 0.020 |
| Pulmonary artery, gradient, mm Hg | 3.20 [2.43;4.35] | 2.80 [2.10;3.63] | 0.043 |

End of table 1

| Parameters | COVID-19 convalescents without PCC, *n* = 62 | Convalescents of COVID-19 with PCC, *n* = 208 | *p* |
|---|---|---|---|
| EF by the Simpson method, % | 67.00 [63.25;69.00] | 67.00 [63.00;70.00] | 0.564 |
| Mean pulmonary artery pressure, mm Hg | 19.50 [14.00;22.75] | 20.00 [15.00;24.00] | 0.408 |
| LVDD (grade 1), abs. (%) | 22 (35.50) | 122 (58.70) | 0.002 |
| LVMM, g | 176.00 [143.50;194.75] | 182.50 [153.00;224.00] | 0.100 |
| LVMI, g/m$^2$ | 88.23 [79.34;99.67] | 92.15 [82.00;110.12] | 0.052 |
| LVRWT, U | 1.51 [1.28;1.89] | 1.62 [1.38;1.93] | 0.049 |
| LVH, abs. (%) | 11 (17.70) | 77 (37.00) | 0.005 |

Note. AO – the diameter of the aortic root, LA – left atrium, RV – size of the right ventricle in a four–chamber section, IVSD – interventricular septum thickness during diastole, LVEDD – left ventricular end–diastolic diameter, LVESD – left ventricular end–systolic diameter, PWd – left ventricular posterior wall thickness during diastole, RA – right atrium, LVDD – left ventricular diastolic dysfunction, LVMM – left ventricular myocardial mass, LVMI – left ventricular myocardial mass index, LVRWT – relative wall thickness of the left ventricle, LVH – left ventricular hypertrophy

When analyzing demographic and anamnestic parameters in the group of COVID-19 convalescents with a cardiovascular phenotype, it was revealed that those with this phenotype were younger than other convalescents with PCC. Before the debut of COVID-19, blood pressure figures reached target values in people with decompensated cardiovascular phenotype, and optimal therapy was selected. The comparative characteristics of drug treatment are given in Table 2.

When analyzing cardiometabolic risk factors in the group with the cardiovascular phenotype, TC was 1.11 times higher, LDL-C was 1.21 times higher, HDL-C was 1.22 times lower, and non-HDL-C was 1.24 times higher than in other convalescents (Table 3).

Table 2

**Comparative Characteristics of Drug Therapy for COVID-19 Convalescents with a Cardiovascular Phenotype and Other COVID-19 Convalescents, abs. (%)**

| Parameter | COVID-19 convalescents with a cardiovascular phenotype, *n* = 16 | Other COVID-19 convalescents with PCC, *n* = 192 | *p* |
|---|---|---|---|
| Angiotensin-converting enzyme inhibitors | 1 (6.3%) | 51 (26.6%) | 0.070 |
| Angiotensin II receptor blockers | 0 (0.0%) | 49 (25.5%) | 0.020 |
| Beta-blockers | 2 (12.5%) | 59 (30.7%) | 0.121 |
| Calcium channel blockers | 0 (0.0%) | 34 (17.7%) | 0.065 |
| Diuretics | 0 (0.0%) | 54 (28.1%) | 0.013 |
| Centrally acting antihypertensive agents | 1 (6.3%) | 8 (4.2%) | 0.698 |

Table 3

**Cardiometabolic Risk Factors in COVID-19 Convalescents with a Cardiovascular Phenotype and Other COVID-19 Convalescents, *Me* [25;75]**

| Parameters | COVID-19 convalescents with a cardiovascular phenotype, *n* = 16 | Other COVID-19 convalescents with PCC, *n* = 192 | *p* |
|---|---|---|---|
| Age, years | 46.00 [41.25;55.00] | 56.00 [46.00;65.00] | 0.016 |
| Men, abs (%) | 9 (56.30) | 85 (44.30) | 0.355 |
| BMI | 28.03 [24.73;32.78] | 29.03 [25.07;33.47] | 0.605 |
| WC, cm | 97.00 [88.50;106.00] | 100.00 [88.00;110.00] | 0.390 |
| Smoking, years, abs. (%) | 6 (37.50) | 66 (34.40) | 0.801 |
| PA < 3 h/week, abs. (%) | 12 (75.00) | 134 (69.80) | 0.621 |
| SBP, mm Hg | 129.75 [118.13;140.00] | 126.75 [115.63;135.00] | 0.692 |
| DBP, mm Hg | 84.75 [73.13;90.00] | 80.00 [75.00;87.38] | 0.231 |
| Heart rate, bpm | 67.50 [57.25;71.50] | 67.00 [62.00;75.00] | 0.295 |
| FBG, mmol/l | 5.95 [5.50;6.45] | 6.30 [5.70;7.00] | 0.108 |
| TC, mmol/l | 5.86 [5.29;6.72] | 5.27 [4.51;6.10] | 0.039 |
| LDL-C, mmol/l | 4.05 [3.62;4.71] | 3.29 [2.50;3.99] | 0.004 |
| HDL-C, mmol/l | 1.06 [0.82;1.40] | 1.29 [1.05;1.60] | 0.040 |
| Triglycerides, mmol/l | 1.40 [1.09;2.42] | 1.40 [0.96;2.09] | 0.515 |
| non-HDL-C, mmol/l | 4.90 [4.20;5.70] | 3.91 [3.12;4.75] | 0.005 |
| Fibrinogen, g/l | 4.00 [2.88;4.61] | 3.55 [2.88;4.00] | 0.198 |

Note. Here and in Table 4: BMI – body mass index, WC – waist circumference, PA < 3 – physical activity less than 3 hours per week, SBP – systolic blood pressure, DBP – diastolic blood pressure, HR – heart rate, TC – total cholesterol, LDL-C –low-density lipoprotein cholesterol, HDL-C – high-density lipoprotein cholesterol, non-HDL-C – high-density non-lipoprotein cholesterol.

According to instrumental research methods, no differences were revealed between the cardiovascular phenotype and other individuals with PCC.

Logistic regression analysis identified the correlations of the cardiovascular phenotype with the level of TCH, LDL-C, HDL-C, and non-HDL-C (Table 4). The odds of having a cardiovascular phenotype increased twofold along with an increase in atherogenic lipid fractions and by 12.5 times along with a decrease in HDL-C.

Table 4

**Logistic Regression Analysis of Parameters Associated with the Cardiovascular Phenotype of Post COVID-19 Condition**

| Parameter | Model 1 $Exp(B)_1$ | *p* | Model 2 $Exp(B)_2$ | *p* | Model 3 $Exp(B)_3$ | *p* | Model 4 $Exp(B)_4$ | *p* |
|---|---|---|---|---|---|---|---|---|
| Age, in year 1 | 0.951 (0.905–0.999) | 0.045 | 0.947 (0.901–0.996) | 0.034 | 0.961 (0.920–1.003) | 0.071 | 0.944 (0.897–0.993) | 0.026 |
| Sex, M/W | 0.677 (0.228–2.004) | 0.481 | 0.728 (0.242–2.196) | 0.574 | 1.008 (0.322–3.156) | 0.989 | 0.803 (0.263–2.453) | 0.700 |
| BMI, per 1 kg/m$^2$ | 1.008 (0.918–1.106) | 0.872 | 1.000 (0.911–1.098) | 0.994 | 0.945 (0.849–1.052) | 0.300 | 0.992 (0.901–1.092) | 0.869 |
| Hypolipidemic therapy, yes/no | 0.329 (0.051–2.128) | 0.243 | 0.346 (0.057–2.119) | 0.251 | 0.247 (0.035–1.735) | 0.160 | 0.316 (0.050–1.987) | 0.219 |
| TC, per 1 mmol/l | 1.594 (1.023–2.483) | 0.039 | - | - | - | - | - | - |
| LDL-C, per 1 mmol/l | - | - | 2.033 (1.213–3.407) | 0.007 | - | - | - | - |
| HDL-C, per 1 mmol/l | - | - | - | - | 0.080 (0.012–0.524) | 0.008 | - | - |
| non-HDL-C, per 1 mmol/l | - | - | - | - | - | - | 1.917 (1.218–3.017) | 0.005 |

## DISCUSSION

A number of studies reflect the cytotoxic effect of SARS-CoV-2 on cardiomyocytes, which is confirmed by increased markers of cardiovascular damage [12–14]. However, it remains controversial whether the long-term cardiovascular manifestations of COVID-19 are caused by the direct action of the virus on the heart tissue or are secondary due to the formation of systemic inflammation and hypoxia [15].

In our study, individuals with PCC were statistically more likely to have abdominal obesity. AO is known to affect immune function and endocrine metabolism. For instance, L. Shang et al. discussed obesity as a risk factor for the development of PCC [16]. H.W. Kim et al. described how, through the secretion of chemokines, perivascular adipose tissue leads to endothelial dysfunction, vasoconstriction, and proliferation of smooth muscle cells, which potentially contributes to the development of cardiovascular diseases [17].

Concomitant chronic diseases are well known to be risk factors in the development of severe forms of COVID-19. A number of studies confirm the association of arterial hypertension in patients with severe and fatal COVID-19 [18, 19]. However, high blood pressure is associated with old age, as well as other cardiovascular risk factors that affect the overall prognosis [3]

M.R. Dweck et al. studied a sample consisting of patients from 69 countries. As a result, changes in Echo parameters were detected in 55% of patients with acute COVID-19 [20]. Long-term studies of the heart were reflected in the work of I. Yaroslavskaya et al., which revealed a decrease in systolic and diastolic function of the left ventricle due to the presence of chronic heart failure and AH [21]. S.G. Kanorskiy et al. found a relationship between PCC and DD of the right ventricle, as well as a significant increase in the maximum and average pressure gradients on the aortic valve and the average pressure gradient on the mitral valve [22]. In our study, convalescents with PCC had grade 1 diastolic dysfunction of the left ventricle and Echo signs of left ventricular hypertrophy, which may be associated with heart damage according to the modern concepts of the mechanisms of damage to the cardiovascular system in COVID-19 [23].

When comparing the groups of convalescents with the cardiovascular phenotype and other phenotypes, we revealed a difference in the lipid profile. HDL-C has an antioxidant and immunomodulatory function. It also binds and neutralizes pathogenic lipids. However, during the inflammatory process, HDL-C is modified, which is accompanied by oxidative processes and the accumulation of oxidized forms of lipids. As a result,

accumulated LDL-C and TG lead to endothelial dysfunction and the development of cardiovascular complications [24].

Several studies have demonstrated an increase in blood lipids, in particular TG and LDL-C, in the acute and post-COVID period, regardless of the COVID-19 severity [25, 26]. In our study, high levels of TC, non-HDL-C, and LDL-C were observed in convalescents with a cardiovascular phenotype and a decrease in HDL-C.

## CONCLUSION

Patients with PCC had changes in echocardiography more often, as well as cardiometabolic risk factors such as AO, AH, and impaired carbohydrate metabolism compared with convalescents without PCC. The cardiovascular phenotype of PCC is more associated with changes in the lipid profile, namely, an increase in total cholesterol, LDL-C, non-HDL-C, and a decrease in HDL-C.

### REFERENCES


1. Ferrario C.M., Trask A.J., Jessup J.A. Advances in biochemical and functional roles of angiotensin-converting enzyme 2 and angiotensin-(1-7) in regulation of cardiovascular function. *Am. J. Physiol. Heart Circ. Physiol* .2005;289(6):2281–2290. DOI: 10.1152/ajpheart.00618.2005.
2. Jia H.P., Look D.C., Hickey M., Shi L., Pewe L., Netland J. et al. Infection of human airway epithelia by SARS coronavirus is associated with ACE2 expression and localization. *Adv. Exp. Med. Biol.* 2006;581:479–484. DOI: 10.1007/978-0-387-33012-9_85.
3. Raman B., Bluemke D.A., Lüscher T.F., Neubauer S. Long COVID: post-acute sequelae of COVID-19 with a cardiovascular focus. *Eur. Heart J.* 2022;43(11):1157–1172. DOI: 10.1093/eurheartj/ehac031.
4. Soriano J.B., Murthy S., Marshall J.C., Relan P., Diaz J.V. A clinical case definition of post-COVID-19 condition by a Delphi consensus. *Lancet Infect. Dis.* 2022;22(4):e102–e107. DOI: 10.1016/S1473-3099(21)00703-9.
5. Dedov I.I., Mokrysheva N.G., Melnichenko G.A., Troshina E.A., Mazurina N.V., Ershova E.V. et al. Obesity. Clinical Guidelines. *Consilium Medicum.* 2021;23(4):311–325. (In Russ.). DOI: 10.26442/20751753.2021.4.200832.
6. Devereux R.B., Reichek N. Echocardiographic determination of left ventricular mass in man: anatomic validation of the method. *Circulation.* 1977;55(4):613–618. DOI: 10.1161/01.cir.55.4.613.
7. Du Bois D., Du Bois E.F. A formula to estimate the approximate surface area if height and weight be known. *Arch. Intern. Med.* 1916;17:863–871. DOI: 10.1001/archinte.1916.00080130010002.
8. Flakskampf F.A. A Course of Echocardiography. Moscow: Medpress-inform, 2016:328 (In Russ.).
9. Clinical Guidelines. Arterial Hypertension. Russian Society of Cardiology. 2020 (In Russ.).
10. Russian Society of Cardiology (RSC). Chronic Heart Failure. 2020 Clinical Guidelines. *Russian Journal of Cardiology.* 2020;25(11):4083. (In Russ.). DOI: 10.15829/1560-4071-2020-4083.
11. Atherosclerosis and Dyslipidemia. Diagnosis and Correction of Lipid Metabolism Disorders for the Prevention and Treatment of Atherosclerosis. *Russian Guidelines, 7th Revision.* 2020;1(38):7–42. (In Russ.). DOI: 10.34687/2219-8202.JAD.2020.01.0002.
12. Chen C., Zhou Y., Wang D.W. SARS-CoV-2: a potential novel etiology of fulminant myocarditis. *Herz.* 2020;45(3):230–232. DOI: 10.1007/s00059-020-04909-z.
13. Huang C., Wang Y., Li X., Ren L., Zhao J., Hu Y. et al. Clinical features of patients infected with 2019 novel coronavirus in Wuhan, China. *Lancet.* 2020;395(10223):497–506. DOI: 10.1016/S0140-6736(20)30183-5.
14. Guzik T.J., Mohiddin S.A., Dimarco A., Patel V., Savvatis K., Marelli-Berg F.M. et al. COVID-19 and the cardiovascular system: implications for risk assessment, diagnosis, and treatment options. *Cardiovasc. Res.* 2020;116(10):1666–1687. DOI: 10.1093/cvr/cvaa106.
15. Giustino G., Croft L.B., Stefanini G.G., Bragato R., Silbiger J.J., Vicenzi M. et al. Characterization of myocardial injury in patients with COVID-19. *J. Am. Coll. Cardiol.* 2020;76(18):2043–2055. DOI: 10.1016/j.jacc.2020.08.069.
16. Shang L., Wang L., Zhou F., Li J., Liu Y.,Yang S. Long-term effects of obesity on COVID-19 patients discharged from hospital. *Immun. Inflamm. Dis.* 2021;9(4):1678–1685. DOI: 10.1002/iid3.522.
17. Kim H.W., de Chantemèle E.J.B., Weintraub N.L. Perivascular adipocytes in vascular disease. *Arterioscler. Thromb. Vasc. Biol.* 2019;39(11):2220–2227. DOI: 10.1161/atvbaha.119.312304.
18. Zhang J., Wu J., Sun X., Xue H., Shao J., Cai W. et al. Association of hypertension with the severity and fatality of SARS-CoV-2 infection: a meta-analysis. *Epidemiol. Infect.* 2020;28:148:e106. DOI: 10.1017/S095026882000117X.
19. Bauer A.Z., Gore R., Sama S.R., Rosiello R., Garber L., Sundaresan D. et al. Hypertension, medications, and risk of severe COVID-19: a Massachusetts community-based observational study. *J. Clin. Hypertens (Greenwich).* 2021;23(1):21–27. DOI: 10.1111/jch.14101.
20. Dweck M.R., Bularga A., Hahn R.T., Bing R., Lee K.K., Chapman A.R. et al. Global evaluation of echocardiography in patients with COVID19. *Eur. Heart J. Cardiovasc. Imaging.* 2020;21(9):949–958. DOI: 10.1093/ehjci/jeaa178.
21. Yaroslavskaya I., Krinochkin D.V., Shirokov N.E., Krinochkina I.R., Gultyaeva E.P. et al. Echocardiographic Characteristics of COVID-19 Pneumonia Survivors Three Months after Hospital Discharge. *Russian Journal of Cardiology*. 2022;62(1):13–23. (In Russ.). DOI: 10.18087/cardio.2022.1.n1859.
22. Kanorsky S.G., Panchenko D.I., Bystrov A.O., Moisova D.L., Gorodin V.N., Ionov A.Yu. Echocardiographic Changes in Patients who Experienced COVID-19 after 6 and 12 Months of Hospital Discharge. *International Journal of Heart and Vascular Diseases.* 2023;11(37):17–24. (In Russ.).
23. Serviente C., Decker S.T., Layec G. From heart to muscle: pathophysiological mechanisms underlying long-term physical

sequelae from SARS-CoV-2 infection. *J. Appl. Physiol. (1985).* 2022;132(3):581–592. DOI: 10.1152/japplphysiol.00734.2021.
24. Sorokin A.V., Karathanasis S.K., Yang Z.H., Freeman L., Kotani K., Remaley A.T. COVID-19-Associated dyslipidemia: implications for mechanism of impaired resolution and novel therapeutic approaches. *FASEB J.* 2020;34:9843–9853. DOI: 10.1096/ fj.202001451.
25. Dennis A., Wamil M., Alberts J., Oben J., Cuthbertson D.J., Wootton D. et al. Multiorgan impairment in low-risk individuals with post-COVID-19 syndrome: A prospective, community-Based study. *BMJ Open.* 2021;11(3):e048391. DOI: 10.1136/bmjopen-2020-048391.
26. Washirasaksiri C., Sayabovorn N., Ariyakunaphan P., Kositamongkol C., Chaisathaphol T., Sitasuwan T. et al. Long-term multiple metabolic abnormalities among healthy and high-risk people following nonsevere COVID-19. *Sci. Rep.* 2023;13(1):14336. DOI: 10.1038/s41598-023-41523-5.

## Author Contribution

Zorina V.V. – data collection, analysis, and interpretation, and drafting of the manuscript. Garbuzova E.V., Afanaseva A.D. – conception and design and critical revision for important intellectual content. Palekhina Yu.Yu., Shchepina Yu.V. – ultrasound examination, data analysis and interpretation. Shramko V.S. – performing biochemical studies, data analysis and interpretation. Schachtschneider E.V., Logvinenko I.I. – project leader, final approval of the manuscript for publication.

## Author Information

**Zorina Valentina V.** – Junior Researcher, Laboratory of the Study of Monogenic Forms of Common Human Diseases, Institute of Cytology and Genetics, Siberian Branch of the Russian Academy of Sciences, Novosibirsk, walentina.zorina@bk.ru, https://orcid.org/0000-0002-7846-7933

**Garbuzova Evgenia V.** – Cand. Sci. (Med.), Researcher, Laboratory of Genetic and Environmental Determinants of the Human Life Cycle, Research Institute of Internal and Preventive Medicine, Branch of the Institute of Cytology and Genetics, Siberian Branch of the Russian Academy of Sciences, Novosibirsk, stryukova.j@mail.ru, https://orcid.org/0000-0001-5316-4664

**Afanaseva Alena D.** – Cand. Sci. (Med.), Head of the Laboratory of Genetic and Environmental Determinants of the Human Life Cycle, Research Institute of Internal and Preventive Medicine, Branch of the Institute of Cytology and Genetics, Siberian Branch of the Russian Academy of Sciences, Novosibirsk, alena.dmytryevna@yandex.ru, https://orcid.org/0000-0001-7875-1566

**Shchepina Yulia V.** – Researcher, Laboratory of Etiopathogenesis and the Clinic of Internal Diseases, Research Institute of Internal and Preventive Medicine, Branch of the Institute of Cytology and Genetics, Siberian Branch of the Russian Academy of Sciences, Novosibirsk, yulia@shchepin.ru, https://orcid.org/0000-0003-3465-7572

**Palekhina Yulia Yu.** – Junior Researcher, Laboratory of Etiopathogenesis and the Clinic of Internal Diseases, Research Institute of Internal and Preventive Medicine, Branch of the Institute of Cytology and Genetics, Siberian Branch of the Russian Academy of Sciences, Novosibirsk, ukolova@hotmail.com, https://orcid.org/0000-0002-9404-6987

**Shramko Victoria S.** – Cand. Sci. (Med.), Researcher, Laboratory of Clinical, Biochemical and Hormonal Studies of Internal Diseases, Research Institute of Internal and Preventive Medicine, Branch of the Institute of Cytology and Genetics, Siberian Branch of the Russian Academy of Sciences, Novosibirsk, nosova@211.ru, https://orcid.org/0000-0002-0436-2549

**Shakhtshneider Elena V.** – Cand. Sci. (Med.), Leading Researcher, Laboratory of Molecular and Genetic Research of Internal Diseases; Head of the Laboratory of the Study of Monogenic Forms of Common Human Diseases, Research Institute of Internal and Preventive Medicine, Branch of the Institute of Cytology and Genetics, Siberian Branch of the Russian Academy of Sciences, Novosibirsk, 2117409@mail.ru, https://orcid.org/0000-0001-6108-1025

**Logvinenko Irina I.** – Dr. Sci. (Med.), Professor, Leading Researcher, Laboratory of Preventive Medicine; Deputy Head for Medical Work, Research Institute of Internal and Preventive Medicine, Branch of the Institute of Cytology and Genetics, Siberian Branch of the Russian Academy of Sciences, Novosibirsk, 111157@mail.ru, https://orcid.org/0000-0003-1348-0253

(✉) **Zorina Valentina V.,** walentina.zorina@bk.ru

Received on September 21, 2024;
approved after peer review on March 6, 2025;
accepted on March 20, 2025

УДК 618.33-07
https://doi.org/10.20538/1682-0363-2025-3-34-41

# Evaluation of the role of biochemical and biophysical parameters of combined prenatal screening of the first trimester in the development of fetal growth restriction

**Izhoykina E.V.[1, 3], Trifonova E.A.[1, 2], Gavrilenko M.M.[2], Kutsenko I.G.[1], Stepanov V.A.[2]**

*[1] Siberian State Medical University of the Ministry of Health of the Russian Federation (SibSMU)*
*2 Moskovsky trakt, 634050 Tomsk, Russian Federation*

*[2] Research Institute of Medical Genetics, Tomsk National Research Medical Center (NRMC), Russian Academy of Sciences*
*10 Naberezhnaya reki Ushaiki St., 634050 Tomsk, Russian Federation*

*[3] I.D. Evtushenko Regional Perinatal Center*
*96/1 Ivan Chernykh St., 634049 Tomsk, Russian Federation*

## ABSTRACT

**Aim.** To evaluate the role of biochemical and biophysical parameters in the combined first-trimester prenatal screening for the development of clinical forms of fetal growth restriction.

**Materials and methods.** Group I (main) included 73 patients, whose pregnancies were complicated by the fetal growth restriction. The main group was divided into two subgroups: Ia with 30 patients whose pregnancies were complicated by fetal growth restriction (FGR) and Ib with 43 patients whose pregnancies were complicated by small for gestational age fetuses (SGA). Group II (control) included 118 patients whose pregnancies resulted in the birth of a live, full-term infant with normal height and weight. All patients underwent combined first-trimester prenatal screening with calculation of biochemical (pregnancy-associated plasma protein A (PAPP-A), free β-subunit of human chorionic gonadotropin (β-hCG) and biophysical (mean arterial pressure (MAP), uterine artery pulsatility index (PI) parameters, the values of which were subsequently analyzed.

**Results.** The level of PAPP-A was statistically significantly lower in the FGR group (0.793 MoM) compared to the control group (1.048 MoM), $p = 0.005$. The level of PAPP-A in the blood below 0.793 MoM increases the risk of fetal growth restriction by 3.244 times (odds ratio (OR) = 3.244; 95% confidence interval (95% CI) 1.394–7.554, $p = 0.005$). An increase in the pulsation index was found in Doppler ultrasound of the uterine arteries in patients with FGR compared to the SGA group (OR = 2.254; 95% CI 0.990–5.129, $p = 0.017$). Statistically significant differences were not found in the studied parameters of the combined first-trimester prenatal screening in relation to SGA.

**Conclusion.** Differences in the biochemical and biophysical parameters of combined prenatal screening for the clinical forms of FGR were identified. Further research is needed to identify new prognostic markers of FGR, which will help reduce perinatal losses. Additional research is required to expand the sample size of the Russian population to clarify the role of the prenatal screening components.

**Keywords:** fetal growth restriction, small for gestational age fetus

**Conflict of interest.** The authors declare the absence of obvious or potential conflicts of interest related to the publication of this article.

**Source of financing.** The authors declare no funding.

**Conformity with the principles of ethics.** All patients signed an informed consent to participate in the study. The study was approved by the local Ethics Committee at Siberian State Medical University (Minutes No. 9330 dated January 30, 2023).

✉ *Izhoykina Ekaterina V.,* katushkabig@mail.ru

**For citation:** Izhoykina E.V., Trifonova E.A., Gavrilenko M.M., Kutsenko I.G., Stepanov V.A. Evaluation of the role of biochemical and biophysical parameters of combined prenatal screening of the first trimester in the of insufficient fetal growth development. *Bulletin of Siberian Medicine.* 2025;24(3):34–41. https://doi.org/10.20538/1682-0363-2025-3-34-41.

# Оценка роли биохимических и биофизических параметров комбинированного пренатального скрининга первого триместра в развитии недостаточного роста плода

**Ижойкина Е.В.[1, 3], Трифонова Е.А.[1, 2], Гавриленко М.М.[2], Куценко И.Г.[1], Степанов В.А.[2]**

*[1] Сибирский государственный медицинский университет (СибГМУ)*
*Россия, 634050, г. Томск, Московский тракт, 2*

*[2] Научно-исследовательский институт (НИИ) медицинской генетики, Томский национальный исследовательский медицинский центр (НИМЦ) Российской академии наук*
*Россия, 634050, г. Томск, Набережная реки Ушайки, 10*

*[3] Областной перинатальный центр (ОПЦ) им. И.Д. Евтушенко*
*Россия, 634063, г. Томск, ул. Ивана Черных, 96/1*

## РЕЗЮМЕ

**Цель:** оценить роль биохимических и биофизических параметров комбинированного пренатального скрининга первого триместра в развитии клинических форм недостаточного роста плода.

**Материалы и методы.** Группа I (основная) – 73 пациентки, чьи беременности были осложнены развитием недостаточного роста плода. Основная группа была разделена на две подгруппы: Ia – 30 пациенток, чьи беременности были осложнены развитием задержки роста плода (ЗРП), Ib – 43 пациентки, чьи беременности были осложнены развитием маловесного для гестационного возраста плода (МГВ). Группа II (контрольная) – 118 пациенток, чьи беременности закончились рождением живого доношенного ребенка с нормальными росто-весовыми показателями. Всем пациенткам проведен комбинированный пренатальный скрининг первого триместра с расчетом значений биохимических (ассоциированный с беременностью плазменный белок А – PAPP-A, свободная β-субъединица хорионического гонадотропина человека – β-hCG) и биофизических (среднее значение артериального давления – САД, пульсационный индекс в маточных артериях – PI MA) параметров, значения которых в дальнейшем были подвергнуты анализу.

**Результаты.** Уровень PAPP-A был статистически значимо ниже в группе ЗРП (0,793 MoM) по сравнению с контрольной группой (1,048 MoM), $p = 0{,}005$. Содержание PAPP-A в крови менее 0,793 MoM увеличивает риск развития задержки роста плода в 3,244 раза (отношение шансов (OR) 3,244; 95%-й доверительный интервал (95% ДИ) 1,394–7,554, $p = 0{,}005$). Выявлено повышение пульсационного индекса при допплерометрии маточных артерий у пациенток с ЗРП по сравнению с группой МГВ (OR = 2,254; 95% ДИ 0,990–5,129, $p = 0{,}017$). Статистически значимые различия изученных параметров комбинированного пренатального скрининга первого триместра с развитием МГВ не были выявлены.

**Заключение.** Выявлены различия по биохимическим и биофизическим параметрам комбинированного пренатального скрининга для клинических форм недостаточного роста плода. Необходим дальнейший поиск новых прогностических маркеров недостаточного роста плода, что приведет к снижению перинатальных потерь. Требуется дополнительное проведение исследований для увеличения объема выборки российской популяции с целью уточнения роли составляющих компонентов пренатального скрининга.

**Ключевые слова:** задержка роста плода, маловесный для гестационного возраста плод

**Конфликт интересов.** Авторы декларируют отсутствие явных и потенциальных конфликтов интересов, связанных с публикацией настоящей статьи.

**Источник финансирования.** Авторы заявляют об отсутствии финансирования при проведении исследования.

**Соответствие принципам этики**. Все пациенты подписали информированное согласие на участие в исследовании. Исследование одобрено этическим комитетом ФГБОУ ВО СибГМУ (протокол № 9330 от 30.01.2023).

**Для цитирования:** Ижойкина Е.В., Трифонова Е.А., Гавриленко М.М., Куценко И.Г., Степанов В.А. Оценка роли биохимических и биофизических параметров комбинированного пренатального скрининга первого триместра в развитии недостаточного роста плода. *Бюллетень сибирской медицины.* 2025;24(3):34–41. https://doi.org/10.20538/1682-0363-2025-3-34-41.

## INTRODUCTION

Reducing perinatal losses is one of the priority areas in obstetrics. Fetal growth restriction (FGR) is a pregnancy complication in which the fetus does not achieve its optimal physical development for the gestational age and is a probable risk factor for complications such as neonatal respiratory distress syndrome, hypothermia, hypoglycemia, pulmonary hemorrhage, intraventricular hemorrhage, necrotizing enterocolitis, and sepsis [1–3]. The development of screening programs for early detection of pregnant women with a high risk of FGR remains relevant. The obstetric community continues to actively search FGR predictors to create mathematical models and algorithms that would have high prognostic significance in stratifying the pathological gestation risk.

In 2020, with the support of the Fetal Medicine Foundation (FMF, UK), a large-scale study was conducted involving 60,875 pregnant women to assess the predicting effectiveness of a birth of a child weighing less than the 10th percentile based on biochemical and biophysical parameters of prenatal screening. According to the results of this study, the best biophysical predictor was the uterine artery pulsatility index (PI), and the best biochemical marker was the placental growth factor (PIGF) [4]. The evaluation of the parameters was conducted in many countries around the world with their subsequent implementation in wide clinical practice [5–8].

In the Russian Federation, the calculation of biochemical (free β-subunit of human chorionic gonadotropin (β-hCG) and pregnancy-associated plasma protein A (PAPP-A)) and biophysical (uterine artery pulsatility index (PI) and mean arterial pressure (MAP)) marker values is performed as part of prenatal screening for fetal developmental disorders in the first trimester. In 2017, a group of Russian researchers assessed the use of first-trimester biochemical screening parameters and the uterine artery PT to form a risk group for FGR. It was shown that the probability of developing FGR is 68% with an increase in the PI value > 2.5 MoM in combination with a decrease in PAPP-A < 0.7 MoM. However, in our country at the time of the study, a different clinical classification of FGR was in effect, based on the fetometry parameter lag from the norm by two or more weeks, which in turn determined the inclusion criteria in this work [9].

In 2019, T.A. Yarygina et al. published the findings of a study devoted to assessing the effectiveness of biophysical and biochemical parameters of prenatal screening in predicting the birth of a SGA child. The analysis conducted in this work established an acceptable quality of the model for predicting the birth of a preterm low birth weight baby only for the PAPP-A biomarker (area under the curve (AUC) 0.74). However, the inclusion criterion in the main group was the value of the estimated fetal weight less than the 10th percentile [10]. Given the small number of studies assessing the effectiveness of biochemical and biophysical parameters of prenatal screening in the development of FGR, further research in this area is required.

The aim of the study was to evaluate the role of biochemical and biophysical parameters of combined first-trimester prenatal screening in the development of clinical forms of FGR.

## MATERIALS AND METHODS

The study group consisted of 191 women who had a singleton spontaneously conceived pregnancy that resulted in a live birth at 24 weeks or more of gestation between 2021 and 2023.

Inclusion criteria for the main group were as follows: singleton pregnancy complicated by the development of FGR. Inclusion criteria for the control group were singleton normal pregnancy resulting in the birth of a healthy newborn with a body weight corresponding to the gestational age. Exclusion criteria for both groups were the presence of severe extragenital pathology in the woman; pregnancy

resulting from assisted reproductive technologies; multiple pregnancy; hereditary diseases in the mother; acute phase or exacerbation of chronic infectious diseases; chromosomal abnormalities, and congenital malformations of the fetus.

All patients underwent combined first-trimester prenatal screening to diagnose fetal developmental disorders at the Medical Genetic Center of the Research Institute of Medical Genetics of Tomsk National Research Medical Center and the I.D. Evtushenko Regional Perinatal Center in Tomsk at a gestational age of 11–13.6 weeks. Prenatal screening included ultrasound examination (US) of the fetus and biochemical examination of the mother's blood with an assessment of the concentration of free β-subunit of human chorionic gonadotropin (β-hCG) and pregnancy-associated plasma protein A (PAPP-A) [10]. Screening was supplemented by determination of the uterine artery pulsatility index (PI) and double measurement of blood pressure (BP) in both arms, followed by the mean BP (MBP) value calculation. The obtained values of PI, MBP, serum protein concentrations considering the crown-rump length of the fetus and the body weight of the pregnant woman were converted into MoM. The standard reference values of 0.5–2.0 MoM were considered. All women signed an informed consent to participate in the study, which was approved by the Ethics Committee at Siberian State Medical University.

Statistical analysis was performed in several stages. The quantitative data were tested for compliance with the normal distribution law using the Kolmogorov–Smirnov test (for a sample size of $n > 50$) and the Shapiro–Wilk test (for $n < 50$). In our study, the distribution was not normal, therefore, quantitative data are presented as the median and the interquartile range $Me$ ($Q_1$; $Q_3$). To compare differences between groups, nonparametric statistical methods were used including the Kruskal–Wallis and Mann–Whitney tests. Differences were considered statistically significant at $p < 0.05$. To adjust for multiple comparisons, the Bonferroni correction was used ($p_{adjusted}$, the adjusted $p$-value, was 0.017). The analysis of four-field contingency tables was performed using the Pearson's chi-squared test, since the value of the expected phenomenon was more than 10. In order to assess the influence of biochemical and biophysical parameters on the development of FGR, the odds ratio (OR) was calculated with a 95% confidence interval (95% CI). Statistical analysis was performed using the statistical packages Excel and SPSS Statistics 26.

## RESULTS

All study participants were divided into two groups. The main (I) included includes patients whose pregnancy was complicated by the development FGR. According to the clinical guidelines in force in the Russian Federation, the group was divided into two subgroups, depending on the clinical form of FGR. Group Ia included patients with antenatally diagnosed FGR ($n = 30$). FGR was defined as an ultrasound value of the estimated fetal weight (EFW) less than the 3rd percentile or an EW less than the 10th percentile in combination with abnormal blood flow according to ultrasound Doppler data. Group Ib includes patients whose pregnancy was complicated by the formation of a small-for-gestational-age (SGA) fetus ($n = 43$). SGA was defined when ultrasound values of the EFW were in the range from the 3rd to the 9th percentile in combination with normal blood flow parameters according to Doppler data.

The control (II) group consisted of patients whose pregnancy ended with the birth of a healthy full-term newborn with normal weight and height ($n = 118$). The postnatal assessment of weight and height in newborns was carried out according to the INTERGROWTH-21st centile tables to confirm the antenatal diagnosis of FGR and SGA fetus, as well as to establish normal growth and weight of newborns in the control group. Data on the course and outcomes of pregnancy were obtained from the primary medical documentation of I.D. Evtushenko Regional Perinatal Center, Tomsk.

All patients participating in the study underwent combined first-trimester prenatal screening with calculation of biochemical and biophysical parameter values, the results of which are presented in Table 1.

$p_{Ia\text{-}II}$ is the level of statistical significance of differences between FGR and control groups; $p_{Ib\text{-}II}$ is the level of statistical significance of differences between SGA and control groups; $p_{Ia\text{-}Ib}$ is level of statistical significance of differences between FGR and SGA groups; $p_{adj} = 0.017$.

It should also be noted that the median values of all presented parameters did not exceed the reference limits. The Kruskal–Wallis test revealed statistically significant differences between the groups in such parameters as PAPP-A and PI levels ($H = 9.113$, $p = 0.010$; $H = 6.594$, $p = 0.37$, respectively). There were no significant differences between the groups in the level of MAP and β-hCG content ($H = 1.695$, $p = 0.428$; $H = 0.905$, $p = 0.636$, respectively).

Table 1

**Results of Biochemical and Biophysical Parameters of Prenatal Screening in the Study Groups, MoM, *Me* ($Q_1$; $Q_3$)**

| Biochemical marker | Main (Ia) group, *n* = 30 | Main (Ib) group, *n* = 43 | Control (II) group, *n* = 118 | *p* |
|---|---|---|---|---|
| PAPP-A | 0.793 (0.548; 0.997) | 0.958 (0.524; 1.346) | 1.048 (0.656; 1.346) | $p_{Ia\text{-}II}$ = 0.005<br>$p_{Ib\text{-}II}$ = 0.062<br>$p_{Ia\text{-}Ib}$ = 0.583 |
| β-hCG | 1.305 (0.605; 1.476) | 1.088 (0.538; 1.301) | 1.124 (0.603; 1.391) | $p_{Ia\text{-}II}$ = 0.644<br>$p_{Ib\text{-}II}$ = 0.437<br>$p_{Ia\text{-}Ib}$ = 0.433 |
| PI | 1.082 (0.801; 1.234 | 0.886 (0.691; 1.061) | 0.956 (0.818; 1.126) | $p_{Ia\text{-}II}$ = 0.06<br>$p_{Ib\text{-}II}$ = 0.155<br>$p_{Ia\text{-}Ib}$ = 0.017 |
| MAP | 1.075 (0.993; 1.099) | 1.078 (0.976; 1.147) | 1.042 (0.952; 1.133) | $p_{Ia\text{-}II}$ = 0.698<br>$p_{Ib\text{-}II}$ = 0.185<br>$p_{Ia\text{-}Ib}$ = 0.638 |

Note. PAPP-A is pregnancy associated plasma protein A; β-hCG is free β-subunit of human chorionic gonadotropin; PI is uterine artery pulsatility index; MAP is mean arterial pressure.

If statistically significant differences between groups were detected using the Kruskal–Wallis test, post-hoc comparisons were then performed using the Mann–Whitney test.

In both main groups, the median for PAPP-A was lower compared with the control group. However, statistically significant differences were obtained only between the main Ia (FGR) group and the control group ($p$ = 0.005). Subsequent calculation of the odds ratio showed that the values of PAPP-A ≤0.793 MoM obtained during prenatal screening increased the risk of developing FGR by 3.244 times (OR = 3.244; 95% CI 1.394–7.554, $p$ = 0.005) and increased the risk of developing a SGA fetus by 2.049 times (OR = 2.049; 95% CI 1.010–4.157, $p$ = 0.045). The median for PI was higher in group Ia (FGR) compared with groups Ib (SGA) and the control. However, statistically significant differences were obtained only between groups Ia (FGR) and Ib (SGA) ($p$ = 0.017). Subsequent calculation of the odds ratio showed that the values of PI MA ≥1.082 MoM obtained during prenatal screening increased the risk of developing FGR by 2.254 times (OR = 2.254; 95% CI 0.990–5.129, $p$ = 0.017). For the remaining indicators analyzed in this work, no statistically significant differences were found using the Mann–Whitney test.

## DISCUSSION

Initially, maternal serum markers were studied in the context of fetal chromosomal abnormalities screening. However, research on its role in predicting "major obstetric syndromes" is currently gaining traction [11–13]. Of the parameters making up the prenatal screening, statistically significant differences between groups were found only for PAPP-A, which is a metalloproteinase in the insulin-like growth factor (IGF) system [14, 15]. It has been shown that PAPP-A increases IGF bioavailability by adjustable splitting of IGF-binding protein 4 (IGFBP4). This process promotes activation of cell proliferation, migration, and differentiation, thereby determining normal fetal growth and development. During pregnancy, PAPP-A synthesis occurs mainly in the syncytiotrophoblast [15].

The most recognized causes of FGR development are inadequate trophoblast invasion into the uterine wall, explaining low PAPP-A levels, which, in turn reduce the IGF bioavailability, which, as noted above, is an important determinant of fetal growth [15–17]. In our study, the median PAPP-A in the FGR group was 0.793 MoM, which is significantly lower compared to the control group.

It is known that abnormal placentation is the main cause of FGR. In this regard, there is a justified interest in studying the level of β-hCG synthesized by syncytiotrophoblast in the blood, which may indicate placental dysfunction and thereby predict the development of complicated pregnancy [14, 15]. Despite a large number of studies devoted to the study of β-hCG levels in FGR, there is still no consensus on this issue. Some studies have noted a decrease in this biomarker level at 11–14 weeks in pregnancies that were subsequently complicated by FGR. For example, P. Sirikunalai et al. showed that the risk of the pathology under consideration increased

significantly at a β-hCG level <0.5 MoM [18]. On the contrary, other authors note an increased level of the biomarker in FGR [11, 19]. These results confirm the necessity of a more in-depth study of the β-hCG level in various forms of FGR. The β-hCG values in our study were slightly higher in the FGR group compared to the control, but the differences were not statistically significant.

Ultrasound diagnostics is the mainstay in assessing the fetus condition in modern obstetrics [1, 5, 6]. The use of ultrasound equipment in antenatal diagnostics, whose operation is based on the Doppler effect, allows us to study the state of the uteroplacental, fetoplacental and fetal blood flow. Since FGR is characterized by a disruption of normal trophoblastic invasion and a lack of uterine spiral arteries remodeling, leading to highly resistant uteroplacental circulation, studying blood flow in the uterine arteries at the end of the first trimester of pregnancy is one of the methods for predicting this pathology [20]. Most researchers agree that PI in the first trimester above the 95$^{th}$ percentile indicates a high risk of developing FGR, rather than a SGA fetus, which is characterized by the absence of increased resistance in the uterine arteries [21–23].

The results of our study showed that the PI value in the FGR group, although not exceeding the reference values, is significantly higher compared to the SGA group, which confirms the idea of the formation of a highly resistant type of blood flow. The absence of significant differences with the control group may be due to the small sample size in our work.

With the widespread implementation of combined first-trimester screening, a significant amount of data has accumulated on the MAP role in predicting the preeclampsia development, which formed the basis for studying the possibility of its use in FGR screening [12, 24]. It should be noted that to date, the role of MAP in terms of isolated FGR prediction has been poorly studied. The median MAP values obtained in our study do not allow us to identify risk groups for the FGR and SGA development in the first trimester.

## CONCLUSION

Fetal gowth restriction as a significant risk factor for perinatal losses still requires a search for prognostic criteria, since intrauterine development is determined by a complex of factors. Researchers are trying to find new prognostic parameters for the early prediction of FGR, hoping that this will lead to a decrease in perinatal losses. However, at present in the Russian Federation, there is a limited number of studies focusing on the use of biochemical and biophysical parameters of prenatal screening to assess the birth of children with insufficient body weight.

Our study showed that the values of biochemical (PAPP-A and β-hCG) and biophysical (MAP and PI) parameters of prenatal screening in the main and control groups did not exceed the reference limits. No significant differences in the values of PAPP-A, β-hCG, MAP, and PI were found between the SGA and control groups. It was shown that the PAPP-A level was significantly lower in the FGR group (0.793 MoM) compared to the control group (1.048 MoM) ($p$ = 0.005), which is consistent with the findings of extensive studies [4, 9, 16]. The median PI was higher in the FGR group (1.082 MoM) and there were statistically significant differences with the SGA group ($p$ = 0.018). The values of β-hCG and MAP between the FGR and control groups had no significant differences.

Thus, further research is required to increase the sample size of the Russian population in order to clarify the data we obtained. It is necessary to study the role of soluble fms-like tyrosine kinase-1 (sFlt-1) and PIGF in the FGR development, the prognostic effectiveness of which has been shown in foreign literature [21, 25]. It seems relevant to continue research to clarify the role of combined prenatal screening parameters in FGR development.

## REFERENCES


1. Russian Society of Obstetricians and Gynecologists. Clinical Guidelines: Insufficient Fetal Growth Requiring Medical Care for the Mother (Fetal Growth Restriction). 2020:71. (In Russ.).
2. Vayssier C., Sentilhes, L., Ego, A., Bernard C., Cambourieu, D., Flamant C. et al. Fetal growth restriction and intra-uterine growth restriction: guidelines for clinical practice from the French College of Gynaecologists and Obstetricians. *European Journal of Obstetrict & Gynecology and Reproductive Biology*. 2015;193:10–18.
3. Sharma D., Shastri S., Sharma P. Intrauterine growth restriction: Antenatal and postnatal aspects. *Clinical Medicine Insights Pediatrics.* 2016;10:67–83. DOI: 10.4137/CMPed.S40070.
4. Papastefanou I., Wright D., Syngelaki A., Souretis K., Chrysanthopoulou E., Nicolaides K.H. Competing-risks model for prediction of small-for-gestational-age neonate from biophysical and biochemical markers at 11–13 weeks' gestation. *Ultrasound in Obstetrics and Gynecology.* 2021;57(1):52–61. DOI: 10.1002/uog.23523.
5. Mosimann B., Pfiffner C., Amylidi-Mohr S., Risch L., Surbek D., Raio L. First trimester combined screening for preeclampsia and small for gestational age - a single centre experience and validation of the FMF screening algorithm. *Swiss Medical Weekly.* 2017;147:w14498. DOI: 10.4414/smw.2017.14498.

6. Sotiriadis A., Figueras F., Eleftheriades M., Papaioannou G.K., Chorozoglou G., Dinas K. et al. First-trimester and combined first- and second-trimester prediction of small-for-gestational age and late fetal growth restriction. *Ultrasound in Obstetrics and Gynecology.* 2019;53(1):55–61. DOI: 10.1002/uog.19055.
7. Zhang J., Han L., Li W., Chen Q., Lei J., Long M. et al. Early prediction of preeclampsia and small-for-gestational-age via multi-marker model in Chinese pregnancies: a prospective screening study. *BMC Pregnancy and Childbirth*. 2019;19:304.
8. Lui R., Rezende K., Guimaraes M., Dourado A.L., Matta F., Amim J. et al. Evaluation of fetal medicine foundation algorithm in predicting small-for-gestational-age neonates. *Journal of Maternal-Fetal and Neonatal Medicine.* 2021;34(6):876–882. DOI: 10.1080/14767058.2019.1622664.
9. Zamaleeva R.S., Cherepanova N.A., Frizin D.V., Frizina A.V. Using Results of First-Trimester Biochemical Screening and Utreine Artery Pulsatility Index for Inclusion in Risk Groups for Fetal Growth Restriction. *Medical Council*. 2017;2:52–56. (In Russ.).
10. Yarygina T.A., Bataeva R.S. Performance of Screening for Small-for-Gestational Age Newborn at First Trimester Using the Algorithm Proposed by the Fetal Medicine Foundation. *Ultrasound & Functional Diagnostics*. 2019;2:16–32. (In Russ.).
11. Boonpiam R., Wanapirak C., Sirichotiyakul S., Sekararithi R., Traisrisilp K., Tongsong T. Quad test for fetal aneuploidy screening as a predictor of small-for-gestational age fetuses: a population-based study. *BMC Pregnancy Childbirth.* 2020;20(1):621. DOI: 10.1186/s12884-020-03298-9.
12. Lemeshevskaya T.V., Pribushenya O.V. Prediction of Preeclampsia during Extended Combined Prenatal Screening of the First Trimester of Pregnancy. *Obstetrics and Gynecology*. 2017;12:52–59. (In Russ.). DOI: 10.18565/aig.2017.12.52-59.
13. Samchuk P.M., Azoeva E.L., Ishchenko A.I., Rozalieva Yu.Yu. Prenatal Screening as a Predictor of Gestational Complications. *Problems of Gynecology, Obstetrics and Perinatology*. 2020;19(6):5–11. (In Russ.). DOI: 10.20953/1726-1678-2020-6-5-11.
14. Izhoykina E.V., Trifonova E.A., Kutsenko I.G., Stepanov I.A., Gavrilenko M.M., Stepanov V.A. Possibility of Predicting Fetal Growth Restriction Based on Determination of Biomarkers in Blood Plasma. *Obstetrics and Gynecology*. 2023;2:18–24. (In Russ.). DOI: 10.18565/aig.2022.269.
15. Costa M.A. The endocrine function of human placenta: an overview. Reproductive Biomedicine Online. 2016;32(1):14–43. DOI: 10.1016/j.rbmo.2015.10.005.
16. Springer S., Worda K., Franz M., Karner E., Krampl-Bettelheim E., Worda C. Fetal growth restriction is associated with pregnancy associated plasma protein a and uterine artery doppler in first trimester. *Journal of Clinical Medicine*. 2023;12(7):2502. DOI: 10.3390/jcm12072502.
17. Conover C.A., Bale L.K., Overgaard M.T., Johnstone E.W., Laursen U.H., Füchtbauer E.M. et al. Metalloproteinase pregnancy-associated plasma protein A is a critical growth regulatory factor during fetal development. *Development.* 2004;131:1187–1194.
18. Sirikunalai P., Wanapirak C., Sirichotiyakul S., Tongprasert F., Srisupundit K., Luewan S. et al. Associations between maternal serum free beta human chorionic gonadotropin (β-hCG) levels and adverse pregnancy outcomes. *Journal of Obstetrics and Gynaecology.* 2016;36(2):178–182. DOI: 10.3109/01443615.2015.1036400.
19. Kiyokoba R., Uchiumi T., Yagi M., Toshima T., Tsukahara S., Fujita Y. et al. Mitochondrial dysfunction-induced high hCG associated with development of fetal growth restriction and pre-eclampsia with fetal growth restriction. *Scientific Reports*. 2022;12(1):4056. DOI: 10.1038/s41598-022-07893-y.
20. Prefumo F., Sebire N.J., Thilaganathan B. Decreased endovascular trophoblast invasion in first trimester pregnancies with high-resistance uterine artery Doppler indices. *Human Reproduction.* 2004;19(1):206–209. DOI: 10.1093/humrep/deh037.
21. Fabjan-Vodusek V., Kumer K., Osredkar J., Verdenik I., Gersak K., Premru-Srsen T. Correlation between uterine artery Doppler and the sFlt-1/PlGF ratio in different phenotypes of placental dysfunction. *Hypertens Pregnancy.* 2019;38(1):32–40.
22. Melchiorre K., Leslie K., Prefumo F., Bhide A., Thilaganathan B. First-trimester uterine artery Doppler indices in the prediction of small-for-gestational age pregnancy and intrauterine growth restriction. *Ultrasound in Obstetrics and Gynecology*. 2009;33(5):524–529. DOI: 10.1002/uog.6368.
23. He B., Hu C., Zhou Y. First-trimester screening for fetal growth restriction using Doppler color flow analysis of the uterine. *Journal of Maternal-Fetal and Neonatal Medicine*. 2021;34(23):3857–3861. DOI: 10.1080/14767058.2019.1701646.
24. Teng H., Wang Y., Han B., Liu J., Cao Y., Wang J. et al. Gestational systolic blood pressure trajectories and risk of adverse maternal and perinatal outcomes in Chinese women. *BMC Pregnancy and Childbirth 21*. 2021;155. DOI: 10.1186/s12884-021-03599-7
25. Gaccioli F., Sovio U., Cook E., Hund M., Charnock-Jones D.S., Smith G.C.S. Screening for fetal growth restriction using ultrasound and the sFlt-1/PlGF ratio in nulliparous women: a prospective cohort study. *Lancet Child Adolesc. Health.* 2018;2(8):569–581.

## Author Contribution

Izhoykina E.V., Gavrilenko M.M. – data collection and processing, drafting of the manuscript. Stepanov I.A. – database formation. Trifonova E.A., Kutsenko I.G., Stepanov V.A. – conception and design.

## Author Information

**Izhoykina Ekaterina V.** – Assistant, Obstetrics and Gynecology Division, Siberian State Medical University, Tomsk, katushkabig@mail.ru, https://orcid.org/0009-0007-9273-6371

**Trifonova Ekaterina A.** – Cand. Sci. (Med.), Senior Researcher, Research Institute of Medical Genetics, Tomsk National Research Medical Center (NRMC), Tomsk, ekaterina.trifonova@medgenetics.ru, https://orcid.org/0000-0003-1311-7403

**Gavrilenko Maria M.** – Junior Researcher, Research Institute of Medical Genetics, Tomsk National Research Medical Center (NRMC), Tomsk, maria.gavrilenko@medgenetics.ru, https://orcid.org/0000-0002-9526-8581

**Kutsenko Irina G.** – Dr. Sci. (Med.), Professor, Head of the Obstetrics and Gynecology Division, Siberian State Medical University, Tomsk, kutsenko.ig@ssmu.ru, https://orcid.org/ 0000-0002-8495-8210

**Stepanov Vadim A.** – Academician of the Russian Academy of Sciences, Dr. Sci. (Biology.), Professor, Head of Tomsk National Research Medical Center (NRMC), Tomsk, vadim.stepanov@medgenetics.ru, https://orcid.org/0000-0002-5166-331X

(✉) **Izhoykina Ekaterina V.,** katushkabig@mail.ru

Received on January 19, 2025;
approved after peer review on February 14, 2025;
accepted on February 27, 2025

УДК 616.345-006.63-033.1:576.311.347]-092.6
https://doi.org/10.20538/1682-0363-2025-3-42-51

# Ultrastructural aspects of mitochondrial translocation in colorectal cancer as a possible pathway of tumorigenesis

**Kit O.I.[1], Shikhlyarova A.I.[1], Frantsiants E.M.[1], Ilchenko S.A.[1], Neskubina I.V.[1], Kirichenko E.Yu.[2], Logvinov A.K.[3], Snezhko A.V.[1], Averkin M.A.[1], Gabrichidze P.N.[1]**

[1] *National Medical Research Centre (NRMC) for Oncology*
*63 14 liniya St., 344037 Rostov-on-Don, Russian Federation*

[2] *Don State Technical University (DSTU)*
*1 Gagarin Sq., 344000 Rostov-on-Don, Russian Federation*

[3] *Southern Federal University (SFU)*
*194/1 Stachki Ave., 344006 Rostov-on-Don, Russian Federation*

## ABSTRACT

**Aim.** To study the ultrastructural features of rectal cancer cells and to detect signs of mitochondrial translocation from the tumor to the resection line area with an assessment of the possibility of the formation of new malignant cells.

**Materials and methods.** The present study encompassed the data obtained from 44 patients with an average age of 66 (58–73) years, who underwent surgical intervention for rectal cancer T2–3N0M0 with differentiation grade G2. A portion of the tumor specimen and intestinal tissue along the resection line were preserved in a formaldehyde-glutaraldehyde fixative solution. Standard methods of section preparation were employed. Sections were subsequently examined using a Jeol JEM-1011 electron microscope (JEOL Inc., Japan).

**Results.** The ultrastructure of rectal adenocarcinoma was characterized by a high density of arrangement and varying sizes and shapes of tumor cells with a large nucleus and deep invaginations of the nuclear membrane, as well as an accumulation of multiple mitochondria at one of the cell poles. The process of pinching off a cytoplasmic fragment, which was found to be densely packed with mitochondria, was observed. This phenomenon was subsequently identified as a mitochondriome. Following this observation, the mitochondria were found to have translocated into healthy intestinal tissues along the resection line. Electron diffraction data revealed the active movement of mitochondria in the form of small spheroids and mitovesicles along the boundaries of the multilayer structure of the rectal submucosa, and subsequent fusion into large organelles capable of implementing nuclear synthesis from transported mitochondrial and nuclear DNA. We observed the presence of individual nuclear structures in conjunction with groups of mitochondria, followed by the self-assembly of abnormal cells.

**Conclusion.** The ultrastructural analysis of rectal adenocarcinoma indicates the need for mitochondrial translocation to free up intracellular space and prevent the metabolic threat of reactive oxygen species (ROS) accumulation in tumor cells. It also points to the key role of mitochondria in initiating tumor energy and information transfer as leaders of these processes. This observation suggests the possibility of early recurrence and metastasis in rectal cancer cases.

**Keywords:** mitochondria, rectal adenocarcinoma, ultrastructural analysis

**Conflict of interest.** The authors declare the absence of obvious or potential conflicts of interest related to the publication of this article.

**Source of financing.** The authors declare no funding for the study.

**Conformity with the principles of ethics.** All patients signed an informed consent to the collection and transfer of biological material for scientific research, state assignments for socially and socially useful purposes. The study was approved by the Ethics Committee of the Federal State Budgetary Institution NMRC for Oncology of the Ministry of Health of the Russian Federation (Minutes No. 1 dated January 30, 2023).

✉ *Neskubina Irina V.,* neskubina.irina@mail.ru

**For citation:** Kit O.I., Shikhlyarova A.I., Frantsiants E.M., Ilchenko S.A., Neskubina I.V., Kirichenko E. Yu., Logvinov A.K., Snezhko A.V., Averkin M.A., Gabrichidze P.N. Ultrastructural aspects of mitochondrial translocation in colorectal cancer as a possible pathway of tumorigenesis. *Bulletin of Siberian Medicine.* 2025;24(3):42–51. https://doi.org/10.20538/1682-0363-2025-3-42-51.

# Ультраструктурные аспекты транслокации митохондрий при раке толстой кишки как возможного пути распространения опухолевого процесса

**Кит О.И.[1], Шихлярова А.И.[1], Франциянц Е.М.[1], Ильченко С.А.[1], Нескубина И.В.[1], Кириченко Е.Ю.[2], Логвинов А.К.[3], Снежко А.В.[1], Аверкин М.А.[1], Габричидзе П.Н.[1]**

*[1] Национальный медицинский исследовательский центр (НМИЦ) онкологии*
*Россия, 344037, г. Ростов-на-Дону, ул. 14-я линия, 63*

*[2] Донской государственный технический университет (ДГТУ)*
*Россия, 344000, г. Ростов-на-Дону, пл. Гагарина, 1*

*[3] Южный федеральный университет (ЮФУ)*
*Россия, 344006, г. Ростов-на-Дону, пр. Стачки 194/1*

## РЕЗЮМЕ

**Цель.** Изучение ультраструктурных особенностей клеток рака прямой кишки и обнаружение признаков транслокации митохондрий из опухоли в область линии резекции с оценкой возможности образования новых злокачественных клеток.

**Материалы и методы.** В исследование включены результаты, полученные от 44 больных (средний возраст 66 (58–73) лет), прооперированных по поводу рака прямой кишки T2–3N0M0 со степенью дифференцировки G2. Часть опухолевого материала и ткани кишки по линии резекции помещали в фиксирующий раствор формальдегида/глутаральдегида. Применяли стандартные методы подготовки срезов, которые исследовали с помощью электронного микроскопа Jeol JEM-1011 (JEOL Inc., Япония).

**Результаты.** Ультраструктура аденокарциномы прямой кишки характеризовалась высокой плотностью расположения и вариабельностью размеров и формы опухолевых клеток с крупным ядром и глубокими инвагинациями ядерной мембраны, скоплением множества митохондрий по одному из полюсов клетки. Было выявлено отшнуровывание фрагмента цитоплазмы, плотно заполненного митохондриями, в виде митохондриома с последующей транслокацией митохондрий в здоровые ткани кишки по линии резекции. По данным электронограмм можно было судить об активном передвижении митохондрий в форме мелких сфероидов и митовизикул вдоль границ многослойной структуры подслизистой оболочки прямой кишки, а затем их слияние в крупные органеллы, способных к реализации ядерного синтеза из транспортированных митохондриальных и ядерных ДНК. Отмечены отдельные ядерные структуры в кооперации с группами митохондрий и последующей самосборкой аномальных клеток.

**Заключение.** Ультраструктурный анализ аденокарциномы прямой кишки свидетельствует не только о необходимости митохондриальной транслокации для освобождения внутриклеточного пространства и предотвращения метаболической угрозы накопления активных форм кислорода в клетках опухоли, но и указывает на ключевую роль митохондрий для старта опухолевого переноса энергии и информации как лидеров этих процессов. Это приводит к мысли о вероятности индукции процессов раннего рецидивирования и метастазирования рака прямой кишки.

**Ключевые слова:** митохондрии, аденокарцинома прямой кишки, ультраструктурный анализ

**Конфликт интересов.** Авторы декларируют отсутствие явных и потенциальных конфликтов интересов, связанных с публикацией настоящей статьи.

**Источник финансирования.** Авторы заявляют об отсутствии финансирования при проведении исследования.

**Соответствие принципам этики.** Все пациенты подписали информированное согласие на взятие и передачу биологического материала для проведения научных исследований, государственных заданий в общественно и социально полезных целях. Исследование одобрено этическим комитетом ФГБУ «НМИЦ онкологии» Минздрава России (протокол № 1 от 30.01.2023).

**Для цитирования:** Кит О.И., Шихлярова А.И., Франциянц Е.М., Ильченко С.А., Нескубина И.В., Кириченко Е.Ю., Логвинов А.К., Снежко А.В., Аверкин М.А., Габричидзе П.Н. Ультраструктурные аспекты транслокации митохондрий при раке толстой кишки как возможного пути распространения опухолевого процесса. *Бюллетень сибирской медицины.* 2025;24(3):42–51. https://doi.org/10.20538/1682-0363-2025-3-42-51.

## INTRODUCTION

In recent years, significant improvements have been made in the treatment of colorectal cancer (CRC) with chemotherapy, molecular targeted therapies, and immune checkpoint inhibitors [1]. However, recurrences and drug resistance prevent successful cancer treatment, resulting in a relatively poor 5-year survival prognosis in approximately 60% of cases [2–4]. Moreover, approximately 20% of patients with CRC have metastasis at the time of diagnosis, whereas 25% of patients develop metastasis at an early stage during follow-up [5]. Therefore, an in-depth study of the key factors and mechanisms of tumor progression, as well as the investigation of new therapeutic targets, is essential.

Metabolic reprogramming is currently the focus of cancer research. Recent evidence suggests that the unique metabolism of tumor cells, characterized by reduced oxidative phosphorylation (OXPHOS) and increased glycolysis, is regulated by mitochondrial dynamics [6–8]. Mitochondria are known as the powerhouses of eukaryotic cells that exhibit dynamic properties such as fusion, fission, and degradation, which is crucial for their optimal functioning in energy production [9]. They play an important role in various cellular processes including cell differentiation, apoptosis, calcium homeostasis, innate immunity, and fatty acid (FA) and amino acid metabolism [10, 11].

Both whole mitochondria and mitochondrial genome or other mitochondrial components are endowed with the ability of intercellular translocation [12]. Mitochondrial transport can be accomplished by tunneling nanotubes (TNTs), gap junctions (GJs), and extracellular vesicles or microvesicles (MVs) ranging from 100 nm to 1μm, which are able to span whole mitochondria, genomic DNA, and mitochondrial DNA [13]. However, mitochondria themselves as active organelles are also transported along the cytoskeleton and can take different shapes, for example, fusing into long or interconnected tubules or dividing into small spheroids, which is regulated by opposing processes of fusion and fission [14]. The continuous processes of mitochondrial membrane fusion and fission help to regulate the morphology and number of mitochondria, ensuring their homogeneity and efficient functioning [15]. In addition, unbalanced mitochondrial fusion and fission during the cell cycle, apparently, may be associated with the processes of mitochondria-dependent metabolic reprogramming, promoting the entry of cancer cells into mitosis, thereby providing an advantage in proliferation and survival [9].

Mitochondrial fusion is defined as the full-collapse fusion of two mitochondria by end-to-end collision [10]. Mitochondria consist of two membranes: the outer mitochondrial membrane (OMM) and the inner mitochondrial membrane (IMM). The fusion of the outer membrane occurs first, followed by fusion of the inner membrane, which occurs in close proximity. The IMM contains the mitochondrial lumen (matrix), an inner fringing membrane parallel to the OMM, and a deep curved polymorphic invagination known as the crista.

The crista increases the surface area of the inner membrane and contains components essential for mitochondrial respiration. When the four lipid bilayers fuse, the contents mix, and the matrix components diffuse to form a single fused mitochondrion [9]. In addition to full fusion, there is the so-called kiss-and-run fusion. In contrast to full-collapse fusion, provisional fusion occurs when two mitochondria join, partially exchange intact membrane proteins, and divide, thereby retaining their original topology. This type of fusion increases the functional stability and plasticity of mitochondria and is necessary to support mitochondrial metabolism [16]. While moderate fusion protects intestinal epithelial cells from mitochondrial damage caused by oxidative stress and prevents CRC, abnormal mitochondrial fusion leads to

adenosine triphosphate overproduction and abnormal tumor proliferation.

Thus, taking into account the level of modern knowledge about mitochondria dislocation and transformation and their biological significance in tumor pathogenesis, it seems relevant to visually assess the topographic signs of mitochondria movement from the primary focus of CRC to the resection line. This will help to approach the formation of a hypothesis about the key role of mitochondria in the initiation of new tumor cell conglomerations as a possible basis for recurrence and metastasis.

The aim of this study was to investigate the ultrastructural features of rectal cancer cells and to detect signs of mitochondrial translocation from the tumor to the resection line, taking into account the possibility of formation of new malignant cells.

## MATERIALS AND METHODS

The study included the data obtained from 44 patients with rectal cancer T2–3N0M0 with an average age of 66 (58–73) years, operated on without adjuvant therapy. The tumor differentiation grade in all patients was G2. During the operation after laparotomy, we performed mobilization of the tumor-affected part of the intestine by dissecting and dividing the feeding blood vessels, performed lymphodissection and resection of the affected organ in the scope of rectal resection with removal of the malignant tumor. A part of tumor material and a fragment of intestinal tissue along the resection line were immediately placed in the formaldehyde-glutaraldehyde fixative solution.

## TRANSMISSION ELECTRON MICROSCOPY

After the pretreatment procedure, the tissue sample was placed in pure Epon-812 resin (SPI Inc., USA) and cured for 72 hours at 70°C. Ultrathin 90-nm sections were obtained using an ultramicrotome equipped with a diamond knife. Sections were mounted on copper slit grids and contrasted with 2% aqueous uranyl acetate solution for 40 minutes and lead citrate for 2 minutes. Sections were examined and photographed using a Jeol JEM-1011 electron microscope (JEOL Inc., Japan).

## RESULTS

According to the histopathology report, the rectal tumor was a low-differentiated adenocarcinoma (high grade G2). The most characteristic features of such tumors were the presence of a mucinous component (5%) with invasion of all layers of the intestinal wall, invasion of visceral peritoneum, foci of necrosis, moderately pronounced chronic inflammation, and presence of signs of lymphovascular and perineural invasion.

Ultrastructural study of the tumor tissue showed typical invasive growth of adenocarcinoma cells varying in shape and size (Fig. 1). The cells were tightly adherent to each other without a pronounced intercellular space between the outer layers of cell membranes. At the same time, electron-dense formations of the “interdigitation” type or desmosomes (indicated by arrows in Fig. 1, *b*) were among the noticeable structures demonstrating close intercellular contacts.

Taking into account the fact that desmosomes provide the necessary mechanical adhesion between cells by connecting intermediate filaments, it confirms direct interaction and exchange, allowing to realize the life support of tumor tissue. In cellular polymorphism, we observed diverse nucleus sizes and shapes. The bizarre shape of the nuclei was associated with numerous invaginations of the nuclear membrane. Often the nucleus occupied a significant part, reaching up to 50–60% of the cell surface, and had a multilobed appearance with deep invaginations of the nucleus shell (Fig. 2).

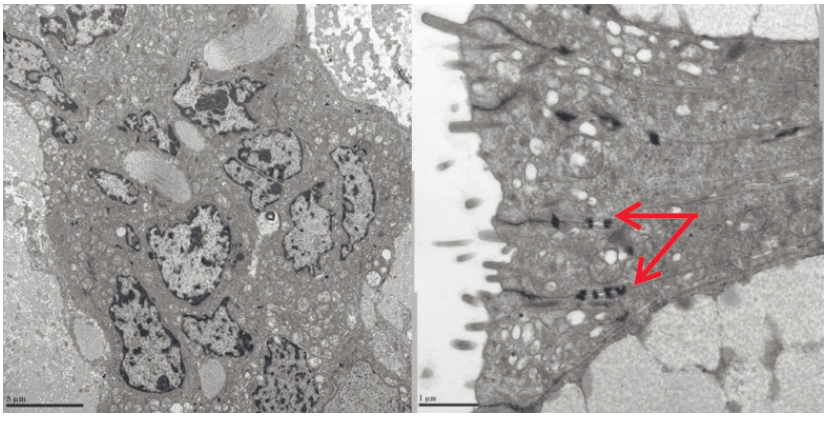

a *b*

Fig. 1. Electron diffraction image of a fragment of a low-differentiated adenocarcinoma with invasion of the rectal wall: *a* – variability in the size and shape of tumor cells with high-density arrangement; *b* – the presence of intercellular contacts in the form of “interdigitation” or desmosomes (indicated by arrows); x10,000. Here and in Figures 2 and 4, images are typical of the preparations of each of the examined patients in the group.

This type of nuclei is characteristic of malignant transformation. The cytoplasm of adenocarcinoma cells was densely filled with organoids, among which the most common ones were mitochondria of different sizes, mainly of irregular round shape with pathological configuration of cristae, and varying electron density of the inner space containing metabolic products (Fig. 2).

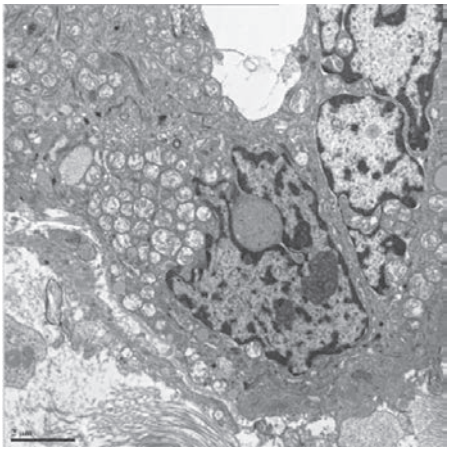

Fig. 2. Electron diffraction image of a fragment of rectal adenocarcinoma tissue. We observe tumor cells with numerous deep invaginations of the nuclear membrane and a cluster of mitochondria at one of the cell poles; ×20,000

It was noticed that in the overwhelming majority of cells the large aggregation of mitochondria as a rule was shifted to one of the cell poles. As a rule, this peculiarity of mitochondria movement to the leading edge of invasive cancer cells is associated with the necessity of energy supply for their movement [17, 18]. It can be assumed that a significant accumulation of mitochondria in the cells could initiate a large mitochondrial transfer, which was realized through the mechanism of cytoplasmic pinching off of the whole aggregation of mitochondria (expulsion) outside the cell as a mitochondriome, as shown in the electron diffraction image below (Fig. 3).

Indeed, it was observed that a separate structure with mitochondria in the area of collagen bundle accumulation was located near the cells. Otherwise, when tumor cells form an excessive accumulation of mitochondria in a state of dysfunction, a large number of ROS can be produced, which poses a threat to cell life [19]. It is under such dangerous conditions that cancer cells tend to displace mitochondria into the intercellular space [20].

Obviously, the separation of the mitochondriome from the cell by pinching off the mitochondria-filled portion of the cytoplasm demonstrates the initial stage of transcellular mitochondrial translocation, which we recorded in our ultrastructural study of rectal cancer. We cannot exclude the assumption that further on, this may represent one of the signaling mechanisms for translocation of mitochondria and associated essential mitochondrial components (mitochondrial DNA and nuclear DNA fragments) into the surrounding space and invasion into the area of healthy tissues. We were able to confirm this by studying electron diffraction images of the intestinal tissue along the resection line of the removed tumor (Fig. 4, 5).

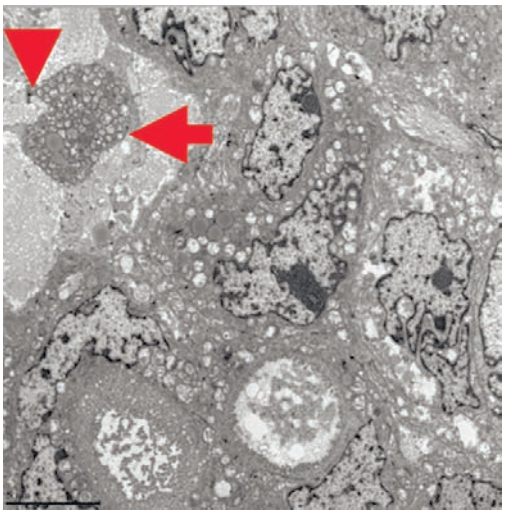

Fig. 3. Electron diffraction image of a fragment of colon adenocarcinoma tissue. It shows pinching off of a cytoplasm fragment forming mitochondriome surrounded by collagen bundles (indicated by an arrow); ×10,000

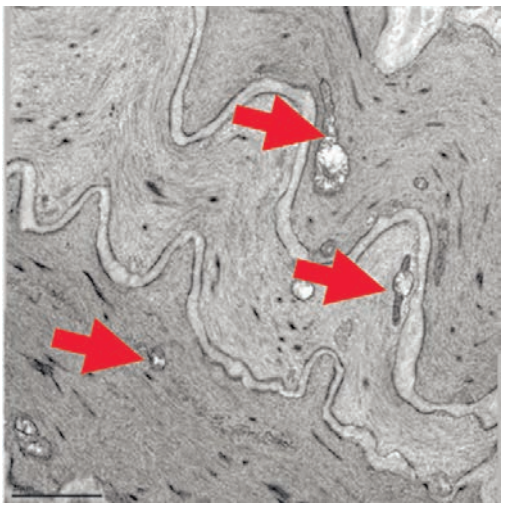

Fig. 4. Electron diffraction image of a fragment of colon tissue along the line of adenocarcinoma resection. The image shows active migration of mitochondria through the layers of the muscularis mucosae. ×25,000

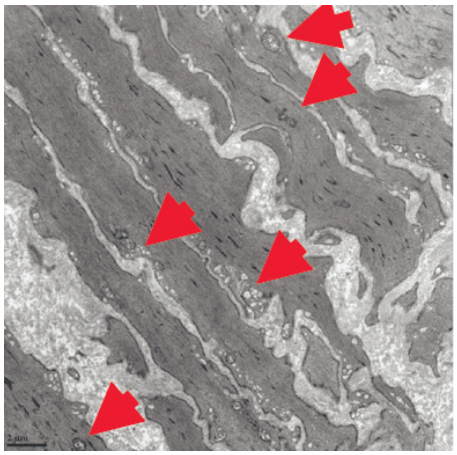

Fig. 5. Electron diffraction image of a fragment of colon tissue along the adenocarcinoma resection line. The image shows movement of many small spheroid-type mitochondria and mitovesicles (indicated by arrows) along the interfaces between the submucosa and the muscularis mucosae. ×12,000

Moving beyond the cell boundaries appeared to enhance mitochondrial migration activity, including the mitochondrial genome to play a signaling role in surrounding intercellular communication, mediating information transfer not only near tumor cells but even over longer distances in the environment of normal healthy tissues.

As can be seen in Fig. 4, mitochondria released from tumor cells show mobility and move independently along the layers of the muscularis mucosae of the colon. Further, it is easy to notice that the overwhelming majority of mitochondria look like small spheroids, which confirms their morphological plasticity and ability to adapt quickly during the transition from tumor environment to healthy tissues (Fig. 5). At the same time, there is a mechanism associated with the formation of so-called mitovesicles, a population of extracellular vesicles of mitochondrial origin during the development of mitochondrial dysfunction. The composition of mitovesicles may include mitochondrial proteins, mtDNA, cytochrome C, and other components.

In other words, at this stage of active independent translocation of mitochondria, we visualized the process of their size reduction, known from the literature as the process of fission, providing adaptive efficient functioning of small spheroid forms and mitovesicles during active movement at the boundary with muscle and mucous tissue (Fig. 6, *a*).

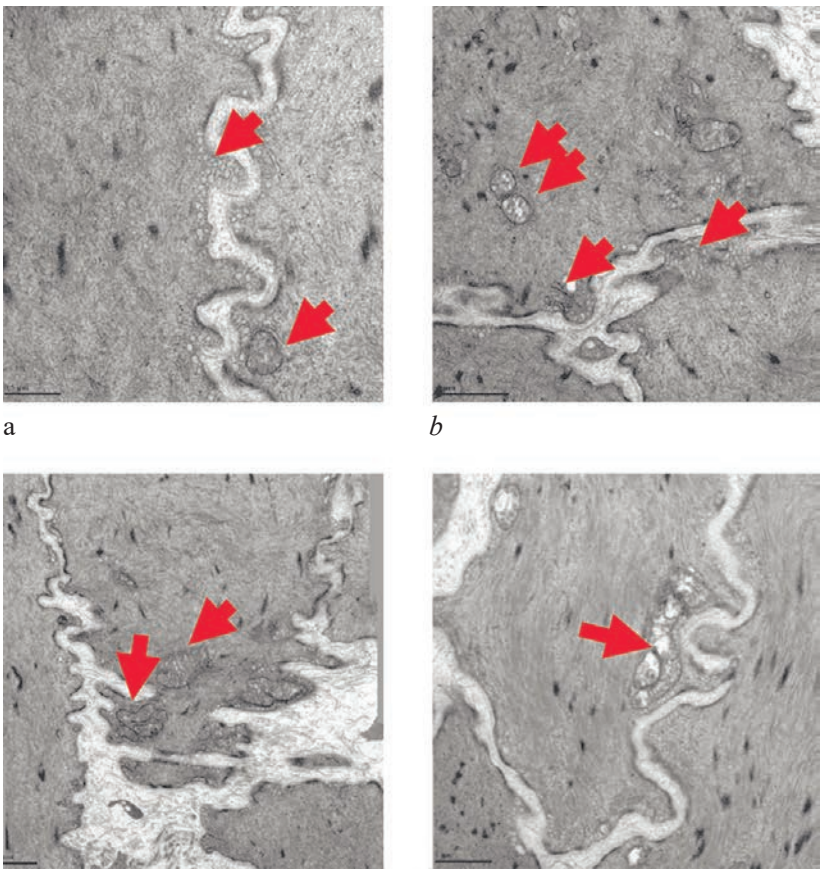

a *b* *c* *d*

Fig. 6. Electron diffraction image of a rectal tissue fragment along the adenocarcinoma resection line: *a* – the presence of small spheroid mitochondria along the healthy tissue interface of submucosa, ×80,000; *b* – accumulation and fusion areas of spheroids and mitovesicles, ×50,000; *c*, *d* – the formation of large abnormal mitochondria in the niches of curved spaces, ×30,000

It was not only the accumulation of a large number of mitovesicles in the curved segments of the boundary but also the presence of single large mitochondria with electron-dense content that drew attention.

The question arose whether these large mitochondria are the result of fusion as a legitimate process of dynamic shaping according to the implementation program of mitochondrial carcinogenesis.First of all, attention was drawn to the fact that in contrast to the "vertical" movement along tissues, in which the expedient form for the process of rapid mitochondrial movement was fission into small spheroids and mitovesicles, in the presence of folded transverse partitions of tissues, there appeared conditions facilitating "horizontal" displacement into a convenient niche and fusion of small forms of mitochondria into larger ones (Fig. 6, *b–d*). The mechanism of such fusion, as already noted, begins with the outer membranes and is then followed by that of the inner membranes, which form a polymorphic invagination with crista protrusions into the matrix. At the same time, matrix components diffuse to form a fused mitochondrion [9]. It is known that the processes of mitochondrial fission are regulated by Drp1 expression, while mitofusin expression regulates fusion [21, 22]. Apparently, such an abnormal fusion and concentration of metabolic and information factors involved mitochondria-dependent metabolic reprogramming to realize nuclear fusion (Fig. 7).

As can be seen from Figure 7, the connective tissue layers of the colon submucosa along the resection line contain only free nuclei and mitochondria, which are single or assembled in groups. It was not possible to determine the time of nuclear assembly, but, apparently, such electron diffraction images illustrate the role of mitochondria in the initiation of self-organization processes of nuclear structures due to the possibility of nuclear material transfer and fusion processes. Figure 8 demonstrates the process of further abnormal self-assembly of tumor cells with the participation of mitochondria surrounding the object they are assembling or being inside it.

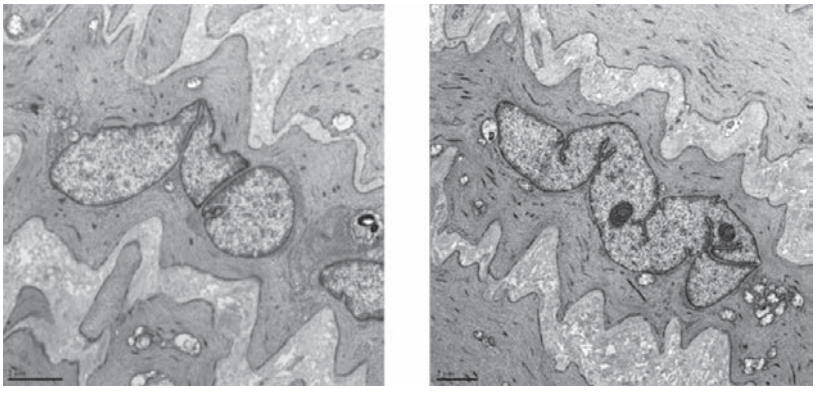

*a* *b*

Fig. 7. Electron diffraction image of a rectal tissue fragment along the adenocarcinoma resection line: *a* – the formation of nuclei fragments in connective tissue layers surrounded by mitochondria, ×20,000; *b* – an elongated shape of the formed nucleus with nuclei in close contact with mitochondria, ×15,000

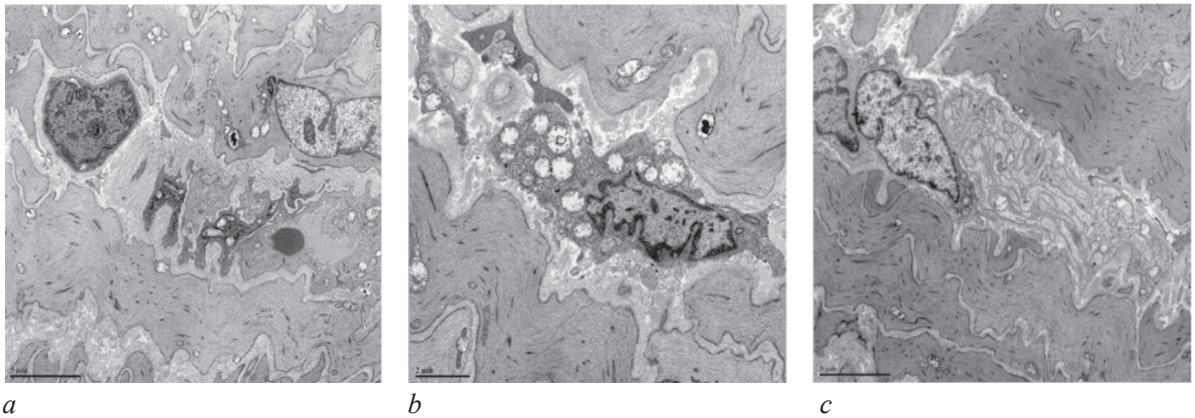

*a* *b* *c*

Fig. 8. Electron diffraction image of a fragment of colon tissue along the line of adenocarcinoma resection: *a* – filling of the dilated area of submucosa with nucleus and unformed fragments of cytoplasm, ×10,000; *b* – the formation of a cellular structure including nucleus and mitochondria, ×20,000; *c* – the formation of a system of tubes and cisterns as a prototype of the Golgi apparatus and endoplasmic network, ×10,000

## DISCUSSION

Summarizing the data of the conducted study, it is possible to present the sequence of dynamic events from primary tumor cells to the appearance of a similar image at a remote distance along the resection line and to highlight the main stages of mitochondrial translocation. Our assumption includes several conditional stages, which are discussed below.

First, the ultrastructural study of colon adenocarcinoma cells allowed us to determine the presence of a significant accumulation of mitochondria, the pathological status of which could pose a threat to the tumor cell due to the accumulation of ROS. In fact, this was a signal not only to free up vital space and prevent metabolic threat to the cell, but also to start the most important process of tumorigenic energy and information transfer by mitochondria, which drive these processes. The analysis of electron diffraction images pointed to such a mechanism of mass transfer of mitochondria outside the cell as the formation of mitochondriomas in pinching off a section of cytoplasm containing a conglomeration of mitochondria. It was this extremely simplified mechanism of separation that allowed for further active movement of mitochondria and mitovesicles in a tumor-free direction.

The second stage, which we associate with mitochondrial translocation itself, is based on electron diffraction data indicating the active movement of mitochondria along the borders of the multilayer structure of the rectal submucosa. The high degree of mitochondrial plasticity contributes to the inclusion of the fission mechanism and the formation of small spherical forms. As noted in the literature, in colorectal cancer cells, enhanced mitochondrial fission is a common phenomenon that promotes or prevents tumor progression. Namely, enhanced mitochondrial fission promotes metabolic reprogramming of cells, leading to cell proliferation, invasion, metastasis, and chemoresistance [22].

Then, as mitochondrial microspheres advanced into the depth of the colon wall tissues, the structure of submucosa changed, forming transverse folds and curves, into the lumen of which spheroids and mitovisicles penetrated. The outer membrane is known to act as a permeable platform that facilitates the convergence of other cellular signals that can be decoded and transmitted to mitochondria [14]. Apparently, this served to turn on the mechanisms of mitochondrial fusion and the formation of large organelles capable of realizing nuclear fusion from transported mitochondrial and nuclear DNA.

Indeed, when analyzing electron diffraction images, we identified areas of the colon submucosa along the resection line, in the layers of which we detected only single nuclei and mitochondria in contact with them. The nuclei were both separate fragments without nuclei and whole nuclei in the form of an elongated structure with several nuclei. However, the characteristic circumstance was the obligatory contact or non-contact interaction of nuclei with mitochondria, which confirms the assumption about the establishment of signaling membrane connections between them, as well as between mitochondria and major organelles such as the endoplasmic reticulum.

This may be evidenced by the next stage, which can apparently be characterized as a self-assembly process based on the same unique signaling mechanisms of membrane system interactions and the formation of abnormal tubes and cavities, which may already represent the prototype tumor cell. It can be assumed that the presence of the nucleus and mitochondria, taking into account their signaling role in triggering the protein synthesis system, could facilitate the proliferative activity of the cell as the basis for recurrence or metastasis.

Undoubtedly, the visually observed pattern of mitochondrial movement can be interpreted as a possibility of new foci of rectal adenocarcinoma growth. However, this problem needs further investigation not only by means of electronic visualization, but also in the application of quantitative immunohistochemical, radioisotopic, and other methods of examination. We believe that the findings of this study may lead to consideration of the enormous and dangerous potential of motor and regulatory activities of mitochondria in malignant neoplasm progression.

## CONCLUSION

The ultrastructural study recorded the process of mitochondrial conglomeration movement from rectal adenocarcinoma cells into the intercellular space in the form of mitochondriomas (passive transfer). Further independent dynamics of mitochondria promotion in the layers of the rectum submucosa at the level of the resection line (active transfer) was accompanied by the transformation of mitochondria sizes (fission and fusion) and the inclusion of trigger mechanisms of self-organization processes. It is assumed that the mobile nature of mitochondria and regulatory signaling

systems of membranes contribute to the reproduction of the processes of nuclear fusion and self-assembly of the prototype tumor cell as possible mechanisms of early recurrence and metastasis of rectal cancer.

## REFERENCES


1. Kit O.I., Gevorkyan Yu.A., Soldatkina N.V., Gusareva M.A., Kharagezov D.A., Milakin A.G. et al. The Complete Clinical Response of Colorectal Cancer to Chemoradiation: Tactics. *Problems in Oncology.* 2017;63(6):838–842. (In Russ.). DOI: 10.37469/0507-3758-2017-63-6-838-842.
2. Luo M., Yang X., Chen N.N., Nizza E.C., Huang K. Drug resistance in colorectal cancer: an epigenetic review. *Biochim. et Biophys. Acta (BBA) – Cancer Reviews.* 2021;1876(2). DOI: 10.1016/ j.bbcan.2021.188623.
3. Hossain M.S., Karunyawati H., Jairoon A.A., Urbi Z., Ooi D.J., John A. et al. Colorectal cancer: a review of carcinogenesis, global epidemiology, current challenges, risk factors, prevention and treatment strategies. *Cancer Diseases.* 2022;14(7). DOI: 10.3390/cancers14071732.
4. Kit O.I., Gevorkyan Yu.A., Soldatkina N.V., Kolesnikov V.E., Bondarenko O.K., Dashkov A.V. Modern Strategy of Metastatic Colorectal Cancer Treatment (Literature Review). *South Russian Journal of Cancer*. 2024;5(3):102–110. (In Russ.). DOI: 10.37748/2686-9039-2024-5-3-9.
5. Biller L.H., Schrag D. Diagnosis and treatment of metastatic colorectal cancer: a review. *JAMA.* 2021;325(7):669–685. DOI: 10.1001/jama.2021.0106.
6. Bonnay F., Veloso A., Steinmann V., Köcher T., Abdusselamoglu M.D., Bajaj S. et al. Oxidative metabolism drives immortalization of neural stem cells during tumorigenesis. *Cell.* 2020;182(6):1490–1507.e19. DOI: 10.1016/j.cell.2020.07.039.
7. Sessions D.T., Kashatus D.F. Mitochondrial dynamics in cancer stem cells. *Cell Life Science*. 2021;78(8):3803–3816. DOI: 10.1007/s00018-021-03773-2.
8. Frantsiyants E.M., Neskubina I.V., Sheiko E.A. Mitochondria of Transformed Cell as a Target of Antitumor Influence. *Research and Practical Medicine Journal*. 2020;7(2):92–108. (In Russ.). DOI: 10.17709/2409-2231-2020-7-2-9.
9. Chen W., Zhao H., Li Y. Mitochondrial dynamics in health and disease: mechanisms and potential targets. *Signal Transl. Purpose Tam.* 2023;8(1):333. DOI: 10.1038/s41392-023-01547.
10. Chan D.K. Mitochondrial dynamics and its involvement in disease. *Annu. Rev. Pathol.* 2020;15:235–259. DOI: 10.1146/annurev-pathmechdis-012419-032711.
11. Zhou Z., Fan W., Zong R., Tang Q. Mitochondrial unfolded protein reaction: a multitasking giant in the fight against human diseases. *Aging Editorial.* 2022;81:101702. DOI: 10.1016/j.arr.2022.101702.
12. Singh B., Modica-Napolitano J.S., Singh K.K. Defining the momiome: Promiscuous information transfer by mobile mitochondria and the mitochondrial genome. *Semin. Cancer Biol.* 2017;47:1–17. DOI: 10.1016/j.semcancer.2017.05.004.
13. Davis C.H., Kim K.Y., Bushong E.A., Mills E.A., Boassa D., Shih T. et al. Transcellular degradation of axonal mitochondria. *Proc. Natl. Acad. Sci. USA.* 2014;111(26):9633–9638. DOI: 10.1073/pnas.1404651111.
14. Giacomello M., Pyakurel A., Glitsu S., Scorrano L. Cell biology of mitochondrial membrane dynamics. *Nat. Rev. Mol. Cell Biol.* 2020;21(4):204–224. DOI: 10.1038/s41580-020-0210-7.
15. Kłos P., Dabravolski S.A. The role of mitochondria dysfunction in inflammatory bowel diseases and colorectal cancer. *Int. J. Mol. Sci.* 2021;22(21):11673. DOI: 10.3390/ijms222111673.
16. Wang S., Xiao W., Shan S., Jiang S., Chen M., Zhang W. et al. Multistep dynamics of mitochondrial fission and fusion in living cells. *PLoS One.* 2012;7(5):e19879. DOI: 10.1371/journal.pone.0019879.
17. Cunniff B., McKenzie A.J., Heintz N.H., Howe A.K. AMPK activity regulates trafficking of mitochondria to the leading edge during cell migration and matrix invasion. *Mol. Biol. Cell.* 2016;27:2662–2674. DOI: 10.1091/mbc.e16-05-0286.
18. Schuler M.-H., Lewandowska A., Di Caprio G., Skillern W., Upadhyayula S., Kirchhausen T. et al. Miro1-mediated mitochondrial positioning shapes intracellular energy gradients required for cell migration. *Mol. Biol. Cell.* 2017;28:2159–2169. DOI: 10.1091/mbc.e16-10-0741.
19. Lyamzaev K.G., Nepryakhina O.K., Saprunova V.B., Bakeeva L.E., Pletjushkina O.Y., Chernyak B. et al. Novel mechanism of elimination of malfunctioning mitochondria (mitoptosis): Formation of mitoptotic bodies and extrusion of mitochondrial material from the cell. *Biochim. Biophys. Acta (BBA) Bioenerg.* 2008;1777:817–825. DOI: 10.1016/j.bbabio.2008.03.027.
20. Nakajima A., Kurihara H., Yagita H., Okumura K., Nakano H. mitochondrial extrusion through the cytoplasmic vacuoles during cell death. *J. Biol. Chem.* 2008;283:24128–24135. DOI: 10.1074/jbc.M802996200.
21. Parone P.A., Da Cruz S., Tondera D., Mattenberger Y., James D.I., Maechler P. et al. Preventing mitochondrial fission impairs mitochondrial function and leads to loss of mitochondrial DNA. *PLoS One.* 2008;3(9):e3257. DOI: 10.1371/journal.pone.0003257.
22. Wu Z., Xiao S., Long J., Huang W., Yu F., Li S. Mitochondrial dynamics and biology of colorectal cancer: mechanisms and potential targets. *Cell Commun. Signal.* 2024;22(1):91. DOI: 10.1186/s12964-024-01490-4.


## Author Contribution

Kit O.I., Snezhko A.V. – final approval of the manuscript for publication. Shikhlyarova A.I., Ilchenko S.A. – justification of the manuscript and critical revision for important intellectual content. Frantsiyants E.M. – conception and design. Neskubina I.V. – critical revision for important intellectual content. Kirichenko E.Yu., Logvinov A.K. – data analysis and interpretation. Averkin M.A., Gabrichidze P.N. – critical revision for important intellectual content.

## Author Information

**Kit Oleg I.** – Academician of the Russian Academy of Sciences, Dr. Sci. (Med.), Professor, General Director of the National Medical Research Centre for Oncology, Rostov-on-Dov, super.gormon@ya.ru, https://orcid.org/0000-0003-3061-6108

**Shikhlyarova Alla I.** – Dr. Sci. (Biology), Professor, Senior Researcher, Laboratory of Malignant Tumor Pathogenesis Study, National Medical Research Centre for Oncology, Rostov-on-Don, shikhliarova.a@mail.ru, https://orcid.org/0000-0003-2943-7655

**Frantsiyants Elena M.** – Dr. Sci. (Biology), Professor, Deputy General Director for Research, National Medical Research Centre for Oncology, Rostov-on-Don, super.gormon@yandex.ru, http://orcid.org/0000-0003-3618-6890

**Ilchenko Sergey A.** – Cand. Sci. (Med.), Oncologist, Abdominal Cancer Unit No. 1, Deputy General Director for Education, National Medical Research Centre for Oncology, Rostov-on-Don, ilchenkosergei@mail.ru, https://orcid.org/0000-0002-0796-3307

**Neskubina Irina V.** – Dr. Sci. (Biology), Senior Researcher, Laboratory of Malignant Tumor Pathogenesis Study, National Medical Research Centre for Oncology, Rostov-on-Don, neskubina.irina@mail.ru, https://orcid.org/0000-0002-7395-3086

**Kirichenko Evgeniya Yu.** – Dr. Sci. (Biology), Acting Head of the Department of Bioengineering, DSTU, Rostov-on-Don, kiriche.evgeniya@yandex.ru, http://orcid.org/0000-0003-4703-1616

**Logvinov Aleksandr K.** – Cand. Sci. (Biology), Researcher, Laboratory of Molecular Neurobiology, Southern Federal University, Rostov-on-Don, a.k.logvinov@yandex.ru, https://orcid.org/0000-0002-8873-3625

**Snezhko Aleksandr V.** – Dr. Sci. (Med.), Professor, Oncologist, Abdominal Cancer Unit No. 1, Deputy General Director for Education, National Medical Research Centre for Oncology, Rostov-on-Don, snezhko.sania@yandex.ru, https://orcid.org/0000-0003-3998-8004

**Averkin Mikhail A.** – Cand.Sci. (Med.), Oncologist, Abdominal Oncology Unit No. 1, Deputy General Director for Education, National Medical Research Centre for Oncology, Rostov-on-Don, mifodiy111@yandex.ru, https://orcid. org/0000-0003-4378-1508

**Gabrichidze Petr N.** – Cand. Sci. (Med.), Oncologist, Consultation and Diagnosis Unit, National Medical Research Centre for Oncology, Rostov-on-Don, q395273@yandex.ru, https://orcid. org/0009-0003-3918-1945

(✉) **Neskubina Irina V.,** neskubina.irina@mail.ru

Received on February 4, 2025;
approved after peer review on February 19, 2025;
accepted on February 27, 2025

УДК 616.126-77:[615.462:678]
https://doi.org/10.20538/1682-0363-2025-3-52-58

# Hydrodynamic performance of a composite heart valve prosthesis

**Klyshnikov K.Yu., Kostyunin A.E., Onishchenko P.S., Glushkova T.V., Akentyeva T.N., Borisova N.N., Kutikhin A.G., Ovcharenko E.A.**

*Research Institute for Complex Issues of Cardiovascular Diseases (RICICD)*
*6 Sosnoviy Blvd., 650002 Kemerovo, Russian Federation*

## ABSTRACT

**The aim** of the study was to conduct a hydrodynamic assessment of the efficiency of heart valve prostheses made of xenopericardium protected by polyvinyl alcohol.

**Materials and methods.** Experimental prostheses based on the UniLine bioprosthesis model were manufactured for the study. The xenopericardium used for the valve cusps was modified with polyvinyl alcohol to improve its resistance to biological and mechanical effects. Hydrodynamic tests were performed on a Pulse Duplicator system, which simulates the function of the "left heart". The key parameters of the prosthesis operation were estimated including average transprosthetic gradient, effective orifice area, locking volume, and regurgitant volume. Unmodified prostheses of similar size were used as a control.

**Results.** Hydrodynamic tests showed that the experimental prostheses demonstrate an increase in the average transprosthetic gradient to 6.59 mm Hg (compared to 5.29 mm Hg in the control group) and a decrease in the effective orifice area to 1.52 cm² (1.69 cm² in the control group). The regurgitant volume also increased to 23.3 ml per cycle, which is higher than the control value of 12.2 ml per cycle. Despite this, all indicators remain within the permissible values established by the state standard (GOST).

**Conclusion.** The use of polyvinyl alcohol to protect the xenopericardium demonstrates potential advantages such as increased resistance of the material to biological effects, but is accompanied by some decrease in the hydrodynamics of the prosthesis. Nevertheless, the efficiency indicators remain within the standards, which opens up opportunities for further improvement of the technology. It is necessary to continue research in order to optimize the material and design to improve both the biocompatibility and functional characteristics of the prosthesis.

**Keywords**: hydrodynamic testing, prosthetic heart valve, transprosthetic gradient, effective orifice area, regurgitation

**Conflict of interest.** The authors declare the absence of obvious or potential conflicts of interest related to the publication of this article.

**Source of financing.** The study was conducted with the support of a grant from the Russian Science Foundation No. 24-75-10048, https://rscf.ru/project/24-75-10048/.

**For citation:** Klyshnikov K.Yu., Kostyunin A.E., Onishchenko P.S., Glushkova T.V., Akentyeva T.N., Borisova N.N., Kutikhin A.G., Ovcharenko E.A. Hydrodynamic performance of a composite heart valve prosthesis. *Bulletin of Siberian Medicine.* 2025;24(3):52–58. https://doi.org/10.20538/1682-0363-2025-3-52-58.

✉ *Akentyeva Tatiana N.,* akentn@kemcardio.ru

# Гидродинамическая эффективность композитного протеза клапана сердца

**Клышников К.Ю., Костюнин А.Е., Онищенко П.С., Глушкова Т.В., Акентьева Т.Н., Борисова Н.Н., Кутихин А.Г., Овчаренко Е.А.**

*Научно-исследовательский институт комплексных проблем сердечно-сосудистых заболеваний (НИИ КПССЗ) Россия, 650002, г. Кемерово, б-р имени академика Л.С. Барбараша, 6*

**РЕЗЮМЕ**

**Целью** исследования стала гидродинамическая оценка эффективности работы протезов клапанов сердца, изготовленных из ксеноперикарда, защищенного поливиниловым спиртом.

**Материалы и методы.** Для исследования были изготовлены экспериментальные протезы на основе модели биопротеза «ЮниЛайн». Ксеноперикард, использованный для створок, был модифицирован поливиниловым спиртом для улучшения его стойкости к биологическим и механическим воздействиям. Гидродинамические испытания проводили на стенде Pulse Duplicator, который моделирует функцию «левого сердца». Оценивали ключевые параметры работы протеза: средний транспротезный градиент, эффективная площадь отверстия, запирающий объем и объем регургитации. В качестве контроля использовали немодифицированные протезы аналогичного размера.

**Результаты.** Гидродинамические испытания показали, что экспериментальные протезы демонстрируют увеличение среднего транспротезного градиента до 6,59 мм рт. ст. (по сравнению с 5,29 мм рт. ст. у контрольной группы) и уменьшение эффективной площади отверстия до 1,52 см² (в контрольной группе – 1,69 см²). Объем регургитации также увеличился до 23,3 мл/цикл, что выше показателя контроля в 12,2 мл/цикл. Несмотря на это, все показатели остаются в пределах допустимых значений, установленных ГОСТом.

**Заключение.** Использование поливинилового спирта для защиты ксеноперикарда демонстрирует потенциальные преимущества в повышении стойкости материала к биологическим воздействиям, однако сопровождается некоторым ухудшением гидродинамических характеристик протеза. Тем не менее показатели эффективности остаются в пределах нормативов, что открывает возможности для дальнейшего совершенствования технологии. Дальнейшая трансляция технологии в клиническую практику требует корректировки характеристик материала для улучшения функциональных показателей протеза.

**Ключевые слова:** гидродинамические испытания, протез клапана сердца, транспротезный градиент, эффективная площадь отверстия, регургитация

**Конфликт интересов.** Авторы декларируют отсутствие явных и потенциальных конфликтов интересов, связанных с публикацией настоящей статьи.

**Источник финансирования.** Исследование выполнено за счет гранта Российского научного фонда № 24-75-10048, https://rscf.ru/project/24-75-10048/.

**Для цитирования:** Клышников К.Ю., Костюнин А.Е., Онищенко П.С., Глушкова Т.В., Акентьева Т.Н., Борисова Н.Н., Кутихин А.Г., Овчаренко Е.А. Гидродинамическая эффективность композитного протеза клапана сердца. *Бюллетень сибирской медицины.* 2025;24(3):52–58. https://doi.org/10.20538/1682-0363-2025-3-52-58.

## INTRODUCTION

Cardiovascular diseases remain the leading causes of death worldwide and a significant burden on the healthcare system [1]. Surgical (SAVR) and transcatheter aortic valve replacement (TAVR) are becoming common treatment modalities, providing patients with the opportunity to prolong their lifespan and improve quality of life.

Thus, 2,526 SAVR (according to data for 2022) [2] and 1,467 TAVR (according to data for 2021) [3] procedures took place in the Russian Federation. Bioprosthetic heart valves used for these interventions are made using bovine or porcine xenopericardium stabilized with preservatives such as glutaraldehyde or ethylene glycol diglycidyl ether [4, 5]. These materials have good bio- and hemocompatibility properties and are used worldwide in manufacturing of

bioprostheses [6]. However, failure of such prostheses observed in clinical practice due to calcification of the xenopericardium, structural degeneration due to prolonged function in the bloodstream, exposure to immune cells and blood proteinases, prevent specialists from referring to this material as "ideal" [7]. Therefore, the field of materials science for implantable medical devices puts emphasis on the complete or partial replacement of xenopericardium with a synthetic polymer material that is more resistant to mechanical and biological influences during functioning and can withstand aggressive environment of the recipient`s body [8–10].

A number of authors propose the development of a fully polymeric heart valve, demonstrating successful *in vitro*, preclinical *in vivo*, and human trial results [8, 11–13]. Other authors modify xenopericardium with additional agents that reduce the immunogenicity of the material or the tendency toward calcification [14, 15]. Our team has developed the concept of a "protected" material, it is centered around the idea of insulating the pericardium with layers of polymer – polyvinyl alcohol (PVA) [16]. The polymer covers and impregnates the pericardial base, thus preventing proteolytic blood enzymes, immune cells, albumin, and other factors from penetrating into the tissue and inducing calcification. Thus, PVA creates a protective layer.

However, the introduction of a new component into xenopericardial material will affect the bio- and hemocompatibility of the device and mechanical properties of the cusps, and, consequently, the function of the bioprosthesis as a whole. The key indicators of the reliability and effectiveness of a heart valve prosthesis can be evaluated using hydrodynamic tests. Hydrodynamic tests performed with high-precision systems are highly informative due to qualitative and quantitative assessment of the key performance indicators of the prosthesis at all phases of its function – opening and closing [17]. The more accurately the system simulates the function of the heart, the more reliable the results of the study of the prosthesis will be.

The aim of this study was to conduct a hydrodynamic assessment of the function of a novel heart valve prosthesis made of a polyvinyl alcohol-protected xenopericardial tissue using a hydrodynamic tester system.

## MATERIAL AND METHODS

### Prosthetic Heart Valves

Experimental prostheses were made on the basis of the UniLine heart valve bioprosthesis for tricuspid heart valves replacement (NeoCor, Russia), which proved itself as an effective medical device for the treatment of acquired heart valve defects [18, 19]. The prosthesis consists of three cusps made from bovine xenopericardium stabilized with ethylene glycol diglycidyl ether. The cusps are mounted on a three-pronged polypropylene support frame, covered inside and outside with synthetic woven lining. The sewing ring is located at the base of the prosthesis (Fig. 1). The device is designed for open implantation in the tricuspid position and suture fixation.

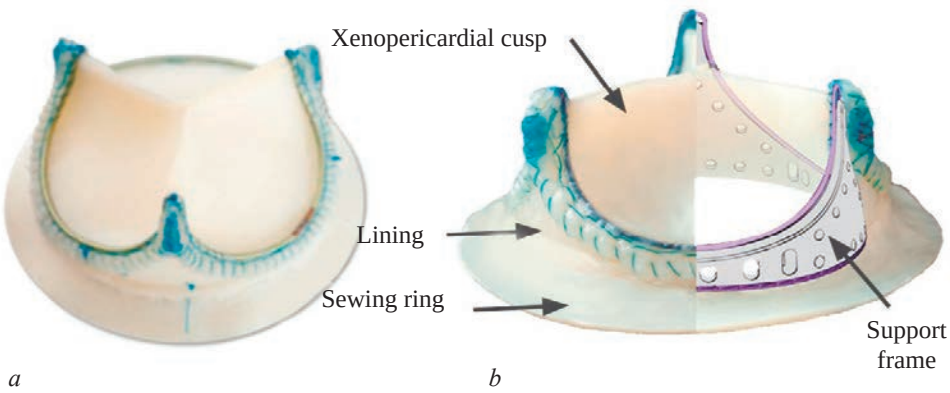


Fig. 1. The UniLine bioprosthesis, standard 26 mm in size, and its main components: *a* – isometric view, *b* – side view

To improve the stability of the biomaterial of this prosthesis, we have proposed an additional polymer modification of the xenopericardial tissue that is used to cut out and manufacture cusps. It is an experimental technology that has been described earlier [16]. For the modification we used a 15% modification solution of PVA, prepared by dissolving this polymer (Mw = 89,000–98,000 99+% hydrolyzed, Sigma-Aldrich, USA) in deionized water at 100° °C for 2.5 hours and constantly stirred. After dissolution, the solution

was cooled to room temperature, and xenopericardial patches were immersed in this solution for 24 hours. Then, the samples were removed from the solution and placed between two glasses, the gap between which was fixed with metal plates. Next, the samples were subjected to three cryostructuring cycles, consisting of the following successive steps: the samples were kept at –40° C for 24 hours, then at –2° C for 12 hours, and finally at +8° C for 12 hours. After cryostructuring, the samples were washed in water for 24 hours to remove unbound PVA, the water was changed regularly.

After that, NeoCor manufactured a series of prototype prostheses using this protected material ($n$ = 5), which we assessed *in vitro*. All devices in this study were of standard 26-mm size.

### Hydrodynamic Tests

The functional properties of experimental protected prostheses were evaluated using the Pulse Duplicator hydrodynamic testing system (Vivitro Labs, Canada). The system is a model of the "left heart", simulating the work of the ventricle and atrium (Fig. 2).

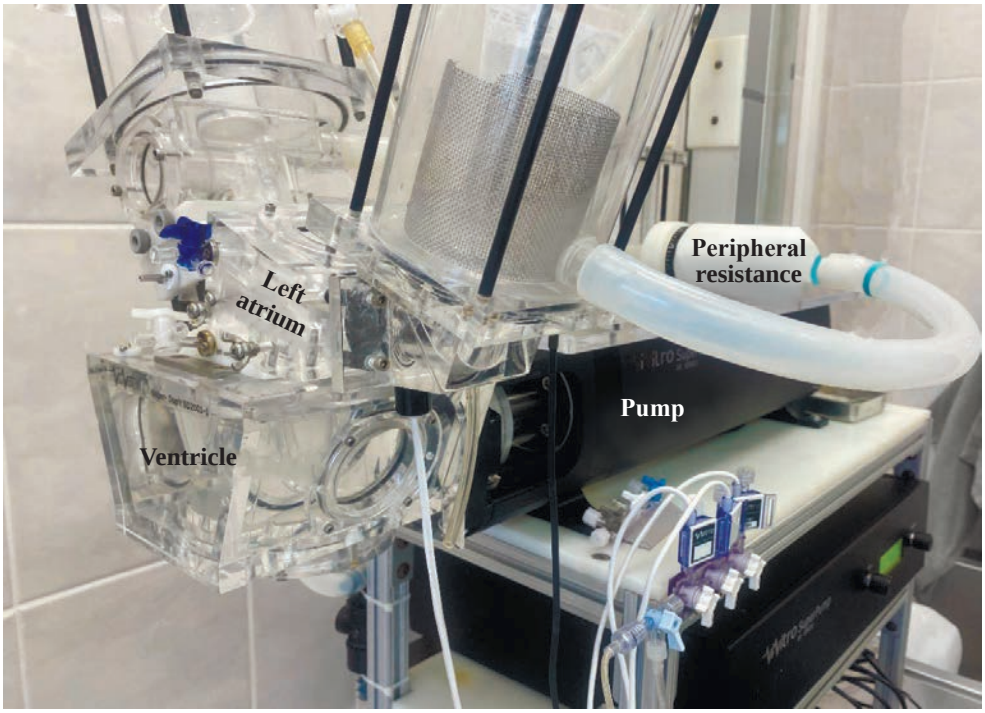


Fig. 2. Pulse Duplicator system and its main components

The study was carried out by reproducing the physiological function of the "heart" as defined by state standards (GOST 31618.1-2012): stroke volume – 70 ml; minute volume – 5 l/min; heart rate – 70 beats/min; the mean back pressure on the prosthesis – 120 mm Hg. Saline solution was used as the test medium. During the study, the following parameters were quantified: mean transprosthetic gradient, effective orifice area, locking volume, and regurgitant volume. All parameters were evaluated during 10 steady "cardiac" cycles for each prosthesis. Moreover, these cardiac cycles were recorded using a FastVideo-250 video camera (NPO ASTEK, Russia).

Unmodified UniLine bioprostheses ($n$ = 5) of the same standard size (26 mm) for the implantation in tricuspid position were used as controls. All tests on controls were carried out under the same conditions.

Statistical data processing was performed using the Statistica 10.0 program (StatSoft, Russia). Given the small sample size, the presence of statistically significant differences in quantitative hydrodynamic parameters between the groups was assessed using the Mann–Whitney $U$-test, a nonparametric criterion for independent samples. The data are presented as the median and the interquartile range $Me$ ($Q_1$–$Q_3$). The differences between the groups were considered statistically significant at $p < 0.05$.

## RESULTS

The results of comparison of prosthesis quantitative characteristics are presented in Table 1. There was no statistically significant decrease in the parameters, however, the experimental samples tended to function less efficiently compared to controls. Their performance

worsened as the effective orifice area decreased while the mean transprosthetic gradient increased. The analysis of the video recordings confirmed these conclusions – the experimental samples opened with a small geometric orifice area, thus showing higher transprosthetic gradients and smaller effective orifice area (Fig. 3).

Table 1

| Hydrodynamic Performance of Experimental and Control Prostheses, *Me* ($Q_1$–$Q_3$) | | | |
|---|---|---|---|
| Parameter | Experimental samples | Controls | *p* |
| Mean transprosthetic gradient, mm Hg | 6.59 [6.10–7.22] | 5.29 [5.19–6.13] | 0.143 |
| Effective orifice area, $cm^2$ | 1.52 [1.51–1.61] | 1.69 [1.60–1.76] | 0.296 |
| Locking volume, ml/cycle | 1.12 [1.22–1.055] | 1.77 [1.405–1.92] | 0.094 |
| Regurgitant volume, ml/cycle | 2.33 [1.93–2.465] | 1.22 [1.115–1.45] | 0.296 |

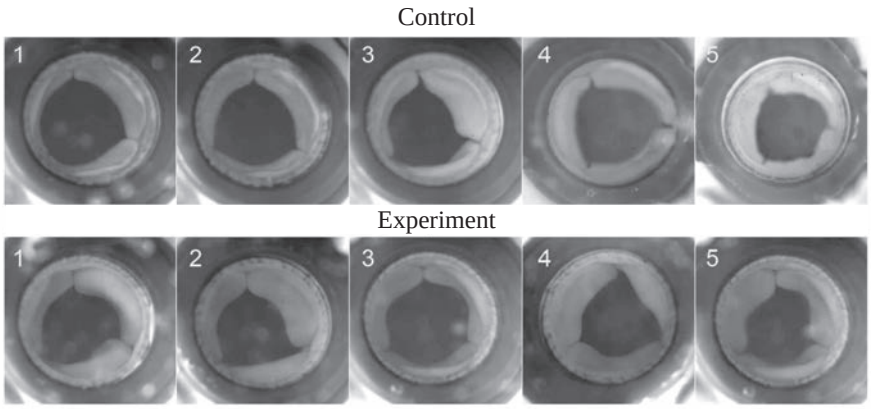


Fig. 3. Pairwise comparison of experimental and control prostheses in sped up video recording at maximum opening (several selected samples)

Regurgitant volume increased as well, however, it remained within the limits allowed by state standards (GOST 31618), there were no significant differences compared to controls.

## DISCUSSION

Bioprosthetic heart valve dysfunction is a significant challenge for engineers and researchers developing these medical devices. The need to create an optimal geometry of cusps and support frame is complicated by the aggressive operating conditions of the device such as exposure to blood components (proteolytic enzymes and immune cells) and extremely long duration of loading (tens of years, 200–400–600 million cycles). Therefore, the research and implementation of new materials resistant to such impacts are important aspects of the development of future bioprosthetic heart valve designs.

Modern promising materials in this field are likely to be synthetic polymer and/or composite. The present study demonstrates the latter using a unique concept – a xenopericardial patch commonly used to create cusps for prostheses protected from the factors and blood cells by a biocompatible polymer material [16]. Such a concept can improve the biocompatibility and stability of prostheses, increase their durability, i.e. delay the onset of dysfunction and, as a result, the need for repeated surgical intervention.

It is worth noting that the introduction of PVA into the composition of the material also affects the biomechanics of the final product in close-to-real conditions. This effect is expected, but its severity and potential significance should be carefully evaluated for further adjustment of the prosthesis design and balancing between the protective properties of PVA and efficiency, primarily in terms of hydrodynamic parameters. This effect was fully demonstrated in our study.

To form the protective layer, we selected a standard 0.5 ± 0.01-mm-thick pericardial patch used in the actual manufacturing of bioprostheses. Modification with PVA changed its the physical and mechanical characteristics – increased the thickness. Despite the fact that PVA itself had an extremely low modulus of elasticity (less than 0.1 MPa) [20], even such small addition to the “xenopericardium + PVA” composite material negatively affected its hydrodynamic characteristics compared to unmodified xenopericardium. It is worth mentioning that any prosthetic heart valves based on biological materials have some variability in their parameters, since the animal tissues themselves are variable. However,

we have noted a clear trend (albeit not statistically significant) towards a decrease in the effectiveness of experimental protected prostheses *in vitro*, which means that it was the introduction of PVA that affected the parameters, not the random variability.

Given the negative experience with PVA-protected xenopericardium, the positive results of such modification. Firstly, despite the worse performance of the prosthesis, its parameters remain within acceptable limits allowed by state standards (GOST 31618.1-2012 "Prosthetic heart valves. Part 1"). Thus, the effective orifice area for this standard size should not be less than 1.4 $cm^2$, and the regurgitant volume should be 10 ml/cycle, i.e. experimental protected prostheses have an acceptable performance.

Secondly, to make cusps based on such composite material, one can use a thinner xenopericardial patch. In this study, the baseline material had a thickness of 0.5 ± 0.01 mm, which increased to 0.55 ± 0.01 mm after the modification with PVA, i.e. it thickened and changed the biomechanics of the device as a whole (its hydrodynamics). The use of a 0.45–0.475-mm-thick xenopericardial material, taking into account the subsequent modification with PVA, should result in better physical and mechanical properties of the composite, similar to the unmodified material used in the prosthesis. It will be difficult to find a thin xenopericardial material since the manufacturing process at NeoCor is already established. However, taking into account the advantages provided by the PVA protection like increased durability and reliability of the prosthesis, it is possible to justify the amendments to technical regulations and selection of new materials (thinner xenopericardium), including the costs.

## CONCLUSION

In conclusion, the use of the PVA-protected xenopericardium opens up new opportunities for the development of a new generation of prosthetic heart valves with longer lifespan and protection from aggressive factors of recipient`s body. The first experience of creating the material and a prosthetic heart valve based on it demonstrate the high potential of the technology, which, however, already requires prototyping adjustments. Further research in this area with a larger scope of tests is needed to assess the long-term effectiveness, safety, and duration of new designs.

In general, the relevance of developing a new prosthetic heart valve based on PVA-protected xenopericardium is scientifically and practically justified. The successful implementation of this type of prosthesis in clinical practice can change the treatment of cardiovascular diseases, improving the quality of life of patients and reducing the financial costs of treatment.

## REFERENCES


1. Virani S.S., Alonso A., Benjamin E.J., Bittencourt M.S., Callaway C.W., Carson A.P. et al. Heart Disease and stroke statistics-2020 update: a report from the American Heart Association. *Circulation*. 2020;141(9):e139–e596. DOI: 10.1161/CIR.0000000000000757.
2. Bockeria L.A., Milievskaya E.B., Pryanishnikov V.V., Yurlov I.A. Cardiovascular Surgery - 2022. Diseases and Congenital Anomalies of the Circulatory System. A.N. Bakulev Centre for Cardiovascular Surgery, 2023. (In Russ.).
3. Alekyan B.G., Grigoryan A.M., Staferov A.V., Karapetyan N.G. X-ray Endovascular Diagnostics and Treatment of Diseases of the Heart and Blood Vessels in the Russian Federation - 2021. *Russian Journal of Endovascular Surgery*. 2022;9:1–254. (In Russ.). DOI: 10.24183/2409-4080-2022-9S.
4. Oveissi F., Naficy S., Lee A., Winlaw D.S., Dehghani F. Materials and manufacturing perspectives in engineering heart valves: a review. *Mater. Today Bio*. 2020;5:100038. DOI: 10.1016/j.mtbio.2019.100038.
5. Mohammadi H., Mequanint K. Prosthetic aortic heart valves: Modeling and design. *Med. Eng. Phys*. 2011;33(2):131–147. DOI: 10.1016/j.medengphy.2010.09.017.
6. Barbarash L.S., Zhuravleva I.Yu. Bioprosthetic Heart Valve Evolution: Two Decades of Advances and Challenges. *Complex Issues of Cardiovascular Diseases*. 2012;1:4–11. (In Russ.).
7. Glushkova T.V., Kostyunin A.E. Calcification of Bioprosthetic Heart Valves Treated with Ethylene Glycol Diglycidyl Ether. *Complex Issues of Cardiovascular Diseases*. 2021;10(2):16–24. (In Russ.). DOI: 10.17802/2306-1278-2021-10-2-16-24.
8. Rotman O.M., Kovarovic B., Chiu W.-C., Bianchi M., Marom G., Slepian M.J. et al. Novel Polymeric Valve for Transcatheter Aortic Valve Replacement Applications: *In Vitro* Hemodynamic Study. *Ann. Biomed. Eng*. 2019;47(1):113–125. DOI: 10.1007/s10439-018-02119-7.
9. Motta S.E., Falk V., Hoerstrup S.P., Emmert M.Y. Polymeric valves appearing on the transcatheter horizon. *Eur. J. Cardio-Thoracic Surg*. 2021;59(5):1057–1058. DOI: 10.1093/ejcts/ezab089.
10. Singh S.K., Kachel M., Castillero E., Xue Y., Kalfa D., Ferrari G. et al. Polymeric prosthetic heart valves: A review of current technologies and future directions. *Front. Cardiovasc. Med*. 2023;10. DOI: 10.3389/fcvm.2023.1137827.
11. Claiborne T.E., Xenos M., Sheriff J., Chiu W.-C., Soares J., Alemu Y. et al. Toward optimization of a novel trileaflet polymeric prosthetic heart valve via device thrombogenicity emulation. *ASAIO J*. 2013;59(3):275–283. DOI: 10.1097/MAT.0b013e31828e4d80.
12. De Gaetano F., Bagnoli P., Zaffora A., Pandolfi A., Serrani M., Bruberrt J. et al. A newly developed tri-leaflet polymeric heart

valve prosthesis. *J. Mech. Med. Biol*. 2015;15(02):1540009. DOI: 10.1142/S0219519415400096.
13. Stasiak J.R., Serrani M., Biral E., Taylor J.V., Zaman A.G., Jones S. et al. Design, development, testing at ISO standards and: In vivo feasibility study of a novel polymeric heart valve prosthesis. *Biomater. Sci*. 2020;8(16):4467–4480. DOI: 10.1039/d0bm00412j.
14. Bondarenko N.A., Surovtseva M.A., Lykov A.P., Kim I.I., Zhuravleva I.Yu., Poveshchenko O.V. Cytotoxicity of Xenogeneic Pericardium Preserved with Epoxy Compounds as Cross-Linking Agents. *Modern Technologies in Medicine.* 2021;13(4):27. (In Russ.). DOI: 10.17691/stm2021.13.4.03.
15. Timchenko T.P. Bisphosphonates as Potential Inhibitors of Calcification in Bioprosthetic Heart Valves (Review). *Modern Technologies in Medicine*. 2022;14(2):68–79. (In Russ.). DOI: 10.17691/stm2022.14.2.07.
16. Ovcharenko E.A., Glushkova T.V., Shishkova D.K., Rezvova M.A., Velikanova E.A., Klyshnikov K.Y. et al. Anti-adhesive properties of epoxy-treated xenopericardium modified with polyvinyl alcohol: in vitro study of leukocyte adhesion in the pulsatile flow model. *Sovrem. Tehnol. Med*. 2024;16(2):40–46. DOI: 10.17691/stm2024.16.2.04.
17. Susin F.M., Bagno A., Gerosa G. Hydrodynamic performance of heart valve prostheses: Open discussion on European Committee for Standardization International Organization for Standardization standard 5840. *J. Thorac. Cardiovasc. Surg*. 2010;139(5):1356–1357. DOI: 10.1016/j.jtcvs.2010.01.025.
18. Kozlov B.N., Petlin K.A., Pryakhin A.S., Seredkina E.B., Panfilov D.S., Shipulin V.M. Immediate and Remote Results of the Use of Bioprostheses UniLine in the Aortic Position. *Clinical and Experimental Surgery. Petrovsky Jounral.* 2017;5(4(18)):37–42. (In Russ.).
19. Karaskov A.M., Zheleznev S.I., Rogulina N.V., Sapegin A.V., Odarenko Yu.N., Levadin Yu.V. et al. Next Generation Russian Biological Prosthesis “Unilin” for Mitral Valve Replacement: First Experience. *Grudnaya i Serdechno-Sosudistaya Khirurgiya.* 2017;59(2):98–104. (In Russ.). DOI: 10.24022/0236-2791-2017-59-2-98-104.
20. Studenikina L.N., Domareva S.Y., Golenskikh Y.E., Matveeva A.V., Melnikov A.A. Increasing the Strength and Water Resistance of Materials Based on Polyvinyl Alcohol with Boric Acid. *Proceedings of the Voronezh State University of Engineering Technologies*. 2022;2(92):249–255. (In Russ.). DOI: 10.20914/2310-1202-2022-2-249-255.

## Author Contribution

Klyshnikov K.Yu., Kostyunin A.E., Onishchenko P.S., Glushkova T.V., Akentyeva T.N., Borisova N.N., Kutikhin A.G. – data collection and interpretation, drafting and editing of the manuscript, full responsibility for the manuscript. Ovcharenko E.A. – data collection and interpretation, drafting and editing of the manuscript, approving the final version of the manuscript for publication, full responsibility for the manuscript.

## Author Information

**Klyshnikov Kirill Yu.** – Cand. Sci. (Med.), Senior Researcher, Research Institute for Complex Issues of Cardiovascular Diseases, Kemerovo, klyshku@kemcardio.ru, https://orcid.org/0000-0003-3211-1250

**Kostyunin Aleksandr E.** – Cand. Sci. (Biology), Senior Researcher, Research Institute for Complex Issues of Cardiovascular Diseases, Kemerovo, kostae@kemcardio.ru, https://orcid.org/0000-0001-6099-0315

**Onishchenko Pavel S.** – Junior Researcher, Research Institute for Complex Issues of Cardiovascular Diseases, Kemerovo, onisps@kemcardio.ru, https://orcid.org/0000-0003-2404-2873

**Glushkova Tatiana V.** – Cand. Sci. (Biology), Senior Researcher, Research Institute for Complex Issues of Cardiovascular Diseases, Kemerovo, glushtv@kemcardio.ru, https://orcid.org/0000-0003-4890-0393

**Akentyeva Tatiana N.** – Junior Researcher, Research Institute for Complex Issues of Cardiovascular Diseases, Kemerovo, akentn@kemcardio.ru, https://orcid.org/0000-0002-0033-9376

**Borisova Natalya N.** – Junior Researcher, Research Institute for Complex Issues of Cardiovascular Diseases, Kemerovo, borinn@kemcardio.ru, https://orcid.org/0009-0004-1138-9653

**Kutikhin Anton G.** – Dr. Sci. (Med.), Department Head, Research Institute for Complex Issues of Cardiovascular Diseases, Kemerovo, kytiag@kemcardio.ru, https://orcid.org/0000-0001-8679-4857

**Ovcharenko Evgeny A.** – Cand. Sic. (Tech.), Laboratory Head, Research Institute for Complex Issues of Cardiovascular Diseases, Kemerovo, ovchea@kemcardio.ru, https://orcid.org/0000-0001-7477-3979

(✉) **Akentyeva Tatiana N.,** akentn@kemcardio.ru

Received on November 29, 2024;
approved after peer review on March 17, 2025;
accepted on March 20, 2025

УДК 615.281-015.46(476)
https://doi.org/10.20538/1682-0363-2025-3-59-67

# Sources of information about antibacterial drugs and antibiotic resistance: results of the study in the Republic of Belarus

**Kolchanova N.E.[1], Sharshakova T.M.[1], Braga A.Y.[1], Chigrina V.P.[2], Tyufilin D.S.[2], Kobyakova O.S.[2], Stoma I.O.[1]**

*[1] Gomel State Medical University*
*5 Lange St., 246000 Gomel, Republic of Belarus*

*[2] Federal Research Institute for Health Organization and Informatics*
*11 Dobrolubov St., 127254 Moscow, Russian Federation*

## ABSTRACT

**Aim.** To analyze sources of information about antibacterial drugs and antibiotic resistance among the population in the Republic of Belarus.

**Materials and methods.** The social study included 1,405 people from all regions of Belarus.

**Results.** The main sources of information about antibacterial drugs were doctor's knowledge (59.4%), medication instructions (45.5%), the Internet (22.7%), and personal (past) experience of using antibacterial drugs (21.0%). In the extended analysis, it was found that in most cases, information about antibacterial drugs was received from a doctor by people with lower-middle income, medication instructions were used more often by respondents with upper-middle income, while individuals with higher education were more likely to receive information from the Internet.

**Conclusion.** To increase awareness of the population of antibacterial drugs, income, age, and socio-occupational characteristics should be considered. Working with health professionals is also essential: holding annual training events in medical organizations and pharmacies, organizing internships for professional development, conversations with patients during doctor's visits, placing information about the correct use of antibacterial drugs in medical organizations in the form of posters, leaflets, and videos.

**Keywords:** antibacterial drugs, sources of information, antibiotic resistance, population, Republic of Belarus

**Conflict of interest.** The authors declare the absence of obvious or potential conflicts of interest related to the publication of this article.

**Source of financing.** The authors state that they received no funding for the study.

**Conformity with the principles of ethics.** The study was approved by the Ethics Committee at Gomel State Medical University (Minutes No. 2 dated March 3, 2023).

**For citation:** Kolchanova N.E., Sharshakova T.M., Braga A.Y., Chigrina V.P., Tyufilin D.S., Kobyakova O.S., Stoma I.O. Sources of information about antibacterial drugs and antibiotic resistance: results of the study in the Republic of Belarus. *Bulletin of Siberian Medicine.* 2025;24(3):59–67. https://doi.org/10.20538/1682-0363-2025-3-59-67.

✉ *Chigrina Valeriya P.,* chigrinavp@mednet.ru

# Источники информации об антибактериальных препаратах и антибиотикорезистентности: результаты исследования в Республике Беларусь

**Колчанова Н.Э.[1], Шаршакова Т.М.[1], Брага А.Ю.[1], Чигрина В.П.[2], Тюфилин Д.С.[2], Кобякова О.С.[2], Стома И.О.[1]**

[1] *Гомельский государственный медицинский университет (ГомГМУ)*
*Республика Беларусь, 246000, г. Гомель, ул. Ланге, 5*

[2] *Центральный научно-исследовательский институт организации и информатизации здравоохранения (ЦНИИОИЗ)*
*Россия, 127254, г. Москва, ул. Добролюбова, 11*

**РЕЗЮМЕ**

**Цель.** Проанализировать источники информации об антибактериальных препаратах и антибиотикорезистентности среди населения в Республике Беларусь.

**Материалы и методы.** В социологическом исследовании приняли участие 1 405 человек из всех областей Республики Беларусь.

**Результаты.** Основными источниками информации населения об антибактериальных препаратах являлись знания врача (59,4%), инструкции к лекарственным препаратам (45,5%), Интернет (22,7%) и личный (прошлый) опыт применения антибактериальных препаратов (21,0%). При расширенном анализе выявлено, что в большинстве случаев информацию об антибактериальных препаратах от врача получали лица со средним финансовым положением, инструкции к лекарственным препаратам чаще остальных использовали респонденты с финансовым положением выше среднего, а лица с высшим образованием чаще получали вышеуказанную информацию из интернет-источников.

**Заключение.** Для увеличения охвата информированности населения об антибактериальных препаратах необходимо учитывать их финансовую, возрастную и социально-профессиональную категории. Важным также является работа с медицинскими работниками: проведение ежегодных обучающих мероприятий в медицинских организациях и аптечных пунктах, стажировка с целью повышения квалификации, проведение тематических бесед с пациентами на приеме, размещение информации в медицинских организациях в виде плакатов, роликов и буклетов о правильном приеме антибактериальных препаратов.

**Ключевые слова:** антибактериальные препараты, источники информации, антибиотикорезистентность, население, Республика Беларусь

**Конфликт интересов.** Авторы декларируют отсутствие явных и потенциальных конфликтов интересов, связанных с публикацией настоящей статьи.

**Источник финансирования.** Авторы декларируют отсутствие внешнего финансирования для проведения исследования и публикации статьи.

**Соответствие принципам этики.** Исследование одобрено этическим комитетом по экспертизе социологических исследований в сфере общественного здравоохранения при ГомГМУ (заключение № 2 от 03.03.2023).

**Для цитирования:** Колчанова Н.Э., Шаршакова Т.М., Брага А.Ю., Чигрина В.П., Тюфилин Д.С., Кобякова О.С., Стома И.О. Источники информации об антибактериальных препаратах и антибиотикорезистентности: результаты исследования в Республике Беларусь. *Бюллетень сибирской медицины.* 2025;24(3):59–67. https://doi.org/10.20538/1682-0363-2025-3-59-67.

## INTRODUCTION

Antibiotic resistance is currently one of the most important problems in public health. The decreasing number of new antibacterial drugs (AD) entering clinical practice is aggravating the situation. As a result, treatment of infections caused by resistant strains of microorganisms is time-consuming and costly and sometimes leads to reduced quality of life or a lethal outcome in patients [1, 2].

One of the reasons for the development of antibiotic resistance is irrational use of ADs. To optimize this situation, a number of initiatives are underway at national, international, and global levels, requiring continuous education of physicians and patients, as well as dissemination of information supported by a strong evidence base [3, 4].

According to the meta-analysis conducted by S. Schuts et al. in 2016, such factors as empirical prescription of ADs in accordance with clinical protocols, de-escalation of antimicrobial therapy, switching from intravenous to oral administration, therapeutic drug monitoring, use of a limited list of antibiotics and counseling patients on rational use of drugs are the most important goals in antibiotic resistance prevention programs [5]. However, achieving the effectiveness of prevention programs is impossible without sufficient public awareness of antibacterial drugs. The main goal of public awareness campaigns should be to support the correct use of ADs, which can be transferred into practice through competent coordination, professional communication, and citizen education.

To analyze the rationality of antimicrobial use and knowledge about antibiotic resistance among different population groups in the Republic of Belarus, it is reasonable to study the main sources of information.

## MATERIALS AND METHODS

In the present study, the online questionnaire method (CAWI) was used. The questionnaire was validated using the focus group method ($n$ = 15). The final version of the questionnaire included 28 questions that constituted six blocks. The developed questionnaire presented: general characteristics of respondents; prescription and purchase of antibacterial drugs; frequency and peculiarities, as well as rationality of taking antibacterial drugs by the population of the Republic of Belarus; knowledge and sources of information of the population about antibacterial drugs and antibiotic resistance. According to the main characteristics: sex, age, level of education, type of settlement, the sample represents the population of the Republic of Belarus. The electronic questionnaire was filled in for all regions of the Republic of Belarus using the Google platform.

Statistical analysis of the results was performed using the Statistica analytical package (Version 10-Index, StatSoft Inc, USA) and R-studio. Before applying the methods of descriptive statistics, the type of distribution of quantitative variables was determined using the Shapiro – Wilk criterion. For traits with normal distribution, the arithmetic mean and the standard deviation $M \pm \sigma$ were calculated. For traits with a distribution other than normal, the median and the lower 25th and upper 75th quartiles $Me$ ($LQ$; $UQ$) were calculated. The Mann – Whitney test was used to assess statistical significance between unrelated groups. The Kruskal – Wallis test was used to compare three or more samples. Differences were recognized as statistically significant at $p$ (observed) < 0.05, unless the use of Bonferroni correction was discussed. In this case, statistical significance was estimated at p (observed) < 0.05/k, where k is the number of hypotheses under consideration.

## RESULTS

The conducted sociological research covered all regional centers of the Republic of Belarus. The total number of respondents amounted to 1,405 people, of which 21.8% ($n$ = 306) were men, 78.2% ($n$ = 1,099) were women, the average age was 40.7 ± 13.3 years.

In terms of socio-professional categories, the majority of participants (76.1%, $n$ = 1,069) belonged to the groups of workers/employees/specialists, as well as to the group of people with middle income (43.1%, $n$ = 606). Half of the respondents had higher education (54.9%, $n$ = 772), and one third had technical or specialized secondary education (34.7%, $n$ = 487).

Fifty-five percent ($n$ = 419) of the respondents received information about the correctness of antibiotic use over the last 12 months, of which 75.2% ($n$ = 316) would like to continue to receive new data on the above-mentioned topics.

The most popular topics presented to the participants for selection as additional information were rational use of ADs (79%), antibiotic resistance (54%), use of AD in food and agriculture (26%) (Fig. 1).

Based on the conducted research, it was revealed that one of the risk factors for self-medication of AD was the lack of public awareness about these drugs.

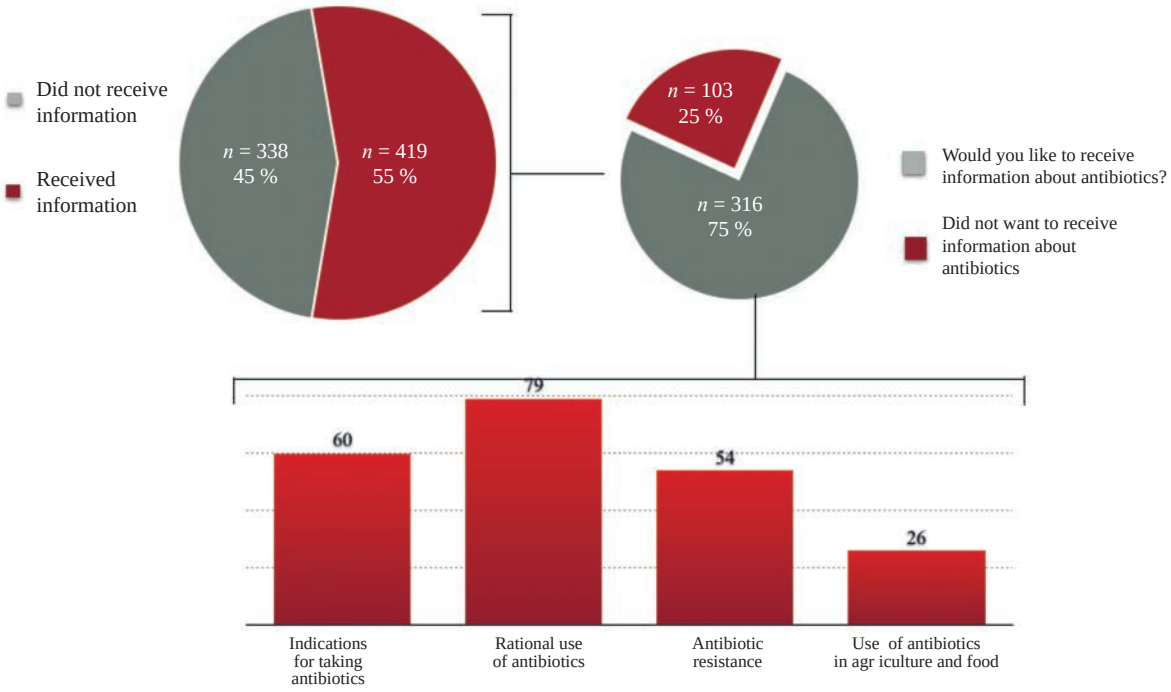


Fig.1. Relevant topics for additional information

Statistically significantly more respondents who did not receive information about the optimal AD use and believed that all ADs were over-the-counter medicines were self-medicating respondents compared to participants who took ADs as prescribed by the doctor (66.7 vs. 80.2%, $p < 0.05$). At the same time, there were fewer citizens who expressed a desire to receive additional information about rational use of AD (17 vs. 26.7%, $p < 0.05$).

According to the questionnaire, each respondent was offered 13 options for sources of information about ADs. The obtained data show that in most cases citizens used doctor's knowledge (64.9%), medication instructions (39.9%) and the Internet (23.5%) as the main sources of information about ADs (Fig. 2).

The majority of middle-income citizens received information about ADs from a doctor (72%; $p < 0.005$) compared to other respondents. The main source of information for 42.1% ($p < 0.05$) of the respondents with upper-middle income was medication instruction. Those with higher education more often preferred to obtain the above information from Internet sources, as well as from brochures and posters in medical organizations (28.7 and 13.3%, respectively; $p < 0.05$).

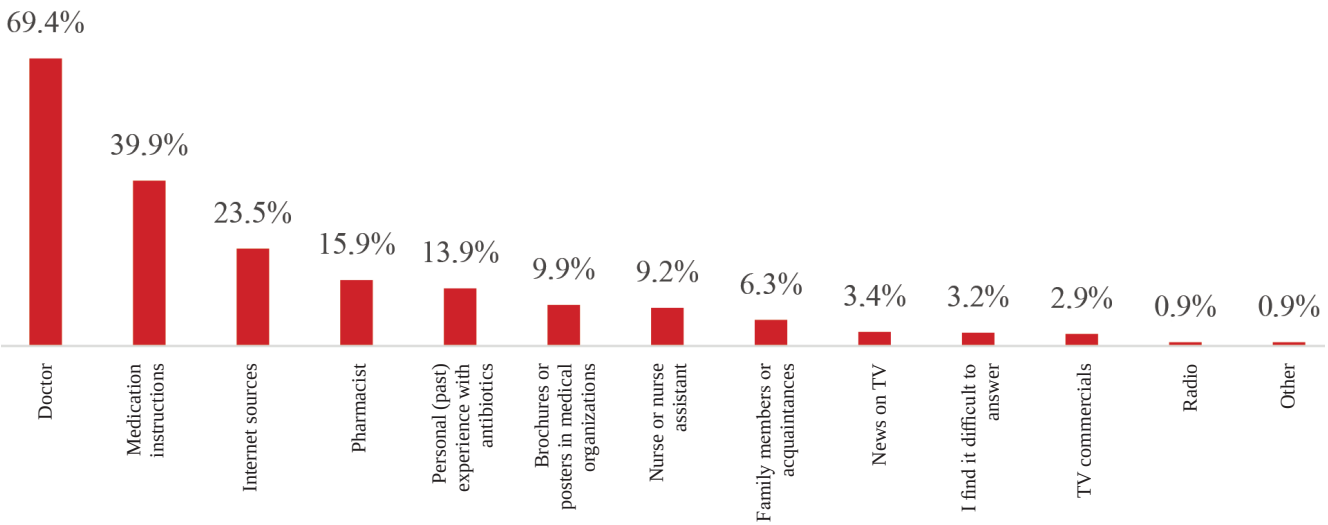


Fig. 2. Sources of information about antibacterial drugs

It is worth noting that the group of persons over 65 years of age from the socio-professional category of pensioners (11.2 and 11.5%, respectively ($p < 0.05$)) relied on TV commercials broadcasting information about ADs. Instructions to medicines as the main source of information about rational use of AD were used by 52.9% ($p < 0.05$) of the respondents over 35 years from the group of employees / managers. Physician's knowledge as the main source of information about ADs was selected in the group of persons with secondary education (72%, $p < 0.05$) (Table 1).

Table 1

**Distribution of the Respondents Depending on Sources of Information about Antibacterial Drugs**

| Parameter | | Physician, % ($n$ = 525, 69.3%) | Medication instruction, % ($n$ = 302, 39.9%) | Internet sources, % ($n$ = 178, 23.5%) | Personal (past) experience, % ($n$ = 105, 13.9%) | Pharmacist, % ($n$ = 120, 15.8%) | Medical nurse/ paramedic, % ($n$ = 70, 9.2%) | TV commercials, % ($n$ = 22, 2.9%) | Family members or acquaintances, % ($n$ = 48, 6.3%) | Brochures or posters in health care organizations, % ($n$ = 75, 9.9%) |
|---|---|---|---|---|---|---|---|---|---|---|
| Age groups | 18–24 years | 76.2 | 44.0 | 19.0 | 11.9 | 23.8 | 13.1 | 2.4* | 9.5 | 7.1 |
| | 25–34 years | 73.9 | 44.9 | 28.4 | 17.6 | 19.9 | 10.2 | 1.7* | 5.1 | 11.9 |
| | 35–44 years | 70.8 | 37.6 | 22.3 | 11.9 | 13.9 | 6.9 | 1.5* | 1.9 | 8.9 |
| | 45–54 years | 65.9 | 38.9 | 29.9 | 16.7 | 10.4 | 6.9 | 2.8* | 7.6 | 12.5 |
| | 55–64 years | 64.0 | 34.8 | 16.9 | 11.2 | 12.4 | 10.1 | 3.4* | 10.1 | 11.2 |
| | 65+ years | 58.1 | 37.1 | 14.5 | 9.7 | 17.7 | 12.9 | 11.2* | 11.2 | 3.2 |
| Socio-professional category | Manager | 72.5 | 52.9* | 19.6 | 11.8 | 11.7 | 7.8 | 3.9 | 3.9 | 17.6 |
| | Self-employed | 44.0 | 20.0 | 20.0 | 20.0 | 12.0 | 4.0 | 0.0 | 8.0 | 0.0 |
| | Entrepreneur | 80.0 | 10.0* | 25.0 | 0.0 | 20.0 | 20.0 | 5.0 | 0.0 | 5.0 |
| | Employee/ specialist | 71.3 | 42.3 | 25.2 | 15.2 | 15.7 | 9.1 | 1.9* | 5.5 | 10.2 |
| | Unemployed | 55.6 | 11.1* | 33.3 | 11.1 | 16.7 | 0.0 | 5.6 | 11.1 | 16.7 |
| | Pensioner | 60.7 | 31.1 | 16.4 | 8.2 | 18.0 | 14.8 | 11.5* | 14.8 | 4.9 |
| | Student | 68.2 | 45.5 | 4.5 | 9.1 | 22.7 | 4.5 | 0.0 | 9.1 | 9.1 |
| Income | Extremely low | 23.8* | 23.8* | 19.0 | 9.5 | 9.5 | 4.8 | 0.0 | 9.5 | 14.3 |
| | Low | 70.5* | 31.8* | 18.6 | 15.5 | 18.6 | 8.5 | 2.4 | 10.1 | 6.2 |
| | Middle | 72.0* | 43.4 | 23.3 | 12.9 | 16.0 | 10.4 | 2.5 | 5.9 | 8.2 |
| | Upper-middle | 69.2* | 42.1* | 29.9 | 14.9 | 17.2 | 9.9 | 4.1 | 4.9 | 14.5 |
| | High | 20.8* | 36.8 | 14.7 | 13.2 | 7.4 | 4.4 | 2.9 | 4.4 | 8.8 |
| Level of education | Completed secondary | 75.9 | 22.4 | 6.9* | 6.9 | 24.1 | 13.8 | 3.4 | 12.1 | 3.4 |
| | Secondary vocational | 70.9 | 30.5 | 20.7 | 11.6 | 16.5 | 12.3 | 2.1 | 6.3 | 7.0* |
| | Unfinished higher education | 58.1 | 38.7 | 16.1 | 9.7 | 19.4 | 13.2 | 3.2 | 9.7 | 6.5 |
| | Higher education | 68.1 | 49.6 | 28.7* | 16.9 | 13.8 | 6.8 | 3.4 | 5.2 | 13.3* |

* $p < 0.05$ between the groups.

Based on the results obtained in the course of the sociological survey, the respondents were characterized depending on their trust in sources of information about AD (Tables 2, 3).

Table 2

**Characteristics of the Respondents Depending on Their Trust in Sources of Information about Antibacterial Drugs**

| Source of information | Respondent characteristics |
|---|---|
| Physician | Female 43.7±14.2 years old, who bought AD according to the doctor's prescription, followed the doctor's recommendations for the use of APs, had a high mean score of knowledge about AD, received information about the correct use of AD during the last 12 months |
| Instructions to AD | A woman who purchased AD from a pharmacy without a doctor's prescription, self-medicated, used leftover AD from a previous course of treatment, with higher education and a high average score of knowledge about AD, who expressed a desire to receive more information about AD |
| Internet sources | A person who purchased AD without a doctor's prescription, with higher education, who had a high average score of knowledge about AD, and expressed a desire to expand their knowledge about AD |
| TV commercials | A person 50.2 ± 16.8 years old who took AD following the advice of a pharmacist, with a low mean score of knowledge about AD |
| Personal experience | A person with higher education, who took AD following the advice of family members or acquaintances, engaged in self-treatment, at the same time having a high average score of knowledge about AD and willing to expand their knowledge about AD |

Table 3

**Characteristics of the Respondents Depending on Sources of Information about Antibacterial Drugs**

| Parameter | Source of information about antibacterial drugs | | | | | | | | | |
|---|---|---|---|---|---|---|---|---|---|---|
| | Physician | | Medication instruction | | Internet sources | | TV commercials | | Personal (past) experience | |
| | Yes | No | Yes | No | Yes | No | Yes | No | Yes | No |
| Female gender, % | 77.5 | 68.9 | 80.8 | 70.9 | – | – | – | – | – | – |
| Settlement type – village, % | – | – | 5.9 | 15.8 | – | – | – | – | – | – |
| Age, years | 40.7 ± 13.7 | 43.7 ± 14.1 | – | – | – | – | 50.2 ± 16.8 | 41.4 ± 13.7 | – | – |
| Higher education, % | – | – | 62.9 | 42.4 | 61.8 | 47.2 | – | – | 61.9 | 48.8 |
| Pensioners, % | – | – | – | – | – | – | 4.5 | 7.3 | – | – |
| Took antibiotics in tablet (capsule) form | 95.2 | 87.1 | – | – | – | – | 81.8 | 93.1 | – | – |
| Took antibiotics in syrup form | 0.8 | 2.6 | – | – | – | – | 9.1 | 1.1 | – | – |
| Took antibiotics in the form of an ointment | | | – | – | – | – | – | – | 2.9 | 0.6 |
| Purchased antibiotics following a prescription or received them during hospitalization, % | 64.6 | 52.2 | – | – | – | – | – | – | – | – |
| Purchased antibiotics from a pharmacy without a doctor’s prescription | 37.1 | 46.6 | 47.0 | 35.4 | 49.4 | 37.1 | – | – | 58.1 | 37.1 |
| Received antibiotics from family members / acquaintances | – | – | – | – | – | – | – | – | 3.8 | 1.2 |
| Took leftover antibiotics from the previous treatment, % | – | – | 10.9 | 4.6 | – | – | – | – | | |
| The source of antibiotic prescription is the physician | 89.3 | 62.9 | – | – | – | – | – | – | 74.3 | 82.4 |
| The source of antibiotic prescription is the paramedic | 1.1 | 3.4 | – | – | – | – | – | – | – | – |
| Source of antibiotic prescription is the pharmacist | – | – | – | – | – | – | 31.8 | 3.9 | – | – |
| The source of antibiotic prescription is users in the Telegram channel | – | – | – | – | – | – | 4.5 | 0.0 | 0.9 | 0.0 |
| The source of antibiotic prescription is a family member or acquaintance | 1.9 | 6.5 | – | – | – | – | – | – | – | – |
| Self-medicattion with antibiotics. | 9.3 | 21.1 | 19.5 | 8.6 | – | – | – | – | 22.9 | 11.3 |
| Rational use of antibiotics, % | 49.3 | 40.5 | – | – | – | – | – | – | – | – |
| Completed the full treatment course with antibiotics, % | 89.3 | 80.6 | – | – | – | – | – | – | – | – |

End of table 3

| Parameter | Source of information about antibacterial drugs | | | | | | | | | |
|---|---|---|---|---|---|---|---|---|---|---|
| | Physician | | Medication instruction | | Internet sources | | TV commercials | | Personal (past) experience | |
| | Yes | No | Yes | No | Yes | No | Yes | No | Yes | No |
| Had tests performed before the initiation of antibacterial therapy | 57.3 | 38.4 | – | – | – | – | – | – | – | – |
| Average score of knowledge about antibiotics | 11. 5 ± 2.2 | 10.5 ± 2.8 | 11.7 ± 2.1 | 10.8 ± 2.5 | 11.8 ± 2.2 | 10.9 ± 2.4 | 9.8 ± 3.1 | 11. 2 ± 2.4 | 11.6 ± 2.3 | 11.1 ± 2.4 |
| Were aware of the ban on the sale of antibiotics without a doctor's prescription, % | 81.7 | 68.1 | 81.8 | 74.7 | – | – | – | – | – | – |
| Received information on correct antibiotic use in the last year, % | 50.5 | 31.5 | – | – | 57.3 | 40.8 | – | – | – | – |
| Would like to receive more information about antibiotic resistance | – | – | 26.8 | 19.6 | – | – | – | – | 33.4 | 20.9 |
| Would like to receive more information about the rational use of antibiotics | – | – | 42.7 | 26.8 | 39.3 | 31.3 | – | – | 45.7 | 31.1 |
| Would like to receive more information about the indications for antibiotic use | – | – | 28.8 | 22.2 | – | – | – | – | – | – |
| Would like to receive more information about the use of antibiotics in agriculture | – | – | 14.2 | 8.8 | 17.4 | 8.9 | – | – | – | – |

Note. The table shows values at which $p < 0.05$ when comparing variables within groups for positive and negative answers from the respondents.

## DISCUSSION

When comparing the data obtained in the present study with the results of a one-stage observational study in the Russian Federation ($n$ = 2,725, 2023), the similarity of information sources about ADs was noted [6]. The top three most common information sources were knowledge and opinion of a doctor (69.4% in the Republic of Belarus and 59.4% in the Russian Federation), medication instructions (39.9% in the Republic of Belarus and 45.5% in the Russian Federation), and Internet sources (23.5% in the Republic of Belarus and 22.7% in the Russian Federation). According to the study by S. Miyano et al. [7], involving 2,045 respondents, doctors and paramedics (46.3%) were also the main source of information about the rational use of ADs, followed by an advice from family members or friends (38.9%) and mass media (26.1%). In an Italian study by R. Zucco et al. with 913 participants, it was found that 73.4% of the respondents received information about ADs from the Internet, and 45% preferred messengers [8].

At the same time, the Republic of Belarus had twice as large a proportion of citizens who received information about the harm of incorrect AP use in the last year (55.0%, $n$ = 419) compared to citizens from the Russian Federation (23.6%, $n$ = 642). The proportion of citizens who wanted to receive information about ADs was identical in both countries (75.2% in the Russian Federation and 75.0% in the Republic of Belarus). The risk group of low public awareness about ADs in both countries was also identical: men with low income, who took ADs without a doctor's prescription following the advice of family members or acquaintances, who self-medicated and did not use drugs normalizing intestinal microflora.

According to the results of the study, obtaining information about the rational use of AD over the last 12 months, and following the recommendations and using the knowledge of a doctor as the main source of information about AD contributed to a decrease in the number of respondents who self-medicated and, as a consequence, to more correct use of ADs. This trend is typical of both the Republic of Belarus and the Russian Federation.

## CONCLUSION

Thus, there is a need to raise public awareness of antibiotic resistance and increase commitment of citizens to optimal use of ADs. Income, age, and socio-professional categories of the population should be taken into account to elevate awareness of the population around ADs.

Working with health professionals is also essential: holding annual training events in medical organizations and pharmacies, organizing internships for professional development, holding conversations with patients during doctor's visits, placing information about the correct use of antibacterial drugs in medical organizations in the form of posters, leaflets, and videos.

### REFERENCES


1. Butler C., Hillier S., Roberts Z. Antibiotic-Resistant Infections in Primary Care are Symptomatic for Longer and Increase Workload: Outcomes for Patients with E Coli Utis. *Br. J. Gen. Pract.* 2006;56 686–692.
2. Costelloe C., Metcalfe C., Lovering A., Mant D., Hay A.D. Effect of Antibiotic Prescribing in Primary Care on Antimicrobial Resistance in Individual Patients: Systematic Review and Meta-Analysis. *BMJ.* 2010;340:c2096. DOI: 10.1136/bmj.c2096.
3. Zueva L.P., Polak M.S., Kaftyreva L.A., Kolosovskaya E.N. Epidemiological Monitoring of Antimicrobial Resistance of Microorganisms Using the WHONET Computer Program. Guidelines. 2004:69. (In Russ.).
4. Kuzmenkov A.Yu., Eidelstein M.V., Kozlov R.S. AMR-map – a System for Monitoring Antibiotic Resistance in Russia. *Clinical Microbiology and Antimicrobial Chemotherapy.* 2021;23(2):198–204. (In Russ.). DOI: 10.36488/cmac.2021.2.198–204.
5. Schuts C., Hulscher L., Prins M. Current Evidence on Hospital Antimicrobial Stewardship Objectives: A Systematic Review and Meta–Analysis. *The Lancet Infectious Diseases.* 2016;16(7):847–856. DOI: 10.1016/s1473-3099(16)00065-7.
6. Chigrina V.P., Tyufilin D.S., Deev I.A., Kobyakova O.S. Sources of Information of the Population of the Russian Federation about Antibacterial Drugs. *Public Health.* 2023;3(2):31–40. (In Russ.). DOI: 10.21045/2782-1676-2023-3-2-31-40.
7. Miyano S., Htoon T., Nozaki I. Public Knowledge, Practices, and Awareness of Antibiotics and Antibiotic Resistance in Myanmar: The Rst National Mobile Phone Panel Survey. *PLoS One.* 2022;17(8):e0273380. DOI: 10.1371/journal.pone.0273380.
8. Zucco R., Lavano F., Anfosso R. Internet and Social Media Use for Antibiotic–Related Information Seeking: Findings From a Survey among Adult Population in Italy. *Int. J. Med. Inform.* 2018;111:131–139. DOI: 10.1016/j.ijmedinf.2017.12.005.


## Author Contribution

Kolchanova N.E. – literature review, acquisition and interpretation of the data, drafting the article, final approval of the manuscript for publication. Sharshakova T.M. – coordination of the study, critical revision of the manuscript for important intellectual content, final approval of the manuscript for publication. Braga A.Y. – literature review, interpretation of the data, compilation of the database, final approval of the manuscript for publication. Chigrina V.P. – statistical processing of the data, critical revision of the manuscript for important intellectual content, drafting the article, final approval of the manuscript for publication. Tyufilin D.S. – acquisition and interpretation of the data, compilation of the database, final approval of the manuscript for publication. Kobyakova O.S. – conception and design of the study, coordination of the study, final approval of the manuscript for publication. Stoma I.O. – coordination of the study, final approval of the manuscript for publication.

## Author Information


**Kolchanova Natalia E.** – Cand. Sci. (Med.), Associate Professor, Department of Otorhinolaryngology with Courses in Ophthalmology and Dentistry, Gomel State Medical University, Gomel, kolchn@yandex.by, https://orcid.org/0000-0002-4501-7821

**Sharshakova Tamara M.** – Dr. Sci (Med.), Professor, Head of the Department of Public Health and Healthcare with Faculty of Advanced Training and Retraining, Gomel State Medical University, Gomel, t_sharshakova@mail.ru, https://orcid.org/0000-0001-5580-5939

**Braga Anna Y.** – Teaching Assistant, Department of General and Clinical Pharmacology, Gomel State Medical University, Gomel, Bragaanna@mail.ru, https://orcid.org/0009-0004-1696-9702

**Chigrina Valeriya P.** – Senior Specialist, Department of Strategic Healthcare Development, Federal Research Institute for Health Organization and Informatics, Moscow, chigrinavp@mednet.ru, https://orcid.org/0000-0002-5044-4836

**Tyufilin Denis S.** – Head of the Department of Strategic Healthcare Development, Federal Research Institute for Health Organization and Informatics, Moscow, tyufilinds@mednet.ru, https://orcid.org/0000-0002-9174-6419

**Kobyakova Olga S.** – Dr. Sci (Med.), Professor, Head of the Federal Research Institute for Health Organization and Informatics, Moscow, kobyakovaos@mednet.ru, https://orcid.org/0000-0003-0098-1403

**Stoma Igor O.** – Dr. Sci. (Med.), Professor, Head of Gomel State Medical University, Gomel, gsmu@gsmu.by, https:/orcid.org/0000-0003-0483-7329

(✉) **Chigrina Valeriya P.,** chigrinavp@mednet.ru

Received on February 26, 2025;
approved after peer review on March 12, 2025;
accepted on March 20, 2025

УДК 617.7-007.681-021.3:575.174.015.3](470+571)
https://doi.org/10.20538/1682-0363-2025-3-68-80

# Interregional differences in *IL-10* and *MMP2* gene polymorphisms in groups of patients with primary open-angle glaucoma in the Russian Federation according to a multicenter study

**Konenkov V.I.[1], Shevchenko A.V.[1], Prokofiev V.F.[1], Arsyutov D.G.[2], Khodjaev N.S.[2], Boiko E.V.[3], Pravosudova M.M.[3], Chuprov A.D.[4], Kuvaitseva Yu.S.[4], Gorbunova N.Yu.[5], Markova A.A.[5], Pshenichnov M.V.[6], Postupaeva N.V.[6], Malysheva Yu.V.[7], Ivanov A.A.[7], Eremina A.V.[8], Trunov A.N.[8], Chernykh V.V.[8]**

*[1] Research Institute of Clinical and Experimental Lymphology – Branch of the Federal Research Center Institute of Cytology and Genetics, Siberian Branch of the Russian Academy of Sciences (IC&G SB RAS)*
*2 Timakov St., 630060 Novosibirsk, Russian Federation*

*[2] S. Fyodorov Eye Microsurgery Federal State Institution*
*59a Beskudnikovsky Blv., 127486 Moscow, Russian Federation*

*[3] Saint Petersburg branch of S. Fyodorov Eye Microsurgery Federal State Institution*
*21a Yaroslav Hashek St., 192283 Saint Petersburg, Russian Federation*

*[4] Orenburg branch of S. Fyodorov Eye Microsurgery Federal State Institution*
*17 Salmyshskaya St., 460047 Orenburg, Russian Federation*

*[5] Cheboksary branch of S. Fyodorov Eye Microsurgery Federal State Institution*
*10 Traktorostroiteley Ave., 428028 Cheboksary, Russian Federation*

*[6] Khabarovsk branch of S. Fyodorov Eye Microsurgery Federal State Institution*
*211 Tikhookeanskaya St., 680033 Khabarovsk, Russian Federation*

*[7] Irkutsk branch of S. Fyodorov Eye Microsurgery Federal State Institution*
*337 Lermontov St., 664033 Irkutsk, Russian Federation*

*[8] Novosibirsk branch of S. Fyodorov Eye Microsurgery Federal State Institution*
*10 Kolhidskaya St., 630096 Novosibirsk, Russian Federation*

## ABSTRACT

**Background.** Primary open-angle glaucoma (POAG) is optic neuropathy, the etiology of which is associated with genetic and non-genetic factors. *IL-10* and *MMP2* SNPs are associated with POAG, but the nature of the association depends on the ethnic profile of the population. For the Russian Federation, whose population includes 190 nationalities, this issue is relevant.

**Aim.** To perform a multicenter comparative analysis of the *IL-10* and *MMP2* SNPs as potential factors for predicting the development of POAG in patients in four regions of the Russian Federation: the Novosibirsk, Leningrad, and Orenburg Regions, and the Chuvash Republic.

**Materials and methods.** We examined 499 POAG patients from 4 branches of S. Fyodorov Eye Microsurgery Federal State Institution (main group), 530 people without visual pathology (control 1), and 100 patients with cataracts (control 2). Genotyping of *IL10* (rs1800896 and rs1800872 SNPs) and *MMP*-2 (rs243865) was performed by real-time polymerase chain reaction (RT-PCR) according to the manufacturer's instructions (Lytex and Syntol, Russia). The differences were considered statistically significant at the Bonferroni-corrected $p < 0.05$.

✉ *Konenkov Vladimir I.,* vikonenkov@gmail.com

**Results.** An increase in the incidence of *IL-10-1082 A* was revealed in POAG patients compared to patients with cataract and healthy individuals. An increase in the incidence of *IL-10 AA* in both regions and a decrease in the frequency of *MMP2-1306 TT* were found. Similar patterns were established for interlocus *IL-10* and *MMP2* genotypes. The group of patients in the Leningrad Region differed the most compared to other regions, which may be due to their long-term residence together with the indigenous Finno – Ugric peoples.

**Conclusion.** The data obtained should be taken into account when developing additional criteria for predicting predisposition to POAG, which is important in case of POAG in the family history.

**Keywords:** *IL-10, MMP2*, SNP, POAG

**Conflict of interest.** The authors declare the absence of obvious or potential conflicts of interest related to the publication of this article.

**Source of financing.** The work was carried out within the agreement on scientific and practical cooperation between the Research Institute of Clinical and Experimental Lymphology and the Novosibirsk Branch of S. Fyodorov Eye Microsurgery Federal State Institution.

**Conformity with the principles of ethics.** All study participants signed an informed consent to personal data processing. The study was approved by the Bioethics Committee at the Research Institute of Clinical and Experimental Lymphology (Minutes No. 177 dated February 2, 2003) and Novosibirsk branch of S. Fyodorov Eye Microsurgery Federal State Institution (Minutes No. 2 dated September 2, 2018).

**For citation:** Konenkov V.I., Shevchenko A.V., Prokofiev V.F., Arsyutov D.G., Khodjaev N.S., Boiko E.V., Pravosudova M.M., Chuprov A.D., Kuvaitseva Yu.S., Gorbunova N.Yu., Markova A.A., Pshenichnov M.V., Postupaeva N.V., Malysheva Yu.V., Ivanov A.A., Eremina A.V., Trunov A.N., Chernykh V.V. Interregional differences in Il-10 and MMP2 gene polymorphisms in groups of patients with primary open-angle glaucoma in the Russian federation according to a multicenter study. *Bulletin of Siberian Medicine.* 2025;24(3):68–80. https://doi.org/10.20538/1682-0363-2025-3-68-80.

# Межрегиональные различия распределения SNP генов *IL-10* и *MMP2* в группах пациентов с первичной открытоугольной глаукомой по данным многоцентрового исследования в Российской Федерации

**Коненков В.И.[1], Шевченко А.В.[1], Прокофьев В.Ф.[1], Арсютов Д.Г.[2], Ходжаев Н.С.[2], Бойко Э.В.[3], Правосудова М.М.[3], Чупров А.Д.[4], Кувайцева Ю.С.[4], Горбунова Н.Ю.[5], Маркова А.А.[5], Пшеничнов М.В.[6], Поступаева Н.В.[6], Малышева Ю.В.[7], Иванов А.А.[7], Еремина А.В.[8], Трунов А.Н.[8], Черных В.В.[8]**

*[1] Научно-исследовательский институт клинической и экспериментальной лимфологии – филиал Федерального исследовательского центра «Институт цитологии и генетики Сибирского отделения Российской академии наук» (НИИКЭЛ – филиал ИЦиГ СО РАН)*
*Россия, 630060, г. Новосибирск, ул. Тимакова, 2*

*[2] Национальный медицинский исследовательский центр (НМИЦ) «Межотраслевой научно-технический комплекс (МНТК) “Микрохирургия глаза” им. акад. С.Н. Федорова»*
*Россия, 127486, г. Москва, Бескудниковский бульвар, 59а*

*[3] Санкт-Петербургский филиал НМИЦ «МНТК “Микрохирургия глаза” им. акад. С.Н. Федорова»*
*Россия, 192283, г. Санкт-Петербург, ул. Ярослава Гашека, 21*

*[4] Оренбургский филиал НМИЦ «МНТК “Микрохирургия глаза” им. акад. С.Н. Федорова*
*Россия, 460047, г. Оренбург, ул. Салмышская, 17*

*[5] Чебоксарский филиал НМИЦ «МНТК “Микрохирургия глаза” им. акад. С.Н. Федорова» Россия, 428028, Чувашская Республика, г. Чебоксары, проспект Тракторостроителей, 10*

[6] *Хабаровский филиал НМИЦ «МНТК "Микрохирургия глаза" им. акад. С.Н. Федорова» Россия, 680033, г. Хабаровск, ул. Тихоокеанская, 211*

[7] *Иркутский филиал НМИЦ «МНТК "Микрохирургия глаза" им. акад. С.Н. Федорова» Россия, 664033, г. Иркутск, ул. Лермонтова, 337*

[8] *Новосибирский филиал НМИЦ «МНТК "Микрохирургия глаза" им. акад. С.Н. Федорова» Россия, 630096, г. Новосибирск, ул. Колхидская, 10*

## РЕЗЮМЕ

**Обоснование.** Первичная открытоугольная глаукома (ПОУГ) – хроническая прогрессирующая оптиконейропатия, этиология которой связана с генетическими и негенетическими факторами. Полиморфизмы SNP генов *IL-10* и *MMP2* ассоциированы с ПОУГ, однако характер ассоциированности зависит от этнического состава населения. Для Российской Федерации, население которой состоит из представителей 190 национальностей, это актуальная проблема.

**Цель** исследования – многоцентровый сравнительный анализ распределения SNP генов *IL-10* и *MMP2* как потенциальных факторов прогноза развития заболевания в группах пациентов с ПОУГ в четырех регионах населения России: Новосибирской, Ленинградской и Оренбургской областей, Чувашской Республики.

**Материалы и методы.** Обследованы 499 пациентов с ПОУГ (основная группа) из четырех филиалов Межотраслевого научно-технического комплекса «Микрохирургия глаза», 530 человек без патологии органов зрения (контроль 1) и 100 пациентов с катарактой (контроль 2). Генотипирование генов *IL-10* (полиморфизмы rs1800896, rs1800872) и *MMP2* (полиморфизм rs243865) проводили методом полимеразной цепной реакции в реальном времени согласно инструкции фирмы производителя («Литех» и «Синтол», Россия). Статистически значимыми считались различия при $p < 0,05$ с учетом поправки Бонферрони.

**Результаты.** Выявлено достоверное преобладание локуса -1082 аллеля *A* (ген *IL-10)* у пациентов с ПОУГ относительно лиц с катарактой и здоровых. Установлено повышение частоты генотипа *AA* (*IL-10)* в обеих позициях и снижение частоты -1306 TT (*MMP2*). Сходные закономерности установлены для межлокусных генотипов *IL-10* и *MMP2.* Получены данные о наличии достоверных различий в характере распределения аллей, генотипов между регионами России. Наиболее отличалась от остальных регионов группа пациентов Ленинградской области, что может быть связано с ее многолетним проживанием совместно с коренным населением финно-угорского происхождения.

**Заключение.** Полученные данные необходимо учитывать при разработках дополнительных критериев прогноза предрасположенности к развитию ПОУГ, что актуально при наличии отягощенного семейного анамнеза.

**Ключевые слова:** *IL-10, MMP2*, SNP, ПОУГ

**Источник финансирования.** Работа выполнена в рамках договора о научно-практическом сотрудничестве между НИИКЭЛ – филиалом ИЦиГ СО РАН и Новосибирским филиалом МНТК «Микрохирургия глаза» им. акад. С.Н. Федорова Минздрава России.

**Конфликт интересов.** Авторы заявляют об отсутствии конфликта интересов при проведении исследования.

**Соответствие принципам этики.** Все участники подписали письменное информированное согласие на участие в исследовании и обработку персональных данных Исследование одобрено комитетами по биомедицинской этике НИИКЭЛ – филиалом ИЦиГ СО РАН (протокол № 177 от 02.02.2003) и Новосибирского филиала МНТК «Микрохирургия глаза» им. акад. С.Н. Федорова Минздрава России (протокол № 2 от 2.09.2018).

**Для цитирования:** Коненков В.И., Шевченко А.В., Прокофьев В.Ф., Арсютов Д.Г., Ходжаев Н.С., Бойко Э.В., Правосудова М.М., Чупров А.Д., Кувайцева Ю.С., Горбунова Н.Ю., Маркова А.А., Пшеничнов М.В., Поступаева Н.В., Малышева Ю.В., Иванов А.А., Еремина А.В., Трунов А.Н., Черных В.В. Межрегиональные различия распределения SNP генов IL-10 и MMP2 в группах пациентов с первичной открытоугольной глаукомой по данным многоцентрового исследования в Российской Федерации. *Бюллетень сибирской медицины.* 2025;24(3):68–80. https://doi.org/10.20538/1682-0363-2025-3-68-80.

## INTRODUCTION

Primary open-angle glaucoma (POAG) is chronic progressive optic neuropathy that unites a group of diseases whose etiology is not fully understood. Its origin and development are predominantly explained by a multifactorial concept involving the variety of genetic and non-genetic factors [1]. Among the causes of incurable blindness in Russia, glaucoma occupies one of the leading places, exceeding the European average by 1.5–2 times [2]. In addition to genetic predisposition, disorders of aqueous humor outflow caused by impaired angiogenesis, damage to the optic nerve, and retinal ganglion cell loss play an essential role in the development of POAG [3]. Both vascular (circulatory and lymphatic vascular) networks and extravascular spaces (extracellular matrix) are involved in the aqueous humor outflow [4].

Matrix metalloproteinases (MMPs) are a family of proteolytic enzymes that break down extracellular matrix (ECM) components and are crucial in many biological processes, including the development and remodeling of tissues both in normal and pathological conditions. This family of zinc-containing endopeptidases, which catalyze degradation reactions of ECM components, consists of more than 20 enzymes in the human body. The substrates for MMP-2 are gelatinases represented by type 4 collagen, aggrecan, gelatin, and fibronectin. The activity of MMPs is affected by their expression level and the expression of tissue inhibitors of MMPs. In the eye, MMP-mediated ECM turnover in the juxtacanalicular region of the ocular trabecular meshwork reduces aqueous humor outflow resistance and helps maintain intraocular pressure homeostasis [5, 6].

MMPs are involved in the pathogenesis of various types of glaucoma; the content of MMP-2 and -9 is significantly higher in glaucomatous eyes compared to healthy ones. These changes were found in watery eye discharge, the iridocorneal angle, and the Tenon capsule in patients with POAG, primary angle-closure glaucoma, and exfoliative glaucoma. An increase in the content of MMP-9 both in the systemic circulation and locally may also indicate impaired cellular remodeling in the structures of the eye, which contributes to the formation of autoimmune inflammation with tissue destruction [7].

Associations have been established between the genotypes 1G/2G *(MMP-1* gene*)*, C/T *(MMP-9* gene*)* ($p < 0.001$), and C/T *(IL-1b* gene*)* ($p < 0.05$) and a decrease in the thickness of the retinal nerve fiber layer in the group of patients with POAG. The results showed a relationship between the reduced rim area and the A/G genotype *(MMP-12* gene*)* ($p < 0.001$). The normal value of this parameter was detected in the group of patients with POAG associated with the genotypes T/C *(TIMP1* gene) ($p < 0.05$) and C/T *(IL1b* gene) ($p < 0.05$). Finally, the results showed an association of the C/T genotype *(MMP-9* gene*)* ($p < 0.001$) with a decrease in the optic disc excavation index in the group of patients with POAG [8].

In humans, the *MMP-2* gene is located on chromosome 16. A total of 37 polymorphisms located in the *MMP-2* gene were studied, most of which are located in the promoter region. The main polymorphisms studied were rs243865, rs2285053, rs243866, and rs243864, which can affect the expression of encoded regulatory proteins.

Cytokines, and in particular the inhibitory immunosuppressive interleukin (IL)-10, play an essential role in regulating the functional activity of MMP. IL-10 stimulates tissue inhibitors of metalloproteinases (TIMPs) and inhibits the expression of MMP, thus influencing the induction of angiogenesis [9].

In humans, IL-10 is encoded by the *IL-10* gene located on the long arm of chromosome 1. The *IL-10* gene promoter is characterized by the presence of polymorphisms that can significantly affect IL-10 expression in different people [10]. Of the 49 polymorphisms identified, 46 are single-nucleotide polymorphisms (SNPs), 2 are microsatellite polymorphisms, and 1 is a small (3-letter) dropout. Twenty-eight polymorphisms occur in the promoter region of the gene, 20 polymorphisms are non-coding intronic or synonymous substitutions, and only 1 polymorphism leads to a change in the amino acid sequence of the protein.

Based on these data, we formulated the aim of the study – to conduct a multicenter comparative analysis of the distribution of three SNPs of the *IL-10* and *MMP2* genes as potential factors for predicting the development of POAG in patients in four regions of the Russian Federation: the Novosibirsk, Leningrad, and Orenburg Regions, and the Chuvash Republic. These studies are relevant for the Russian Federation, where, according to the latest population census, more than 190 nationalities of various ethnicities live.

## MATERIALS AND METHODS

We performed a comparative, multicenter, case – control genetic study of 499 patients with POAG (main group) from four regions of the Russian Federation.

The patients were treated and followed up in Novosibirsk (199 people), Cheboksary (100 people), Orenburg (100 people), and Saint Petersburg (100 people) branches of S. Fyodorov Eye Microsurgery Federal State Institution. The study included patients aged 36–91 years, with a median of 71.0 [66.0; 76.0] years; 259 men (51.9%) and 240 women (48.1%).

Control group 1 (530 people) included apparently healthy individuals (157 men and 373 women) aged 18–69 years. Control group 2 encompassed 100 patients with cataract who received treatment in the Novosibirsk branch of S. Fyodorov Eye Microsurgery Federal State Institution. Relatives of the patients were not included either in the main or in the control groups.

The study was approved by the Bioethics Committees at Research Institute of Clinical and Experimental Lymphology – Branch of the Institute of Cytology and Genetics, Siberian Branch of Russian Academy of Sciences (Minutes No. 177 dated 02.02.2003) and the Novosibirsk Branch of S. Fyodorov Eye Microsurgery Federal State Institution (Minutes No. 2 dated 2.09.2018) and was carried out in accordance with the WMA Declaration of Helsinki "Ethical Principles of Conducting Medical Research Involving Humans as Subjects" (Fortaleza, Brazil, October 2013). A written informed consent was obtained from all participants to participation in the study and to personal data processing.

The inclusion criterion for the main group was stage II–III POAG with the axial length of 22.5–24.5 mm.

The exclusion criteria were the presence of any hereditary and genetic diseases, autoimmune diseases and tumors of any localization (including multiple sclerosis, diabetes mellitus of any form, cataracts (total cataract, if it made it difficult to conduct an instrumental examination), neovascular, pigmentary glaucoma, low-tension glaucoma, keratitis and uveitis of various etiology and localization, central retinal vein occlusion, central serous chorioretinopathy, wet macular degeneration, eye injuries and burns in the medical history.

The diagnosis of POAG was verified according to the developed and approved criteria set out in the clinical guidelines "Primary open-angle glaucoma" (http://avo-portal.ru/documents/fkr/Klinicheskie_rekomendacii_POUG_2022.pdf).

To assess intraocular pressure (IOP), applanation tonometry data were used. Structural pathological neuroretinal alterations were assessed following protocols for the optic disc and retinal nerve fiber layer examination (according to optical coherence tomography). Typical defects in the visual field were confirmed by the perimeter index *MD* (average deviation of photosensitivity) and narrowing of the boundaries of the visual field along the nasal isopters. Grade 3–4 opening of the iridocorneal angle was confirmed by gonioscopy. Given the fact that the Russian classification of POAG includes four clinical and pathogenetic forms (pseudoexfoliative glaucoma, chronic (simple) glaucoma, low-tension glaucoma, and pigmentary glaucoma), biomicroscopy of the anterior segment of the eye was performed. Its results allowed for the differential diagnosis and correct selection of patients. The study included patients with pseudoexfoliative glaucoma and primary simple glaucoma.

Single-nucleotide polymorphisms of the *IL10* gene (-592 C/A, rs1800872 and -1082 G/A, rs1800896) were genotyped using real-time polymerase chain reaction (RT-PCR) with the SYBR Green dye (Lytech and Syntol, Russia) on the DT-96 amplifier (DNA Technology, Russia) according to the manufacturer's instructions. DNA isolation and RT-PCR were performed using a unified instrument and reagent database at the Laboratory for Clinical Immunogenetics of the Research Institute of Clinical and Experimental Lymphology (Novosibirsk).

Statistical processing of the results was carried out using IBM SPSS Statistics 23 and specialized programs for volumetric processing of biological information, including multidimensional genetic analysis: Arlequin 3.5.2, SNPStats, and Cytoscape 3.10.3. When analyzing the results of the genetic study, the allele and genotype frequency, their poly-locus combinations, the odds ratio (OR), and the 95% confidence interval (95% CI) were calculated. The distribution of genotypes across the studied polymorphic loci was checked for compliance with the Hardy – Weinberg equilibrium using the exact Fisher's criterion. The significance level of differences in the frequency of genetic trait distribution (alleles, simple and complex genotypes) in the compared groups was determined by the two-tailed Fisher's exact test for 2 x 2 contingency tables (P_TMF2). To eliminate the effect of multiple comparisons, the Bonferroni correction was applied. The critical significance level when testing statistical hypotheses was assumed to be 0.05.

## RESULTS

At the first stage of the study, it was necessary to identify groups comparing the results identified among patients with POAG with the controls. As the latter, we identified groups of healthy individuals without signs of visual organ dysfunction (control 1) as the most representative and a group of patients with cataract who did not have an increase in IOP (control 2, 100 people). The comparison group (control 1) included 530 people that matched with the main POAG group (499 people) based on gender and age. The results of comparing the distribution of the studied parameters are presented in Table 1.

Table 1

**Results of the Frequency Distribution of rs243865 in the *MMP-2* Gene, rs1800896 and rs1800872 in the *IL-10* Gene in Groups of Patients with POAG and Healthy Individuals**

| Polymorphic region of the gene | Alleles/ genotypes | POAG | Donors | | | | |
|---|---|---|---|---|---|---|---|
| | | Frequency, % | | OR | OR_CI95 | *p*_TMF2 | *p*_COR |
| IL10-592 | C | 77.5 | 79.9 | 0.86 | 0.69–1.07 | 0.187 | 0.374 |
| IL10-592 | A | 22.6 | 20.1 | 1.16 | 0.93–1.44 | 0.187 | 0.374 |
| IL10-1082 | A | 63.1 | 49.8 | 1.73 | 1.38–2.16 | 0.000 | 0.000 |
| IL10-1082 | G | 36.9 | 50.2 | 0.58 | 0.46–0.73 | 0.000 | 0.000 |
| MMP2-1306 | C | 75.7 | 74.6 | 1.06 | 0.84–1.33 | 0.639 | 1.278 |
| MMP2-1306 | T | 24.4 | 25.4 | 0.95 | 0.75–1.19 | 0.639 | 1.278 |
| IL10-592 | CC | 60.7 | 62.6 | 0.93 | 0.72–1.20 | 0.556 | 1.669 |
| IL10-592 | CA | 33.5 | 34.8 | 0.94 | 0.72–1.23 | 0.687 | 2.061 |
| IL10-592 | AA | 5.8 | 2.7 | 2.25 | 1.15–4.37 | 0.017 | 0.052 |
| IL10-1082 | AA | 38.5 | 22.8 | 2.12 | 1.48–3.04 | 0.000 | 0.000 |
| IL10-1082 | AG | 49.3 | 54.0 | 0.83 | 0.60–1.14 | 0.260 | 0.781 |
| IL10-1082 | GG | 12.2 | 23.2 | 0.46 | 0.31–0.69 | 0.000 | 0.001 |
| MMP2-1306 | CC | 55.7 | 57.1 | 0.95 | 0.71–1.26 | 0.718 | 2.155 |
| MMP2-1306 | CT | 39.9 | 35.1 | 1.23 | 0.92–1.64 | 0.184 | 0.552 |
| MMP2-1306 | TT | 4.4 | 7.8 | 0.54 | 0.39–0.98 | 0.045 | 0.136 |
| IL10-592:IL10-1082 | CC-AA | 17.0 | 10.8 | 1.69 | 1.04–2.75 | 0.033 | 0.260 |
| IL10-592:IL10-1082 | CC-AG | 32.7 | 32.9 | 0.99 | 0.71–1.39 | 1.000 | 8.000 |
| IL10-592:IL10-1082 | CC-GG | 11.0 | 18.9 | 0.53 | 0.34–0.82 | 0.006 | 0.050 |
| IL10-592:IL10-1082 | CA-AA | 16.6 | 9.9 | 1.81 | 1.10–2.99 | 0.022 | 0.174 |
| IL10-592:IL10-1082 | CA-AG | 15.6 | 20.7 | 0.71 | 0.47–1.06 | 0.109 | 0.869 |
| IL10-592:IL10-1082 | CA-GG | 1.2 | 4.5 | 0.26 | 0.09–0.72 | 0.011 | 0.085 |
| IL10-592:IL10-1082 | AA-AA | 4.8 | 1.8 | 2.75 | 0.94–8.03 | 0.060 | 0.483 |
| IL10-592:IL10-1082 | AA-AG | 1.0 | 0.5 | 2.24 | 0.26–19.26 | 0.672 | 5.378 |
| IL10-592:MMP2-1306 | CC-CC | 35.1 | 32.9 | 1.10 | 0.82–1.49 | 0.544 | 4.352 |
| IL10-592:MMP2-1306 | CC-CT | 22.7 | 24.6 | 0.90 | 0.64–1.25 | 0.551 | 4.411 |
| IL10-592:MMP2-1306 | CC-TT | 3.0 | 5.1 | 0.58 | 0.28–1.18 | 0.136 | 1.09 |
| IL10-592:MMP2-1306 | CA-CC | 17.2 | 21.4 | 0.76 | 0.54–1.09 | 0.141 | 1.131 |
| IL10-592:MMP2-1306 | CA-CT | 14.8 | 10.5 | 1.48 | 0.95–2.29 | 0.088 | 0.706 |
| IL10-592:MMP2-1306 | CA-TT | 1.4 | 2.9 | 0.48 | 0.18–1.30 | 0.193 | 1.547 |
| IL10-592:MMP2-1306 | AA-CC | 3.4 | 2.2 | 1.54 | 0.63–3.76 | 0.399 | 3.194 |
| IL10-592:MMP2-1306 | AA-CT | 2.4 | 0.3 | 7.69 | 0.99–54.42 | 0.021 | 0.169 |
| IL10-1082:MMP2-1306 | AA-CC | 20.2 | 11.9 | 1.88 | 1.17–3.01 | 0.007 | 0.065 |
| IL10-1082:MMP2-1306 | AA-CT | 17.2 | 9.5 | 1.98 | 1.18–3.31 | 0.008 | 0.072 |
| IL10-1082:MMP2-1306 | AA-TT | 1.0 | 1.4 | 0.70 | 0.17–2.95 | 0.700 | 6.300 |
| IL10-1082:MMP2-1306 | AG-CC | 28.7 | 27.6 | 1.05 | 0.73–1.51 | 0.855 | 7.697 |
| IL10-1082:MMP2-1306 | AG-CT | 18.0 | 21.9 | 0.78 | 0.53–1.17 | 0.251 | 2.257 |
| IL10-1082:MMP2-1306 | AG-TT | 2.6 | 3.8 | 0.68 | 0.28–1.65 | 0.467 | 4.196 |

End of Table 1

| Polymorphic region of the gene | Alleles/ genotypes | POAG | Donors | | | | |
|---|---|---|---|---|---|---|---|
| | | Frequency, % | | OR | OR_CI95 | *p*_TMF2 | *p*_COR |
| IL10-1082:MMP2-1306 | GG-CC | 6.8 | 15.2 | 0.41 | 0.24–0.68 | 0.001 | 0.009 |
| IL10-1082:MMP2-1306 | GG-CT | 4.6 | 7.1 | 0.63 | 0.32–1.23 | 0.201 | 1.805 |
| IL10-1082:MMP2-1306 | GG-TT | 0.8 | 1.4 | 0.56 | 0.12–2.51 | 0.428 | 3.856 |
| IL10-592:IL10-1082:MMP2-1306 | CC-AA-CC | 9.6 | 3.8 | 2.67 | 1.24–5.76 | 0.009 | 0.187 |
| IL10-592:IL10-1082:MMP2-1306 | CC-GG-CC | 6.2 | 11.5 | 0.51 | 0.29–0.89 | 0.021 | 0.437 |
| IL10-592:IL10-1082:MMP2-1306 | CA-AA-CT | 7.8 | 2.4 | 3.46 | 1.34–8.90 | 0.006 | 0.120 |
| IL10-592:IL10-1082:MMP2-1306 | CA-GG-CC | 0.6 | 3.8 | 0.15 | 0.04–0.58 | 0.004 | 0.076 |
| IL10-592:IL10-1082:MMP2-1306 | AA-AA-CT | 2.2 | 0.0 | 5.15 | 0.67–39.89 | 0.040 | 0.832 |

Note. Here and in Table 2: *p*_TMF2 – significance of the two-ailed Fisher's exact test; *p*_COR – Bonferroni-corrected significance.

As seen from the data presented, the distribution of *IL-10* gene alleles at position *-592* and *MMP2* gene alleles at position *-1306* was similar in both compared groups, whereas at position *-1082*, significant predominance of allele *A* among patients was revealed.

For the SNP genotypes of the *IL-10* gene, an increase in the frequency of homozygous *AA* variants at both positions and a decrease in the frequency of the homozygous *TT* variant of the *MMP2* gene in the position *-1306* were found. A slight increase in the frequency of *CC-AA* and *CA-AA* genotypes was also detected in the group of patients with POAG, along with a decrease in the frequency of *IL-10* genotypes containing the *G* allele.

Similar patterns were established for the interlocus genotypes of the *IL-10* and *MMP2* genes, which are characterized by a combination of alleles A and C at positions -592 and -1082 and double homozygotes GG / CC at position -1082. Minor multidirectional changes were revealed for three-locus combinations.

The conducted studies of patients from the Novosibirsk branch S. Fyodorov Eye Microsurgery Federal State Institution showed that, unlike the control group of patients with cataracts who did not have an increase in IOP, a significant decrease in the frequency of the homozygous *TT* variant of the *MMP-2* gene at position *-1306* (OR = 0.33; *p*_ cor = 0.0258) was also found among patients with POAG. Moreover, this pattern persisted in the complex genotype *IL10-1082:MMP2-1306 AA-TT* (OR = 0.07; *p*_cor = 0.0207) and with lower reliability in the complex genotype *IL10-592:IL10-1082:MMP2-1306 CC-AA-TT* (OR = 0.08; *p*_ TMF2 = 0.0039; *p*_cor = 0.08). This conclusion was also verified by comparing the data obtained in a group of patients with POAG with the results of the study of healthy individuals (526 people) used as an additional control group. The frequency of distribution of the homozygous *TT* variant at *MMP2-1306* position among patients with POAG was also significantly lower (OR = 0.54; *p* = 0.045) than among healthy individuals without identified eye diseases.

Based on the above data, these results can be interpreted as indirect evidence that the level of MMP-2 expression in patients with POAG should be higher, which can be regarded as one of the possible factors of ECM disorders in this eye disease. For our multinational country, it is interesting to see how common the data obtained are for a number of regions of the Russian Federation, or whether there are significant differences in these distributions. To get an answer to this question, we conducted a joint study with branches of S. Fyodorov Eye Microsurgery Federal State Institution located in such regions as Saint Petersburg, Orenburg, Cheboksary, and Novosibirsk. The results of this multicenter study are presented in Table 2.

The results presented in Table 2 show that interregional differences were revealed in a number of analyzed genetic parameters between the patient groups from the Novosibirsk Region and the Chuvash Republic, which is probably due to different representation of the Mongoloid population in these regions, with predominantly white population. It was found that the frequency of the *TT* genotype in the position *-1306* of the *IL-10* gene was increased among patients from the NSR, while it was completely absent in patients from the CHR.

**Differences between the Distribution Parameters of rs243865 of the *MMP-2* Gene and rs1800896 and rs1800872 of the *IL-10* Gene in Groups of Patients with POAG according to the Data of Four Branches of S. Fyodorov Eye Microsurgery Federal State Institution (Frequency is Indicated in %)**

| Polymorphic genotypes | | NSR | CHR | OR | LR | *p*_ TMF2 | *p*_ TMF2 | *p*_ TMF2 | *p*_ TMF2 | *p*_ TMF2 | *p*_ TMF2 | *p*_cor | *p* _cor | *p*_cor | *p*_cor | *p*_cor | *p*_cor |
|---|---|---|---|---|---|---|---|---|---|---|---|---|---|---|---|---|---|
| | | 1 | 2 | 3 | 4 | 1-2 | 1-3 | 1-4 | 2-3 | 2-4 | 3-4 | 1-2 | 1-3 | 1-4 | 2-3 | 2-4 | 3-4 |
| *MMP2-1306* | *C* | 74.9 | 74.5 | 78.0 | 76.0 | 0.920 | 0.419 | 0.841 | 0.481 | 0.817 | 0.722 | 1.842 | 0.838 | 1.682 | 0.962 | 1.634 | 1.443 |
| *MMP2-1306* | *T* | 25.1 | 25.5 | 22.0 | 24.0 | 0.920 | 0.419 | 0.841 | 0.481 | 0.817 | 0.727 | 1.842 | 0.830 | 1.682 | 0.962 | 1.634 | 1.443 |
| *MMP2-1306* | *CC* | 55.3 | 49.0 | 58.0 | 61.0 | 0.327 | 0.711 | 0.387 | 0.257 | 0.118 | 0.773 | 0.982 | 2.134 | 1.160 | 0.770 | 0.353 | 2.320 |
| *MMP2-1306* | *CT* | 39.2 | 51.0 | 40.0 | 30.0 | 0.063 | 0.901 | 0.127 | 0.155 | 0.004 | 0.182 | 0.190 | 2.702 | 0.382 | 0.466 | 0.011 | 0.546 |
| *MMP2-1306* | *TT* | 5.5 | 0.0 | 2.0 | 9.0 | 0.018 | 0.232 | 0.326 | 0.497 | 0.003 | 0.058 | 0.055 | 0.695 | 0.980 | 1.493 | 0.010 | 0.176 |
| *IL10-592:MMP2-1306* | *CC-CC* | 30.2 | 31.0 | 39.0 | 45.0 | 0.895 | 0.152 | 0.015 | 0.299 | 0.058 | 0.474 | 7.157 | 1.2144 | 0.116 | 2.096 | 0.463 | 3.791 |
| *IL10-592:MMP2-1306* | *CC-CT* | 17.1 | 34.0 | 18.0 | 27.0 | 0.001 | 0.872 | 0.049 | 0.015 | 0.357 | 0.175 | 0.010 | 6.978 | 0.394 | 0.106 | 2.855 | 1.401 |
| *IL10-592:MMP2-1306* | *CC-TT* | 4.0 | 0.0 | 0.0 | 7.0 | 0.055 | 0.053 | 0.273 | | 0.014 | 0.014 | 0.442 | 0.442 | 2.185 | | 0.112 | 0.112 |
| *IL10-592:MMP2-1306* | *CA-CC* | 21.6 | 14.0 | 16.0 | 13.0 | 0.122 | 0.283 | 0.084 | 0.843 | 1.000 | 0.689 | 0.974 | 2.266 | 0.674 | 5.903 | 8.000 | 5.508 |
| *IL10-592:MMP2-1306* | *CA-CT* | 20.1 | 14.0 | 19.0 | 1.0 | 0.207 | 0.879 | 0.000 | 0.446 | 0.001 | 0.000 | 1.659 | 7.028 | 0.001 | 3.125 | 0.005 | 0.001 |
| *IL10-592:MMP2-1306* | *CA-TT* | 1.5 | 0.0 | 2.0 | 2.0 | 0.553 | 1.000 | 1.000 | 0.497 | 0.498 | 1.000 | 4.426 | 8.000 | 8.000 | 3.483 | 3.980 | 8.000 |
| *IL10-592:MMP2-1306* | *AA-CC* | 3.5 | 4.0 | 3.0 | 3.0 | 1.000 | 1.000 | 1.000 | 1.000 | 1.000 | 1.000 | 8.000 | 8.000 | 8.000 | 7.000 | 8.000 | 8.000 |
| *IL10-592:MMP2-1306* | *AA-CT* | 2.0 | 3.0 | 3.0 | 2.0 | 0.690 | 0.690 | 1.000 | 1.000 | 1.000 | 1.000 | 5.521 | 5.521 | 8.000 | 7.000 | 8.000 | 8.000 |
| *IL10-1082:MMP2-1306* | *AA-CC* | 20.6 | 18.0 | 19.0 | 23.0 | 0.646 | 0.879 | 0.656 | 1.000 | 0.484 | 0.603 | 5.817 | 7.907 | 5.900 | 7.000 | 4.355 | 5.426 |
| *IL10-1082:MMP2-1306* | *AA-CT* | 12.6 | 26.0 | 21.0 | 14.0 | 0.003 | 0.063 | 0.719 | 0.505 | 0.051 | 0.264 | 0.048 | 0.567 | 6.474 | 3.535 | 0.458 | 2.376 |
| *IL10-1082:MMP2-1306* | *AA-TT* | 0.5 | 0.0 | 2.0 | 2.0 | 1.000 | 0.260 | 0.260 | 0.497 | 0.498 | 1.000 | 9.000 | 2.340 | 2.340 | 3.483 | 4.478 | 9.000 |
| *IL10-1082:MMP2-1306* | *AG-CC* | 27.1 | 21.0 | 36.0 | 32.0 | 0.262 | 0.141 | 0.417 | 0.028 | 0.109 | 0.655 | 2.357 | 1.273 | 3.757 | 0.195 | 0.977 | 5.891 |
| *IL10-1082:MMP2-1306* | *AG-CT* | 21.6 | 19.0 | 16.0 | 12.0 | 0.652 | 0.283 | 0.057 | 0.710 | 0.241 | 0.542 | 5.870 | 2.550 | 0.511 | 4.971 | 2.167 | 4.874 |
| *IL10-1082:MMP2-1306* | *AG-TT* | 3.5 | 0.0 | 0.0 | 6.0 | 0.100 | 0.100 | 0.371 | | 0.029 | 0.029 | 0.898 | 0.898 | 3.340 | | 0.260 | 0.260 |
| *IL10-1082:MMP2-1306* | *GG-CC* | 7.5 | 10.0 | 3.0 | 6.0 | 0.509 | 0.196 | 0.811 | 0.082 | 0.435 | 0.498 | 4.582 | 1.760 | 7.301 | 0.573 | 3.918 | 4.479 |
| *IL10-1082:MMP2-1306* | *GG-CT* | 5.0 | 6.0 | 3.0 | 4.0 | 0.787 | 0.554 | 0.780 | 0.498 | 0.748 | 1.000 | 7.085 | 4.990 | 7.021 | 3.484 | 6.728 | 9.000 |
| *IL10-1082:MMP2-1306* | *GG-TT* | 1.5 | 0.0 | 0.0 | 1.0 | 0.553 | 0.553 | 1.000 | | 1.000 | 1.000 | 4.9 | 4.980 | 9.000 | | 9.000 | 9.000 |
| *IL10-592:IL10-1082:MMP2-1306* | *CC-AA-CC* | 8.0 | 7.0 | 8.0 | 17.0 | 0.822 | 1.000 | 0.030 | 1.000 | 0.048 | 0.086 | 16.442 | 19.000 | 0.600 | 16.000 | 0.968 | 1.626 |
| *IL10-592:IL10-1082:MMP2-1306* | *CC-AA-CT* | 1.5 | 17.0 | 5.0 | 11.0 | 0.000 | 0.123 | 0.001 | 0.012 | 0.308 | 0.191 | 0.002 | 2.335 | 0.010 | 0.184 | 6.166 | 3.638 |
| *IL10-592:IL10-1082:MMP2-1306* | *CC-AA-TT* | 0.0 | 0.0 | 0.0 | 1.0 | | | 0.334 | | 1.000 | 1.000 | | | 6.688 | | 20.00 | 19.00 |
| *IL10-592:IL10-1082:MMP2-1306* | *CC-AG-CC* | 15.1 | 14.0 | 29.0 | 23.0 | 0.864 | 0.006 | 0.108 | 0.015 | 0.145 | 0.420 | 17.282 | 0.105 | 2.168 | 0.245 | 2.890 | 7.988 |
| *IL10-592:IL10-1082:MMP2-1306* | *CC-AG-CT* | 10.6 | 14.0 | 10.0 | 12.0 | 0.446 | 1.000 | 0.700 | 0.514 | 0.834 | 0.822 | 8.922 | 19.000 | 1.994 | 8.234 | 16.678 | 15.612 |

Endof Table 2

| Polymorphic genotypes | | NSR | CHR | OR | LR | *p*_ TMF2 | *p*_ TMF2 | *p*_ TMF2 | *p*_ TMF2 | *p*_ TMF2 | *p*_ TMF2 | *p*_cor | *p* _cor | *p*_cor | *p*_cor | *p*_cor | *p*_cor |
|---|---|---|---|---|---|---|---|---|---|---|---|---|---|---|---|---|---|
| | | 1 | 2 | 3 | 4 | 1-2 | 1-3 | 1-4 | 2-3 | 2-4 | 3-4 | 1-2 | 1-3 | 1-4 | 2-3 | 2-4 | 3-4 |
| *IL10-592:IL10-1082:MMP2-1306* | *CC-AG-TT* | 2.5 | 0.0 | 0.0 | 5.0 | 0.173 | 0.173 | 0.311 | | 0.059 | 0.059 | 3.456 | 3.283 | 6.216 | | 1.188 | 1.129 |
| *IL10-592:IL10-1082:MMP2-1306* | *CC-GG-CC* | 7.0 | 10.0 | 2.0 | 5.0 | 0.375 | 0.100 | 0.619 | 0.033 | 0.283 | 0.445 | 7.504 | 1.896 | 12.386 | 0.528 | 5.656 | 8.451 |
| *IL10-592:IL10-1082:MMP2-1306* | *CC-GG-CT* | 5.0 | 3.0 | 3.0 | 4.0 | 0.554 | 0.554 | 0.780 | 1.000 | 1.000 | 1.000 | 11.088 | 10.534 | 15.602 | 16.000 | 20.000 | 19.000 |
| *IL10-592:IL10-1082:MMP2-1306* | *CC-GG-TT* | 1.5 | 0.0 | 0.0 | 1.0 | 0.553 | 0.553 | 1.000 | | 1.000 | 1.000 | 11.066 | 10.513 | 20.000 | | 20.000 | 19.000 |
| *IL10-592:IL10-1082:MMP2-1306* | *CA-AA-CC* | 10.1 | 8.0 | 9.0 | 3.0 | 0.676 | 0.839 | 0.037 | 1.000 | 0.213 | 0.134 | 13.524 | 15.935 | 0.742 | 16.000 | 4.268 | 2.542 |
| *IL10-592:IL10-1082:MMP2-1306* | *CA-AA-CT* | 9.6 | 6.0 | 13.0 | 1.0 | 0.378 | 0.428 | 0.005 | 0.146 | 0.118 | 0.001 | 7.566 | 8.134 | 0.108 | 2.342 | 2.368 | 0.025 |
| *IL10-592:IL10-1082:MMP2-1306* | *CA-AA-TT* | 0.5 | 0.0 | 2.0 | 1.0 | 1.000 | 0.260 | 1.000 | 0.498 | 1.000 | 1.000 | 20.000 | 4.940 | 20.000 | 7.960 | 20.000 | 19.000 |
| *IL10-592:IL10-1082:MMP2-1306* | *CA-AG-CC* | 11.1 | 6.0 | 6.0 | 9.0 | 0.207 | 0.207 | 0.689 | 1.000 | 0.593 | 0.593 | 4.144 | 3.937 | 13.790 | 16.000 | 11.856 | 11.263 |
| *IL10-592:IL10-1082:MMP2-1306* | *CA-AG-CT* | 10.6 | 5.0 | 6.0 | 0.0 | 0.130 | 0.284 | 0.000 | 1.000 | 0.059 | 0.029 | 2.600 | 5.404 | 0.004 | 16.000 | 1.1880 | 0.549 |
| *IL10-592:IL10-1082:MMP2-1306* | *CA-AG-TT* | 1.0 | 0.0 | 0.0 | 1.0 | 0.553 | 0.553 | 1.000 | | 1.000 | 1.000 | 11.066 | 10.5130 | 20.000 | | 20.000 | 19.000 |
| *IL10-592:IL10-1082:MMP2-1306* | *CA-GG-CC* | 0.5 | 0.0 | 1.00 | 1.0 | 1.000 | 1.000 | 1.000 | 1.000 | 1.000 | 1.000 | 20.000 | 19.000 | 20.000 | 16.000 | 20.000 | 19.000 |
| *IL10-592:IL10-1082:MMP2-1306* | *CA-GG-CT* | 0.0 | 3.0 | 0.00 | 0.0 | 0.037 | | | 0.246 | 0.246 | | 0.734 | | | 3.939 | 4.924 | |
| *IL10-592:IL10-1082:MMP2-1306* | *AA-AA-CC* | 2.5 | 3.0 | 2.0 | 3.0 | 1.000 | 1.000 | 1.000 | 1.000 | 1.000 | 1.000 | 20.000 | 19.000 | 20.000 | 16.000 | 20.000 | 19.000 |
| *IL10-592:IL10-1082:MMP2-1306* | *AA-AA-CT* | 1.5 | 3.0 | 3.0 | 2.0 | 0.405 | 0.405 | 1.000 | 1.000 | 1.000 | 1.000 | 8.108 | 7.703 | 20.000 | 16.000 | 20.000 | 19.000 |
| *IL10-592:IL10-1082:MMP2-1306* | *AA-AG-CC* | 1.0 | 1.0 | 1.0 | 0.0 | 1.000 | 1.000 | 0.553 | 1.000 | 1.000 | 1.000 | 20.000 | 19.000 | 11.066 | 16.000 | 20.000 | 19.000 |
| *IL10-592:IL10-1082:MMP2-1306* | *AA-AG-CT* | 0.5 | 0.0 | 0.0 | 0.0 | 1.000 | 1.000 | 1.000 | | | | 20.000 | 19.000 | 20.000 | | | |

Note. 1-NSR – Novosibirsk Region, 2-CHR – Chuvash Republic, 3-OR – Orenburg Region,4-LR – Leningrad Region.

At the same time, an increase in the frequency of two-locus genotypes (CC-CT IL10-592:MMP2-1306; AA-CTIL10-1082:MMP2-1306) and three-locus genotypes (IL10-592:IL10-1082:MMP2-1306 CC-AA-CT, and CA-GG-CT IL10-592:IL10-1082:MMP2-1306) was noted in this region. The latter was identified exclusively in patients from the CHR and never occurred in patients of the other three regions. Perhaps this is due to the greater proportion of the Mongoloid population in this region of the Russian Federation.

The group of patients from the Orenburg Region appeared to be more similar in the distribution of the studied parameters to the population of the NSR. In this group, only one difference was found related to an increase in the frequency of the CC-AG-CC IL10-92:IL10-1082:MMP2-1306 genotype.

The group of patients from the Leningrad Region differed the most compared to other regions, which may be due to their long-term residence together with the indigenous Finno – Ugric peoples. Among patients in this region, an increase in the frequency of CC-CC IL10-592:MMP2-1306; CC-CTIL10-592:MMP2-1306; CC-AA-CC IL10-592:IL10-1082:MMP2-1306; CC-AA-CT IL10-592:IL10-1082:MMP2-1306 genotypes was revealed. Along with this, there was a decrease in the distribution frequency of genotypes CA-CT IL10-592:MMP2-1306; CA-AA-CC IL10-592:IL10-1082:MMP2-1306; CA-AA-CTIL10-592:IL10-1082:MMP2-1306, and CA-AG-CT IL10-592: IL10-1082:MMP2-1306. At the same time, the frequency of the last two traits ranged from 0.00 to 1.00.

## DISCUSSION

The interim conclusion in this section of the study may be significant differences in the detection rates of the studied polygenic parameters for the association of POAG with SNPs of functionally related genes, with the establishment of significant differences between significant groups of patients in the studied regions of the Russian Federation. This speaks of a necessity to use regional standards in the development of prognostic criteria for individual's predisposition to the development of POAG, even in case of POAG in the family history. For such a multinational country as the Russian Federation, this is a prerequisite for the development of personalized approaches in medicine.

Since vascular and capillary networks are integrated into the ECM space, regulation of its metabolism and regulation of angiogenesis are also interdependent. The processes of angiogenesis are under the control of numerous families of cytokines, chemokines, and growth factors with complex effects on the vascular and extravascular pathways of aqueous humor, blood, and lymph and their interactions with each other [11, 12]. In addition to a large family of proangiogenic factors, cytokines with an antiangiogenic effect, of which IL-10 is one of the most important, also play a significant role in maintaining the homeostasis of aqueous humor outflow.

The single nucleotide polymorphism *IL-10 -1082* and the haplotype *-1082, -819, -592* are associated with different expression of IL-10 *in vitro*, while haplotype *-1082 A/ -819 T/ -592 A* is associated with reduced expression of IL-10 compared to haplotype *-1082 G/ -819 C/ -592 C*. It is believed that up to 75% of individual differences in IL-10 expression may be due to genetic differences [13].

There is evidence that IL-10 exerts its immunosuppressive effect, including by inhibiting angiogenesis. For example, IL-10 has been shown to stimulate TIMPs and inhibit the expression of MMPs, thus affecting the induction of angiogenesis [9].

In addition, during neuroinflammation, characteristic of POAG, M2 macrophages, producing IL-10, are able to inhibit the synthesis of MMP-9, which leads to a decrease in macrophage infiltration of tissues, blockade of T cell activation and differentiation, and destruction of myelin [14]. Activation of nuclear factor kappa B (NFκB) during neuroinflammation also leads to a decrease in IL-10 synthesis [15].

The *MMP-2* rs243865 polymorphism is represented by the substitution C→T at position -1306 in the promoter. This variant disrupts binding to stimulating protein 1 (Sp1), which is a gene transcription factor, which leads to a decrease in MMP-2 expression [16]. In the meantime, the presence of the C allele in this position in the human genome leads to an increase in the concentration of MMP-2 in the circulation [17].

Thus, the substitutions of all three SNPs studied by us in promoter regions are associated with the expression of regulatory proteins encoded by these genes, and their presence in the human genome has an impact on the state of ECM, which may trigger a genetic predisposition to diseases associated with these processes.

It is important to note that the detected patterns of the association of POAG with SNPs of *IL-10* and *MMP2* genes in the Russian population are not exhaustive in terms of the involvement of polymorphic regions of cytokine genes.

Thus, associations of the predisposition to the development of POAG among the population of

Southern Russia with SNPs of the *TNFα* and *IL1b* genes were established, and respondents with the rare 308A allele and carriers of the 308G/A +308A/A genotypes showed an increase in the TNFα level in tear fluid – 49 (14.0–90.0) pg / ml compared to patients with the 308G/G genotype [18].

Our studies of the population of Western Siberia have shown a decrease in the frequency of the minor IL 1B-31*CC genotype, the IL8-251*TT genotype, and the complex IL8-251*TT:IL17-197*AA genotype. Differences in the distribution of genotypes positively and negatively correlated with the pathology were identified [19].

In the work by A. Golshan-Tafti et al. (2024), which included 442 cases and 672 controls, the IL-10 -592C>A, -819T>C, and -1082A>G polymorphisms were studied. A significant association was found between -592C>A, -819T>C, and -1082A>G in the *IL-10* gene and predisposition to POAG among the Mongoloid population [20].

It was shown that polymorphic loci *MMP-1* rs1799750 and *MMP-9* rs2250889, which play the most significant role in the formation of susceptibility to POAG (they are part of the largest number of SNP × SNP interaction models associated with the development of the disease), exert an important function in the body. The *MMP1*rs1799750 polymorphism is located in the regulatory region of DNA motifs interacting with regulatory proteins CFOS and GATA2 and is associated with the expression level of three genes (*MMP1, MMP10*, and *WTAPP1*).

The polymorphic locus rs2250889 determines a non-synonymous substitution in the *MMP-9* gene (p.Arg574Pro), is localized in an evolutionarily conserved DNA region, and is associated with the transcription level of three genes (*PLTP, PCIF1*, and *NEURL2*) and the level of alternative splicing of the *SLC12A5* gene transcript [7].

According to the 2019 meta-analysis data for the rs1799750 SNP in the *MMP* gene, a comprehensive analysis of four studies (885 POAG cases and 875 control cases) showed that rs1799750 significantly correlated with POAG in the recessive model [21].

## CONCLUSION

The data obtained should be taken into account not only when analyzing the possible involvement of cytokine and metalloproteinase gene polymorphisms in the genetic predisposition to the development of POAG, but also when trying to elaborate additional criteria for predicting individual predisposition to the development of POAG, which is especially relevant with a family history of the disease. In some cases, markers of a relative risk of developing the pathology in the group analysis reach very substantial values, although not reliable.

Undoubtedly, the transition from the analysis of the association of single SNPs of a single gene to a comprehensive analysis using interlocus combinations of SNPs of a number of functionally related genes is promising. While reducing the prevalence of such polygenic traits in patient groups, it will significantly increase the information and prognostic value of identifying such genetic complexes as additional personalized prognostic features. For conducting such clinical and genetic studies, regional standards for comparing data obtained in patient groups and in randomized comparison groups can be recommended.

## REFERENCES

1. Primary Open-Angle Glaucoma. Clinical Guidelines. M.: Ministry of Healthcare of Russia, 2020:58. (In Russ.).
2. Libman E.S., Shakhova E.V. Blindness and Disability due to Pathology of Vision in Russia. *Vestnik Oftal'mologii*. 2006;1:35–37. (In Russ.).
3. Youngblood H., Hauser M.A., Liu Y. Update on the Genetics of Primary Open-Angle Glaucoma. *Exp. Eye Res*. 2019;188 107795. DOI: 10.1016/j.exer.107795.
4. Ramos T., Parekh M., Meleady P., O'Sullivan F., Stewart R.M.K., Kaye S.B. et al. Specific Decellularized Extracellular Matrix Promotes the Plasticity of Human Ocular Surface Epithelial Cells. *Front. Med. (Lausanne*). 2022;9:974212:1–20. DOI: 10.3389/fmed.2022.974212.
5. Weinreb R.N., Robinson M.R., Dibas M., Stamer W.D. Matrix Metalloproteinases and Glaucoma Treatment. *J. Ocul. Pharmacol. Ther.* 2020;36(4):208–228. DOI: 10.1089/jop.2019.0146.
6. Shadrina A.S., Plieva Y.Z., Kushlinskiy D.N. Morozov A.A., Filipenko M.L., Chang V.L. et al. Classification, Regulation of Activity, and Genetic Polymorphism of Matrix Metalloproteinases in Health and Disease. *Almanac of Clinical Medicine*. 2017;45(4):266–279. (In Russ.). DOI: 10.18786/2072-0505-2017-45-4-266-279.
7. Svinareva D.I. The Contribution of Gene – Gene Interactions of Polymorphic Loci of Matrix Metalloproteinases to Susceptibility to Primary Open-Angle Glaucoma in Men. *Research Results in Biomedicine*. 2020;6(1):63–77. (In Russ.). DOI: 10.18413/2658-6533-2020-6-1-0-6.
8. Markiewicz L., Majsterek I., Przybylowska K., Dziki L., Waszczyk M., Gacek M. et al. Gene Polymorphisms of the MMP1, MMP9, MMP12, IL1b and TIMP1 and the Risk of Primary Open-Angle Glaucoma. *Acta Ophthalmol*. 2013;91:e516–e523. DOI: 10.1111/aos.
9. Stearns M.E., Wang M., Hu Y., Garcia F.U., Rhim A.B. Interleukin 10 Blocks Matrix Metalloproteinase-2 and Membrane Type 1-Matrix Metalloproteinase Synthesis in Primary Human

Prostate Tumor Lines. *J. Clin Cancer Res*. 2003;9(3):1191–1199.
10. Ouyang W., O'Garra A. Il-10 Family Cytokines Il-10 and Il-22: From Basic Science to Clinical Translation. *Immunity.*2019;50(4):871–891. DOI: 10.1016/j.immuni.2019.03.020.
11. Rakhmanov V.V., Sokolov D.I., Selkov S.A., Astakhov Yu.S., Astakhov S.Yu. Role of Cytokines in the Pathogenesis of Glaucoma. *Vestnik RAMN*. 2020;75(6):609–616. (In Russ.). DOI: 10.15690/vramn1289.
12. Geindreau M., Bruchard M., Vegran F. Role of Cytokines and Chemokines in Angiogenesis in a Tumor Context. *Cancers.* 2022;14(10):2446. DOI: 10.3390/cancers14102446.
13. Howell M.W. Interleukin-10 Gene Polymorphisms and Cancer. Madame Curie Bioscience Database [Internet]. National Center for Biotechnology Information; 2010-2013. Bookshelf Copyright Notice, 2011. URL: https://www.ncbi.nlm.nih.gov/books/about/copyright/
14. Nurdianto A.R., Arwati H., Dachlan Y.P., Febiyanti D.A. The Relationship of Hemoglobin, Interleukin-10 and Tumor Necrosis Factor Alpha Levels in Asymptomatic Malaria Patients in Trenggalek. Jawa Timur, Indonesia. *Mol. Cell Biomed Sci*. 2019;3(1):13–16. DOI: 10.21705/mcbs.v3i1.37.
15. Sidharta B.R.A., Purwanto B., Wasita B., Widyaningsih V., Soetrisno S. Single or Divided Administration of Cisplatin Can Induce Inflammation and Oxidative Stress in Male Sprague-Dawley Rats. *Indones. Biomed J*. 2022;14(2):164–171. DOI: 10.18585/inabj.v14i2.1745.
16. Dofara S.G., Chang S.L. Dioreo C. Gene Polymorphisms and Circulating Levels of MMP-2 and MMP-9: a Review of Their Role in Breast Cancer Risk. *Anticancer Research*. 2020;40(7):3619–3631. DOI: 10.21873/anticanres.14351.
17. Belo V.A., Luizon M.R., Carneiro P.C., Gomes V.A., Lacchini R., Lanna C.M. Effect of Metabolic Syndrome Risk Factors and MMP-2 Genetic Variations on Circulating MMP-2 Levels in Childhood Obesity. *Mol. Biol. Rep*. 2013;40(3):2697–704. DOI: 10.1007/s11033-012-2356-7.
18. Barycheva L.Yu., Kakulia D.M., Minasyan M.M., Kuznetsova V.V., Kozmova N.A. Polymorphism of Proinflammatory Interleukin Genes in Primary Open-Angle Glaucoma. *Medical Immunology*. 2024;26(2):303–312. (In Russ.). DOI: 10.15789/1563-0625-POP-2878.
19. Shevchenko A.V., Prokof'ev V.F., Konenkov V.I., Chernykh V.V., Ermakova O.V., Trunov A.N. Analysis of IL1B (rs1143627), IL4 (rs2243250), IL6 (rs1800795), IL8 (rs4073), IL10 (rs1800896, rs1800872), IL17A (rs227593) Cytokine Gene Polymorphism and Its Complex Genotypes among Caucasian Patients of Western Siberia with Primary Open-Angle Glaucoma. *Immunology*. 2021;42(3):211–221. (In Russ.). DOI: 10.33029/0206-4952-2021-42-3-211-221.
20. Golshan-Tafti A., Bahrami M., Mohsenzadeh-Yazdi R., Dastgheib S.A., Aghasipour M., Shiri A. et al. Consolidating Data on the Association of IL-6 And IL-10 Polymorphisms with the Development of Glaucoma: A Meta-Analysis. *Ophthalmic Genetics.* 2024;45(4):321–331. DOI: 10.1080/13816810.2024.2336964.
21. Chen M., Yu H., Xu J., Ma J., Chen X., Chen B. et al. Association of Gene Polymorphisms with Primary Open Angle Glaucoma: A Systematic Review and Meta-Analysis. *Invest. Ophthalmol. Vis. Sci*. 2019;(60):1105–1121. DOI: 10.1167/iovs.18-25922.

## Author Contribution

Konenkov V.I. – carrying out a multicenter clinical and ophthalmological examination, writing Introduction and Conclusion sections of the article. Shevchenko A.V. – conducting genotyping, editing the Results section of the article. Prokofiev V.F. – conducting bioinformatic analysis of the results, editing sections of the article, performing statistical analysis. Arsyutov D.G. – carrying out a multicenter clinical and ophthalmological examination, editing the article. Khodjaev N.S., Boiko E.V., Chuprov A.D., Gorbunova N.Yu., Pshenichnov M.V., Chernykh V.V. – carrying out a clinical and ophthalmological examination, verifying the diagnosis of primary open-angle glaucoma, approving groups of patients included in the study, taking into account the criteria for inclusion and exclusion from the study. Pravosudova M.M., Kuvaitseva Yu.S., Markova A.A., Postupaeva N.V., Malysheva Yu.V., Ivanov A.A., Eremina A.V. – conducting a clinical and ophthalmological examination, compiling groups of patients included in the study. Trunov A.N. – carrying out a clinical and ophthalmological examination, verifying the diagnosis of primary open-angle glaucoma, editing the article.

## Author Information

**Konenkov Vladimir I.** – Dr. Sci. (Med.), Professor, Academician of RAS, Research Supervisor at the Research Institute of Clinical and Experimental Lymphology, Branch of IC&G SB RAS, Novosibirsk, vikonenkov@gmail.com, https://orcid.org/0000-0001-7385-6270

**Shevchenko Alla V.** – Dr. Sci. (Biol.), Research Institute of Clinical and Experimental Lymphology, Branch of IC&G SB RAS, Novosibirsk, shalla64@mail.ru, https://orcid.org/0000-0001-5898-950X

**Prokofiev Viktor F.** – Cand. Sci. (Med.), Research Institute of Clinical and Experimental Lymphology, Branch of IC&G SB RAS, Novosibirsk, vf_prok@mail.ru, https://orcid.org/0000-0001-7290-1631

**Arsyutov Dmitry G.** – Cand. Sci. (Med.), S. Fyodorov Eye Microsurgery Federal State Institution, Moscow, fcc@mntk.ru, https://orcid.org/000-0002-2618-5256

**Khodjaev Nazrulla S.** – Dr. Sci. (Med.), Professor, S. Fyodorov Eye Microsurgery Federal State Institution, Moscow, nskhodjaev@mail.ru, https://orcid.org/0000-0002-7614-628X

**Boiko Ernest V.** – Dr. Sci. (Med.), Professor, Honored Doctor of the Russian Federation, Director of Saint Petersburg branch of S.Fyodorov Eye Microsurgery Federal State Institution, Saint Petersburg, boiko111@list.ru, https://orcid.org/0000-0002-7413-7478

**Pravosudova Marina M.** – Cand. Sci. (Med.), Head of the Clinical Expert Department of Saint Petersburg branch of S. Fyodorov Eye Microsurgery Federal State Institution, Saint Petersburg, mpravosudova52@gmail.com, https://orcid.org/0009-0003-8322-579X

**Chuprov Aleksandr D.** – Dr. Sci. (Med.), Professor, Director of Orenburg branch of S. Fyodorov Eye Microsurgery Federal State Institution, Orenburg, nauka@ofmntk.ru, https://orcid.org/0000-0001-7011-4220

**Kuvaitseva Yuliya S.** – Ophthalmologist, Orenburg branch of S. Fyodorov Eye Microsurgery Federal State Institution, Orenburg, nauka@ofmntk.ru, https://orcid.org/0000-0001-9544-1308

**Gorbunova Nadezhda Yu.** – Cand. Sci. (Med.), Head of the Glaucoma Surgery Department, Cheboksary branch of S. Fyodorov Eye Microsurgery Federal State Institution, Cheboksary, ngorbunova_21@mail.ru, https://orcid.org/0000-0002-7388-5634

**Markova Anna A.** – Cand. Sci. (Med.), Ophthalmologist, Glaucoma Surgery Department, Cheboksary branch of S. Fyodorov Eye Microsurgery Federal State Institution, Cheboksary, dr.anya@list.ru, https://orcid.org/0000-0002-4252-6487

**Pshenichnov Maxim V.** – Cand. Sci. (Med.), Khabarovsk branch of S. Fyodorov Eye Microsurgery Federal State Institution, Khabarovsk, naukakhvmntk@mail.ru, https://orcid.org/0000-0002-4879-1900

**Postupaeva Natalia V.** – Cand. Sci. (Med.), Ophthalmologist, Khabarovsk branch of S. Fyodorov Eye Microsurgery Federal State Institution, Khabarovsk, naukakhvmntk@mail.ru, https://orcid.org/0000-0002-5364-4964

**Malysheva Yulia V.** – Irkutsk branch of S. Fyodorov Eye Microsurgery Federal State Institution, Irkutsk, mal-julia@bk.ru, https://orcid.org/0000-0002-4200-5649

**Ivanov Andrey A.** – Irkutsk branch of S. Fyodorov Eye Microsurgery Federal State Institution, Irkutsk, ivanov.andrei.med@yandex.ru, https://orcid.org/0009-0001-4235-9252

**Eremina Alena V.** – Cand. Sci. (Med.), Novosibirsk branch of S. Fyodorov Eye Microsurgery Federal State Institution, Novosibirsk, sci@mntk.nsk.ru, https://orcid.org/0000-0002-6913-0925

**Trunov Aleksandr N.** – Dr. Sci. (Med.), Professor, Novosibirsk branch of S. Fyodorov Eye Microsurgery Federal State Institution, Novosibirsk, trunov1963@yandex.ru, https://orcid.org/0000-0002-7592-8984

**Chernykh Valeriy V.** – Dr. Sci. (Med.), Professor, Novosibirsk branch of S. Fyodorov Eye Microsurgery Federal State Institution, Novosibirsk, sci@mntk.nsk.ru, https://orcid.org/0000-0002-7623-3359

(✉) **Konenkov Vladimir I.,** vikonenkov@gmail.com

Received on April 28, 2025;
approved after peer review on June 04, 2025;
accepted on June 19, 2025

УДК 616.24-002-037-036.8:579.842.16]:[616.15-074:616.15]
https://doi.org/10.20538/1682-0363-2025-3-81-88

# Predicting a fatal outcome in patients with pneumonia caused by carbapenem-resistant *Klebsiella pneumoniae* by hematological indices

**Levchenko K.V.[1], Mitsura V.M.[2]**

[1] *Gomel State Medical University*
*5 Lange St., 246000 Gomel, Republic of Belarus*

[2] *Republican Research Center for Radiation Medicine and Human Ecology*
*290 Ilyich St., 246040 Gomel, Republic of Belarus*

## ABSTRACT

**Aim.** To determine the most significant indicators for predicting a fatal outcome in patients with pneumonia caused by carbapenem-resistant *K. pneumoniae*.

**Materials and methods**. A total of 114 cases of pneumonia caused by *K. pneumoniae*, including those associated with COVID-19, were retrospectively analyzed. Depending on the outcome of the disease, two groups were formed: group 1 included 54 patients discharged from the hospital upon completion of treatment; group 2 encompassed 60 patients with an unfavorable (fatal) outcome. Patients who did not have a concomitant COVID-19 infection were analyzed separately. The profile of concomitant diseases, hemogram parameters, C-reactive protein (CRP) level, and hematological indices (neutrophil-to-lymphocyte ratio (NLR), monocyte-to-lymphocyte ratio (MLR), platelet-to-lymphocyte ratio (PLR)) were studied, and the risk of death according to the CURB-65 score was assessed.

**Results.** Patients with an unfavorable outcome were characterized by higher leukocyte and neutrophil counts, higher NLR, MLR, PLR, and CRP levels, higher risk according to the CURB-65 score, and lower lymphocyte and platelet concentrations. According to the results of the ROC analysis, the most significant prognostic indicators of an unfavorable outcome were lymphocytes, neutrophils, NLR, CURB-65, CRP, and TLR. The diagnostic value of the CURB-65 score (3–5 points) in predicting the risk of an unfavorable outcome was the following: test sensitivity was 47.5%, specificity was 98.2%, positive predictive value was 96.6%, negative predictive value was 63.1%, accuracy was 71.7%. For NLR (at a threshold value > 6), sensitivity was 85.0%, specificity was 87.0%, positive predictive value was 87.9%, negative predictive value was 83.9%, accuracy was 86.0%. For MLR, the diagnostic accuracy was 79.0%, and for PLR – 73.7%.

**Conclusion.** The parameter of choice that can be used at the early stage to predict the fatal outcome of pneumonia caused by carbapenem-resistant *K. pneumoniae* should be NLR (> 6) due to its high sensitivity (85%) and specificity (87%) and ease of use. In addition, the CURB-65 score can be used at NLR > 3.

**Keywords:** prediction of a fatal outcome, carbapenem-resistant *Klebsiella pneumoniae*, COVID-19, CURB-65 score, hematological indices

**Conflict of interest.** The authors declare the absence of obvious or potential conflicts of interest related to the publication of this article.

**Source of financing.** The authors state that they received no funding for the study.

**Conformity with the principles of ethics.** All study participants signed an informed consent. The study was approved by the Ethics Committee at Gomel State Medical University.

**For citation:** Levchenko K.V., Mitsura V.M. Predicting a fatal outcome in patients with pneumonia caused by carbapenem-resistant *Klebsiella pneumoniae* by hematological indices. *Bulletin of Siberian Medicine.* 2025;24(3):81–88. https://doi.org/10.20538/1682-0363-2025-3-81-88.

✉ *Levchenko Kristina V.,* kristy_levchenko@mail.ru

# Прогнозирование летального исхода у пациентов с пневмонией, вызванной карбапенем-резистентной *Klebsiella pneumoniae*, при помощи гематологических индексов

**Левченко К.В.[1], Мицура В.М.[2]**

[1] *Гомельский государственный медицинский университет*
*Республика Беларусь, 246000, г. Гомель, ул. Ланге, 5*

[2] *Республиканский научно-практический центр радиационной медицины и экологии человека*
*Республика Беларусь, 246040, г. Гомель, ул. Ильича, 290*

## РЕЗЮМЕ

**Цель.** Определение наиболее значимых показателей для прогнозирования летального исхода у пациентов с пневмонией, вызванной карбапенем-резистентной *K. pneumoniae.*

**Материалы и методы.** Ретроспективно проанализировано 114 случаев пневмонии, вызванной *K. pneumoniae*, в том числе на фоне коронавирусной инфекцией (COVID-19). В зависимости от исхода заболевания сформировано две группы: группа 1 – 54 пациента, выписанных из стационара по завершении лечения; группа 2 – 60 пациентов с неблагоприятным (летальным) исходом. Отдельно проанализированы пациенты, у которых не выявлено сопутствующей инфекции COVID-19. Изучена структура сопутствующих заболеваний, определены показатели гемограммы, С-реактивного белка (СРБ), а также гематологические индексы: отношение нейтрофилов и лимфоцитов (НЛИ), моноцитов и лимфоцитов (МЛИ), тромбоцитов и лимфоцитов (ТЛИ). Риск летального исхода оценивался по шкале CURB-65.

**Результаты.** Для пациентов с неблагоприятным исходом характерны более высокие показатели лейкоцитов в общем анализе крови, нейтрофилов, значения НЛИ, МЛИ, ТЛИ, СРБ, более высокий риск по шкале CURB-65 и низкий уровень лимфоцитов, тромбоцитов. По результатам проведенного ROC-анализа, наиболее значимыми прогностическими показателями неблагоприятного исхода является уровень лимфоцитов, нейтрофилов, НЛИ, показатели CURB-65, СРБ, ТЛИ. Диагностическая значимость шкалы CURB-65 (3–5 баллов) в прогнозировании риска неблагоприятного исхода составляет: чувствительность теста – 47,5%, специфичность – 98,2; положительная прогностическая ценность – 96,6; отрицательная прогностическая ценность – 63,1; точность – 71,7%. Для НЛИ (при пороговом значении более 6) получены следующие данные: по чувствительности (85,0%), специфичности (87,0%), положительной прогностической ценности (87,9%), отрицательной прогностической ценности (83,9%), точности (86,0%). Диагностическая точность для МЛИ составила 79,0%, для ТЛИ – 73,7%.

**Заключение.** Предпочтительным показателем, который можно использовать на первом этапе для прогнозирования летального исхода пневмонии, вызванной карбапенем-резистентной *K. pneumoniae*, следует считать НЛИ (при уровне более 6) ввиду высокой чувствительности (85%) и специфичности (87%), а также простоты применения. В дополнение к этому можно использовать расчет баллов по шкале CURB-65 при значениях 3 балла и выше.

**Ключевые слова:** прогнозирование летального исхода, карбапенем-резистентная *K. pneumoniae*, COVID-19, шкала CURB-65, гематологические индексы

**Конфликт интересов.** Авторы декларируют отсутствие явных и потенциальных конфликтов интересов, связанных с публикацией настоящей статьи.

**Источник финансирования.** Авторы заявляют об отсутствии финансирования при проведении исследования.

**Соответствие принципам этики.** Все участники исследования подписали информированное согласие. Протокол исследования одобрен этическим комитетом УО «Гомельский государственный медицинский университет».

**Для цитирования:** Левченко К.В., Мицура В.М. Прогнозирование летального исхода у пациентов с пневмонией, вызванной карбапенем-резистентной *Klebsiella pneumoniae*, при помощи гематологических индексов. *Бюллетень сибирской медицины.* 2025;24(3):81–88. https://doi.org/10.20538/1682-0363-2025-3-81-88.

## INTRODUCTION

*K.pneumoniae* is the most common pathogen of healthcare-associated infections worldwide. These pathogens belong to the group of clinically significant ESKAPE pathogens – *Enterococcus faecium, Staphylococcus aureus, Klebsiella pneumoniae, Acinetobacter baumannii, Pseudomonas aeruginosa,* and *Enterobacter spp.*, which is associated with the development of severe infections and the difficulty of selecting an effective antibiotic (AB) regimen [1–3]. In the profile of nosocomial pneumonia, there is an increase in the prevalence of carbapenem-resistant *K.pneumoniae*. Carbapenem resistance is a marker of multidrug and extensive antibiotic resistance [4, 5].

*K. pneumoniae*, previously almost never seen among the causative agents of community-acquired pneumonia, is now often isolated from the biomaterial of patients diagnosed with pneumonia in the first 48 hours of hospital stay. High frequency of an unfavorable outcome has been noted among patients with pneumonia associated with K. pneumoniae and other ESKAPE pathogens, especially in combination with COVID-19 infection [2, 6, 7]. Detection of carbapenem-resistant *K. pneumoniae* in patients' biomaterial increases the risk of an unfavorable outcome [8, 9].

Risk factors for a fatal outcome of community-acquired pneumonia have been identified: late hospitalization (5 days or more after the onset of the disease); underestimation of the severity of the patient's condition during the initial examination; concomitant somatic symptom pathology, bilateral nature of pneumonia; errors in initial antibacterial therapy. In order to predict an unfavorable outcome, the levels of procalcitonin, C-reactive protein (CRP), presepsin, pro-adrenomedullin, and progranulin are assessed. However, to date it is difficult to identify a single marker with an absolute predictive ability regarding a fatal outcome in a patient with pneumonia [10].

Researchers from Saint Petersburg reported that it is possible to accurately predict the likelihood of a fatal outcome in patients with severe community-acquired pneumonia upon their admission to the intensive care unit (ICU) by assessing serum markers, such as surfactant protein D, hypoxia-inducible factor 1α, angiotensin-converting enzyme 2, and levels of interleukins 6 and 10 [11].

At the stage of diagnosis, important tasks for the physician include determining the risk of an adverse outcome and deciding whether to treat the patient in the internal medicine department or in the ICU. Currently, the CURB-65 score (confusion, uremia, respiratory rate, blood pressure, age ≥ 65 years) and the Pneumonia severity index (PSI) are widely used and recommended for predicting 30-day mortality and a need for intensive care in a hospital setting. However, the CURB-65 assessment system may be preferable for identifying high-risk patients and due to its ease of use [12].

Neutrophil-to-lymphocyte ratio (NLR), monocyte-to-lymphocyte ratio (MLR), and platelet-to-lymphocyte ratio (PLR) are biomarkers used for prediction of adverse outcomes in many diseases. NLR has high practical significance for predicting mortality in patients with pneumonia, as it correlates with mortality in patients with community-acquired pneumonia better than traditional assessment systems (PSI, CURB-65), leukocyte count, and CRP [13–16]. NLR has been shown to be an independent risk factor for death from nosocomial pneumonia during the COVID-19 pandemic [17]. MLR and PLR are increasingly recognized as markers of inflammation and have good prognostic value in patients with cancer, cardiovascular disease, and some infectious diseases, but the prognostic value of these parameters for hospitalized patients with pneumonia is questionable [16, 18]. For early diagnosis and assessment of the disease severity as well as for prediction of the disease outcome, preference is given to non-invasive prediction methods that do not require additional costs.

**The aim of this study** was to determine the most significant indicators for predicting a fatal outcome in patients with pneumonia caused by carbapenem-resistant *K. pneumoniae*.

## MATERIALS AND METHODS

A retrospective analysis of 114 cases of pneumonia caused by *K.pneumoniae* was conducted. The object of the study were adult patients treated at the Gomel Regional Tuberculosis Clinical Hospital (GRTCH) for pneumonia caused by *K.pneumoniae* in 2021–2024, including those with COVID-19 co-infection, confirmed in the laboratory before and during hospitalization. Inclusion criteria: age 18 years and older, isolation of carbapenem-resistant *K.pneumoniae* from sputum, bronchoalveolar lavage fluid (BALF) in diagnostically significant quantities ($10^6$ CFU / ml or more).

The profile of concomitant diseases, hemogram parameters, and CRP were studied. Hematological indices were calculated based on a complete blood count, which was taken on the day of sputum and BALF specimen collection for microbiological testing, before the initiation of antibacterial therapy (19 patients) and thereafter (95 patients). The median detection of *K. pneumoniae* in the studied samples was 17.0 [11.0–27.0] days from the onset of the disease, 13.0 [6.0–20.0] days from the date of hospitalization.

The study group consisted of 45 women and 69 men. The median age of patients was 68.0 [59.0–75.8] years (minimum age – 21 years, maximum age – 91 years). Fifty-five people (48.2%; 38.8–57.8) were patients of pulmonology departments, and 59 patients (51.8%; 42.2–61.2) were treated in the ICU. Mechanical ventilation was used in 28 patients (24.6%; 17.0–33.5). COVID-19 infection was detected in 65 patients (57.0%; 47.4–66.3). A fatal outcome was observed in 60 patients (52.6%; 43.1–62.3).

Depending on the outcome of the disease, two groups were formed: group 1 included 54 patients discharged from the hospital upon completion of treatment. Group 2 encompassed 60 patients with an unfavorable (fatal) outcome. Patients who did not have concomitant COVID-19 infection were analyzed separately. The characteristics of the groups are presented in Table 1.

Table 1

**Characteristics of the Groups of Patients Hospitalized with Pneumonia Caused by *K. Pneumoniae***

| Parameter | Group 1, $n = 54$ | Group 2, $n = 60$ | $p$ |
|---|---|---|---|
| Sex: male/female | 39/15 | 30/30 | 0.016* |
| Age, *Me* [$Q_{25}$–$Q_{75}$] | 61.0 (52.5–70.8) | 70.0 (62.0–77.3) | 0.001* |
| Treatment in the ICU, abs. (%) | 10 (18.5) | 29 (48.3) | <0.001* |
| Mechanical ventilation used, abs. (%) | 2 (3.7) | 26 (43.3) | <0.001* |
| COVID-19 infection, abs. (%) | 22 (40.7) | 43 (71.7) | <0.001* |
| Aggravated premorbid background, abs. (%) | 51 (94.4) | 59 (98.3) | 0.26 |

* differences are statistically significant.

Cardiovascular diseases (ischemic heart disease, arterial hypertension, arrhythmias) were present in 55 people (91.7%; 81.6–97.2) in group 2 and in 38 patients (70.4%; 56.4-82.0) in group 1 ($\chi^2 = 8.58$, $p = 0.004$). Metabolic disorders (obesity, diabetes mellitus) were present in 21 patients (38.9%; 25.9–53.1) in group 1 and in 28 patients (46.7%; 33.7–60.0) in group 2 without statistically significant differences ($p = 0.40$). Chronic nonspecific lung diseases were present in 9 patients (16.7%; 7.9–29.3) in group 1 and in 8 patients (13.3%; 5.9–24.6) in group 2 without statistically significant differences ($p = 0.62$).

Cancer was detected in 11 patients (20.4%; 10.6–33.5) in group 1 and in 8 patients (13.3%; 5.9–24.6) in group 2 without statistically significant differences ($p = 0.32$). Chronic liver diseases were present in 5 patients (7.9%; 3.7–14.5) in group 1 and in 4 patients (6.7%; 1.9–16.2) in group 2 ($p = 0.61$). Chronic kidney diseases were observed in 9 patients (16.7%; 7.9–29.3) in group 1 and in 7 patients (11.7%; 4.8–22.6) in group 2 ($p = 0.44$). To predict 30-day mortality, the CURB-65 pneumonia severity assessment score was used [12].

Statistical processing of the obtained data was performed using the Statistica v. 12.5 and MedCalc, v. 18.9.1 software packages. The median and the interquartile range *Me* [$Q_{25}$–$Q_{75}$] were calculated to present the data. Comparison of groups by quantitative characteristics was performed using the Mann – Whitney U-test. For relative values, the 95% confidence interval (95% CI) was determined using the Clopper – Pearson method. The significance of differences in the relative values was calculated using the Pearson's $\chi^2$ test. To assess the impact of various factors on hospital mortality, the odds ratio (OR) was calculated with 95% CI. To study the relationship between variables, the Spearman's rank correlation coefficient ($r_s$) was calculated. To assess the significance of quantitative variables in predicting a certain outcome, the ROC analysis was used with the calculation of area under the curve (AUC), 95% CI for AUC, and determination of the cutoff point using the Youden criterion and sensitivity and specificity for this cutoff point. The differences were considered statistically significant at $p < 0.05$.

## RESULTS

The hemogram parameters obtained on the day of sputum and BALF specimen collection and the calculated hematological indices are presented in Table 2.

Table 2 shows that patients in group 2 were characterized by higher WBC and neutrophil counts, NLR, MLR, PLR, and CRP, lower levels of lymphocytes and platelets, and a higher risk according to the CURB-65 score.

Table 2

**Laboratory Parameters of Patients in the Analyzed Groups, *Me* [$Q_{25}$–$Q_{75}$]**

| Parameter | Group 1, *n* = 54 | Group 2, *n* = 60 | *p* |
|---|---|---|---|
| White blood cells (WBC), × $10^9$ / L | 8.9 [7.6–12.3] | 13.4 [9.6–17.2] | 0.0003* |
| Neutrophils, % | 68.0 [61.2–75.0] | 88.0 [82.0–91.0] | <0.0001* |
| Lymphocytes, % | 18.5 [15.0–27.0] | 7.0 [4.0–11.8] | <0.0001* |
| Monocytes, % | 6.5 [4.0–8.0] | 5.0 [3.0–7.9] | 0.147 |
| Platelets, × $10^9$ / l | 279.5 [211.0–331.0] | 213.0 [163.0–255.0] | 0.004* |
| Hemoglobin, g / l | 116.5 [97.0–131.0] | 108.5 [94.5–123] | 0.19 |
| Red blood cells, × $10^{12}$ / l | 3.8 [3.1–4.4] | 3.8 [3.3–4.4] | 0.982 |
| CRP, mg / l | 41.8 [23.0–88.0] | 140.0 [95.0–140.0] | <0.0001* |
| MLR | 0.32 [0.19–0.42] | 0.94 [0.41–1.25] | <0.0001* |
| NLR | 3.74 [2.37–5.07] | 12.25 [7.31–22.38] | <0.0001* |
| PLR | 12.36 [9.11–20.64] | 33,53 [18.44–55.67] | <0.0001* |
| CURB-65 score | 1.0 [0.0–1.0] | 2.0 [2.0–4.0] | <0.0001* |
| CURB-65, *n* (%) | | | |
| 0–1 points | 45 (83.3) | 13 (21.7) | $\chi^2$ = 46.5; <0.0001 |
| 2 points | 8 (14.8) | 18 (30.0) | |
| 3–5 points | 1 (1.9) | 28 (46.7) | |

* differences are statistically significant.

Various factors that could affect the mortality of hospitalized patients were analyzed. Risk factors associated with a fatal outcome were the presence of COVID-19 infection (OR 3.68; 95% CI 1.69–8.03), CURB-65 scores of 3–5 (OR 46.37; 95% CI 6.02–357.5), the use of mechanical ventilation (OR 19.88; 95% CI 4.43–89.27), and hospitalization in the ICU (OR 4.12; 95% CI 1.75–9.66), which does not contradict the data of foreign authors [19, 20].

A direct correlation was established between the CURB-65 score and WBC count ($r_s$ = 0.33, $p$ = 0.0004), neutrophil count ($r_s$ = 0.65, $p$ < 0.001), CRP ($r_s$ = 0.42, $p$ < 0.001), PLR ($r_s$ = 0.64, $p$ < 0.001), MLR ($r_s$ = 0.60, $p$ < 0.001), and NLR ($r_s$ = 0.78, $p$ < 0.001). An inverse correlation was established between the CURB-65 score and the lymphocyte count ($r_s$ = –0.79, $p$ < 0.001).

The ROC analysis was performed to determine the prognostic value and threshold values of the parameters. The parameters that have significant differences when compared in the study groups were included (WBC, neutrophils, lymphocytes, platelets, CRP, NLR, MLR, PLR, CURB-65 score).

For WBC, the AUC values were 0.69 (0.60–0.77), test sensitivity was 71.2%, specificity was 68.5% at a cutoff point of > 10.4, and the Youden index was 0.40. For neutrophils, the AUC values were 0.93 (0.87–0.97), test sensitivity was 85.0%, specificity was 94.4% at a cutoff point of > 79, and the Youden index was 0.79. For lymphocytes, the AUC values were 0.92 (0.85–0.96), test sensitivity was 93.3%, specificity was 77.8% at a cutoff point ≤ 14.37, and the Youden index was 0.71. For platelets, the AUC values were 0.66 (0.56–0.74), test sensitivity was 76.7%, specificity was 55.6% at a cutoff point ≤ 255, and the Youden index was 0.32. The AUC values obtained for CRP were 0.80 (0.71–0.87), test sensitivity was 75.0%, specificity was 77.8% at a cutoff point > 97, and the Youden index was 0.53.

The AUC values for MLR (Fig. 1) were 0.79 (0.70–0.86), test sensitivity was 70.0%, specificity was 85.2% at a cutoff point > 0.55, and the Youden index was 0.55. For NLR, the AUC values were (Fig. 2) 0.93 (0.86–0.97), test sensitivity was 85.0%, specificity was 87.0% at a cutoff point of > 6, and the Youden index was 0.72. For PLR, the AUC values were 0.80 (0.72–0.87), test sensitivity was 56.7%, specificity was 92.6% at a cutoff point of > 28.15, the Youden index was 0.49 (Fig. 3). For the CURB-65 score, the AUC values were 0.87 (0.80–0.93), test sensitivity was 46.7%, specificity was 98.2% at a cutoff point of > 2, the Youden index was 0.60 (Fig. 4).

According to the results of the analysis, the most significant prognostic indicators of an unfavorable outcome were lymphocytes, neutrophils, NLR, CURB-65, CRP, and PLR. To exclude the influence of COVID-19 co-infection on the threshold values of prognostic indicators, the ROC analysis was performed including the NLR values calculated for patients who did not have confirmed COVID-19 co-infection (*n* = 49). The AUC values were 0.92 (0.81–0.98), test sensitivity was 82.4%, specificity was 87.5% at a cutoff point of > 6, the Youden index was 0.73.

The diagnostic value of the CURB-65 score (3–5 points) in predicting the risk of an unfavorable outcome in patients was calculated using the Medcalc Diagnostic Test Evaluation Online Calculator (https://www.medcalc.org/calc/diagnostic_test.php). The test sensitivity was 47.5%, specificity was 98.2%, positive predictive value was 96.6%, negative predictive value was 63.1%, and accuracy was 71.7%.

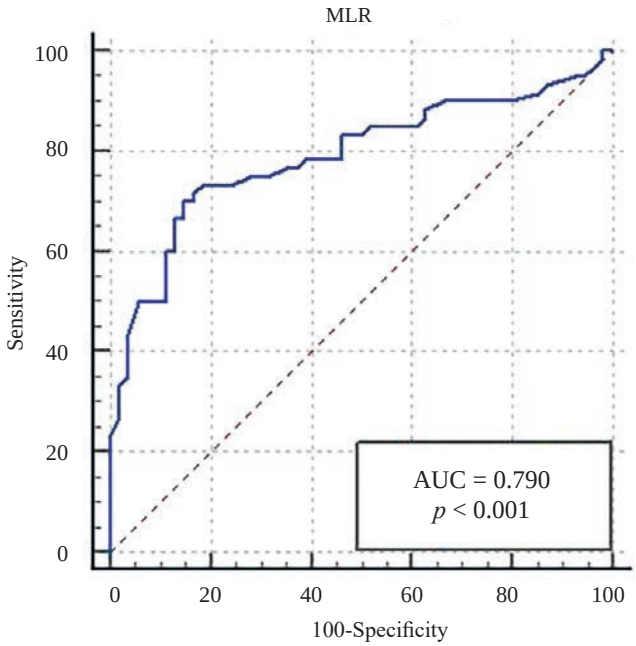


Fig. 1. ROC-curve for the prognostic value of MLR

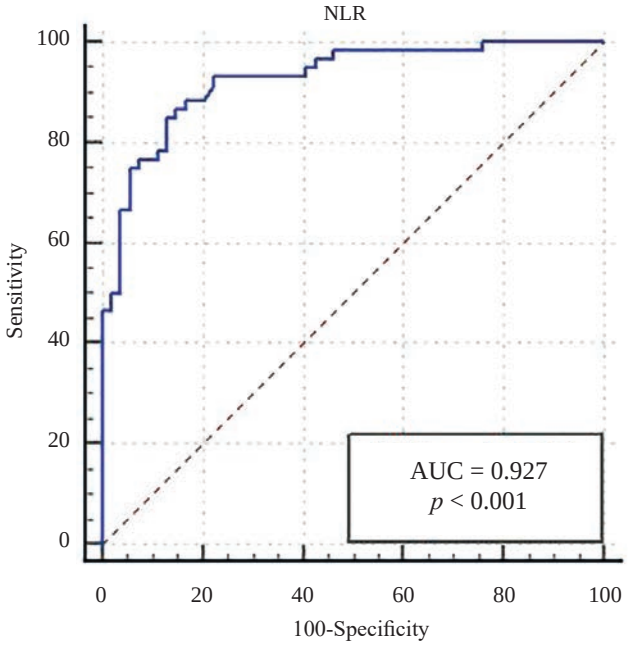


Fig. 2. ROC-curve for the prognostic value of NLR

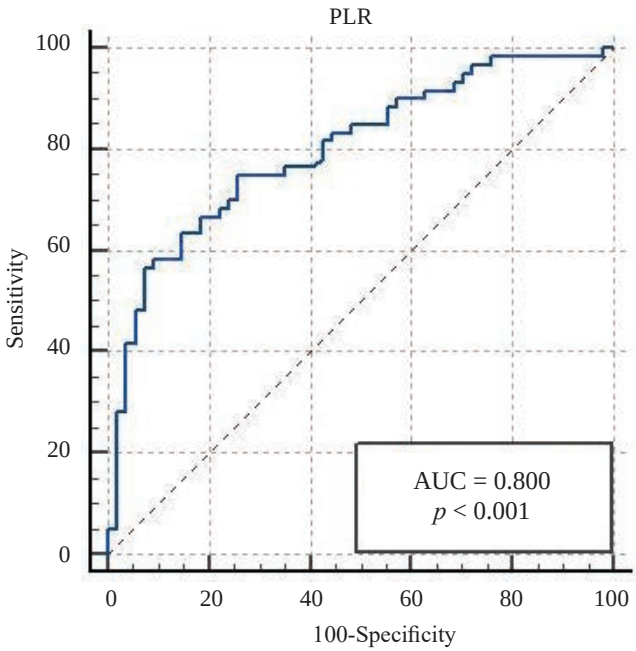


Figю 3. ROC-curve for the prognostic value of PLR

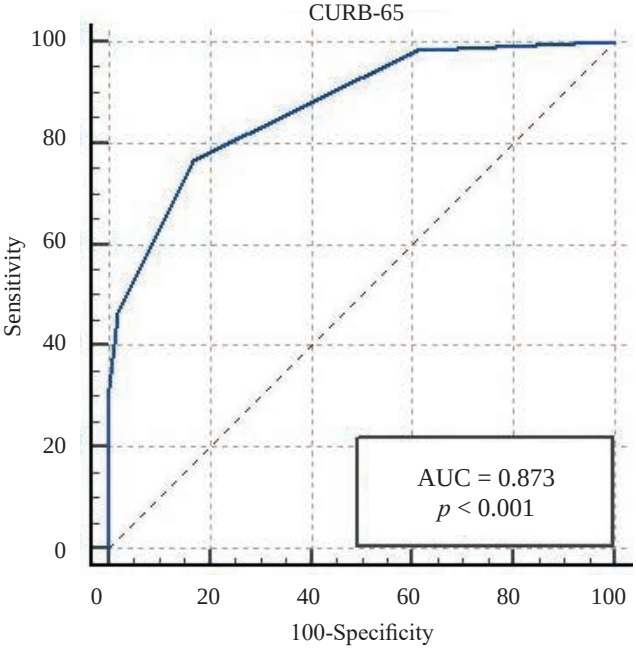


Fig. 4. ROC-curve for the prognostic value of CURB-65 score

For NLR (at a threshold value > 6), sensitivity was 85.0%, specificity was 87.0%, positive predictive value was 87.9%, negative predictive value was 83.9%, and accuracy was 86.0%. For MLR, the diagnostic accuracy was 79.0%, and for PLR – 73.7%.

## DISCUSSION

To predict a fatal outcome in patients with pneumonia caused by carbapenem-resistant *K. pneumoniae*, including those with COVID-19 co-infection, various laboratory parameters, scores, and indices can be used. In a similar study conducted by A. Singh et al., the average values of NLR, PLR, and CRP were higher in the group of patients with severe COVID-19 infection and a fatal outcome than in those with moderate disease and discharged, respectively. It is proposed to consider these indicators for predicting a fatal outcome. MLR is not a reliable prognostic biomarker, since when analyzing the ROC curve, the AUC 95% CI was < 0.50. NLR, on the contrary, had

the highest AUC (0.923), with the highest specificity (0.83%) and sensitivity (0.88%) [21], which is consistent with our data.

According to the study by O. Bardakci, the group of deceased patients had higher CURB-65 scores compared to survivors, both in patients with COVID-19-associated pneumonia and in patients with community-acquired pneumonia without COVID-19 infection. It was assumed that NLR and PLR are as reliable as the CURB-65 risk assessment score [22]. Z. Wang et al. reported that NLR was an easily accessible biomarker for predicting mortality in patients with carbapenem-resistant K. pneumoniae infection [23].

In a study by E. Cataudella et al., NLR predicted 30-day mortality in elderly patients with pneumonia ($p < 0.001$) and showed better results than the PSI score ($p < 0.05$), CURB-65 score, CRP, and leukocyte count ($p < 0.001$) [15]. However, there is also somewhat different information. According to Y. Kaya et al., deceased patients with community-acquired pneumonia had higher NLR levels compared to survivors (13.5 ± 9 versus 7.9 ± 6.8, $p = 0.010$). Still, when comparing ROC curves, the prognostic value of NLR did not exceed the CURB-65 and PSI scores [24]. According to our data, NLR is a more sensitive indicator in assessing the risk of an unfavorable outcome than the CURB-65 score, and PLR and MLR are inferior to the CURB-65 score in diagnostic accuracy. Considering that NLR has greater sensitivity and the CURB-65 score has greater specificity, we believe it is optimal to use them in combination.

## CONCLUSION

In patients with pneumonia caused by carbapenem-resistant *K. pneumoniae*, the prognosis of a fatal outcome can be determined using laboratory parameters (leukocytes, neutrophils, lymphocytes, platelets, NLR, MLR, and PLR), as well as CURB-65 score. Although this scoring system is widely used and has proven itself as a simple way to assess the patient's condition and predict mortality and the need for intensive care, it showed low specificity (47%) and diagnostic accuracy (71.7%). Therefore, NLR (at a level > 6) should be considered as the indicator of choice that can be used at the first stage to predict a fatal outcome of pneumonia caused by carbapenem-resistant *K. pneumoniae* due to its high sensitivity (85%) and specificity (87%) as well as due to ease of use. In addition, the calculation of the CURB-65 score can be used at NLR > 3.

## REFERENCES


1. Lee J., Sunny S., Nazarian E., Fornek M., Abdallah V., Episcopia B. et al. Carbapenem-Resistant Klebsiella Pneumoniae in Large Public Acute-Care Healthcare System, New York, New York, USA, 2016–2022. *Emerg Infect Dis.* 2023;29(10):1973-1978. DOI: 10.3201/eid2910.230153.
2. Fasciana T., Antonelli A., Bianco G., Lombardo D., Codda G., Roscetto E. et al. Multicenter Study On The Prevalence Of Colonization Due To Carbapenem-Resistant Enterobacterales Strains Before And During The First Year Of COVID-19, Italy 2018–2020. *Front. Public Health.* 2023;11(1270924). DOI: 10.3389/fpubh.2023.1270924.
3. Miller W.R., Arias C.A. ESKAPE Pathogens: Antimicrobial Resistance, Epidemiology, Clinical Impact and Therapeutics. *Nat Rev Microbiol*. 2024;22:598–616. DOI: 10.1038/s41579-024-01054-w.
4. Sawa T., Kooguchi K., Moriyama K. Molecular Diversity of Extended-Spectrum B-Lactamases and Carbapenemases, and Antimicrobial Resistance. *J Intensive Care.* 2020;8:13. DOI: 10.1186/s40560-020-0429-6.
5. Guo H., Wu Y., Li L., Wang J., Xu J., He F. Global Emergence of Carbapenem-Resistant Klebsiella Pneumoniae Co-Carrying Multiple Carbapenemases. *Comput Struct Biotechnol J*. 2023;21:3557-3563. DOI: 10.1016/j.csbj.2023.07.013.
6. Choi M.H., Kim D., Lee K.H., Cho J.H., Jeong S.H. Changes in the Prevalence of Pathogens Causing Hospital-Acquired Bacterial Pneumonia and the Impact of their Antimicrobial Resistance Patterns on Clinical Outcomes: A Propensity-Score-Matched Study. *International Journal of Antimicrobial Agents*. 2023;62(3):106886. DOI: 10.1016/j.ijantimicag.2023.106886.
7. Vikhe V.B., Faruqi A.A., Patil R.S., Patel H., Khandol D., Reddy A. A Study on the Etiology and Clinical Manifestations of Community-Acquired Pneumonia in Adults in Western India. *Cureus* 2024;16(6): e63132. DOI:10.7759/cureus.63132.
8. Kuloglu T.O., Unuvar G.K., Cevahir F., Kilic A.U., Alp E. Risk Factors and Mortality Rates of Carbapenem-Resistant Gram-Negative Bacterial Infections in Intensive Care Units. *J Intensive Med*. 2024;4(3):347-354. DOI: 10.1016/j.jointm.2023.11.007.
9. Yao Y., Zha Z., Li L., Tan H., Pi J., You C. et al. Healthcare-Associated Carbapenem-Resistant Klebsiella Pneumoniae Infections are Associated with Higher Mortality Compared to Carbapenem-Susceptible K. Pneumoniae Infections in the Intensive Care Unit: A Retrospective Cohort Study. *J Hosp Infect.* 2024; 148:30-38. DOI: 10.1016/j.jhin.2024.03.003.
10. Vinokurova D.A., Kulikov E.S., Fedosenko S.V., Starovoytova E.A., Chernogoryuk G.E., Yun V.E. et al. Risk Factors of Death and Prognostic Markers of the Adverse Outcome of Community-Acquired Pneumonia in Adult Patients. *Siberian Medical Review*. 2024;(1):22-32. (In Russ.). DOI: 10.20333/25000136-2024-1-22-32.
11. Volchkova E.V., Titova O.N., Kuzubova N.A., Lebedeva E.S. Potential Predictors of Severe Course and Outcome of Community-Acquired Pneumonia. *Pulmonology*. 2023; 33 (2): 225–232. (In Russ.). DOI: 10.18093/0869-0189-2023-33-2-225-232.

12. Zaki H.A., Hamdi A.B., Shaban E., Mohamed E.H., Basharat K., Elsayed W.A. et al. The Battle of the Pneumonia Predictors: A Comprehensive Meta-Analysis Comparing the Pneumonia Severity Index (PSI) and the CURB-65 Score in Predicting Mortality and the Need for ICU Support. *Cureus*. 2023;15(7): e42672. DOI:10.7759/cureus.42672.
13. Buonacera A., Stancanelli B., Colaci M., Malatino M. Neutrophil to Lymphocyte Ratio: An Emerging Marker of the Relationships between the Immune System and Diseases. *International Journal of Molecular Sciences* 2022;23(7):3636. DOI: 10.3390/ijms23073636.
14. Feng D.Y., Zou X.L., Zhou Y.Q., Wu W.B., Yang H.L., Zhang T.T. Combined Neutrophil-to-Lymphocyte Ratio and CURB-65 Score as an Accurate Predictor of Mortality for Community-Acquired Pneumonia in the Elderly. *Int J Gen Med.* 2021;14:1133-1139. DOI: 10.2147/IJGM.S300776.
15. Cataudella E., Giraffa C.M., Di Marca S., Pulvirenti A., Alaimo S., Pisano M. et al. Neutrophil-To-Lymphocyte Ratio: An Emerging Marker Predicting Prognosis in Elderly Adults with Community-Acquired Pneumonia. *J. Am. Geriatr. Soc.* 2017;65(8):1796–1801. DOI: 10.1111/jgs.14894.
16. Enersen, C.C., Egelund, G.B., Petersen, P.T, Andersen S., Ravn P., Rohde G. et al. The Ratio of Neutrophil-To-Lymphocyte and Platelet-To-Lymphocyte and Association with Mortality in Community-Acquired Pneumonia: A Derivation-Validation Cohort Study. *Infection* 2023;51(5):1339-1347. DOI: 10.1007/s15010-023-01992-2.
17. Liu Y., Du X., Chen J., Jin Y., Peng L., Wang H.X. et al. Neutrophil-to-Lymphocyte Ratio as an Independent Risk Factor for Mortality in Hospitalized Patients with COVID-19. *J. Infect.* 2020;81: e6–e12. DOI: 10.1016/j.jinf.2020.04.002.
18. Ng W.W.S., Lam S.M., Yan W.W., Shum H.P. NLR, MLR, PLR and RDW to Predict Outcome and Differentiate between Viral and Bacterial Pneumonia in the Intensive Care Unit. *Sci Rep.* 2022; 12(1):15974. DOI: 10.1038/s41598-022-20385-3.
19. Wu C., Lin Z., Jie Y. Analysis of Risk Factors and Mortality of Patients with Carbapenem-Resistant Klebsiella Pneumoniae Infection. *Infection and Drug Resistance*. 2022;15:2383-2391. DOI: 10.2147/IDR.S362723.
20. Guo J., Zhou B., Zhu M., Yuan Y., Wang Q., Zhou H. et al. CURB-65 May Serve as a Useful Prognostic Marker in COVID-19 Patients within Wuhan, China: A Retrospective Cohort Study. *Epidemiol Infect.* 2020 Oct 1;148:e241. DOI: 10.1017/S0950268820002368.
21. Singh A, Bhadani PP, Surabhi, Sinha R, Bharti S, Kumar T. et al. Significance of Immune-Inflammatory Markers in Predicting Clinical Outcome Of COVID-19 Patients. *Indian J Pathol Microbiol.* 2023 Jan-Mar;66(1):111-117. DOI: 10.4103/ijpm.ijpm_658_21.
22. Bardakci O., Das M., Akdur G., Akman C., Siddikoglu D., Akdur O. et al. Haemogram Indices are as Reliable as CURB-65 to Assess 30-Day Mortality in Covid-19 Pneumonia. *Natl Med J India* 2022;35(4):221-228. DOI: 10.25259/NMJI_474_21.
23. Wang Z, Li R, Yuan Z, Zhang Z, Qian K. The Prognostic Value of Neutrophil-to-Lymphocyte Ratio in Adult Carbapenem-Resistant Klebsiella Pneumoniae Infection: A Retrospective Cohort Study. *Front Cell Infect Microbiol.* 2024 Nov 28; 14:1461325. DOI: 10.3389/fcimb.2024.1461325.
24. Kaya Y, Taş N, Çanakçı E, Cebeci Z, Özbilen M, Keskin H et al. Relationship of Neutrophil-To-Lymphocyte Ratio with Presence and Severity of Pneumonia. *J Clin Anal Med* 2018;9(5): 452-7. DOI: 10.4328/JCAM.5817.

## Author Contribution

Levchenko K.V. – review of publications on the article topic, study design, collection of material, drafting of the article, statistical processing, analysis and interpretation of the data. Mitsura V.M. – study design, statistical processing, analysis and interpretation of the data, editing of the manuscript, critical revision of the manuscript for important intellectual content, final approval of the manuscript for publication.

## Author Information

**Levchenko Kristina V.** – Assistant Lecturer, Department of Phthisiopulmonology, Faculty of Professional Development and Retraining, Gomel State Medical University, Gomel, Republic of Belarus, kristy_levchenko@mail.ru, https://orcid.org/0000-0002-0368-0473

**Mitsura Viktor M.** – Dr. Sci. (Med.), Professor, Deputy Director for Science, Republican Research Center for Radiation Medicine and Human Ecology, Gomel, Republic of Belarus, mitsura_victor@tut.by, https://orcid.org/0000-0002-0449-5026

(✉) **Levchenko Kristina V.,** kristy_levchenko@mail.ru

Received 30.10.2024;
approved after peer review 07.02.2025;
accepted 27.02.2025

УДК 616.5-003.93-085.451.16:[582.284+547.922.15]
https://doi.org/10.20538/1682-0363-2025-3-89-96

# Wound-Healing effect of substances based on lanolin and *Ganoderma applanatum* and *Fomitopsis pinicola* (xylotrophic basidiomycetes) extracts

**Petrova I.M., Ermoshin A.A., Khatsko S.L.**

*Ural Federal University named after the first President of Russia B.N.Yeltsin*
*19 Mira St., 620002 Yekaterinburg, Russian Federation*

## ABSTRACT

**Aim.** To evaluate the wound-healing effect of substances based on lanolin and *Ganoderma applanatum* and *Fomitopsis pinicola* extracts.

**Materials and methods.** The experiment used 20 white laboratory rats. The study included 3rd-degree burn modeling with wound exposure to an ointment containing *Ganoderma applanatum* and *Fomitopsis pinicola* extracts. A morphological investigation of skin was carried out with an assessment of the following parameters: epidermis thickness, fibroblast count, number of blood vessels, vessel area, and number of vessels with erythrocyte stasis, leukocyte stasis, and leukocyte diapedesis.

**Results.** *Ganoderma applanatum* and *Fomitopsis pinicola* extracts intensified regenerative processes. By day 14 of the experiment, epithelialization of the defect and scar formation took place. Application of the extract-containing ointments reduced exudation, microcirculatory disorders, and inflammatory infiltration.

**Conclusion.** The results suggested the beneficial effect of the *Ganoderma applanatum* and *Fomitopsis pinicola* extracts on the wound-healing process and demonstrated their potential for skin regeneration.

**Keywords:** skin regeneration, burn wounds, wound-healing agents, xylotrophic basidiomycetes, *Ganoderma* extract, *Fomitopsis* extract

**Conflict of interest.** The authors declare the absence of obvious or potential conflicts of interest related to the publication of this article.

**Source of financing.** The authors state that they received no funding for the study.

**Conformity with the principles of ethics.** The study was approved by the Ethics Committee at Ural Federal University named after the first President of Russia B.N.Yeltsin (Minutes No.1 dated March 13, 2023).

**For citation:** Petrova I.M., Ermoshin A.A., Khatsko S.L. Wound-Healing effect of substances based on lanolin and *Ganoderma applanatum* and *Fomitopsis pinicola* (xylotrophic basidiomycetes) extracts. *Bulletin of Siberian Medicine.* 2025;24(3):89–96. https://doi.org/10.20538/1682-0363-2025-3-89-96.

✉ *Petrova Irina M.,* Irina.Petrova@urfu.ru

# Оценка ранозаживляющего действия субстанций на основе ланолина и экстрактов ксилотрофных базидиомицетов *Ganoderma applanatum* и *Fomitopsis pinicola*

**Петрова И.М., Ермошин А.А., Хацко С.Л.**

*Уральский федеральный университет (УрФУ) им. первого Президента России Б.Н. Ельцина*
*Россия, 620002, г. Екатеринбург, ул. Мира, 19*

**РЕЗЮМЕ**

**Цель:** оценить ранозаживляющее действие субстанций на основе ланолина и экстрактов ксилотрофных базидиомицетов *Ganoderma applanatum* и *Fomitopsis pinicola.*

**Материалы и методы.** Эксперимент проводили на 20 белых лабораторных крысах. Животным моделировали термический ожог III степени с последующим воздействием на раны мазью, содержащей экстракты трутовых грибов. Проводили морфологическое описание препаратов кожи с оценкой следующих показателей: толщина эпидермиса, количество фибробластов, количество кровеносных сосудов, площадь сосудов, количество сосудов с явлениями эритростаза, лейкостаза и лейкодиапедеза.

**Результаты.** При воздействии экстрактов трутовых грибов отмечается интенсификация регенераторных процессов. К 14-м сут эксперимента имела место полная эпителизация, а на месте дефекта формировался рубец с развитым волокнистым компонентом. Использование мазей способствует уменьшению экссудативных явлений, микроциркуляторных расстройств и воспалительной инфильтрации.

**Заключение.** Показано, что использование экстрактов *Ganoderma applanatum* и *Fomitopsis pinicola* при лечении ожоговой раны благоприятно сказывается на течении раневого процесса. Полученные результаты позволяют осуществлять дальнейшее изучение экстрактов трутовых грибов в качестве ранозаживляющих агентов.

**Ключевые слова:** регенерация кожи, ожоговые раны, ранозаживляющие средства, ксилотрофные базидиомицеты, экстракт *Ganoderma*, экстракт *Fomitopsis*

**Конфликт интересов.** Авторы декларируют отсутствие явных и потенциальных конфликтов интересов, связанных с публикацией настоящей статьи.

**Источник финансирования.** Авторы декларируют отсутствие внешнего финансирования для проведения исследования и публикации статьи.

**Соответствие принципам этики.** Исследование одобрено этической комиссией ИЕНиМ УрФУ (протокол № 1 от 13.03.2023).

**Для цитирования:** Петрова И.М., Ермошин А.А., Хацко С.Л. Оценка ранозаживляющего действия субстанций на основе ланолина и экстрактов ксилотрофных базидиомицетов *Ganoderma applanatum* и *Fomitopsis pinicola*. *Бюллетень сибирской медицины.* 2025;24(3):89–96. https://doi.org/10.20538/1682-0363-2025-3-89-96.

## INTRODUCTION

In recent years, researchers have increasingly focused on discovering natural medicinal compounds. In particular, studies demonstrating the wound-healing effects of preparations derived from polypores have emerged [1]. Xylotrophic basidiomycetes (wood-decaying polypores) represent a vast but largely untapped source of novel pharmaceutical products. The most frequently cited polypore in traditional medicine, *Ganoderma lucidum*, has been used as a therapeutic agent in China for over two millennia [2]. Modern studies confirm that preparations derived from *Ganoderma lucidum* exhibit hypoglycemic, anti-inflammatory, antitumor, and immunomodulatory properties [3, 4]. For another, less-studied species of the *Ganoderma* genus – *G. applanatum,* the presence of similar effects has been confirmed by more recent research [5, 6].

The long-standing use of *Ganoderma* fungi and current scientific interest in them stem from their rich

content of metabolites: polysaccharides, phenolic compounds, alkaloids, sterols, flavonoids, amino acids, and others [7, 8]. The activity spectrum of these compounds is broad [9, 10] but occasionally contradictory. For instance, certain terpenes of *G. applanatum* exhibit anti-angiogenic effects [11], while lanostane triterpenoids demonstrate opposing pro-angiogenic effects [12].

In addition to polypores of the *Ganoderma* genus, fungi from the *Fomitopsis* genus have been widely used in traditional medicine, with *Fomitopsis pinicola* being one of its species [13]. However, *Fomitopsis* remains significantly understudied compared to the more extensively researched *Ganoderma*. Recent studies have identified new potential anti-inflammatory agents in *F. pinicola* fruiting bodies [14, 15].

In summary, both *G. applanatum* and *F. pinicola* are strong candidates for evaluating their effects on regeneration processes. The feasibility and safety of using xylotrophic macromycetes for developing wound-healing agents are further supported by the growing demand for raw materials from these fungi in cosmetology [16]. Thus, this study is aimed at assessing the wound-healing effects of substances based on lanolin and xylotrophic basidiomycetes *Ganoderma applanatum* and *Fomitopsis pinicola* extracts.

## MATERIALS AND METHODS

The study was conducted on 20 outbred white laboratory rats (males, aged 6 months). All experiments were approved by the Bioethics Committee at the Institute of Natural Sciences and Mathematics, Ural Federal University. A third-degree burn was modeled by applying a medical steel weight (2 cm diameter, 20 g) heated to 100 °C to the interscapular skin area for 30 seconds. Prior to this, the animals received an intramuscular injection of Analgin (0.2 ml). The animals were randomly divided into 4 groups ($n$ = 5):

CONTR, Control – rats with untreated wounds;

LAN, Lanolin – rats with wounds treated with lanolin;

LAN+extGND – rats with wounds treated with an ointment based on lanolin and a condensed alcoholic and aqueous *Ganoderma applanatum* extract;

LAN+extFP – rats with wounds treated with an ointment based on lanolin and a condensed alcoholic and aqueous *Fomitopsis pinicola* extract.

Ointments were applied to the wound area once daily (0.2 g) for 14 days. The animals were removed from the experiment on day 14 via diethyl ether overdose. Wounds were photographed with a Nikon D3000 camera on days 1, 3, 7, and 14. Wound areas were evaluated using the ImageJ software.

Fruiting bodies of *G. applanatum* and *F. pinicola* were collected in summer in a mixed forest in the vicinity of the Ural Federal University biological station (Russia, Sverdlovsk Region, the village of Klyuchi, 30 km south of Yekaterinburg). The specimens were dried in a shaded ventilated room for up to one week. Then the material was fixed by heating at 105 °C for 15 minutes to eliminate insect eggs and larvae and dried to constant mass at 50 °C. Extracts were prepared via sequential extraction with 95%, 70%, and 40% ethanol and distilled water (biomass : solvent ratio of 1:10; extraction time – 90 minutes at 50 °C). Combined extracts were evaporated on a rotary evaporator to aqueous residue, then adjusted with hydroalcoholic mixture. To prepare the 5% ointment, 7.5 ml of the extract (equivalent to 750 mg fungal biomass) was added at vigorous stirring to 7.5 g lanolin melted at 50 °C in a water bath until homogeneous consistency was achieved.

The chemical composition of the extracts was assessed by diluting stock suspension 20-fold with distilled water. Spectrophotometric methods were used to determine the content of phenolic compounds (via Folin – Ciocalteu's phenol reagent and 7.5 % sodium carbonate aqueous solution, with gallic acid as the standard), flavonoids (as complexes with aluminum chloride, with rutin as the standard), and free amino acids (with the ninhydrin reagent and glycine as the standard). The methods were adapted for the microplate immune-assay [17].

Extracted mass was determined gravimetrically by evaporating aliquots of stock suspension and recalculating the obtained value to ointment content. The qualitative analysis followed standard pharmacognostic methods. Saponins were determined by the foam formation in the aqueous solution and precipitation with lead acetate. Tannins were detected by the ferric (III) chloride test and precipitation test with potassium dichromate or lead acetate. Anthraquinones were determined in the color reaction with magnesium acetate. Dragendorff's, Marme's, Marquis, and Bouchardat's reagents were used for detecting alkaloids. Individual amino acids were identified by thin-layer chromatography (TLC) in n-butanol:acetic acid:water (4:1:1) [18]. All tests were performed in 4 analytical replicates.

For the histological analysis, standard procedures were employed. Tissue specimens (3 μm) were

stained with hematoxylin and eosin and Van Gieson's picrofuchsin. The ToupView software was applied for the histological analysis. The epidermal thickness, fibroblast count, and vessel area and number (including some that exhibit stasis or diapedesis) were analyzed according to 10 randomly selected fields with conversion to 1 mm$^2$.

The statistical analysis was performed using Microsoft Excel, Mathematica 12.0, and Statistica 12.0 packages. Data sets were compared by the Kruskal – Wallis test with the Dunn's post-hoc analysis. The results were presented as the median and the interquartile range *Me* [$Q_1$; $Q_3$]. The values of $p < 0.05$ were considered statistically significant.

## RESULTS

The table below summarizes the chemical composition of the tested extracts.

Table

**Chemical Composition of the *Ganoderma Applanatum* and *Fomitopsis Pinicola* Extracts, *Me* [$Q_1$; $Q_3$]**

Bioactive substances in 1 g ointments containing *Ganoderma applanatum* and *Fomitopsis pinicola* extracts

| Fungi species | Extractives, mg / ml | Phenolics, mg / ml | Flavonoids, mg / ml | Free amino acids | | Qualitative composition | | | |
|---|---|---|---|---|---|---|---|---|---|
| | | | | mg / ml | Quantity | Alkaloids | Saponins | Anthraqui-nones | Tannins |
| G. applanatum | 4.5 [4.5 ; 4.9] | 0.403 [0.398 ; 0.420] | 0.008 [0.007 ; 0.009] | 0.018 [0.015; 0.023] | 6 | - | - | - | - |
| F. pinicola | 5.5 [5.5 ; 6.3] | 0.42 [0.373 ; 0.432] | 0.016 [0.015 ; 0.016]* | 0.014 [0.013 ; 0.017] | 6 | + | + | – | - |

* significant differences compared to the *G. applanatum* group ($p < 0.05$).

The comparative analysis revealed higher extractability for *F. pinicola*. Both extracts contained negligible free amino acids and carbohydrates (below detection limit via TLC or anthrone colorimetry). Phenolics accounted for no more than 10 % of total extracted substances, with similar levels in both extracts. Flavonoids were detected at higher concentrations than free amino acids. *F. pinicola* exhibited twice the flavonoid content of *G. applanatum*. Notably, flavonoids comprised a larger proportion of phenolics in *F. pinicola*. Alkaloids and saponins were also present in *F. pinicola* extracts, indicating their greater metabolic diversity.

Wound-healing dynamics (Fig. 1) showed accelerated healing in fungal extract-treated groups, with earlier crust formation and sloughing as well as wound closure. Thus, by the end of the experiment, a decrease in wound area in the LAN+extGND group significantly exceeded that of not only the control group, but also of the LAN group.

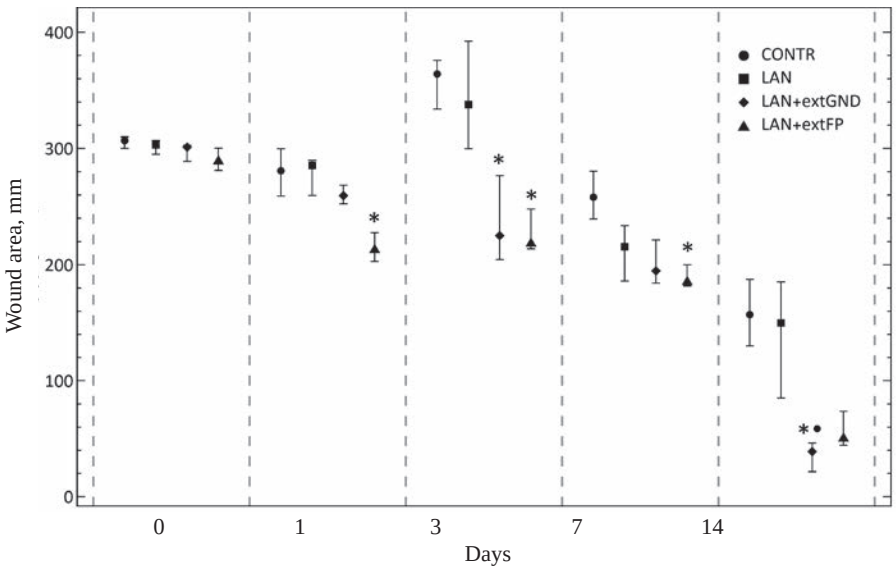


Fig. 1. Wound area reduction:
* significant differences compared to the CONTR group, $p < 0.05$;
● significant differences compared to the LAN group, $p < 0.05$

The histological analysis on day 14 revealed persistent leukocyte necrotic layers with fibrin clusters and damaged tissue in the CONTR and LAN groups. Epithelialization was limited to wound margins. Dermal infiltration and dilated vessels with stasis and diapedesis were observed (Fig. 2). Van Gieson's staining showed thin and disorganized pale crimson collagen bundles (Fig. 3).

In the LAN+extGND and LAN+extFP groups, the defect was closed by neo-epidermis with marked acanthosis, so that epidermis thickness increased compared to the control group (Fig. 4, *a*). Subjacent granulation tissue contained a large number of fibroblasts and neovessels. In the LAN+extGND group, inflammation was absent in most regenerated skin areas (Fig. 2). Massive twisted bundles of collagen fibers were detected deep in the regenerated skin, indicating intensive fibrous component development (Fig. 3). In the LAN+extFP group, moderate perivascular leukocyte infiltration persisted (Fig. 2) with less pronounced fiber formation (Fig. 3).

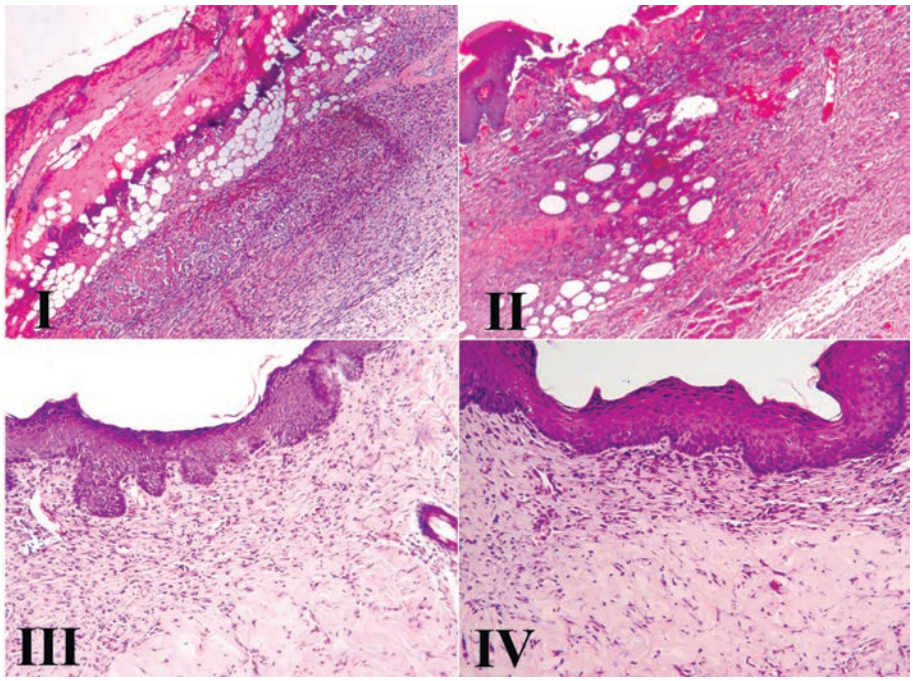


Fig. 2. Morphological structure of the skin in the experimental groups:
I – CONTR, II – LAN,
III – LAN+extGND,
IV – LAN+extFP;
hematoxylin and eosin staining;
×100

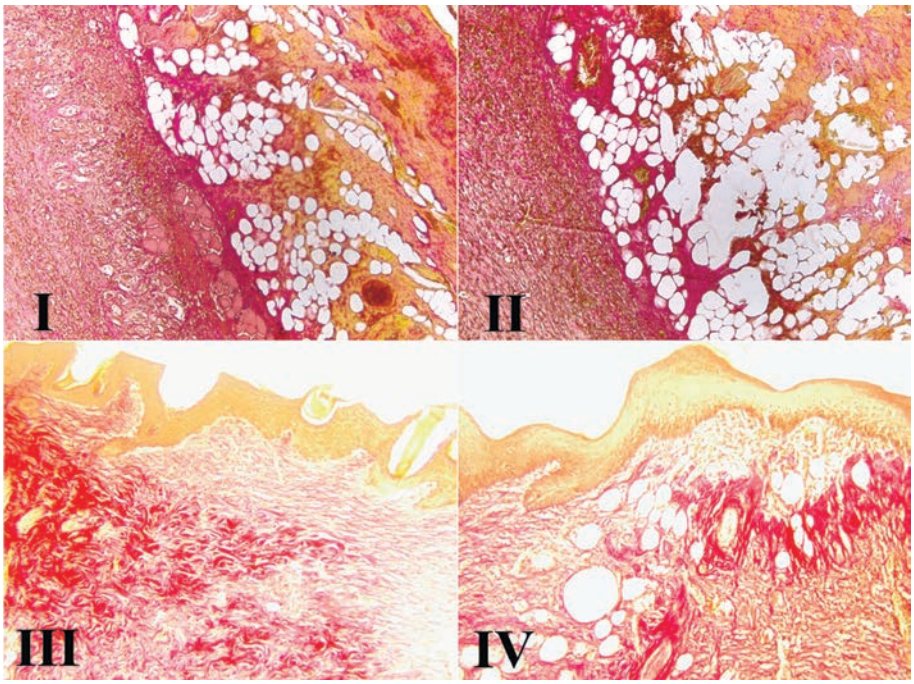


Fig. 3. Morphological structure of the skin in the experimental groups:
I – CONTR, II – LAN,
III – LAN+extGND,
IV – LAN+extFP;
Van Gieson's staining; ×100

The CONTR and LAN groups exhibited microcirculatory disfunction, such as vasodilation, leukocyte stasis and diapedesis, and vascular congestion. Both fungal extract groups showed reduced vascular reactions. The LAN+extFP group demonstrated smaller vessel area (Fig. 4, *b*). Despite a comparable vessel number (Fig. 4, *c*), the LAN+extGND group showed a decreased vessel number with leukocyte stasis and diapedesis (Fig. 4, *d*). Both groups also had a reduced number of vessels with blood stasis (Fig. 4, *e*).

Inflammation hindered scar formation in the CONTR and LAN groups, therefore it comprised mainly hematogenous cells. By contrast, in the fungal extract groups, a large number of fibroblasts were found (Fig. 4, *f*). Moreover, for the LAN+extGND group, the differences were noted compared to not only the control group, but also to the LAN group.

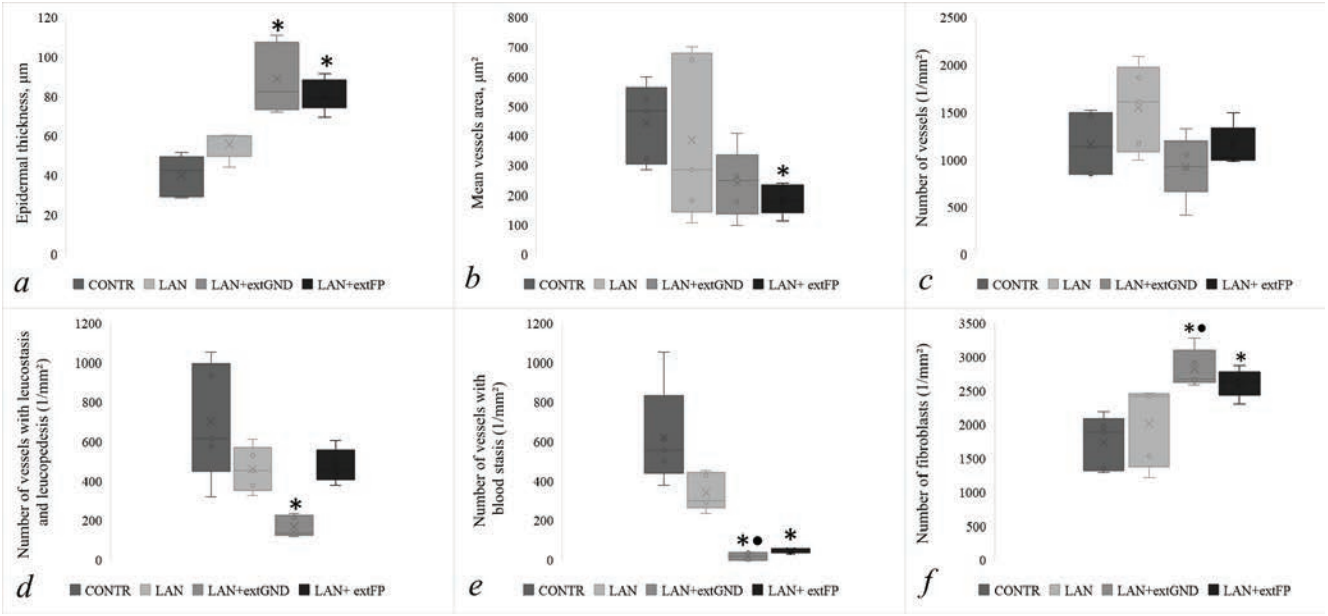


Fig. 4. Results of the morphological and quantitative assessment of the regenerated skin: * significant differences compared to the CONTR group, $p < 0.05$; ● significant differences compared to the LAN group, $p < 0.05$

## DISCUSSION

Accelerated wound healing in the experimental fungal extract groups correlated with reduced exudation, improved microcirculation, and diminished inflammation, promoting faster tissue restoration and smaller wound areas. Acanthosis in the LAN+extGND group signaled active re-epithelialization, while mature collagen bundles indicated scar maturation. Nevertheless, a high vascularization degree characterized the scar as normal rather than fibrous. Reduced leukocyte stasis and diapedesis in the LAN+extGND group aligned with anti-inflammatory effects of the *G. applanatum* extract compounds.

In the LAN+extFP group, epithelialization was also pronounced, however, the fibrous component formation was not as intense. In addition, the infiltrate presence indicated a slight anti-inflammatory effect. Despite weaker anti-inflammatory effects, the *F. pinicola* extract modulated vascular reactions. It can be assumed that disparate bioactivity of extracts apparently stemed from alkaloids and saponins identified in *F. pinicola*, as well as higher flavonoid content. Both extracts likely owed their anti-inflammatory effects to phenolic compounds with antioxidant activity. Moreover, phenolic content was the same in both fungi extracts. According to numerous studies, the most potent effect of *G. applanatum* extract may be related to triterpene compounds [7].

In both fungal extract groups, a large number of fibroblasts was observed, probably associated with the inflammation and microcirculation modulation. An enhanced fibroblast count might suggest stimulating effects of fungal metabolites on cell proliferation. This is also supported by enhanced re-epithelialization, caused by proliferative activity of keratinocytes.

Greater collagen deposition under *G. applanatum* extract treatment implied a potential impact on the synthetic activity of fibroblasts. However, a detailed extract composition and effects of extractive compounds require further study.

## CONCLUSION

Burn injury regeneration under fungi extract treatment proceeds through classical stages but with shortened duration and neo-tissue formation by day 14 of the experiment. Both extracts accelerated epithelialization and scar maturation probably via cell proliferation stimulation. Anti-inflammatory effects and vascular modulation were evident for *G. applanatum* and *F. pinicola*, which increased the regeneration efficiency.

### REFERENCES


1. Cheng P.G., Phan C.W., Sabaratnam V., Abdullah N., Abdulla M.A., Kuppusamy U.R. Polysaccharides-Rich Extract of Ganoderma Lucidum (M.A. Curtis:Fr.) P. Karst Accelerates Wound Healing in Streptozotocin-Induced Diabetic Rats. *J. Evid. Based Complementary Altern. Med*. 2013;1: 671252. DOI: 10.1155/2013/671252.
2. Luangharn T., Karunarathna S.C., Dutta A.K., Paloi S., Promputtha I., Hyde K.D. et al. Ganoderma (Ganodermataceae, Basidiomycota) Species from the Greater Mekong Subregion. *J. Fungi.* 2021;7(10):819. DOI: 10.3390/jof7100819.
3. Lin Z.B., Zhang H.N. Anti-Tumor and Immunoregulatory Activities of Ganoderma Lucidum and Its Possible Mechanisms. *Acta Pharmacol. Sin.* 2004;25(11):1387–1395.
4. Li F., Zhang Y., Zhong Z. Antihyperglycemic Effect of Ganoderma Lucidum Polysaccharides on Streptozotocin-Induced Diabetic Mice. *Int. J. Mol. Sci.* 2011;12(9):6135–6145. DOI: 10.3390/ijms12096135.
5. Ma C.-w., Feng M., Zhai X., Hu M., You L., Luo W. et al. Optimization for the Extraction of Polysaccharides from Ganoderma Lucidum and Their Antioxidant and Antiproliferative Activities. *J. Taiwan Inst. Chem. E*. 2013;44(6):886–894. DOI: 10.1016/j.jtice.2013.01.032.
6. Shi M., Zhang Z., Yang Y. Antioxidant and Immunoregulatory Activity of Ganoderma Lucidum Polysaccharide (GLP). *Carbohydr. Polym*. 2013;95(1):200–206. DOI: 10.1016/j.carbpol.2013.02.081.
7. Galappaththi M.C.A., Patabendige N.M., Premarathne B.M., Hapuarachchi K.K., Tibpromma S., Dai D.Q. et al. A Review of Ganoderma Triterpenoids and Their Bioactivities. *Biomolecules.* 2022;13 (1):24. DOI: 10.3390/biom13010024.
8. Wang Y.Y., Khoo K.H., Chen S.T., Lin C.C., Wong C.H., Lin C.H. Studies on the Immuno-Modulating and Antitumor Activities of Ganoderma Lucidum (Reishi) Polysaccharides: Functional and Proteomic Analyses of a Fucose-Containing Glycoprotein Fraction Responsible for the Activities. *Bioorg. Med. Chem.* 2002;10(4):1057–1062. DOI: 10.1016/s0968-0896(01)00377-7.
9. Kao C.H.J., Jesuthasan A.C., Bishop K.S., Glucina M.P., Ferguson L.R. Anti-Cancer Activities of Ganoderma Lucidum: Active Ingredients and Pathways. *Funct. Food Health Dis.* 2013;3:48–65. DOI: 10.31989/ffhd.v3i2.65.
10. Cör Andrejč D., Knez Ž., Knez Marevci M. Antioxidant, Antibacterial, Antitumor, Antifungal, Antiviral, Anti-Inflammatory, and Nevro-Protective Activity of Ganoderma Lucidum: An Overview. *Front. Pharmacol.* 2022;13:934982. DOI: 10.3389/fphar.2022.934982.
11. Kimura Y., Taniguchi M., Baba K. Antitumor and Antimetastatic Effects on Liver of Triterpenoid Fractions of Ganoderma Lucidum: Mechanism of Action and Isolation of an Active Substance. *Anticancer Res.* 2002;22(6A):3309–3318.
12. Jiang C., Ji J., Li P., Liu W., Yu H., Yang X. et al. New Lanostane-Type Triterpenoids with Proangiogenic Activity from the Fruiting Body of Ganoderma Applanatum. *Nat. Prod. Res.* 2022;36(6):1529–1535. DOI: 10.1080/14786419.2021.1898388.
13. Grienke U., Zöll M., Peintner U., Rollinger J.M. European Medicinal Polypores – A Modern View on Traditional Uses. *J. Ethnopharmacol.* 2014;154(3):564–583. DOI: 10.1016/j.jep.2014.04.030.
14. Sum W.C., Ebada S.S., Matasyoh J.C., Stadler M. Recent Progress in the Evaluation of Secondary Metabolites from Basidiomycota. *Curr. Res. Biotechnol.* 2023;6:100155. DOI: 10.1016/j.crbiot.2023.100155.
15. Tai S.H., Kuo P.C., Hung C.C., Lin Y.H., Hwang T.L., Lam S.H. et al. Bioassay-Guided Purification of Sesquiterpenoids from the Fruiting Bodies of Fomitopsis Pinicola and Their Anti-Inflammatory Activity. *RSC Adv.* 2019;9(59):34184–34195. DOI: 10.1039/c9ra05899k.
16. Taofiq O., González-Paramás A.M., Martins A., Barreiro M.F., Ferreira I.C.F.R. Mushrooms Extracts and Compounds in Cosmetics, Cosmeceuticals and Nutricosmetics – A Review. *Ind. Crops Prod.* 2016;90:38–48. DOI: 10.1016/j.indcrop.2016.06.012.48.
17. Kiseleva I.S., Ermoshin A.A., Galishev B.A., Shen D., Ma C., He J. Chemical Composition and Antioxidant Activity of Fomitopsis Pinicola Growing on Coniferous and Deciduous Substrates. *For. Ideas.* 2022;28(2):287–297.
18. Ermoshin A.A., Kiseleva I.S., Nikkonen I.V., Nsengiumva D.S., Duan S., Ma C. et al. Antioxidant Activity and Chemical Composition of Extracts from Fruiting Bodies of Xylotrophic Fungi Growing on Birch. *Journal of Siberian Federal University. Biology.* 2021;14(3):339–353. DOI: 10.17516/1997-1389-0354.


## Author Information

**Petrova Irina M.** – Senior Lecturer, Department of Biology and Fundamental Medicine, Institute of Natural Sciences and Mathematics, Ural Federal University, Yekaterinburg, Irina.Petrova@urfu.ru, https:/orcid.org/0000-0002-4358-5219

**Ermoshin Alexander A.** – Cand. Sci. (Biology), Associate Professor, Department of Experimental Biology and Biotechnologies, Institute of Natural Sciences and Mathematics, Ural Federal University, Yekaterinburg, Alexander.Ermoshin@urfu.ru, https:/orcid.org/0000-0003-2784-4898

**Khatsko Sergey L.** – Head of Anatomical and Physiological Experimental Laboratory, Institute of Natural Sciences and Mathematics, Ural Federal University, Yekaterinburg, sergey.khatsko@urfu.ru, https:/orcid.org/0000-0001-5921-6680

(✉) **Petrova Irina M.,** Irina.Petrova@urfu.ru

Received on July 16, 2024;
approved after peer review on February 13, 2025;
accepted on February 27, 2025

УДК 616.12-005.4:616.132.2-089.819.5:612.127.4]-092.4
https://doi.org/10.20538/1682-0363-2025-3-97-106

# Effects of nitric oxide on sympathoadrenal system activity in patients with ischemic heart disease in coronary artery bypass grafting

**Rebrova T. Yu., Podoksenov Yu.K., Korepanov V.A., Churilina E.A., Kamenshchikov N.O., Muslimova E.F., Vorozhtsova I.N., Afanasiev S.A.**

*Cardiology Research Institute, Tomsk National Research Medical Center (NRMC), Russian Academy of Sciences*
*111a Kievskaya St., 634012 Tomsk, Russian Federation*

## ABSTRACT

**Aim.** To investigate changes in laboratory parameters of sympathoadrenal system activity and β-adrenergic receptor reactivity of erythrocyte membranes (β-ARMe) in ischemic heart disease (IHD) patients with clinical forms of arterial hypertension of high cardiovascular risk during coronary artery bypass grafting with anesthetic management including nitric oxide.

**Materials and methods.** In this randomized study with parallel distribution, 36 patients (male – 66.7%; average age – 68 [63; 70] years) with IHD and clinical forms of arterial hypertension of high cardiovascular risk were enrolled. According to the indications, all patients underwent elective coronary artery bypass grafting (CABG) using extracorporeal circulation (ECC). Patients were randomly divided into the main and control groups. Patients of the main group intraoperatively received NO at the concentration of 80 ppm first in the breathing circuit and then in the ECC circuit. Patients of the control group underwent CABG with standard mechanical lung ventilation and ECC. Before connecting to the ECC, at the end of ECC, and 1 day after CABG, all patients underwent clinical, laboratory, and instrumental tests in accordance with the clinical standards, β-ARMe was assessed, and the concentration of norepinephrine and epinephrine in the blood plasma was determined by ELISA.

**Results.** At the presurgical stage and 1 day after CABG, the groups did not differ in clinical and biochemical parameters. At the presurgical stage, the median values of β-ARMe in the main and control groups slightly exceeded the upper limits of normal and did not differ significantly. CABG was not accompanied by changes in β-ARMe in the control group. Intrasurgical NO donation also did not affect the level of β-ARMe. One day after CABG, neither intergroup differences in β-ARMe nor significant changes in the parameter during follow-up in each group were noted. In both control and main groups, a significant increase in the levels of epinephrine and norepinephrine was detected 1 day after CABG compared to the baseline level. At the same time, there were no intergroup differences in the level of catecholamines either before ECC or 1 day after CABG.

**Conclusion.** In cardiac surgery with extracorporeal circulation, the use of NO for the purpose of organ protection does not affect the level of β-ARMe and changes in the mediator response of the sympathetic system to stress in patients with IHD and clinical forms of hypertension of high cardiovascular risk.

**Keywords:** nitric oxide, coronary artery bypass grafting, β-adrenergic receptor reactivity of erythrocyte membranes, epinephrine, norepinephrine

**Conflict of interest.** The authors declare the absence of obvious or potential conflicts of interest related to the publication of the article.

**Source of financing.** The study was carried out within the state assignment of the Ministry of Science and Higher Education of the Russian Federation, state registration No. 122020300183-4.

**Conformity with the principles of ethics.** All patients signed an informed consent to participate in the study. The

✉ *Rebrova Tatiana Yu.,* rebrova@cardio-tomsk.ru

study protocol was approved by the Bioethics Committee at the Cardiology Research Institute of Tomsk NRMC (Minutes No. 208 dated January 20, 2021).

**For citation:** Rebrova T.Yu., Podoksenov Yu.K., Korepanov V.A., Churilina E.A., Kamenshchikov N.O., Muslimova E.F, Vorozhtsova I.N., Afanasiev S.A. Effects of nitric oxide on sympathoadrenal system activity in patients with ischemic heart disease in coronary artery bypass grafting. *Bulletin of Siberian Medicine.* 2025;24(3):97–106. https://doi.org/10.20538/1682-0363-2025-3-97-106.

# Эффекты оксида азота на показатели активности симпато-адреналовой системы пациентов с ишемической болезнью сердца при операции коронарного шунтирования

**Реброва Т.Ю., Подоксенов Ю.К., Корепанов В.А., Чурилина Е.А., Каменщиков Н.О., Муслимова Э.Ф., Ворожцова И.Н., Афанасьев С.А.**

*Научно-исследовательский институт (НИИ) кардиологии, Томский национальный исследовательский медицинский центр (НИМЦ) Российской академии наук*
*Россия, 634012, г. Томск, ул. Киевская, 111а*

## РЕЗЮМЕ

**Цель.** Изучить динамику лабораторных показателей активности симпатоадреналовой системы и показателя β-адренореактивности мембран эритроцитов у больных ишемической болезнью сердца (ИБС) с клиническими формами артериальной гипертонии (АГ) высокого кардиоваскулярного риска на этапах выполнения операции коронарного шунтирования с анестезиологическим обеспечением, включающим применение оксида азота.

**Материалы и методы.** В рандомизированное исследование с параллельным распределением были включены 36 пациентов (из них 66,7% – мужчины; средний возраст 68 [63; 70] лет) с диагнозом ИБС с клиническими формами АГ высокого кардиоваскулярного риска. Согласно показаниям пациентам были выполнены плановые операции коронарного шунтирования (КШ) в условиях искусственного кровообращения (ИК). Пациенты были рандомизированы в основную и контрольную группы. Пациенты основной группы интраоперационно получали NO в концентрации 80 ppm первоначально в ингаляционный контур, а затем в контур ИК. Пациентам контрольной группы операция КШ была выполнена в условиях стандартной искусственной вентиляции легких и ИК. Всем пациентам перед подключением ИК, в конце ИК и через 1 сут после операции КШ выполняли комплекс клинических и лабораторно-инструментальных исследований согласно стандартам медицинской практики, оценивали β-адренореактивность мембран эритроцитов (β-АРМэ) и определяли концентрацию в плазме крови норадреналина и адреналина методом ИФА.

**Результаты.** На дооперационном этапе и спустя 1 сут после операции КШ сформированные группы не различались по клиническим и биохимическим показателям. На дооперационном этапе медианы показателей β-АРМэ в основной и контрольных группах незначительно превышали верхнюю границу нормы и значимо не различались. Выполнение КШ не сопровождалось изменениями показателя β-АРМэ у пациентов в контрольной группе. Интраоперационная донация NO также не отразилась на уровне β-АРМэ. Через 1 сут после операции КШ не отмечено как межгрупповых различий β-АРМэ, так и значимых изменений показателя на сроках наблюдения в отдельно взятой группе. У пациентов контрольной и основной групп выявлено значимое повышение уровня адреналина и норадреналина спустя 1 сут после операции КШ по сравнению с исходным уровнем. В то же время не получено межгрупповых различий по уровню катехоламинов как до ИК, так и через сутки после операции КШ.

**Заключение.** Использование NO с целью органопротекции не влияет на уровень β-АРМэ и динамику медиаторного ответа симпатической системы на стресс у больных ИБС, имеющих клинические формы АГ высокого кардиоваскулярного риска, при кардиохирургических операциях с использованием искусственного кровообращения.

**Ключевые слова:** оксид азота, коронарное шунтирование, адренореактивность эритроцитов, адреналин, норадреналин

**Конфликт интересов.** Авторы декларируют отсутствие явных и потенциальных конфликтов интересов, связанных с публикацией настоящей статьи.

**Источники финансирования.** Исследование выполнено в рамках государственного задания Министерства науки и высшего образования Российской Федерации, № государственной регистрации 122020300183-4.

**Соответствие принципам этики.** Все пациенты подписали информированное согласие на включение в исследование. Исследование одобрено комитетом по биомедицинской этике НИИ кардиологии Томского НИМЦ (протокол № 208 от 20.01.2021).

**Для цитирования:** Реброва Т.Ю., Подоксенов Ю.К., Корепанов В.А., Чурилина Е.А., Каменщиков Н.О., Муслимова Э.Ф., Ворожцова И.Н., Афанасьев С.А. Эффекты оксида азота на показатели активности симпатоадреналовой системы пациентов с ишемической болезнью сердца при операции коронарного шунтирования. *Бюллетень сибирской медицины.* 2025;24(3):97–106. https://doi.org/10.20538/1682-0363-2025-3-97-106.

## INTRODUCTION

The use of extracorporeal circulation (ECC) has significantly expanded the possibilities of invasive heart interventions. However, applying ECC increases the risk of damage to other vital organs [1, 2]. To a large extent, this is due to the formation of reactive oxygen species, which lead to the alteration of the membrane structures of the endothelium and cellular components of the blood [3, 4]. ECC, along with other negative factors accompanying extensive surgical interventions, causes the development of perioperative stress in the patient body. It is well known that the sympathoadrenal system (SAS) is activated in the body during a stress response [5, 6]. The majority of patients who require surgical intervention using ECC have a chronic form of ischemic heart disease (IHD) combined with hypertension. It has been shown that such patients are characterized by predominance of sympathetic regulation over parasympathetic one. This results in consistently high levels of catecholamines in the blood of patients. Hypersympathicotonia, along with changes in the lipid bilayer of cell membranes in conditions of chronic vascular pathology, triggers remodeling of transmembrane and cell surface proteins. Previous studies have shown that beta-adrenergic receptor reactivity of erythrocyte membranes (β-ARMe) quite fully reflects not only the state of β-adrenergic receptors (β-AR) of erythrocytes but also the general β-adrenergic receptor reactivity of the body and its changes during the treatment of the prior disease [7, 8].

The use of nitric oxide (NO) is one of the novel approaches to organ protection during cardiac surgery requiring ECC. It consists in introducing NO donors, NO synthase inducers, or gaseous NO into the breathing circuit. Depending of the concentration used, NO can have a damaging or protective effect [9]. Despite the publications over the past decade [10–12], the fundamental pathophysiological mechanisms of organ-protective effects and the safety of exogenous NO supply during ECC remain under study.

The aim of the study was to investigate changes in laboratory parameters of SAS activity and β-ARMe in IHD patients with clinical forms of arterial hypertension of high cardiovascular risk during coronary artery bypass grafting with anesthetic management including nitric oxide.

## MATERIALS AND METHODS

This randomized study with parallel distribution enrolled 36 patients. Of these, 24 (66.7%) were men. The average age in the sample was 68 [63; 70] years. All patients were diagnosed with IHD with a clinical form of hypertension of high cardiovascular risk.

The inclusion criteria were the following: diagnosis of IHD with a clinical form of hypertension of high cardiovascular risk, elective coronary artery bypass grafting (CABG), bypass surgery of 2–4 vessels using ECC, age over 18 years, a signed voluntary informed consent.

The exclusion criteria were the following: absence of a patient's voluntary informed consent; a history of cancer; critical condition before CABG; taking norepinephrine, epinephrine or dopamine 3 days before CABG; left ventricular ejection fraction < 30%; blood transfusion in the last 4 months before CABG;

methemoglobinemia (congenital and acquired); bleeding diathesis; intracranial hemorrhage; severe left ventricular failure (NYHA functional class III and IV).

The study was approved by the local Ethics Committee of the Cardiology Research Institute of Tomsk NRMC (Minutes No. 208 dated January 20, 2021). All patients signed an informed consent to participate in the study. According to the indications, all patients underwent CABG using ECC. The patients were randomly divided into 2 groups: study group and control group. Patients of the study group received NO intraoperatively: first in the breathing circuit, then in the ECC circuit. For patients of the control group, CABG was performed using standard mechanical ventilation and ECC.

Baseline clinical and demographic characteristics of the study and control groups did not differ (Table 1).

Table 1

**Baseline Clinical and Demographic Characteristics of Patients**

| Characteristics | Study group, *n* = 18 | Control group, *n* = 18 | *p* |
|---|---|---|---|
| Age, years, *Me* [25; 75] | 68 [36; 70] | 68 [61; 70] | 0.849 |
| Men, *n* (%) | 12 (66.7 %) | 12 (66.7%) | 1 |
| Women, *n* (%) | 6 (33.3%) | 6 (33.3%) | 1 |
| BMI, kg / m$^2$, *M* ± *SD* | 31.7 ± 4.8 | 30.7 ± 5.3 | 0.555 |
| LVEF, %, *Me* [25; 75] | 60 [46; 65] | 56 [45; 65] | 0.924 |
| CRD, *n* (%) | 4 (22.2 %) | 7 (38.9 %) | 0.471 |
| AF, *n* (%) | 4 (22.2 %) | 3 (16.7 %) | 1 |
| Grade I AP, *n* (%) | 1 (5.6 %) | 1 (5.6 %) | 0.850 |
| Grade II AP, *n* (%) | 6 (33.3 %) | 4 (22.2 %) | 0.850 |
| Grade III AP, *n* (%) | 11 (61.1 %) | 13 (72.2 %) | 0.850 |
| PICS, *n* (%) | 11 (61.1 %) | 13 (72.2 %) | 0.725 |
| Grade 3 hypertension, *n* (%) | 18 (100 %) | 18 (100 %) | 1 |
| NYHA FC I CHF, *n* (%) | 2 (11.1 %) | 2 (11.1 %) | 0.510 |
| NYHA FC II CHF, *n* (%) | 7 (38.9 %) | 11 (61.1 %) | 0.510 |
| NYHA FC III CHF, *n* (%) | 8 (44.4 %) | 5 (27.8 %) | 0.510 |
| NYHA FC IV CHF, *n* (%) | 1 (5.6 %) | 0 (0.0 %) | 0.510 |
| DM, *n* (%) | 7 (38.9 %) | 5 (27.8 %) | 0.725 |
| Class 1 CKD, *n* (%) | 1 (5.6 %) | 3 (16.7 %) | 0.139 |
| Class 2 CKD, *n* (%) | 7 (38.9 %) | 12 (66.7 %) | 0.139 |
| Class 3a CKD, *n* (%) | 9 (50.0 %) | 3 (16.7 %) | 0.139 |
| Class 4 CKD, *n* (%) | 1 (5.6 %) | 0 (0.0%) | 0.139 |
| GFR, ml / min / 1.73 m$^2$ | 79.8 ± 13.2 | 62.2 ± 13.9 | 0.0004 |
| Smoking, *n* (%) | 11 (61.1 %) | 7 (38.9 %) | 0.318 |

Note. BMI – body mass index; LVEF – left ventricular ejection fraction; CRD – cardiac rhythm disorder; AF – atrial fibrillation; AP – angina pectoris; PICS – postinfarction cardiosclerosis; CHF – chronic heart failure; FC – functional class; DM – diabetes mellitus; CKD – chronic kidney disease; GFR – glomerular filtration rate.

Anesthetic management prior to CABG included premedication with narcotic analgesics, benzodiazepines, and antihistamines. Fentanyl (3.0–5.0 μg / kg) and propofol (1.5 μg / kg) were used to induce anesthesia. Pipecuronium bromide (0.1 μg / kg) was used for neuromuscular blockade. Anesthesia was maintained by inhalation of sevoflurane (2–3 vol.%) and infusion of fentanyl (3.0–5.0 μg / kg / h). Mechanical ventilation was performed using the Drager Primus apparatus (Drager AG, Germany) along a semi-closed breathing circuit in the Controlled Mandatory Ventilation mode with controlled volume of $FiO_2$ = 0.3 and higher, depending on the clinical situation. To measure central venous pressure and conduct infusion and transfusion therapy, central venous catheterization was performed. Blood pressure monitoring and arterial blood sampling for acid – base balance and gas monitoring were carried out through catheters inserted in the right and left radial arteries. To maintain anesthesia during ECC, propofol infusion (4 mg / kg / h) and fentanyl infusion (3.0–5.0 μg / kg / h) were performed via the infusion pump.

During CABG, we carried out extensive intraoperative monitoring of the patient's condition, which included: continuous ECG analysis, capnometry, capnography for invasive blood pressure measurement, pulse oximetry, diuresis measurement, thermometry with a sensor in the oropharynx, monitoring of the $NO/NO_2$ ratio. To assess the adequacy of anesthesia and ECC, acid – base balance, hematocrit, hemoglobin, and lactate were monitored using the STAT PROFILE Critical Care Xpress analyzer (NOVA Biomedical, USA).

ECC was performed using the Stockert apparatus (Stockert GmbH, Germany) in the nonpulsatile mode. The perfusion index was 2.5 l / min / m$^2$. Connection to the ECC circuit was carried out in a standard manner via the aorta – right atrium. To ensure hypocoagulation, heparin was administered before ECC at a dose of 3 mg / kg, maintaining activated coagulation time > 480 s. During ECC, the temperature in the oropharynx was maintained at 35.5–36.6 °C, the hemoglobin level ≥ 80 g / l, and the mean arterial pressure at 50–80 mm Hg. Myocardial protection was achieved by perfusion of the ascending aorta or coronary artery (in case of aortic regurgitation) with a cold (5–8 °C) crystalloid solution (Custodiol HTK-Bretschneider; Dr Franz Köhle rChemie GmbH, Bensheim, Germany) at a dose of 3 ml / kg for 6–8 minutes according to the manufacturer's instruction. Local hypothermia with ice slurry was used. After the end of ECC, heparin was inactivated with protamine in a 1:1 ratio.

Patients of the study group, immediately after tracheal intubation, received NO intraoperatively

at a concentration of 80 ppm in the breathing circuit and then, after the start of ECC, to the ECC circuit. After disconnection from the ECC, NO delivery was resumed in the anesthesia machine circuit at the concentration of 80 ppm until the end of surgery. Delivery and monitoring of $NO/NO_2$ were carried out using plasma-chemical NO synthesis AIT-NO-01 system (Tianox, RFNC-VNIIEF, enterprise of Rosatom State Atomic Energy Corporation, Sarov, Russia). The maximum permissible $NO_2$ concentration in the study group was 2 ppm.

All patients underwent a complex of clinical, laboratory, and instrumental tests in accordance with clinical standards at the following stages of surgery: before connecting to ECC, at the end of ECC, 1 day after CABG. In the meantime, we assessed body β-ARMe measurements using the Beta-ARM Agat kit (Agat-Med LLC, Russia, https://www.agat.ru/documents/instructions/4994/). This method is based on inhibition of hemolysis of erythrocytes placed in hypoosmotic medium in the presence of a selective β-blocker. According to the manufacturer's protocol, β-ARMe values in 93% of apparently healthy individuals are in the range of 2.0–20.0%, which reflects an increase in osmotic fragility of erythrocytes following binding of the adrenergic blocker to β-ARs. Higher values of β-ARMe reflect reduced osmotic fragility of erythrocytes and, therefore, weaker binding of the adrenergic blocker to β-ARs due to a decrease in the number of receptors on the cell membrane or their desensitization.

To assess the activity of SAS, before connecting to the ECC and 1 day after CABG, the concentrations of norepinephrine and epinephrine in the blood plasma of the patients of both groups were determined using ELISA kits for the quantitative determination of catecholamines (IBL CatCombi ELISA, Germany).

Statistical processing of the obtained data was carried out using the Statistica 10.0 software package. Normality of data distribution was checked using the Shapiro – Wilk test, since the number of patients in the study sample was less than 50. Normally distributed variables were presented as the mean and standard deviation $M \pm SD$. When the distribution was not normal, the data were presented as the median and the interquartile range *Me* [25; 75]. Qualitative data were presented as absolute and relative values – *n* (%). Quantitative variables of independent samples were compared by the *t*-test for normally distributed values or the Mann – Whitney *U*-test for non-normally distributed variables. Quantitative variables in dependent samples were compared using the *t*-test for normally distributed values or the Wilcoxon test for non-normally distributed variables. To compare qualitative variables in two samples, the Fisher's exact test was used. The differences were considered to be statistically significant at $p < 0.05$.

## RESULTS

Table 2 demonstrates parameters characterizing the perioperative period. Procedure of NO donation into the breathing and then into the perfusion circuit led to an increase in the duration of the surgery, which did not reach statistical significance. The study and control groups did not differ in the ECC duration, the time of aorta clamping, or the volume of intraoperative blood loss. The groups were comparable in terms of blood pressure levels before and during ECC. There were also no intergroup differences in the acid – base balance, hematocrit, hemoglobin, and lactate levels at the stages of the surgery.

Table 3 demonstrates clinical and biochemical blood parameters in the study and control groups.

Table 2

**Parameters of the Perioperative Period**

| Parameters | Study group, *n* = 18 | Control group, *n* = 18 | *p* |
|---|---|---|---|
| Surgery duration, min, *Me* [25; 75] | 300 [260; 330] | 270 [240; 300] | 0.058 |
| ECC duration, min, $M \pm SD$ | 95.50 ± 25.50 | 82.00 ± 15.04 | 0.062 |
| Aorta clamping duration, min, $M \pm SD$ | 58.75 ± 18.67 | 48.50 ± 15.47 | 0.089 |
| Mean BP before ECC, mm Hg, $M \pm SD$ | 104.59 ± 40.56 | 122.73 ± 36.83 | 0.128 |
| Mean BP during ECC, mm Hg, $M \pm SD$ | 56.29 ± 6.89 | 53.35 ± 5.23 | 0.064 |
| Blood loss during surgery, ml, *Me* [25; 75] | 1,000 [800; 1,000] | 1,000 [800; 1,000] | 0.949 |
| Homeostasis parameters during CABG | | | |
| Before ECC | | | |
| pH, *Me* [25; 75] | 7.39 [7.37; 7.43] | 7.40 [7.37; 7.41] | 0.646 |
| Lactate, mmol / l, *Me* [25; 75] | 1.1 [0.9; 1.4] | 1.1 [0.9; 1.4] | 1 |

End of table 2

| Parameters | Study group, *n* = 18 | Control group, *n* = 18 | *p* |
|---|---|---|---|
| Hb, g / l, *Me* [25; 75] | 130 [123; 141] | 132 [120; 137] | 0.812 |
| Hct, %, *M* ± *SD* | 36.90 ± 3.75 | 38.44 ± 3.38 | 0.216 |
| At the end of ECC | | | |
| pH, *Me* [25; 75] | 7.41 [7.38; 7.40] | 7.38 [7.37; 7.42] | 0.223 |
| Lactate, mmol / l, *Me* [25; 75] | 1.50 [1.30; 2.10] | 1.35 [1.00; 1.60] | 0.064 |
| Hb, g / l, *Me* [25; 75] | 94.5 [85.0; 101.0] | 95.0 [87.0; 101.0] | 0.776 |
| Hct, %, *M* ± *SD* | 25.61 ± 3.18 | 27.00 ± 3.14 | 0.197 |
| At the end of CABG | | | |
| pH, *Me* [25; 75] | 7.35 [7.35; 7.40] | 7.38 [7.37; 7.40] | 0.448 |
| Lactate, mmol / l, *Me* [25; 75] | 1.5 [1.2; 2.1] | 1.4 [1.1; 1.6] | 0.107 |
| Hb, g / l, *Me* [25; 75] | 100.5 [92.0; 108.0] | 103.5 [93.0; 112.0] | 0.579 |
| Hct, %, *M* ± *SD* | 27.56 ± 3.22 | 28.89 ± 3.46 | 0.239 |
| One day after CABG | | | |
| pH, *M* ± *SD* | 7.42 [7.40; 7.44] | 7.43 [7.38; 7.44] | 0.591 |
| Lactate, mmol / l, *M* ± *SD* | 1.9 [1.5; 2.1] | 1.8 [1.5; 2.3] | 0.739 |
| Hb, g / l, *M* ± *SD* | 104 [92; 115] | 106 [86; 119] | 0.800 |
| Hct, %, M ± SD | 30.13 ± 3.99 | 29.57 ± 4.79 | 0.702 |

Note. ECC – extracorporeal circulation; BP – blood pressure; CABG – coronary artery bypass grafting; pH – hydrogen ion concentration or acid value; Hb – hemoglobin; Hct – hematocrit.

Table 3

**Changes in Clinical and Biochemical Blood Parameters at the Stages of the Study**

| Parameters | Study group, *n* = 18 | Control group, *n* = 18 | ***p*** |
|---|---|---|---|
| Before CABG | | | |
| Leukocytes, $10^9$ / l, *M* ± SD | 7.19 ± 1.76 | 7.52 ± 2.32 | 0.637 |
| Platelets, $10^9$ / l, *M* ± *SD* | 240.78 ± 71.89 | 223.61 ± 50.25 | 0.412 |
| ESR, mm / h, *Me* [25; 75] | 6 [4; 15] | 6 [5; 8] | 0.832 |
| CK, U / l, *Me* [25; 75] | 73 [47; 120] | 93 [76; 127] | 0.223 |
| CK-MB, U / l, *Me* [25; 75] | 19 [16; 24] | 20 [15; 24] | 0.899 |
| Glucose, mmol / l, *Me* [25; 75] | 5.9 [5.3; 6.5] | 7.2 [5.7; 7.9] | 0.101 |
| Urea, mmol / l, *Me* [25; 75] | 5.7 [5.0; 6.7] | 4.3 [4.2; 7.8] | 0.250 |
| Creatinine, µmol / l, *Me* [25; 75] | 94 [87; 119] | 82 [76; 88] | 0.001 |
| CRP, mg / l, *Me* [25; 75] | 5.1 [1.2; 13.2] | 3.5 [1.0; 12,4] | 0.486 |
| Total protein, g / l, *M* ± SD | 70.29 ± 6.12 | 72.93 ± 9.08 | 0.399 |
| ALT, U / l, *Me* [25; 75] | 18.2 [16.0; 23.0] | 21.8 [10.0; 42.6] | 0.569 |
| AST, U / l, *Me* [25; 75] | 18.6 [13.0; 24.9] | 22.4 [16.0; 26.0] | 0.429 |
| Total bilirubin, µmol / l, *Me* [25; 75] | 12.8 [10.0; 18,7] | 11.6 [9.7; 19.5] | 0.857 |
| One day after CABG | | | |
| Leukocytes, $10^9$ / l, *M* ± *SD* | 11.59 ± 3.01, *p** = 0.035 | 11.22 ± 2.99, *p** = 0.48 | 0.719 |
| Platelets, $10^9$ / l, *M* ± *SD* | 183.44 ± 71.68, *p** = 0.678 | 165.89 ± 47.31, *p** = 0.834 | 0.392 |
| CK, U / l, *Me* [25; 75] | 754 [558; 993], *p** = 0.001 | 783 [569; 1,250], *p** = 0.001 | 0.564 |
| CK-MB, U / l, *Me* [25; 75] | 34 [32; 43], *p** = 0.001 | 35 [28; 42], *p** = 0.045 | 0.817 |
| Glucose, mmol / l, *Me* [25; 75] | 9.2 [7.6; 10.9], *p** = 0.036 | 9.7 [8.2; 11.6], *p** = 0.05 | 0.643 |
| Urea, mmol / l, *Me* [25; 75] | 7.1 [5.9; 8.3], *p** = 0.002 | 6.6 [5.8; 8.3], *p** = 0.449 | 0.607 |
| Creatinine, µmol / l, *Me* [25; 75] | 104.5 [84.0; 133.0], *p** = 1.0 | 94,0 [76.0; 116.0], *p** = 0.05 | 0.211 |
| CRP, mg / l, *Me* [25; 75] | 149 [128; 169], *p** = 0.000 | 139 [115; 160], *p** = 0.000 | 0.628 |
| Total protein, g / l, *M* ± SD | 53.67 ± 4.89, *p** = 0.001 | 53.33 ± 5.61, *p** = 0.013 | 0.875 |
| ALT, U / l, *Me* [25; 75] | 35 [27; 46], *p** = 0.009, | 32 [15; 43], *p** = 0.239 | 0.646 |
| AST, U / l, *Me* [25; 75] | 57 [39; 68], *p** = 0.001 | 53 [43; 72], *p** = 0.002 | 0.962 |
| Total bilirubin, µmol / l, *Me* [25; 75] | 10.7 [8.6; 18.7], *p** = 0.802 | 12.1 [8.7; 27.7], *p** = 0.795 | 0.681 |

Note. ALT – alanine transaminase; AST – aspartate transaminase; CK – creatine kinase; CK-MB – creatine kinase, myocardial band.

In our study, the surgical intervention did not result in significant differences between the groups. At the same time, in both groups, there was a significant increase in CK, CK-MB, ALT, and AST and a decrease in total protein one day after CABG compared to the preoperative period. The increase in the activity of serum biomarkers of cell damage and the decrease in total protein in the postoperative period are certainly due to the large volume of surgical intervention on the tissues of the chest and heart. In the postoperative period, a significant increase in the concentration of urea in the blood plasma was noted only in the study group. However, this did not result in significant intergroup differences at this follow-up stage.

Table 4 demonstrates clinical parameters of the patients of the study and control groups, reflecting the features of their early postoperative period. According to the data presented, the use of NO during CABG did not lead to statistically significant differences between the groups. However, there were no intraoperative myocardial infarctions and oliguria / anuria in the study group. On the contrary, in the control group, the incidence of myocardial infarction and oliguria / anuria was 22.2% each. Due to a small sample size, intergroup differences did not reach a critical level of significance.

Table 4

**Characteristics of the Early Postoperative Period**

| Characteristics | Study group, *n* = 18 | Control group, *n* = 18 | *p* |
|---|---|---|---|
| Reoperation, *n* (%) | 0 (0.0%) | 1 (5.6%) | 1 |
| Intraoperative complications, *n* (%) | 1 (5.6%) | 1 (5.6%) | 1 |
| Mechanical ventilation duration, min, *Me* [25; 75] | 550 [395; 1,040] | 480 [390; 625] | 0.517 |
| Tracheostomy, n (%) | 1 (5.6%) | 1 (5.6%) | 1 |
| Pneumonia, *n* (%) | 4 (22.2%) | 6 (33.3%) | 0.711 |
| RF (need for oxygen support), *n* (%) | 3 (16.7%) | 4 (22.2%) | 1 |
| Diuresis 1 day after CABG (ml), *Me* [25; 75] | 3,275 [2,350; 3,900] | 3,550 [2,400; 3,900] | 0.874 |
| Oliguria / anuria (< 0.5 ml / kg / h), *n* (%) | 0 (0.0%) | 4 (22.2%) | 0.104 |
| AMI, *n* (%) | 0 (0.0%) | 4 (22.2%) | 0.104 |
| AF in the postoperative period, *n* (%) | 3 (16.7%) | 7 (38.9%) | 0.264 |
| Delirium, *n* (%) | 3 (16.7%) | 3 (16.7%) | 1 |
| Stroke, *n* (%) | 1 (5.6%) | 2 (11.1%) | 1 |
| Stool (days after CABG), *Me* [25; 75] | 4 [3; 4] | 4 [3; 5] | 0.319 |
| Bed days in ICU, *Me* [25; 75] | 1 [1; 6] | 1 [1; 6] | 1 |
| Bed days in the in-patient department, *Me* [25; 75] | 17.5 [16.0; 26.0] | 19.5 [16.0; 31.0] | 0.527 |

Note. RF – respiratory failure; AMI – acute myocardial infarction; AF – atrial fibrillation; ICU – intensive care unit.

The results of assessing catecholamine concentrations in the blood of patients are shown in Fig.1. In our study, in patients of the study and control groups, epinephrine concentration significantly increased 1 day after CABG compared to the level before ECC ($p = 0.005$ and $p = 0.003$, respectively) (Fig. 1, *a*). At the same time, the median concentrations of epinephrine in the study group before CABG and 1 day after it were higher compared to the control group. However, these differences did not reach statistical significance ($p = 0.063$ and $p = 0.095$, respectively).

Changes in the norepinephrine levels were similar in both the control ($p < 0.001$) and study groups ($p = 0.006$) (Fig. 1, *b*) without significant intergroup

Table 5

**Beta-ARMe in Patients with Nitric Oxide Donation during CABG, *Me* [25; 75]**

| Stages of observation | Study group, *n* = 18 | Control group, *n* = 18 | *p* |
|---|---|---|---|
| β-ARMe before CABG | 21.9 [14.3; 26.1] | 21.2 [13.3; 26.2] | 0.972 |
| β-ARMe at the end of CABG | 18.6 [13.5; 34.2] | 20.8 [15.3; 27.5] | 0.851 |
| β-ARMe 1 day after CABG | 25.3 [18.8; 42.7] $p^*$ = 0.169 | 21.0 [14.3; 30.9] $p^*$ = 0.838 | 0.187 |

Note. CABG – coronary artery bypass grafting; β-ARMe – β-adrenergic reactivity of erythrocyte membranes; *p* – significance level of differences between the groups. $p^*$ – significance level of intragroup differences before CABG and 1 day after CABG.

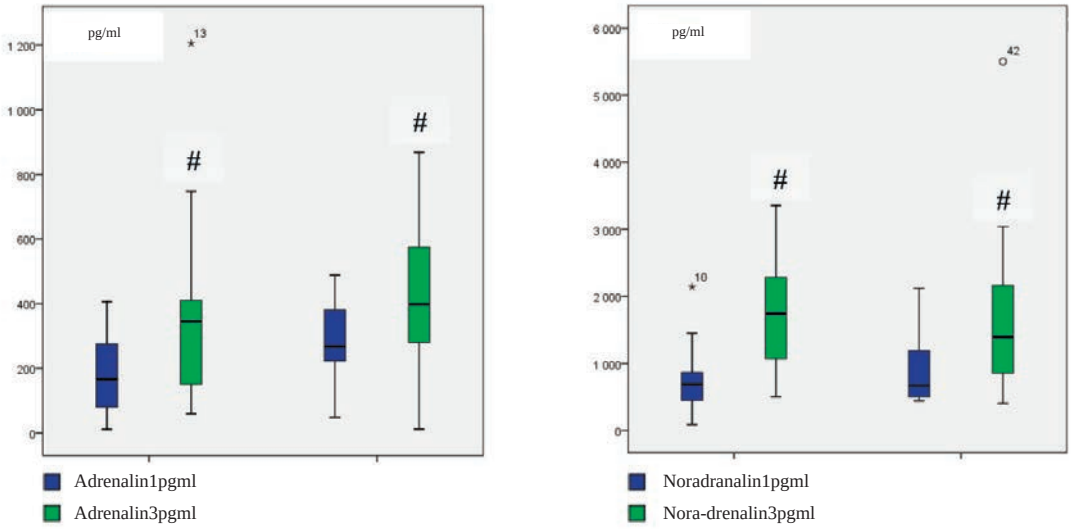


Fig. 1. Concentrations of epinephrine (*a*) and norepinephrine (*b*) in the study and control groups at the stages of CABG: # significant intragroup difference

– before ECC; – 1 day after CABG

differences both before ECC ($p$ = 0.318) and 1 day after CABG ($p$ = 0.0560).

Table 5 reflects baseline β-ARMe values and their subsequent changes. For both groups of patients, the baseline values of β-ARMe were at the upper range limit. CABG was not accompanied by significant changes in β-ARMe at the end of the surgery and 1 day after its completion. Intraoperative NO donation did not cause significant changes in this parameter in patients of the study group in perioperative and postoperative periods.

## DISCUSSION

Connecting the patient's body to the ECC circuit is a crucial stage of CABG that increases the risk of vital organ damage [13, 14]. One of the novel approaches to organ protection is the use of NO. Effects of NO are dose-dependent, which results from the formation of physiologically active metabolites of NO and its interaction with various molecular targets [9, 10]. In particular, it has been shown for cardiomyocytes that activation of iNOS or NO donation suppresses function of ryanodine receptors through the cGMP-independent pathway [15]. This mechanism limits beta-adrenergic sensitivity of the myocardium and may be an important signaling pathway for the damaging effects of NO.

The absence of significant differences in baseline β-ARMe values in the study and control groups indicates the absence of functional overload in the SAS receptor pathway in patients with IHD and clinical forms of arterial hypertension of high cardiovascular risk enrolled in the study. In the postoperative period, the stability of β-ARMe in the study group was further evidence of NO application safety during CABG. It may be suggested that NO has no effects associated with a direct influence on the activity of the SAS receptor component. At the same time, it was shown that in both the study and control groups at the postoperative stage, the increase in the blood concentration of norepinephrine (by 1.5 and 2.0 times, respectively) and epinephrine (by 2.1 and 2.5 times, respectively) was revealed, which reflected the involvement of the SAS in maintaining the body homeostasis of operated patients. However, the absence of changes in β-ARMe both in the period of ECC disconnection and 1 day after CABG in patients of the control group speaks of adequate premedication. It could be concluded that intraoperative NO donation did not affect the parameters of SAS mediator metabolism, which also confirms the safety of the NO dose used.

## CONCLUSION

In cardiac surgery with extracorporeal circulation, the use of NO for the purpose of organ protection does not affect the level of β-ARMe and changes in the mediator response of the sympathetic system to stress in patients with IHD and clinical forms of hypertension of high cardiovascular risk.

*The limitation of the study* was a small number of patients who were enrolled and completed the full course of examination.

## REFERENCES


1. Ostermann M., Lumlertgul N., Wilson F.P. Predictive models for acute ridney injury following cardiac surgery: the importance of accurate and actionable prediction. *JAMA*. 2022;327(10):927–929. DOI: 10.1001/jama.2022.1823. PMID: 35258544.
2. Zou M., Yu L., Lin R., Feng J., Zhang M., Ning S. et al. Cerebral autoregulation status in relation to brain injury on electroencephalogram and magnetic resonance imaging in children following cardiac surgery. *J. Am. Heart Assoc*. 2023;12(12):e028147. DOI: 10.1161/JAHA.122.028147.
3. Ottolenghi S., Sabbatini G., Brizzolari A., Samaja M., Chiumello D. Hyperoxia and oxidative stress in anesthesia and critical care medicine. *Minerva Anestesiol*. 2020;86(1):64–75. DOI: 10.23736/S0375-9393.19.13906-5.
4. Rebrova T.Yu., Shipulin V.M., Afanasiev S.A., Vorobiova E.V., Kiiko O.G. The Experience of the Application of Ascorbic Acid as an Antioxidant after Coronary Artery Bypass Grafting. *Kardiologiya*. 2012;52(7):73–76. (In Russ.).
5. Gutsol L.O., Guzovskaya E.V., Serebrennikova S.N., Seminsky I.Zh. Stress (General Adaptation Syndrome): Lecture. *Baikal Medical Journal*. 2022;1(1):70–80. (In Russ.). DOI: 10.57256/2949-0715-2022-1-1-70-80.
6. Muslimova E., Rebrova T., Kondratieva D., Korepanov V., Sonduev E., Kozlov B. et al. Expression of the β1-adrenergic receptor (*ADRB1*) gene in the myocardium and β-adrenergic reactivity of the body in patients with a history of myocardium infraction. *Gene*. 2022;844;146820. DOI: 10.1016/j.gene.2022.146820.
7. Malkova M.I., Bulashova O.V., Khazova E.V. Determination of the Body's Adrenoreactivity by Adrenoreception of the Cell Membrane in Cardiovascular Pathology. *Practical Medicine.* 2013;71(3):20–23. (In Russ.).
8. Muslimova E.F., Rebrova T.Yu., Korepanov V.A., Akhmedov Sh.D., Afanasyev S.A. Beta-Adrenergic Reactivity of Erythrocyte Membranes and Expression of Beta1-Adrenergic Receptors of Cardiomyocytes in Patients with Heart Failure with Different Left Ventricular Ejection Fraction. *Siberian Journal of Clinical and Experimental Medicine*. 2024;39(1):44–49. (In Russ.). DOI: 10.29001/2073-8552-2023-561.
9. Porrini C., Ramarao N., Tran S.L. Dr. NO and Mr. Toxic - the versatile role of nitric oxide. *Biol. Chem*. 2020;401(5):547–572. DOI: 10.1515/hsz-2019-0368.
10. Signori D., Magliocca A., Hayashida K., Graw J.A., Malhotra R., Bellani G. et al. Inhaled nitric oxide: role in the pathophysiology of cardio-cerebrovascular and respiratory diseases. *Intensive Care Med. Exp*. 2022;10(1):28. DOI: 10.1186/s40635-022-00455-6.
11. Bhatia V., Elnagary L., Dakshinamurti S. Tracing the path of inhaled nitric oxide: Biological consequences of protein nitrosylation. *Pediatr. Pulmonol*. 2021;56(2):525–538. DOI: 10.1002/ppul.25201.
12. Ntessalen M., Procter N.E.K, Schwarz K., Loudon B.L., Minnion M., Fernandez B.O. et al. Inorganic nitrate and nitrite supplementation fails to improve skeletal muscle mitochondrial efficiency in mice and humans. *Am. J. Clin. Nutr*. 2020;111(1):79–89. DOI: 10.1093/ajcn/nqz245.
13. Bokeria L.A., Milievskaya E.B., Pryanishnikov V.V., Orlov I.A. Cardiovascular Surgery – 2023. Diseases and Congenital Anomalies of the Circulatory System. **M**.: NMITSS named after A.N. Bakulev, Ministry of Health of the Russian Federation, 2024:344. (In Russ.).
14. Dzhitava T.G., Shamsiev G.A., Abdulloev O.K., Filaretova O.V., Agafonov I.A., Kusraev G.A. et al. Determining Factors of Early Recovery of Patients who Underwent Open Heart Surgery. *Thoracic and Cardiovascular Surgery*. 2024;66(1):99–112. (In Russ.). DOI: 10.24022/0236-2791-2024-66-1-99-112.
15. Ziolo M.T., Katoh H., Bers D.M. Expression of inducible nitric oxide synthase depresses beta-adrenergic-stimulated calcium release from the sarcoplasmic reticulum in intact ventricular myocytes. *Circulation*. 2001;104(24):2961–2966. DOI: 10.1161/hc4901.100379.

## Author Contribution

Rebrova T. Yu. – epinephrine / norepinephrine determination by ELISA, analysis and interpretation of the data, drafting of the manuscript. Churilina E.A. – collection, processing, and statistical analysis of clinical data. Podoksenov Yu. K. – study design, analysis and interpretation of clinical data, critical revision of the manuscript for important intellectual content. Korepanov V.A. – determination of beta-adrenergic reactivity of erythrocytes, statistical analysis of laboratory parameters. Kamenshchikov N.O. – development of inclusion / exclusion criteria, selection and inclusion of patients in the study according to the criteria, obtaining an informed consent from the patients. Muslimova E.F. – compilation of the database, analysis and interpretation of the data. Vorozhtsova I.N. – discussion of the results, final approval of the manuscript for publication. Afanasiev S.A. – conception and design of the study, final approval of the manuscript for publication.

## Author Information

**Rebrova Tatiana Yu.** – Cand. Sci. (Med), Researcher, Laboratory of Molecular and Cell Pathology and Gene Diagnostics, Cardiology Research Institute, Tomsk NRMC, Tomsk, rebrova@cardio-tomsk.ru, http://orcid.org/ 0000-0003-3667-9599

**Podoksenov Yuri K.** – Dr. Sci. (Med), Leading Researcher, Department of Cardiovascular Surgery; Senior Researcher, Laboratory of Critical Care Medicine, Cardiology Research Institute, Tomsk NRMC, Tomsk, uk@cardio-tomsk.ru, http://orcid.org/ 0000-0002-8939-2340.

**Korepanov Viacheslav A.** – Junior Researcher, Laboratory of Molecular and Cell Pathology and Gene Diagnostics, Cardiology Research Institute, Tomsk NRMC, Tomsk, vakorep41811@gmail.com, http://orcid.org/ 0000-0002-2818-1419

**Churilina Elena A.** – Junior Researcher, Laboratory of Critical Care Medicine, Cardiology Research Institute, Tomsk NRMC, Tomsk, eas@cardio-tomsk.ru, http://orcid.org/ 0000-0003-3562-9979

**Kamenshchikov Nikolay O.** – Cand. Sci. (Med), Head of the Laboratory of Critical Care Medicine, Cardiology Research Institute, Tomsk NRMC, Tomsk, no@cardio-tomsk.ru, https://orcid.org/0000-0003-4289-4439

**Muslimova Elvira F.** – Cand. Sci. (Med), Researcher, Laboratory of Molecular and Cell Pathology and Gene Diagnostics, Cardiology Research Institute, Tomsk NRMC, Tomsk, muslimova@cardio-tomsk.ru, http://orcid.org/0000-0001-7361-2161

**Vorozhtsova Irina N.** – Dr. Sci. (Med.), Professor, Department of Science and Education Office, Tomsk NRMC, Tomsk, abv1953@mail.ru, http://orcid.org/ 0000-0002-1610-0896

**Afanasiev Sergey A.** – Dr. Sci. (Med), Professor, Head of the Laboratory of Molecular and Cell Pathology and Gene Diagnostics, Cardiology Research Institute, Tomsk NRMC, Tomsk, tursky@cardio-tomsk.ru, http://orcid.org/ 0000-0001-6066-3998

(✉) **Rebrova Tatiana Yu.,** rebrova@cardio-tomsk.ru

Received on February 06, 2025;
approved after peer review on February 18, 2025;
accepted on February 27, 2025

УДК 617.55-089-06:616.94]-037-036.88
https://doi.org/10.20538/1682-0363-2025-3-107-115

# Early clinical and laboratory predictors of in-hospital mortality in patients with postoperative abdominal sepsis

**Rodionova Yu.O., Fedosenko S.V., Ivanova A.I., Arzhanik M.B., Semenova O.L., Starovoitova E.A., Nesterovich S.V., Efimova D.A., Kalyuzhin V.V.**

*Siberian State Medical University of the Ministry of Health of the Russian Federation (SibSMU)*
*2 Moskovsky trakt, 634050 Tomsk, Russian Federation*

## ABSTRACT

**Aim.** To identify early clinical and laboratory predictors of death in patients with postoperative abdominal sepsis in the first 48 hours after its verification.

**Materials and methods.** A retrospective study was conducted on 40 patients with abdominal sepsis hospitalized in the surgical department of Siberian State Medical University in 2019–2023. All patients were divided into groups according to the outcome of hospitalization (discharge or death). Clinical and anamnestic data, Sequential Organ Failure Assessment (SOFA) and quick SOFA (qSOFA) scores, and dynamic changes in biochemical and hematological markers were evaluated (T1– at verification, T2 – after 48 hours). The Mann – Whitney *U* test, $\chi^2$ test, Wilcoxon test, and ROC analysis were applied.

**Results.** The mortality rate was 45%. Statistically significant predictors of mortality were: SOFA score > 4, serum urea > 12.1 mmol / l, calcium ≤ 1.8 mmol / l, platelet count ≤ 264 × $10^9$ / l, no platelet increase > 15 × $10^9$ / l, neutrophil reactivity intensity (NEUT-RI) > 57.6 fluorescence intensity (FI) at T1 and > 53.8 FI at T2. Prognostic values were also established for reticulocyte parameters and reactive lymphocyte content.

**Conclusion.** Early assessment of clinical and laboratory parameters, especially indicators of kidney function, calcium metabolism, blood count, and the intensity of the inflammatory response, has high prognostic value in postoperative sepsis and can be used for risk stratification and optimization of therapy.

**Keywords:** sepsis, surgical sepsis, abdominal sepsis, fatal outcome, predictors of fatal outcome

**Conflict of interest.** The authors declare the absence of obvious or potential conflicts of interest related to the publication of this article.

**Source of financing.** The authors state that they received no funding for the study.

**Conformity with the principles of ethics.** The study was approved by the Ethics Committee at Siberian State Medical University (Minutes No. 8616/1 dated March 29, 2021).

**For citation:** Rodionova Yu.O., Fedosenko S.V., Ivanova A.I., Arzhanik M.B., Semenova O.L., Starovoitova E.A., Nesterovich S.V., Efimova D.A., Kalyuzhin V.V. Early clinical and laboratory predictors of in-hospital mortality in patients with postoperative abdominal sepsis. *Bulletin of Siberian Medicine.* 2025;24(3):107–115. https://doi.org/10.20538/1682-0363-2025-3-107-115.

✉ *Rodionova Yulia O.,* rodionova.yo@ssmu.ru

# Ранние клинико-лабораторные предикторы госпитальной летальности у пациентов с хирургическим абдоминальным сепсисом

**Родионова Ю.О., Федосенко С.В., Иванова А.И., Аржаник М.Б., Семенова О.Л., Старовойтова Е.А., Нестерович С.В., Ефимова Д.А., Калюжин В.В.**

*Сибирский государственный медицинский университет (СибГМУ)*
*Россия, 634050, г. Томск, Московский тракт, 2*

**РЕЗЮМЕ**

**Цель исследования.** Идентификация ранних клинико-лабораторных предикторов летального исхода у пациентов с хирургическим абдоминальным сепсисом в первые 48 ч от момента верификации состояния.

**Материалы и методы.** Проведено ретроспективное исследование 40 пациентов с абдоминальным сепсисом, госпитализированных в хирургическое отделение Сибирского государственного медицинского университета в 2019–2023 гг. Все пациенты были разделены на группы по исходу госпитализации (выписка или летальный исход). Оценивали клинико-анамнестические данные, показатели шкал Sequential Organ Failure Assessment (SOFA) и quick SOFA, биохимические и гематологические маркеры в динамике (Т1 – верификация, Т2 – через 48 ч). Применялись *U*-критерий Манна – Уитни, критерий Пирсона $\chi^2$, критерий Вилкоксона, ROC-анализ.

**Результаты.** Уровень летальности составил 45%. Статистически значимыми предикторами летального исхода явились: оценка по шкале SOFA более 4 баллов, уровень мочевины в сыворотке крови более 12,1 ммоль/л, снижение концентрации в сыворотке крови общего кальция 1,8 ммоль/л и менее, количество тромбоцитов в общем анализе крови 264 × $10^9$/л и менее, отсутствие прироста количества тромбоцитов более 15 × $10^9$/л, интенсивность реактивности нейтрофилов (NEUT-RI) более 57,6 единиц интенсивности флуоресценции (ИФ) на Т1 и более 53,8 ИФ на Т2. Также установлены прогностические значения для ретикулоцитарных параметров и содержания реактивных лимфоцитов.

**Заключение.** Ранняя оценка клинико-лабораторных показателей, особенно показателей функции почек, кальциевого обмена, параметров гемограммы и интенсивности воспалительного ответа, имеет высокую прогностическую значимость при хирургическом сепсисе и может быть использована для стратификации риска и оптимизации терапии.

**Ключевые слова:** сепсис, хирургический сепсис, абдоминальный сепсис, летальный исход, предикторы летального исхода

**Конфликт интересов.** Авторы декларируют отсутствие явных и потенциальных конфликтов интересов, связанных с публикацией настоящей статьи.

**Источник финансирования.** Авторы заявляют об отсутствии финансирования при проведении исследования.

**Соответствие принципам этики.** Протокол исследования одобрен локальным этическим комитетом Сибирского государственного медицинского университета (решение № 8616/1 от 29.03.2021).

**Для цитирования:** Родионова Ю.О., Федосенко С.В., Иванова А.И., Аржаник М.Б., Семенова О.Л., Старовойтова Е.А., Нестерович С.В., Ефимова Д.А., Калюжин В.В. Ранние клинико-лабораторные предикторы госпитальной летальности у пациентов с хирургическим абдоминальным сепсисом. *Бюллетень сибирской медицины.* 2025;24(3):107–115. https://doi.org/10.20538/1682-0363-2025-3-107-115.

## INTRODUCTION

Sepsis as a complication of intra-abdominal infections is widespread in surgical practice and remains a leading cause of non-traumatic mortality in emergency surgical departments both in Russia and abroad [1]. Abdominal sepsis (AS) presents a serious clinical problem due to the diversity of nosological forms, the broad spectrum of pathogens (aerobic and anaerobic bacteria, fungi), as well as limitations in microbiological diagnosis [2].

Clinical heterogeneity complicates the assessment of epidemiological indicators of AS. According to

data from I. Martin-Loeches et al. (2019), mortality in complicated intra-abdominal infections without sepsis is 2–3%, whereas in cases progressing to sepsis and septic shock in intensive care units, it reaches up to 50% [3].

The effectiveness of treatment for AS largely depends on early verification of the condition, selection of the optimal surgical approach, and timely antimicrobial therapy [4]. In the context of nonspecific clinical presentations and limited diagnostic value of individual laboratory markers, the role of a comprehensive assessment of clinical and laboratory parameters increases for predicting outcomes. The aim of this study was to perform a comparative analysis of clinical and laboratory predictors of death in patients with postoperative AS within the first 48 hours after diagnosis verification, depending on the hospitalization outcome.

## MATERIALS AND METHODS

A retrospective comparative study was conducted based on a protocol approved by the local Ethics Committee of Siberian State Medical University (Minutes No.8616/1 dated March 29, 2021). The study included a consecutive sample of 40 patients with postoperative AS hospitalized in the surgical department of Siberian State Medical University clinics from January 1, 2019 to April 30, 2023. The patients were divided into two groups according to the hospitalization outcome (discharge or death) for analyzing clinical, anamnestic, and laboratory parameters within the first 48 hours after AS verification.

Inclusion criteria were the presence of an abdominal bacterial infection focus and a score of ≥ 2 on the quick Sepsis-Related Organ Failure Assessment (qSOFA) scale, which considers systolic blood pressure (BP) < 100 mm Hg, respiratory rate ≥ 22 per minute, and altered mental status (Glasgow coma score < 15). The diagnosis of sepsis was confirmed using the Sequential Organ Failure Assessment (SOFA) scale, with a score of ≥ 2.

The study evaluated the duration of hospital stay and hospitalization outcome, anthropometric data, comorbidities (including immunodeficiency states), qSOFA and SOFA scores, duration of sepsis, data from intensive care unit stay, including mechanical ventilation and vasopressor support. A dynamic assessment of key clinical parameters was performed: BP, heart rate, level of consciousness, peripheral oxygen saturation. Biochemical blood parameters were also measured: C-reactive protein (CRP), lactate, procalcitonin (PCT), creatinine, urea, total and direct bilirubin, sodium, potassium, and calcium (at verification and after 48 hours).

Statistical analysis was performed using the Statistica 12.0 software (StatSoft, USA). Quantitative data were presented as the median and the interquartile range $Me$ ($Q_1$; $Q_3$). Qualitative data were presented as $n$ (%). Independent samples were compared using the Mann – Whitney $U$ test for continuous variables and the $\chi^2$ (Fisher's exact) test for categorical variables. Dependent variables were analyzed using the Wilcoxon signed-rank test. The Receiver Operating Characteristic (ROC) analysis was performed in MedCalc 18.9.1 to calculate the area under the curve (AUC), with a 95% confidence interval (CI), Youden's index for cutoff points, sensitivity, and specificity. The significance level was set at $p < 0.05$.

## RESULTS

A total of 40 patients were included in the study, of whom 27 (67.5%) were men and 13 (32.5%) – women. The overall mortality rate was 45%, with 18 deceased patients and 22 survivors. The groups did not differ significantly in age (median 59.5 years [45.0; 72.0] vs. 65.0 years [61.0; 76.0]; $p = 0.068$), body mass index (BMI) (24.81 vs. 24.02 kg / m²; $p = 0.815$), or gender distribution ($p = 0.435$).

Most patients ($n = 37$) were admitted in the emergency room, while only 3 were hospitalized electively. In the group with fatal outcomes, 16 patients had emergency admissions and 2 – elective admissions; in the survivor group, these numbers were 21 and 1, respectively. Surgical intervention was required in 36 patients (90%). Among survivors, 20 patients underwent surgery (1 patient required reoperation), whereas in the deceased group, 16 patients underwent surgery (with 5 patients undergoing reoperation).

Comorbid conditions included: ischemic heart disease in 12 patients (30%), hypertension in 23 patients (57.5%), history of myocardial infarction in 8 patients (20%), stroke in 5 patients (12.5%), type 2 diabetes mellitus in 6 patients (15%), chronic heart failure in 5 patients (12.5%), bronchial asthma in 1 patient (2.5%), chronic obstructive pulmonary disease in 1 patient (2.5%), liver cirrhosis in 2 patients (5%), and chronic kidney disease in 2 patients (5%). Alcohol abuse was identified in 4 patients (10%), and drug addiction – in 2 patients (5%). No significant differences between the groups were found in the prevalence of comorbid conditions or results of objective examinations ($p > 0.05$, Table 1).

Table 1

**Objective Data at the Time of Sepsis Verification, *Me* ($Q_1$; $Q_3$)**

| Parameter | Patients with a favorable outcome | Patients with a fatal outcome | *p* |
|---|---|---|---|
| Body temperature | 38 (38; 38) | 38 (37.8; 38) | 0.302 |
| HR in 1 min | 100 (89; 102) | 101 (80; 109) | 0.643 |
| RR in 1 min | 25 (24; 26) | 25 (24; 28) | 0.490 |
| SPB, mm Hg | 97.5 (90; 102) | 100 (92; 105) | 0.657 |
| DBP, mm Hg | 60 (50; 60) | 60 (60; 70) | 0.253 |
| Pulse pressure, mm Hg | 40 (30; 42) | 40 (30; 40) | 0.966 |
| SpO2, % | 94 (93; 96) | 95 (90; 97) | 0.891 |

Note. HR – heart rate; RR – respiratory rate; SBP – systolic blood pressure; DBP – diastolic blood pressure; $SpO_2$ – peripheral oxygen saturation (measured during breathing ambient air).

At the time of AS diagnosis, the SOFA score for patients with fatal outcomes was 6 (5; 7), whereas for survivors, it was 4 (3; 5) ($p = 0.001$).

Among the biochemical parameters assessed within the first 48 hours, statistically significant intergroup differences were observed only in serum calcium and urea levels (Table 2).

Table 2

**Dynamics of Biochemical Serum Test Results, *Me* ($Q_1$; $Q_3$)**

| Parameter | Patients with a favorable outcome | Patients with a fatal outcome | *p* |
|---|---|---|---|
| Calcium, mmol / l, T1 | 2.02 (1.80; 2.05) | 1.80 (1.76; 2.01) | 0.040 |
| Calcium, mmol / l, T2 | 2.01 (1.80; 2.15) | 1.90 (1.80; 2.12) | 0.685 |
| $p_{T_1\text{-}T_2}$ | 0.327 | 0.018 | – |
| Total bilirubin, μmol / l, T1 | 21.0 (9.0; 27.0) | 16.5 (12.0; 30.0) | 0.945 |
| Total bilirubin, μmol / l, T2 | 16.1 (8.1; 24.5) | 11.7 (9.0; 22.0) | 0.581 |
| $p_{T_1\text{-}T_2}$ | 0.306 | 0.022 | – |
| Conjugated bilirubin, μmol / l, T1 | 8.8 (7.0; 15.8) | 9.5 (6.0; 14.8) | 0.891 |
| Conjugated bilirubin, μmol / l, T2 | 9.2 (4.0; 16.3) | 6.8 (4.0; 10.3) | 0.569 |
| $p_{T_1\text{-}T_2}$ | 0.277 | 0.116 | – |
| Urea, T1 | 6.9 (4.3; 12.1) | 15.5 (7.6; 19.9) | 0.012 |
| Urea, T2 | 7.0 (3.3; 13.1) | 12.2 (4.8; 22.6) | 0.076 |
| $p_{T_1\text{-}T_2}$ | 0.178 | 0.683 | – |
| Creatinine, μmol / l, T1 | 81.0 (66.7; 161.0) | 143.4 (92.8; 219.0) | 0.070 |
| Creatinine, μmol / l, T2 | 80.0 (55.0; 107.4) | 70.9 (59.0; 160.0) | 0.356 |
| $p_{T_1\text{-}T_2}$ | 0.005 | 0.060 | – |
| C-reactive protein, mg / l, T1 | 300.7 (201.0; 487.0) | 262.5 (198.9; 480.0) | 0.683 |

Endof Table 2

| Parameter | Patients with a favorable outcome | Patients with a fatal outcome | *p* |
|---|---|---|---|
| C-reactive protein, mg / l, T2 | 198.0 (154.4; 320.0) | 198.0 (140.0; 289.0) | 0.784 |
| $p_{T_1\text{-}T_2}$ | 0.001 | 0.064 | – |
| Procalcitonin, ng / ml, T1 | 3.39 (0.72; 7.44) | 4.71 (0.48; 8.68) | 0.479 |
| Procalcitonin, ng / ml, T2 | 2.16 (0.70; 7.28) | 3.81 (0.65; 10.30) | 0.515 |
| $p_{T_1\text{-}T_2}$ | 0.170 | 0.600 | – |
| Lactate, mmol / l, T1 | 4.5 (3.6; 5.0) | 4.5 (3.7; 4.8) | 0.848 |
| Lactate, mmol / l, T2 | 3.9 (2.9; 4.9) | 3.9 (3.5; 4.8) | 0.957 |
| $p_{T_1\text{-}T_2}$ | 0.039 | 0.021 | – |

Note. Here and in Tables 3–5: T – time point of measurement (T1 – baseline value; T2 – after 48 hours).

In both groups, baseline serum calcium levels indicated hypocalcemia (normal range: 2.15–2.50 mmol / l); however, in survivors, calcium was significantly higher than in non-survivors (Table 2).

In the group with fatal outcomes, serum urea levels upon admission and after 48 hours exceeded reference values; at the time of AS diagnosis, urea was 2.3 times higher than in survivors ($p = 0.012$). Only in the survivor group was there a significant decrease in serum creatinine concentration after 48 hours ($p = 0.005$) (Table 2).

All patients exhibited elevated levels of inflammatory markers: CRP and PCT. Differences between the groups did not reach statistical significance; however, in survivors, a significant reduction ($p = 0.001$) in CRP was observed after 48 hours (Table 2).

Elevated serum lactate concentrations persisted in both groups throughout the observation period, with no intergroup differences (Table 2).

The analysis of the blood count did not reveal statistically significant differences between the groups for most parameters (Table 3).

Table 3

**Dynamics of Peripheral Blood Erythropoiesis Parameters within the First 48 Hours from Sepsis Verification, *Me* ($Q_1$; $Q_3$)**

| Parameter | Patients with a favorable outcome | Patients with a fatal outcome | *p* |
|---|---|---|---|
| Erythrocytes, $10^{12}$ / l, T1 | 3.09 (2.70; 4.02) | 3.59 (2.82; 4.18) | 0.549 |
| Erythrocytes, $10^{12}$ / l, T2 | 3.13 (2.64; 3.84) | 3.42 (2.58; 3.83) | 0.891 |
| $p_{T_1\text{-}T_2}$ | 0.149 | 0.040 | – |

End of Table 2

| Parameter | Patients with a favorable outcome | Patients with a fatal outcome | *p* |
|---|---|---|---|
| Hemoglobin, g / l, T1 | 89 (75;106) | 91 (78;120) | 0.663 |
| Hemoglobin, g / l, T2 | 82.5 (76; 109) | 85 (74; 108) | 0.745 |
| $p_{T_1\text{-}T_2}$ | 0.232 | 0.028 | – |
| Hematocrit, %, T1 | 26.7 (24.5; 33.5) | 27.7 (25.7; 34.8) | 0.422 |
| Hematocrit, %, T2 | 25.9 (23.7; 32.9) | 26.6 (23.0; 30.5) | 0.986 |
| $p_{T_1\text{-}T_2}$ | 0.211 | 0.034 | – |
| ESR, mm / h, T1 | 55 (40; 67) | 50.5 (29; 57) | 0.086 |
| ESR, mm / h, T2 | 58 (45; 66) | 45 (29; 57) | 0.111 |
| $p_{T_1\text{-}T_2}$ | 0.506 | 0.906 | – |
| MCV, fl:T1 | 86.4 (83.1; 92.1) | 85.9 (83.3; 89.2) | 0.900 |
| MCV, fl:T2 | 87.1 (84.1; 91.8) | 87.2 (79.6; 88.7) | 0.562 |
| $p_{T_1\text{-}T_2}$ | 0.058 | 0.972 | – |
| MCH, pg: T1 | 28.7 (27.4; 31.2) | 28.5 (26.4; 29.5) | 0.455 |
| MCH, pg: T2 | 28.7 (27.5; 30.7) | 28.7 (26.7; 29.3) | 0.516 |
| $p_{T_1\text{-}T_2}$ | 0.305 | 0.433 | – |
| MCHC, g / l: T1 | 332 (321; 337) | 327 (313; 339) | 0.398 |
| MCHC, g / l: T2 | 329 (319; 333) | 329 (320; 335) | 0.973 |
| $p_{T_1\text{-}T_2}$ | 0.117 | 0.875 | – |
| RDW-CV, %: T1 | 14.7 (13.4; 17.3) | 16.3 (14.9; 19.0) | 0.143 |
| RDW-CV, %: T2 | 15.1 (14.0; 16.3) | 15.2 (14.0; 18.6) | 0.446 |
| $p_{T_1\text{-}T_2}$ | 0.035 | 0.017 | – |
| MicroR, %: T1 | 3.9 (2.7; 4.4) | 8.5 (2.3; 13.3) | 0.153 |
| MicroR, %: T2 | 3.9 (1.5; 4.5) | 6.8 (2.3; 11.4) | 0.142 |
| $p_{T_1\text{-}T_2}$ | 0.345 | 0.345 | – |
| MacroR, %: T1 | 2.9 (2.7; 4.5) | 3.7 (3.1; 5.0) | 0.491 |
| MacroR, %: T2 | 3.7 (2.9; 5.4) | 3.9 (2.8; 4.5) | 0.898 |
| $p_{T_1\text{-}T_2}$ | 0.046 | 0.237 | – |

Note. MCV, fl – mean corpuscular volume, femtoliters (fl); MCH – mean corpuscular hemoglobin content; MCHC – mean corpuscular hemoglobin concentration; RDW-CV – red cell distribution width – coefficient of variation; microR – microcyte ratio; macroR – macrocyte ratio; ESR – erythrocyte sedimentation rate.

In both groups, at admission and after 48 hours from the onset of sepsis, elevated erythrocyte sedimentation rates were observed without statistically significant intergroup differences or changes over time (Table 3). At baseline and after 48 hours, all patients were diagnosed with normocytic normochromic anemia accompanied by erythropoiesis and anisocytosis – an increased red cell distribution width – coefficient of variation (RDW-CV), which, in the context of medical history, corresponds to compensatory posthemorrhagic anemia. In patients with unfavorable outcomes, a significant decrease ($p < 0.05$) in erythrocyte count, hematocrit, and hemoglobin levels was noted over 48 hours in the context of increasing RDW-CV.

Table 4

**Dynamics of Peripheral Blood Leukocyte Counts in the First 48 Hours from the Moment of Sepsis Verification, *Me* ($Q_1$; $Q_3$)**

| Parameter | Patients with a favorable outcome | Patients with a fatal outcome | *p* |
|---|---|---|---|
| Leukocytes, $10^9$ / l, T1 | 11.93 (7.85; 17.75) | 17.94 (7.15; 29.71) | 0.314 |
| Leukocytes, $10^9$ / l, T2 | 9.49 (6.80; 14.43) | 13.18 (10.19; 23.97) | 0.076 |
| $p_{T_1\text{-}T_2}$ | 0.016 | 0.600 | – |
| Neutrophils, %, T1 | 84.0 (77.4; 87.6) | 89.7 (71.9; 92.3) | 0.079 |
| Neutrophils, %, T2 | 74.9 (70.9; 83.7) | 84.7 (79.5; 91.7) | 0.124 |
| $p_{T_1\text{-}T_2}$ | 0.016 | 0.753 | – |
| Neutrophils, $10^9$ / l, T1 | 9.24 (6.32; 13.68) | 15.98 (5.14; 25.1) | 0.254 |
| Neutrophils, $10^9$ / l, T2 | 7.26 (4.66; 10.78) | 10.59 (9.01; 21.35) | 0.056 |
| $p_{T_1\text{-}T_2}$ | 0.017 | 0.422 | – |
| IG, %, T1 | 1.4 (0.5; 2.4) | 2.0 (1.0; 3.0) | 0.525 |
| IG, %, T2 | 2.9 (0.7; 4.8) | 2.0 (0.6; 9.8) | 0.749 |
| $p_{T_1\text{-}T_2}$ | 0.043 | 0.345 | – |
| IG, $10^9$ / l, T1 | 0.25 (0.09; 0.26) | 0.14 (0.13; 0.65) | 0.874 |
| IG, $10^9$ / l, T2 | 0.40 (0.16; 0.69) | 0.09 (0.05; 0.95) | 0.749 |
| $p_{T_1\text{-}T_2}$ | 0.237 | 0.463 | – |
| Platelets, $10^9$ / l, T1 | 311 (234; 370) | 252 (133; 394) | 0.422 |
| Platelets, $10^9$ / l, T2 | 356 (254; 397) | 212 (120; 264) | 0.011 |
| $p_{T_1\text{-}T_2}$ | 0.487 | 0.028 | – |
| Platelets, % | 0.76 (–10.78; 14.15) | –9.78 (–31.34; 1.33) | 0.035 |
| NEUT-GI, T1 | 156.1 (152.0; 159.7) | 156.3 (151.7; 157.5) | 0.405 |
| NEUT-GI, T2 | 154.5 (151.9; 160.4) | 154.5 (152.4; 156.2) | 0.592 |
| $p_{T_1\text{-}T_2}$ | 0.422 | 0.086 | – |
| NEUT-GI, % | 0.25 (–1.04; 2.37) | 1.38 (0.26; 2.91) | 0.367 |
| NEUT-RI, T1 | 52.0 (49.1; 56.6) | 58.3 (53.2; 64.8) | 0.032 |
| NEUT-RI, T2 | 50.1 (48.7; 53.6) | 62.9 (58.0; 64.4) | 0.002 |
| $p_{T_1\text{-}T_2}$ | 0.363 | 0.594 | – |
| NEUT-RI, % | –2.93 (–6.60; 3.32) | –3.90 (–6.98; 4.11) | 0.900 |

Note. IG, % – relative number of immature granulocytes; IG – absolute number of immature granulocytes; NEUT-GI – neutrophil granularity intensity, scattering intensity; NEUT-RI –neutrophil reactivity intensity, fluorescence intensity.

At the time of sepsis diagnosis, neutrophilic leukocytosis was observed in both groups. In patients with fatal outcomes, the leukocyte count was nearly twice the upper limit of reference values. Despite the absence of statistically significant differences in leukocyte and neutrophil levels (including immature forms) at both measurement points, survivors showed

a reduction in the severity of neutrophilic leukocytosis after 48 hours (Table 4). In the group of diseased patients, a significant decrease in platelet count was observed over time, which after 48 hours resulted in statistically significant differences between the groups ($p = 0.011$).

Both groups exhibited a pronounced inflammatory response in the blood (leukocytosis, neutrophil shift). However, in survivors, a positive dynamic was observed after 48 hours: the leukocyte level decreased from 11.93 (7.85; 17.75) to 9.49 (6.80; 14.43) × $10^9$ / l ($p = 0.016$), neutrophil percentage decreased from 84.0 (77.4; 87.6)% to 74.9 (70.9; 83.7)% ($p = 0.016$), and their absolute count decreased from 9.24 (6.23; 13.68) to 7.26 (4.66; 10.78) × $10^9$ / l ($p = 0.017$).

At the time of sepsis diagnosis, NEUT-RI was higher in the group of deceased patients: 58.3 (53.2; 64.8) vs. 51.95 (49.10; 56.60) FI in survivors ($p = 0.032$). After 48 hours, NEUT-RI decreased in survivors to 50.05 (48.70; 53.60) FI and increased in non-survivors to 62.9 (58.0; 64.4) FI, with differences between the groups persisting ($p = 0.002$). Regarding NEUT-GI, no significant differences between the groups were found at either time point ($p > 0.05$; Table 3).

*Verification of potential early predictors of mortality in postoperative sepsis using ROC analysis.* The following should be considered as significant clinical and anamnestic factors associated with the risk of death in postoperative sepsis: duration of hospitalization ≤11 bed- – days (AUC 0.720 (0.555; 0.850); $p = 0.009$, with sensitivity of 44.4% and specificity of 95.45%), as well as such indicators at the time of sepsis diagnosis as SOFA score > 4 (AUC 0.795 (0.638; 0.906); $p < 0.001$ with sensitivity of 77.78% and specificity of 72.73%), the Glasgow score ≤12 (AUC 0.616 (0.449; 0.785); $p = 0.049$ with sensitivity of 27.78% and specificity of 95.45%), as well as baseline serum urea concentration > 12.1 mmol / l (AUC 0.732 (0.569; 0.960); $p = 0.004$ with sensitivity of 61.11% and specificity of 67.27%) and serum calcium ≤ 1.8 mmol / l (AUC 0.765 (0.525; 0.923), $p = 0.013$ with sensitivity of 70% and specificity of 70%). A number of potential predictors of an unfavorable outcome were identified during the analysis of hemogram parameters (Table 5).

Table 5

**Hemogram Parameters as Early Predictors of a Fatal Outcome in Postoperative Sepsis**

| Parameter | AUC | 95% CI | *p* | Cutoff point | Sensitivity | Specificity |
|---|---|---|---|---|---|---|
| Neutrophils, $10^9$ / l, T2 | 0.696 | (0.518; 0.839) | 0.046 | > 10.15 | 69.23 | 72.73 |
| Monocytes, %, T1 | 0.711 | (0.536; 0.849) | 0.038 | ≤ 4.8 | 66.67 | 85.71 |
| Eosinophils, %, T2 | 0.730 | (0.541; 0.872) | 0.017 | ≤ 1.2 | 81.82 | 60.00 |
| Platelets, $10^9$ / l, T2 | 0.760 | (0.587; 0.888) | 0.003 | ≤ 264 | 76.92 | 72.73 |
| Platelets, $10^9$ / l (T2–T1) | 0.733 | (0.556; 0.867) | 0.006 | ≤ 15 | 100.00 | 45.45 |
| PCT, %, T2 | 0.782 | (0.604; 0.906) | 0.001 | ≤ 0.27 | 75.00 | 76.19 |
| RET-He, pg (T2–T1) | 0.766 | (0.493; 0.936) | 0.036 | ≤ 0.8 | 75.00 | 75.00 |
| RET-He – RBC-He, pg, T1 | 0.903 | (0.680; 0.990) | < 0.0001 | > –1.5 | 81.82 | 87.50 |
| RET-He – RBC-He, pg, T2 | 0.821 | (0.543; 0.966) | 0.012 | > –1.9 | 100.00 | 62.50 |
| NEUT RI, FI, T1 | 0.736 | (0.540; 0.881) | 0.019 | > 57.6 | 77.78 | 85.71 |
| NEUT RI, FI, T2 | 0.889 | (0.688; 0.91) | < 0.0001 | > 53.8 | 53.85 | 93.75 |
| RE LYMP, %, T1 | 0.730 | (0.534; 0.877) | 0.016 | ≤ 0.28 | 83.33 | 58.82 |

Note. PCT – plateletcrit; RET-He – hemoglobin concentration in reticulocytes; RET-He – RBC-He – the difference between the measured mean concentration of hemoglobin in reticulocytes (RET-He) and mature erythrocytes (RBC-He); NEUT-RI – neutrophil reactivity intensity; RE LYMP – reactive lymphocytes.

Particular attention is drawn to potential predictors of a fatal outcome recorded in the dynamics of AS. Thus, an increase in the level of neutrophils > 10.15 × $10^9$ / l after 48 hours, a relative number of monocytes ≤ 4.8% at the time of AS detection, eosinophils ≤ 1.2% after 48 hours, as well as a decrease in the number of platelets to ≤ 264 × $10^9$ / l or the absence of their increase by more than 15 × $10^9$ / l from the baseline level may indicate an unfavorable prognosis. Predictors also include: platelet count ≤ 0.27% after 48 hours, a decrease in reticulocyte hemoglobin concentration by ≥ 0.8 pg and / or ≥ 5.38%, a decrease in the difference in hemoglobin content between reticulocytes and mature red blood cells to –1.5 pg at baseline and > –1.9 pg after 48 hours, an increase in NEUT-RI > 57.6 FI when sepsis is detected and / or > 53.8 FI after 48 hours, and a relative number of reactive lymphocytes ≤ 0.28% at baseline (Table 5).

## DISCUSSION

The results of the study confirm the significance of the early assessment of clinical and laboratory parameters in patients with AS for predicting outcomes. The mortality rate in the studied cohort was 45%, which exceeds the average values (30–38%) reported for patients with sepsis and septic shock [6]. This may be associated with a larger number of emergency surgeries in the deceased group, the severity of condition upon admission, and pronounced multiple organ failure.

The SOFA score is traditionally used to evaluate the risk of mortality in sepsis, demonstrating high sensitivity (89%) and specificity (69%) [7]. In the work by R. Garg et al., SOFA score of ≥ 9 was associated with increased mortality [8]. In our study, the SOFA score > 4 predicted mortality with sensitivity of 77.78% and specificity of 72.73%.

Hypocalcemia, previously described in critical conditions, including sepsis [9], was also observed in our patients. In the group with fatal outcomes, calcium levels were significantly lower compared to survivors. According to the literature, during sepsis, active forms of oxygen and proinflammatory mediators are released, which activate calcium-sensitive receptors, potentially contributing to the development of hypotension and endothelial dysfunction [10].

Acute kidney injury (AKI) is a frequent and severe manifestation of organ dysfunction in sepsis, detected in 60% of patients [11]. It is associated with an increase in in-hospital mortality up to 18% and an independent rise in the risk of death [12]. Indicators such as creatinine, urea, and diuresis are used to assess AKI [13]. In our patients with fatal outcomes, urea levels were statistically higher, and the value > 12.1 mmol / l was an independent predictor of death in AS.

PCT and CRP are among the most studied markers of bacterial infection [14]. Although levels of both markers were elevated in all patients, no statistically significant differences were found between the groups. This may be explained by the universal nature of the inflammatory response in sepsis. However, the dynamics of these indicators had prognostic value: in survivors, a decrease in CRP was observed after 48 hours, reflecting the effectiveness of therapy. In the group with fatal outcomes, levels of CRP and PCT either did not decrease or increased, indicating progression of inflammation and organ dysfunction. Thus, a comprehensive assessment of inflammatory markers in combination with clinical and biochemical data is essential.

Lactate is an important marker of tissue hypoperfusion and metabolic dysfunction in sepsis [15]. According to Sepsis-3 criteria, septic shock is diagnosed in the presence of persistent systemic arterial hypotension requiring vasopressor support, combined with a lactate level ≥ 2 mmol / l after fluid resuscitation [5]. In our study, lactate levels were elevated in all patients upon admission and remained elevated after 48 hours, with no significant differences between the groups. This may reflect similar early metabolic disturbances across the cohort.

The analysis of the erythrogram revealed normocytic normochromic anemia, typical of inflammation and blood loss. At baseline, all patients exhibited decreased hemoglobin, erythrocyte count, and hematocrit levels, with more pronounced reductions in the deceased group, and further declines observed after 48 hours. This supports existing literature data on septic anemia, which is caused by the effects of proinflammatory cytokines, impaired erythropoiesis, and surgical blood loss [16].

The red cell distribution width (RDW-CV) was elevated in both groups; however, a significant increase was observed after 48 hours in the patients who died. This may indicate activation of erythropoiesis and iron redistribution in response to inflammation. Elevated RDW-CV has been previously associated with a poor prognosis in sepsis [17].

Evaluation of reticulocyte parameters revealed a decrease in hemoglobin concentration within reticulocytes (RET-He) among patients with fatal outcomes, along with a decrease in the difference between RET-He and hemoglobin levels in mature erythrocytes. This indicates impaired hemoglobinization and suppression of erythropoiesis, consistent with the pathogenesis of septic anemia and disturbances in iron metabolism [18].

Coagulopathy is a key prognostic factor in sepsis, ranging from isolated thrombocytopenia to disseminated intravascular coagulation (DIC). In our study, 48 hours after diagnosis, deceased patients showed a statistically significant decrease in platelet count (212 (120; 264) × $10^9$ / l, $p$ = 0.028). These findings align with existing literature: thrombocytopenia occurs in 10–70% of sepsis patients, especially in intensive care units. Mechanisms include consumption of platelets in microcirculation, impaired production, sequestration in the liver and spleen, and apoptosis [19]. A critical level below 150 × $10^9$ / l is associated with an increased risk of mortality [20]. Our data support this conclusion.

Leukocytosis in sepsis is an important criterion of systemic inflammatory response syndrome (SIRS), characterized by high sensitivity (0.85) but low specificity (0.41) [21]. Both groups exhibited neutrophilic leukocytosis; however, it was more pronounced among the deceased. In survivors, the leukocyte count decreased from 11.93 (7.85; 17.75) to 9.49 (6.80; 14.43) × $10^9$ / l ($p$ = 0.016) after 48 hours, and neutrophil percentage decreased from 84.0 (77.4; 87.6) to 74.9 (70.9; 83.7)% ($p$ = 0.016), which may indicate a positive response to treatment.

The value of NEUT-RI at diagnosis was higher among deceased patients (58.3 [53.2; 64.8] FI) compared to survivors (51.95 [49.10; 56.60] FI) ($p$ = 0.032). After 48 hours, NEUT-RI continued to increase in the deceased group, whereas it tended to decrease among survivors ($p$ = 0.002). Elevated NEUT-RI has been previously associated with a poor prognosis in sepsis [22], a finding confirmed by our study results.

## CONCLUSION

The results of this study confirm the clinical significance of the early comprehensive assessment of clinical and laboratory parameters for predicting hospital outcomes in patients with postoperative AS. The most prognostically valuable indicators within the first 48 hours after sepsis verification included: the severity of organ dysfunction (SOFA score > 4), hypocalcemia (≤ 1.8 mmol / l), hyperuricemia (> 12.1 mmol / l), a decrease and insufficient increase in platelet count, elevated neutrophil reactivity, as well as reduced hemoglobinization of reticulocytes and levels of reactive lymphocytes.

Additionally, the absence of positive dynamics in inflammatory markers (CRP, procalcitonin), neutrophilic leukocytosis, and hematological parameters during the first two days were associated with unfavorable outcomes. These parameters can serve as accessible and informative criteria for risk stratification and personalized therapy in patients with AS. The obtained findings require confirmation in larger cohort and prospective clinical trials.

## REFERENCES


1. Vincent J.L., Marshall J.C., Namendys-Silva S.A., François B., Martin-Loeches I., Lipman J. et al.; ICON Investigators. Assessment of the Worldwide Burden of Critical Illness: The Intensive Care over Nations (ICON) Audit. *Lancet Respir. Med*. 2014;2(5):380–386. DOI: 10.1016/S2213-2600(14)70061-X.
2. Blot S., Antonelli M., Arvaniti K., Blot K., Creagh-Brown B., de Lange D. et al.; Abdominal Sepsis Study (AbSeS) Group on Behalf of the Trials Group of the European Society of Intensive Care Medicine. Epidemiology of Intra-Abdominal Infection and Sepsis in Critically Ill Patients: "Abses", A Multinational Observational Cohort Study and ESICM Trials Group Project. *Intensive Care Med.* 2019;45(12):1703–1717. DOI: 10.1007/s00134-019-05819-3.
3. Martin-Loeches I., Timsit J.F., Leone M., de Waele J., Sartelli M., Kerrigan S. et al. Clinical Controversies in Abdominal Sepsis. Insights for Critical Care Settings. *J. Crit. Care.* 2019;53:53–58. DOI: 10.1016/j.jcrc.2019.05.023.
4. Sartelli M., Coccolini F., Kluger Y., Agastra E., Abu-Zidan F.M., Abbas A.E.S. et al. WSES/GAIS/SIS-E/WSIS/AAST Global Clinical Pathways for Patients with Intra-Abdominal Infections. *World J. Emerg. Surg.* 2021;16(1):49. DOI: 10.1186/s13017-021-00387-8.
5. Singer M., Deutschman C.S., Seymour C.W., Shankar-Hari M., Annane D., Bauer M. et al. The Third International Consensus Definitions for Sepsis and Septic Shock (Sepsis-3). *JAMA.* 2016;315(8):801–810. DOI: 10.1001/jama.2016.0287.
6. Bauer M., Gerlach H., Vogelmann T., Preissing F., Stiefel J., Adam D. Mortality in Sepsis and Septic Shock in Europe, North America and Australia Between 2009 and 2019- Results from a Systematic Review and Meta-Analysis. *Crit. Care.* 2020;24(1):239. DOI: 10.1186/s13054-020-02950-2.
7. Qiu X., Lei Y.P., Zhou R.X. SIRS, SOFA, qSOFA, and NEWS in the Diagnosis of Sepsis and Prediction of Adverse Outcomes: A Systematic Review and Meta-Analysis. *Expert Rev. Anti. Infect. Ther.* 2023;21(8):891–900. DOI: 10.1080/14787210.2023.2237192.
8. Garg R., Tellapragada C., Shaw T., Eshwara V.K., Shanbhag V., Rao S. et al. Epidemiology of Sepsis and Risk Factors for Mortality in Intensive Care Unit: A Hospital Based Prospective Study in South India. *Infect. Dis. (Lond.).* 2022;54(5):325–334. DOI: 10.1080/23744235.2021.2017475.
9. Gallardo J., Fardella P., Pumarino H., Campino C. Niveles de Calcio Plasmático en Pacientes Críticos con y Sin Sepsis [Plasma Calcium Levels in Critical Patients with and Without Sepsis]. *Rev. Med. Chil.* 1991;119(3):262–266. (In Span.).
10. Sood A., Singh G., Singh T.G., Gupta K. Pathological Role of the Calcium-Sensing Receptor in Sepsis-Induced Hypotensive Shock: Therapeutic Possibilities and Unanswered Questions. *Drug. Dev. Res.* 2022;83(6):1241–1245. DOI: 10.1002/ddr.21959.
11. Balkrishna A., Sinha S., Kumar A., Arya V., Gautam A.K., Valis M. et al. Sepsis-Mediated Renal Dysfunction: Pathophysiology, Biomarkers and Role of Phytoconstituents in its Management. *Biomed. Pharmacother.* 2023;165:115183. DOI: 10.1016/j.biopha.2023.115183.
12. White K.C., Serpa-Neto A., Hurford R., Clement P., Laupland K.B., See E. et al; Queensland Critical Care Research Network (QCCRN). Sepsis-Associated Acute Kidney Injury in the Intensive Care Unit: Incidence, Patient Characteristics, Timing, Trajectory, Treatment, and Associated Outcomes. A Multicenter, Observational Study. *Intensive Care Med.* 2023;49(9):1079–1089. DOI: 10.1007/s00134-023-07138-0.
13. Seymour C.W., Liu V.X., Iwashyna T.J., Brunkhorst F.M., Rea T.D., Scherag A. et al. Assessment of Clinical Criteria for Sepsis: For the Third International Consensus Definitions for Sepsis and Septic Shock (Sepsis-3). *JAMA.* 2016;315(8):762–774. DOI: 10.1001/jama.2016.0288.

Erratum in: *JAMA.* 2016;315(20):2237. DOI: 10.1001/jama.2016.5850.
14. Pierrakos C., Velissaris D., Bisdorff M., Marshall J.C., Vincent J.L. Biomarkers of Sepsis: Time for a Reappraisal. *Crit. Care.* 2020;24(1):287. DOI: 10.1186/s13054-020-02993-5.
15. Weinberger J., Klompas M., Rhee C. What is the Utility of Measuring Lactate Levels in Patients with Sepsis and Septic Shock? *Semin. Respir. Crit. Care Med.* 2021;42(5):650–661. DOI: 10.1055/s-0041-1733915.
16. An M.M., Liu C.X., Gong P. Effects of Continuous Renal Replacement Therapy on Inflammation-Related Anemia, Iron Metabolism and Prognosis in Sepsis Patients with Acute Kidney Injury. *World J. Emerg. Med.* 2023;14 (3):186–192. DOI: 10.5847/wjem.j.1920-8642.2023.052.
17. Hong C., Xiong Y., Xia J., Huang W., Xia A., Xu S. et al. LASSO-Based Identification of Risk Factors and Development of a Prediction Model for Sepsis Patients. *Ther. Clin. Risk Manag.* 2024;20:47–58. DOI: 10.2147/TCRM.S434397.
18. Piagnerelli M., Cotton F., Herpain A., Rapotec A., Chatti R., Gulbis B. et al. Time Course of Iron Metabolism In Critically Ill Patients. *Acta Clin. Belg.* 2013;68(1):22–27. DOI: 10.2143/ACB.68.1.2062715.
19. Giustozzi M., Ehrlinder H., Bongiovanni D., Borovac J.A., Guerreiro R.A., Gąsecka A. et al. Coagulopathy and Sepsis: Pathophysiology, Clinical Manifestations and Treatment. *Blood Rev.* 2021;50:100864. DOI: 10.1016/j.blre.2021.100864.
20. Wada H., Thachil J., Di Nisio M., Matino D., Kurosawa S., Gando S. et al. The Diagnostic and Prognostic Value of Thrombocytopenia in Critically Ill Patients. *J. Thromb. Haemost*. 2019;17(6):1057–1070. DOI: 10.1111/jth.14478.
21. Qiu X., Lei Y.P., Zhou R.X. SIRS, SOFA, qSOFA, and NEWS in the Diagnosis of Sepsis and Prediction of Adverse Outcomes: A Systematic Review and Meta-Analysis. *Expert Rev. Anti. Infect. Ther.* 2023;21(8):891–900. DOI: 10.1080/14787210.2023.2237192.

## Author Contribution

Rodionova Yu.O. – compilation of the database, acquisition and interpretation of clinical data, drafting of the article, review of the literature. Fedosenko S.V. – conception and design of the study, coordination of the study, drafting of the article, review of the literature, final approval of the manuscript for publication. Ivanova A.I., Semenova O.L. – statistical processing of the data, interpretation of the data. Arzhanik M.B. – statistical processing of the data, interpretation of the data, critical revision of the manuscript for important intellectual content. Starovoitova E.A., Kalyuzhin V.V. – critical revision of the manuscript for important intellectual content, final approval of the manuscript for publication. Nesterovich S.V., Efimova D.A. – collection of clinical data, coordination of the study.

## Author Information

**Rodionova Yulia O.** – Teaching Assistant, Division of Intermediate-Level Therapy with a Course in Clinical Pharmacology,, SibSMU, Head of the Department of Clinical Pharmacology, Clinical Pharmacologist, SibSMU Clinics, Tomsk, rodionova.yo@ssmu.ru, http://orcid.org/0000-0001-6819-6968

**Fedosenko Sergey V.** – Dr. Sci. (Med.), Associate Professor, Professor of the Division of General Medical Practice and Polyclinic Therapy, SbSMU, Tomsk, s-fedosenko@mail.ru, http://orcid.org/0000-0001-6655-3300

**Ivanova Anastasia I.** – Student, Biomedical Department, SibSMU, Tomsk, nastya-170502@mail.ru, http://orcid.org/0009-0001-7948-1665

**Arzhanik Marina B.** – Cand. Sci. (Pedagogy), Associate Professor, Division of Medical and Biological Cybernetics, SibSMU, Tomsk, arzh_m@mail.ru, http://orcid.org/0000-0003-4844-9803

**Semenova Oksana L.** – Senior Lecturer, Division of Medical and Biological Cybernetics, SibSMU, Tomsk, oksleon@list.ru, http://orcid.org/0000-0002-6866-5020

**Starovoitova Elena A.** – Dr. Sci. (Med.), Associate Professor, Head of the Division of General Medical Practice and Polyclinic Therapy, SibSMU, Tomsk, elena-starovoytova@yandex.ru, http://orcid.org/0000-0002-4281-1157

**Nesterovich Sofia V.** – Cand. Sci. (Med.), Internal Medicine Doctor of the Expert Department, SibSMU, Tomsk, snesterovich@mail.ru, http://orcid.org/0000-0003-2098-2964

**Efimova Daria A.** – Cand. Sci. (Med.), Head of Internal Medicine Clinic, Internal Medicine Doctor, SibSMU, Tomsk, vinokurova.da@ssmu.ru, https://orcid.org/0000-000208422-8349

**Kalyuzhin Vadim V.** – Dr. Sci. (Med.), Professor, Head of the Advanced Therapy Division with a Course in Rehabilitation, Physiotherapy and Sports Medicine, SibSMU, Tomsk, kalyuzhinvv@mail.ru, https://orcid.org/0000-0001-9640-2028

(✉) **Rodionova Yulia O.,** rodionova.yo@ssmu.ru

.
Received on June 02, 2025;
approved after peer review on June 09, 2025;
accepted on June 18, 2025

УДК 616.127-008.853.6-036.11-02:[616.98:578.834.1]
https://doi.org/10.20538/1682-0363-2025-3-116-126

# Acute myocardial injury in new coronavirus infection: contribution of mast cells

**Budnevsky A.V.[1], Avdeev S.N.[2], Ovsyannikov E.S.[1], Tokmachev R.E.[1], Feigelman S.N.[1], Shishkina V.V.[1], Perveeva I.M.[3], Chernik T.A.[1], Arkhipova E.D.[1], Budnevskaya S.A.[1]**

[1] *N.N. Burdenko Voronezh State Medical University*
*10 Studencheskaya St., 394036 Voronezh, Russian Federation*

[2] *I.M. Sechenov First Moscow State Medical University*
*8-2 Trubetskaya St., 119048 Moscow, Russian Federation*

[3] *Voronezh Regional Clinical Hospital No. 1*
*151 Moskovsky Ave., 394066 Voronezh, Russian Federation*

**ABSTRACT**

The new coronavirus infection, COVID-19, led to a global pandemic in 2019–2023. The infection affects not only the lung tissue, but also other organs and systems, including the heart. This causes the frequent development of myocarditis, arrhythmia, and acute coronary syndrome in these patients, as well as worsening of coronary heart disease and chronic heart failure. One of the important mechanisms of heart damage in COVID-19 is the excessive activation of mast cells, which produce cytokines and chemokines with pro-inflammatory activity, thus causing a so-called "cytokine storm" – a special severe form of systemic inflammatory response that can be fatal.

**The aim** of the literature review was to analyze and summarize published data on cardiovascular complications in COVID-19, including the effect of mast cell proteases on myocardial damage.

**Keywords:** COVID-19, mast cells, cytokine storm, heart

**Conflict of interest.** The authors declare the absence of obvious and potential conflicts of interest related to the publication of this article.

**The source of financing.** The authors declare no funding for the study.

**For citation:** Budnevsky A.V., Avdeev S.N., Ovsyannikov E.S., Tokmachev R.E., Feigelman S.N., Shishkina V.V., Perveeva I.M., Chernik T.A., Arkhipova E.D., Budnevskaya S.A. Acute myocardial injury in new coronavirus infection: contribution of mast cells. *Bulletin of Siberian Medicine.* 2025;24(3):116–126. https://doi.org/10.20538/1682-0363-2025-3-5-13.

# Острое повреждение миокарда при новой коронавирусной инфекции: вклад тучных клеток

**Будневский А.В.[1], Авдеев С.Н.[2], Овсянников Е.С.[1], Токмачев Р.Е.[1], Фейгельман С.Н.[1], Шишкина В.В.[1], Первеева И.М.[3], Черник Т.А.[1], Архипова Е.Д.[1], Будневская С.А.[1]**

[1] *Воронежский государственный медицинский университет (ВГМУ) им. Н.Н. Бурденко*
*Россия, 394036, г. Воронеж, ул. Студенческая, 10*

✉ *Feigelman Sofia N.,* s.feygelman@gmail.com

[2] *Первый Московский государственный медицинский университет им. И.М. Сеченова (Сеченовский Университет) Россия, 119048, г. Москва, ул. Трубецкая, 8-2*

[3] *Воронежская областная клиническая больница № 1 (ВОКБ № 1) Россия, 394066, г. Воронеж, Московский проспект, 151*

**РЕЗЮМЕ**

Новая коронавирусная инфекция COVID-19, вызвавшая масштабную пандемию в 2019–2023 гг., поражает не только легочную ткань, но и другие органы и системы, в том числе сердце, что обусловливает частое развитие у данных пациентов миокардита, аритмий, острого коронарного синдрома, а также ухудшение течения ишемической болезни сердца и хронической сердечной недостаточности. Одним из важных механизмов повреждения сердца при COVID-19 является избыточная активация тучных клеток, которые вырабатывают цитокины и хемокины, обладающие провоспалительной активностью, вызывая, таким образом, «цитокиновый шторм» – особую тяжелую форму системной воспалительной реакции, которая может заканчиваться летальным исходом.

**Цель** литературного обзора заключалась в проведении анализа и обобщении опубликованных данных о сердечно-сосудистых осложнениях при COVID-19, включая влияние протеаз тучных клеток на поражение миокарда.

**Ключевые слова:** COVID-19, тучные клетки, протеазы, цитокиновый шторм, сердце

**Конфликт интересов.** Авторы декларируют отсутствие явных и потенциальных конфликтов интересов, связанных с публикацией настоящей статьи.

**Источник финансирования.** Авторы заявляют об отсутствии финансирования при проведении исследования.

**Для цитирования:** Будневский А.В., Авдеев С.Н., Овсянников Е.С., Токмачев Р.Е., Фейгельман С.Н., Шишкина В.В., Первеева И.М., Черник Т.А., Архипова Е.Д., Будневская С.А. Острое повреждение миокарда при новой коронавирусной инфекции: вклад тучных клеток. *Бюллетень сибирской медицины.* 2025;24(3):116–126. https://doi.org/10.20538/1682-0363-2025-3-116-126.

## LITERATURE REVIEW METHODS

A systematic literature review was conducted including original articles on myocardial damage associated with the novel coronavirus infection, COVID-19, as well as the role of mast cell proteases in the development of cardiovascular complications among patients with this disease. PubMed and eLIBRARY were used as electronic search engines. The primary search was performed using the keywords “COVID-19”, “mast cells”, and “heart”. Based on these criteria, we found and reviewed 436 articles published between 1996 and 2024.

When reviewing the summaries of the selected articles, we excluded 134 publications from the PubMed electronic database and 32 publications from eLIBRARY as they were not relevant to the topic of our systematic literature review. After a detailed analysis of full-text publications, we excluded 207 articles. For example, we excluded 12 studies that examined the effect of mast cells on coronary heart disease, chronic heart failure, and acute coronary syndrome in patients without COVID-19. In two clinical trials, the sample size was too small (less than 30 individuals), and in three publications, full access to the results was blocked. Finally, we included 41 studies in our review.

## BRIEF EPIDEMIOLOGY OF COVID-19

During the period of sanitary and epidemiological monitoring in the 21st century, there were three significant episodes of mass coronavirus infection. A common feature of these epidemics was that humans were primarily infected from animals, forming a natural source of anthropozoonotic infection [1].

The severe acute respiratory syndrome (SARS) epidemic was first reported in 2002 in China. Cases were recorded in 37 other countries, and in 2003, the causative agent SARS-CoV was identified [2]. During this time, 8,096 cases of the disease were confirmed,

of which 774 were fatal. Since 2004, no new cases of SARS-CoV have been reported [3].

The second epidemic caused by a coronavirus occurred in 2012 in Saudi Arabia. It was caused by the Middle East respiratory syndrome-related coronavirus (MERS-CoV) [4]. According to the World Health Organization (WHO), the epidemic had a high mortality rate of 36% among those infected. Due to the spread of the virus from infected dromedaries to humans, high-risk groups included shepherds and workers at slaughterhouses [1]. In addition, people with chronic lung diseases, chronic kidney diseases, obesity, diabetes, and immunodeficiency conditions were also at an increased risk of infection [5, 6]. The epidemic spread to 27 countries, mostly in the Arabian Peninsula and surrounding areas, and cases of MERS-CoV continue to be identified at present [6].

The third wave of the coronavirus infection in December 2019 was identified as the most widespread, soon receiving the status of a pandemic. On January 13, the first case of the infection was recorded outside of China, and on January 30, person-to-person spread of the virus was confirmed [7]. A coronavirus called severe acute respiratory syndrome coronavirus 2 (SARS-CoV-2) was identified as the etiological factor of COVID-19 [8]. Bats, minks, and some members of the felidae family are thought to be the natural reservoirs of SARS-CoV-2, as well as a number of other potential intermediate hosts, including pangolins, ferrets, and snakes [9]. Humans are susceptible to this virus due to its affinity for the human angiotensin-converting enzyme 2 (ACE2) receptor [10]. At the same time, the contagiousness, virulence, replication rate, and other characteristics of different genetic variants of the SARS-CoV-2 virus vary [11]. A sick person or an asymptomatic carrier can transmit SARS-CoV-2. Airborne transmission is the most significant way of spreading the virus, followed by transmission through airborne dust particles and household contact. Fecal-oral transmission is considered less likely [12].

In the Russian Federation during the pandemic caused by the novel coronavirus infection, five significant increases in morbidity and mortality, known as waves, were recorded. The average incidence rate for all recorded waves was 248 cases per 10,000 people, with an overall average mortality rate of 2.4%. The highest incidence occurred in the fifth wave, and the highest mortality was in the fourth one [13]. When studying global patterns of morbidity fluctuations during the pandemic, it was found that waves subside after an average of 48 days, regardless of the initial conditions [14]. Due to the improved epidemic situation, the World Health Organization declared an end to COVID-19 as a public health emergency on May 5, 2023. As of now, COVID-19 can be considered a seasonal disease [12].

## Etiology and Pathogenesis of Coronavirus Infections, Including Novel Coronavirus Infection (COVID-19)

Phylogenetic analysis of the SARS-CoV-2 virus genome allowed it to be assigned to the genus *Betacoronavirus*, the family Coronaviridae. This RNA-containing enveloped pleomorphic virus has round particles ranging from 60 to 140 nm in diameter. The SARS-CoV-2 genome is 50% identical to that of SARS-CoV and 75% identical to that of MERS–CoV [15].

SARS-CoV and SARS-CoV-2 viruses, as well as pathogens of mild respiratory infections – alphacoronaviruses HCoV-NL63 and HCoV-229E and betacoronaviruses HCoV-OC43 and HCoV-HKU1, use the ACE2 receptor to enter cells, which was first identified in 2003 [16, 17]. ACE2 is an 805-amino-acid carboxypeptidase that cleaves one amino acid from the C-terminus of its substrates. Being a part of the renin-angiotensin-aldosterone system, ACE2 converts angiotensin I and angiotensin II into angiotensin-(1–9) and angiotensin-(1–7), respectively [18].

The coronavirus virion consists of nucleocapsid (N), membrane (M), envelope (E), and spike (S) proteins. The penetration of viral particles into the cell is mediated by S-glycoprotein, which embedding into the membrane of the virion in several copies of the homotrimer gives it a crown-shaped appearance. Glycoproteins of many viruses, including HIV-1, Ebola, and avian influenza viruses, are cleaved into two subunits in infected cells — extracellular and transmembrane (this cleavage occurs prior to the virus release from the producing cell). Similarly, the S-protein of some coronaviruses is cleaved into S1 and S2 subunits during their biosynthesis in infected cells, but the S-protein of other coronaviruses is cleaved only when the next target cell is reached. SARS-CoV-2, like MERS-CoV, belongs to the first category: its S-protein is cleaved by protein convertases in virus production cells [17].

Thus, the S-protein of a mature virion consists of two non-covalently bound subunits: the S1 subunit binds to ACE2, and the S2 subunit attaches the S-protein to the membrane [19]. The interaction of receptors with viral glycoproteins in the presence of

specific triggers causes significant conformational changes in both subunits, which bring the viral and cell membranes closer together, eventually creating a fusion pore through which the viral genome enters the cytoplasm of the cell. For SARS-CoV-2, one of these triggers is the cleavage of an additional region within the S2 subunit, called the "S2' region", which is exposed after interaction with ACE2. The cleavage of the S2' region by transmembrane protease, serine 2 (TMPRSS2) on the cell surface or by cathepsin L in the endosomal vesicle after ACE2-mediated endocytosis releases the merging peptide, initiating the formation of a pore that ensures the penetration of the viral genome into the cell [20–22].

Analysis of animal models and human transcriptome databases demonstrates that the expression of ACE2 in the lower parts of the lungs is represented only by type II alveolar cells, however, it is much higher in the epithelium of the bronchi and nose, especially in ciliated cells. The difference in ACE2 levels across the respiratory tract may explain the variable infection gradient of SARS-CoV-2, while the ciliated cells of the nasal cavity are the main target for virus replication in the early stages of the disease [23].

Despite the fact that the airborne transmission of SARS-CoV-2 infection is the dominant route, the highest level of ACE2 expression is observed in the intestine, testicles, kidneys, myocardium, and thyroid gland [24]. Cardiac infection with SARS-CoV-2 was often detected at autopsy, and the presence of ACE2 in colon and kidney cells has been proposed as an explanation for gastrointestinal and renal complications caused by SARS-CoV-2 [25, 26]. The expression of ACE2 in the gastrointestinal tract is consistent with the fact that many coronaviruses are transmitted not only using the airborne route but also by the fecal-oral route [26]. Inflammatory cytokines released during the "cytokine storm" in severe COVID-19, such as IL-1β and type I and III interferons, can increase the expression of ACE2, potentially creating a positive feedback loop for viral replication [27].

Concomitant diseases, including arterial hypertension, hyperlipidemia, diabetes mellitus, chronic lung diseases, old age, and smoking, are risk factors for COVID-19 infection, and some of them may affect ACE2 expression. Widespread epidemiological data suggest that smoking increases the risk of severe disease, but it is not fully known whether smoking causes an increase in ACE2 expression and whether it is associated with worsening of the infection [12]. Many biochemical studies have demonstrated that the expression of ACE2 is increased in lung tissue samples from smokers and patients with chronic obstructive pulmonary disease, as well as in the lungs of mice exposed to cigarette smoke [28, 29].

## THE ROLE OF MAST CELLS IN THE PATHOGENESIS OF COVID-19

Mast cells (MCs) are cells of innate immunity of myeloid origin, which also participate in the reactions of acquired immunity. They are present everywhere in the body, but are mainly concentrated in the lungs, respiratory tract, heart, gastrointestinal tract, skin, nasal cavity, and meninges. MCs differ in their ultrastructure, morphology, mediator content, receptor expression, and response to stimuli, and they play an important role in the first line of defense against viruses and bacteria entering the body. Recent data indicate that after entering the body, coronaviruses activate cells of the innate immune system – monocytes/macrophages, neutrophils, T-cells, natural killers (NK-cells), MCs, and epithelial and endothelial cells. Activation of MCs in response to a viral infection performs a protective function, directly countering infection and influencing the immune system [30–32].

The immune response to COVID-19 can be divided into physiological and pathological – excessively active, contributing to damage to the lungs, heart, and other organs, which can significantly aggravate the course of the disease. Initially, SARS-CoV-2 infection causes a local immune response, including the attraction of MCs, macrophages, and monocytes to the infection site, their production of interferons and cytokines, as well as activation of the adaptive immune response of T and B cells.

In most cases, this process eliminates the infection, but in some cases, immune system dysfunction occurs, which leads to severe damage to internal organs. When the immune response is disrupted, immune cells hyperactivate with excessive infiltration of monocytes, macrophages, and T-cells in the lungs, which causes excessive production of pro-inflammatory cytokines, the so-called "cytokine storm" or "cytokine release syndrome," which can eventually lead to acute respiratory distress syndrome, pulmonary edema, and other multiple injuries to internal organs, including the heart [33–35].

A "cytokine storm" is a potentially dangerous exaggerated inflammatory response that involves the activation of macrophages, leukocytes, MCs, and endothelial cells as a result of an autocrine and paracrine effect associated with the release of

large amounts of pro-inflammatory cytokines and chemokines (for example, IL-6, IL-8, IL-1β, tumor necrosis factor α (TNFα), CCL2 (chemokine (C-C motif) ligand), CCL5, IL-17, IL-18, IL-33, CXCL-10 (C-X-C motif chemokine ligand), IFNγ, IL-12, and granulocyte-macrophage colony-stimulating factor) [36]. Lymphopenia caused by a "cytokine storm" prevents the immune system from producing antiviral antibodies, which are necessary for the destruction of viruses [37]. Elevated IL-6 levels correlate with the need for mechanical ventilation and mortality, and leukotrienes and reactive oxygen species released by neutrophils cause lung damage by destroying endothelial cells and pneumocytes [38].

Damage to the cardiovascular system as a result of the "cytokine storm" is probably caused by endothelial dysfunction, instability or rupture of atherosclerotic plaques, apoptosis of cardiomyocytes, and myocarditis. The mechanisms of endothelial dysfunction in patients with COVID-19 are not limited to increased concentrations of pro-inflammatory cytokines and include direct infection with viral particles of endothelial cells, angiotensin II hyperactivity, complement activation, and other variants of immune regulation disorders, such as the formation neutrophil extracellular traps (NETs) [39].

SARS-CoV-2 viruses have been detected in endothelial cells of various tissues, which may contribute to an imbalance between ACE2 and angiotensin II. It was found that complement activation was directly correlated with microthrombosis in a small number of COVID-19 patients, and NET formation was associated with acute respiratory distress syndrome caused by COVID-19. The complement system recognizes viral pathogens, thereby activating the innate immune response to viral infections, while NET cells stimulate the secretion of IL-1β by macrophages and are involved in the development of atherosclerosis, causing endothelial damage and dysfunction.

Moreover, endothelial cells undergoing apoptosis have been shown to activate the complement system, which can further enhance cytokine secretion, contributing to microthrombosis. Thus, direct infection of endothelial cells with SARS-CoV-2 virus particles, subsequent angiotensin II hyperactivity, and the pro-inflammatory effects of complement activation and NET formation cause both direct and indirect disruptions to the cardiovascular system, exacerbating the "cytokine storm" [33].

An increase in the level of cytoplasmic $Ca^{2+}$ within endothelial cells is a critical factor in disrupting interendothelial connections and, consequently, increasing vascular permeability. The reason for the increased influx of $Ca^{2+}$ is the activation of channels with a temporary receptor potential, which is induced by TNFα, causing destabilization of microtubules [33]. J.H. Tinsley et al. demonstrated the role of cytokines (TNFα, IL-1β, and IL-6) in increasing vascular permeability through the signaling pathways of protein kinase C and myosin light chain kinase (MLCK) in cultured endothelial cells of rat heart microvessels. The results obtained have been reproduced *in vivo* in a model of heart failure in rodents with ischemia/reperfusion [40].

Thus, the influx of $Ca^{2+}$ into endothelial cells caused by the "cytokine storm" may be one of the mechanisms underlying the disruption of interendothelial connections and increased vascular permeability. In addition, cytokine-induced stimulation of protein kinase C and MLCK leads to direct damage to heart tissue and can exacerbate existing cardiovascular diseases, which is quite common in patients with severe COVID-19 [33].

## The Relationship between the Number of Mast Cells and Laboratory Blood Values in COVID-19 Patients

Positive correlations were found between the content of tryptase-positive MCs and the level of band neutrophils in the complete blood count in COVID-19 patients, which can be explained both by the local effect of MCs on the chemotaxis of neutrophils in the focus of inflammation and by the systemic effect of MCs on the number of neutrophils in peripheral blood [41].

The positive correlation between the content of tryptase-positive MCs and the level of eosinophils in the blood of COVID-19 patients is due to the effect of tryptase on the activation status of eosinophils due to the release of eosinophil peroxidase and beta-hexosaminidase. In addition, MCs are involved in the pathogenesis of other diseases accompanied by blood eosinophilia: eosinophilic esophagitis, bronchial asthma, chronic rhinosinusitis, etc. [41].

The positive correlation between the content of tryptase-positive MCs and the level of blood basophils in COVID-19 patients may hypothetically be due to activating signals common to MCs and basophils: through Fc epsilon RI receptors, fragments of complement C3a, C4a, and C5a; mediators of activated neutrophils, and some neurotransmitters [41].

Negative correlations were found between the absolute content of single carboxypeptidase A3 (CPA3)-positive MCs in the autopsy material of lungs of patients with COVID-19 and the content of monocytes in the blood. It is known that monocytes, macrophages, and MCs infected with SARS-CoV-2 produce pro-inflammatory cytokines and chemokines that contribute to the development of local tissue inflammation and a systemic reaction in the form of a "cytokine storm." Low expression of ACE2 by monocytes/macrophages in patients with COVID-19 may also contribute to the development of pathological reactions due to the pro-inflammatory properties of angiotensin II and dysfunction of the renin-angiotensin system [41].

No statistically significant correlations were found between the number of MCs and total leukocyte count [41].

Positive correlations were found between the content of CPA3-positive MCs and the level of hemoglobin in the blood. Increased levels of glycolysis intermediates were observed in the red blood cells of patients with COVID-19, which is accompanied by oxidation and fragmentation of membrane proteins. Laboratory tests in patients with COVID-19 demonstrate a decrease in hemoglobin concentration and a pathologically increased concentration of ferritin. The level of ESR negatively correlated with the content of tryptase-positive and chymase-positive MCs [41].

No statistically significant correlations were found between the number of MCs and the level of CRP [41].

## FEATURES OF DAMAGE TO THE CARDIOVASCULAR SYSTEM IN COVID-19

Although macrophages are the predominant cells of the innate immune system in the heart, MCs also play an important role in the development of a large number of cardiometabolic diseases. Mast cells are present in the endocardium, myocardium, and epicardium, in the left and right ventricles and atria, as well as around coronary and microcirculatory vessels, in atherosclerotic plaques, and near sensory neurons [42]. For example, in the left ventricle of the human heart, the density of MCs is usually about 5.3 MCs/mm$^3$, and the number of macrophages is about 10 times greater. The density of MCs in heart tissues in patients with dilated cardiomyopathy and ischemic cardiomyopathy is approximately 18 MCs/mm$^3$ [43].

Cardiovascular complications, which often develop in COVID-19, include arrhythmias, worsening of coronary heart disease (CHD), heart failure, cardiogenic shock, myocarditis, or myopericarditis, which can occur both during the acute phase of COVID-19 and in the post-COVID period [44, 45]. Patients with pre-existing heart diseases and risk factors are more susceptible to cardiovascular complications of COVID-19, more severe course of the disease, and death [46, 47]. Nevertheless, these conditions can occur even in patients without concomitant diseases [47]. Regardless of the clinical pattern, acute myocardial injury, defined as an increase in serum troponin levels above the 99th percentile of the upper limit of normal, was associated with a more severe course of COVID-19 and an increased risk of death [48, 49].

The high prevalence of co-occurring acute myocardial injury and clinically pronounced heart failure in patients with severe COVID-19 strongly supports the diagnosis of acute myocarditis, which was initially confirmed by two series of autopsies of patients with COVID-19 at the beginning of the pandemic [50, 51]. However, as subsequent series of autopsies were published, it became clear that these studies represent only isolated cases. Of 277 autopsies of COVID-19 deaths reported in 22 articles in the first year of the pandemic, less than 8% showed histological signs of myocarditis [52]. Moreover, only a small part of the described cases would meet the Dallas or Marburg criteria of the World Health Organization, which makes acute lymphocytic myocarditis in COVID-19 patients a rare disease (<1.4%) [53, 54]. In contrast to these signs of myocarditis, other acute histopathological changes in the heart including macro- and microvascular thrombosis, damage to endothelial cells, focal necrosis, injury to cardiomyocytes distributed across the heart muscle, and infiltrates of immune cells without damage to adjacent cardiomyocytes are much more common in COVID-19 [55, 56].

Thus, an increase in the number of macrophage infiltrates was observed in the interstitial myocardium of deceased COVID-19 patients, which, according to the Dallas criteria, does not correspond to the diagnosis of myocarditis [53, 57]. Nevertheless, the density of interstitial CD68+ macrophages in the myocardium was significantly higher in those who died from COVID-19 with myocarditis than in those who died from COVID-19 without myocarditis. In rare cases of lymphocytic myocarditis caused by

COVID-19, the density of CD3+ T-cells and CD4+ T helper cells in the myocardium, but not CD8+ cytotoxic T-cells, was also increased compared with those who died from COVID-19 without myocarditis [58, 59]. It is assumed that infiltrating macrophages in the myocardium of patients with COVID-19 probably originate from circulating monocytes [60].

It is worth noting that myocarditis occurs 10–15 days after the onset of COVID-19 symptoms. The degree of myocardial damage is mainly due to the activity of viral replication, immune, and other mechanisms. Acquired T-cell immunity plays a key role in the development of this disease. Most scientists believe that delayed myocardial inflammation may be associated with at least two pathogenetic mechanisms. Firstly, the "cytokine storm" contributes to the occurrence of subclinical autoimmune myocarditis. Secondly, myocardial damage and/or molecular mimicry can cause autoimmune reaction [61].

During the first wave of the pandemic, a single-center study using both hematoxylin and eosin staining and immunohistochemical staining assessed hearts of 69 COVID-19 patients regarding six acute histopathological changes, which were observed in 97% of the deceased. Microthrombi were found in 70% of the deceased, which makes them the most frequently detected acute histopathology of the heart. Damage to microvascular endothelial cells was observed in 36%, scattered necrosis of individual cardiomyocytes in 36%, focal myocardial necrosis without any adjacent inflammatory infiltrate in 20%, focal inflammatory infiltrates without concomitant damage to cardiomyocytes in 17%, and focal myocarditis in only 4.6% of the deceased. SARS-CoV-2 virus particles were detected in the cardiomyocytes of 62% of the deceased [62].

The effects of COVID-19 on the heart can largely be characterized as apoptosis of cells (pericytes, endothelial cells, and cardiomyocytes), severe disorders of the innate immune response, and coagulopathy in the form of hypercoagulation. Coronary microvascular pericytes are the most likely primary target for SARS-CoV-2 infection, although some experimental data confirm the primary infection of cardiomyocytes. Infection of pericytes leads to their dysfunction and death, which further leads to a loss of functional support for endothelial cells. It is believed that the death of endothelial cells and cardiomyocytes is largely due to the inflammatory reaction caused by SARS-CoV-2, which also activates fibroblasts, which play an important role in immune-mediated thrombosis in COVID-19. Dysregulation of the kallikrein-kinin system, the complement system, and the coagulation cascade all contribute to the occurrence of cardiovascular complications in COVID-19. Many details of the described pathological mechanisms, including the sequence of events, are not fully understood [55].

According to O. Dmytrenko et al., SARS-CoV-2 affects the cardiovascular system through direct infection of myocardial cells and systemic inflammation. Infection of cardiomyocytes through ACE2 leads to disruption of the sarcomere structure, decreased contractility, and release of cytokines and chemokines, which can lead to the death of infected cells. Replication contributes to the further spread of the virus. Moreover, severe injury in COVID-19 causes a systemic inflammatory reaction that promotes the attraction of immune cells and increases prothrombotic activity [63].

## CONCLUSION

In patients with COVID-19, researchers tend to pay more attention to the study of damage to the cardiovascular system, the most common manifestations of which include arrhythmias, myocardial damage, and thromboembolic complications. The main clinical symptoms include exercise intolerance, chest pain, and fatigue. Recent studies conducted by several groups of scientists have demonstrated the presence of SARS-CoV-2 RNA and proteins in the myocardium of patients with COVID-19. Cardiomyocytes and pericytes of the heart were found to be the most susceptible to infection, which promotes the release of immune mediators, changes in basic cell functions, and ultimately the death of infected cells. The noted virus-mediated effect on MC activation is in the form of increased degranulation, while increased release of mediators also contributes its pathogenetic effects to the mechanism of development of myocardial damage. However, most of the literature data are still contradictory.

It should be noted that different studies have analyzed different pathologies, often focusing on specific heart damage (for example, myocardial necrosis, endothelial damage, or inflammatory infiltration). In some studies, only conventional hematoxylin and eosin staining was used, while others used immunohistochemical staining. In addition, there were no standardized methods and criteria. Moreover, studies conducted using autopsy material cover several waves of the COVID-19 pandemic, and

different strains of SARS-CoV-2 can affect the heart in different ways.

Thus, it can be assumed that even systematic reviews are limited by biased data selection and presentation [57]. Further research is needed to better understand the mechanisms of heart damage in COVID-19.

## REFERENCES


1. Lvov D.K., Alkhovsky S.V. Source of the COVID-19 Pandemic: Ecology and Genetics of Coronaviruses (Betacoronavirus: Coronaviridae) SARS-CoV, SARS-CoV-2 (Subgenus Sarbecovirus), and MERS-CoV (Subgenus Merbecovirus). *Problems of Virology*. 2020;65(2):62–70. (In Russ.).
2. Machhi J., Herskovitz J., Senan A.M., Dutta D., Nath B., Oleynikov M.D. et al. The natural history, pathobiology, and clinical manifestations of SARS-CoV-2 infections. *J. Neuroimmune Pharmacol*. 2020;15(3):359–386. DOI: 10.1007/s11481-020-09944-5.
3. Zarubin E.A., Kogan E.A. Pathogenesis and Morphological Changes in the Lung in COVID-19. *Arkhiv Patologii*. 2021;83(6):54–59. (In Russ.).
4. Zaki A.M., van Boheemen S., Bestebroer T.M., Osterhaus A.D., Fouchier R.A. Isolation of a novel coronavirus from a man with pneumonia in Saudi Arabia. *N. Engl. J. Med*. 2012;367(19):1814–1820. DOI: 10.1056/NEJMoa1211721.
5. Rahman A, Sarkar A. Middle East respiratory syndrome coronavirus (MERS-CoV) infection: Analyses of risk factors and literature review of knowledge, attitude and practices. *Zoonoses Public Health*. 2022;69(6):635–642. DOI: 10.1111/zph.12952.
6. Apostolopoulos V., Chavda V., Alshahrani N.Z., Mehta R., Satapathy P., Rodriguez-Morales A.J. et al. MERS outbreak in Riyadh: A current concern in Saudi Arabia. *Infez. Med*. 2024;32(2):264–266. DOI: 10.53854/liim-3202-15.
7. Tian H., Liu Y., Li Y., Wu C.H., Chen B., Kraemer M.U.G. et al. An investigation of transmission control measures during the first 50 days of the COVID-19 epidemic in China. *Science*. 2020;368(6491):638–642. DOI: 10.1126/science.abb6105.
8. Yu W.B., Tang G.D., Zhang L., Corlett R.T. Decoding the evolution and transmissions of the novel pneumonia coronavirus (SARS-CoV-2/HCoV-19) using whole genomic data. *Zool Res*. 2020;41(3):247–257. DOI: 10.24272/j.issn.2095-8137.2020.022.
9. Magateshvaren Saras M.A., Patro L.P.P., Uttamrao P.P., Rathinavelan T. Geographical distribution of SARS-CoV-2 amino acids mutations and the concomitant evolution of seven distinct clades in non-human hosts. *Zoonoses Public Health*. 2022;69(7):816–825. DOI: 10.1111/zph.12971.
10. Andersen K.G., Rambaut A., Lipkin W.I., Holmes E.C., Garry R.F. The proximal origin of SARS-CoV-2. *Nat. Med*. 2020;26(4):450–452. DOI: 10.1038/s41591-020-0820-9.
11. Bolze A., Luo S., White S., Cirulli E.T., Wyman D., Dei Rossi A. et al. SARS-CoV-2 variant Delta rapidly displaced variant Alpha in the United States and led to higher viral loads. *Cell Rep. Med*. 2022;3(3):100564. DOI: 10.1016/j.xcrm.
12. Ministry of Health of the Russian Federation. Interim Guidelines: Prevention, Diagnosis and Treatment of Novel Coronavirus Infection (COVID 19). 14th ed. (December 27, 2021). (In Russ.). URL: https://static-0.minzdrav.gov.ru/system/attachments/attaches/000/064/610/original/%D0%92%D0%9C%D0%A0_COVID-19_V18.pdf
13. Karpova L.S., Komissarov A.B., Stolyarov K.A., Popovtseva N.M., Stolyarova T.P., Pelikh M.Yu. et al. Features of the COVID-19 Epidemic Process in Each of the of the Five Waves of Morbidity in Russia. *Epidemiology and Vaccinal Prevention*. 2023;22(2):23–36. (In Russ.). DOI: 10.31631/2073-3046-2023-22-2-23-36.
14. Bali Swain R., Lin X., Wallentin F.Y. COVID-19 pandemic waves: Identification and interpretation of global data. *Heliyon*. 2024;10(3):e25090. DOI: 10.1016/j.heliyon.2024.e25090.
15. Zhu N., Zhang D., Wang W., Li X., Yang B., Song J. et al. China novel coronavirus investigating and research team. a novel coronavirus from patients with pneumonia in China, 2019. *N. Engl. J Med*. 2020;382(8):727–733. DOI: 10.1056/NEJMoa2001017.
16. Wang Q., Zhang Y., Wu L., Niu S., Song C., Zhang Z. et al. Structural and functional basis of SARS-CoV-2 entry by using human ACE2. *Cell*. 2020;181(4):894–904.e9. DOI: 10.1016/j.cell.2020.03.045.
17. Hofmann H., Pyrc K., van der Hoek L., Geier M., Berkhout B., Pöhlmann S. Human coronavirus NL63 employs the severe acute respiratory syndrome coronavirus receptor for cellular entry. *Proc. Natl. Acad. Sci. USA*. 2005;102(22):7988–7993. DOI: 10.1073/pnas.0409465102.
18. Donoghue M., Hsieh F., Baronas E., Godbout K., Gosselin M., Stagliano N. et al. A novel angiotensin-converting enzyme-related carboxypeptidase (ACE2) converts angiotensin I to angiotensin 1-9. *Circ. Res*. 2000;87(5):e1–9. DOI: 10.1161/01.res.87.5.e1.
19. Shang J., Wan Y., Luo C., Ye G., Geng Q., Auerbach A. et al. Cell entry mechanisms of SARS-CoV-2. *Proc. Natl. Acad. Sci. USA*. 2020;117(21):11727–11734. DOI: 10.1073/pnas.2003138117.
20. Baklaushev V.P., Kulemzin S.V., Gorchakov A.A., Yusubalieva G.M., Lesnyak V.N., Sotnikova A.G. COVID-19. Etiology, Pathogenesis, Diagnosis and Management. *Clinical Practice*. 2020;1:7–20. (In Russ.). DOI: 10.17816/clinpract26339.
21. Huang I.C., Bosch B.J., Li F., Li W., Lee K.H., Ghiran S. et al. SARS coronavirus, but not human coronavirus NL63, utilizes cathepsin L to infect ACE2-expressing cells. *J. Biol. Chem*. 2006;281(6):3198–3203. DOI: 10.1074/jbc.M508381200.
22. Bayati A., Kumar R., Francis V., McPherson P.S. SARS-CoV-2 infects cells after viral entry via clathrin-mediated endocytosis. *J. Biol. Chem*. 2021;296:100306. DOI: 10.1016/j.jbc.2021.100306.
23. Hou Y.J., Okuda K., Edwards C.E., Martinez D.R., Asakura T., Dinnon K.H. 3rd et al. SARS-CoV-2 reverse genetics reveals a variable infection gradient in the respiratory tract. *Cell*. 2020;182(2):429–446.e14. DOI: 10.1016/j.cell.2020.05.042.
24. Wang Y., Wang Y., Luo W., Huang L., Xiao J., Li F. et al. A comprehensive investigation of the mRNA and protein level of ACE2, the putative receptor of SARS-CoV-2, in human tis-

sues and blood cells. *Int. J. Med. Sci*. 2020;17(11):1522–1531. DOI: 10.7150/ijms.46695.
25. Lindner D., Fitzek A., Bräuninger H., Aleshcheva G., Edler C., Meissner K. et al. Association of cardiac infection with SARS-CoV-2 in confirmed COVID-19 autopsy cases. *JAMA Cardiol*. 2020;5(11):1281–1285. DOI: 10.1001/jamacardio.2020.3551.
26. Jackson C.B., Farzan M., Chen B., Choe H. Mechanisms of SARS-CoV-2 entry into cells. *Nat. Rev. Mol. Cell Biol*. 2022;23(1):3–20. DOI: 10.1038/s41580-021-00418-x.
27. Zhuang M.W., Cheng Y., Zhang J., Jiang X.M., Wang L., Deng J. et al. Increasing host cellular receptor-angiotensin-converting enzyme 2 expression by coronavirus may facilitate 2019-nCoV (or SARS-CoV-2) infection. *J. Med. Virol*. 2020;92(11):2693–2701. DOI: 10.1002/jmv.26139.
28. Jacobs M., Van Eeckhoutte H.P., Wijnant S.R.A., Janssens W., Joos G.F., Brusselle G.G. et al. Increased expression of ACE2, the SARS-CoV-2 entry receptor, in alveolar and bronchial epithelium of smokers and COPD subjects. *Eur. Respir. J*. 2020;56(2):2002378. DOI: 10.1183/13993003.02378-2020.
29. Leung J.M.., Yang CX., Tam A., Shaipanich T., Hackett T.L., Singhera G.K. et al. ACE-2 expression in the small airway epithelia of smokers and COPD patients: implications for COVID-19. *Eur. Respir. J*. 2020;55(5):2000688. DOI: 10.1183/13993003.00688-2020.
30. Kolesnikova N.V. Mast cells in allergic and infectious inflammation. *Russian Medical Inquiry.* 2022;6(2):79–84 (In Russ.). DOI: 10.32364/2587-6821-2022-6-2-79-84.
31. Budnevsky A.V., Avdeev S.N., Ovsyannikov E.S., Shishkina V.V., Esaulenko D.I., Filin A.A. et al. The Role of Mast cells and their proteases in lung damage associated with COVID-19. *Pulmonologiya*. 2023;33(1):17–26. (In Russ.). DOI: 10.18093/0869-0189-2023-33-1-17-26.
32. Budnevskiy A.V., Avdeev S.N., Ovsyannikov E.S., Alekseeva N.G., Shishkina V.V., Savushkina I.A. et al. Certain Aspects of Mast Cell Carboxypeptidase A3 Involvement in the Pathogenesis of COVID-19. *Tuberculosis and Lung Diseases.* 2024;102(1):26–33. (In Russ.). DOI: 10.58838/2075-1230-2024-102-1-26-33.
33. Ellison-Hughes G.M., Colley L., O'Brien K.A., Roberts K.A., Agbaedeng T.A., Ross M.D. The role of MSC therapy in attenuating the damaging effects of the cytokine storm induced by COVID-19 on the heart and cardiovascular system. *Front. Cardiovasc. Med*. 2020;7:602183. DOI: 10.3389/fcvm.2020.602183.
34. Budnevsky A.V., Avdeev S.N., Ovsyannikov E.S., Savushkina I.A., Choporov O.N., Shishkina V.V. et al. On the Role of Mast Cells and Their Proteases in the Severe COVID-19. *The Russian Archives of Internal Medicine*. 2024;14(3):181–189. (In Russ.). DOI: 10.20514/2226-6704-2024-14-3-181-189.
35. Budnevsky A.V., Avdeev S.N., Kosanovic D., Shishkina V.V., Filin A.A., Esaulenko D.I. et al. Role of mast cells in the pathogenesis of severe lung damage in COVID-19 patients. *Respiratory Research*. 2022;23(1):1–10. DOI: 10.1186/s12931-022-02284-3.
36. Azkur A.K., Akdis M., Azkur D., Sokolowska M., van de Veen W., Brüggen M.C. et al. Immune response to SARS-CoV-2 and mechanisms of immunopathological changes in COVID-19. *Allergy*. 2020;75(7):1564–1581. DOI: 10.1111/all.14364.
37. Manjili R.H., Zarei M., Habibi M., Manjili M.H. COVID-19 as an acute inflammatory disease. *J. Immunol*. 2020;205(1):12–19. DOI: 10.4049/jimmunol.2000413.
38. Vardhana S.A., Wolchok J.D. The many faces of the anti-COVID immune response. *J. Exp. Med*. 2020;217(6):e20200678. DOI: 10.1084/jem.20200678.
39. Ravindran M., Khan M.A., Palaniyar N. Neutrophil extracellular trap formation: physiology, pathology, and pharmacology. *Biomolecules*. 2019;9(8):365. DOI: 10.3390/biom9080365.
40. Tinsley J.H., Hunter F.A., Childs E.W. PKC and MLCK-dependent, cytokine-induced rat coronary endothelial dysfunction. *J. Surg. Res*. 2009;152(1):76–83. DOI: 10.1016/j.jss.2008.02.022.
41. Budnevsky A.V., Avdeev S.N., Kosanovic D., Ovsyannikov E.S., Savushkina I.A., Alekseeva N.G. et al. Involvement of mast cells in the pathology of COVID-19: clinical and laboratory parallels. *Cells*. 2024;13(8):711. DOI: 10.3390/cells13080711.
42. Poto R., Marone G., Galli S.J., Varricchi G. Mast cells: a novel therapeutic avenue for cardiovascular diseases? *Cardiovasc. Res*. 2024;120(7):681–698. DOI: 10.1093/cvr/cvae066.
43. Patella V., Marino I., Arbustini E., Lamparter-Schummert B., Verga L., Adt M. et al. Stem cell factor in mast cells and increased mast cell density in idiopathic and ischemic cardiomyopathy. *Circulation*. 1998;97(10):971–978. DOI: 10.1161/01.cir.97.10.971.
44. Daugherty S.E., Guo Y., Heath K., Dasmariñas M.C., Jubilo K.G., Samranvedhya J. et al. Risk of clinical sequelae after the acute phase of SARS-CoV-2 infection: retrospective cohort study. *BMJ*. 2021;373:n1098. DOI: 10.1136/bmj.n1098.
45. Xie Y., Xu E., Bowe B., Al-Aly Z. Long-term cardiovascular outcomes of COVID-19. *Nat. Med*. 2022;28(3):583–590. DOI: 10.1038/s41591-022-01689-3.
46. Tomasoni D., Inciardi R.M., Lombardi C.M., Tedino C., Agostoni P., Ameri P. et al. Impact of heart failure on the clinical course and outcomes of patients hospitalized for COVID-19. Results of the Cardio-COVID-Italy multicentre study. *Eur. J. Heart Fail*. 2020;22(12):2238–2247. DOI: 10.1002/ejhf.2052.
47. Zhou F., Yu T., Du R., Fan G., Liu Y., Liu Z. et al. Clinical course and risk factors for mortality of adult inpatients with COVID-19 in Wuhan, China: a retrospective cohort study. *Lancet*. 2020;395(10229):1054–1062. DOI: 10.1016/S0140-6736(20)30566-3.
48. Guo T., Fan Y., Chen M., Wu X/, Zhang L/, He T. et al. cardiovascular implications of fatal outcomes of patients with coronavirus disease 2019 (COVID-19). *JAMA Cardiol*. 2020;5(7):811–818. DOI: 10.1001/jamacardio.2020.1017.
49. Shi S., Qin M., Shen B., Cai Y., Liu T., Yang F. et al. Association of cardiac injury with mortality in hospitalized patients with COVID-19 in Wuhan, China. *JAMA Cardiol*. 2020;5(7):802–810. DOI: 10.1001/jamacardio.2020.0950.
50. Falasca L., Nardacci R., Colombo D., Lalle E., Di Caro A., Nicastri E. et al. Postmortem findings in Italian patients with COVID-19: a descriptive full autopsy study of cases with and

without comorbidities. *J. Infect. Dis*. 2020;222(11):1807–1815. DOI: 10.1093/infdis/jiaa578.
51. Schurink B., Roos E., Radonic T., Barbe E., Bouman C.S.C., de Boer H.H. et al. Viral presence and immunopathology in patients with lethal COVID-19: a prospective autopsy cohort study. *Lancet Microbe*. 2020;1(7):e290–e299. DOI: 10.1016/S2666-5247(20)30144-0.
52. Halushka M.K., Vander Heide R.S. Myocarditis is rare in COVID-19 autopsies: cardiovascular findings across 277 postmortem examinations. *Cardiovasc. Pathol*. 2021;50:107300. DOI: 10.1016/j.carpath.2020.107300.
53. Aretz H.T., Billingham M.E., Edwards W.D., Factor S.M., Fallon J.T., Fenoglio J.J. Jr. et al. Myocarditis. A histopathologic definition and classification. *Am. J. Cardiovasc. Pathol*. 1987;1(1):3–14.
54. Richardson P., McKenna W., Bristow M., Maisch B., Mautner B., O'Connell J. et al. Report of the 1995 World Health Organization/International Society and Federation of Cardiology Task Force on the Definition and Classification of Cardiomyopathies. *Circulation*. 1996;93:841–842. DOI: 10.1161/01.cir.93.5.841.
55. Tsai E.J., C˘iháková D., Tucker N.R. Cell-specific mechanisms in the heart of COVID-19 patients. *Circ. Res*. 2023;132(10):1290–1301. DOI: 10.1161/CIRCRESAHA.123.321876.
56. Pellegrini D., Kawakami R., Guagliumi G. et al. Microthrombi as a Major Cause of Cardiac Injury in COVID-19: A Pathologic Study. *Circulation*. 2021;143(10):1031–1042. DOI: 10.1161/CIRCULATIONAHA.120.051828.
57. Sewanan L.R., Clerkin K.J., Tucker N.R., Tsai E.J. How does COVID-19 affect the heart? *Curr. Cardiol. Rep*. 2023;25(3):171–184. DOI: 10.1007/s11886-023-01841-6.
58. Basso C., Leone O., Rizzo S., De Gaspari M., van der Wal A.C., Aubry M.C. et al. Pathological features of COVID-19-associated myocardial injury: a multicentre cardiovascular pathology study. *Eur. Heart J*. 2020;41(39):3827–3835. DOI: 10.1093/eurheartj/ehaa664.
59. Bearse M., Hung Y.P., Krauson A.J., Bonanno L., Boyraz B., Harris C.K. et al. Factors associated with myocardial SARS-CoV-2 infection, myocarditis, and cardiac inflammation in patients with COVID-19. *Mod. Pathol*. 2021;34(7):1345–1357. DOI: 10.1038/s41379-021-00790-1.
60. Chen S.T., Park M.D., Del Valle D.M., Buckup M., Tabachnikova A., Simons N.W. et al. A shift in lung macrophage composition is associated with COVID-19 severity and recovery. *Sci. Transl. Med*. 2022;14(662):eabn5168. DOI: 10.1126/scitranslmed.abn5168.
61. Shao H.H., Yin R.X. Pathogenic mechanisms of cardiovascular damage in COVID-19. *Mol. Med*. 2024;30(1):92. DOI: 10.1186/s10020-024-00855-2.
62. Brener M.I., Hulke M.L., Fukuma N., Golob S., Zilinyi R.S., Zhou Z. et al. Clinico-histopathologic and single-nuclei RNA-sequencing insights into cardiac injury and microthrombi in critical COVID-19. *JCI Insight*. 2022;7(2):e154633. DOI: 10.1172/jci.insight.154633.
63. Dmytrenko O., Lavine K.J. Cardiovascular tropism and sequelae of SARS-CoV-2 infection. *Viruses*. 2022;14(6):1137. DOI: 10.3390/v14061137.

## Author Contribution

Budnevsky A.V. – conception and design, final approval of the manuscript for publication. Avdeev S.N. – conception and design. Ovsyannikov E.S., Tokmachev R.E., Shishkina V.V., Perveeva I.M. – justification of the manuscript or critical revision for important intellectual content. Feigelman S.N., Chernik T.A., Budnevskaya S.A., Arkhipova E.D. – data analysis and interpretation.

## Author Information

**Budnevsky Andrey V.** – Dr. Sci. (Med.), Professor, Distinguished Inventor of the Russian Federation, Head of Faculty Therapy Department, Vice-Rector for Research, N.N. Burdenko VSMU, Voronezh, Russia, budnev@list.ru, https://orcid.org/0000-0002-1171-2746

**Avdeev Sergey N.** – Academician of the Russian Academy of Sciences, Dr. Sc. (Medicine), Professor, Head of Pulmonology Department, I.M. Sechenov First Moscow State Medical University, Moscow, Russia, serg_avdeev@list.ru, https://orcid.org/0000-0002-5999-2150

**Ovsyannikov Evgeniy S.** – Dr. Sci. (Med.), Associate Professor, Professor, Faculty Therapy Department, N.N. Burdenko VSMU, Voronezh, Russia, ovses@yandex.ru, https://orcid.org/0000-0002-8545-6255

**Tokmachev Roman E.** – Cand. Sci. (Med.), Director of the Research Institute of Experimental Biology and Medicine, Associate Professor, Faculty Therapy Department, N.N. Burdenko VSMU, Voronezh, r-tokmachev@mail.ru, https://orcid.org/0000-0001-6379-4635

**Feigelman Sofia N.** – Assistant, Faculty Therapy Department, N.N. Burdenko VSMU, Voronezh, s.feygelman@gmail.com, https://orcid.org/0000-0003-4128-6044

**Shishkina Victoria V.** – Cand. Sci. (Med.), Associate Professor, Senior Researcher, Research Institute of Experimental Biology and Medicine, Head of Histology Department, N.N. Burdenko VSMU, Voronezh, 4128069@gmail.com, https://orcid.org/0000-0001-9185-4578

**Perveeva Inna M.** – Cand. Sci. (Med.), Senior Researcher, Research Institute of Experimental Biology and Medicine, N.N. Burdenko VSMU, Pulmonologist, Voronezh Regional Clinical Hospital No. 1, Voronezh, perveeva.inna@yandex.ru, https://orcid.org/0000-0002-5712-9302

**Chernik Tatiana A.** – Cand. Sci. (Med.), Associate Professor, Faculty Therapy Department, Deputy Head of the Center for Scientific Research, Development and Transfer of Medical Technologies, N.N. Burdenko VSMU, Voronezh, ch01@mail.ru, https://orcid.org/0000-0003-1371-0848

**Arkhipova Ekaterina D.** – Postgraduate Student, Faculty Therapy Department, N.N. Burdenko VSMU, Voronezh, e.pavlykevich@bk.ru, https://orcid.org/0009-0002-4960-334X

**Budnevskaya Sofia A.** – Student of the Faculty of Medicine, N.N. Burdenko VSMU, Voronezh, sofa_budnevskaya@mail.ru, https://orcid.org/0009-0000-0623-0243

(✉) **Feigelman Sofia N.,** s.feygelman@gmail.com

Received on February 11, 2025;
approved after peer review on March 3, 2025;
accepted on March 20, 2025

УДК 616.89-008.441.13-092:616.8-097
https://doi.org/10.20538/1682-0363-2025-3-127-137

# Neurotransmitters, factors of neuroimmune inflammation and endocrine regulation in alcohol dependence

**Vetlugina T.P., Epimakhova E.V., Prokopieva V.D., Shumilova S.N., Voevodin I.V.**

*Mental Health Research Institute, Tomsk National Research Medical Center (NRMC), Russian Academy of Sciences*
*4 Aleutskaya St., 634014 Tomsk, Russian Federation*

**ABSTRACT**

Alcohol dependence remains a global medical and social issue, despite the advancements in studying its pathogenesis and the diversity of available treatment methods. This determines the relevance of further research aimed at revealing the complex neurobiological effects of ethanol on the human body. A fundamental knowledge of the mechanisms of formation and course of alcohol dependence is the theoretical basis for the development of new pathogenetically substantiated methods of prevention, diagnosis, and treatment of alcohol-related disorders, which will contribute to enhancing the social functioning of patients and reducing the economic burden of socially sensitive diseases.

**The aim** of the review was to analyze recent studies conducted by Russian and foreign authors on the role of neurotransmitters, neuroimmune inflammation factors, and endocrine regulation in the pathogenesis of alcohol dependence.

**Keywords:** alcohol dependence, alcoholism, neurotransmitters, neuroimmune inflammation, corticotropin-releasing factor, cortisol.

**Conflict of interest.** The authors declare the absence of obvious or potential conflicts of interest related to the publication of this article.

**Source of financing.** The publication was prepared with the financial support of the grant of the Russian Science Foundation (Project No. 25-25-00188, https://rscf.ru/en/project/25-25-00188/)

**For citation:** Vetlugina T.P., Epimakhova E.V., Prokopieva V.D., Shumilova S.N., Voevodin I.V. Neurotransmitters, factors of neuroimmune inflammation and endocrine regulation in alcohol dependence. *Bulletin of Siberian Medicine.* 2025;24(3):127–137. https://doi.org/10.20538/1682-0363-2025-3-127-137.

# Нейромедиаторы, факторы нейроиммунного воспаления и эндокринной регуляции при алкогольной зависимости

**Ветлугина Т.П., Епимахова Е.В., Прокопьева В.Д., Шумилова С.Н., Воеводин И.В.**

*Научно-исследовательский институт (НИИ) психического здоровья, Томский национальный исследовательский медицинский центр (НИМЦ) Российской академии наук*
*Россия, 634014, г. Томск, ул. Алеутская, 4*

**РЕЗЮМЕ**

Алкогольная зависимость остается глобальной медико-социальной проблемой, несмотря на достигнутые успехи в изучении патогенеза заболевания и многообразие существующих методов лечения. Это определяет актуальность дальнейших исследований, направленных на раскрытие сложных нейробиологических эффектов этанола на организм человека. Фундаментальные знания механизмов формирования и течения

✉ *Vetlugina Tamara P.,* vetluga21@mail.ru

алкогольной зависимости являются теоретической базой для разработки новых патогенетически обоснованных методов профилактики, диагностики и лечения расстройств, связанных с алкоголем, что будет способствовать повышению социального функционирования пациентов, снижению экономических потерь от социально-значимых заболеваний.

**Цель:** анализ современных исследований российских и зарубежных авторов, касающихся изучения роли нейромедиаторов, факторов нейроиммунного воспаления и эндокринной регуляции в патогенезе алкогольной зависимости.

**Ключевые слова:** алкогольная зависимость, алкоголизм, нейромедиаторы, нейроиммунное воспаление, кортикотропин-рилизинг фактор, кортизол

**Конфликт интересов.** Авторы декларируют отсутствие явных и потенциальных конфликтов интересов, связанных с публикацией настоящей статьи.

Источник финансирования. Статья подготовлена при финансовой поддержке гранта Российского научного фонда (проект № 25-25-00188, https://rscf.ru/en/project/25-25-00188/).

**Для цитирования:** Ветлугина Т.П., Епимахова Е.В., Прокопьева В.Д., Шумилова С.Н., Воеводин И.В. Нейромедиаторы, факторы нейроиммунного воспаления и эндокринной регуляции при алкогольной зависимости. *Бюллетень сибирской медицины.* 2025;24(3):127–137. https://doi.org/10.20538/1682-0363-2025-3-127-137.

## INTRODUCTION

Alcohol dependence (alcoholism) as one of the primary addictive disorders remains a serious medical and social problem in Russia and worldwide due to a steady increase in the incidence of this pathology, the severity of its consequences, and limited treatment efficacy. Alcohol abuse leads to rising crime rates, violence, and orphanhood and causes a notably high level of disability and mortality among men aged 40–60, who at this age are the most productive in social and professional spheres. One of the approaches to solving the problem of reducing the growth rate of addiction is the development of new methods of diagnosis, individualized prediction, and effective therapies developed using fundamental knowledge about the disease pathogenesis.

The brain neurotransmitter systems, primarily the dopaminergic system, whose functional state is related to the activity of other systems, play a crucial role in the formation of addiction [1–3]. Alcohol and its metabolites, in particular acetaldehyde, activate peripheral immune cells and microglia leading to an increase in the production of pro-inflammatory cytokines and other mediators of neuroimmune inflammation, affecting the severity of the disease and cognitive and behavioral characteristics [4, 5]. Chronic alcohol consumption and repeated withdrawal cycles are stressors stimulating the hypothalamic-pituitary-adrenal axis (HPA axis) and glucocorticoid synthesis causing dysregulation of the brain reward system and perpetuating alcohol-seeking behavior [6, 7].

The aim of this review was to analyze recent studies conducted by both Russian and foreign authors regarding the role of neurotransmitters, neuroimmune inflammatory factors, and endocrine regulation in the pathogenesis of alcohol dependence.

We searched the electronic databases PubMed (https://pubmed.ncbi.nlm.nih.gov/) and the scientific electronic library eLIBRARY (https://www.elibrary.ru/) for studies published during the last 15 years. The search was conducted using the following key words: alcohol dependence, alcoholism, neurobiology of alcoholism, neurotransmitters, inflammatory factors, cytokines, and hormones. The review includes 88 publications (clinical and experimental studies, meta-analyses, randomized controlled trials, and reviews) relevant to the problem under study.

## NEUROMEDIATORS

Ethanol crosses the blood-brain barrier altering neurochemical processes in the brain and leading to the remodeling of synapses that regulate emotions, motivation, and overall human behavior. Currently, the primary neurophysiological mechanism underlying addiction to psychoactive substances (PAS) is considered to be the emotionally positive reactions that arise in response to the chemical effects of alcohol and other PAS on brain regions linked to the reward system [2, 8, 9].

Long-term studies conducted at the National Scientific Center for Narcology (Moscow, Russia) have established the leading role of dopamine (DA)

in the development of addiction to alcohol and other PAS. A vicious cycle underlying addiction formation has been described, characterized by alternating periods of increased and decreased DA levels during alcohol consumption, withdrawal syndrome, and remission. It has been shown that DA levels positively correlate with the severity of withdrawal symptoms. Elevated DA levels during the initial period of remission formation subsequently decrease and, as a rule, remain below normal, which may indicate that DA deficiency is the basis of persistent pathological craving for PAS [8].

Chronic ethanol consumption leads to long-term changes in the dopaminergic system, affecting neural networks associated with reward mechanisms and addictive behavior [9]. Experimental studies have demonstrated that both acute and chronic alcohol intoxication cause the most pronounced changes in the activity of the mesolimbic dopaminergic system in rats, confirming the involvement of this system in the neurobiology of alcohol effects [10, 11]. Alcohol activates dopaminergic neurons in the ventral tegmental area of the midbrain leading to an increased dopamine release in the cortico-limbic regions of the forebrain. Inhibition of D2 dopamine receptors by their antagonist, sulpiride, reduced voluntary alcohol intake in animals [12, 13].

It has been shown that long-term potentiation or suppression of cortical activity transmitted to the striatum, which expresses D1 dopamine receptors, controls alcohol-seeking behavior in experimental animals [14]. In animals with a progressively increasing preference for alcohol, a more pronounced reduction in the expression of D1 and D2 receptor mRNA in the striatum was observed compared to rats that maintained consistently low levels of alcohol consumption and those with consistently high preference scores [15].

Neuroimaging methods used in clinical research have expanded our understanding of the neurochemistry of alcoholism. Reviewing 30 years of functional magnetic resonance imaging (fMRI) use, D. Nutt et al. (2021) highlight the significant contribution of these studies to uncovering the mechanisms of reward and neuroadaptation resulting from chronic alcohol use, as well as the role of DA neurotransmission. At the same time, the authors note certain contradictions in the currently available data and emphasize the need for further longitudinal studies in this direction to identify biological markers for predicting addiction development and to develop new therapeutic approaches for patients at all stages of the disease [2].

A longitudinal study of social drinkers (habitual drinking) was conducted using positron emission tomography (PET) to investigate the potential use of striatal D2 dopamine receptors as predictors of alcohol dependence development. When participants were re-evaluated 8–16 years after PET scanning, the authors found no evidence of a link between D2 receptor availability and the subsequent development of alcohol use disorder [16]. These results also underscore the need for continued research using neuroimaging methods.

Overall, the data obtained by various authors on the role of dopaminergic neurotransmission depend on research methods, the brain region studied, the duration of alcohol use, and the type of alcohol-seeking behavior examined. Nevertheless, DA and the brain regions where this neurotransmitter is actively synthesized and functions remain key in the formation of addiction syndrome and are primary targets in translational research [17, 18].

Other neurotransmitters also play an important role in the development of alcohol dependence, particularly gamma-aminobutyric acid (GABA), glutamate, and serotonin.

Chronic ethanol exposure disrupts the balance between inhibitory and excitatory neurotransmitters, with GABA being the primary inhibitory neurotransmitter in the brain. B.M. Roberts, E.F.Lopes, S.J.Cragg, analyzing publications on the modulation of dopamine release in the striatum through axonal mechanisms, provide evidence that GABA inhibits the activity of dopaminergic neurons, basal and induced DA synthesis, and suppresses DA release, thereby reducing overall DA neurotransmission. GABA can modulate DA output by affecting metabotropic $GABA_A$ and $GABA_B$ receptors [20].

A randomized double-blind placebo-controlled study evaluated the role of the $GABA_B$ receptor in the neurobiology of alcohol-related behavior. In patients with alcohol dependence, administration of the selective $GABA_B$ receptor agonist baclofen had a positive effect on some clinical characteristics of the disorder, and the maximum plasma concentration of baclofen negatively correlated with alcohol craving [20, 21]. These findings, along with preclinical studies, demonstrate that $GABA_B$ receptor modulators, particularly baclofen, normalize impaired GABAergic transmission and have high translational potential for the treatment of alcohol use disorders [22].

Glutamate is the primary excitatory neurotransmitter. Glutamatergic signaling mediated by ionotropic (NMDA, AMPA) and metabotropic (G protein-coupled – mGluR) glutamate receptors is crucial. Ethanol-induced dysfunction of these receptors in various brain regions leads to significant alterations in glutamatergic neurotransmission [23]. Studies using PET imaging in individuals with alcohol dependence have provided evidence of the role of metabotropic glutamate receptor subtype 5 (mGluR5) in the clinical features of the disorder. Researchers observed increased mGluR5 binding in various brain regions with a particularly strong signal in the amygdala, which was associated with reduced alcohol craving [24].

Experimental data analysis has shown that a single (acute) administration of ethanol typically inhibits glutamatergic neurotransmission, while chronic ethanol use enhances it leading to a hyperexcitable state and anxiety characteristic of withdrawal syndrome. Prolonged ethanol exposure increases glutamatergic activity, accompanied by neuroplasticity changes in key brain regions, including the basolateral and central nuclei of the amygdala. These impairments may reduce behavioral flexibility, promote seeking behavior, and increase the likelihood of relapse [25, 26]. These findings support the hypothesis that some effects of chronic ethanol exposure are mediated by its impact on synaptic transmission of GABA and glutamate playing a significant role in maintaining dependence.

The potential use of various drugs (pregabalin and gabapentin) that modulate the GABA and glutamate systems is investigated for the treatment of patients with alcoholism. These studies have demonstrated that these neurotransmitter systems could be promising pharmacological targets for the pathogen-specific therapy of alcohol dependence [27, 28]. Such studies make it possible to obtain new data on the mechanisms of development of alcohol dependence and to identify biomarkers of treatment effectiveness.

Serotonin (5-hydroxytryptamine, 5-HT) is a neurotransmitter that regulates mood, sleep, appetite, learning, memory, and other physiological functions. Various types of serotonin receptors in the central nervous system (CNS) convert the chemical signal induced by serotonin into functional changes in the signal-receiving cell. D.Most, L. Ferguson, R.A. Harris (2014) analyzing studies of the molecular basis of alcoholism provide evidence of serotonin involvement in mediating both acute and chronic effects of alcohol. Increased serotonergic transmission has been associated with lower alcohol consumption, while reduced transmission is linked to higher consumption both in experimental models and in individuals with alcohol dependence [30].

The administration of serotonergic agents (SSRIs and buspirone) resulted in reduced alcohol consumption across all models of alcoholism [30, 31]. Studies on serotonin levels in platelets of alcohol-dependent patients admitted for treatment demonstrated an increase in its concentration by day 12 of therapy, with this rise coinciding with a reduction in withdrawal symptom severity and improved clinical condition in the patients [32]. When examining individuals with alcohol and nicotine dependence who were divided into groups based on different phenotypes (age of alcohol use initiation, presence of withdrawal syndrome, alcohol-induced psychosis, aggression, etc.), thrombocytes of non-smoking patients exhibited an association between low 5-HT levels and the severity of alcohol dependence, whereas smokers showed a correlation with late-onset alcohol abuse. It has been suggested that platelet 5-HT could serve as a peripheral biomarker for different phenotypes of alcohol-related disorders [33]. The functions of serotonin and the role of the serotonergic system in addictive behavior are discussed in detail in a monograph [34].

In summary, literature analysis demonstrates that alcohol-induced modulation of the brain dopaminergic, GABAergic, glutamatergic, and serotonergic systems is a crucial molecular mechanism underlying the development of alcohol dependence and a potential target for treatment.

## NEUROIMMUNE INFLAMMATORY FACTORS

Neuroimmune inflammation plays a significant role in the pathogenesis of alcohol dependence. Experimental studies have shown that acute and chronic ethanol consumption activates resident brain macrophages – microglia. Microglia activation leads to an increased secretion of cytokine mediators, such as high-mobility group protein B1 (HMGB1), which, through various subtypes of Toll-like receptors (TLR), triggers intracellular molecular cascades of reactions, resulting in increased expression of pro-inflammatory cytokines and the development of neuroinflammation. TLR4-dependent signaling plays a key role in this process [35, 36]. Neuroimmune inflammation adversely affects the function of neurons in brain

structures associated with behavior and emotions, contributing to the development and persistence of alcohol-related pathology.

Several recent reviews have analyzed the results of studies on the contribution of neuroimmune activation and neuroimmune inflammation to the formation of alcohol dependence [5, 37–39]. Repeated cycles of binge drinking/alcohol withdrawal cause persistent induction of HMGB1, mRNA, and TLR receptors in the brain, possibly underlying the loss of behavioral control, impulsivity, and anxiety, which promote reward-seeking behavior and increase the risk of developing alcohol use disorders [40, 41].

When alcohol is consumed, the gastrointestinal tract is exposed to the highest concentration of exogenous ethanol. Alcohol and its metabolite, acetaldehyde, disrupt the tight junctions between intestinal epithelial cells and increase intestinal permeability. Dysfunction of the intestinal barrier facilitates the release of bacterial components, such as the bacterial endotoxin lipopolysaccharide (LPS), other pathogen-associated molecular patterns (PAMPs), and intracellular proteins into the bloodstream. These molecules activate the immune system, primarily through TLR4 on immune cells, elevating levels of circulating cytokines that act as inducers of inflammation in the absence of pathogens, which is referred to as "sterile inflammation" [42–44]. Clinical studies have identified elevated levels of serum LPS, peptidoglycan, and other inflammatory markers, particularly IL-8 and IL-1β, in actively drinking individuals. These levels correlated with the amount of alcohol consumed and with alcohol craving, decreasing after abstinence [45, 46].

Analysis of available data indicates alterations in the serum cytokine profile in patients with alcoholism, generally towards an increase in pro-inflammatory mediators, contributing to the formation of alcohol-related pathologies [47–49]. Associations have been identified between inflammation mediators and the severity of alcohol dependence, as well as with cognitive and behavioral characteristics [4, 50]. The results of a meta-analysis of cytokine studies in patients with alcohol use disorder revealed that the overwhelming majority of publications confirm the presence of an abnormal circulating pro-/anti-inflammatory cytokine profile in patients compared to controls, with variations depending on the disease stage. Elevated levels of pro-inflammatory cytokines (interleukins IL-6, TNFα, IL-8, and IL-12) are associated with the severity of dependence, alcohol withdrawal syndrome, and alcohol craving [51]. Based on these findings, a number of cytokines/chemokines have been proposed as promising biomarkers of excessive alcohol consumption and prediction of the course of alcoholism [4, 50].

Peripheral cytokines, particularly IL-1α, IL-1β, IL-6, and TNFα, penetrate the blood-brain barrier through various mechanisms and enhance neuroinflammation and neuroadaptive changes in the CNS [52]. A series of reviews provide data from studies indicating that cytokines influence surrounding neurons by regulating neurotransmitter function and neurotransmission [37, 53–55].

## ENDOCRINE REGULATING FACTORS

The effects of alcohol on the endocrine system have been thoroughly researched. Long-term alcohol consumption and repeated withdrawal cycles are believed to be stressors leading to endocrine dysregulation and neuroadaptive changes, the mechanisms of which are discussed in a number of reviews [6, 56–58]. The information presented in these reviews can be briefly summarized in the following statements: prolonged alcohol consumption and withdrawal are powerful stressors that stimulate the HPA axis and glucocorticoid synthesis; HPA axis activation leads to multiple neuroadaptive changes in the brain reward and stress systems which sustain increased motivation for alcohol consumption and largely determine pathological alcohol craving and relapse in dependent patients.

According to the literature, alcohol can directly activate the HPA by affecting corticotropin-releasing factor (CRF), disrupting the regulation of CRF signaling in hypothalamic and extrahypothalamic brain regions. Activation of the CRF system may contribute to alcohol-related behavioral changes, the development of negative emotional reactions, especially during withdrawal states, compulsive responses, and stress-induced resumption of psychoactive substances (PAS) [59, 60]. The actions of CRF are mediated by two subtypes of G-protein-coupled receptor (CRF1 and CRF2), with stress-related behavioral responses primarily mediated by CRF1 receptors [61].

Corticotropin-releasing factor (corticotropin-releasing hormone or corticoliberin), a neuropeptide expressed by neurons throughout the CNS, is a key regulator of the brain stress system and a key factor in the transition from remission to substance seeking to alleviate the negative emotional states of acute withdrawal and prolonged abstinence [62–64].

Experimental and clinical studies have attempted to promote corticotropin-releasing factor receptor 1 (CRF1) antagonists as potential therapeutic agents.

The CRF1 antagonist verucerfonte has been shown to suppress stress-induced alcohol seeking in rats [65]. A double-blind placebo-controlled study found no clinical effect of the CRF1 antagonist pexacerfonte in individuals with alcohol dependence and high anxiety [66]. M.M.Weera, N. W.Gilpin (2024) analyzed studies on the therapeutic potential of CRF1 antagonists and noted that clinical trials involving individuals with anxiety, depression, and alcohol use disorder have largely yielded negative results. At the same time, further research in this direction may lead to new therapeutic approaches for alleviating symptoms in patients with these conditions [68].

The main stress-releasing hormone is cortisol, a glucocorticoid steroid hormone secreted by the adrenal cortex in response to effect of adrenocorticotropic hormone (ACTH). ACTH secretion, in turn, is stimulated by corticotropin-releasing factor. High levels of cortisol correlating with the severity of the clinical condition have been detected in biological fluids (serum, plasma, and CSF) of patients with alcohol withdrawal syndrome, alcohol delirium, and alcohol abusers [7, 68–70].

As part of a double-blind placebo-controlled clinical and laboratory study, the use of the glucocorticoid receptor (GR) antagonist mifepristone was tested as treatment of alcohol dependence. Patients receiving mifepristone compared with placebo showed a significant reduction in alcohol craving and alcohol consumption during one-week treatment phase and one-week post-therapy period [71]. In a randomized double-blind placebo-controlled study involving patients with alcohol dependence, the effect of a single oral administration of cortisol on craving was investigated [72]. It was found that cortisol administration significantly increased craving on the first day of testing in less severe cases but decreased it in patients with more severe forms. The authors conclude that the different effects of cortisol on craving, depending on disease severity, are still difficult to explain and emphasize the importance of developing new treatment approaches targeting alcohol-mediated neurobiological dysregulation.

G.F. Koob, N.D.Volkow (2016) conceptualize substance use disorder as a three-stage cycle: binge/intoxication; withdrawal/negative affect; and preoccupation/anticipation [9]. Neurotransmission dysregulation occurs within three functional domains: incentive salience/pathological habits, negative emotional states, and executive function, which are mediated by key elements of neural circuits (basal ganglia, extended amygdala, and prefrontal cortex). Impaired executive function during the preoccupation/anticipation stage leads to alcohol craving and perpetuation of the addiction cycle. Each stage is characterized by specific alterations in neurotransmitter and neuromodulator systems, manifesting in the core components of neural circuits – the basal ganglia, extended amygdala, and prefrontal cortex. In summary, stage-specific changes include increased dopamine and glutamate neurotransmission; reduced function of the dopamine component in the reward system; recruitment of stress-related neurotransmitters; and dysregulation of peptidergicneuromodulatory systems (glutamate/GABA). The application of this three-stage model may facilitate the individualization of pharmacological treatments for alcohol dependence [73].

Literature reviews discuss the concept of positive and negative reinforcement as an important aspect of the neurobiology of psychoactive substances (PAS) use [74–77]. The positive reinforcing effects of alcohol, which induce pleasurable sensations, are primarily mediated by dopamine, opioid peptides, serotonin, and GABA. Negative reinforcement associated with negative emotional states involves increased recruitment of corticotropin-releasing factor and glutamatergic systems, along with reduced GABA transmission.

## CONCLUSION

The analysis of the current state of the problem discussed in the review demonstrates that the main aim of research is to develop new strategies to improve the effectiveness of therapy for alcoholism and prevent early relapses of the disease. To do this, crecently conducted and future studies should focus on further elucidation of the complex neurobiological effects of ethanol, identification of molecular pharmacological targets, and the search for measurable objective markers of disease stages.

Alcoholism is a chronic disease with alternating periods of relapse and remission. There are various approaches to defining remission and calculating its duration. In Russian addiction medicine, remission is typically calculated starting from 1 month of complete abstinence from alcohol and disappearance of intoxication symptoms [78]. Despite the diversity of alcoholism treatment methods, the issue of achieving

and maintaining therapeutic remission remains relevant. After completing a course of treatment, only 50% of patients maintained sobriety for up to three months, while 34% continued to consume alcohol despite treatment [79]. Furthermore, only 7.1% of individuals with alcohol abuse reported abstinence for two years [80].

A one-year follow-up of 877 patients after outpatient treatment revealed that about 65% of those surveyed experienced at least one transition from remission to relapse during the follow-up period. [81]. The state of remission in alcohol dependence is unstable and dynamic; it cannot be considered equivalent to mental health, as the clinical structure permanently includes alcohol craving of varying degrees of severity, which is the core syndrome of dependence, and its actualization (activation of craving) is considered to be one of the main causes of disease relapse [78, 82–85].

The problem of finding ways to prevent relapse, particularly the search for predictive markers of craving activation to improve the effectiveness of therapy and the stability of remission, is becoming increasingly important. In psychiatry and addiction medicine, alongside the importance of expensive neuroimaging and omics technologies, the potential of a rapidly expanding field of research focused on identifying peripheral biomarkers that provide affordable non-invasive methods of monitoring the course of the disease and the effectiveness of therapy has been highlighted. Researchers most often consider factors related to inflammation, oxidative stress, and endocrine mediators of the stress response as potential biomarkers [86–88].

It is important to emphasize the significant expediency of using as craving markers not individual parameters but a complex of peripheral biomarkers reflecting the interrelated processes of alcohol dependence pathogenesis – neurotransmission, neuroimmune inflammation, and endocrine regulation. Such an approach would enhance the value and reliability of clinical and biological research findings, which could be used for a personalized approach to treatment based on individual patient profiles.

## REFERENCES


1. Anokhina I.P. Main Biological Mechanisms of Psychoactive Substance Addiction. *Journal of Addiction Problems.* 2013;6:40–59. (In Russ.). URL: https://www.elibrary.ru/item.asp?id=21074215
2. Nutt D., Hayes A., Fonville L., Zafar R., Palmer E.O.C., Paterson L. et al. Alcohol and the brain. *Nutrients.* 2021;13(11):3938. DOI: 10.3390/nu13113938.
3. Gimenez-Gomez P., Le T., Martin G.E. Modulation of neuronal excitability by binge alcohol drinking. *Front. Mol. Neurosci.* 2023;16:1098211. DOI: 10.3389/fnmol.2023.1098211.
4. Manzardo A.M., Poje A.B., Penick E.C., Butler M.G. Multiplex immunoassay of plasma cytokine levels in men with alcoholism and the relationship to psychiatric assessments. *Int. J. Mol. Sci.* 2016;17(4):472. DOI: 10.3390/ijms17040472.
5. Coleman L.G.Jr, Crews F.T. innate immune signaling and alcohol use disorders. *Handb. Exp. Pharmacol.* 2018;248:369–396. DOI: 10.1007/164_2018_92.
6. Proskuryakova T.V., Shamakina I.M., Shokhonova V.A., Tarabarko I.E., Anokhina I.P. Activity of the Hypothalamic-Pituitary-Adrenal System under Conditions of Single and Chronic Exposure to Psychoactive Substances and during Their Withdrawal. *Narcology.* 2017;16(10):84–98. (In Russ.). URL: https://elibrary.ru/item.asp?id=30622038.
7. Blaine S.K., Nautiyal N., Hart R., Guarnaccia J.B., Sinha R. Craving, cortisol and behavioral alcohol motivation responses to stress and alcohol cue contexts and discrete cues in binge and non-binge drinkers. *Addict. Biol.* 2019;24(5):1096–1108. DOI: 10.1111/adb.12665.
8. Anokhina I.P. Main Biological Mechanisms of Psychoactive Substance Addiction. *Journal of Addiction Problems*. 2017;(2-3):15–41. (In Russ.). URL: https://www.elibrary.ru/item.asp?id=30103919
9. Koob G.F., Volkow N.D. Neurobiology of addiction: a neurocircuitry analysis. *Lancet Psychiatry.* 2016;3(8):760–773. DOI: 10.1016/S2215-0366(16)00104-8.
10. Mikhailova M.A., Gainetdinov R.R. Effect of Acute Ethanol Injection on the Mesolimbic Dopamine System on Freely-Moving Rats. *Russian Journal of Physiology*. 2019;105(7):853–860. (In Russ.). DOI: 10.1134/S0869813919070069.
11. Lelevich S.V., Gushcha V.K., Doroshenko E.M. Neurotransmitter Disturbances in Some Parts of the Rat Brain and Their Correction under Chronic and Intermittent Alcohol Intoxication. *Bulletin of Yanka Kupala Grodno State University. Issue 5. Economics. Sociology. Biology.* 2020;10(1):150–158. (In Russ.). URL: https://elibrary.ru/item.asp?id=42367025
12. Ding Z.M., Ingraham C.M., Rodd Z.A., McBride W.J. The reinforcing effects of ethanol within the posterior ventral tegmental area depend on dopamine neurotransmission to forebrain cortico-limbic systems. *Addict. Biol*. 2015;20:458–468. DOI: 10.1111/adb.12138.
13. Engleman E.A., Ingraham C.M., Rodd Z.A., Murphy J.M., McBride W. J., Ding Z.M. The reinforcing effects of ethanol within the prelimbic cortex and ethanol drinking: Involvement of local dopamine D2 receptor-mediated neurotransmission. *Drug and Alcohol Dependence.* 2020;214:108165. DOI: 10.1016/j.drugalcdep.2020.108165.
14. Ma T., Cheng Y., Roltsch Hellard E., Wang X., Lu J., Gao X., et al. Bidirectional and long-lasting control of alcohol-seeking behavior by corticostriatal LTP and LTD. *Nature Neuroscience*. 2018;21:373–383. DOI: 10.1038/s41593-018-0081-9.
15. Anokhin P.K., Razumkina E.V., Shamakina I.Yu. Comparative Analysis of mRNA Expression of Dopamine Receptors, Tyrosine Hydroxylase and Dopamine Transport Protein in the Mesolimbic System of Rats with Different Levels of Alco-

hol Consumption. *Neurochemistry.* 2019;36(2):119–127. (In Russ.). DOI: 10.1134/S1027813319010035.
16. Jangard S., Jayaram-Lindström N., Isacsson N.H., Matheson G.J., Plavén-Sigray P., Franck J., et al. Striatal dopamine D2 receptor availability as a predictor of subsequent alcohol use in social drinkers. *Addiction.* 2023;118(6):1053–1061. DOI: 10.1111/add.16144.
17. Anikhina I.P. New Insight into the Role of Dopamine in the Development of Alcoholism. *Journal of Addiction Problems*. 2021;201(6):17–27. (In Russ.). DOI: 10.47877/0234-0623_2021_06_17.
18. Kibitov A.O., Rybakova K.V., Brodyansky V.M., Berntsev V.A., Skurat E.P., Krupitsky E.M. Comparative Pharmacogenetic Study of Disulfiram or Cyanamide Efficacy for Alcohol
19. Dependence: the Key Role of Dopamine Neurotransmission Gene Polymorphisms. V.M. Bekhterev Review of Psychiatry and Medical Psychology. 2024;58(1):115–130. (In Russ.). DOI: 10.31363/2313-7053-2024-833.
20. Roberts B.M., Lopes E.F., Cragg S.J. Axonal modulation of striatal dopamine release by local γ-aminobutyric acid (GABA) signalling. *Cells.* 2021;10(3):709. DOI: 10.3390/cells10030709.
21. Farokhnia M., Sheskier M.B., Lee M.R., Le A.N., Singley E., Bouhlal S. et al. Neuroendocrine response to GABA-B receptor agonism in alcohol-dependent individuals: Results from a combined outpatient and human laboratory experiment. *Neuropharmacology.* 2018;137:230–239. DOI: 10.1016/j.neuropharm.2018.04.011.
22. Farokhnia M., Deschaine S.L., Sadighi A., Farinelli L.A., Lee M.R., Akhlaghi F. et al. A deeper insight into how GABA-B receptor agonism via baclofen may affect alcohol seeking and consumption: lessons learned from a human laboratory investigation. *Mol. Psychiatry*. 2021;26 (2):545–555. DOI: 10.1038/s41380-018-0287-y.
23. Augier E. Recent advances in the potential of positive allosteric modulators of the $GABA_B$ receptor to treat alcohol use disorder. *Alcohol and Alcoholism*. 2021;56(2):139–148. DOI: 10.1093/alcalc/agab003.
24. Kibitov A.O., Kuznetsova M.N. Molecular Mechanisms of Alcohol Dependence: the Role of Brain Glutamate Receptors. *Journal of Addiction Problems.* 2019;5(176):58–98. (In Russ.). URL: https://elibrary.ru/item.asp?id=32497447
25. Akkus F., Mihov Y., Treyer V., Ametamey S.M., Johayem A., Senn S. et al. Metabotropic glutamate receptor 5 binding in male patients with alcohol use disorder. *Transl. Psychiatry.* 2018;8:1–8. DOI: 10.1038/s41398-017-0066-6.
26. Akhmadeev A.V., Kalimullina L.B. Disturbances of Glutamatergic Transmission in the Basolateral Nucleus of the Amygdala during the Development of Alcohol Dependence. *Russian Journal of Physiology.* 2016;102(4):385–397. (In Russ.). URL: https://www.elibrary.ru/item.asp?id=25717819
27. Roberto M., Kirson D., Khom S. The role of the central amygdala in alcohol dependence. *Cold Spring Harb. Perspect. Med*. 2021;11(2):a039339. DOI: 10.1101/cshperspect.a039339.
28. Kibitov A.O., Brodyansky V.M., Rybakova K.V., Krupitsky E.M. Modulation of GABA and Glutamate Systems as a Promising Pharmacological Target for Pathogenetic Therapy of Alcohol Dependence: Possibilities of Pharmacogenetic Analysis Based on a Double-Blind Placebo-Controlled Study. *Journal of Addiction Problems*. 2018;1(161):48–86. (In Russ.). URL: https://elibrary.ru/item.asp?id=32497447
29. Prisciandaro J.J., Hoffman M., Brown T.R., Voronin K., Book S., Bristol E. et al. Effects of Gabapentin on Dorsal Anterior Cingulate Cortex GABA and Glutamate Levels and Their Associations With Abstinence in Alcohol Use Disorder: A Randomized Clinical Trial. *Am. J. Psychiatry*. 2021;178(9):829–837. DOI: 10.1176/appi.ajp.2021.20121757.
30. Most D., Ferguson L., Harris R.A. Molecular basis of alcoholism. *Handb. Clin. Neurol*. 2014;125:89–111. DOI: 10.1016/B978-0-444-62619-6.00006-9.
31. Ciccocioppo R., Economidou D., Cippitelli A., Cucculelli M., Ubaldi M., Soverchia L. et al. Genetically selected Marchigian Sardinian alcohol-preferring (msP) rats: an animal model to study the neuro-biology of alcoholism. *Addict. Biol*. 2006;11(3-4):339–355. DOI: 10.1111/j.1369-1600.2006.00032.x.
32. Ko Y.E., Hwa L.S. Serotonin regulation of intermittent and continuous alcohol drinking in male and female C57BL/6J mice with systemic SB242084 and buspirone. *Alcohol. Alcohol.* 2023;58(3):280–288. DOI: 10.1093/alcalc/agad019.
33. Llinás S.G., Caballero A.J., Peñalver J.C., Valdés R. Platelet serotonin concentration and clinical status in alcohol withdrawal syndrome, preliminary results. *MEDICC Rev*. 2014;16(1):37–42. DOI: 10.37757/MR2014.V16. N1.8.
34. Nedic Erjavec G., Bektic Hodzic J., Repovecki S., Nikolac Perkovic M., Uzun S., Kozumplik O. et al. Alcohol-related phenotypes and platelet serotonin concentration. *Alcohol.* 2021;97:41–49. DOI: 10.1016/j.alcohol.2021.09.001.
35. Bokhan N.A., Ivanova S.A., Levchuk L.A. Serotonin System in the Modulation of Depressive and Addictive Behavior. Tomsk: National Research Tomsk State University Publishing House, 2013:102. (In Russ.). ISBN: 978-5-91701-090-8.
36. Airapetov M.I., Eresko S.O., Lebedev A.A., Bychkov E.R., Shabanov P.D. Alcoholization and Withdrawal of Ethanol Lead to Activation of the Neuroimmune Response in the Prefrontal Cortex of the Rat Brain. *Biomedical Chemistry.* 2019;65(5):380–384. (In Russ.). DOI: 10.18097/PBMC20196505380.
37. Pascual M., Calvo-Rodriguez M., Núñez L., Villalobos C., Ureña J., Guerri C. Toll-like receptors in neuroinflammation, neurodegeneration, and alcohol-induced brain damage. *IUBMB Life*. 2021;73(7):900–915. DOI: 10.1002/iub.2510.
38. Roberto M., Patel R.R., Bajo M. Ethanol and cytokines in the central nervous system. *Handb. Exp. Pharmacol.* 2018;248:397–431. DOI: 10.1007/164_2017_77.
39. Airapetov M., Eresko S., Lebedev A., Bychkov E., Shabanov P. The role of Toll-like receptors in neurobiology of alcoholism. *Biosci. Trends*. 2021;15(2):74–82. DOI: 10.5582/bst.2021.01041.
40. Niedzwiedz-Massey V.M., Douglas J.C., Rafferty T., Johnson J.W., Holloway K.N., Berquist M.D. et al. Effects of chronic and binge ethanol administration on mouse cerebellar and hippocampal neuroinflammation. *Am. J. Drug Alcohol. Abuse.* 2023;49(3):345–358. DOI: 10.1080/00952990.2022.2128361.
41. Crews F.T., Lawrimore C.J., Walter T.J., Coleman L.G.Jr. The role of neuroimmune signaling in alcoholism. *Neu-*

*ropharmacology.* 2017;122:56–73. DOI:10.1016/j.neuropharm.2017.01.031.
42. Crews F.T., Coleman L.G. Jr., Macht V.A., Vetreno R.P. Alcohol, HMGB1, and innate immune signaling in the brain. *Alcohol. Res.* 2024;44(1):04. DOI: 10.35946/arcr.v44.1.04.
43. Blednov Y.A., Benavidez J.M., Geil C., Perra S., Morikawa H., Harris R.A. Activation of inflammatory signaling by lipopolysaccharide produces a prolonged increase of voluntary alcohol intake in mice. *Brain Behav. Immun*. 2011;25(Suppl. 1):S92–S105. DOI: 10.1016/j.bbi.2011.01.008.
44. Kany S., Janicova A., Relja B. Innate immunity and alcohol. *J. Clin. Med.* 2019;8(11):1981. DOI: 10.3390/jcm8111981.
45. Czerwińska-Błaszczyk A., Pawlak E., Pawłowski T. The significance of toll-like receptors in the neuroimmunologic background of alcohol dependence. *Front. Psychiatry.* 2022;12: 97123. DOI: 10.3389/fpsyt.2021.797123.
46. Leclercq S., De Saeger C., Delzenne N., de Timary P., Stärkel P. Role of inflammatory pathways, blood mononuclear cells, and gut-derived bacterial products in alcohol dependence. *Biol. Psychiatry.* 2014;76(9):725–733. DOI: 10.1016/j.biopsych.2014.02.003.
47. Liangpunsakul S., Toh E., Ross R.A., Heathers L.E., Chandler K., Oshodi A. et al. Quantity of alcohol drinking positively correlates with serum levels of endotoxin and markers of monocyte activation. *Sci. Rep.* 2017;7(1):4462. DOI: 10.1038/s41598-017-04669-7.
48. Panchenko L.F., Terebilina N.N., Pirozhkov S.V., Naumova T.A., Baronets V.Yu., Balashova A.A. et al. Serum Markers of Fibrosis and Endothelial Dysfunction in Patients with Alcoholism with Varying Degrees of Liver Fibrosis. *Pathological Physiology and Experimental Therapy.* 2015;59(3):18–27 (In Russ.). URL: https://www.elibrary.ru/item.asp?id=26000984
49. Gao B., Ahmad M.F., Nagy L.E., Tsukamoto H. Inflammatory pathways in alcoholic steatohepatitis. *J. Hepatol.* 2019;70(2):249–259. DOI: 10.1016/j.jhep.2018.10.023.
50. Girard M., Malauzat D., Nubukpo P. Serum inflammatory molecules and markers of neuronal damage in alcohol-dependent subjects after withdrawal. *World J. Biol. Psychiatry.* 2019;20(1):76–90. DOI: 10.1080/15622975.2017.1349338.
51. Hillmer A.T., Nadim H., Devine L., Jatlow P., O'Malley S.S. Acute alcohol consumption alters the peripheral cytokines IL-8 and TNF-alpha. *Alcohol.* 2020;85:95–99. DOI: 10.1016/j.alcohol.2019.11.005.
52. ёAdams C., Conigrave J.H., Lewohl J., Haber P., Morley K.C. Alcohol use disorder and circulating cytokines: A systematic review and meta-analysis. *Brain Behav. Immun*. 2020;89:501–512. DOI: 10.1016/j.bbi.2020.08.002.
53. Pan W., Stone K.P., Hsuchou H., Manda V.K., Zhang Y., Kastin A.J. Cytokine signaling modulates blood-brain barrier function. *Curr. Pharm. Des*. 2011;17(33):3729–3740. DOI: 10.2174/138161211798220918.
54. Capuron L., Miller A.H. Immune system to brain signaling: Neuropsychopharmacological implications. *Pharmacol. Ther.* 2011;130(2):226–238. DOI: 10.1016/j.pharmthera.2011.01.014.
55. Patel R.R., Khom S., Steinman M.Q., Varodayan F.P., Kiosses W.B., Hedges D.M. et al. IL-1β expression is increased and regulates GABA transmission following chronic ethanol in mouse central amygdala. *Brain Behav. Immun*. 2019;75:208–219. DOI: 10.1016/j.bbi.2018.10.009.
56. Varodayan F.P., Pahng A.R., Davis T.D., Gandhi P., Bajo M., Steinman M.Q. et al. Chronic ethanol induces a pro-inflammatory switch in interleukin-1β regulation of GABAergic signaling in the medial prefrontal cortex of male mice. *Brain Behav. Immun*. 2023;110:125–139. DOI: 10.1016/j.bbi.2023.02.020.
57. Becker H.C. Influence of stress associated with chronic alcohol exposure on drinking. *Neuropharmacology*. 2017;122:115–126. DOI: 10.1016/j.neuropharm.2017.04.028.
58. Blaine S.K., Sinha R. Alcohol, stress, and glucocorticoids: From risk to dependence and relapse in alcohol use disorders. *Neuropharmacology.* 2017;122:136–147. DOI: 10.1016/j.neuropharm. 2017.01.037.
59. Wemm S.E., Sinha R. Drug-induced stress responses and addiction risk and relapse. *Neurobiol. Stress*. 2019;10:100148. DOI: 10.1016/j.ynstr.2019.100148.
60. Schreiber A.L., Gilpin N.W. Corticotropin-releasing factor (CRF) neurocircuitry and neuropharmacology in alcohol drinking. *Handb. Exp. Pharmacol*. 2018;248:435–471. DOI: 10.1007/164_2017_86.
61. Simpson S., Shankar K., Kimbrough A., George O. Role of corticotropin-releasing factor in alcohol and nicotine addiction. *Brain Res.* 2020;1740:146850. DOI: 10.1016/j.brainres.2020.146850.
62. Domi E., Domi A., Adermark L., Heilig M., Augier E. Neurobiology of alcohol seeking behavior. *J. Neurochem*. 2021;157(5):1585–1614. DOI: 10.1111/jnc.15343.
63. Koob G.F. The role of CRF and CRF-related peptides in the dark side of addiction. *Brain Res.* 2010;1314:3–14. DOI: 10.1016/j.brainres.2009.11.008.
64. Haass-Koffler C.L., Bartlett S.E. Stress and addiction: contribution of the corticotropin releasing factor (CRF) system in neuroplasticity. *Front. Mol. Neurosci*. 2012;5:91. DOI: 10.3389/fnmol.2012.00091.
65. Heilig M. Stress-related neuropeptide systems as targets for treatment of alcohol addiction: A clinical perspective. *J. Intern. Med.* 2023;293(5):559–573. DOI: 10.1111/joim.13636.
66. Schwandt M.L., Cortes C.R., Kwako L.E., George D.T., Momenan R., Sinha R. et al. The CRF1 antagonist verucerfont in anxious alcohol-dependent women: translation of neuroendocrine, but not of anti-craving effects. *Neuropsychopharmacology.* 2016;41(12):2818–2829. DOI: 10.1038/npp.2016.61.
67. Lee M.R., Rio D., Kwako L., George D.T., Heilig M., Momenan R. Corticotropin-Releasing Factor receptor 1 (CRF1) antagonism in patients with alcohol use disorder and high anxiety levels: effect on neural response during Trier Social Stress Test video feedback. *Neuropsychopharmacology.* 2023;48(5):816–820. DOI: 10.1038/s41386-022-01521-z.
68. Weera M.M., Gilpin N.W. Central amygdala CRF1 cells control nociception and anxiety-like behavior. *Neuropsychopharmacology*. 2024;49(1):341–342. DOI: 10.1038/s41386-023-01693-2.
69. Anokhina I.P., Veretinskaya A.G., Kuznetsova M.N., Vekshina N.L. Dopamine, Cortisol and Adrenocorticotropic Hormone in the Blood and Cerebrospinal Fluid of Patients with Alcohol Withdrawal Syndrome and Delirium. *Journal of*

*Addiction Problems.* 2014;3:73–81. (In Russ.). URL: https://www.elibrary.ru/item.asp?id=21670127
70. Vetlugina T.P., Lobacheva O.A., Nikitina V.B., Prokopyeva V.D., Mandel A.I., Bokhan N.A. Hormones of the Stress-Realizing System in Alcohol Dependence: the Possibility of Predicting the Duration of Remission. *S.S. Korsakov Journal of Neurology and Psychiatry.* 2020;5(120):73–78. (In Russ.). DOI: 10.17116/jnevro202012005173.
71. Vetlugina T.P., Prokopyeva V.D., Nikitina V.B., Lobacheva O.A., Yarygina E.G., Mandel A.I. et al. Search for Biological Factors Associated with the Stability of Therapeutic Remission in Alcohol Dependence. *Siberian Herald of Psychiatry and Addiction Psychiatry.* 2021;2(111):5–12. (In Russ.). DOI: 10.26617/1810-3111-2021-2(111)-5-12.
72. Vendruscolo L.F., Estey D., Goodell V., Macshane L.G., Logrip M.L., Schlosburg J.E. et al. Glucocorticoid receptor antagonism decreases alcohol seeking in alcohol-dependent individuals. *J. Clin. Invest*. 2015;125(8):3193–3197. DOI: 10.1172/JCI79828.
73. Soravia L.M., Moggi F., de Quervain D.J. Effects of cortisol administration on craving during in vivo exposure in patients with alcohol use disorder. *Transl. Psychiatry*. 2021;11(1):6. DOI: 10.1038/s41398-020-01180-y.
74. Koob G.F. alcohol use disorder treatment: problems and solutions. *Annu. Rev. Pharmacol. Toxicol.* 2024;64:255–275. DOI: 10.1146/annurev-pharmtox-031323-115847.
75. Roberto M., Spierling S.R., Kirson D., Zorrilla E.P. Corticotropin-Releasing Factor (CRF) and Addictive Behaviors. *Int. Rev. Neurobiol*. 2017;136:5–51. DOI: 10.1016/bs.irn.2017.06.004.
76. Witkiewitz K., Litten R.Z., Leggio L. Advances in the science and treatment of alcohol use disorder. *Sci. Adv.* 2019;5(9): eaax4043. DOI: 10.1126/sciadv.aax4043.
77. Anokhin P.K., Shagiakhmetov F.Sh., Kokhan V.S., Shamakina I.Yu. Dynorphin/Kappa-Opioid System of the Brain, Anti-Reward and Alcohol Abuse. *Journal of Addiction Problems*. 2020;5(188):47–63. (In Russ.). DOI: 10.47877/0234-0623_2020_5_47.
78. Sinha R. Alcohol's Negative emotional side: the role of stress neurobiology in alcohol use disorder. *Alcohol. Res.* 2022;42(1):12. DOI: 10.35946/arcr.v42.1.12.
79. Vinnikova M.A. Remissions in Addiction Syndrome: Possibilities of Formation, Stages of the Course, and Clinical Forms. *Journal of Addiction Problems*. 2017;4-5:83–102. (In Russ.).
80. Meliksetyan A.S. Features of the Course of Remission in Patients with Chronic Alcoholism. *Narcology.* 2014;13(12):35–43. (In Russ.). URL: https://elibrary.ru/item.asp?id=22627611.
81. Abdin E., Subramaniam M., Vaingankar J.A., Chong S.A. The role of sociodemographic factors in the risk of transition from alcohol use to disorders and remission in Singapore. *Alcohol. Alcohol*. 2014;49(1):103–108. DOI: 10.1093/alcalc/agt126.
82. Maisto S.A., Hallgren K.A., Roos C.R., Witkiewitz K. Course of remission from and relapse to heavy drinking following outpatient treatment of alcohol use disorder. *Drug Alcohol. Depend.* 2018;187:319–326. DOI: 10.1016/j.drugalcdep.2018.03.011.
83. Altshuler V.B. Clinical Manifestations and Patterns of the Course of Alcoholism. *Journal of Addiction Problems*. 2013;3:112–142 (In Russ.). URL: https://elibrary.ru/item.asp?id=19101632.
84. Gofman A.G. Remission in Patients with Alcoholism. *Journal of Addiction Problems*. 2013;4:110–118. (In Russ.). URL: https://elibrary.ru/item.asp?id=20159402.
85. Bernard L., Cyr L., Bonnet-Suard A., Cutarella C., Bréjard V. Drawing alcohol craving process: A systematic review of its association with thought suppression, inhibition and impulsivity. *Heliyon.* 2021;7(1):e05868. DOI: 10.1016/j.heliyon.2020.e05868.
86. Martins J.S., Fogelman N., Wemm S., Hwang S., Sinha R. Alcohol craving and withdrawal at treatment entry prospectively predict alcohol use outcomes during outpatient treatment. *Drug Alcohol. Depend.* 2022;231:109253. DOI: 10.1016/j.drugalcdep.2021.109253.
87. Uzbekov M.G., Gurovich I.Ya., Ivanova S.A. Potential Biomarkers of Mental Illnesses in the Aspect of a Systemic Approach. *Social and Clinical Psychiatry.* 2016;26(1):77–94. (In Russ.). URL: https://www.elibrary.ru/item.asp?id=26539116
88. Milivojevic V., Sinha R. Central and peripheral biomarkers of stress response for addiction risk and relapse vulnerability. *Trends Mol. Med.* 2018;24(2):173–186. DOI: 10.1016/j.molmed.2017.12.010
89. Coccini T., Ottonello M., Spigno P., Malovini A., Fiabane E., Roda E. et. al. Biomarkers for alcohol abuse/withdrawal and their association with clinical scales and temptation to drink. A prospective pilot study during 4-week residential rehabilitation. *Alcohol.* 2021; 94: 43–56. DOI: 10.1016/j.alcohol.2021.04.004.

## Author Information

**Vetlugina Tamara P.** – Dr. Sci. (Biology), Professor, Honored Scientist of the Russian Federation, Chief Researcher, Laboratory of Clinical Psychoneuroimmunology and Neurobiology, Mental Health Research Institute, Tomsk NRMC, Tomsk, vetluga21@mail.ru, https://orcid.org/0000-0003-2068-0931

**Epimakhova Elena V.** – Cand. Sci. (Biology), Researcher, Department of Addictive Disorders, Mental Health Research Institute, Tomsk NRMC, Tomsk, elenaepimakhova@mail.ru, https://orcid.org/0000-0002-9304-4496

**Prokopieva Valentina D.** – Dr. Sci. (Biology), Leading Researcher, Laboratory of Clinical Psychoneuroimmunology and Neurobiology, Mental Health Research Institute, Tomsk NRMC, Tomsk, valyaprok@mail.ru, https://orcid.org/0000-0002-4811-984X

**Shumilova Sofia N.** – Junior Researcher, Laboratory of Clinical Psychoneuroimmunology and Neurobiology, Mental Health Research Institute, Tomsk NRMC, Tomsk, sofashumilova97@gmail.com, https://orcid.org/0000-0001-9248-4150

**Voevodin Ivan V.** – Dr. Sci. (Medicine), Leading Researcher, Endogenous Disorder Department, Mental Health Research Institute, Tomsk NRMC, Tomsk, i_voevodin@list.ru, https://orcid.org/0000-0002-3988-7660

(✉) **Vetlugina Tamara P.,** vetluga21@mail.ru

Received on March 12, 2025;
approved after peer review on March 31, 2025;
accepted on April 17, 2025

УДК 616.1-003.84:576.385.362
https://doi.org/10.20538/1682-0363-2025-3-138-148

# The role of biomolecules in the development and progression of vascular calcification in cardiovascular diseases

**Demina E.D., Shramko V.S.**

*Research Institute of Internal and Preventive Medicine – Branch of Federal Research Center Institute of Cytology and Genetics, Siberian Branch of the Russian Academy of Sciences (IIPM – Branch of IC&G SB RAS)*
*175/1 B. Bogatkov St., 630089 Novosibirsk, Russian Federation*

**ABSTRACT**

Cardiovascular diseases (CVD) remain the most pressing problem in the healthcare system. Complex interactions between changes in the intima – media thickness of arteries and blood components (accumulation of lipids, complex carbohydrates, fibrous tissue, calcification, etc.) are involved in the pathogenesis of CVD. Various biomolecules play a crucial role in the development and progression of coronary artery calcification, the most common calcification inhibitors being osteopontin, osteoprotegerin, sclerostin, fetuin-A, inorganic pyrophosphate, matrix Gla protein, fibroblast growth factor 23 (FGF-23), Klotho, bone morphogenetic proteins (BMP), in particular BMP-7, and the most common activators being leptin, BMP-2, BMP-4, parathyroid hormone, calcitriol, etc. Currently, the most studied biomolecules associated with calcium metabolism are osteoprotegerin, osteopontin, osteonectin, osteocalcin, and Klotho protein.

The paper describes in detail the poorly studied effects of calcification inhibitors (sclerostin, fetuin-A, matrix Gla protein, FGF-23, inorganic pyrophosphate, BMP-7) and some calcification activators (leptin, BMP-2 and BMP-4, parathyroid hormone, and calcitriol).

**The aim** of this study was to analyze and systematize data on the role of biomolecules in the development and progression of vascular calcification in cardiovascular diseases.

**Keywords:** cardiovascular diseases, atherosclerosis, biomolecules, vascular calcification, blood

**Conflict of interest.** The authors declare the absence of obvious or potential conflicts of interest related to the publication of this article.

**Source of financing.** The article was written within the budgetary topic in the state assignment No. FWNR-2024-0004.

**For citation:** Demina E.D., Shramko V.S. The role of biomolecules in the development and progression of vascular calcification in cardiovascular diseases. *Bulletin of Siberian Medicine.* 2025;24(3):138–148. https://doi.org/10.20538/1682-0363-2025-3-138-148.

# Роль биомолекул в развитии и прогрессировании кальцификации сосудов при сердечно-сосудистых заболеваниях

**Демина Е.Д., Шрамко В.С.**

*Научно-исследовательский институт терапии и профилактической медицины (НИИТПМ) – филиал Института цитологии и генетики Сибирского отделения Российской академии наук (ИЦиГ СО РАН)*
*Россия, 630089, г. Новосибирск, ул. Бориса Богаткова, 175/1*

✉ *Demina Elizaveta D.,* chaussova.liza@gmail.com

**РЕЗЮМЕ**

Сердечно-сосудистые заболевания (ССЗ) остаются наиболее актуальной проблемой в системе здравоохранения. В патогенез ССЗ вовлечены сложные взаимодействия между изменениями интима-медиа артерий и компонентами крови (накопление липидов, сложных углеводов, фиброзной ткани, кальцификация и др.). В развитии и прогрессировании кальцификации коронарных артерий огромную роль играют различные биомолекулы, где в качестве ингибиторов кальцификации чаще всего выступают остеопонтин, остеопротегерин, склеростин, фетуин-А, неорганический пирофосфат, матриксный Gla-протеин, фактор роста фибробластов 23 (FGF-23), Клото, белки морфогенеза костей (BMP), в частности BMP-7; а активаторов – лептин, BMP-2, BMP-4, паратиреоидный гормон, кальцитриол и др. В настоящее время наиболее изученными биомолекулами, ассоциированными с кальциевым обменом, считаются остеопротегерин, остеопонтин, остеонектин, остеокальцин и белок Клото.

В работе описаны малоизученные эффекты ингибиторов кальцификации (склеростин, фетуин А, матриксный Gla-протеин, FGF-23, неорганический пирофосфат, BMP-7), а также некоторых активаторов кальцификации (лептин, BMP-2 и BMP-4, паратиреоидный гормон и кальцитриол).

**Цель** данного исследования заключается в анализе и систематизации данных о роли биомолекул в развитии и прогрессировании кальцификации сосудов при ССЗ.

**Ключевые слова:** сердечно-сосудистые заболевания, атеросклероз, биомолекулы, кальцификация сосудов, кровь

**Конфликт интересов.** Авторы декларируют отсутствие явных и потенциальных конфликтов интересов, связанных с публикацией настоящей статьи.

**Источник финансирования.** Статья подготовлена в рамках бюджетной темы по государственному заданию № FWNR-2024-0004.

**Для цитирования:** Демина Е.Д., Шрамко В.С. Роль биомолекул в развитии и прогрессировании кальцификации сосудов при сердечно-сосудистых заболеваниях. *Бюллетень сибирской медицины.* 2025;24(3):138–148. https://doi.org/10.20538/1682-0363-2025-3-138-148.

## INTRODUCTION

Cardiovascular diseases (CVD) remain the most pressing problem in healthcare, despite the significant progress in the diagnosis and treatment of cardiovascular pathology in last decades [1, 2]. The pathogenesis of atherosclerotic CVD involves complex interactions between changes in arterial intima – media thickness and blood components (accumulation of lipids, complex carbohydrates, fibrous tissue, calcification, etc.) [3]. For a long time, atherosclerosis can be asymptomatic due to a latent stage of the disease, which is already accompanied by morphologic changes in the coronary arteries. However, following atherosclerotic plaque (AP) progression, there is gradual stenosis of coronary and other arteries, which results in such complications as angina pectoris, cerebrovascular insufficiency, myocardial infarction (MI), sudden cardiacdeath, etc. [4].

Currently, at least three histologic types of unstable APs are distinguished:

1) lipid – fibroatheroma with a thin fibrous cap;

2) inflammatory – erosive – with increased proteoglycan or inflammation leading to erosion or thrombosis;

3) dystrophic – necrotic – with necrosis and / or calcification [3].

Vascular calcification is a part of atherosclerotic process; at the same time, the degree of mineralization can reflect the severity of AP [5]. Calcium deposition in coronary arteries reduces vasodilatory effects and changes the stability of AP [6]. Several authors have demonstrated that a fairly common mechanism of AP instability is the formation of a calcified nodule consisting of calcified plates similar to bone spicules that surround the area of fibrosis [7]. Nevertheless, the relationship between arterial calcification and the risk of plaque rupture is still controversial.

Various biomolecules play an essential role in the development and progression of coronary artery calcification (CAC), the most common inhibitors of calcification being osteopontin [8], osteoprotegerin [9], sclerostin [9], fetuin-A [10], inorganic

pyrophosphate [11, 12], matrix Gla protein [13], fibroblast growth factor 23 (FGF-23) [14, 15], Klotho [16], bone morphogenetic proteins (BMP), in particular BMP-7 [17], and the most common activators being leptin [18], BMP-2 and BMP-4 [19, 20], parathyroid hormone [21], calcitriol [22], and others.

Currently, the most studied molecules associated with vascular calcification are considered to be osteoprotegerin, osteopontin, osteonectin, osteocalcin, and Klotho protein. Therefore, this review will consider the less studied ones.

## MATERIALS AND METHODS

References for this article were searched in PubMed and eLIBRARY.RU databases using the following keyword combinations: “sclerostin and CVD”, “fetuin-A and CVD”, “matrix Gla protein and CVD”, “fibroblast growth factor 23 and CVD”, “inorganic pyrophosphate and CVD”, “bone morphogenetic protein 2 and CVD”, “bone morphogenetic protein 4 and CVD”, “bone morphogenetic protein 7 and CVD”, “leptin and CVD”, “parathyroid hormone and CVD”, “calcitriol and CVD” in Russian and English. A total of 563 full-text articles for the period 2013–2025 were retrieved. Eighty-one articles were selected for review, containing information on the association of the above biomolecules with CVD, in particular, with coronary heart disease and coronary atherosclerosis.

## CALCIFICATION INHIBITORS

### Sclerostin

Sclerostin is a secreted glycoprotein that is expressed predominantly in osteocytes, but also in other tissues and organs, such as vascular smooth muscle cells (VSMCs) [23], and contains three distinct domains. It was found that sclerostin inhibits bone formation via the Wnt/β-catenin signaling pathway [24, 25].

A number of studies have shown an association between serum sclerostin levels and the incidence of CVD and / or cardiovascular mortality. In particular, W. He et al. found that higher serum sclerostin levels were associated with a better 3-year prognosis after percutaneous coronary intervention in elderly patients with stable coronary heart disease (CHD) [26]. Moreover, serum sclerostin is an independent prognostic parameter for predicting adverse cardiovascular and cerebrovascular events, MI, and all-cause mortality. In a prospective study, C.Y. Yang et al. [27] found an inverse relationship between serum sclerostin levels and aortic calcification in patients on long-term hemodialysis. The authors suggested that higher sclerostin levels led to fewer cardiovascular events (hazard ratio 0.982 for every 1 pmol / l of sclerostin increase). In a study on mice [28], it was shown that sclerostin can play a protective role, contributing to the maintenance of structural and functional integrity of the aorta by suppressing inflammation and degradation of extracellular matrix, which in turn prevents the development of aortic aneurysm and atherosclerosis. At the same time, a prospective population-based study by G. Klingenschmid et al. [29] revealed no association between serum sclerostin levels and cardiovascular events, such as stroke. Similarly, in the meta-analysis by M. Kanbay et al. [30], serum sclerostin levels were not associated with cardiovascular and all-cause mortality.

### Fetuin-A

Fetuin-A is a serum protein with a molecular mass of 48 kDa synthesized by liver cells. Fetuin-A is thought to be involved in the regulation of bone and vascular calcification through the formation of stable colloidal mineral – protein complexes called calciprotein particles. Removal of these particles and, consequently, excess minerals from the circulation prevents local accumulation of minerals and calcification of soft tissues [31, 32].

In a study by L.E. Laugsand et al. [33], an increase in serum fetuin-A concentration was associated with a lower risk of CVD among participants without type 2 diabetes, while a reverse trend was observed among participants with type 2 diabetes. In a prospective cohort study, N. Kubota et al. concluded that despite the ability of fetuin-A to inhibit ectopic calcium deposition, its low serum level probably had no significant effect on the progression of aortic stenosis [34].

Another prospective study by M. Krajnc et al. found that serum fetuin-A may be inversely associated with the progression of CAC in patients

with type 2 diabetes [10]. In a one-stage cohort study by A.T. Makhieva et al., involving 84 patients with stage 5 chronic kidney disease (CKD), decreased blood levels of fetuin-A contributed to an increased risk of heart valve and aortic wall calcification both alone and in combination with decreased Klotho protein levels [35].

In addition, the work by L.B. Drygina et al. presented data on the relationship of fetuin-A levels with markers of endothelial dysfunction and the presence of atherosclerosis with vascular calcification [32]. Moreover, it was found that in individuals with very high calcium score (more than 400 Agatston units), the level of fetuin-A in serum was significantly lower than in patients with high calcium score (100–400 units) [36].

**Matrix Gla Protein**

Matrix gamma-carboxyglutamic acid protein (Gla protein, MGP) is a vitamin K-dependent mineral-binding protein with a molecular weight of 15 kDa, present in bone, cartilage, and vascular smooth muscles [37]. The biological activity of MGP depends on vitamin K, a cofactor for the enzyme gamma-glutamyl carboxylase, which converts inactive uncarboxylated MGP to active carboxylated MGP [38]. MGP also serves as an inhibitor of BMPs, in particular BMP-2. It is proposed that decreased MGP activity leads to unimpeded expression of BMP-2, which leads to osteochondrogenic differentiation of vascular smooth muscle cells and, subsequently, to vascular calcification. [39].

There are conflicting data on the role of MGP in patients with atherosclerosis. It is suggested that only the functional form of MGP (post-translationally modified, including carboxylated Gla residues and phosphorylated serine hydroxyl groups) has the ability to inhibit vascular calcification. However, low levels of this functional MGP are associated with increased vascular calcification in certain patient groups. At the same time, various non-functional fractions of MGP may serve as potential markers of CVD risk, correlating with cardiovascular mortality and the severity of vascular calcification.

Biologically inactive dephospho-uncarboxylated MGP (dp-ucMGP) in the study by O. Mayer Jr. et al. was described as a potential biomarker for predicting mortality in patients with heart failure and aortic stenosis. Over a mean follow-up period of 2,050 days (5.6 years), patients with plasma dp-ucMGP ≥ 977 pmol / l had a higher risk of five-year all-cause and cardiovascular mortality [40]. The study by R. Capoulade et al. showed that the total dpMGP level was associated with a faster rate of aortic stenosis progression ($r = 0.24$; $p = 0.008$) in patients under 57 years [41].

In a multicenter study by A. A. Berlot et al., a positive association was found between the inactive form of matrix Gla protein, dp-ucMGP, and the progression of coronary artery calcification, ascending (ATAC), and descending thoracic aorta (DTAC) calcification. For each standard deviation (SD, 178 pmol / l) in the increase in plasma dp-ucMGP, CAC increased by 3.44 Agatston units per year (AU / year) (95% confidence interval (CI): 1.68–5.21), $p < 0.001$), ATAC increased by 0.63 AU / year (95% CI: 0.27–0.98), $p = 0.001$), and DTAC increased by 8.61 AU / year (95% CI: 4.55–12.67), $p < 0.001$) [42].

In addition, there is increasing evidence suggesting that multiple single nucleotide polymorphisms in the *MGP* gene may significantly influence susceptibility to vascular calcification and atherosclerosis. A meta-analysis by K. Sheng et al., including 23 case-control studies, demonstrated a significant association between the rs1800801 polymorphism in the *MGP* gene and vascular calcification, especially in the Caucasian population [43].

**Fibroblast Growth Factor 23 (FGF-23)**

Fibroblast growth factor 23 (FGF-23) is a 30-kDa hormone secreted by osteocytes and osteoblasts. It affects fibroblast growth factor receptors type 1–4 (FGFR1–4) and acts with the Klotho protein as a co-receptor in the kidneys, heart, intestines, and parathyroid gland [14, 15]. The role of FGF-23 in the development of CVD and calcification of atherosclerotic plaques is not completely clear.

In a prospective study by P. L. Lutsey et al., involving 15,792 men and women (aged 45–64 years), high serum FGF-23 levels were associated with an increased risk of CHD, heart failure, and cardiovascular mortality. However, at FGF-23 levels < 40 pg / ml, no association between FGF-23 and cardiovascular risk was noted, and at > 40 pg / ml, a positive association was observed. After

demographic adjustments, individuals in the group with the highest FGF-23 (≥ 58.8 pg / ml) had a higher risk of CHD (adjusted hazard ratio, 95% CI: 1.40–1.94, $p = 0.02$) compared to those with FGF-23 < 40 pg / ml [44].

The Multinational Study of Atherosclerosis (MESA) was conducted to evaluate the association of serum FGF-23 with major subclinical and clinical CVD events in 6,546 individuals aged 45–85 years. Exclusion criteria for this study were MI, angina, stroke, transient ischemic attack, heart failure, atrial fibrillation, nitroglycerin consumption, angioplasty, coronary artery bypass grafting, valve replacement, pacemaker or defibrillator placement, and any cardiac or arterial surgery. Participants with serum FGF-23 concentrations in the upper quartile (46.4–223 pg / ml) were found to have CAC (as determined by computed tomography (CT)) more often than those with FGF-23 levels in the lower quartile (< 30.5 pg / ml) (95% CI: 1.09–1.46) [45].

In a cross-sectional study by M.N. Turan et al., high plasma intact FGF-23 levels were an independent predictor of severe CAC, after adjustment for age, gender, diabetes, time on dialysis, and intima – media thickness [46]. A prospective cohort study of 204 outpatients found a positive association between plasma FGF-23 levels and plaque calcification. In men, FGF-23 was associated with an increase in the proportion of fat in plaques, while in women, it was associated with increased calcium content in these formations [47]. However, not all studies showed that the level of FGF-23 was reliably associated with arterial calcification. Thus, in the study by Y. Takashi Y., the simple regression analysis showed that the serum level of FGF23 was not associated with the aortic calcification index [48].

## Pyrophosphates

Inorganic pyrophosphate (PPi) is one of the strongest inhibitors of hydroxyapatite formation, which leads to its ectopic deposition in the vascular wall, and, consequently, to the development of vascular calcification in soft tissues. Normally, PPi is expressed in the walls of blood vessels. Vascular calcification is associated with a decrease in PPi concentration and an increase in phosphate (Pi) levels. Mutations in the *ABCC6* gene (*ATP-BINDING CASSETTE, SUBFAMILY C, MEMBER 6*), encoding the ABCC6 transporter protein, which regulates the release of ATP from the liver into the blood, lead to a decrease in PPi levels. In addition to ABC proteins, PPi levels are regulated primarily by two enzymes: tissue-nonspecific alkaline phosphatase (TNAP), which converts PPi into two molecules of inorganic phosphate (Pi), and ectonucleotide pyrophosphatase / phosphodiesterase 1 (ENPP-1), which breaks down circulating adenosine triphosphate (ATP) into adenosine monophosphate (AMP) and PPi [49–51].

PPi deficiency can lead to vascular and soft tissue calcification, while excessive PPi elevation can cause premature loss of deciduous teeth, osteomalacia, stress fractures, etc. [52]. A study by D. Dedinszki et al. showed that orally administered PPi can suppress connective tissue calcification in mice modeling pseudoxanthoma elasticum and generalized arterial calcification [11].

The study by W. Gu et al. aimed to investigate the effects of adenosine disodium triphosphate (ADTP) and sodium alendronate (AL) as exogenous sources of PPi on atheromatous calcification in mice. The results showed that ADTP and AL, when administered intraperitoneally daily at a dose of 0.6 and 1.2 mg / kg / day for 2 months, reduced atheromatous calcification in mice by increasing serum PPi levels [53]. In a study by K.A. Lomashvili et al., it was shown that mice lacking the ENPP1 enzyme (Enpp1−/-) had reduced plasma PPi levels, which could subsequently cause spontaneous aortic calcification [12]. A number of studies on aortic valve calcification models showed that PPi significantly reduced calcium accumulation in aortic cusps and rings [54–56].

## Bone Morphogenetic Proteins

BMPs belong to the transforming growth factor β (TGFβ) superfamily and regulate cellular differentiation and tissue mineralization [17]. Currently, at least 33 ligands have been identified in the TGFβ protein family, of which more than 20 belong to the BMP superfamily [57].

BMP-7 is expressed in the collecting ducts of the kidneys, lungs, and heart. BMP-7 is a pleiotropic growth factor and plays a critical role in the development of various tissues and organs. It supports many physiological processes, such as bone development, fracture healing, and brown adipose

tissue differentiation in the body. Decreased BMP-7 expression is associated with various diseases, including osteoporosis, CVD, and diabetes [58].

In the context of CVD, BMP-7 has attracted the attention of researchers due to its ability to participate in processes associated with atherosclerosis. It can modulate inflammatory responses and promote vascular wall remodeling, which potentially reduces the progression of atherosclerosis. [59]. A study by D. Merino et al. showed an inverse correlation between blood BMP-7 levels and cardiac hypertrophy, as well as diastolic dysfunction [60]. In a study by X. Yu et al., it was found that serum BMP-7 concentrations were significantly reduced in patients with CHD [61]. A study in mice showed that intravenous administration of BMP-7 at a dose of 200 μg / kg inhibited the formation of atherosclerotic plaques [62]. In a study by P. Urbina et al., it was shown that in laboratory mice with prediabetic cardiomyopathy, administration of BMP-7 at a dose of 200 μg / kg for 3 days significantly improved cardiac function, as evidenced by an increase in the shortening fraction and ejection fraction compared to the control group that did not receive BMP-7 ($p < 0.05$) [63].

## CALCIFICATION ACTIVATORS

### Leptin

Leptin is a hormone secreted mainly by adipose tissue. It regulates energy balance and body weight through a negative feedback mechanism [64, 65]. Leptin affects vascular calcification through activation of smooth muscle cell proliferation and production of proinflammatory cytokines [18].

Many studies have shown that hyperleptinemia is closely associated with CVD. Thus, a meta-analysis by V. A. Myasoedova et al., including 10 studies involving 2,360 patients, indicated a potential link between elevated blood leptin levels and severe aortic stenosis [66].

In a study by P. Szulc et al., involving 548 men aged 50–85 years, high serum leptin levels (> 8.93 ng / ml) were associated with greater severity and rapid progression of abdominal aortic calcification, resulting in higher cardiovascular risk [18] and also increased the risk of developing CHD [67].

In a study by Y. Liu et al., the median serum leptin level was higher in 200 patients with aortic valve calcification than in 197 controls (20.07 vs. 9.03 ng / ml; $p < 0.01$). In the same study, patients with aortic valve calcification had a higher proportion of advanced CHD (88.50 vs. 68.00%) ($p < 0.01$) than patients without calcification [68].

N. Roy et al. found that higher leptin levels were associated with progression of coronary atherosclerosis in patients on hemodialysis. However, lower leptin levels were associated with all-cause mortality [69]. A meta-analysis including 13 epidemiological studies involving 4,257 patients with CVD showed that high blood leptin levels were not independently associated with CHD [70].

### BMP-2 and BMP-4

BMP-2 and BMP-4 affect VSMCs through transcription proteins (Msx2, Cbfa1), as a result of which muscle cells lose their contractile function and, like osteoblasts, synthesize alkaline phosphatase, bone sialoprotein, type I collagen, and osteocalcin [71]. Thus, BMP-2 and BMP-4 stimulate osteogenic differentiation of VSMCs, thereby promoting calcification and the development of atherosclerosis [19].

In the study by M. Scimeca et al., the multivariate analysis showed significant associations between increased BMP-2 expression and the presence of unstable plaques, as well as a significant positive relationship between hypertriglyceridemia and BMP-4 expression [20].

In the study by M. Zhang et al., involving 124 patients with type 2 diabetes, it was found that plaque volume index and plaque calcium density were positively correlated with BMP-2 in blood plasma ($p = 0.035$ and $p = 0.0025$, respectively) [72].

N. Wang et al., examining 204 patients with hypertension, found that plasma BMP-4 levels were significantly higher in the group with high cardio-ankle vascular index (CAVI) than in the group with low CAVI [38.51 (31.79–50.83) pg / ml vs. 31.15 (29.38–32.37) pg / ml; $p < 0.001$]. CAVI was used to determine the state of arterial stiffness [73].

### Parathyroid Hormone

Parathyroid hormone (PTH) is a hormone synthesized by the parathyroid glands that increases the concentration of calcium in the blood due to its

release from bone tissue. In addition, PTH activates the renin – angiotensin – aldosterone system, which results in an increase in renin levels and, ultimately, in an increase in blood pressure [74].

There are studies on the relationship between PTH and vascular calcification [21]. A group of authors [75] showed that an increase in PTH levels in blood plasma was associated with an increase in the prevalence of atherosclerosis, assessed by magnetic resonance angiography, and mortality from atherosclerotic lesions of peripheral and large vessels in two independent cohorts with a total of 1,304 patients.

It was also found that PTH had a synergistic effect on calcification in combination with phosphate. In a study conducted by S. Fernández-Villabrille et al. on rats, it was found that the highest calcium content in the aorta was observed in animals with elevated serum phosphate levels, which was accompanied by a significant increase in PTH concentrations [76].

### Calcitriol

Calcitriol [1,25(OH)2D] is an active form of vitamin D3 (cholecalciferol), which plays an important role in the regulation of calcium and phosphorus metabolism. Calcitriol precursors include calcidiol (25-hydroxyvitamin D [25(OH) D]), low circulating concentrations of which are commonly used to define vitamin D deficiency [77].

There are conflicting data on the role of calcidiol (25-hydroxyvitamin D [25(OH)D]) in vascular calcification and its association with CVD incidence and mortality. In the study by C. Robinson-Cohen et al., lower serum 25(OH)D concentrations were associated with an increased risk of CHD among participants who were Caucasian or Chinese, but not African American or Hispanic [78].

In a study of 11,022 patients (mean age 54.3 ± 17.2 years), Caucasians with 25(OH)D values < 20 ng / ml had higher all-cause mortality than those whose 25(OH)D was 20–50 ng / ml [79].

Other studies suggest an inverse J-shaped relationship between serum 25(OH)D and all-cause mortality [80]. In a study by C.T. Sempos et al., involving 15,099 individuals aged ≥ 20 years, women were found to have an increased risk of death when blood 25(OH)D concentrations ranged from 100 to 119 nmol / l, whereas for men, the increased risk occurred at values ≥ 120 nmol / l [81].

## CONCLUSION

Understanding and more detailed study of biomolecules involved in the development and progression of vascular calcification in patients with CVD is a promising area of research. Data on the relationships of various molecules associated with calcium metabolism with lipid and lipoprotein indices and / or inflammatory biomarkers of CVD may be of interest for obtaining new data clarifying and complementing the mechanisms of development of CVD and its complications.

### REFERENCES


1. Boytsov S.A., Pogosova S.A., Ansheles A.A., Badtieva V.A., Balakhonova T.V., Barbarash O.L. et al. Cardiovascular Prevention 2022. Russian National Guidelines. *Russian Journal of Cardiology*. 2023;28(5):5452. (In Russ.). DOI: 10.15829/1560-4071-2023-5452.
2. Begun D.N., Morozova T.A., Surikova A.V. Circulatory Disorders as a Medical and Social Problem. *Young Scientist.* 2019;8(246):25–28. (In Russ.).
3. Ragino Yu. I. Unstable Atherosclerotic Plaque and Its Laboratory Biochemical Markers. Novosibirsk: Nauka, 2019:120. (In Russ.).
4. Sergienko I.V., Ansheles A.A. Pathogenesis, Diagnosis, and Treatment of Atherosclerosis: Practical Aspects. *Russian Cardiology Bulletin.* 2021;16(1):64–72. (In Russ.). DOI: 10.17116/Cardiobulletin20211601164.
5. Kashtanova E.V., Polonskaya Ya.V., Ragino Yu.I. Calcification of Coronary Arteries and Its Role in Atherosclerosis Development. *Terapevticheskii Arkhiv.* 2021;93(1):84–86. (In Russ.). DOI: 10.26442/00403660.2021.01.200598.
6. Barbarash O.L., Kashtalap V.V., Shibanova I.A., Kokov A.N. Fundamental and Applied Aspects of Coronary Artery Calcification. *Russian Journal of Cardiology*. 2020;25(3S):40–49. (In Russ.). DOI: 10.15829/1560-4071-2020-4005.
7. Torii S., Sato Y., Otsuka F., Kolodgie F.D., Jinnouchi H., Sakamoto A., et al. Eruptive calcified nodules as a potential mechanism of acute coronary thrombosis and sudden death. *J. Am. Coll. Cardiol*. 2021;77(13):1599–1611. DOI: 10.1016/j.jacc.2021.02.016.
8. Abdalrhim A.D., Marroush T.S., Austin E.E., Gersh B.J., Solak N., Rizvi S.A. et al. Plasma Osteopontin Levels and Adverse Cardiovascular Outcomes in the PEACE Trial. *PLoS One.* 2016;11(6):e0156965. DOI: 10.1371/journal.pone.0156965.
9. Morena M., Jaussent I., Dupuy A.M., Bargnoux A.S., Kuster N., Chenine L. et al. Osteoprotegerin and sclerostin in chronic kidney disease prior to dialysis: potential partners in vascular calcifications. *Nephrol. Dial Transplant*. 2015;30(8):1345–1356. DOI: 10.1093/ndt/gfv081.
10. Krajnc M., Pečovnik Balon B., Krajnc I. Non-traditional risk factors for coronary calcification and its progression in patients with type 2 diabetes: The impact of postprandial

glycemia and fetuin-A. *J. Int. Med. Res*. 2019;47(2):846–858. DOI: 10.1177/0300060518814080.
11. Dedinszki D., Szeri F., Kozák E., Pomozi V., Tőkési N., Mezei T.R. et al. Oral administration of pyrophosphate inhibits connective tissue calcification. *EMBO Mol. Med*. 2017;9(11):1463–1470. DOI: 10.15252/emmm.201707532.
12. Lomashvili K.A., Narisawa S., Millán J.L., O'Neill W.C. Vascular calcification is dependent on plasma levels of pyrophosphate. *Kidney Int*. 2014;85(6):1351–1356. DOI: 10.1038/ki.2013.521.
13. Marulanda J., Eimar H., McKee M.D., Berkvens M., Nelea V., Roman H. et al. Matrix Gla protein deficiency impairs nasal septum growth, causing midface hypoplasia. *J. Biol. Chem*. 2017;292(27):11400–11412. DOI: 10.1074/jbc.M116.76980224.
14. Alehagen U., Aaseth J., Larsson A., Alexander J. Decreased Concentration of Fibroblast Growth Factor 23 (FGF-23) as a Result of Supplementation with Seleniumand Coenzyme Q10 in an Elderly Swedish Population: ASub-Analysis. *Cells.* 2022;11(3):509. DOI: 10.3390/cells11030509.
15. Xiao Y., Peng C., Huang W., Zhang J., Xia M., Zhang Y. et al. Circulating fibroblast growth factor 23 is associated with angiographic severity and extent of coronary artery disease. *PLoS One*. 2013;8(8):e72545. DOI: 10.1371/journal.pone.0072545.
16. Bergmark B.A., Udell J.A., Morrow D.A., Jarolim P., Kuder J.F., Solomon S.D. et al. Klotho, fibroblast growth factor-23, and the renin-angiotensin system - an analysis from the PEACE trial. *Eur. J. Heart Fail.* 2019;21(4):462–470. DOI: 10.1002/ejhf.1424.
17. Morrell N.W., Bloch D.B., ten Dijke P., Goumans M.J., Hata A., Smith J. et al. Targeting BMP signalling in cardiovascular disease and anaemia. *Nat. Rev. Cardiol*. 2016;13(2):106–120. DOI: 10.1038/nrcardio.2015.156.
18. Szulc P., Amri E.Z., Varennes A., Panaia-Ferrari P., Fontas E., Goudable J. et al. Positive Association of High Leptin Level and Abdominal Aortic Calcification in Men - The Prospective MINOS Study. *Circ. J.* 2018; 82(12):2954–2961. DOI: 10.1253/circj.CJ-18-0517.
19. Yang P., Troncone L., Augur Z.M., Kim S.S.J., McNeil M.E., Yu P.B. The role of bone morphogenetic protein signaling in vascular calcification. *Bone*. 2020; 141:115542. DOI: 10.1016/j.bone.2020.115542.
20. Scimeca M., Anemona L., Granaglia A., Bonfiglio R., Urbano N., Toschi N.et al. Plaque calcification is driven by different mechanisms of mineralization associated with specific cardiovascular risk factors. *Nutr. Metab. Cardiovasc. Dis.* 2019; 29(12):1330–1336. DOI: 10.1016/j.numecd.2019.08.009.
21. Carrillo-López N., Panizo S., Alonso-Montes C., Martínez-Arias L., Avello N., Sosa P. et al. High-serum phosphate and parathyroid hormone distinctly regulate bone loss and vascular calcification in experimental chronic kidney disease. *Nephrol. Dial Transplant*. 2019;34(6):934–941. DOI: 10.1093/ndt/gfy287.
22. Hahn D., Hodson E.M., Craig J.C. Interventions for metabolic bone disease in children with chronic kidney disease. *Cochrane Database Syst. Rev*. 2015; 2015(11):CD008327. DOI: 10.1002/14651858.CD008327.pub2.
23. He F., Li L., Li P., Deng Y., Yang Y., Deng Y. et al. Cyclooxygenase-2/sclerostin mediates TGF-β1-induced calcification in vascular smooth muscle cells and rats undergoing renal failure. *Aging (Albany NY)*. 2020;12:21220–21235. DOI: 10.18632/aging.103827.
24. Yu S., Huang W., Zhang H., Guo Y., Zhang B., Zhang G., et al. Discovery of the small molecular inhibitors against sclerostin loop3 as potential anti-osteoporosis agents by structural based virtual screening and molecular design. *Eur. J. Med. Chem*. 2024;271:116414. DOI: 10.1016/j.ejmech.2024.116414.
25. Galea G.L., Lanyon L.E., Price J.S. Sclerostin's role in bone's adaptive response to mechanical loading. *Bone.* 2017;96:38–44. DOI: 10.1016/j.bone.2016.10.008.
26. He W., Li C., Chen Q., Xiang T., Wang P., Pang J. Serum sclerostin and adverse outcomes in elderly patients with stable coronary artery disease undergoing percutaneous coronary intervention. *Aging Clin. Exp. Res*. 2020;32(10):2065–2072. DOI: 10.1007/s40520-019-01393-2.
27. Yang C.Y., Chang Z.F., Chau Y.P., Chen A., Yang W.C., Yang A.H. et al. Circulating Wnt/β-catenin signalling inhibitors and uraemic vascular calcifications. *Nephrol. Dial Transplant.* 2015;30(8):1356–1363. DOI: 10.1093/ndt/gfv043.
28. Krishna S.M., Seto S.W., Jose R.J., Li J., Morton S. K., Biros E. et al. Wnt signaling pathway inhibitor sclerostin inhibits angiotensin ii-induced aortic aneurysmand atherosclerosis. *Arterioscler. Thromb. Vasc. Biol*. 2017;37(3):553–566. DOI: 10.1161/ATVBAHA.116.308723.
29. Klingenschmid G., Tschiderer L., Himmler G., Rungger G., Brugger S., Santer P. et al. Associations of Serum Dickkopf-1 and Sclerostin With Cardiovascular Events: Results From the Prospective Bruneck Study. *J. Am. Heart Assoc*. 2020;9(6):e014816. DOI: 10.1161/JAHA.119.014816.
30. Kanbay M., Solak Y., Siriopol D., Aslan G., Afsar B., Yazici D. et al. Sclerostin, cardiovascular disease and mortality: a systematic review and meta-analysis. *Int. Urol. Nephrol.* 2016;48(12):2029–2042. DOI: 10.1007/s11255-016-1387-8.
31. Brylka L., Jahnen-Dechent W. The role of fetuin-A in physiological and pathological mineralization. *Calcif Tissue Int.* 2013;93(4):355–364. DOI: 10.1007/s00223-012-9690-6.
32. Drygina L.B., Khirmanov V.N. Clinical and Laboratory Markers of Atherosclerotic Calcification. *Medical Alphabet*. 2021;1(30):43–47. (In Russ.). DOI: 10.33667/2078-5631-2021-30-43-47.
33. Laugsand L.E., Ix J.H., Bartz T.M., Djousse L., Kizer J.R., Tracy R.P. et al. Fetuin-A and risk of coronary heart disease: A Mendelian randomization analysis and a pooled analysis of AHSG genetic variants in 7 prospective studies. *Atherosclerosis*. 2015;243(1):44–52. DOI: 10.1016/j.atherosclerosis.2015.08.031.

34. Kubota N., Testuz A., Boutten A., Robert T., Codogno I., Duval X. et al. Impact of fetuin-A on progression of calcific aortic valve stenosis - The COFRASA - GENERAC study. *Int. J. Cardiol.* 2018;265:5257. DOI: 10.1016/j.ijcard.2018.03.070.
35. Makhieva A.T., Mambetova A.M. Fetuin-A as a Marker for Assessing the Risk of Mineral and Bone Disorders and Coronary Artery Calcification in Patients with Chronic Stage 5 Kidney Disease. *Nephrology*. 2022;26(4):105–109. (In Russ.). DOI: 10.36485/1561-6274-2022-26-4-105-109.
36. Drygina L.B., Khirmanov V.N. Coronary Artery Calcification and Metabolic Disorders in Chernobyl Disaster Liquidators. *Medico-Biological and Socio-Psychological Problems of Safety in Emergency*. 2021;(2):11–17. (In Russ.). DOI: 10.25016/2541-7487-2021-0-2-11-17.
37. Bjørklund G., Svanberg E., Dadar M., Card D.J., Chirumbolo S., Harrington D.J. et al. The role of matrix gla protein (MGP) in vascular calcification. *Curr. Med. Chem.* 2020;27(10):1647–1660. DOI: 10.2174/0929867325666180716104159.
38. Chin K.Y. The Relationship between Vitamin K and Osteoarthritis: A Review of Current Evidence. *Nutrients.* 2020;12(5):1208. DOI: 10.3390/nu12051208.
39. Durham A.L., Speer M.Y., Scatena M., Giachelli C.M., Shanahan C.M. Role of smooth muscle cells in vascular calcification: implications in atherosclerosis and arterial stiffness. *Cardiovasc. Res*. 2018;114(4):590–600. DOI: 10.1093/cvr/cvy010.
40. Mayer O. Jr., Seidlerová J., Bruthans J., Filipovský J., Timorácká K., Vaněk J. et al. Desphospho-uncarboxylated matrix Gla-protein is associated with mortality risk in patients with chronic stable vascular disease. *Atherosclerosis*. 2014;235(1):162–168. DOI: 10.1016/j.atherosclerosis.2014.04.027.
41. Capoulade R., Côté N., Mathieu P., Chan K.L., Clavel M.A., Dumesnil J.G. et al. Circulating levels of matrix gla protein and progression of aortic stenosis: a substudy of the Aortic Stenosis Progression Observation: Measuring Effects of rosuvastatin (ASTRONOMER) Trial. *Can. J. Cardiol.* 2014;30(9):1088–1095. DOI: 10.1016/j.cjca.2014.03.025.
42. Berlot A.A., Fu X., Shea M.K., Tracy R., Budoff M., Kim R.S. et al. Matrix Gla protein and the long-term incidence and progression of coronary artery and aortic calcification in the Multi-Ethnic Study of Atherosclerosis. *Atherosclerosis*. 2024;392:117505. DOI: 10.1016/j.atherosclerosis.2024.117505.
43. Sheng K., Zhang P., Lin W., Cheng J., Li J., Chen J. Association of Matrix Gla protein gene (rs1800801, rs1800802, rs4236) polymorphism with vascular calcification and atherosclerotic disease: a meta-analysis. *SciRep*. 2017;7(1):8713. DOI: 10.1038/s41598-017-09328-5.
44. Lutsey P.L., Alonso A., Selvin E., Pankow J.S., Michos E.D., Agarwal S.K. et al. Fibroblast growth factor-23 and incident coronary heart disease, heart failure, and cardiovascular mortality: the Atherosclerosis Risk in Communities study. *J. Am. Heart Assoc*. 2014;3(3):e000936. DOI: 10.1161/JAHA.114.000936.
45. Kestenbaum B., Sachs M.C., Hoofnagle A.N., Siscovick D.S., Ix J.H., Robinson-Cohen C. et al. Fibroblast growth factor-23 and cardiovascular disease in the general population: the Multi-Ethnic Study of Atherosclerosis. *Circ. Heart Fail*. 2014;7(3):409–417. DOI: 10.1161/CIRCHEARTFAILURE.113.000952.
46. Turan M.N., Kircelli F., Yaprak M., Sisman A.R., Gungor O., Bayraktaroglu S. et al. FGF-23 levels are associated with vascular calcification, but not with atherosclerosis, in hemodialysis patients. *Int. Urol. Nephrol*. 2016;48(4):609–617. DOI: 10.1007/s11255-016-1231-1.
47. Holden R.M., Hétu M.F., Li T.Y., Ward E., Couture L.E., Herr J.E. et al. The heart and kidney: abnormal phosphate homeostasis is associated with atherosclerosis. *J. Endocr. Soc*. 2018;3(1):159–170. DOI: 10.1210/js.2018-00311.
48. Takashi Y., Wakino S., Minakuchi H., Ishizu M., Kuroda A., Shima H. et al. Circulating FGF23 is not associated with cardiac dysfunction, atherosclerosis, infection or inflammation in hemodialysis patients. *J. Bone Miner. Metab.* 2020;38(1):70–77. DOI: 10.1007/s00774-019-01027-7.
49. Murcia Casas B., Carrillo Linares J.L., Baquero Aranda I., Rioja Villodres J., Merino Bohórquez V., González Jiménez A. et al. Lansoprazole Increases Inorganic Pyrophosphate in Patients with Pseudoxanthoma Elasticum: A Double-Blind, Randomized, Placebo-Controlled Crossover Trial. *Int. J. Mol. Sci*. 2023;24(5):4899. DOI: 10.3390/ijms24054899.
50. Bartstra J.W., de Jong P.A., Kranenburg G., Wolterink J.M., Isgum I., Wijsman A. et al. Etidronate halts systemic arterial calcification in pseudoxanthoma elasticum. *Atherosclerosis*. 2020;292:37–41. DOI: 10.1016/j.atherosclerosis.2019.10.004.
51. Jansen R.S., Duijst S., Mahakena S., Sommer D., Szeri F., Váradi A. et al. ABCC6-mediated ATP secretion by the liver is the main source of the mineralization inhibitor inorganic pyrophosphate in the systemic circulation-brief report. *Arterioscler. Thromb. Vasc. Biol.* 2014;34(9):1985–1989. DOI: 10.1161/ATVBAHA.114.304017.
52. Maruyama S., Visser H., Ito T., Limsakun T., Zahir H., Ford D. et. al. Phase I studies of the safety, tolerability, pharmacokinetics, and pharmacodynamics of DS-1211, a tissue-nonspecific alkaline phosphatase inhibitor. *Clin. Transl. Sci*. 2022;15(4):967–980. DOI: 10.1111/cts.13214.
53. Gu W., Wei Y., Tang Y., Zhang S., Li S., Shi Y. et al. Supplement of exogenous inorganic pyrophosphate inhibits atheromatous calcification in Apolipoprotein E knockout mice. *Heliyon.* 2023;9(8):e19214. DOI: 10.1016/j.heliyon.2023.e19214.
54. Rathan S., Yoganathan A.P., O'Neill C.W. The role of inorganic pyrophosphate in aortic valve calcification. *J. Heart Valve Dis*. 2014;23(4):387–394.
55. Villa-Bellosta R. Synthesis of extracellular pyrophosphate increases in vascular smooth muscle cells during phosphate-induced calcification. *Arterioscler. Thromb. Vasc. Biol*. 2018;38(9):2137–2147. DOI: 10.1161/ATVBAHA.118.311444. PMID: 30002059.

56. Rattazzi M., Bertacco E., Iop L., D'Andrea S., Puato M., Buso G. et al. Extracellular pyrophosphate is reduced in aortic interstitial valve cells acquiring a calcifying profile: implications for aortic valve calcification. *Atherosclerosis.* 2014;237(2):568–576. DOI: 10.1016/j.atherosclerosis.2014.10.027.
57. Tang H., Zhang X., Xue G., Xu F., Wang Q., Yang P. et al. The biology of bone morphogenetic protein signaling pathway in cerebrovascular system. *Chin. Neurosurg. J.* 2021;7(1):36. DOI: 10.1186/s41016-021-00254-0.
58. Aluganti Narasimhulu C., Singla D.K. The role of bone morphogenetic protein 7 (BMP-7) in inflammation in heart diseases. *Cells.* 2020;9(2):280. DOI: 10.3390/cells9020280.
59. Elmadbouh I., Singla D.K. BMP-7 Attenuates inflammation-induced pyroptosis and improves cardiac repair in diabetic cardiomyopathy. *Cells.* 2021;10(10):2640. DOI: 10.3390/cells10102640.
60. Merino D., Villar A.V., García R., Tramullas M., Ruiz L., Ribas C. et al. BMP-7 attenuates left ventricular remodelling under pressure overload and facilitates reverse remodelling and functional recovery. *Cardiovasc. Res*. 2016;110(3):331–345. DOI: 10.1093/cvr/cvw076.
61. Yu X., Guan W., Zhang Y., Deng Q., Li J., Ye H. et al. Large-scale gene analysis of rabbit atherosclerosis to discover new biomarkers for coronary artery disease. *Open Biol*. 2019;9(1):180238. DOI: 10.1098/rsob.180238.
62. Singla D.K., Singla R., Wang J. BMP-7 Treatment increases m2 macrophage differentiation and reduces inflammation and plaque formation in Apo E-/-mice. *PLoS One*. 2016;11(1):e0147897. DOI: 10.1371/journal.pone.0147897.
63. Urbina P., Singla D.K. BMP-7 attenuates adverse cardiac remodeling mediated through M2 macrophages in prediabetic cardiomyopathy. *Am. J. Physiol. Heart Circ. Physiol.* 2014;307(5):H762–772. DOI: 10.1152/ajpheart.00367.2014.
64. Wang C., Chang L., Wang J., Xia L., Cao L., Wang W. et al. Leptin and risk factors for atherosclerosis: A review. *Medicine (Baltimore).* 2023;102(46):e36076. DOI: 10.1097/MD.0000000000036076.
65. Sweeney T., Ogunmoroti O., Ndumele C.E., Zhao D., Varma B., Allison M.A. et al. Associations of adipokine levels with the prevalence and extent of valvular and thoracic aortic calcification: The Multi-Ethnic Study of Atherosclerosis (MESA). *Atherosclerosis.* 2021;338:15–22. DOI: 10.1016/j.atherosclerosis.2021.11.002.
66. Myasoedova V.A., Bertolini F., Valerio V., Moschetta D., Massaiu I., Rusconi V. et al. The Role of Adiponectin and Leptin in Fibro-Calcific Aortic Valve Disease: A Systematic Review and Meta-Analysis. *Biomedicines.* 2024;12(9):1977. DOI: 10.3390/biomedicines12091977.
67. Criqui M.H., Denenberg J.O., McClelland R.L., Allison M.A., Ix J.H., Guerci A. et al. Abdominal aortic calcium, coronary artery calcium, and cardiovascular morbidity and mortality in the Multi-Ethnic Study of Atherosclerosis. *Arterioscler. Thromb. Vasc. Biol.* 2014;34(7):1574–1579.
68. Liu Y., Gu Y., Shen Y., Lin B., Li Y., He X. et al. association between serum leptin level and calcific aortic valve disease. *J. Am. Heart Assoc*. 2019;8(19):e012495. DOI: 10.1161/JAHA.119.012495.
69. Roy N., Haddad D., Yang W., Rosas S.E. Adipokines and coronary artery calcification in incident dialysis participants. *Endocrine*. 2022;77(2):272–280. DOI: 10.1007/s12020-022-03111-x.
70. Yang H., Guo W., Li J., Cao S., Zhang J., Pan J. et al. Leptin concentration and risk of coronary heart disease and stroke: A systematic review and meta-analysis. *PloS One*. 2017;12(3):e0166360. DOI: 10.1371/journal.pone.0166360.
71. Patidar A., Singh D.K., Winocour P., Farrington K., Baydoun A.R. Human uraemic serum displays calcific potential in vitro that increases with advancing chronic kidney disease. *Clin. Sci. (Lond.).* 2013;125:237–245. DOI: 10.1042/CS20120638.
72. Zhang M., Sara J.D., Wang F.L., Liu L.P., Su L.X., Zhe J. et al. Increased plasma BMP-2 levels are associated with atherosclerosis burden and coronary calcification in type 2 diabetic patients. *Cardiovasc Diabetol*. 2015;14:64. DOI: 10.1186/s12933-015-0214-3.
73. Wang N., Guo Y., Dong Y., Li X., Liu Q., Liu Q. et al. Association of plasma bone morphogenetic protein-4 levels with arterial stiffness in hypertensive patients. *J. Clin. Lab. Anal.* 2022;36(11):e24746. DOI: 10.1002/jcla.24746.
74. Feng M., Xu M., Wang Q., Xia S., Yu C., Li M. et al. Association of parathyroid hormone with risk of hypertension and type 2 diabetes: a dose-response meta-analysis. *BMC Cardiovasc. Disord.* 2024;24(1):13. DOI: 10.1186/s12872-023-03682-1.
75. Hagström E., Michaëlsson K., Melhus H., Hansen T., Ahlström H., Johansson L. et al. Plasma-parathyroid hormone is associated with subclinical and clinical atherosclerotic disease in 2 community-based cohorts. *Arterioscler. Thromb. Vasc. Biol.* 2014;34(7):1567–1573. DOI: 10.1161/ATVBAHA.113.303062.
76. Fernández-Villabrille S., Martín-Vírgala J., Martín-Carro B., Baena-Huerta F., González-García N., Gil-Peña H. et al. RANKL, but Not R-spondins, is involved in vascular smooth muscle cell calcification through LGR4 interaction. *Int. J. Mol. Sci*. 2024;25(11):5735. DOI: 10.3390/ijms25115735.
77. Hsu S., Prince D.K., Williams K., Allen N.B., Burke G.L., Hoofnagle A.N.et al. Clinical and biomarker modifiers of vitamin D treatment response: the Multi-Ethnic Study of Atherosclerosis. *Am. J. Clin. Nutr*. 2022;115(3):914–924. DOI: 10.1093/ajcn/nqab390.
78. Robinson-Cohen C., Hoofnagle A.N., Ix J.H., Sachs M.C., Tracy R.P., Siscovick D.S. Racial differences in the association of serum 25-hydroxyvitamin D concentration with coronary heart disease events. *JAMA*. 2013;310(2):179–188. DOI: 10.1001/jama.2013.7228.
79. Dudenkov D.V., Mara K.C., Petterson T.M., Maxson J.A., Thacher T.D. Serum 25-Hydroxyvitamin D Values and Risk of All-Cause and Cause-Specific Mortality: A Population-Based Cohort Study. *Mayo*

*Clin. Proc*. 2018;93(6):721–730. DOI: 10.1016/j.mayocp.2018.03.006.
80. Amrein K., Quraishi S.A., Litonjua A. ., Gibbons F.K., Pieber T.R., Camargo C.A. et al. Evidence for a U-shaped relationship between prehospital vitamin D status and mortality: a cohort study. *J. Clin. Endocrinol. Metab*. 2014;99(4):1461–1469. DOI: 10.1210/jc.2013-3481.
81. Sempos C.T., Durazo-Arvizu R.A., Dawson-Hughes B., Yetley E.A., Looker A.C., Schleicher R L. et al. Is there a reverse J-shaped association between 25-hydroxyvitamin D and all-cause mortality? Results from the U.S. nationally representative NHANES. *J. Clin. Endocrinol. Metab*. 2013;98(7):3001–3009. DOI: 10.1210/jc.2013-1333.

## Author Contribution

Demina E.D. – drafting of the article. Shramko V.S. – conception and design. The authors approved the final version of the article before publication.

## Author Information

**Demina Elizaveta D.** – Junior Researcher, Laboratory for Clinical Biochemical and Hormonal Studies of Internal Diseases, IIPM – Branch of IC&G SB RAS, Novosibirsk, chaussova.liza@gmail.com, https://orcid.org/0009-0005-0611-1486

**Shramko Viktoriya S.** – Cand. Sci. (Med.), Researcher, Laboratory for Clinical Biochemical and Hormonal Studies of Internal Diseases, IIPM – Branch of IC&G SB RAS; Head of the Department of Clinical Biochemical and Molecular Genetic Research Methods, IIPM – Branch of IC&G SB RAS, Novosibirsk, Nosova@211.ru, https://orcid.org/0000-0002-0436-2549

(✉) **Demina Elizaveta D.,** chaussova.liza@gmail.com

Received on March 27, 2025;
approved after peer review on May 19, 2025;
accepted on May 22, 2025

УДК 616-006-031-073.916
https://doi.org/10.20538/1682-0363-2025-3-149-162

# Potential of PSMA-targeted imaging of tumors with various localizations

**Medvedeva A.A.[1, 2], Vysotskaya V.V.[1], Muravleva A.V.[1], Zeltchan R.V.[1, 2], Rybina A.N.[1, 2], Gol'dberg V.E.[1], Chernov V.I.[1, 2, 3]**

*[1] Cancer Research Institute, Tomsk National Research Medical Center (NRMC), Russian Academy of Sciences*
*5 Kooperativny St., 634009 Tomsk, Russian Federation*

*[2] National Research Tomsk Polytechnic University (NR TPU)*
*30 Lenin Ave., 634050 Tomsk, Russian Federation*

*[3] National Research Center Kurchatov Institute*
*1 Academician Kurchatov Sq., 123098 Moscow, Russian Federation*

*[4] Siberian State Medical University (SibSMU)*
*2 Moskovsky trakt, 634050 Tomsk, Russian Federation*

## ABSTRACT

Diagnosis and therapy of malignant neoplasms are increasingly focused on the use of molecular targets involved in the multistage process of tumor pathogenesis. Prostate-specific membrane antigen (PSMA) is currently one of such molecular markers for prostate cancer, and over the past two decades, there have been active developments in PSMA-directed theranostics for prostate cancer therapy. However, numerous studies in recent years have shown that PSMA, despite its name, is not a specific molecular marker only for prostate cancer screening. It was revealed that the expression of this receptor in other neoplasms is associated with neovascular endothelium, which was the prerequisite for the beginning of studies on the clinical application of PSMA-directed visualization of tumors with various localizations.

This lecture analyzes the possibilities of using PSMA-targeted radionuclide diagnosis for various histologic types of tumors, as well as the features of PSMA expression in some tumors. The authors of the lecture demonstrate existing clinical examples of the results of diagnostic studies and the use of targeted radionuclide therapy. The lecture presents possible applications of PSMA-targeted visualization methods for obtaining additional information about the features of the tumor process.

**Keywords:** PSMA, PET/CT, cancer, endothelial, radionuclide, therapy, diagnosis

**Conflict of interest.** The authors declare the absence of obvious or potential conflicts of interest related to the publication of this article.

**Source of financing.** The authors state that they received no funding for the study.

**For citation:** Medvedeva A.A., Vysotskaya V.V., Muravleva A.V., Zeltchan R.V., Rybina A.N., Gol'dberg V.E., Chernov V.I. Potential of PSMA-targeted imaging of tumors with various localizations. *Bulletin of Siberian Medicine.* 2025;24(3):149–162. https://doi.org/10.20538/1682-0363-2025-3-149-162.

✉ *Medvedeva Anna A.,* medvedeva@tnimc.ru

# Потенциал ПСМА-таргетной визуализации опухолей различных локализаций

**Медведева А.А.[1,2], Высоцкая В.В.[1], Муравлева А.В.[1,4], Зельчан Р.В.[1,2], Рыбина А.Н.[1,2], Гольдберг В.Е.[1], Чернов В.И.[1,2,3]**

*[1] Научно-исследовательский институт (НИИ) онкологии, Томский национальный исследовательский медицинский центр (НИМЦ) Российской академии наук*
*Россия, 634009, г. Томск, Кооперативный пер., 5*

*[2] Национальный исследовательский Томский политехнический университет (НИ ТПУ)*
*Россия, 634050, г. Томск, пр. Ленина, 30*

*[3] Национальный исследовательский центр (НИЦ) «Курчатовский институт»*
*Россия, 123098, г. Москва, пл. Академика Курчатова, 1*

*[4] Сибирский государственный медицинский университет (СибГМУ)*
*Россия, 634050, г. Томск, Московский тракт, 2*

**РЕЗЮМЕ**

Диагностика и терапия злокачественных новообразований в современной онкологии все больше ориентируется на использование молекулярных мишеней, участвующих в многостадийном процессе патогенеза опухолей. Простат-специфический мембранный антиген (ПСМА) является на сегодняшний день одним из таких молекулярных маркеров для рака предстательной железы, и в течение последних двух десятилетий отмечается активное развитие ПСМА-тераностики опухолей простаты. Однако многочисленные исследования последних лет показали, что ПСМА, несмотря на свое название, не является специфичным молекулярным маркером только для ткани предстательной железы. Выявлено, что экспрессия этого рецептора в других новообразованиях ассоциирована в большей степени с неоваскулярным эндотелием, что послужило началу исследований по клиническому применению ПСМА-направленной визуализации опухолей различных локализаций.

В данной лекции проанализированы возможности применения ПСМА-направленной радионуклидной диагностики, главным образом методов позитронной эмиссионной томографии, для различных гистологических вариантов неоплазий, а также особенности ПСМА-экспрессии некоторых опухолей. Авторы лекции демонстрируют существующие клинические примеры не только результатов диагностических исследований, но в ряде случаев и применения таргетной радионуклидной терапии. В лекции представлены возможные точки приложения ПСМА-направленных методов визуализации с точки зрения получения дополнительной информации об особенностях течения опухолевого процесса.

**Ключевые слова:** ПСМА, ПЭТ/КТ, рак, эндотелиальный, радионуклидный, терапия, диагностика

**Конфликт интересов.** Авторы декларируют отсутствие явных и потенциальных конфликтов интересов, связанных с публикацией настоящей статьи.

**Источник финансирования.** Авторы заявляют об отсутствии финансирования при проведении исследования.

**Для цитирования:** Медведева А.А., Высоцкая В.В., Муравлева А.В., Зельчан Р.В., Рыбина А.Н., Гольдберг В.Е., Чернов В.И. Потенциал ПСМА-таргетной визуализации опухолей различных локализаций. *Бюллетень сибирской медицины.* 2025;24(3):149–162. https://doi.org/10.20538/1682-0363-2025-3-149-162.

## INTRODUCTION

Diagnosis and therapy of malignant neoplasms in modern oncology are increasingly focused on the use of molecular targets involved in the multistage process of tumor pathogenesis. This was facilitated by numerous studies on the mechanisms of cancer development and the identification of key targets of the pathogenesis of particular carcinogenesis. One of such molecular markers of prostate cancer (PCa) is prostate-specific membrane antigen (PSMA), type II integral membrane glycoprotein (glutamate

carboxypeptidase II, or GCPII) [1, 2]. Glutamate carboxypeptidase II was found to consist of three domains: a short N-terminal intracellular portion, a hydrophobic transmembrane region, and an extracellular C-terminal domain [3, 4]. A specific feature of PSMA is its dual nature: it is not only a receptor protein, but also an enzyme that plays a key role in prostate carcinogenesis, glutamatergic neurotransmission (NAALADase), and folic acid absorption (folate hydrolase FOLH1) [5]. Thus, numerous studies have shown that PSMA is characterized as a multifunctional agent involved in the development and course of PCa, in particular in proliferation, apoptosis, and cellular and tissue homeostasis, and also exerting an enzymatic function [6, 7]. Studies have shown a direct correlation between the level of PSMA expression and the degree of prostate tumor malignancy, the stage of the disease, and aggressive behavior of the tumor [8].

Increased expression of PSMA on the cell membrane of PCa has made it a suitable target for molecular imaging and radioligand therapy in patients with PCa [9]. Over the past decades, numerous small-molecule PSMA-binding agents have been developed to create diagnostic and therapeutic radiopharmaceuticals for imaging and treatment of PCa [10–12]. Clinical trials convincingly demonstrate the effectiveness of these radiopharmaceuticals not only in diagnosis, but also in the treatment of this disease.

Further studies have shown that PSMA, despite its name, is not specific to prostate tissue alone. The extracellular domain of PSMA serves as a promising therapeutic target for PCa, but it has also been found to be selectively expressed in the vasculature of other solid tumors [13–16]. This antigen is found in healthy tissues of the salivary glands, duodenal mucosa, renal tubular cells, a subpopulation of neuroendocrine cells in the colonic crypts, as well as in tumor cells – for example, in some subtypes of transitional cell carcinoma, renal cell carcinoma, and colon cancer. However, in contrast to the mechanisms of PSMA expression in PCa cells, its expression in other neoplasms is associated to a greater extent with neovascular endothelium. It should be noted, that this antigen was not detected in the vascular epithelium of healthy tissues or benign formations.

The aim of this lecture was to analyze the current possibilities of using PSMA-targeted radionuclide diagnosis for various histologic types of tumors, taking into account the features of PSMA expression in the tumors. The lecture is intended for researchers and specialists in the field of nuclear medicine and oncology.

## FEATURES OF PSMA DIAGNOSIS OF VARIOUS TUMORS

***Thyroid cancer*** (TC) is the most common endocrine malignancy worldwide and its incidence is increasing annually, largely due to improved screening methods [17]. Most newly diagnosed TC are small and asymptomatic papillary lesions, belonging to a significant number of subclinical indolent tumors that would probably not be detected during the patients' lifetime in most cases. However, the increase in the number of newly diagnosed tumors also concerns high-risk TC, aggressive histopathological subtypes, as well as tumors detected at a late stage of the disease, with gross extrathyroidal extension [18]. In this context, the observed increase in mortality rates among patients with advanced TC suggests aggressive postoperative treatment and accurate risk stratification. Post-therapy whole-body imaging after radioactive iodine administration has historically played a significant role in assessing tumor burden and radioiodine sensitivity of residual or recurrent disease [18].

Unfortunately, only approximately 30% of patients with TC metastases demonstrate radioactive iodine uptake. In most cases, metastatic tumors are either initially radioiodine-negative, or lose their ability to accumulate it over time, or progression of the disease is observed after treatment with radioactive iodine, which indicates the development of radioiodine refractoriness [18, 19]. In widespread clinical practice, with the development of TC resistance to radioactive iodine, the main method of radiodiagnosis for detecting relapse of the disease, metastases to the lymph nodes, and distant metastases is contrast-enhanced computed tomography (CT). In addition, this method is also the main tool for assessing the response to treatment with tyrosine kinase inhibitors [18, 20].

In terms of nuclear imaging methods, besides routine radioactive iodine scintigraphy, the most studied method for diagnosing radioiodine-resistant thyroid cancer (rrTC) is fluorine-18 fluorodeoxyglucose ($[^{18}F]$F-FDG) positron emission tomography (PET). According to the recommendations, this study is advisable for patients with TC with elevated serum thyroglobulin levels and a negative result of whole-body radioactive iodine scintigraphy after therapy [18]. The diagnostic accuracy of this method is influenced

by several factors, including dedifferentiation and tumor load – higher sensitivity of the study is observed in patients with aggressive histologic subtypes. High-intensity [$^{18}$F]F-FDG uptake on PET images is considered an independent prognostic factor for overall survival in patients with TC [20, 21].

In the presence of signs of tumor progression, patients with radioiodine-refractory differentiated TC are recommended to receive targeted therapy with tyrosine kinase inhibitors (lenvatinib, sorafenib) [22–26]. Their mechanism of action on tumors is mediated by suppression of the kinase activity of vascular endothelial growth factor (VEGF) receptors [26, 27]. Since PSMA is frequently expressed on the cell membrane of neovascular endothelial cells of various solid tumors, nuclear imaging methods targeting PSMA may be used as a biomarker of neoangiogenesis and may possibly be involved in predicting the efficacy of antiangiogenic therapy.

Several studies have demonstrated that intense PSMA staining in the endothelium of some TC subtypes, including papillary and follicular cancer, correlated with a more aggressive clinical course. In particular, it was shown, that patients with moderate or strong PSMA expression were more likely to develop rrTC [28–30]. Moreover, anaplastic TC, despite its well-known aggressive behavior, was characterized by lower PSMA expression compared to well-differentiated tumors, which may probably be associated with a lower density of microvessels in this variant of the disease compared to highly differentiated TC [28, 31].

The diagnostic accuracy assessment of PET/CT with PSMA ligands demonstrated relatively weak performance in a number of studies [32–35]. Only two studies reported high incidence of pathological findings (100%) [36, 37]. More intense uptake of PSMA ligands was observed in follicular cancers, whereas low-intensity or absent radiopharmaceutical uptake was observed in dedifferentiated tumors [33, 35, 36]. At the same time, the intensity of PSMA ligand accumulation did not correlate with the results of the immunohistochemical analysis, especially in dedifferentiated TC. Moreover, when analyzing standardized uptake value (SUVmax), all authors noted significant heterogeneity of this parameter (from 1.0 to 39.7). A number of studies also described the comparative analysis of PET findings with PSMA ligands and with [$^{18}$F]F-FDG and showed that studies with PSMA-targeted radiopharmaceuticals demonstrated lower diagnostic efficiency, however, the histopathologic variants of tumors were not taken into account in the comparison [32–36].

It should be noted that in the presented references, as a rule, [$^{68}$Ga]Ga-PSMA-11 was used as a diagnostic radiopharmaceutical targeting PSMA receptors. Two studies report theranostics-based use of [$^{177}$Lu]Lu-PSMA-617 in three patients with rrTC [35, 36]. Two of the included patients exhibited a minor and temporary response to treatment, followed by an increase in serum thyroglobulin levels and disease progression several months after the end of therapy, while one patient experienced disease progression one month after treatment.

***Kidney cancer*** is a common type of tumor, ranking 14th among all newly diagnosed malignant tumors in the world, according to WHO data, and accounting for 3% of the total number of diagnosed tumors [38, 39]. Currently new data are emerging regarding the genomic and molecular characteristics of renal malignancies, but histopathological characteristics are still taken into account when prescribing therapy and analyzing the prognosis of the disease [40, 41]. Clear cell renal cell carcinoma (ccRCC) is the most common histologic type of kidney cancer, characterized by high immunogenicity. In addition, ccRCC is considered to be a highly vascularized tumor due to excessive production of platelet-derived growth factor (PDGF) and VEGF by tumor cells [41]. Standard examination including CT and/or MRI may be considered insufficient since 20–30% of patients with apparently resectable tumors experience progression within a relatively short time after surgery [42].

The most studied nuclear medicine method for detecting ccRCC is PET/CT with [$^{18}$F]F-FDG. [43]. However, this study does not play a key role in the treatment of this category of patients and is currently not recommended as a diagnostic method for ccRCC [44–46]. This limitation is mainly due to the physiological renal excretion of [$^{18}$F]F-FDG, which naturally complicates visualization of the primary tumor [43]. In addition, ccRCC in general is characterized by a relatively low level of [$^{18}$F]F-FDG uptake, but the underlying mechanism of this phenomenon is not fully understood. Nevertheless, a recent study showed that [$^{18}$F]F-FDG uptake reflected the level of FBP1 (fructose-1,6-bisphosphatase 1) expression, which is an essential intermediate of glycolysis. More intense accumulation of FBP1 was observed in ccRCC tumors with low FBP1 expression [48].

As already mentioned, ccRCC is considered to be a highly vascularized tumor and this may be a

rationale for the use of nuclear medicine methods with radiopharmaceuticals targeting PSMA receptors, which are expressed, among other things, on the surface of neovascular endothelial cells [13–16]. This is especially relevant in light of the fact that the combination of immunotherapy and antineoangiogenetic therapy is the standard of care for metastatic ccRCC. This means that PSMA-guided PET/CT may become a valuable tool for predicting treatment outcomes and assessing the response to this therapy in patients with ccRCC [44–46].

Besides, it should be noted, that surgical treatment with radical or partial nephrectomy remains the only effective method of treating localized renal cancer and postoperative changes may complicate the differentiation of local tumor recurrence from postoperative changes using [$^{18}$F]F-FDG PET, since accumulation of this radiopharmaceutical can also be observed in foci of inflammation, abscesses, and areas of fat necrosis [46]. In a number of studies, PET/CT with PSMA ligands demonstrated higher accuracy in determining tumor burden in patients with ccRCC, visualizing more metastatic foci than conventional diagnostic methods, thus leading to a reduction in false-positive results and changing patient treatment strategy in a significant percentage of cases [49–55].

The few studies on this topic have analyzed the level of [$^{68}$Ga]Ga-PSMA-11 accumulation depending on the stage of the disease and histopathological type of ccRCC and it was shown that SUVmax was significantly higher in tumors with a more aggressive phenotype [49–52]. In the study by Y. Liu et al. [56], comparison of the results of PET studies with [$^{18}$F]F-FDG and [$^{18}$F]F-DCFPyL showed the advantage of using PSMA ligand in detecting bone metastases and disease recurrence. Regarding the visualization of metastatic lesions in visceral organs and lymph nodes, the higher detection rate with [$^{18}$F]F-DCFPyL was not statistically significant, but SUVmax and tumor-to-background ratio were significantly higher than those of [$^{18}$F]F-FDG.

Similar results were presented in the works by V. S. Ilyakov et al. [57, 58], where the authors analyzed comparative PET studies with [$^{18}$F]F-PSMA-1007 and [$^{18}$F]F-FDG in patients with locally advanced, metastatic ccRCC and suspected local recurrence after surgical treatment. Regarding the use of [$^{99m}$Tc]Tc-HYNIC-PSMA, its high physiological accumulation in the kidneys is likely to be a limiting factor for the use of this radiopharmaceutical in the diagnosis of primary renal tumor (Fig. 1). However, the use of single-photon emission computed tomography (SPECT) with PSMA ligands can also be considered as an alternative method for identifying advanced forms of the disease, or, in the future, as a method for selecting patients for therapy.

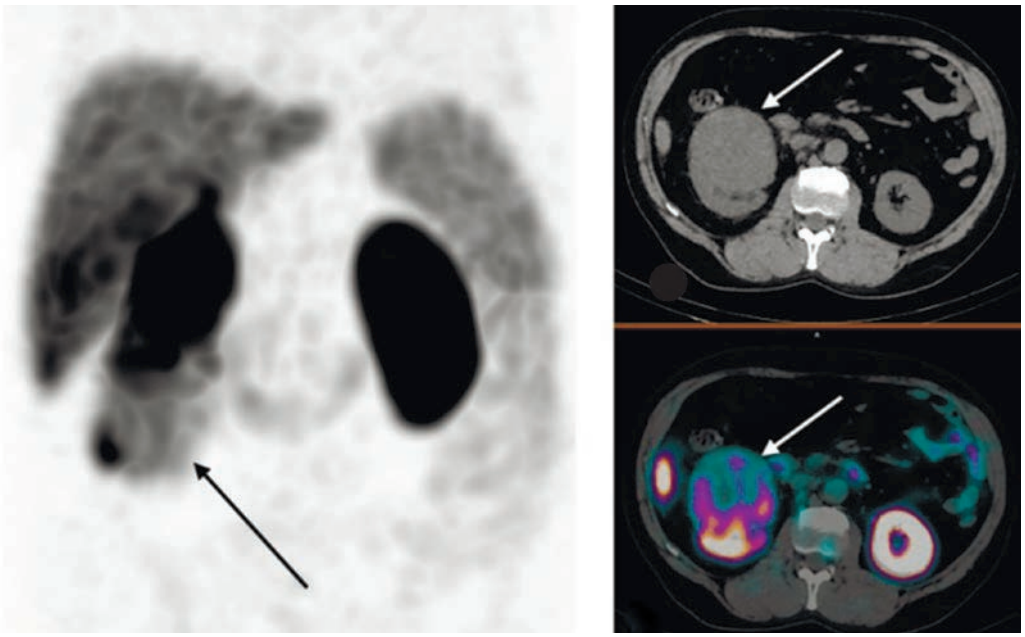

*a* *b*

Fig. 1. MIP- reconstruction (*a*), CT and combined SPECT / CT images (*b*) at 2 h after administration of [$^{99m}$Tc]Tc-HYNIC-PSMA in a patient with ccRCC, grade2: the arrow indicates the tumor, SUVmax 7.72 (self-reported).

***Breast cancer*** (BC) is one of the leading malignant tumors in the world in terms of incidence, ranking fifth in terms of deaths. Over the past 10 years, the annual standardized growth rate of incidence has amounted to 1.97% in Russia [59]. Breast cancer diagnosis requires a personalized and multimodal approach taking into account age, medical history, heredity, and the structure of the mammary glands. The use of conventional imaging methods is included in the standards for examining patients with BC, as well as nuclear medicine methods, which have already become a routine method for examining this category of patients. In recent years, [$^{18}$F]F-FDG PET/CT has become widely used to assess the extent of BC in cases where standard examination methods are ambiguous [60]. One of the limitations of this method is false negative results in some types of tumors and false positive results in some benign processes. Few studies to date demonstrate the potential of nuclear medicine methods with PSMA-targeted radiopharmaceuticals for imaging malignant BC [61–65], but most of them are represented by isolated clinical cases.

In the studies by A.G.Wernicke et al. [66], PSMA expression was assessed in the tumor-associated vasculature related with invasive breast carcinomas in 106 patients – 92 cases were primary BC, 14 patients had tumor metastases to the brain. Analysis of the obtained results showed that the tumor-associated vasculature was PSMA-positive in 68/92 (74%) cases of primary BC and in 14/14 (100%) cases of metastatic BC. PSMA receptors were not detected in healthy breast tissue or carcinoma cells and in almost all cases (98%) in healthy breast tissue vasculature. The authors found a statistically significant correlation between increased PSMA expression in the tumor-associated vasculature and tumor size, Ki-67 proliferation index, receptor status, and overall survival.

Several studies have also noted marked vascular PSMA expression in higher grade, Her2-positive, and triple-negative tumors [67, 68]. Thus, in the study by Y. Tolkach et al. [67], a negative correlation was shown between vascular PSMA expression and tumor hormone receptor expression. There was no correlation between pN stage, locoregional progression status, development of distant metastases, tumor size, and PSMA expression.

The study by N. Andryszak et al. [68] compared findings of PET/CT with [$^{18}$F]F-PSMA-1007 and [$^{18}$F]F-FDG in patients with triple-negative BC ($n$ = 10). The detection rate of triple-negative tumors with [$^{18}$F]F-PSMA-1007 was comparable to [$^{18}$F]F-FDG in most patients. However, in patients with distant metastases, a higher number of metastatic lesions were detected using [$^{18}$F]F-PSMA-1007 due to more intense accumulation (higher SUVmax values) compared to [$^{18}$F]F-FDG. In addition, [$^{18}$F]F-PSMA-1007 demonstrated higher diagnostic efficiency in detecting metastatic lesions in areas with high physiological accumulation of [$^{18}$F]F-FDG, such as the brain and adjacent bones of the skull.

The literature also described a case of detecting metastatic BC following SPECT/CT with [$^{99m}$Tc]Tc-EDDA/HYNIC-PSMA, which was performed on a patient with suspected bone metastases from prostate cancer. Radiopharmaceutical accumulations were visualized in the projection of bone structures and the left mammary gland, where hormone-positive infiltrating ductal carcinoma was confirmed by biopsy results [69]. Our clinical experience also indicates the possibility of using SPECT/CT with [$^{99m}$Tc]Tc-HYNIC-PSMA for visualization of the primary tumor and metastases in this pathology (Fig. 2). A case of radionuclide PSMA therapy in a patient with metastatic BC with disease progression after 2 courses of [$^{177}$Lu]Lu-PSMA-617 is described [64].

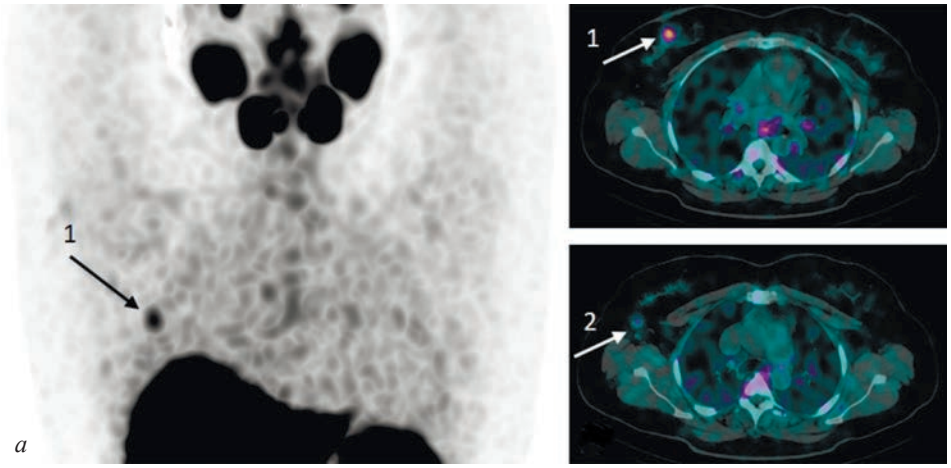


Fig. 2. MIP- reconstruction (*a*) and combined SPECT/CT images (*b*) at 2 h after administration of [$^{99m}$Tc]Tc-HYNIC-PSMA in a patient with BC, metastasis to the axillary lymph node: 1 – breast tumor, SUVmax 5.1; 2 – enlarged lymph node, SUVmax 1.93 (self-reported)

***Hepatocellular carcinoma*** (HCC) is the most common type of liver cancer, accounting for approximately 90% of cases [70, 71]. The diagnosis of HCC is complicated by the latent course of the disease, fluctuations in serum alpha-fetoprotein levels, and inconclusive radiological results [72]. The most studied nuclear medicine methods for HCC are PET/CT with [$^{18}$F]F-FDG and labeled choline (with $^{18}$F or $^{11}$C). Both methods demonstrate a potential role in identifying extrahepatic lesions in HCC, however, their use is limited by the broader capabilities of CT and magnetic resonance imaging (MRI). In addition, [$^{18}$F]F-FDG PET/CT is known to have limitations for staging and restaging of HCC [73]. Since the enzymes of well-differentiated HCC are similar to those observed in a healthy liver, [$^{18}$F]F-FDG-6-phosphate formed after phosphorylation of [$^{18}$F]F-FDG may be dephosphorylated and released from the cells, which explains low uptake of [$^{18}$F]F-FDG and, consequently, low sensitivity of the assay.

The possibilities of PSMA-guided radionuclide diagnosis of HCC are currently presented in a few literary sources. In all the presented sources, [$^{68}$Ga]Ga-PSMA-11 was used as the radiopharmaceutical, which is undoubtedly justified, since the biodistribution feature of [$^{18}$F]F-PSMA-1007, due to its lipophilicity, is the dominant hepatic clearance, which, in theory, makes it less suitable for visualizing HCC [74–79]. On the whole, the results of the studies demonstrate the advantages of using PSMA ligands over [$^{18}$F]F-FDG both in terms of the number of detected lesions and the intensity of accumulation in the detected tumor foci [74, 75, 77].

In the study by M. Kesler et al. [74], [$^{68}$Ga]Ga-PSMA-11 uptake was shown to correlate with tumor vascularization, and HCC lesions are most often hypervascular. Radiopharmaceutical uptake was observed in 36 of 37 liver tumors, and only ten of these lesions were FDG-positive. Besides, the method allowed the authors to differentiate tumor formations and regenerative nodes in the context of cirrhotic changes and this fact may have high practical significance, since the cirrhotic liver has a nodular architecture with altered vascularization, which complicates the differentiation of regenerative nodes and HCC using traditional visualization methods.

Additionally, PSMA PET/CT showed slightly higher efficiency in detecting hepatic and extrahepatic HCC lesions compared to CT and MRI [74,76–78]. When comparing semi-quantitative parameters of PET with PSMA ligands (SUVmax) with the results of laboratory studies, in particular the level of alpha-fetoprotein and CA 19-9, no statistically significant correlation was found [76, 77]. Generally, the results of the studies demonstrate fairly variable absorption of PSMA ligands: according to different authors, the average SUVmax values vary from 8.3 to 16.7, while the average tumor-to-background values have a smaller spread – from 2 to 3.6 [74–79].

The rich blood supply of HCC plays a crucial role in tumor growth and metastasis. First-line therapy for locally advanced and metastatic HCC consists of a combination of immunotherapy and anti-neoangiogenic therapy [70]. In this situation, PET/CT with PSMA radioligands may become a valuable tool for predicting therapy outcomes and assessing a treatment response. It should also be noted that HCC is often diagnosed at late stages of the disease, which limits the possibilities of standard treatment for these patients. In this regard, the concept of a theranostic approach targeting PSMA receptors may become a relevant direction in the treatment of this disease. The study by N. Hirmas et al. [78] presented the results of [$^{177}$Lu]Lu-PSMA-617 administration to two patients who were diagnosed with liver lesions with high uptake of [$^{68}$Ga]Ga-PSMA-11 (SUVmax more than 10). However, in both cases, intratherapeutic dosimetry based on SPECT/CT showed that the radiation dose to the tumor was 10 times lower than that typically achieved in a single cycle of external beam radiotherapy for HCC. In this regard, radionuclide therapy with [$^{177}$Lu]Lu-PSMA-617 was suspended after one administration. Considering that nearly 95% of HCCs exhibit high levels of endothelial PSMA expression, it may be used as a therapeutic target for radioligand therapy [79–81]. The study of this issue may become quite relevant.

***Lymphomas*** are among the most difficult malignant pathologies in terms of diagnosis and therapy. In addition, lymphomas are a fairly heterogeneous group of diseases in oncohematology. The incidence of this pathology is steadily increasing – the number of cases has increased by 22% over the past ten years [59]. Treatment of lymphomas is almost always associated with chemotherapy courses of varying degrees of toxicity and duration, which leads to the development of a number of complications, including delayed ones. With the advent of PET/CT with [$^{18}$F]F-FDG, the quality of lymphoma diagnosis has significantly improved, including monitoring during therapy, which has made it possible to optimize the therapeutic effect and, accordingly, reduce the number of complications

[82]. Thus, [$^{18}$F]F-FDG is currently the drug of choice for radionuclide diagnosis of Hodgkin's lymphoma and non-Hodgkin's lymphoma (NHL); however, some subtypes of indolent NHL are FDG-negative [83, 84].

In connection with the active introduction of PSMA theranostics into widespread clinical practice, reports of clinical cases of lymphoma visualization using diagnostic PSMA ligands have begun to appear in the literature. However, these were isolated publications involving a small number of subjects and, as a rule, these were incidental findings in patients with prostate cancer, which were subsequently confirmed by the results of the histological examination. In existing studies, increased accumulation of PSMA-targeted radiopharmaceuticals for PET diagnosis is described in various histologic variants of lymphomas – follicular lymphoma, Hodgkin's lymphoma, diffuse large B-cell lymphoma [85–90]. In the study by S.P.M. de Souza et al. [91], a direct comparative study of [$^{18}$F]F-FDG and [$^{68}$Ga]Ga-PSMA PET/CT was conducted in 10 patients with confirmed diagnosis of Hodgkin's lymphoma ($n$ = 3) and NHL ($n$ = 7). It was shown that [$^{18}$F]F-FDG accumulated in 59 of 59 abnormal sites, while [$^{68}$Ga]Ga-PSMA – in 47 of 59 sites. Overall, its accumulation was characterized by lower uptake in lesions, regardless of FDG uptake intensity. However, PET/CT with [$^{68}$Ga]Ga-PSMA demonstrated greater potential in detecting brain lesions compared to FDG, which is logical given the biodistribution characteristics of [$^{18}$F]F-FDG. Generally, it should be noted that regardless of the histologic variant of lymphomas included in the few studies, they, as a rule, demonstrated low intensity of PSMA ligand uptake.

Our research results also demonstrate the possibility of using SPECT/CT with PSMA-targeted radiopharmaceuticals for the diagnosis of lymphomas, including for the evaluation of therapy results (Fig. 3).

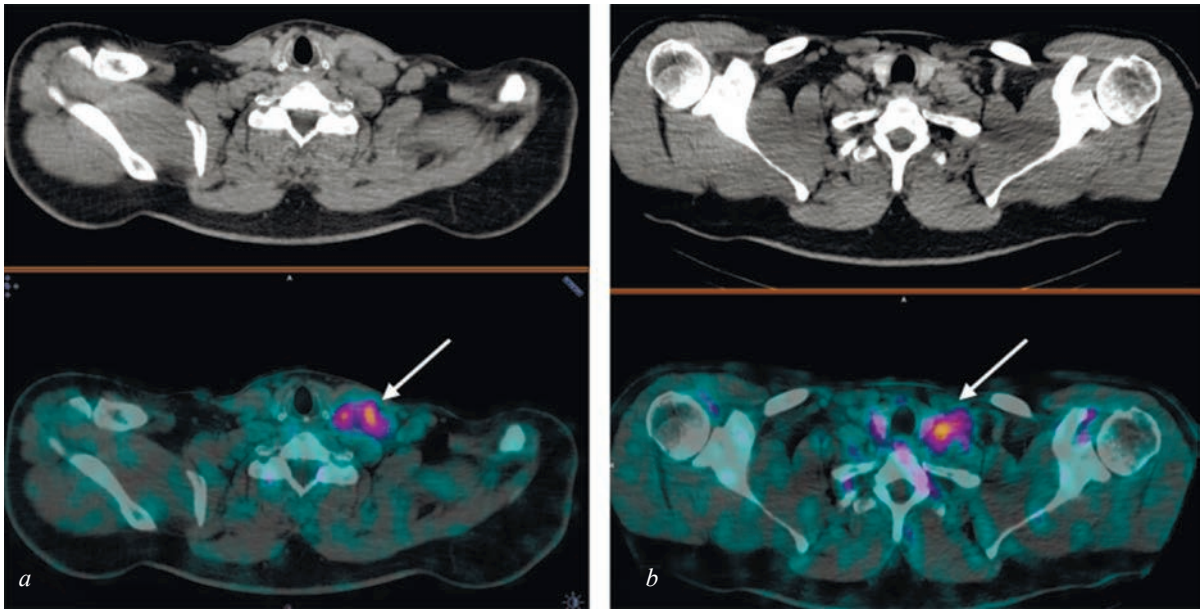


Fig. 3. CT and combined SPECT/CT images at 2 h after administration of [$^{99m}$Tc]Tc-HYNIC-PSMA in a patient with Hodgkin's lymphoma, with damage to the cervical and supraclavicular lymph nodes, the arrow indicates the tumor: *a* – before therapy, SUVmax 4.03; *b* – after 4 courses of polychemotherapy according to the BEACOPP protocol, SUVmax 1.46 (self-reported)

## DISCUSSION

To date, there are no large, well-designed studies investigating the role of PSMA-guided imaging techniques in non-prostate tumors. However, the limited available data, mostly retrospective in nature, demonstrate some correlation between PSMA ligand accumulation and PSMA receptor expression in different tumor types. It is logical that most of the tumors studied are those for which [$^{18}$F] F-FDG PET imaging has low sensitivity either due to high physiological uptake in surrounding healthy tissue, such as brain tumors, or due to low glucose metabolism or specific characteristics that limit the intensity of [$^{18}$F]F-FDG uptake, such as increased glucose-6-phosphatase activity in differentiated HCC.

A number of tumors show mixed evidence for the utility of PSMA imaging. For example, in urothelial

carcinoma, according to research data, there is relatively poor expression of PSMA receptors, which, of course, limits the use of diagnostic PSMA ligands. Also, low information content of the method is observed in malignant neoplasms of the gastrointestinal tract and pancreas, which is associated with low expression of PSMA in tumor tissue and high physiological absorption of PSMA ligands in background organs [92]. In breast carcinoma, the method demonstrates significant variation in the expression of these receptors in both primary and metastatic tumors, as well as in different patients, which confirms the heterogeneity of this disease.

Preliminary results indicate fairly high diagnostic sensitivity and specificity of PSMA-guided imaging in clear cell renal carcinoma, glioma, and hepatocellular carcinoma, which has led to changes in treatment strategy in some clinical situations. However, the currently published results require confirmation by larger prospective studies that further evaluate the impact of the data obtained on patient treatment outcomes.

Numerous studies have already proven that the expression of PSMA receptors is associated with neovascular endothelial cells in many tumors [35]. This fact makes these receptors an interesting target for antiangiogenic therapy. For example, according to the hypothesis of R. Jain, treatment with antiangiogenic agents is supposed to improve the effectiveness of chemotherapy by improving the delivery conditions [93]. At the same time, preclinical studies show that when chemotherapy drugs are administered outside the so-called "normalization window" in the context of antiangiogenic therapy, it turns out to be ineffective [94]. It is suggested, that suboptimal clinical results obtained with the use of bevacizumab as an antiangiogenic agent in combination with chemotherapy may have resulted from improper sequencing of the chemotherapeutic agents. In this regard, PSMA-guided imaging could be a potential tool to identify the "window of normalization," which in turn could potentially optimize the efficacy of VEGF-targeted therapy [95].

Radioligand therapy with [$^{177}$Lu]Lu-PSMA is currently actively used in many countries for the treatment of metastatic castrate-resistant PCa. Retrospective and prospective data show favorable safety and efficacy of this therapy, high response rates, and significant improvement in quality of life and survival [96–101]. Taking into account that in addition to PCa a number of tumor processes demonstrate high PSMA expression, it is considered relevant to study the issue of a PSMA-directed theranostic approach in relation to these nosologies. Despite the limited clinical examples of the use of radioligand therapy with [$^{177}$Lu]Lu-PSMA in various solid tumors with insufficient efficacy published to date, this area requires further, larger-scale studies.

## CONCLUSION

Although the exact role of PSMA in neoplasia and neoangiogenesis remains unclear, it can be assumed that PSMA-guided imaging may be useful not only in relation to PCa, but also in other tumor nosologies. It is likely that the routine use of conventional imaging methods for many tumors will continue to be a priority, both in primary diagnosis and in staging the process and assessing therapy. However, PSMA-guided imaging methods may in the future provide useful prognostic information, assisting in patient selection for systemic therapy by providing data on PSMA expression associated with some tumors with aggressive behavior [49–52, 67, 68].

It should also be noted that one of the important modern strategies in cancer treatment is the selective inhibition of angiogenesis, either by interfering with angiogenic growth factors or by directly targeting tumor-associated blood vessels [102, 103, 104]. In this regard, the use of diagnostic PSMA ligands may become a valuable tool for planning personalized treatment, increasing the effectiveness and safety of antitumor treatment. Another rather relevant direction may be PSMA theranostics of various malignant tumors, and radionuclide diagnostics with PSMA ligands in this situation will become a necessary option for patient routing.

## REFERENCES

1. Horoszewicz J.S., Kawinski E., Murphy G.P. Monoclonal antibodies to a new antigenic marker in epithelial prostatic cells and serum of prostatic cancer patients. *Anticancer Res.* 1987;7(5B): 927–935.
2. Israeli R.S., Powell C.T., Corr J.G., Fair W.R., Heston W.D. Expression of the prostate-specific membrane antigen. *Cancer Res.* 1994;54(7):1807–1811.
3. Haberkorn U., Eder M., Kopka K., Babich J.W. and Eisenhut M. New strategies in prostate cancer: Prostate Specific Membrane Antigen (PSMA) ligands for diagnosis and therapy. *Clin. Cancer Res*. 2016;22(1):9–15. DOI: 10.1158/1078-0432.CCR-15-0820.
4. Wang X., Tsui B., Ramamurthy G., Zhang P., Meyers J., Kenney M. E. et al. Theranostic agents for photodynamic therapy of prostate cancer by targeting prostate-specific membrane

antigen. *Mol. Cancer Ther.* 2016;15(8):1834–1844. DOI: 10.1158/1535-7163.MCT-15-0722.
5. Bacich D.J., Ramadan E., O'Keefe D.S., Bukhari N., Wegorzewska I., Ojeifo O. et al. Deletion of the glutamate carboxypeptidase II gene in mice reveals a second enzyme activity that hydrolyzes N-acetylaspartylglutamate. *J. Neurochem*. 2002;83(1):20–29. DOI: 10.1046/j.1471-4159.2002.01117.x.
6. Chehonin V.P., Grigorieiv M.E., Jerkov U.A., Lebedev D.V. The Role of Prostate Specific Membrane Antigen in the Diagnostic of Prostate Cancer. *Voprosy Medicinskoi Khimii.* 2002;48:31–43.(In Russ.).
7. Chang S.S. Overview of prostate-specific membrane antigen. *Reviews in Urology*. 2004;6 (10):13–18.
8. Bouchelouche K., Choyke P. L. and Capala J. Prostate specific membrane antigen – a target for imaging and therapy with radionuclides. *Discov. Med.* 2010;9(44):55–61.
9. Farolfi A., Fendler W., Iravani A., Haberkorn U., Hicks R., Herrmann K., et al. Theranostics for advanced prostate cancer: current indications and future developments. *Eur. Urol. Oncol.* 2019;2:152–162. DOI: 10.1016/j.euo.2019.01.001.
10. Eder M., Schäfer M., Bauder-Wüst U., Hull W-E., Wängler C., Mier W. et al. 68Ga-complex lipophilicity and the targeting property of a urea-based PSMA inhibitor for PET imaging. *Bioconjug. Chem.* 2012;23(4):688–697. DOI: 10.1021/bc200279b.
11. Chernov V.I., Medvedeva A.A., Sinilkin I.G., Zeltchan R.V., Bragina O.D. Development of Radiopharmaceuticals for Nuclear Medicine in Oncology. *Medical Imaging*. 2016;2:63–66. (In Russ.).
12. Medvedeva A.A., Chernov V.I., Zelchan R.V., Rybina A.N. Bragina O.D., Zebzeeva O.S. Safety of Use, Pharmacokinetics, and Dosimetric Characteristics of the Radiopharmaceutical [99mTc]Tc-HYNIC-PSMA. *Voprosy Onkologii.* 2025;71(1):117–127. (In Russ.). DOI: 10.37469/0507-3758-2025-71-1-OF-2175.
13. Wester H-J., Schottelius M. PSMA-targeted radiopharmaceuticals for imaging and therapy. *Semin. Nucl. Med.* 2019;49:302–312. DOI: 10.1053/j.semnuclmed.2019.02.008.
14. Rizzo A., Dall'Armellina S., Pizzuto D.A., Perotti G., Zagaria L., Lanni V. et al. PSMA Radioligand Uptake as a Biomarker of Neoangiogenesis in Solid Tumours: Diagnostic or Theragnostic Factor? *Cancers.* 2022;14:4039. DOI: 10.3390/cancers14164039.
15. Silver D.A., Pellicer I., Fair W.R., Heston W.D., Cordon-Cardo C. Prostate-specific membrane antigen expression in normal and malignant human tissues. *Clin. Cancer Res.* 1997;3:81–85.
16. Spatz S., Tolkach Y., Jung K., Stephan C., Busch J., Ralla B. et al. Comprehensive evaluation of prostate-specific membrane antigen expression in the vasculature of renal tumors: implications for imaging studies and prognostic role. *J. Urol.* 2018;199(2):370–377. DOI: 10.1016/j.juro.2017.08.079.
17. McLeod D.S.A., Zhang L., Durante C., Cooper D.S. Contemporary debates in adult papillary thyroid cancer management. *Endocr. Rev*. 2019;40:1481–1499. DOI: 10.1210/er.2019-00085.
18. Haugen B.R., Alexander E.K., Bible K.C., Doherty G.M., Mandel S.J., Nikiforov Y.E. et al. 2015 American Thyroid Association Management Guidelines for Adult Patients with Thyroid Nodules and Differentiated Thyroid Cancer: The American Thyroid Association Guidelines Task Force on Thyroid Nodules and Differentiated Thyroid Cancer. *Thyroid.* 2016;26:1–133. DOI: 10.1089/thy.2015.0020.
19. Fugazzola L., Elisei R., Fuhrer D., Jarzab B., Leboulleux S., Newbold K. et al. 2019 European Thyroid Association Guidelines for the Treatment and Follow-Up of Advanced Radioiodine-Refractory Thyroid Cancer. *Eur. Thyroid J*. 2019;8:227–245. DOI: 10.1159/000502229.
20. Eisenhauer E.A., Therasse P., Bogaerts J., Schwartz L.H., Sargent D., Ford R. et al. New response evaluation criteria in solid tumours: revised RECIST guideline (version 1.1). *Eur. J. Cancer*. 2009;45:228–247. DOI: 10.1016/j.ejca.2008.10.026.
21. Treglia G., Goichot B., Giovanella L., Hindié E., Jha A., Pacak K. et al. Prognostic and predictive value of nuclear imaging in endocrine oncology. *Endocrine.* 2020;67:9–19. DOI: 10.1007/s12020-019-02131-4.
22. Piccardo A., Trimboli P., Foppiani L., Treglia G., Ferrarazzo G., Massollo M. et al. PET/CT in thyroid nodule and differentiated thyroid cancer patients. The evidence-based state of the art. *Rev. Endocr. Metab. Disord*. 2019;20:47–64. DOI: 10.1007/s11154-019-09491-2.
23. Moiseenko V.M., Gladkov O.M., Stenina M.B., Den'gina N.V., Karabina E.V., Plykina A.A. *Practical Recommendations of the Russian Society of Clinical Oncology.* 2024;14 (3s2). (In Russ.).
24. Cabanillas M.E., Ryder M., Jimenez C. Targeted therapy for advanced thyroid cancer: kinase inhibitors and beyond. *Endocr. Rev*. 2019;40:1573–1604. DOI: 10.1210/er.2019-00007
25. Haddad R.I., Nasr C., Bischoff L., Busaidy N.L., Byrd D., Callender G. et al. NCCN guidelines insights: thyroid carcinoma, version 2. 2018. *J. Natl. Compr. Cancer Netw.* 2018;16:1429–1440. DOI: 10.6004/jnccn.2018.0089.
26. Elia G., Patrizio A., Ragusa F., Paparo S.R., Mazzi V., Balestri E. et al. Molecular features of aggressive thyroid cancer. *Front. Oncol.* 2022;12:1099280. DOI: 10.3389/fonc.2022.1099280.
27. Schlumberger M., Tahara M., Wirth L.J., Robinson B., Brose M.S., Elisei R. et al. Lenvatinib versus placebo in radioiodine-refractory thyroid cancer. *N. Engl. J. Med*. 2015;372:621–630. DOI: 10.1056/NEJMoa1406470
28. Moore M., Panjwani S., Mathew R., Crowley M., Liu Y-F., Aronova A. et al. Well-differentiated thyroid cancer neovasculature expresses prostate-specific membrane antigen-a possible novel therapeutic target. *Endocr. Pathol.* 2017;28:339–344. DOI: 10.1007/s12022-017-9500-9.
29. Sollini M., di Tommaso L., Kirienko M., Piombo C., Erreni M., Lania A.G. et al. PSMA expression level predicts differentiated thyroid cancer aggressiveness and patient outcome. *EJNMMI Res.* 2019;9:93. DOI: 10.1186/s13550-019-0559-9.
30. Heitkötter B., Steinestel K., Trautmann M., Grünewald I., Barth P., Gevensleben H. et al. Neovascular PSMA expression is a common feature in malignant neoplasms of the thyroid. *Oncotarget.* 2018;9:9867–9874. DOI: 10.18632/oncotarget.23984.
31. Herrmann G., Schumm-Draeger P.M., Muller C., Atai E., Wenzel B., Fabian T. et al. T-lymphocytes, CD68-positive

cells and vascularisation in thyroid carcinomas. *J. Cancer Res. Clin. Oncol.* 1994;120:651–656. DOI: 10.1007/BF01245376.
32. Lutje S., Gomez B., Cohnen J., Umutlu L., Gotthardt M., Poeppel T.D. et al. Imaging of prostate-specific membrane antigen expression in metastatic differentiated thyroid cancer using 68Ga-HBED-CC-PSMA PET/CT. *Clin. Nucl. Med.* 2017;42:20–25. DOI: 10.1097/RLU.0000000000001454.
33. Lawhn-Heath C., Yom S.S., Liu C., Villanueva-Meyer J.E., Aslam M., Smith R. et al. Gallium-68 prostate-specific membrane antigen ([68Ga]Ga-PSMA-11) PET for imaging of thyroid cancer: A feasibility study. *EJNMMI Res.* 2020;10:128. DOI: 10.1186/s13550-020-00720-3.
34. Verma P., Malhotra G., Meshram V., Chandak A., Sonavane S., Lila A.R. et al. Prostate-specific membrane antigen expression in patients with differentiated thyroid cancer with thyroglobulin elevation and negative iodine scintigraphy using 68Ga-PSMA-HBED-CC PET/CT. *Clin. Nucl. Med*. 2021;46:e406–e409. DOI: 10.1097/RLU.0000000000003655.
35. Wachter S., Di Fazio P., Maurer E., Manoharan J., Keber C., Pfestroff A. et al. Prostate-specific membrane antigen in anaplastic and poorly differentiated thyroid cancer – a new diagnostic and therapeutic target? *Cancers.* 2021;13:5688. DOI: 10.3390/cancers13225688.
36. De Vries L.H., Lodewijk L., Braat A.J.A.T., Krijger G.C., Valk G.D., Lam M.G.E.H. et al. 68Ga-PSMA PET/CT in radioactive iodine-refractory differentiated thyroid cancer and first treatment results with $^{177}$Lu-PSMA-617. *EJNMMI Res*. 2020;10:18. DOI: 10.1186/s13550-020-0610-x.
37. Pitalua-Cortes Q., Garcна-Perez F.O., Vargas-Ahumada J., Gonzalez-Rueda S., Gomez-Argumosa E., Ignacio-Alvarez E. et al. Head-to-head Comparison of 68Ga-PSMA-11 and 131I in the follow-up of well-differentiated metastatic thyroid cancer: a new potential theragnostic agent. *Front. Endocrinol.* 2021;12:794759. DOI: 10.3389/fendo.2021.794759.
38. Siegel R.L., Miller K.D., Fuchs H.E., Jemal A. Cancer statistics, 2022. *CA A Cancer J. Clin.* 2022;72:7–33. DOI: 10.3322/caac.21708.
39. Capitanio U., Bensalah K., Bex A., Boorjian S.A., Bray F., Coleman J. et al. Epidemiology of Renal Cell Carcinoma. *Eur. Urol.* 2019;75:74–84. DOI: 10.1016/j.eururo.2018.08.036.
40. Srinivasan R., Ricketts C.J., Sourbier C., Linehan W.M. New strategies in renal cell carcinoma: targeting the genetic and metabolic basis of disease. *Clin. Cancer Res.* 2015;21:10–17. DOI: 10.1158/1078-0432.CCR-13-2993.
41. Heng D.Y., Xie W., Regan M.M., Warren M.A., Golshayan A.R., Sahi C. et al. Prognostic Factors for Overall Survival in Patients with Metastatic Renal Cell Carcinoma Treated with Vascular Endothelial Growth Factor – Targeted Agents: Results from a Large, Multicenter Study. *J. Clin. Oncol.* 2009;27:5794–5799. DOI: 10.1200/JCO.2008.21.4809.
42. Tyson M.D., Chang S.S. Optimal surveillance strategies after surgery for renal cell carcinoma. *J. Natl. Compr. Cancer Netw.* 2017;15:835–840. DOI: 10.6004/jnccn.2017.0102.
43. Lindenberg L., Mena E., Choyke P.L., Bouchelouche K. PET imaging in renal cancer. *Curr. Opin. Oncol*. 2019;31:216–221. DOI: 10.1097/CCO.0000000000000518.
44. Motzer R.J., Jonasch E., Agarwal N., Alva A., Baine M., Beckermann K. et al. Kidney Cancer, Version 3.2022, NCCN Clinical Practice Guidelines in Oncology. *J. Natl. Compr. Cancer Netw*. 2022;20:71–90. DOI: 10.6004/jnccn.2022.0001.
45. Escudier B., Porta C., Schmidinger M., Rioux-Leclercq N., Bex A., Khoo V. et al. Renal cell carcinoma: ESMO Clinical Practice Guidelines for diagnosis, treatment and follow-up. *Ann. Oncol*. 2019;30:706–720. DOI: 10.1093/annonc/mdz056.
46. Ljungberg B., Albiges L., Abu-Ghanem Y., Bedke J., Capitanio U., Dabestani S. et al. European Association of Urology Guidelines on Renal Cell Carcinoma: The 2022 Update. *Eur. Urol.* 2022;82:399–410. DOI: 10.1016/j.eururo.2022.03.006.
47. Garg G., Benchekroun M.T., Abraham T. FDG-PET/CT in the postoperative period: utility, expected findings, complications, and pitfalls. *Semin. Nucl. Med*. 2017;47:579–594. DOI: 10.1053/j.semnuclmed.2017.07.005.
48. Chen R., Zhou X., Huang G., Liu J. Fructose 1,6-bisphosphatase 1 expression reduces $^{18}$F-FDG uptake in clear cell renal cell carcinoma. *Contrast Media Mol. Imaging.* 2019;2019:9463926. DOI: 10.1155/2019/9463926.
49. Rhee H., Blazak J., Tham C.M., Ng K.L., Shepherd B., Lawson M. et al. Pilot study: Use of gallium-68 PSMA PET for detection of metastatic lesions in patients with renal tumor. *EJNMMI Res.* 2016;6:76. DOI: 10.1186/s13550-016-0231-6.
50. Gao J., Xu Q., Fu Y., He K., Zhang C., Zhang Q. et al. Comprehensive evaluation of 68Ga-PSMA-11 PET/CT parameters for discriminating pathological characteristics in primary clear-cell renal cell carcinoma. *Eur. J. Nucl. Med. Mol. Imaging.* 2021;48:561–569. DOI: 10.1007/s00259-020-04916-6.
51. Udovicich C., Callahan J., Bressel M., Ong W.L., Perera M., Tran B. et al. Impact of prostate-specific membrane antigen positron emission tomography/computed tomography in the management of oligometastatic renal cell carcinoma. *Eur. Urol. Open Sci.* 2022;44:60–68. DOI: 10.1016/j.euros.2022.08.001.
52. Li Y., Zheng R., Zhang Y., Huang C., Tian L., Liu R. et al. Special issue "The advance of solid tumor research in China": 68Ga-PSMA-11 PET/CT for evaluating primary and metastatic lesions in different histological subtypes of renal cell carcinoma. *Int. J. Cancer*. 2023;152:42–50. DOI: 10.1002/ijc.34189.
53. Meyer A.R., Carducci M.A., Denmeade S.R., Markowski M.C., Pomper M.G., Pierorazio P.M. et al. Improved identification of patients with oligometastatic clear cell renal cell carcinoma with PSMA-targeted $^{18}$F-DCFPyL PET/CT. *Ann. Nucl. Med*. 2019;33:617–623. DOI: 10.1007/s12149-019-01371-8.
54. Raveenthiran S., Esler R., Yaxley J., Kyle S. The use of 68Ga-PET/CT PSMA in the staging of primary and suspected recurrent renal cell carcinoma. *Eur. J. Nucl. Med. Mol. Imaging.* 2019;46:2280–2288. DOI: 10.1007/s00259-019-04432-2.
55. Gühne F., Seifert P., Theis B., Steinert M., Freesmeyer M., Drescher R. PSMA-PET/CT in patients with recurrent clear cell renal cell carcinoma: histopathological correlations of imaging findings. *Diagnostics*. 2021;11:1142. DOI: 10.3390/diagnostics11071142.
56. Liu Y., Wang G., Yu H., Wu Y., Lin M., Gao J. et al. Comparison of $^{18}$F-DCFPyL and $^{18}$F-FDG PET/computed tomography for the restaging of clear cell renal cell carcinoma: Preliminary

results of 15 patients. *Nucl. Med. Commun.* 2020;41:1299–1305. DOI: 10.1097/MNM.0000000000001285

57. Ilyakov V.S., Pronin A.I., Parnas A.V., Subbotin A.S., Krylov A.S., Geliashvili T.M. et al. PET/CT with 18F-PSMA-1007 in Diagnostics of Primary and Recurrent Lesions of Clear-Cell Renal Cell Carcinoma in Comparison with 18F-FDG: Prospective Study. *Oncology Journal: Radiation Diagnostics, Radiation Therapy.* 2024;7(2):15–26. (In Russ.). DOI: 10.37174/2587-7593-2024-7-2-15-26.
58. Ilyakov V.S., Pronin A.I., Parnas A.V., Subbotin A.S., Krylov A.S., Geliashvili T.M. et al. PET/CT with $^{18}$F-PSMA-1007 in Diagnostics of Metastatic Lesions of Clear-Cell Renal Cell Carcinoma in Comparison with 18F-FDG: Prospective Study. *Oncology Journal: Radiation Diagnostics, Radiation Therapy*. 2024;7(3):41–47. (In Russ.). DOI: 10.37174/2587-7593-2024-7-3-41-47.
59. Malignant Neoplasms in Russia in 2023 (Morbidity and Mortality) / edited by A.D. Kaprin [et al.] − M.: P.A. Herzen Moscow Oncology Research Institute − branch of the Federal State Budgetary Institution "NMITs of Radiology" of the Ministry of Health of the Russian Federation, 2024:276. (In Russ.).
60. Clinical Guidelines of the Ministry of Health of the Russian Federation. 2021. (In Russ.). URL: https://cr.minzdrav.gov.ru.
61. Kasoha M., Unger C., Solomayer E.F., Bohle R.M., Zaharia C., Khreich F. et al. Prostate-specific membrane antigen (PSMA) expression in breast cancer and its metastases. *Clin. Exp. Metastasis*. 2017;34:479–490. DOI: 10.1007/s10585-0$^{18}$-9878-x.
62. Passah A., Arora S., Damle N.A., Tripathi M., Bal C., Subudhi T.K. et al. 68Ga –prostate-specific membrane antigen PET/CT in triple-negative breast cancer. *Clin. Nucl. Med.* 2018; 43: 460–461. DOI: 10.1097/RLU.0000000000002071.
63. Arslan E., Ergül N., Beyhan E., Erol Fenercioglu Ö., Sahin R., Cin M. et al. The roles of 68 Ga-PSMA PET/CT and $^{18}$ F-FDG PET/CT imaging in patients with triple-negative breast cancer and the association of tissue PSMA and claudin 1, 4, and 7 levels with PET findings. *Nucl. Med. Commun.* 2023;44:284–290. DOI: 10.1097/MNM.0000000000001663.
64. Marta G.N., Wimana Z., Taraji L., Critchi G., Aftimos P.G., Piccart-Gebhart M.J. et al. Prostate-specific membrane antigen (PSMA) expression in patients with metastatic triple negative breast cancer: Initial results of the PRISMA study. *JCO.* 2023;41:1025. DOI: 10.1200/JCO.2023.41.16_suppl.1025.
65. Parnas A.V., Odzharova A.A., Pronin A.I., Ilyakov V.S., Meshcheryakova N.A., Kamolova Z.Kh. et al. Pssibilities of PET/CT with 18F-PSMA-1007 in the Diagnosis of Triple Negative Breast Cancer: a Case Study. *Oncology Journal: Radiation Diagnostics, Radiation Therapy*. 2021;4(4):88–92. (In Russ.). DOI: 10.37174/2587-7593-2021-4-4-88-92.
66. Wernicke A.G., Varma S., Greenwood E.A., Christos P.J., Chao K.S., Liu H. et al. Prostate-specific membrane antigen expression in tumor-associated vasculature of breast cancers. *APMIS. 2014;*122(6):482–489. DOI: 10.1111/apm.12195.
67. Tolkach Y., Gevensleben H., Bundschuh R., Koyun A., Huber D., Kehrer C. et al. Prostate-specific membrane antigen in breast cancer: a comprehensive evaluation of expression and a case report of radionuclide therapy. *Breast Cancer Res. Treat.* 2018;169(3):447–455. DOI: 10.1007/s10549-018-4717-y.
68. Andryszak N., Świniuch D., Wójcik E., Ramlau R., Ruchała M., Czepczyński R. Head-to-pead comparison of [18F] PSMA-1007 and [18F]FDG PET/CT in patients with triple-negative breast cancer. *Cancers (Basel).* 2024;16(3):667. DOI: 10.3390/cancers16030667.
69. Zárate-García C.D., Cardoza-Ochoa D.R., Sánchez-Vera Y., González-Díaz J.I. Incidental diagnosis of metastatic breast cancer in a man With $^{99m}$ Tc-PSMA SPECT/CT. *Clin Nucl Med.* 2023;48(4):e163-e164. DOI: 10.1097/RLU.0000000000004549.
70. Llovet J.M., Kelley R.K., Villanueva A., Singal A.G., Pikarsky E., Roayaie S. et al. Hepatocellular carcinoma. *Nat. Rev. Dis*. *Prim.* 2021;7:6. DOI: 10.1038/s41572-020-00240-3.
71. McGlynn K.A., Petrick J.L., London W.T. Global epidemiology of hepatocellular carcinoma: an emphasis on demographic and regional variability. *Clin. Liver Dis.* 2015; 19:223–238. DOI: 10.1016/j.cld.2015.01.001.
72. Navin P., Venkatesh S. Hepatocellular carcinoma: state of the art imaging and recent advances. *J. Clin. Transl. Hepatol*. 2019;28:72–85. DOI: 10.14218/JCTH.2018.00032.
73. Sharma B., Martin A., Zerizer I. Positron emission tomography-computed tomography in liver imaging. *Semin. Ultrasound CT MR.* 2013;34:66–80. DOI: 10.1053/j.sult.2012.11.006.
74. Kesler M., Levine C., Hershkovitz D., Mishani E., Menachemn Y., Lerman H. et al. 68Ga-PSMA is a novel PET-CT tracer for imaging of hepatocellular carcinoma: A prospective study. *J. Nucl. Med.* 2018. DOI: 10.2967/jnumed.118.214833.
75. Kuyumcu S., Has-Simsek D., Iliaz R., Sanli Y., Buyukkaya F., Akyuz F. et al. Evidence of prostate-specific membrane antigen expression in hepatocellular carcinoma using 68Ga-PSMA PET/CT. *Clin. Nucl. Med.* 2019;44:702–706. DOI: 10.1097/RLU.0000000000002701.
76. Kunikowska J., Cieślak B., Gierej B., Patkowski W., Kraj L., Kotulski M. et al. [68 Ga]Ga-prostate-specific membrane antigen PET/CT: a novel method for imaging patients with hepatocellular carcinoma. *Eur. J. Nucl. Med. Mol. Imaging.* 2021;48:883–892. DOI: 10.1007/s00259-020-05017-0.
77. Gündoğan C., Ergül N., Çakır M.S., Kılıçkesmez Ö., Gürsu R.U., Aksoy T. et al. 68Ga-PSMA PET/CT Versus $^{18}$F-FDG PET/CT for imaging of hepatocellular carcinoma. *Mol. Imaging Radionucl*. Ther. 2021;30:79–85. DOI: 10.4274/mirt.galenos.2021.92053.
78. Hirmas N., Leyh C., Sraieb M., Barbato F., Schaarschmidt B.M., Umutlu L. et al. 68Ga-PSMA-11 PET/CT Improves Tumor Detection and Impacts Management in Patients with Hepatocellular Carcinoma. *J. Nucl. Med.* 2021;62:1235–1241. DOI: 10.2967/jnumed.120.257915
79. Thompson S.M., Suman G., Torbenson M.S., Chen Z.-M.E., Jondal D.E., Patra A. et al. PSMA as a theranostic target in hepatocellular carcinoma: immunohistochemistry and 68 Ga-PSMA-11 PET using cyclotron-produced 68Ga. *Hepatol. Commun*. 2022;6:1172–1185. DOI: 10.1002/hep4.1861.
80. Denmeade S.R., Mhaka A.M., Rosen D.M., Brennen W.N., Dalrymple S., Dach I. et al. Engineering a prostate-specific membrane antigen-activated tumor endothelial cell prodrug for cancer therapy. *Sci. Transl. Med.* 2012;4(140):140ra86. DOI: 10.1126/scitranslmed.3003886.

81. Lu Q., Long Y., Gai Y., Liu Q., Jiang D., Lan X. [($^{177}$)Lu]Lu-PSMA-617 theranostic probe for hepatocellular carcinoma imaging and therapy. *Eur. J. Nucl. Med. Mol. Imaging.* 2023;50(8):2342–2352. DOI: 10.1007/s00259-023-06155-x.
82. Chernov V.I., Dudnikova E.A., Goldberg V.E., Kravchuk T.L., Danilova A.V., Zelchan R.V. et al. Positron Emission Tomography in the Diagnosis and Monitoring of Lymphomas. *Meditsinskaya Radiologiya i Radiatsionnaya Bezopasnost'*. 2018;63(6):41–50. (In Russ.). DOI: 10.12737/article_5c0b8d72a8bb98.40545646.
83. Weiler-Sagie M., Bushelev O., Epelbaum R., Dann E.J., Haim N., Avivi I. et al. ($^{18}$)F-FDG avidity in lymphoma readdressed: a study of 766 patients. *J. Nucl. Med.* 2010;51: 25–30. DOI: 10.2967/jnumed.109.067892.
84. Calvo-Vidal M.N., Cerchietti L. The metabolism of lymphomas. *Curr. Opin. Hematol*. 2013;20:345–354. DOI: 10.1097/MOH.0b013e3283623d16.
85. Kanthan G.L., Coyle L., Kneebone A., Schembri G.P., Hsiao E. Follicular lymphoma showing avid uptake on 68Ga PSMA-HBED-CC PET/CT. *Clin. Nucl. Med.* 2016; 41(6): 500–501. DOI: 10.1097/RLU.0000000000001169.
86. Miceli A., Riondato M., D'Amico F., Donegani M.I., Piol N., Mora M. et al. Concomitant prostate cancer and hodgkin lymphoma: a differential diagnosis guided by a combined 68Ga-PSMA-11 and $^{18}$F-FDG PET/CT Approach. *Medicina (Kaunas).* 2021;57(9):975. DOI: 10.3390/medicina57090975.
87. Dhiantravan N., Hovey E., Bosco A., Wegner E.A. Concomitant prostate carcinoma and follicular lymphoma: "flip-flop" appearances on PSMA and FDG PET/CT Scans. *Clin. Nucl. Med.* 2019;44(10):797–798. DOI: 10.1097/RLU.0000000000002727.
88. Caputo S.A., Jang A., Talbert J., Saba N.S., Sartor O. Prostate-specific membrane antigen PET positivity in a lung mass: diagnosis of diffuse large B-cell lymphoma. *Clin. Nucl. Med*. 2023;48(2):190–191. DOI: 10.1097/RLU.0000000000004503.
89. Vamadevan S., Le K., Bui C., Mansberg R. Prostate-Specific Membrane Antigen Uptake in Small Cleaved B-Cell Follicular Non-Hodgkin Lymphoma. *Clin Nucl Med.* 2016 Dec; 41(12):980–981. DOI: 10.1097/RLU.0000000000001378.
90. Milrod C.J., Brown C., Mega A.E. Increased PSMA-targeted $^{18}$ F-DCFPyL uptake in peripheral T-cell lymphoma. *Clin. Nucl. Med*. 2024;49(7):e338-e339. DOI: 10.1097/RLU.0000000000005264.
91. De Souza S.P.M., Tobar N., Frasson F., Perini E.A., de Souza C.A., Delamain M.T. et al. Head-to-head comparison between 68Ga-PSMA and $^{18}$F-FDG-PET/CT in lymphomas: a preliminary analysis. *Nucl. Med. Commun*. 2021;42(12):1355–1360. DOI: 10.1097/MNM.0000000000001465.
92. Vuijk F.A., Kleiburg F., Noortman W.A, Heijmen L., Shahbazi S.F., van Velden F.H.P. et al. Prostate-specific membrane antigen targeted Pet/CT imaging in patients with colon, gastric and pancreatic cancer. *Cancers.* 2022;14:6209. DOI: 10.3390/cancers14246209.
93. Jain R. Normalization of tumor vasculature: an emerging concept in antiangiogenic therapy. *Science.* 2005;307:58–62. DOI: 10.1126/science.1104819.
94. Vangestel C., Van de Wiele C., Van Damme N., Staelens S., Pauwels P., Reutlingsperger C. et al. $^{99m}$Tc-(CO)3 His-Annexin A5 micro-SPECT demonstrates increased cell death by irinotecan during the vascular normalization window caused by bevacizumab. *J. Nucl. Med.* 2011;526:1786–1794. DOI: 10.2967/jnumed.111.092650.
95. Grant C., Caromile L., Ho V., Durrani K., Rahman M., Claffey K. et al. Prostate specific membrane antigen (PSMA) regulates angiogenesis independently of VEGF during ocular neovascularization. *PLoS ONE.* 2012;7:e41285. DOI: 10.1371/journal.pone.0041285.
96. Rahbar K., Ahmadzadehfar H., Kratochwil C., Haberkorn U., Schäfers M., Essler M. et al. German Multicenter Study Investigating $^{177}$Lu-PSMA-617 Radioligand Therapy in Advanced Prostate Cancer Patients. *J. Nucl. Med.* 2017;58(1):85–90. DOI: 10.2967/jnumed.116.183194.
97. Rahbar K., Boegemann M., Yordanova A., Eveslage M., Schäfers M., Essler M. et al. PSMA targeted radioligandtherapy in metastatic castration resistant prostate cancer after chemotherapy, abiraterone and/or enzalutamide. A retrospective analysis of overall survival. *Eur. J. Nucl. Med. Mol. Imaging*. 2018;45(1):12–19. DOI: 10.1007/s00259-017-3848-4.
98. Yordanova A., Linden P., Hauser S., Meisenheimer M., Kürpig S., Feldmann G. et al. Outcome and safety of rechallenge [$^{177}$Lu]Lu-PSMA-617 in patients with metastatic prostate cancer. *Eur. J. Nucl. Med. Mol. Imaging*. 2019;46(5):1073–1080. DOI: 10.1007/s00259-018-4222-x.
99. Khreish F., Kochems N., Rosar F., Sabet A., Ries M., Maus S. et al. Response and outcome of liver metastases in patients with metastatic castration-resistant prostate cancer (mCRPC) undergoing $^{177}$Lu-PSMA-617 radioligand therapy. *Eur. J. Nucl. Med. Mol. Imaging.* 2021;48(1):103–112. DOI: 10.1007/s00259-020-04828-5.
100. Violet J., Sandhu S., Iravani A., Ferdinandus J., Thang S.P., Kong G. et al. Long-Term Follow-up and Outcomes of Retreatment in an Expanded 50-Patient Single-Center Phase II Prospective Trial of $^{177}$Lu-PSMA-617 Theranostics in Metastatic Castration-Resistant Prostate Cancer. *J. Nucl. Med.* 2020;61(6):857–865. DOI: 10.2967/jnumed.119.236414.
101. Sartor O., de Bono J., Chi K.N., Fizazi K., Herrmann K., Rahbar K. et al. Lutetium-$^{177}$-PSMA-617 for metastatic castration-resistant prostate cancer. *N. Engl. J. Med*. 2021; 385(12):1091–1103. DOI: 10.1056/NEJMoa2107322.
102. Neri D., Bicknell R. Tumour vascular targeting. *Nat. Rev. Cancer* 2005;5:436–446. DOI: 10.1038/nrc1627.
103. Seaman S., Stevens J., Yang M.Y., Logsdon D., Graff-Cherry C., St Croix B. Genes that distinguish physiological and pathological angiogenesis. *Cancer Cell.* 2007;11:539–54. DOI: 10.1016/j.ccr.2007.04.017.
104. St Croix B., Rago C., Velculescu V., Traverso G., Romans K.E., Montgomery E. et al. Genes expressed in human tumor endothelium. *Science* 2000;289:1197202. DOI: 10.1126/science.289.5482.1197.

## Author Information

**Medvedeva Anna A.** – Dr. Sci. (Med.), Senior Researcher, Department of Nuclear Medicine, Cancer Research Institute, Tomsk NRMC, Russian Academy of Sciences, Tomsk, medvedeva@tnimc.ru, http://orcid.org/0000-0002-5840-3625

**Vysotskaya Vitalina V.** – Research Assistant, Chemotherapy Department, Cancer Research Institute, Tomsk NRMC, Russian Academy of Sciences, Tomsk, vitad@mail.ru, http://orcid.org/0000-0003-3800-6988

**Muravleva Albina V.** – Physician of the Chemotherapy Department, Cancer Research Institute, Tomsk NRMC, Russian Academy of Sciences; Division of Intermediate-Level Therapy with a Course in Clinical Pharmacology and Endocrinology, SibSMU, Tomsk, albina_danilova7487@mail.ru, http://orcid.org/0000-0002-0233-2418

**Zeltchan Roman V.** – Dr. Sci. (Med.), Leading Researcher, Department of Nuclear Medicine, Cancer Research Institute, Tomsk NRMC, Russian Academy of Sciences, Tomsk, zelchan@yandex.ru, http://orcid.org/0000-0002-4568-1781

**Rybina Anastasiya N.** – Cand. Sci. (Med.), Radiologist, Department of Nuclear Medicine, Cancer Research Institute, Tomsk NRMC, Russian Academy of Sciences, Tomsk, pankovaan@mail.ru, http://orcid.org/0000-0002-6488-0647

**Gol'dberg Victor. E.** – Dr. Sci. (Med.), Professor, Head of the Chemotherapy Department, Cancer Research Institute, Tomsk NRMC, Tomsk, goldbergve@mail.ru, http://orcid.org/0000-0003-4753-5283

**Chernov Vladimir I.** – Corresponding Member of RAS, Dr. Sci. (Med.), Professor, Head of the Department of Radionuclide Diagnostics, Cancer Research Institute, Tomsk NRMC, Tomsk; NR TPU, Tomsk, chernov@tnimc.ru, http://orcid.org/0000-0001-8753-7916

(✉) **Medvedeva Anna A.,** medvedeva@tnimc.ru

Received on February 03, 2025;
approved after peer review on March 13, 2025;
accepted on March 20, 2025

УДК 616-002.5-085.37:577.161.2.02:578.828HIV
https://doi.org/10.20538/1682-0363-2025-3-163-171

# The role of vitamin D in immunoadjuvant therapy for tuberculosis depending on the HIV status of patients

**Filinyuk O.V., Khokhlyuk V.V., Volkovskaya A.O.**

*Siberian State Medical University*
*2 Moskovsky trakt, 634050 Tomsk, Russian Federation*

**ABSTRACT**

Search queries were conducted in the PubMed and eLIBRARY.ru databases using keywords, including publications from 2018–2024. A review of the literature on vitamin D deficiency in patients with tuberculosis (TB), human immunodeficiency virus (HIV), and TB/HIV combination is presented, which revealed heterogeneous prevalence. The roles of vitamin D in the body immune response to TB are shown depending on the presence of HIV infection. The data on the therapeutic use of single and prolonged administration of vitamin D at various doses in adjuvant TB therapy are presented. The prospects for the use of vitamin D in the combined treatment of TB patients are outlined depending on the HIV status, especially with multidrug-resistant pathogens requiring study in Russian clinical trials.

**Keywords:** tuberculosis, HIV, immunity, vitamin D, adjuvant immunotherapy, host therapy

**Conflict of interest.** The authors declare the absence of obvious or potential conflicts of interest related to the publication of this article.

**Source of financing.** The authors state that they received no funding for the study.

**For citation:** Filinyuk O.V., Khokhlyuk V.V., Volkovskaya A.O. The role of vitamin D in immunoadjuvant therapy for tuberculosis depending on the HIV status of patients. *Bulletin of Siberian Medicine.* 2025;24(3):163–171. https://doi.org/10.20538/1682-0363-2025-3-163-171.

# Роль витамина D в иммуноадъювантной терапии туберкулеза в зависимости от ВИЧ-статуса пациентов

**Филинюк О.В., Хохлюк В.В., Волковская А.О.**

*Сибирский государственный медицинский университет (СибГМУ)*
*Россия, 634050, г. Томск, Московский тракт, 2*

**РЕЗЮМЕ**

В базах данных PubMed и eLIBRARY.RU по ключевым словам были проведены поисковые запросы, включающие публикации за 2018–2024 гг. Представлен анализ литературы о дефиците витамина D у больных при туберкулезе (ТБ), вирусе иммунодефицита человека (ВИЧ), в сочетании ТБ и ВИЧ, который выявил неоднородную распространенность. Показана роль витамина D в иммунологическом ответе организма при ТБ в зависимости от наличия ВИЧ-инфекции. Приведены данные терапевтического при-

✉ *Filinyuk Olga V.,* filinyuk.olga@yandex.ru

менения в качестве адъюванта к химиотерапии туберкулеза витамина D в различных дозировках в однократном и пролонгированном введении. Обозначены перспективы использования витамина D в комбинированном лечении больных ТБ в зависимости от ВИЧ-статуса, особенно со множественной лекарственной устойчивостью возбудителя, требующие изучения в российских клинических исследованиях.

**Ключевые слова:** туберкулез, ВИЧ, иммунитет, витамин D, адъювантная иммунотерапия, терапия хозяина

**Конфликт интересов.** Авторы декларируют отсутствие явных и потенциальных конфликтов интересов, связанных с публикацией настоящей статьи.

**Источник финансирования.** Авторы заявляют об отсутствии финансирования при проведении исследования.

**Для цитирования:** Филинюк О.В., Хохлюк В.В., Волковская А.О. Роль витамина D в иммуноадъювантной терапии туберкулеза зависимости от ВИЧ-статуса пациентов. *Бюллетень сибирской медицины.* 2025;24(3):163–171. https://doi.org/10.20538/1682-0363-2025-3-163-171.

## INTRODUCTION

In the Russian Federation, there are three key factors significantly influencing further epidemiological situation associated with tuberculosis. The first factor is a high level of multidrug resistance (MDR) of the causative agent of the disease. Currently, every third patient with newly diagnosed respiratory tuberculosis is infected with Mycobacterium tuberculosis (MBT) that is resistant to at least rifampicin. On the whole, Russia has not seen significant changes in the detection rate of such cases recently. However, in Siberian regions, such as the Kemerovo, Tomsk, and Novosibirsk regions, a steady increase in the detection rate has been noted since 2019, exceeding the national value of the parameter [1].

The second problem is associated with a large number of patients with human immunodeficiency virus (HIV) and tuberculosis (TB). In these regions, despite the overall decrease in the proportion of HIV-infected individuals among the population, the incidence of TB and HIV infection is high. In 2023, it was 48.7, 43.2, and 35.8 cases per 100,000 population, respectively [2, 3]. The third aspect is insufficient effectiveness of anti-TB therapy, which is also related to the above two circumstances. Currently, Russia has not achieved the values for the effectiveness of TB treatment recommended by the World Health Organization, especially in treatment regimens for patients with multidrug- / extensively drug-resistant MBT.

Therefore, in addition to introducing new anti-TBs drugs into clinical practice, methods of immune-mediated therapeutic strategies are being actively developed. Their candidates and technologies will not only enhance the potential of etiological treatment but also have immunomodulatory effects [4, 5].

In this regard, the aim of this work was to summarize current data on the role of vitamin D in the immunological response to TB infection, as well as the results of its use as adjuvant therapy in patients with TB, HIV infection, and TB / HIV. The research involved the analysis of scientific papers published in English and Russian. Search queries were conducted in the PubMed and eLIBRARY.ru databases using the following keywords in English: tuberculosis, HIV, immunity, vitamin D, adjuvant immunotherapy, host therapy. The search was mainly limited to the time frame of 2018–2024.

At the initial stage of the analysis, current data on the role of vitamin D in protecting the body from infectious agents, including TB and HIV infection, were identified. At the second stage, following the results of systematic reviews and meta-analyses, information on vitamin D levels in patients with TB and TB/HIV was updated. In the third phase of the study, individual publications were analyzed, which represented randomized controlled trials on vitamin D levels compared to healthy controls, depending on patients' age, localization of the process, disease duration, MBT sensitivity to anti-TB drugs, and the presence of HIV infection.

## THE EFFECT OF VITAMIN D ON MECHANISMS OF NONSPECIFIC AND SPECIFIC BODY DEFENSE AGAINST INFECTIOUS AGENTS

Table 1 presents the main immunomodulatory properties of vitamin D, summarized in recent scientific reviews [6–10]. In the human body, vitamin D is

obtained through foods or produced in the skin under sunlight exposure. Ultraviolet radiation induces the conversion of 7-dehydrocholesterol into previtamin D3, which is then transformed into vitamin D3 or cholecalciferol. In the liver, vitamin D3 undergoes 25-hydroxylation to form 25-hydroxyvitamin D (25(OH)D), calcidiol, the primary circulating form of vitamin D, a prohormone without inherent hormonal activity. Subsequently, most of the 25(OH)D is converted in the kidneys by 1-α-hydroxylase into the bioactive hormonal form 1,25-dihydroxyvitamin D3 (1,25(OH)2D3) under strict regulation by parathyroid hormone, calcium, and phosphorus levels. In this activated state, vitamin D not only exerts classical endocrine effects, controlling calcium metabolism in blood serum and bone tissue, but also affects the immune system, whose effector cells (monocytes, macrophages, dendritic cells, T- and B lymphocytes) possess vitamin D receptors (VDR).

To date, compelling evidence has been obtained regarding the regulation of 1,25(OH)2D3 innate immune responses in the antimicrobial and antiviral defense of the human body, whose target genes *CYP24A1* and *CYP27B1* induce the expression of genes encoding antimicrobial peptides (AMP), β-defensin 2, and hepcidin. Among these, human cationic antimicrobial protein cathelicidin (hCAP18/LL-37) activates not only the signaling pathways for recognizing and binding to scavenger receptors on the cell surface of pathogens but also induces chemotaxis of neutrophils, monocytes, macrophages, and T cells to the site of infection, facilitating the removal of various pathogens by triggering endocytosis, apoptosis, and autophagy of infected cells. Calcitriol directly affects processes in adaptive immunity, regulates the division of T lymphocytes, slows down the transformation of precursor B cells into plasma cells, inhibits the production of interleukins (IL) and costimulatory molecules associated with Th1 cells, and promotes the production of cytokines associated with the Th2 response [6–10].

Table 1

**The Role of Vitamin D in Protecting the Body Against Infectious Agents**

| Immune components, cells | Mechanism, effect |
|---|---|
| Nonspecific immunity | |
| Dendritic cells (DC) | Modulation of DC towards a less mature and more tolerant phenotype with changes in both morphology (more adhesive spindle-shaped cells) and production of cytokines and surface markers; decreased expression of the major histocompatibility complex (MHC) II, differentiation cluster (CD80), costimulatory molecules (CD86) and adhesion molecules (CD54), as well as increased expression of chemokine receptors (CCR5), antigen uptake (DEC205), costimulatory protein of antigen-presenting cells (CD40), mature macrophage molecules (F4/80). |
| Macrophages, monocytes | Acceleration of monocyte maturation into macrophages, enhancement of infected macrophage function through activation of a number of adaptor proteins and kinases that participate in the induction of key antimicrobial factors: CYP24A1, CYP27B1, (CAMP/LL37), DEFB2/DEFB4/HBD2; stimulation of autophagy and autophagosome activity. |
| Cytokine modulation | Suppression of lipopolysaccharide-mediated production of proinflammatory ILs in monocytes and production of IL-2, IL-6, IL-9, IL-17, IL-21, TNFα, induction of transcription of the gene encoding IL-1β, activation of the receptor activator of nuclear factor kappa-B ligand (RANKL) and cyclooxygenase-2 (COX 2), enhancement of expression of the anti-inflammatory cytokine IL-10 in natural killer cells (NK cells) and Th2 cells, which leads to inhibition of IL-12 and IL-23 production and reduction of IFNγ expression. |
| Specific immunity | |
| T lymphocytes | Suppression of T lymphocyte proliferation; reduced activation of T lymphocytes by B lymphocytes through decreased expression of costimulatory molecules (CD860) and increased expression of the differentiation cluster (CD74). |
| Th1 and Th2 cells | Shifting the balance towards the Th2 cell phenotype and inhibition of Th1 cells by reducing the proliferation of autoreactive T lymphocytes, increasing the level of regulatory T cells (Treg), inducing IL-10 and apoptosis of autoreactive T lymphocytes. |
| B lymphocytes and plasma cells | Suppression of plasma cell formation by differentiating mature B cells (through modulation of CD40 and nuclear transcription factor (NF-κB)), induction of apoptosis of activated B lymphocytes. |

In TB, elements of the MBT cell wall are recognized by Toll-like receptors (TLRs), subtypes of which are stimulated by bacterial ligands. TLR2 together with TLR1 detect antigens of the TB cell wall, mediated through TLR4, which are activated by the 38-kDa MBT antigen. Through the 19-kDa bacterial lipopolysaccharide of the MBT cell membrane, macrophages are stimulated, where 25(OH)

D is converted into an active metabolite through hydroxylation and binds to VDR whose signal passes into the nucleus. This increases gene transcription for hCAP18/LL-37, and cathelicidin and other AMPs are formed [9, 10]. Digestive capacity is enhanced, apoptosis is enhanced, and the antimycobacterial and antiviral potential of infected macrophages is realized, as cathelicidin affects retrovirus replication in HIV infection [11]. Additionally, 25(OH)D increases the level of cytokines (IL-4, 5, 6, 10, 18, INFγ), enhancing both cellular and antibody-mediated immune responses. At the same time, the influence of vitamin D on the expression, secretion, and activity of a number of matrix metalloproteinases (MMPs) has been proven. 25(OH)D reduces the expression of MMP-7, MMP-9, and MMP-10 in human peripheral blood monocytes and increases the expression of tissue MMP inhibitor (TIMP-1), which helps reduce the severity of pulmonary parenchyma destruction and the formation of cavitation during TB inflammation [12].

## VITAMIN D DEFICIENCY IN PATIENTS WITH TUBERCULOSIS AND HIV INFECTION

Recent scientific research continues to actively explore the relationship between the detected vitamin D deficiency in TB. The conflicting results of vitamin D levels determined in systematic reviews are explained by the population/genetic/racial characteristics of patients, differing in territorial affiliation, duration of exposure and intensity of natural ultraviolet radiation, standard of living and socio-economic status, as well as age, gender, nutrition, and the presence of concomitant pathology, primarily liver-related one [13–15].

Vitamin D deficiency can also be caused by congenital anomalies in vitamin D metabolism associated with mutations in the cytochrome P450 system (CYP3A4, CYP24A1), which lead to dysregulation of the activity of 24-, 25-, 1α-hydroxylase enzymes that accelerate its inactivation and excretion, as well as mutations in vitamin D receptors leading to the development of target organ resistance [16]. It has been proven that taking certain medications, such as thiazide diuretics, phenytoin, phenobarbital, carbamazepine, and theophylline, affects vitamin D metabolism. Among anti-TB drugs, isoniazid induces the cytochrome P450 enzyme system, thereby changing the level of 25-hydroxylases and 1-hydroxylases, while rifampicin activates CYP3A4 [9, 17]. Among antiviral drugs used to treat HIV-infected patients, efavirenz alters vitamin D levels and induces CYP24A1 enzymes that promote the breakdown of 25(OH)D and active vitamin D 1,25(OH)2D3 into inactive water-soluble metabolites [18].

Until 2024, optimal vitamin D concentrations in blood serum were recognized as values ranging from 30 to 100 ng / ml (75–250 nmol / l). Insufficiency was recognized at 20–30 ng / ml (50–75 nmol / l), and deficiency was noted at < 20 ng / ml (< 50 nmol / l). Currently, clinical guidelines from global endocrinology experts have determined that vitamin D deficiency in the human body, which should be artificially replenished, needs to be re-evaluated [19]. This is especially important considering the growing evidence of the role of vitamin D in innate immunity against infections, diabetes mellitus, cancer, autoimmune, cardiovascular, and other diseases.

In this regard, scientific publications of randomized controlled trials (RCTs) of recent years deserve consideration, including data on vitamin D levels in the blood serum of patients with TB of various localizations, comparable in age and gender with healthy controls (Table 2). Unfortunately, there is no current comparative analysis of 25(OH)D content in the blood serum in the Russian cohort of patients. During the specified period, only values for children and adolescents with TB were published [20, 21]. The study by L.V. Panova deserves attention, where out of 75 patients under the age of 18 years, 49.3% had a concentration of 25(OH)D in the blood serum of less than 10 ng / ml, and significant differences were found in the level of 25(OH) D in the groups of newly diagnosed patients and those with repeat admissions: 13.10 ± 1.04 ng / ml and 8.74 ± 1.07 ng / ml, respectively.

Table 2

**Vitamin D Levels in the Blood Serum of Patients with Tuberculosis (according to Case – Control Studies, 2018–2024)**

| Country | Sample (*n*), TB / HC | Age (years), men / women | Tuberculosis localization, *n* | *M* ± *m* or *Me* ($Q_1$; $Q_3$), ng / ml | Year, reference |
|---|---|---|---|---|---|
| Russia | 75, 75 / no HC | TB – up to 17, 29/46 | PTB, 75 | 13.10 ± 1.04 (newly detected TB) 8.74 ± 1.07 (TB relapse) | 2024, [20] |
| Russia | 31, 31 / no HC | TB – up to 14, 13/18 | PTB, 31 | 14.60 ± 1.30 | 2024, [21] |

End of table 2

| Country | Sample (*n*), TB / HC | Age (years), men / women | Tuberculosis localization, *n* | *M* ± *m* or *Me* ($Q_1$; $Q_3$), ng / ml | Year, reference |
|---|---|---|---|---|---|
| India | 116, 58/58 | TB – 50, 31/27<br>HC – 49, 32/26 | PTB, 29<br>EPTB , 29 | PTB – 15.30 (8.63, 23.47)<br>EPTB – 13.40 (8.47, 25.72)<br>HC – 19.08 (13.92, 26.17) | 2024, [16] |
| India | 400, 200/200 | TB – 32, 130/70<br>HC – 33, 120/80 | PTB, 122<br>EPTB, 78 | PTB – 18.02 ± 7.58<br>EPTB – 17.26 ± 6.58<br>HIV (-) – 17.65 ± 7.26<br>HIV (+) – 17.48 ± 7.13<br>DS-TB – 17.82 ± 7.36<br>MDR-TB – 17.25 ± 6.50<br>HC – 32.34 ± 13.79 | 2024, [22] |
| Egypt | 89, 47/42 | TB – 32, 25/22<br>HC – 31, 22/20 | PTB, 47 | TB – 17.1 ± 5.5<br>HC – 51.8 ± 27.3 | 2024, [23] |
| Uganda | 95, 78/22 | TB – 28, 37/46<br>HC – 28, 9/13 | PTB, 78 | TB – 17 (12.6, 21.4)<br>LTB – 23 (16, 29.2)<br>HC – 22 (16.7, 27.8) | 2022, [24] |
| India | 100, 50/50 | All over 18 years,<br>TB – 88/12<br>HC – 88/12 | PTB, 50 | TB – 19 (7.75, 27.25)<br>HC – 25 (19.75, 32.00) | 2021, [25] |
| Peru | 889, 180/709 | TB – over 25 years 50.6%, 94/86<br>HC – over 25 years 49.5%, 366/343 | PTB, 180 | TB – 21.5 (17.1, 25.6)<br>HC – 21.9 (44.5-67.1) | 2019, [13] |
| Brazil | 72 24/48 | TB – 32, 24/0<br>HC – 33, 48/0 | PTB, 24 | TB – 27.7 ± 7.85<br>HC – 37.1 ± 8.94 | 2018, [26] |

Note. TB / HC – tuberculosis / healthy controls, PTB – pulmonary tuberculosis, EPTB – extrapulmonary tuberculosis, LTB – latent tuberculosis infection, DS-TB – drug-susceptible tuberculosis, MDR-TB multidrug-resistant tuberculosis.

Recent studies from Asia and Africa have demonstrated vitamin D deficiency in adult TB patients, and that characteristics of the disease (localization, drug sensitivity of MBT, presence of HIV) do not affect its concentration [16, 22]. In these studies, vitamin D deficiency was considered as a predisposing factor for the development of TB, as its insufficiency was recorded in patients at the initiation of anti-TB treatment. A case-control study from India showed that the prevalence of vitamin D insufficiency in TB patients according to accepted criteria was 68.9% compared to 51.7% in the control group, with medians of 14.35 ng / ml (8.65, 25.48) and 19.08 ng / ml (13.92, 26.17), respectively [16]. In another study from the same country, the concentration of 25(OH)D in pulmonary tuberculosis (PTB) was slightly higher (18.02 ng / ml) and did not change significantly in patients with extrapulmonary TB (EPTB), in TB patients with cooccurring HIV, and in patients with drug-resistant TB. Similar data were presented by scientists from African countries.

On the contrary, research results from South America (Brazil, Peru) did not reveal vitamin D insufficiency, medians of 25(OH)D in TB patients exceeded 20 ng / ml and were comparable to values in people with latent tuberculosis infection (LTB) and patients who had disease progression. Researchers from European countries indicated a range of vitamin D close to normal (from 20 to 30 ng / ml) in TB patients with its associations with the disease, its spread (tuberculosis of multiple localizations), and comorbid HIV [27].

A notable randomized clinical trial from India compared the concentrations of vitamin D, calcium, and parathyroid hormone in the blood serum of patients with PTB not only with healthy controls but also depending on MBT sensitivity to anti-TB drugs. Randomization in the study groups excluded patients with concomitant pathology of the liver, kidneys, heart, gastrointestinal tract, and as well as with HIV infection. For the first time in such studies, the dietary and insolation characteristics of patients were determined in parallel. The results of the trial convincingly demonstrated that patients with MDR-TB had lower baseline concentrations of vitamin D in their blood serum than patients with DS-TB and controls. At the same time, vitamin D consumption through food had a greater impact on its level than weekly exposure to sunlight [28].

In HIV-infected patients, a similar situation was observed in cohort studies with gender-, age-, and residence-matched controls. Only studies from China, India, and the United States recorded vitamin D levels below 20 ng / ml (15.93 (13.92, 17.94) ng / ml, 19.7 (17.64, 21.76) ng / ml, and 19.09 (13.43, 24.750) ng / ml, respectively). In other countries, according to systematic reviews and meta-analyses, these values in HIV-infected individuals did not significantly differ from the controls [29]. Despite this, a relationship was found between vitamin D deficiency and the risk of disease progression to the stage of acquired immunodeficiency syndrome and all-cause mortality, as vitamin D deficiency prevalence reached 85% [18]. Meanwhile, inflammatory processes characteristic of HIV infection and immune system activation, leading to increased levels of IL-6 and TNFα and impaired renal 1α-hydroxylase activity, exacerbate vitamin D insufficiency in patients with TB/HIV co-infection [30].

## ADJUVANT VITAMIN D THERAPY FOR TUBERCULOSIS AND HIV INFECTION

In clinical phthisiology practice, increasing evidence is accumulating about the positive effects of combination treatment. In studies of patients with TB undergoing chemotherapy with vitamin D administration (total dose of 600,000 IU), positive clinical and radiological dynamics are demonstrated in the form of weight gain in patients, reduced intoxication, cough, and normalization of hematological parameters, as well as a pronounced decline of infiltrative and destructive processes in the lungs compared to the control group [31, 32]. This applies to both adults and children (1,000 IU / day) [33, 34]. There is evidence that a single administration of vitamin D at a dose of 200,000 IU during PTB treatment leads to reduction of sputum conversion time compared to the group receiving only standard anti-TB treatment [35].

In patients with type 2 diabetes mellitus and PTB, a negative acid-fast bacillus smear was obtained after 6 weeks of anti-TB treatment and vitamin D intake (total of 60,000 IU per week) compared to 8 weeks of conventional treatment in the control group [36]. In some studies, vitamin D administration regimens were prolonged. A relatively similar positive effect was achieved after daily intake of vitamin D at a dose of 10,000 IU (250 μg / day) for 6 weeks for PTB and oral administration of 50,000 IU once a week for 6 weeks (total of 300,000 IU) with a maintenance dose of 1,000 IU per day for 3 months of treatment for EPTB [37].

The largest ($n$ = 4,000) double-blind, placebo-controlled study assessing the impact of combining vitamin D and antiretroviral therapy on the development of TB and mortality in adult HIV-infected patients was conducted in Tanzania [38]. Antiviral treatment and oral administration of four doses of vitamin D (50,000 IU) once a week with a prolonged administration of 2,000 IU per day did not affect mortality and did not increase patient one-year survival compared to patients in the placebo control group. Later, a comprehensive systematic review and meta-analysis including 14 studies formulated the same conclusions [39]. Additionally, scientists did not find the expected positive effect on the number of CD4+ cells in microliters of peripheral blood and viral load. Similarly, in TB, as well as in TB/HIV co-infection, mortality and recurrence rates did not differ in comparison groups depending on patients' vitamin D intake. No effect of vitamin D intake on sputum conversion time was found, either by smear microscopy or culture.

Thus, based on the published research, no statistical differences have been found in the effectiveness of TB treatment, including cooccurring HIV / TB treatment, in patient groups depending on vitamin D intake. The noted positive clinical effects of combined anti-TB treatment with vitamin D intake, such as faster reduction of intoxication symptoms, normalization of acute-phase proteins in peripheral blood, and impact on destructive processes in the lungs, require further study.

## CONCLUSION

In the global medical community, research focused on developing host-directed therapy has intensified [4, 5, 39, 40]. Today's challenges for phthisiology require not only progress in creating new anti-TB drugs and repurposing existing medicinal compounds but also re-engineering of multifunctional personalized immunotherapy. Immune activators or suppressors based on chemical compounds, drugs with immunomodulatory properties, interleukins, granulocyte-macrophage colony-stimulating factor, cell therapy based on allogeneic immune effector cells, as well as new drugs obtained through nano- and biotechnologies, can make an effective contribution to schemes for combined anti-TB therapy aimed primarily at reducing treatment duration and increasing safety and clinical effectiveness.

Stimulation of receptor-induced expression of antimicrobial peptides, induction of autophagy, as well as regulation of proinflammatory cytokine secretion and modulation of matrix metalloproteinase production comprise the potential of immunoadjuvant therapy for TB patients using vitamin D. Currently, due to the lack of data, Russian specialists have not reached a consensus regarding the use of vitamin D in chemotherapy regimens (standard / individual), age categories of patients (newly diagnosed / relapse / chronic course), localization of the process, as well as comorbid HIV. Therefore, initiating clinical trials on the use of vitamin D in TB and HIV infection, taking into account individual patient characteristics, is a pressing issue for developing clinical guidelines.

## REFERENCES


1. Starodubov V.I., Tsybikova E.B., Kotlovskiy M.Yu., Lapshina I.S. The Incidence of Tuberculosis in Russian Federation in the Period before and during the COVID-19 Pandemic. *Infektsionnye Bolezni: Novosti, Mneniya, Obuchenie*. 2023;12(3):18–25. (In Russ.). DOI: 10.33029/2305-3496-2023-12-3-18-25.
2. Stavitskaya N.V., Felker I.G., Nemkova E.K. Diagnosis of Drug Resistance of M. tuberculosis in the Regions of the Siberian Federal District. *Tuberculosis and Lung Diseases*. 2024;102(3):48–57. (In Russ.). DOI: 10.58838/2075-1230-2024-102-3-48-57.
3. Stavitskaya N.V., Nemkova E.K., Tashkova G.V. Key Indicators of Anti-Tuberculosis Activities in the Siberian and Far Eastern Federal Districts (*Statistical Materials*). Novosibirsk, 2024:158. https://cloud.mail.ru/public/nKcw/UEEQ7GSeo. (In Russ.).
4. Mi J., Wu X., Liang J. The advances in adjuvant therapy for tuberculosis with immunoregulatory compounds. *Front. Microbiol*. 2024;15. DOI: 10.3389/fmicb.2024.1380848.
5. Mozhokina G.N., Samoylova A.G., Abramchenko A.V., Romanova M.I., Vasilyeva I.A. Strategy of the Host-Directed Therapy for Tuberculosis: the Importance of Interferon-Gamma in the Pathogenesis and Therapy of Tuberculosis Infection. *Tuberculosis and Lung Diseases.* 2024;102(1):72–81. (In Russ.). DOI: 10.58838/2075-1230-2024-102-1-72-81.
6. Ismailova A., White J.H. Vitamin D, infections and immunity. *Rev. Endocr. Metab. Disord*. 2022;23:265–277. DOI: 10.1007/s11154-021-09679-5.
7. Bikle D.D. Vitamin D Regulation of Immune Function. *Curr. Osteoporos Rep*. 2022;20(3):186–193. DOI: 10.1007/s11914-022-00732-z.
8. Lavryashina M.B., Imekina D.O., Thorenko B.A., Ulyanova M. V., Meyer A.V., Tarasova O.L. et al. The Signaling Cascade of the Vitamin D System in Macrophages against Mycobacterium Tuberculosis. *Infection and Immunity*. 2023;13(2):234–242. (In Russ.). DOI: 10.15789/2220-7619-VDS-2033.
9. Papagni R., Pellegrino C., Di Gennaro F., Patti G., Ricciardi A., Novara R. et al. Impact of vitamin D in prophylaxis and treatment in tuberculosis patients. *Int. J. Mol. Sci*. 2022;23(7). DOI: 10.3390/ijms23073860.
10. Junaid K., Rehman A. Impact of vitamin D on infectious disease-tuberculosis-a review. *Clinical Nutrition Experimental.* 2019;25:1–10. DOI: 10.1016/j.yclnex.2019.02.003.
11. Ayelign B., Workneh M., Molla M.D., Dessie G. Role of vitamin-D supplementation in TB/HIV co-infected patients. *Infect. Drug Resist*. 2020; 13:111–118. DOI: 10.2147/IDR.S228336.
12. Coussens A., Timms P.M., Boucher B.J., Boucher B.J., Venton T.R., Ashcroft A.T. et al. 1alpha,25-dihydroxyvitamin D3 inhibits matrix metalloproteinases induced by Mycobacterium tuberculosis infection. *Immunology*. 2009;127(4):539–548. DOI: 10.1111/j.1365-2567.
13. Aibana O., Huang C-C., Aboud S., Arnedo-Pena A., Becerra M.C., Bellido-Blasco J.B. et al. Vitamin D status and risk of incident tuberculosis disease: A nested case-control study, systematic review, and individual-participant data meta-analysis. *PLoS Med.* 2019;16(9):1002907. DOI: 10.1371/journal.pmed.1002907.
14. Zhou Y., Wu Q., Wang F., Chen S., Zhang Y., Wang W. et al. Association of variant vitamin statuses and tuberculosis development: a systematic review and meta-analysis. *Ann. Med*. 2024;56(1). DOI: 10.1080/07853890.2024.2396566.kafle.
15. Kafle S., Basnet A.K., Karki K., Thapa Magar M., Shrestha S., Yadav R.S. Association of Vitamin D Deficiency with Pulmonary Tuberculosis: A Systematic Review and Meta-Analysis. *Cureus.* 2021;13(9):e17883. DOI: 10.7759/cureus.17883.
16. Mamadapur V.K., Nagaraju S., Prabhu M.M. Comparative study of vitamin D levels in newly diagnosed tuberculosis and a normal population. *Medicina.* 2024;60(5):685. DOI: 10.3390/medicina60050685.
17. Chesdachai S., Zughaier S.M., Hao L., Kempker R.R., Blumberg H.M., Ziegler T.R. et al. The effects of first-line anti-tuberculosis drugs on the actions of vitamin D in human macrophages. *J. Clin. Transl. Endocrinol*. 2016;6:23–29. DOI: 10.1016/j.jcte.2016.08.005.
18. Allavena C., Delpierre C., Cuzin L., Rey D., Viget N., Bernard J. et al. High frequency of vitamin D deficiency in HIV-infected patients: effects of HIV-related factors and antiretroviral drugs. *Journal of Antimicrobial Chemotherapy*. 2012;67(9):2222–2230. DOI: 10.1093/jac/dks176.
19. McCartney C.R., McDonnell M.E., Corrigan M.D., Lash R.W. Vitamin D Insufficiency and Epistemic Humility: An Endocrine Society Guideline Communication. *J. Clin. Endocrinol. Metab*. 2024;109(8):1948–1954. DOI: 10.1210/clinem/dgae322.
20. Panova L.V., Averbakh M.M., Ovsyankina E.S., Zakharova I.N., Karasev A.V., Khokhlova Y.Y. et

al. The vitamin D Status and the Levels of β1- and β2-Defensins in Children and Adolescents with Different Forms of Pulmonary TB. *Medical Council*. 2024;18(1):90–96. (In Russ.). DOI: 10.21518/ms2024-006.
21. Yarovaya J.A., Lozovskaya M.E., Krylova S.A., Gurina O.P., Blinov A.E., Shibakova N.D. Vitamin D Status in Children with Latent Tuberculosis Infection and Patients with Tuberculosis. *Medical Council*. 2024;(19):214–222. (In Russ.). DOI: 10.21518/ms2024-393.
22. Zafar S., Siddiqui Z., Agrawal N., Madhurmay Singh M. A Comparative Analysis of Vitamin D Status among Tuberculosis Patients and Healthy Household Contacts: A Case–Control Study from Central India. *Apollo Medicine*. 2024;21(4):308–313. DOI: 10.1177/09760016241245580.
23. Eletreby R., Elsharkawy A., Mohamed R., Hamed M., Kamal Ibrahim E., Fouad R. Prevalence of vitamin D deficiency and the effect of vitamin D3 supplementation on response to anti-tuberculosis therapy in patients with extrapulmonary tuberculosis. *BMC Infect. Dis*. 2024;24(1):681. DOI: 10.1186/s12879-024-09367-0.
24. Acen E.L., Biraro I.A., Bbuye M., Kateete D.P., Joloba M. L., Worodria W. Hypovitaminosis D among newly diagnosed pulmonary TB patients and their household contacts in Uganda. *Sci. Rep*. 2022;12(1):5296. DOI: 10.1038/s41598-022-09375-7.
25. Jaimni V., Shasty B.A., Madhyastha S.P., Shetty G.V., Acharya R.V., Bekur R. et al. Association of vitamin D deficiency and newly diagnosed pulmonary tuberculosis. *Pulm. Med*. 2021; 2021:5285841. DOI: 10.1155/2021/5285841.
26. Maceda E.B., Gonçalves C.C.M., Andrews J.R., Andrews J.R., Ko A.I., Yeckel C.W. et al. Serum vitamin D levels and risk of prevalent tuberculosis, incident tuberculosis and tuberculin skin test conversion among prisoners. *Sci. Rep.* 2018;8(1):997. DOI: 10.1038/s41598-018-19589-3.
27. Nielsen N.O., Skifte T., Andersson M., Wohlfahrt J., Soborg B., Koch A. et al. Both high and low serum vitamin D concentrations are associated with tuberculosis: a case – control study in Greenland. *British Journal of Nutrition*. 2010;104(10):1487–1491. DOI: 10.1017/S0007114510002333.
28. Rathored J., Sharma S.K., Chauhan A., Singh B., Banavaliker J.N., Sreenivas V. et al. Low serum vitamin D in North Indian multi-drug-resistant pulmonary tuberculosis patients: the role of diet and sunlight. *Ann. Med*. 2023;55(2):2291554. DOI: 10.1080/07853890.2023.2291554.
29. Wang Y., Huang X., Wu Y., Li A., Tian Y., Ren M. et al. Risk of Vitamin D Deficiency Among HIV-Infected Individuals: A Systematic Review and Meta-Analysis. *Front. Nutr*. 2021;8: 722032. DOI: 10.3389/fnut.2021.722032.
30. Xie K., Zhang Y., Zhang M., Wu H., Zheng L., Ji J. et al. Association of vitamin D with HIV infected individuals, TB infected individuals, and HIV-TB co-infected individuals: a systematic review and meta-analysis. *Front. Public Health*. 2024;12:1344024. DOI: 10.3389/fpubh.2024.1344024.
31. Salahuddin N., Ali F., Hasan Z., Rao N., Aqeel M., Mahmood F. Vitamin D accelerates clinical recovery from tuberculosis: results of the SUCCINCT Study [Supplementary Cholecalciferol in recovery from tuberculosis]. A randomized, placebo-controlled, clinical trial of vitamin D supplementation in patients with pulmonary tuberculosis. *BMC Infect. Dis*. 2013;13:22. DOI: 10.1186/1471-2334-13-22.
32. Martineau A.R., Timms P.M., Bothamley G.H., Hanifa Y., Islam K., Claxton A.P. et al. High-dose vitamin D3 during intensive-phase antimicrobial treatment of pulmonary tuberculosis: a double-blind randomised controlled trial. *Lancet*. 2011;377(9761):242–250. DOI: 10.1016/S0140-6736(10)61889-2.
33. Tamara L., Kartasasmita C.B., Alam A., Gurnida D.A. Effects of Vitamin D supplementation on resolution of fever and cough in children with pulmonary tuberculosis: A randomized double-blind controlled trial in Indonesia. *J. Glob. Health*. 2022;12:04015. DOI: 10.7189/jogh.12.04015.
34. Wen Y., Li L., Deng Z. Calcitriol supplementation accelerates the recovery of patients with tuberculosis who have vitamin D deficiency: a randomized, single-blind, controlled clinical trial. *BMC Infect. Dis*. 2022;22(1):436. DOI: 10.1186/s12879-022-07427-x.
35. Hassanein E.G., Mohamed E.E., Baess A.I., El-Sayed E.T., Yossef A.M. The role of supplementary vitamin D in treatment course of pulmonary tuberculosis. *Egypt. J. Chest. Dis. Tuberculosis*. 2016;65(3):629–635. DOI: 10.1016/j.ejcdt.2016.03.004.
36. Kota S.K., Jammula S., Tripathy P.R., Panda S., Modi K.D. Effect of vitamin D supplementation in type 2 diabetes patients with pulmonary tuberculosis. Diabetes metabolic syndrome. *Clin. Res. Reviews*. 2011;5(2):85–89. DOI: 10.1016/j.dsx.2012.02.021.
37. Eletreby R., Elsharkawy A., Mohamed R. Prevalence of vitamin D deficiency and the effect of vitamin D3 supplementation on response to anti-tuberculosis therapy in patients with extrapulmonary tuberculosis. *BMC Infect. Dis* 24. 2024;681. DOI: 10.1186/s12879-024-09367-0.
38. Sudfeld C.R., Mugusi F., Muhihi A., Aboud S., Nagu T.J., Ulenga N. et al. Efficacy of vitamin D (3) supplementation for the prevention of pulmonary tuberculosis and mortality in HIV: a randomised, double-blind, placebo-controlled trial. The lancet HIV. 2020;7(7):463–471. DOI: 10.1016/S2352-3018(20)30108-9
39. Cai L., Wang G., Zhang P., Hu X., Zhang H., Wang F. et al. The progress of the prevention and treatment of vitamin D to tuberculosis. *Front. Nutr.* 2022;9:873890. DOI: 10.3389/fnut.2022.873890.
40. Sun Q., Li S., Gao M., Pang Y. Therapeutic strategies for tuberculosis: progress and lessons learned. *Biomedical and Environmental Sciences.* 2024;37(11):1310–1323. DOI: 10.3967/bes2024.168.

## Author Information

**Filinyuk Olga V.** – Dr. Sci. (Med.), Professor, Head of the Division of Phthisiology and Pulmonology, SibSMU, Tomsk, filinyuk.olga@yandex.ru, https://orcid.org/0000-0002-5526-2513
**Khokhlyuk Vasilina V.** – Student, SibSMU, Tomsk, khokhliuk2001@mail.ru, http://orcid.org/0009-0005-3385-0575
**Volkovskaya Anastasia O.** – Student, SibSMU, Tomsk, nastya120701@yandex.ru, http://orcid.org/0009-0001-1233-5874

(✉) **Filinyuk Olga V.,** filinyuk.olga@yandex.ru

Received on February 03, 2025;
approved after peer review on March 13, 2025;
accepted on March 20, 2025

УДК 616-006.6:615.375:577.27
https://doi.org/10.20538/1682-0363-2025-3-172-178

# Dendritic cells as a basis for designing anti-cancer vaccines

**Frantsiyants E.M., Bandovkina V.A., Surikova E.I., Cheryarina N.D., Kaplieva I.V., Menshenina A.P., Shikhlyarova A.I., Neskubina I.V.**

*National Medical Research Centre for Oncology*
*63 14th Liniya, 344037 Rostov-on-Don, Russian Federation*

**ABSTRACT**

Dendritic cells (DCs) have been shown to play a pivotal role in orchestrating the immune response against tumors, thereby acting as a link between innate and adaptive immunity. DCs capture, process, and present tumor antigens to T cells, which triggers a specific immune response aimed at destroying cancer cells. DCs are a heterogeneous population that includes several subtypes, such as conventional DCs (cDC1, cDC2) and plasmacytoid DCs (pDC). Each subtype has unique functions: cDC1s specialize in activating CD8+ T cells, while pDCs produce interferons in response to viral infections. In a tumor microenvironment, DCs are often depleted of their functionality due to immunosuppressive factors, such as IL-6 and PGE2, which impedes their ability to activate T cells. Furthermore, an imbalance between oxidative phosphorylation and glycolysis regulated by the AMPK/mTOR axis may lead to the immunosuppressive phenotype of DCs.

A promising direction in cancer immunotherapy is the creation of DC-based vaccines that can restore the immunogenicity of cold tumors lacking T cell infiltration. Such vaccines can be created by generating DCs *in vitro* or modifying them to enhance the presentation of tumor antigens.

Despite significant advances, the biology of DCs remains poorly understood. This lecture highlights the importance of DCs in developing new cancer treatment strategies and opens up prospects for more effective immunotherapeutic approaches.

**Keywords:** dendritic cells, antitumor vaccine

**Conflict of interest.** The authors declare the absence of obvious or potential conflicts of interest related to the publication of this article.

**Source of financing.** The authors state that they received no funding for the study.

**For citation:** Frantsiyants E.M., Bandovkina V.A., Surikova E.I., Cheryarina N.D., Kaplieva I.V., Menshenina A.P., Shikhlyarova A.I., Neskubina I.V. Dendritic cells as a basis for designing anti-cancer vaccines. *Bulletin of Siberian Medicine.* 2025;24(3):172–178. https://doi.org/10.20538/1682-0363-2025-3-172-178.

# Дендритные клетки как основа конструирования противораковых вакцин

**Франциянц Е.М., Бандовкина В.А., Сурикова Е.И., Черярина Н.Д., Каплиева И.В., Меньшенина А.П., Шихлярова А.И., Нескубина И.В.**

*Национальный медицинский исследовательский центр (НМИЦ) онкологии*
*Россия, 344037, г. Ростов-на-Дону, ул. 14-я линия, 63*

**РЕЗЮМЕ**

Дендритные клетки (ДК) играют ключевую роль в организации иммунного ответа против опухолей, выступая связующим звеном между врожденным и адаптивным иммунитетом. Они захватывают,

✉ *Bandovkina Valerija A.,* valerryana@yandex.ru

обрабатывают и представляют опухолевые антигены Т-клеткам, что запускает специфический иммунный ответ, направленный на уничтожение раковых клеток. Представляют собой неоднородную популяцию, включающую несколько подтипов, таких как обычные ДК (cDC1, cDC2) и плазмоцитоидные ДК (pDC). Каждый подтип выполняет уникальные функции: cDC1 специализируются на активации CD8+ Т-клеток, а pDC вырабатывают интерфероны. В микроокружении опухоли ДК часто теряют свою функциональность из-за иммуносупрессивных факторов, таких как IL-6 и PGE2, что затрудняет их способность активировать Т-клетки. Кроме того, нарушение баланса между окислительным фосфорилированием и гликолизом, регулируемым осью AMPK/mTOR, может приводить к иммуносупрессивному фенотипу ДК.

Перспективным направлением в иммунотерапии рака является создание вакцин на основе ДК, которые могут восстанавливать иммуногенность «холодных» опухолей, лишенных инфильтрации Т-клеток. Такие вакцины созданы путем генерации ДК *in vitro* или их модификации для усиления презентации опухолевых антигенов.

Несмотря на значительные успехи, биология ДК остается недостаточно изученной. Эта работа подчеркивает важность ДК в разработке новых стратегий лечения рака и открывает перспективы для создания более эффективных иммунотерапевтических подходов.

**Ключевые слова:** дендритные клетки, противоопухолевая вакцина

**Конфликт интересов.** Авторы декларируют отсутствие явных и потенциальных конфликтов интересов, связанных с публикацией настоящей статьи.

**Источник финансирования.** Авторы заявляют об отсутствии финансирования при проведении исследования.

**Для цитирования:** Франциянц Е.М., Бандовкина В.А., Сурикова Е.И., Черярина Н.Д., Каплиева И.В., Меньшенина А.П., Шихлярова А.И., Нескубина И.В. Дендритные клетки как основа конструирования противораковых вакцин. *Бюллетень сибирской медицины.* 2025;24(3):172–178. https://doi.org/10.20538/1682-0363-2025-3-172-178.

## INTRODUCTION

The immune system plays a key role in recognizing and destroying tumor cells, and in recent years, significant advances have been made in developing therapeutic strategies aimed at activating the immune system to fight tumors [1].

Cell-based therapeutic anti-cancer vaccines use autologous tumor cells derived from the patient, allogeneic tumor cell lines, or autologous antigen-presenting cells to mimic the natural immune process and stimulate an adaptive immune response against tumor antigens. Such vaccines have been developed over decades and various approaches have been used to create vaccine constructs for anticancer therapy. In general, they can be divided into cell-based vaccines, viral vector-based vaccines, and molecular vaccines consisting of peptides, deoxyribonucleic acid (DNA) or ribonucleic acid (RNA) [2].

Tumor cell-based vaccines have an important advantage: they contain multiple neoantigens, thus avoiding the need for prior identification of specific target antigens. However, their efficacy may be limited by inadequate presentation of antigens to the immune system. If the antigens are not effectively presented by dendritic cells, the immune response may be weak, reducing the efficacy of the vaccine [3]. Tumor neoantigens are proteins produced as a result of mutations in tumor cells that can undergo processing and presentation for recognition by T lymphocytes [4].

The aim of this lecture was to discuss the use of dendritic cells in the development of novel cancer treatment strategies.

## THE ROLE OF DENDRITIC CELLS IN ANTITUMOR IMMUNITY

Dendritic cells (DCs) play a key role in producing effective T-cell responses against tumors and are the basis of modern immunotherapy strategies aimed at replenishing depleted T cells in the tumor microenvironment. Cancer therapy with DC-based vaccines has attracted considerable attention. However, their functional behavior is determined by multiple factors. The type of DCs, transcription program, location, intratumor factors, and inflammatory environment all influence DCs, which may result in enhancement or suppression of antitumor immunity [5].

Conventional DCs (cDCs) are formed in the bone marrow from a common monocyte – dendritic cell progenitor (MDP), from which a common DC progenitor (CDP) originates. In the bone marrow, it gives rise to cDC1 (pre-cDC1) and cDC2 (pre-cDC2) precursors, whose terminal differentiation occurs in peripheral tissues under the influence of the antigenic and inflammatory microenvironment. Plasmacytoid DCs (pDCs) are thought to develop from a separate CDP subpopulation; however, there is an alternative view that their progenitor may be an IL-7R+ lymphoid precursor [6–8]. Using technologies based on the study of single cells, it was found that rDCs originating from lymphoid and myeloid tissues have different functional and transcriptional profiles despite similar phenotypic markers [9].

Immature DCs localize in the bloodstream or peripheral tissues and are activated by signals delivered through pattern recognition receptors (PRRs), including Toll-like receptors (TLRs), retinoic acid-inducible gene-I (RIG-I)- like receptor, nucleotide-binding oligomerization domain-like receptors, and C-type lectin receptors (CLRs). These PRRs allow DCs to respond rapidly to pathogen-associated molecular patterns (PAMP) or danger-associated molecular patterns (DAMP). Under conditions of homeostasis, DCs take up harmless antigens that are to be transferred. When DCs are activated through PRR stimulation, they increase the expression of chemokine receptors, such as chemokine C-C receptor type 7 (CCR7), which promotes DC migration to the draining lymph node. In addition, PRR activation leads to increased expression of MHC molecules, co-stimulatory surface molecules (CD40, CD80, CD86), and cytokines (IL-12, IL-10, IL-23, TNFα), which promotes the transition from resting immature DCs to functional mature DCs capable of activating T cells in the lymph node [10].

Possessing multiple PRRs, DCs recognize DAMP signals and safety-associated signals, which is crucial for triggering appropriate T-cell responses. In addition, they efficiently integrate signals from the local tissue microenvironment to fine-tune T cell responses. Under normal physiologic conditions, DCs play a key role in maintaining immune homeostasis by activating T cells to destroy infected or malignant cells and stimulating regulatory T cells to attenuate chronic inflammation. Immune dysregulation contributes to cancer and tumor-induced immunosuppression, including T-cell depletion, which poses significant obstacles to cancer immunotherapy. Restoration of functional activity of depleted T cells to stimulate antitumor response is the main goal of modern immunotherapeutic strategies [11].

DCs are professional antigen-presenting cells optimized for activation of T-cell responses. DCs play a central role in orchestrating effective CD8+ T-cell responses against tumors [12]. At the initial stage of antitumor immune responses, recognition of tumor antigens by T cells depends on their presentation by DCs. This process begins with the capture of tumor antigens by DCs, which intracellularly bind to major histocompatibility complex (MHC) molecules. These MHC peptide complexes (pMHC) are then transported to the cell surface to prime and activate effector T cells in the lymph node draining the tumor. DCs are professional antigen-presenting cells (APCs). Their expressed major histocompatibility complex type I (MHC-I) molecules present antigens for recognition to CD8+ and MHC-II – to CD4+ T lymphocytes, where, with the participation of costimulatory molecules, proliferation of a clone of T cells specifically recognizing a certain antigen takes place. The assistance of CD4+ T cells, especially activated effector memory Th1 cells, enhances the activation of CD8+ T cells through CD40 signaling to DCs [13]. This interaction promotes antigen cross-presentation, migration of T cells to the tumor, and induction of their effector functions and immunological memory formation [14]. In the tumor microenvironment (TME), cytotoxic T cells (CD8+) recognize specific antigens on the surface of tumor cells, leading to their destruction. Following tumor cell death, new antigens are released and captured by APCs, which restarts the cycle of anti-tumor immune responses. Importantly, APCs that capture and process tumor antigens may differ from those that activate tumor antigen-specific T cells in lymph nodes. Several mechanisms of antigen transfer between different types of DCs have been proposed, including cross-presentation of phagocytized fragments from donor DCs, presentation via MHC, and synaptic transmission of antigen-loaded vesicles [15].

## SUBTYPES OF DENDRITIC CELLS

DCs are a heterogeneous population consisting of multiple subtypes with unique functions that have been identified over the past decade in both mice and humans. However, the exact number of DC subtypes, their interrelationships, and differences from other mononuclear phagocytes remain a subject of research

[16]. DCs can be divided into subtypes depending on their function and phenotypic markers. Initially, conventional DCs (cDCs) were distinguished from plasmacytoid DCs (pDCs) on the basis of their ability to directly present antigens to T cells [17]. Current studies of transcription factors regulating DC differentiation in mice have greatly expanded the understanding of their subtypes. The development of advanced technologies, such as single-cell RNA sequencing (scRNA-seq), has made it possible to clarify and improve the classification of DCs [16]. DCs are classified into three major subtypes: type 1 conventional DCs (cDC1), type 2 conventional DCs (cDC2), and plasmacytoid DCs (pDCs). These subtypes, interacting with one another, play a key role in the formation and regulation of the adaptive immune response.

Numerous studies have shown that human DCs express high levels of MHC class II molecules, such as HLA-DR, a molecule required for antigen presentation, and lack key markers of T cells, B cells, natural killer cells (NK cells), granulocytes, and monocytes. In the blood, DC subtypes include CD11C+ cDCs, composed of CD141+ or CD1C+ cells, and pDCs, composed of CD123+ cells. Conventional DCs efficiently stimulate antigen-specific CD4+ and CD8+ T cells, while pDCs specialize in the production of type I interferons in response to viruses. The pDC and cDC subtypes differ in the expression of numerous receptors, signaling pathways, and effectors and play different roles in the immune response [19].

However, the definition of DCs can still be distorted by the limited number of markers available for cell identification, isolation, and manipulation. Such distortions, in turn, may affect the definition of the function and ontogenesis of each DC subtype.

The study by A.K.Villani et al. [16] allowed to develop a more accurate classification of DCs, including six DC subtypes and four monocyte subtypes, as well as to identify a circulating, dividing dendritic cell precursor. In contrast to previous studies that categorized human blood DCs as one population of pDCs and two populations of cDCs, the authors identified six DC populations: DC1 corresponds to CD141/BDCA-3+ cDC1, which specializes in antigen cross-presentation and is labeled with CLEC9A; DC2 and DC3 represent subpopulations of CD1C/BDCA-1+ cDC2; DC4 corresponds to CD1C-CD141-CD11C+ DC, which is best labeled with CD16 and shares signatures with monocytes; DC5 is a unique DC subtype such as DCs; and DC6 is an interferon-producing pDC that has been isolated in a purer form than previously identified pDCs defined by standard markers (e.g., CD123, CD303/BDCA-2+) but containing an admixture of other DCs (AS DCs).

Given the unique ability of cDC1 to present tumor antigens to CD8 T cells, as well as their ability to interact with CD4 T cells, they are considered to be the main subset of DCs that regulate antitumor responses of T cells. However, cDC2 has been shown to be a critical factor in antitumor immunity under certain conditions [5]. In one preclinical model with diphtheria toxin receptor (DTR) knockout cDC1, depletion of intratumor regulatory T cells (Treg) enhanced migration of cDC2 into the tumor-draining lymph node and eliminated the dysfunction, leading to productive priming and activation of effector CD4 T cells [19].

Tumor-infiltrating DCs are characterized by different functional states that play a key role in antitumor immunity. To identify DC states associated with productive antitumor T-cell immunity, E. Duong et al. [20] compared spontaneously regressing and progressing tumors. In Batf3-deficient (Batf3-/-) mice lacking type 1 DCs, CD8+ T-cell responses to tumor were lost in progressing tumors but preserved in regressing tumors. Transcriptional profiling of intratumor DCs in regressing tumors revealed an activation state of CD11b+ conventional DCs (DC2) characterized by interferon-stimulated gene expression (ISG+ DCs). ISG+ DCs demonstrated an enhanced ability to activate CD8+ T cells *ex vivo* compared to DC1. In contrast to DC1, which perform antigen cross-presentation, ISG+ DCs presented intact tumor cell-derived peptide-MHC class I complexes. Continuous production of type I interferon by regressing tumor cells resulted in an ISG+ DC state, and activation of these cells with exogenous interferon β restored antitumor immunity in Batf3-/- mice. The genetic signature of ISG+ DCs was also detected in human tumors, suggesting their potential role in antitumor protection. At the same time, under conditions of high IL-6 and PGE2 expression, intratumor cDC2 may acquire a pro-tumor phenotype characterized by CD14 expression and impaired antigen presentation [21].

## METABOLIC PROGRAMMING OF DENDRITIC CELLS

In DCs, metabolism is closely linked to maturation signals and is therefore a key factor in the activation or tolerogenicity of DCs in the tumor microenvironment. In general, differences in the

regulation of glycolysis and oxidative phosphorylation programs are associated with anti-inflammatory or proinflammatory DC phenotypes. The metabolic needs of DCs have only recently been discovered, and metabolic phenotypes, dependent on subtype and environmental conditions, are closely related to their functions. In immature DCs, the mammalian AMP-activated protein kinase (AMPK)/mammalian target of rapamycin (mTOR) axis is thought to play a key role in maintaining the metabolic balance. AMPK promotes oxidative metabolism and counteracts mTOR, which activates glycolytic pathways after TLR signaling [5].

The analysis of metabolic pathway activation at the level of individual cells revealed simultaneous involvement of several metabolic pathways at different stages of monocyte-derived DC differentiation. GM-CSF/IL4 induce rapid glycolysis-dominated reprogramming of monocytes, accompanied by temporary joint activation of glycolysis and mitochondrial pathways, which subsequently leads to TLR4-dependent DC maturation. Disruption of the balance between mTOR and AMPK phosphorylation, as well as increased activity of oxidative phosphorylation, glycolysis, and fatty acid metabolism lead to two key features of tolerogenic DCs – hyperactivity and an immunosuppressive DC phenotype. These cells are resistant to maturation, meaning that they fail to fully develop into mature DCs, but instead retain an immature, dedifferentiated phenotype and express unique immunoregulatory receptors that enhance their immunosuppressive properties. Data obtained at the individual cell level provide important information on the metabolic pathways that regulate the immune profiles of human DCs [22].

In recent years, more and more studies have confirmed that immune cells depend on certain metabolic characteristics to perform their functions, and that the extracellular environment can influence their metabolism and vice versa. DC subtypes move in a variety of environments from the bone marrow, where they develop, to peripheral tissues, where they differentiate and capture antigens before migrating to the lymph node for antigen presentation and T cell activation. It is likely that DC subtypes regulate their ability to stimulate the immune response depending on the unique metabolic programs that are activated in them. The metabolic needs of DCs have been studied relatively recently, and their metabolic phenotypes, which depend on cell subtype and environmental conditions, are closely related to their functional properties [10].

## DENDRITIC CELLS OF CANCER PATIENTS

DCs play a key role in the tumor microenvironment (TME). As the main antigen-presenting cells in tumors, DCs modulate the antitumor immune response by regulating the intensity and duration of responses carried out by infiltrating cytotoxic T lymphocytes. Unfortunately, due to the immunosuppressive nature of TME, and high plasticity of DCs, tumor-associated DCs often acquire a dysfunctional phenotype that contributes to the evasion of the immune response. Recent advances in the study of intratumor DC biology have identified potential molecular targets to improve their functional activity, which is involved in cancer immunotherapy [23]. The data indicate that both the number and function of DCs are reduced in cancer patients, and to a greater extent in metastatic tumors than in localized tumors [24]. Moreover, the powerful immunosuppressive environment created by tumors suppresses antigen presentation, maturation and normal function of DCs by several mechanisms, preventing an effective immune response to the tumor [25]. Given what is known about DC development and function, therapeutic anti-cancer vaccines based on these cells have been developed [26]. Vaccines based on DCs are able to transform the so-called cold tumors, characterized by the absence of infiltration by T cells, their dysfunction or exhaustion, into hot tumors, which stimulates the development of an effective anti-tumor immune response.

It has been shown that DCs can be generated *in vitro* in cancer patients or can be isolated from peripheral blood (natural DCs) and modified to enhance their functional competence. The use of DCs that have been activated by tumor antigens to induce the immune response has been proposed as a therapeutic strategy for certain tumors. The goal of DC-based vaccines is to stimulate the patient's own immune system to trigger an antitumor response that destroys malignant cells. In addition, this response can form immunological memory that can prevent recurrence of the disease [27].

## CONCLUSION

Although the importance of dendritic cells in antitumor immunity is becoming increasingly clear, the biology of dendritic cells is still not fully understood. The functional behavior of dendritic cells is determined

by multiple factors, including their subtype, transcriptional programs, localization, intratumor conditions, and inflammatory environment. All of these influence whether dendritic cells will promote an effective T cell response or, conversely, inhibit it.

## REFERENCES


1. Hu Z., Ott P.A., Wu C.J. Towards personalized, tumour-specific, therapeutic vaccines for cancer. *Nat. Rev. Immunol*. 2018;18(3):168–182. DOI: 10.1038/nri.2017.131.
2. Hollingsworth R.E., Jensen K. Therapeutic cancer vaccines revisited. *NPJ Vaccines*. 2019;8(4):7. DOI: 10.1038/s41541-019-0103-y.
3. Melief C.J., van Hall T., Arens R., Ossendorp F., van der Burg S.H. Therapeutic cancer vaccines. *J. Clin. Invest*. 2015;125(9):3401–3412. DOI: 10.1172/JCI80009.
4. Schumacher T.N., Schreiber R.D. Neoantigens in cancer immunotherapy. *Science*. 2015;348(6230):69–74. DOI: 10.1126/science.aaa4971.
5. Chen M.Y., Zhang F., Goedegebuure S.P., Gillanders W.E. Dendritic cell subtypes and their implications for cancer immunotherapy. *Front. Immunol*. 2024;15:1393451. DOI: 10.3389/fimmu.2024.1393451.
6. Liu K., Victora G.D., Schwickert T.A., Guermonprez P., Meredith M.M., Yao K. et al. In vivo analysis of dendritic cell development and homeostasis. *Science*. 2009;324(5925):392–397. DOI: 10.1126/science.1170540.
7. Breton G., Li J., Liu Q., Nussenzweig M.K. Identification of human dendritic cell progenitors by multiparameter flow cytometry. *Nat. Protoc*. 2015;10(9):1407–1422. DOI: 10.1038/nprot.2015.092.
8. Rodrigues P.F., Trsan T., Cvijetic G., Khantakova D., Panda S.K., Liu Z. et al. Progenitors of distinct lineages shape the diversity of mature type 2 conventional dendritic cells. *Immunity.* 2024;57(7):1567–1585.e5. DOI: 10.1016/j.immuni.2024.05.007.
9. Dress R.J., Dutertre C.A., Giladi A., Schlitzer A., Low I., Shadan N.B. et al. Plasmacytoid dendritic cells develop from Ly6D+ lymphoid progenitors distinct from the myeloid lineage. *Nat. Immunol.* 2019;20(7):852–864. DOI: 10.1038/s41590-019-0420-3.
10. Møller S.H., Wang L., Ho P.C. Metabolic programming in dendritic cells tailors immune responses and homeostasis. *Cell Mol. Immunol*. 2022;19(3):370–383. DOI: 10.1038/s41423-021-00753-1.
11. Zebley C.C., Youngblood B. Mechanisms of T cell exhaustion guiding next-generation immunotherapy. *Trends Cancer*. 2022;8(9):726–734. DOI: 10.1016/j.trecan.2022.04.004.
12. Wu R., Murphy K.M. DCs at the center of help: Origins and evolution of the three-cell-type hypothesis. *J. Exp. Med*. 2022;219(7):e20211519. DOI: 10.1084/jem.20211519.
13. Borst J., Ahrends T., Bąbała N., Melief C.J.M., Kastenmüller W. CD4+ T cell help in cancer immunology and immunotherapy. *Nat. Rev. Immunol*. 2018;18(10):635–647. DOI: 10.1038/s41577-018-0044-0.
14. Melssen M., Slingluff C.L. Jr. Vaccines targeting helper T cells for cancer immunotherapy. *Curr. Opin. Immunol*. 2017;47:85–92. DOI: 10.1016/j.coi.2017.07.004.
15. Ruhland M.K., Roberts E.W., Cai E., Mujal A.M., Marchuk K., Beppler C. et al. Visualizing synaptic transfer of tumor antigens among dendritic cells. *Cancer Cell.* 2020;37(6):786–799. DOI: 10.1016/j.ccell.2020.05.002.
16. Villani A.K., Satija R., Reynolds G., Sarkizova S., Shekhar K., Fletcher J. et al. Single-cell RNA analysis identifies novel types of dendritic cells, monocytes, and progenitors in human blood. *Science*. 2017;356(6335):eaah4573. DOI: 10.1126/science.aah4573.
17. Swiecki M., Colonna M. The multifaceted biology of plasmacytoid dendritic cells. *Nat. Rev. Immunol.* 2015;15(8):471–485. DOI: 10.1038/nri3865.
18. Schraml B.W., Reis and Souza K. Defining dendritic cells. *Curr. Opin. Immunol*. 2015;32:13–20. DOI: 10.1016/j.coi.2014.11.001.
19. Binnewies M., Mujal A.M., Pollack J.L., Combes A.J., Hardison E.A., Barry K.C. et al. Unleashing type-2 dendritic cells to drive protective antitumor CD4+ T cell immunity. *Cell.* 2019;177(3):556–571.e16. DOI: 10.1016/j.cell.2019.02.005.
20. Duong E., Fessenden T.B., Lutz E., Dinter T., Yim L., Blatt S. et al. Type I interferon activates MHC class I-dressed CD11b+ conventional dendritic cells to promote protective anti-tumor CD8+ T cell immunity. *Immunity.* 2022;55(2):308–323.e9. DOI: 10.1016/j.immuni.2021.10.020.
21. Saito Y., Komori S., Kotani T., Murata Y., Matozaki T. The role of type-2 conventional dendritic cells in the regulation of tumor immunity. *Cancers (Basel).* 2022;14(8):1976. DOI: 10.3390/cancers14081976.
22. Adamik J., Munson P.V., Hartmann F.J., Combes A.J., Pierre P., Krummel M.F. et al. Distinct metabolic states guide maturation of inflammatory and tolerogenic dendritic cells. *Nat. Commun*. 2022;13(1):5184. DOI: 10.1038/s41467-022-32849-1.
23. Tang M., Diao J., Cattral M.S. Molecular mechanisms involved in dendritic cell dysfunction in cancer. *Cell Mol. Life Sci*. 2017;74(5):761–776. DOI: 10.1007/s00018-016-2317-8.
24. Lurje I., Hammerich L., Tacke F. Dendritic cell and T cell crosstalk in liver fibrogenesis and hepatocarcinogenesis: implications for prevention and therapy of liver cancer. *Int. J. Mol. Sci.* 2020;21(19):7378. DOI: 10.3390/ijms21197378.
25. Lehmann B.D., Colaprico A., Silva T.C., Chen J., An H., Ban Y. et al. Multi-omics analysis identifies therapeutic vulnerabilities in triple-negative breast cancer subtypes. *Nat. Commun.* 2021;12(1):6276. DOI: 10.1038/s41467-021-26502-6.
26. Wculek S.K., Cueto F.J., Mujal A.M., Melero I., Krummel M.F., Sancho D. Dendritic cells in cancer immunology and immunotherapy. *Nat. Rev. Immunol*. 2020;20(1):7–24. DOI: 10.1038/s41577-019-0210-z.
27. Hato L., Vizcay A., Eguren I., Pérez-Gracia J.L., Rodríguez J., Gállego Pérez-Larraya J. et al. Dendritic cells in cancer immunology and immunotherapy. *Cancers* (*Basel)*. 2024;16(5):981. DOI: 10.3390/cancers16050981.

## Author Contribution

Frantsiyants E.M. – conception and design; final approval of the manuscript for publication. Bandovkina V. A. – justification of the manuscript and critical revision of the manuscript for important intellectual content. Surikova E. I. – critical revision of the manuscript for important intellectual content. Cheryarina N. D. – critical revision of the manuscript for important intellectual content. Kaplieva I. V. – justification of the manuscript and critical revision of the manuscript for important intellectual content. Menshenina A.P. – critical revision of the manuscript for important intellectual content. Shikhlyarova A.I. – justification of the manuscript and critical revision of the manuscript for important intellectual content. Neskubina I.V. – critical revision of the manuscript for important intellectual content.

## Author Information

**Frantsiyants Elena M.** – Dr. Sci. (Biology), Professor, Deputy Director General for Science, National Medical Research Centre for Oncology, Rostov-on-Don, super.gormon@yandex.ru, http://orcid.org/0000-0003-3618-6890

**Bandovkina Valerija A.** – Dr. Sci. (Biology), Leading Researcher, Laboratory for Studying Malignant Tumor Pathogenesis, National Medical Research Centre for Oncology, Rostov-on-Don, valerryana@yandex.ru, https://orcid.org/0000-0002-2302-8271

**Surikova Ekaterina I.** – Cand. Sci. (Biology), Senior Researcher, Laboratory for Studying Malignant Tumor Pathogenesis, National Medical Research Centre for Oncology, Rostov-on-Don, sunsur2000@mail.ru, https://orcid.org/0000-0002-4318-7587

**Cheryarina Natalia D.** – Laboratory Assistant, Laboratory for Studying Malignant Tumor Pathogenesis, National Medical Research Centre for Oncology, Rostov-on-Don scalolas.92@yandex.ru, https://orcid.org/0000-0002-3711-8155

**Kaplieva Irina V.** – Dr. Sci. (Med.), Head of Laboratory for Studying Malignant Tumor Pathogenesis, National Medical Research Centre for Oncology, Rostov-on-Don, kaplirina@yandex.ru, https://orcid.org 0000-0002-3972-2452

**Menshenina Anna P.** – Dr. Sci. (Med.), Associate Professor, Leading Researcher, Department of Tumors of the Reproductive System, National Medical Research Centre for Oncology, Rostov-on-Don, anna.menshenina.00@mail.ru, http://orcid.org/0000-0002-7968-5078

**Shikhlyarova Alla I.** – Dr. Sci. (Biology), Professor, Senior Researcher, Laboratory for Studying Malignant Tumor Pathogenesis, National Medical Research Centre for Oncology, Rostov-on-Don, shikhliarova.a@mail.ru, https://orcid.org/0000-0003-2943-7655

**Neskubina Irina V.** – Cand. Sci. (Biology), Senior Researcher, Laboratory for Studying Malignant Tumor Pathogenesis, National Medical Research Centre for Oncology, Rostov-on-Don, neskubina.irina@mail.ru, https://orcid.org/0000-0002-7395-3086

(✉) **Bandovkina Valerija A.,** valerryana@yandex.ru

Received on March 25, 2025;
approved after peer review on April 15, 2025;
accepted on April 17, 2025

УДК 616.831-006.81-021.3-079.2/.4
https://doi.org/10.20538/1682-0363-2025-3-179-186

# Diagnostic difficulties of primary diffuse leptomeningeal melanocytosis of the central nervous system: clinical case

**Vtorushin S.V.[1, 2], Vasilchenko D.V.[1], Tonkikh O.S.[1], Vtorushin K.S.[1], Degtyarenko N.V.[1], Krakhmal N.V.[1, 2]**

[1] *Siberian State Medical University (SibSMU)*
*2 Moskovsky trakt, 634050 Tomsk, Russian Federation*

[2] *Cancer Research Institute, Tomsk National Research Medical Center (NRMC), Russian Academy of Sciences*
*5 Kooperativny St., 634009 Tomsk, Russian Federation*

**ABSTRACT**

Primary diffuse leptomeningeal melanocytosis (PDLM) is a rare neoplastic lesion of the central nervous system, characterized by diffuse infiltration of the leptomeninges by melanocytes without apparent invasion into the brain parenchyma. Diagnosing the disease is challenging due to its nonspecific clinical presentation and the lack of clear neuroimaging criteria, necessitating morphological and immunohistochemical studies for definitive verification.

This article presents a clinical case of a patient with progressive neurological impairments, diagnostic challenges, and postmortem verification of PDLM. The key differential diagnostic aspects, the morphological structure of the tumor, and its immunohistochemical profile are described. Additionally, neuroimaging data are provided, demonstrating characteristic changes associated with PDLM. The presented clinical case highlights the necessity of a multidisciplinary approach to managing patients with chronic meningeal lesions of unknown etiology and underscores the importance of further research in molecular diagnostics and potential treatment strategies.

**Keywords:** primary diffuse meningeal melanocytosis, neuroimaging, immunohistochemistry, pathology

**Conflict of interest.** The authors declare the absence of obvious or potential conflict of interest related to the publication of this article.

**Source of financing.** The authors state that they received no funding for the study.

**For citation:** Vtorushin S.V., Vasilchenko D.V., Tonkikh O.S., Vtorushin K.S., Degtyarenko N.V., Krakhmal N.V. Diagnostic difficulties of primary diffuse leptomeningeal melanocytosis of the central nervous system: clinical case. *Bulletin of Siberian Medicine.* 2025;24(3):179–186. https://doi.org/10.20538/1682-0363-2025-3-179-186.

# Диагностические сложности первичного диффузного меланоцитоза ЦНС: клиническое наблюдение

**Вторушин С.В.[1, 2], Васильченко Д.В.[1], Тонких О.С.[1], Вторушин К.С.[1], Дегтяренко Н.В.[1], Крахмаль Н.В.[1, 2]**

[1] *Сибирский государственный медицинский университет (СибГМУ)*
*Россия, 634050, г. Томск, Московский тракт, 2*

✉ *Krakhmal Nadezhda V.,* krakhmal@mail.ru

[2] *Научно-исследовательский институт онкологии (НИИ онкологии) Томского национального исследовательского медицинского центра (НИМЦ) Российской академии наук*
*Россия, 634009, г. Томск, пер. Кооперативный, 5*

**РЕЗЮМЕ**

Первичный диффузный лептоменингеальный меланоцитоз (ПДЛМ) – редкое опухолевое поражение центральной нервной системы, характеризующееся диффузной инфильтрацией мягких мозговых оболочек мела*н*оцитарными клетками без явной инвазии в паренхиму головного мозга. Диагностика заболевания представляет сложность в связи с неспецифичностью клинической картины и отсутствием четких нейровизуализационных критериев, что требует проведения морфологического и иммуногистохимического исследований для окончательной верификации диагноза.

В статье представлен клинический случай пациента с прогрессирующими неврологическими нарушениями, диагностическими сложностями и постмортальной верификацией ПДЛМ. Описаны ключевые дифференциально-диагностические аспекты, особенности морфологического строения опухоли и ее иммуногистохимический профиль. Также представлены данные нейровизуализационных исследований, демонстрирующие характерные изменения, сопровождающие ПДЛМ. Описанный случай демонстрирует необходимость междисциплинарного подхода при ведении пациентов с хроническими менингеальными поражениями неустановленной этиологии и подчеркивает значимость дальнейших исследований в области молекулярной диагностики и потенциальных терапевтических стратегий.

**Ключевые слова:** первичный диффузный менингеальный меланоцитоз, нейровизуализация, иммуногистохимия, патоморфология

**Конфликт интересов.** Авторы декларируют отсутствие явных и потенциальных конфликтов интересов, связанных с публикацией настоящей статьи.

**Источник финансирования.** Авторы заявляют об отсутствии финансирования при проведении исследования.

**Для цитирования:** Вторушин С.В., Васильченко Д.В., Тонких О.С., Вторушин К.С., Дегтяренко Н.В., Крахмаль Н.В. Диагностические сложности первичного диффузного меланоцитоза ЦНС: клиническое наблюдение. *Бюллетень сибирской медицины.* 2025;24(3):179–186. https://doi.org/10.20538/1682-0363-2025-3-179-186.

## INTRODUCTION

Primary leptomeningeal melanocytic neoplasms (PLMN) represent a heterogeneous group of extremely rare tumors of the central nervous system (CNS), possessing unique histological and molecular characteristics that fundamentally distinguish them from other melanocytic or pigmented lesions, including cerebral and leptomeningeal melanoma metastases. Incidence rates for this group of neoplasms in the general population have not yet been established due to the lack of representative cohort studies, and clinical and biological data on the pathogenesis and natural course of the disease remain highly limited [1].

PLMN of the CNS originate from melanocytes, which are derived from the neural crest and migrate into the leptomeningeal membranes during embryogenesis [2]. According to the current WHO classification of CNS tumors (WHO 2021), this group manifests either as a solitary, well-demarcated, and voluminous leptomeningeal mass or as a diffuse / multifocal leptomeningeal dissemination.

The WHO currently differentiates four categories of primary melanocytic tumors of the CNS: meningeal melanocytosis and melanomatosis, melanocytoma (benign / low-grade malignancy), and meningeal melanoma (malignant), each characterized by specific features of the clinical course, malignant potential, and corresponding prognostic indicators [3].

Primary diffuse leptomeningeal melanocytosis (PDLM) is characterized by diffuse proliferation of histologically benign leptomeningeal melanocytes without apparent invasion into the brain parenchyma, whereas primary diffuse melanomatosis appears as an aggressive dissemination of histologically atypical or malignant melanocytes through the leptomeningeal membranes with invasion into the brain tissue [3]. Epidemiological data indicate that the incidence of

meningeal melanocytomas is 1 case per 10,000,000 population per year, while the annual incidence of meningeal melanomas is only 0.005 case per 100,000 population [4].

A major diagnostic challenge for clinicians and pathologists in these lesions is the differential diagnosis of PLMN from metastatic melanoma and other pigmented primary CNS tumors. This aspect has critical clinical significance for determining prognosis and selecting an appropriate treatment strategy [5, 6]. The diagnostic algorithm is further complicated by the fact that PDLM may present with a wide range of nonspecific symptoms, including cephalic disorder, nausea, vomiting, and seizures (primarily due to the development of obstructive hydrocephalus), changes in mental status, and focal neurological symptoms, often leading to diagnosis by exclusion [7, 8].

PDLM like other primary CNS tumors exhibits characteristic neuroimaging patterns. On computed tomography (CT) scans, melanocytic tumors appear as hyperdense lesions with typical contrast enhancement. Magnetic resonance imaging (MRI) provides more detailed visualization, demonstrating hyperintensity of tumors on T1-weighted images and iso- or hypointensity on T2-weighted images. However, MRI findings can only suggest a melanocytic nature of the tumor but cannot differentiate a primary tumor from a secondary one [9, 10].

Despite the existing arsenal of diagnostic methods, morphological examination of tumor tissue using immunohistochemical techniques remains the gold standard for verifying primary melanocytic tumors of the CNS [11]. Timely and accurate diagnosis of PDLM is crucial for determining the treatment strategy and assessing the prognosis, given the malignant potential of benign lesions and the overall trend toward poor outcomes in diffuse disease. However, the lack of a standardized treatment approach makes patient management extremely challenging [12, 13]. The study of clinical cases, such as the one presented in this article, contributes to a better understanding of disease progression, diagnosis, and potential treatment strategies.

## CLINICAL CASE

Patient N., 48 years old, was admitted to the inpatient emergency unit with a moderate condition and a polymorphic clinical presentation, including progressive lower extremity weakness, generalized asthenia, visual disturbances, cephalic disorder predominantly localized in the frontal region, and cervicalgia.

*Medical History*. The onset of the disease was noted in early January 2024, when the aforementioned symptoms first appeared. The patient initiated the diagnostic process independently and underwent MRI of the brain and cervical spine, which revealed signs of moderately pronounced internal compensatory hydrocephalus and degenerative dystrophic changes in the cervical spine (C6/C7 disc protrusion, uncovertebral and facet joint arthrosis, spondylosis, and vertebral artery asymmetry).

After an unsuccessful attempt at self-medication using nonspecific therapeutic agents, the patient was initially hospitalized in the neurology department. Following the inpatient examination and treatment, a diagnosis of “Migraine without aura with autonomic symptoms and rare moderate-intensity episodes” was established. However, the prescribed therapy upon discharge was ineffective, and no positive clinical dynamics were observed.

Subsequently, the clinical symptoms progressed, with the onset of diplopia, nausea, systemic dizziness, and intensifying lower-limb paraparesis, leading to significant limitations in motor activity. Notably, no hyperthermic syndrome was detected. The patient was admitted to the infectious diseases department with a fully developed clinical presentation, and after excluding an infectious etiology, he was transferred to a specialized neurology unit for further therapeutic decision-making and plasmapheresis.

At the initial neurological examination, a combination of neurological abnormalities was identified, including flaccid lower-limb paraparesis, sensory disturbances, peripheral facial nerve paresis, and signs of bulbar syndrome. Based on the medical history and neurological status, a preliminary diagnosis was established: “Acute inflammatory demyelinating polyneuropathy with flaccid tetraparesis (mild in the upper limbs, pronounced in the lower limbs), mild left-sided facial nerve palsy, early manifestations of bulbar syndrome without respiratory impairments”.

During hospital stay in the neurology department, the patient underwent repeat MRI of the brain, which revealed the following pathological changes: symmetrical triventricular open / normal-pressure hydrocephalus, involvement of the corpus callosum, symmetrical involvement of the tectospinal tracts (suggestive of a degenerative process or sequelae of toxic damage), and changes in the leptomeningeal membranes of the basal brain regions, characteristic of leptomeningitis (Fig. 1–3).

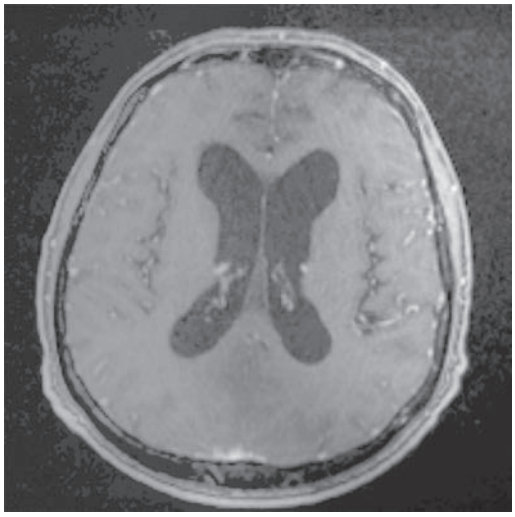

Fig. 1. Multislice Computed Tomography of the Brain.

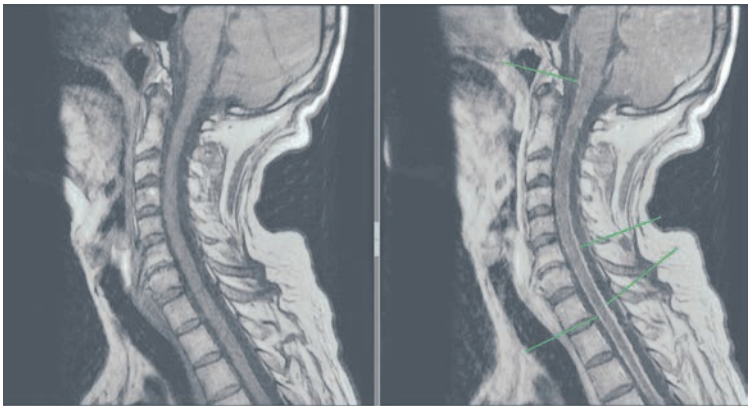

Fig. 2. Multislice Computed Tomography of the Brain.

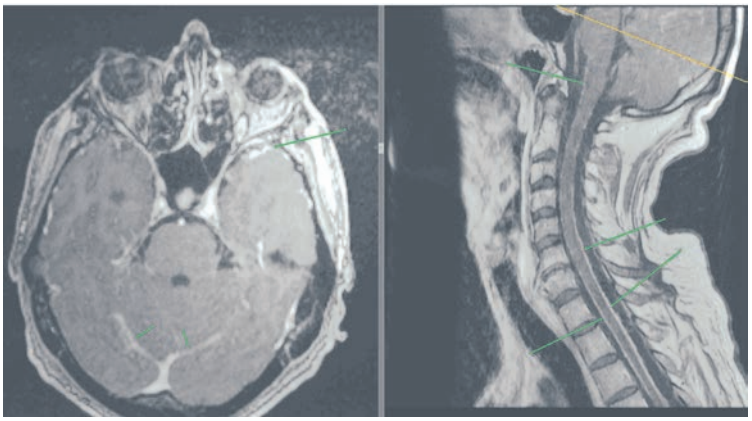

Fig. 3. Multislice Computed Tomography of the Brain. Axial T1-weighted image of the brain and sagittal T1-weighted image of the cervical spine were performed after the administration of the contrast agent. Multiple areas of enhanced MR signal from the pia mater of the brain and spinal cord.

Axial T1-weighted image of the brain after the administration of a contrast agent. Small areas of enhanced MR signal from the pia mater, more pronounced in the occipital region, narrowing of cerebrospinal fluid space at high convexity, expansion of the lateral ventricles in the context of hydrocephalus.

Despite comprehensive conservative therapy, the patient's condition was characterized by a steadily declining trajectory, and at day 18 of hospital stay, amidst progressing neurological deficits, a fatal outcome occurred.

The final clinical diagnosis was formulated as follows: "Chronic leptopachymeningitis of unspecified etiology, progressive course with cranial nerve involvement (bilateral involvement of the optic, oculomotor, and abducent nerves, left-sided facial nerve involvement); bulbar dysfunction;

flaccid tetraparesis predominantly affecting the lower extremities".

Sagittal T1-weighted images of the cervical and upper thoracic spine before and after the administration of the contrast agent. Areas of enhanced MR signal from the unevenly thickened pia mater of the spinal cord are more pronounced at the upper thoracic spine.

## PATHOLOGIC EXAMINATION

At autopsy, an area of discoloration of the meninges to a brownish, translucent, dull shade was observed bilaterally at the lateral sulcus of the brain, extending to the transverse temporal gyri between the frontal and parietal lobes. Similar changes were identified in the pia mater at the transition zone between the medulla oblongata and the spinal cord, as well as in the cerebellar region. Fragments of the meninges from these areas were collected for a subsequent microscopic examination. The microscopic analysis revealed that the pia mater was totally affected by a diffusely growing tumor composed of large and medium-sized epithelioid polygonal, round, and oval cells. Tumor cells exhibited eosinophilic cytoplasm, relatively monomorphic nuclei with coarse chromatin, and distinctly visible small, round, eosinophilic nucleoli. A distinguishing feature was the presence of brown pigment granules within the cytoplasm of most tumor cells. The tumor displayed areas of microalveolar architecture. The mitotic activity of the tumor was low, with 1–2 mitoses per 10 high-power fields at ×40/0.65 magnification. There were no necrotic tissue changes, and no evidence of tumor cell invasion into the neuroparenchyma was detected (Fig. 4).

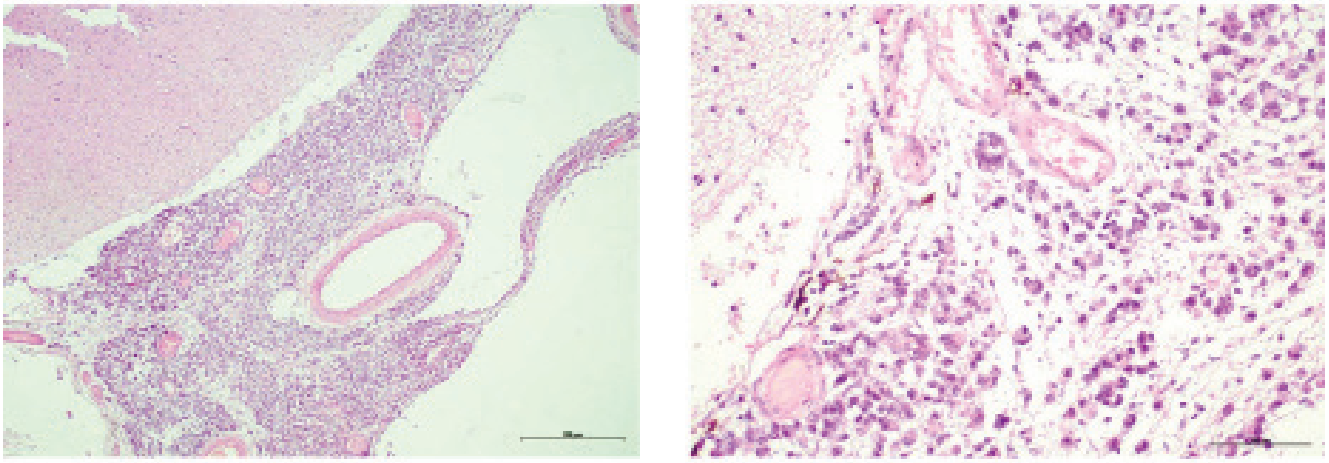

*a* *b*

Fig. 4. Primary Diffuse Meningeal Melanocytosis of the Pia Mater (Microphoto). The pia mater is diffusely infiltrated by small-cell tumor with brown pigment granules in some cells. Hematoxylin and eosin stain: *a* – ×4/0.10; b – ×10/0.25.

## IMMUNOHISTOCHEMISTRY AND MOLECULAR GENETIC STUDY

To verify the histogenesis of the meningeal neoplasm, an immunohistochemical study was performed using the Leica Bond – Max fully automated staining system (Germany). Tumor cells exhibited positive expression of melanocytic markers: SOX10 (clone EP268, Cell Marque) and Melan-A (clone A103, Dako). The Ki-67 proliferative activity index (clone SP6, Cell Marque) was 2% in most parts of the tumor (Fig. 5). Additionally, a molecular genetic study was conducted to detect mutations in the *BRAF* gene, which are characteristic of certain melanocytic neoplasms.

The results indicated the absence of activating *BRAF* mutations, which is relevant for differential diagnosis and understanding the molecular pathogenesis of this tumor. Given the absence of extracranial melanocytic tumors in the patient that could be considered as a primary lesion, the diffuse involvement of the pia mater without invasion of tumor cells into the brain parenchyma, and the results of immunohistochemistry and molecular genetic studies, the histological type of the tumor was verified as primary diffuse leptomeningeal melanocytosis.

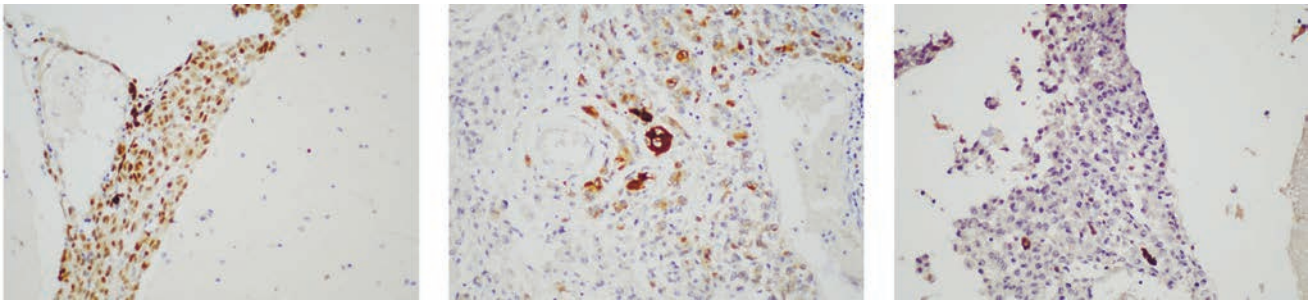

*a* *b* *c*

Fig. 5. Immunohistochemistry of the Pia Mater Tissue Samples with a Tumor. Immunohistochemistry: *a* – positive nuclear expression of SOX10 in tumor cells, ×4 / 0.10; *b* – positive cytoplasmic expression of Melan-A in tumor cells, ×10 / 0.25; *c* – positive nuclear expression of Ki67 in single cells, ×10 / 0.25.

## FINAL PATHOLOGIC DIAGNOSIS

*Primary Disease*. Primary diffuse meningeal melanocytosis with involvement of the pia mater of both cerebral hemispheres, medulla oblongata, pons, cerebellum, and cervical segment of the spinal cord, as well as cranial nerve involvement (bilateral involvement of the optic, oculomotor, and abducent nerves, left-sided facial nerve involvement); bulbar dysfunction; flaccid tetraparesis (based on medical history data).

*Complications.* Triventricular symmetrical open normal-pressure hydrocephalus (MRI findings). Hospital-acquired total polysegmental bilateral fibrinous purulent pneumonia with abscess formation. Sepsis. Acute cardiovascular failure. Acute respiratory failure. Brain edema.

*Comorbidities.* Atherosclerosis of the aorta, type II–IV atherosclerotic plaques with a distribution of up to 30%.

## DISCUSSION

PDLM is a rare CNS pathology characterized by diffuse infiltration of the leptomeninges by melanocytes without apparent invasion into the brain parenchyma. The described fatal clinical case demonstrates significant diagnostic challenges, highlighting the importance and necessity of a multidisciplinary approach to managing patients with progressive neurological symptoms of unclear etiology. The clinical manifestation of PDLM is nonspecific, including cephalic disorder, progressive muscle weakness, visual disturbances, cognitive impairments, and seizures.

In the presented case, there was gradual progression of neurological symptoms mimicking various neurological diseases, particularly demyelinating polyneuropathy, which explains the substantial delay in establishing the final diagnosis. Contrast-enhanced MRI allowed for visualization of pathological changes characteristic of leptomeningeal involvement. However, a definitive diagnosis was only made post-mortem following the pathologic examination. This underscores the limited capacity of modern neuroimaging methods in the differential diagnosis of primary melanocytic neoplasms of the CNS, which is consistent with literature data [14, 15].

The autopsy confirmed diffuse infiltration of the leptomeninges by pigmented cells with low proliferative activity. The application of immunohistochemical markers SOX10 and Melan-A allowed for reliable identification of the melanocytic nature of tumor cells, while the low Ki-67 proliferation index (< 2%) indicated a formally benign biological potential of the tumor.

During the differential diagnosis, metastatic melanoma, leptomeningeal carcinomatosis, and melanotic astrocytoma were considered. The absence of primary extracranial melanocytic lesion, the lack of invasive growth into the brain parenchyma, and low mitotic activity allowed to exclude malignant neoplasms from the differential diagnosis list. The prognostic evaluation of PDLM remains uncertain due to the rarity of the condition and the lack of sufficient data on its natural course. In this case, despite the absence of classical histological signs of malignancy, an aggressive clinical course was observed. The most likely determining factors in the progression of the disease were diffuse infiltration of the leptomeninges and the subsequent development of secondary hydrocephalus.

Treatment strategies for PDLM are limited due to the lack of pathogenetically grounded treatment

methods. The literature describes cases of surgical intervention in localized forms of the disease and potential use of chemotherapy and radiation therapy in cases of malignant transformation; however, the effectiveness of these therapeutic modalities in diffuse PDLM remains debatable and requires further study.

## CONCLUSION

The presented clinical case underscores the necessity of including primary diffuse meningeal melanocytosis in the differential diagnosis algorithm for patients with chronic meningeal lesions of unknown etiology. Modern neuroimaging methods provide diagnostic value, yet they lack sufficient specificity to establish a definitive diagnosis, which must rely on comprehensive morphological and immunohistochemical studies.

Promising research areas include investigation of the molecular genetic characteristics of PDLM, which could potentially contribute to the development of innovative diagnostic approaches and targeted treatment strategies. Accumulating and systematizing data on this rare pathology within multicenter studies may help optimize diagnostic algorithms and therapeutic approaches, thereby improving patient prognosis in PDLM.

### REFERENCES


1. Pellerino A., Verdijk R.M., Nichelli L., Andratschke N.H., Idbaih A., Goldbrunner R. Primary Meningeal Melanocytic Tumors of the Central Nervous System: A Review from the Ultra-Rare Brain Tumors Task Force of the European Network for Rare Cancers (EURACAN). *Cancers (Basel).* 2024;16(14):2508. DOI: 10.3390/cancers16142508.
2. Kumar A., Gunasekaran P.K., Aggarwal D., Janu V., Manjunathan S., Laxmi V. et al. Primary Diffuse Leptomeningeal Melanomatosis in an Indian Child With Review of Literature. *Pediatric Neurology*. 2024;152:23–29. DOI: 10.1016/j.pediatrneurol.2023.12.007.
3. Louis D.N., Perry A., Wesseling P., Brat D.J., Cree I.A., Figarella-Branger D. et al. The 2021 WHO Classification of Tumors of the Central Nervous System: a summary. *Neuro-Oncology*. 2021;23(8):1231–1251. DOI: 10.1093/neuonc/noab106.
4. Machado S., dos Santos D.F., De Martino Luppi A., Guimarães V.V., da Silva A.A.L. Primary diffuse leptomeningeal melanocytosis: a rare and challenging diagnosis. *Journal of Neuroscience and Neurological Disorders*. 2024;8:47–49. DOI: 10.29328/journal.jnnd.1001096.
5. Burgos R., Cardona A.F., Santoyo N., Ruiz-Patiño A., Cure-Casilimas J., Rojas L. et al. Case report: differential genomics and evolution of a meningeal melanoma treated with ipilimumab and nivolumab. *Frontiers in Oncology*. 2022;11:691017. DOI: 10.3389/fonc.2021.691017.
6. Sareh S., Habibi Z., Vasei M., Safavi M., Sharari A.S., Pak N. et al. Primary diffuse leptomeningeal melanomatosis leading to raised intracranial pressure in a pediatric patient. *Clinical Case Reports*. 2025;13(2):e9705. DOI: 10.1002/ccr3.9705.
7. Selvarajan J.M.P., Epari S., Sahu A., Dasgupta A., Chatterjee A., Gupta T. Pearls & oy-sters: primary diffuse leptomeningeal melanocytosis: a diagnostic conundrum. *Neurology*. 2023;101(5):e576–e580. DOI: 10.1212/WNL.0000000000207195.
8. Saadeh Y.S., Hollon T.C., Fisher-Hubbard A., Savastano L.E., McKeever P.E., Orringer D.A. Primary diffuse leptomeningeal melanomatosis: description and recommendations. *Journal of Clinical Neuroscience*. 2018;50:139–143. DOI: 10.1016/j.jocn.2018.01.052.
9. Hossain F.A., Marquez H.J., Veltkamp D.L., Xie S.Q., Klesse L.J., Timmons C.F. eat al. CT and MRI findings in leptomeningeal melanocytosis. *Radiology Case Reports*. 2019;15(3):186–189. DOI: 10.1016/j.radcr.2019.11.006.
10. Hou W., Yu J., Gao S., Chu Y. Primary cervical meningeal melanocytoma with a dumbbell shape: Case report and review of the literature. *Medicine (Baltimore)*. 2023;102(14):e33435. DOI: 10.1097/MD.0000000000033435.
11. Tekatas A., Gemici Y.I., Tuncel S.A., Caglı B., Tastekin E., Unlu E. et al. A rare cause of headache and increased intracranial pressure: primary leptomeningeal melanomatosis. *Turkish Journal of Neurology.* 2014;20:138–140. DOI: 10.4274/tnd.26122.
12. Palacka P., Slopovsky J., Makovnik M., Kajo K., Obertova J., Mego M. A case report of a patient with inoperable primary diffuse leptomeningeal melanomatosis treated with whole-brain radiotherapy and pembrolizumab. *Medicine (Baltimore)*. 2022;101(3):e28613.
    DOI: 10.1097/MD.0000000000028613.
13. Baumgartner A., Stepien N., Mayr L., Madlener S., Dorfer C., Schmook M.T. et al. Novel insights into diagnosis, biology and treatment of primary diffuse leptomeningeal melanomatosis. *Journal of Personalized Medicine*. 2021;11(4):292. DOI: 10.3390/jpm11040292.
14. Lewis D., Dawson T.P., Hyde R., Rata G.A., Alalade A.F., Ghosh K. et al. A rare case of multifocal craniospinal leptomeningeal melanocytoma: A case report and scoping review. *Brain and Spine*. 2024;4:102797. DOI: 10.1016/j.bas.2024.102797.
15. Lang-Orsini M., Wu J., Heilman C.B., Kravtsova A., Weinstein G., Madan N. et al. Primary meningeal melanoma masquerading as neurofibromatosis type 2: illustrative case. *Journal of Neurosurgery: Case Lessons*. 2021;2(20):CASE21444. DOI: 10.3171/CASE21444.

## Author Information

**Vtorushin Sergey V.** – Dr. Sc. (Medicine), Professor, Deputy Director for Research and Translational Medicine, Head of the Department of General and Molecular Pathology, Cancer Research Institute, Tomsk NRMC, Tomsk; Professor of the Pathology Division, SibSMU, Tomsk, wtorushin@rambler.ru, http://orcid.org/0000-0002-1195-4008

**Vasilchenko Dmitry V.** – Cand. Sc. (Medicine), Leading Researcher, Central Research Laboratory, SibSMU, Tomsk; Pathologist, Pathology Department, Clinics of Siberian State Medical University, Tomsk, vasilchenkodmitry1991@gmail.com, http://orcid.org/0000-0002-9780-0770

**Tonkikh Olga S.** – Cand. Sc. (Medicine), Teaching Assistant, Division of Pediatrics with a Course in Endocrinology, SibSMU, Tomsk; Head of Tomographic Imaging Department, Clinics of Siberian State Medical University, Tomsk, tonkih.os@ssmu.ru, https://orcid.org/0000-0003-0589-0260

Vtorushin Konstantin S. – Student, Pathology Division, SibSMU, Tomsk, konstantinvtorushin.doctor@mail.ru, http://orcid.org/0009-0000-4085-3612

**Degtyarenko Nataliya V.** – Neurologist, Head of Neurology Clinic, Clinics of Siberian State Medical University, Tomsk, degtyarenko.nv@ssmu.ru

**Krakhmal Nadezhda V.** – Cand. Sc. (Medicine), Senior Researcher, General and Molecular Pathology Division, Cancer Research Institute, Tomsk NRMC, Tomsk; Teaching Assistant, Pathology Division, SibSMU, Tomsk; Pathologist, Pathology Department, Clinics of Siberian State Medical University, Tomsk, krakhmal@mail.ru, http://orcid.org/0000-0002-1909-1681

(✉) **Krakhmal Nadezhda V.,** krakhmal@mail.ru

Received on March 06, 2025;
approved after peer review on March 13, 2025;
accepted on March 20, 2025

## Издательский дом Сибирского государственного медицинского университета представляет серию книг

# «Наследие томской медицины»

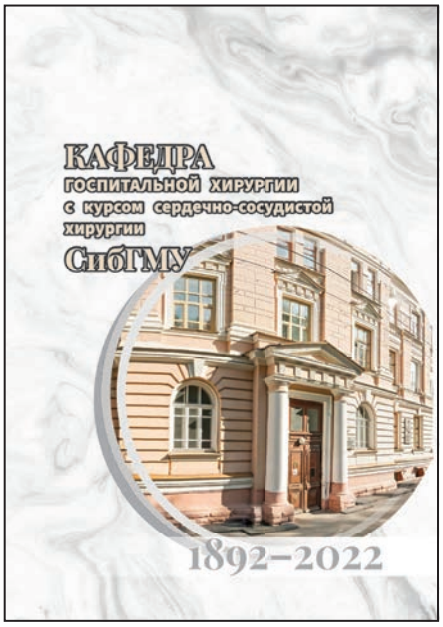


Книга посвящена 130-летнему юбилею кафедры госпитальной хирургии СибГМУ. Приведены биографические данные 79 сотрудников клиники и кафедры госпитальной хирургии в период с 1892 по 2022 г. Им предшествует подробная статья, характеризующая основные научно-практические достижения коллектива на каждом историческом отрезке. В издании упомянуты не только выдающиеся хирурги, звезды мировой величины, но и рядовые профессора, доценты, ассистенты, врачи-ординаторы, многие из которых связали с кафедрой и клиникой всю свою трудовую биографию. При изложении материала наряду с традиционными источниками информации использованы автобиографические документы, данные из семейных архивов, производственные характеристики нередко с сохранением авторского стиля.

Это позволяет полнее ощутить атмосферу в обществе и рабочем коллективе в разные годы существования клиники. Текстовая информация сопровождена богатым иллюстративным материалом, многие фотографии опубликованы впервые.

Издание предназначено для хирургов, студентов старших курсов врачебных факультетов, специалистов по истории медицины.


Трёхтомная иллюстрированная летопись одного из старейших и наиболее авторитетных медицинских вузов России – Сибирского (Томского) государственного медицинского университета является по сути первой серьёзной попыткой осветить более чем 140-летнюю историю этого прославленного университета.Особенностью издания является его богатейший иллюстративный материал, включающий более четырёх тысяч фотографий (в том числе ранее практически неизвестных), и никогда не публиковавшиеся до этого крайне любопытные и интересные факты о жизни университета, его студентов и профессоров, воспоминания и рассказы выпускников и преподавателей вуза.

Для самого широкого круга читателей, интересующихся историей российских университетов, отечественного высшего медицинского образования и науки, развитием клинических и научно-медицинских школ, здравоохранения, историей Томска, Сибири, России…

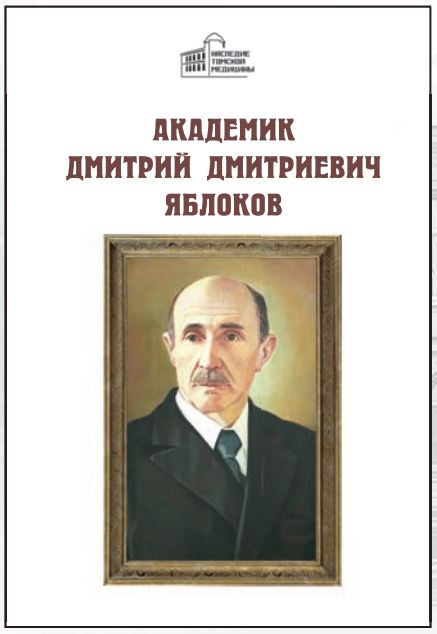


В книге представлены биография и обзор научной, педагогической и общественной деятельности выдающегося ученого, терапевта, клинициста, академика АМН СССР, Героя Социалистического труда, лауреата Сталинской премии Дмитрия Дмитриевича Яблокова (1896-1993).

Для врачей, студентов, всех интересующихся историей медицины.

# bulletin.ssmu.ru

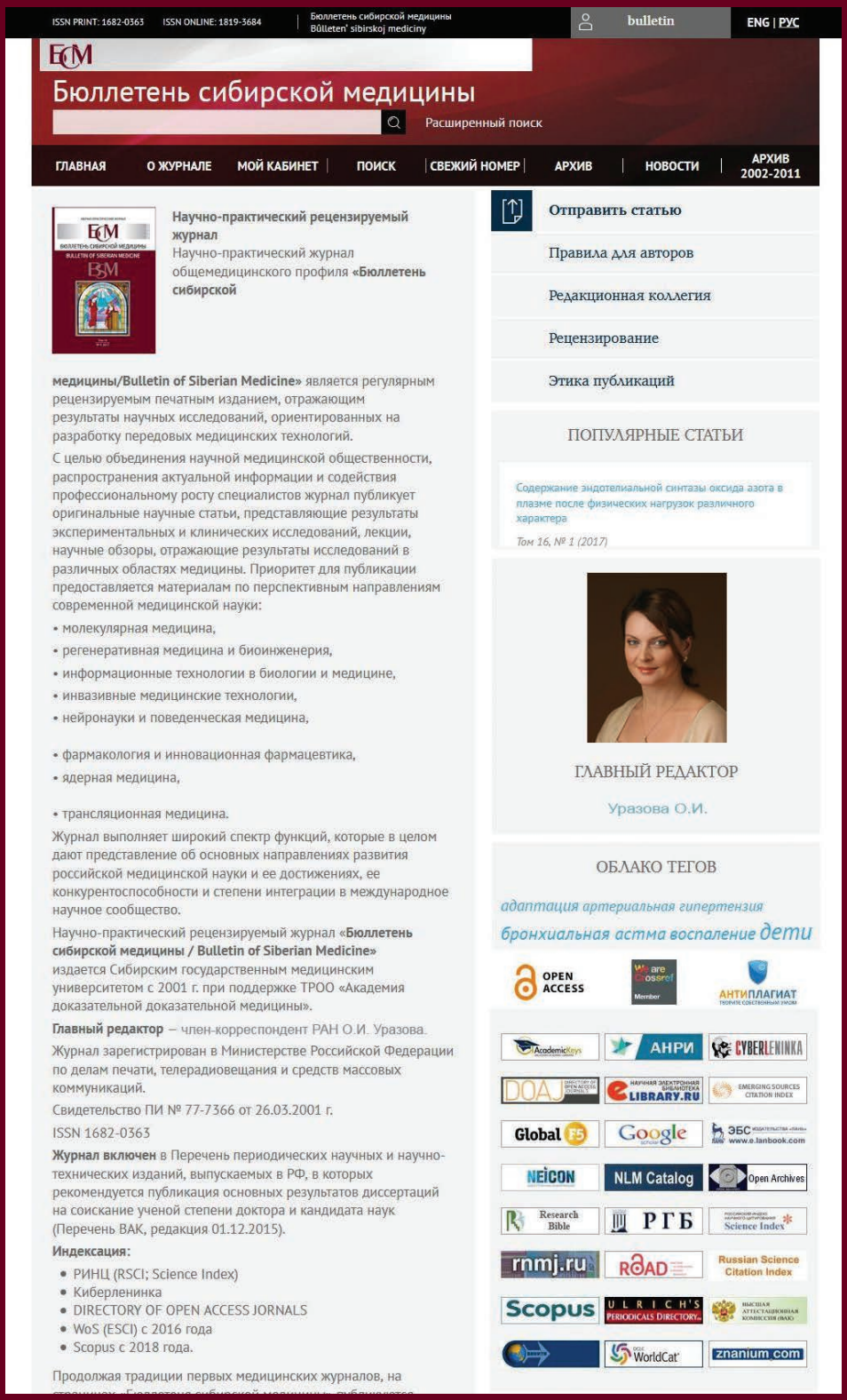


ISSN 1682-0363 (print)
ISSN 1819-3684 (online)
БЮЛЛЕТЕНЬ СИБИРСКОЙ МЕДИЦИНЫ
2025. Т. 24. № 3. 1–186